# NATURAL PRODUCTS AND BRAIN ENERGY METABOLISM: ASTROCYTES IN NEURODEGENERATIVE DISEASES, VOLUME I

EDITED BY: Fushun Wang, Shijun Xu, Fang Pan, Jason H. Huang and Alexei Verkhratsky

PUBLISHED IN: Frontiers in Pharmacology

frontiers Research Topics

ISSN 1664-8714
ISBN 978-2-83250-520-5
DOI 10.3389/978-2-83250-520-5

## About Frontiers

Frontiers is more than just an open-access publisher of scholarly articles: it is a pioneering approach to the world of academia, radically improving the way scholarly research is managed. The grand vision of Frontiers is a world where all people have an equal opportunity to seek, share and generate knowledge. Frontiers provides immediate and permanent online open access to all its publications, but this alone is not enough to realize our grand goals.

## Frontiers Journal Series

The Frontiers Journal Series is a multi-tier and interdisciplinary set of open-access, online journals, promising a paradigm shift from the current review, selection and dissemination processes in academic publishing. All Frontiers journals are driven by researchers for researchers; therefore, they constitute a service to the scholarly community. At the same time, the Frontiers Journal Series operates on a revolutionary invention, the tiered publishing system, initially addressing specific communities of scholars, and gradually climbing up to broader public understanding, thus serving the interests of the lay society, too.

## Dedication to Quality

Each Frontiers article is a landmark of the highest quality, thanks to genuinely collaborative interactions between authors and review editors, who include some of the world's best academicians. Research must be certified by peers before entering a stream of knowledge that may eventually reach the public - and shape society; therefore, Frontiers only applies the most rigorous and unbiased reviews.
Frontiers revolutionizes research publishing by freely delivering the most outstanding research, evaluated with no bias from both the academic and social point of view. By applying the most advanced information technologies, Frontiers is catapulting scholarly publishing into a new generation.

## What are Frontiers Research Topics?

Frontiers Research Topics are very popular trademarks of the Frontiers Journals Series: they are collections of at least ten articles, all centered on a particular subject. With their unique mix of varied contributions from Original Research to Review Articles, Frontiers Research Topics unify the most influential researchers, the latest key findings and historical advances in a hot research area! Find out more on how to host your own Frontiers Research Topic or contribute to one as an author by contacting the Frontiers Editorial Office: frontiersin.org/about/contact

# NATURAL PRODUCTS AND BRAIN ENERGY METABOLISM: ASTROCYTES IN NEURODEGENERATIVE DISEASES, VOLUME I

Topic Editors:
**Fushun Wang,** Nanjing University of Chinese Medicine, China
**Shijun Xu,** Chengdu University of Traditional Chinese Medicine, China
**Fang Pan,** Shandong University, China
**Jason H. Huang,** Baylor Scott and White Health, United States
**Alexei Verkhratsky,** The University of Manchester, United Kingdom

**Citation:** Wang, F., Xu, S., Pan, F., Huang, J. H., Verkhratsky, A., eds. (2022). Natural Products and Brain Energy Metabolism: Astrocytes in Neurodegenerative Diseases, Volume I. Lausanne: Frontiers Media SA.
doi: 10.3389/978-2-83250-520-5

# Table of Contents

frontiers | Frontiers in Pharmacology

TYPE Editorial
PUBLISHED 03 October 2022
DOI 10.3389/fphar.2022.1039904



OPEN ACCESS

EDITED AND REVIEWED BY
Nicholas M. Barnes,
University of Birmingham,
United Kingdom

*CORRESPONDENCE
Fushun Wang,
13814541138@163.com
Shijun Xu,
xushijun@cdutcm.edu.cn

SPECIALTY SECTION
This article was submitted to Neuropharmacology, a section of the journal Frontiers in Pharmacology

RECEIVED 08 September 2022
ACCEPTED 13 September 2022
PUBLISHED 03 October 2022

CITATION
Wang F, Xu S, Pan F, Verkhratsky A and Huang JH (2022), Editorial: Natural products and brain energy metabolism: Astrocytes in neurodegenerative diseases. *Front. Pharmacol.* 13:1039904. doi: 10.3389/fphar.2022.1039904



# Editorial: Natural products and brain energy metabolism: Astrocytes in neurodegenerative diseases

Fushun Wang[1]*, Shijun Xu[2]*, Fang Pan[3], Alex Verkhratsky[4] and J. H Huang[5,6]

[1]Institute of Brain and Psychological Science, Sichuan Normal University, Chengdu, China, [2]School of Pharmacy, Chengdu University of Traditional Chinese Medicine, Chengdu, China, [3]Department of Medical Psychology, Shandong University Medical School, Jinan, China, [4]Department of Physiology, The University of Manchester, Manchester, United Kingdom, [5]Department of Neurosurgery, Baylor Scott & White Health, Temple, TX, United States, [6]Department of Surgery, Texas A&M University College of Medicine, Temple, TX, United States

KEYWORDS

**astrocyte, mitochondria, energy supply, glymphatic, emotinoal arousal, monoamine**

Editorial on the Research Topic
Natural products and brain energy metabolism: Astrocytes in neurodegenerative diseases

The brain weighs approximately 2% of the body, but utilizes about 20% of the total energy and oxygen supply, thus energy supply is critically important for the brain. In addition, the brain has no energy reserve, except some glycogens in the astrocytes, and the neurons can only use ATP, which comes from glucose degradation in the essential structure mitochondria. Mitochondria impairment, such as electron transport chain damage, can induce decreased ATP levels, decreased antioxidant defense, which is prevalent in many neurodegenerative disorders. For example, ATP dysfunction has been suggested to be the major impaired in depression (Cao, et al., 2013). Numerous studies suggest that energy metabolism disorders are hallmarks of brain aging and are particularly involved in many neurodegenerative disorders, such as Alzheimer's diseases and major depression disorder. However, even though the regulatory mechanisms are important to ensure adequate supply for the neurons, how the brain accomplishes this complex task is still unclear.

## Emotional arousal regulates brain energy supply

It is critically important to understand the central facets of physiology and pathophysiology of energy supply in the brain, however, the energy supply regulation

in the brain is not clear, for example how emotion affects energy supply, and does it activated by monoamine neurotransmitters. Emotion plays an important role in the regulation of the energy supply for the brain. Emotion parallels with behavior all the time, from the initiation of a behavior, the process of behavior to the end of the behavior. Emotion is the tendency for behavior, is also the motivation of a behavior. Emotion is also important for appraisal of behavioral consequences, marking the behavior as reward or punishment (Gu, et al., 2019). Emotions have two dimensions: arousal and valence. Emotional arousal can activate the sympathetic nervous system to increase the heart beat and breath rate to increase blood supply, including glucose and oxygen for the brain and induced "fight or flight" behaviors (Liang et al., 2021). Emotional valence is related to physiological needs and can activate the parasympathetic nervous system to increase activities of digestive system, and also increase breath depth (Zheng et al., 2016).

Emotion is nothing but neurotransmitters (Gu, et al., 2019). The emotional neurotransmitters not only affect the periphery organs *via* autonomous nervous system, but also affect the energy supply in the brain. For example, the monoamine transmitters stimulate $Na^+$, $K^+$-ATPase activity in astrocytes and facilitate their role in ion concentrations (Wang et al., 2012, 2013). Previously, we proposed a "three primary color model of basic emotions, which suggested that the emotions are composed of three primary emotions: joy, fear (anger) and disgust (Wang et al., 2020, 2022). The three primary emotions depend on three monoamines: Joy-dopamine (DA), fear (anger)- norepinephrine (NE) and disgust-serotonin (5-HT) (He et al., 2021). The relationship of cerebral neurotransmitters DA, NE, 5-HT to the energy state of the brain has been investigated by many studies, for example, it is found that many environmental and homeostatic challenges can induce monoamine release, and induce rapid preparatory changes in neural activities as well as increased brain energy metabolism (Beley et al., 1991).

## Astrocytes in energy supply for the brain

Blood glucose is the major source of energy supply for the brain, which can be taken up by both neurons and astrocytes, however, astrocyte has been known to play a major support role in energy supply in the brain. "Glycogenetic" hypothesis suggests that astrocyte plays a more important role in glycolytic metabolism, while neurons function as high mitochondrial oxidative activity to use energy. Glycogen reservoir in astrocytes can be used as brain energy supply by turning glycogen to glucose and release glucose at high extracellular $K^+$ and glutamate release during brain arousal (Petit et al., 2021).

Monoamine neurotransmitters are exquisitely suitable for regulation of astrocytic glucose uptake and release. Astrocytes can turn glycogen to glucose at emergent energy demand, when monoamine neurotransmitters are released at emotional arousal. Emotional arousal can induce NE release in the locus coeruleus and also other monoamine neurotransmitters, which are glycogenolytic agents (DiNuzzo et al., 2015). Emotional arousal induced activation of noradrenergic locus coeruleus can reversibly block astrocytic glucose uptake by glycogen mobilization in astrocytes, possibly *via* $Ca^{2+}$ signaling in astrocytes (Ding, et al., 2013). Accumulating evidence indicates that emotions can affect energy metabolism *via* astrocytic $Ca^{2+}$ signaling, which can affect the glucose, ions and also gliotransmitter release. Previously, we have found that NE induced *via* astrocytic $Ca^{2+}$ signaling can affect extracellular $K^+$ (Wang et al., 2012). In addition, these astrocytic $Ca^{2+}$ signaling can also affect the function of mitochondria, whose normal functions rely on $Ca^{2+}$. Indeed, chronic stresses have been found to induce mitochondrial abnormalities and cause energy shortage in neurons (Iwata et al., 2019). In addition, energy supply shortage is a major cause for a cascade of neurosynaptic dysfunctions, which leads to Alzheimer's disease, Parkinson disease, stress, and depression etc.

## Astrocytes in clearance of metabolic waste

Astrocyte is known as an energy support system for the brain, and also a clearance system to clear off the metabolic waste in the brain microenvironment. The Glymphatic system is a unique clearance system in the brain to extrude water and macromolecular waste (Mestre et al., 2020). The glymphatic system is a drainage system that is composed of perivascular spaces and astrocytes to connect the brain interstitial fluids and cerebrospinal fluid (Iliff, et al., 2013). These fluids flow along the paravascular space of the arteries and veins to essentially clear off the metabolites. The function of glymphamatic system is controlled by monoamine neurotransmitters, especially NE, which can block the function of glymphamatic system by modulating astrocytic functions (Ding et al., 2016). Thus sleep is very important for normal function of glymphamatic system to effectively control the clearance of toxic peptides such as tau protein.

The glymphatic system, which was found in our lab in 2012, has recently been found to play an important player in many neurodegenerative diseases, because of vasculature impairment, or astrocytic dysfunction. The glymphatic system is a brain-wide perivascular pathway that is potentially offering new therapeutic targets to improve cerebral drainage and immune survey in

human CNS diseases (Ma et al., 2021). Indeed, many genetic and pharmacological approaches have proved that "housekeeping" effects of astrocytes are involved in many neurodegenerative diseases by supplying energy and clearance of metabolites.

## Natural product for energy supply

Many natural plants have been used to treat the neurodegenerative disorders in Traditional Chinese Medicine or other alternative treatments. Some natural products have been identified and proved to be effective in treating the neurodegenerative disorder, such as flavonoids, polyphenols, alkaloids. The discovery of strong active compounds from plants has been validated for efficacy, and structural modification based on the groups is an effective method for new drug discovery. For example, Huperzine A from Huperzia serrata is proven to improve memory impairment in Alzheimer's disease, and huperzine A-derived Shiplin is currently in Phase III clinical studies. This lesson could reveal a new opportunity for natural compounds as candidates for neurodegenerative diseases therapy.

## This topic collected papers

In this Research Topic, we welcomed high-quality studies about natural products regulating energy metabolism at neurodegenerative diseases. We got 35 submissions and accepted 15 paper *via* peer-reviewed processes, all the accepted papers are introduced below:

In the paper titled "Curcumin as a holistic treatment for tau pathology", the author Sivanantharajah reviewed recent studies about traditional herbs, spices and other nutraceuticals that can be used to effectively treat AD. They found that the spice Turmeric with its active ingredient curcumin can effectively be used to treat tau pathology.

In the experimental study titled "Tanhuo Formula Inhibits Astrocyte Activation and Apoptosis in Acute Ischemic Stroke", Nie et al. introduced an old Chinese formula Tanhuo formula. They first analyzed its bioactive compounds and then tested their effects on the activities of astrocytes, and found that Tanhuo formula can effectively block neural cell apoptosis *via* caspase-3 pathway to block the excessive abnormal and the release of TNF-α and IL-6.

In the review titled "Berberine: a promising treatment for neurodegenerative diseases", the authors Cheng et al., gave a short review about berberine, which is alkaloid compound from a kind of Chinese herb. Many recent studies have reported the effects of berberine on neurodegenerative disorders, such as Parkinson's disease, Alzheimer's disease, Huntington's disease and so on. The review suggested that the major function of berberine is inhibiting oxidative stress and endoplasmic reticulum stress, enhancing mitochondria activity, which can in turn induce neuronal damage and apoptosis.

In another paper titled "Current evidence and future directions of berberine intervention in depression", Zhu et al. also reviewed the effects of berberine, natural monomer compound of Coptis chinensis, and its effects on the typical emotional disorder (major depressive disorders), and suggested the berberine might be used as encouraging antidepressants to modulate depressed emotion.

In the experimental study about berberine titled "Berberine Alleviate Cisplatin-induced Peripheral Neuropathy by Modulating Inflammation Signal *via* TRPV1", the authors Meng et al. studied the effects of berberine on transient receptor potential vanilloid (TRPV1) in dorsal root ganglia inflammation *via* inhibiting NF-κB and activating the JNK/p38 MAPK pathways in early injury, which inhibited the overexpression of TRPV1. The study suggested that berberine can reverse neuropathic pain response *via* inhibiting TRPV1 expression.

In another review, the authors Li et al. introduced another kind of natural product, echinacoside, which is a kind of phenylethanoid glycoside (PhG) in Cistanche tubulosa. In the paper "Therapeutic potential and molecular mechanisms of Echinacoside in neurodegenerative diseases", they reviewed many recent studies about its mechanisms in neuroprotective efficacy in the prevention and treatment of neurodegenerative diseases, and proposed that the major effect of echinacoside is improving mitochondrial function and reducing anti-oxidative stress.

In the review paper titled "Progress in the mechanism of autophagy and traditional Chinese medicine herb involved in dementia", Tao et al. summarized recent *in vitro* and *in vivo* studies about Chinese herbs in treating dementia, and found that the extracts of these Chinese herbs work on reducing generation of reactive oxygen species and inhibiting inflammation and neurotoxicity.

In the experimental paper titled "Yi-zhi-fang-dai formula exerts neuroprotective effects against pyroptosis and blood-brain barrier-glymphatic dysfunctions to prevent amyloid-beta ccute accumulation after cerebral ischemia and reperfusion in rats", the authors Lyu et al. studied a kind of Chinese herb Yi-zhi-fang-dai formula, and its effects on pyroptosis and glymphatic dysfunctions. The study suggested that the Chinese herb Yi-zhi-fang-dai formula could inactivate pyroptosis *via* inhibiting caspase-1/11 activation and gasdermin D cleavage, and induce AQP-4 depolarization thus increase glymphatic function to reduce neuronal damage.

In the experimental paper titled "Rhein relieves oxidative stress in an Aβ1-42 oligomer-burdened neuron model by activating the SIRT1/PGC-1α-regulated mitochondrial biogenesis", the authors Yin et al. studied the antioxidant activity of natural product rhein, and also its effects in clearance of β-amyloid (Aβ) in Alzheimer's disease. The study

found that rhein could significantly reduce reactive oxygen species, and activate mitochondrial biogenesis by increased cytochrome C oxidase and superoxide dismutase activities.

In the experimental paper "Neuronal Regeneration by Downregulating Notch Signaling Pathway in the Treatment of Generalized Anxiety Disorder", the authors Liu et al. introduced a study about a kind of Chinese herb named danzhi xiaoyao powder and its effects on the symptoms of generalized anxiety disorder. The results suggested that the power could improve the weight growth and improve appetite and reduce the anxious mood *via* notch signaling pathway in the hippocampus. The study suggested that danzhi xiaoyao powder is a good therapy method for mood disorders.

In the experimental study, He et al. introduced a kind of classic Chinese herb formula, qiangji decoction in the paper "Qiangji Decoction alleviates neurodegenerative changes and hippocampal neuron apoptosis induced by D-galactose *via* regulating AMPK/SIRT1/NF-κB signaling pathway". The herbs have been widely used in the traditional Chinese medicine, but the mechanisms are not clear. This paper found the major effect of qiangji decoction is reducing inflammation *via* reducing TNF-α, IL-1β and IL-6 in the hippocampus *via* regulating AMPK/SIRT1/NF-κB signaling pathway in hippocampal neuron apoptosis.

In the experimental study, Zheng et al. introduced a kind of Chinese herb ginkgo biloba extract and donepezil on Alzheimer's disease. In the paper titled "Effects of ginkgo biloba extract and donepezil on functional recovery in Alzheimer's disease: a multi-level characterized study based on clinical features and resting-state functional magnetic resonance imaging", they used neuroimage study and found that the herbs could change the ALFF values in right gyrus rectus and decreased PerAF values in left fusiform gyrus. And the authors concluded that the imaging metrics in specific brain regions may serve as biomarkers for therapeutic efficacy of medicines.

The authors Zheng et al. introduced a study on the mechanism of sytisine on temporal lobe epilepsy, in the paper titiled "Cytisine exerts an anti-epileptic effect *via* α7nAChRs in a rat model of temporal lobe epilepsy". Cytisine is an agonist of α7 nicotinic acetylcholine receptors (α7nAChRs) and has shown neuroprotection in many neurological diseases. This study found that sytisine could increase hippocampal function *via* enhancing ACh levels and α7nAChR expression, and decrease glutamate level to reduce seizures. The authors Arrodi et al. introduced one paper titled "Modulatory effects of alpha- and gamma-tocopherol on the mitochondrial respiratory capacity and membrane potential in Alzheimer's disease an *in vitro* model of Alzheimer's disease", which suggested that mitochondrial abnormalities are an early feature in the pathogenesis of AD. They found that alpha-tocopherol or gamma-tocopherol could modulate mitochondrial function by increasing the production of ATP and reducing mitochondrial reactive oxygen species *via* altering mitochondrial metabolic pathways such as oxidative phosphorylation.

In the paper titled "Tortoise plastron and dear antler gelatin prevents against neuronal mitochondrial dysfunction *in vitro*: implication for a potential therapy of Alzheimer's disease", Cheng et al. investigated the role of mitochondrial dysfunction in the pathogenesis of Alzheimer's disease. In addition, they investigated the effects of tortoise plastron gelatin and dear antler gelatin in preventing neuronal mitochondria function. The found that these two natural products could increase cell viability by modulating intracellular ATP and calcium level, and also regulate mitochondrial membrane potential (MMP) and ultrastructure, and finally inducing anti-dementia effects.

In all, these studies demonstrate that astrocytic function and neuronal mitochondria function play important roles in many neurodegenerative disorders. In addition, this topic introduced many natural drugs in treating these diseases. We expected that this Research Topic will stimulate interest in the study of the mechanisms of modulating the energy supply.

## Author contributions

FW and SX designed the stduy, FW and FP wrote the paper, AV and JH did the revision.

## Funding

This study was supported by the grants from the project supported by National Natural Science Foundation of China, China (No. 82171392).

## Conflict of interest

The authors declare that the research was conducted in the absence of any commercial or financial relationships that could be construed as a potential conflict of interest.

## Publisher's note

# References

Beley, A., Bertrand, N., and Beley, P. (1991). Cerebral ischemia: Changes in brain choline, acetylcholine, and other monoamines as related to energy metabolism. *Neurochem. Res.* 16 (5), 555–561. doi:10.1007/BF00974874

Cao, X., Li, L. P., Wang, Q., Wu, Q., Hu, H. H., Zhang, M., et al. (2013). Astrocyte-derived ATP modulates depressive-like behaviors. *Nat. Med.* 19 (6), 773–777. doi:10.1038/nm.3162

Ding, F., O'Donnell, J., Thrane, A. S., Zeppenfeld, D., Kang, H., Xie, L., et al. (2013). α1-Adrenergic receptors mediate coordinated Ca2+ signaling of cortical astrocytes in awake, behaving mice. *Cell Calcium* 54 (6), 387–394. doi:10.1016/j.ceca.2013.09.001

Ding, F., O'Donnell, J., Xu, Q., Kang, N., Goldman, N., and Nedergaard, M. (2016). Changes in the composition of brain interstitial ions control the sleep-wake cycle. *Science* 352 (6285), 550–555. doi:10.1126/science.aad4821

DiNuzzo, M., Giove, F., Maraviglia, B., and Mangia, S. (2015). Monoaminergic control of cellular glucose utilization by glycogenolysis in neocortex and Hippocampus. *Neurochem. Res.* 40 (12), 2493–2504. doi:10.1007/s11064-015-1656-4

Gu, S., Wang, F., Patel, N. P., Bourgeois, J. A., and Huang, J. H. (2019). A model for basic emotions using observations of behavior in Drosophila. *Front. Psychol.* 10, 781. doi:10.3389/fpsyg.2019.00781

He, Z., Jiang, Y., Gu, S., Wu, D., Qin, D., Feng, G., et al. (2021). Emotion induced monoamine neuromodulator release affects functional neurological disorders. *Front. Cell Dev. Biol.* 9, 633048. doi:10.3389/fcell.2021.633048

Iliff, J. J., Lee, H., Yu, M., Feng, T., Logan, J., Nedergaard, M., et al. (2013). Brain-wide pathway for waste clearance captured by contrast-enhanced MRI. *J. Clin. Invest.* 123 (3), 1299–1309. doi:10.1172/JCI67677

Iwata, K. (2019). Mitochondrial involvement in mental disorders; energy metabolism, genetic, and environmental factors. *Methods Mol. Biol.* 1916, 41–48. doi:10.1007/978-1-4939-8994-2_2

Liang, F., Feng, R., Gu, S., Jiang, S., Zhang, X., Li, N., et al. (2021). Neurotransmitters and electrophysiological changes might work as biomarkers for diagnosing affective disorders. *Dis. Markers* 2021, 9116502. doi:10.1155/2021/9116502

Ma, T., Wang, F., Xu, S., and Huang, J. H. (2021). Meningeal immunity: Structure, function and a potential therapeutic target of neurodegenerative diseases. *Brain Behav. Immun.* 2021 (21), 264–276. doi:10.1016/j.bbi.2021.01.028

Mestre, H., Mori, Y., and Nedergaard, M. (2020). The brain's glymphatic system: Current controversies. *Trends Neurosci.*43 (7), 458–466. doi:10.1016/j.tins.2020.04.003

Petit, J. M., Eren-Koçak, E., Karatas, H., Magistretti, P., and Dalkara, T. (2021). Brain glycogen metabolism: A possible link between sleep disturbances, headache and depression. *Sleep. Med. Rev.* 59, 101449. doi:10.1016/j.smrv.2021.101449

Wang, F., Smith, N. A., Xu, Q., Fujita, T., Baba, A., Matsuda, T., et al. (2012). Astrocytes modulate neural network activity by $Ca^2$+-dependent uptake of extracellular K+. *Sci. Signal.* 5 (218), ra26. doi:10.1126/scisignal.2002334

Wang, F., Smith, N. A., Xu, Q., Goldman, S., Peng, W., Huang, J. H., et al. (2013). Photolysis of caged Ca2+ but not receptor-mediated Ca2+ signaling triggers astrocytic glutamate release. *J. Neurosci.* 33 (44), 17404–17412. doi:10.1523/jneurosci.2178-13.2013

Wang, F., Yang, J., Pan, F., Ho, R. C., and Huang, J. H. (2020). Editorial: Neurotransmitters and emotions. *Front. Psychol.* 11, 21. doi:10.3389/fpsyg.2020.00021

Wang, F., Pan, F., Tang, Y. Y., and Huang, J. H. (2022). Editorial: Uncertainty induced emotional disorders during the COVID-19. *Front. Psychol.* 13, 943966. doi:10.3389/fpsyg.2022.943966

Zheng, Z., Gu, S., Lei, Y., Lu, S., Wang, W., Li, Y., et al. (2016). Safety needs mediate stressful events induced mental disorders. *Neural Plast.* 2016. 8058093. doi:10.1155/2016/8058093

frontiers in Pharmacology

ORIGINAL RESEARCH
published: 13 May 2021
doi: 10.3389/fphar.2021.690256

# Tortoise Plastron and Deer Antler Gelatin Prevents Against Neuronal Mitochondrial Dysfunction *In Vitro*: Implication for a Potential Therapy of Alzheimer's Disease

*Dan Cheng*[1], *Xin-Jing Yang*[1,2], *Lu Zhang*[1], *Zong-Shi Qin*[1], *Wen-Qi Li*[1], *Hai-Chun Xu*[3] *and Zhang-Jin Zhang*[1,2]*

[1]School of Chinese Medicine, LKS Faculty of Medicine, The University of Hong Kong, Hong Kong, China, [2]Department of Chinese Medicine, The University of Hong Kong-Shenzhen Hospital (HKU-SZH), Shenzhen, China, [3]Shenyang Jing'an Mental Health Hospital, Shenyang, China

OPEN ACCESS

**Edited by:**
Fushun Wang,
Nanjing University of Chinese Medicine, China

**Reviewed by:**
Guo-qing Zheng
Ying Xu,
Shanghai University of Traditional Chinese Medicine, China
Qinru Sun,
Xi'an Jiaotong University, China

***Correspondence:**
Zhang-Jin Zhang
zhangzj@hku.hk

**Specialty section:**
This article was submitted to Neuropharmacology, a section of the journal Frontiers in Pharmacology

**Received:** 02 April 2021
**Accepted:** 29 April 2021
**Published:** 13 May 2021

**Citation:**
Cheng D, Yang X-J, Zhang L, Qin Z-S, Li W-Q, Xu H-C and Zhang Z-J (2021) Tortoise Plastron and Deer Antler Gelatin Prevents Against Neuronal Mitochondrial Dysfunction In Vitro: Implication for a Potential Therapy of Alzheimer's Disease. Front. Pharmacol. 12:690256. doi: 10.3389/fphar.2021.690256

Mitochondrial dysfunction with oxidative damage plays the fundamental roles in the pathogenesis of Alzheimer's disease. In traditional Chinese medicine (TCM) practice, animal tissue-derived gelatins are often used as nootropic agents to treat cognitive deterioration and senile dementia. Tortoise plastron gelatin (TPG) and deer antler gelatin (DAG) are the two most commonly used gelatins for this purpose. This study sought to examine the effects of the two gelatins in preventing neuronal mitochondria from oxidative damage. PC12 cells, a cell line derived from rat pheochromocytoma, exposed to the neurotoxin $A\beta_{25–35}$ served as an *in vitro* model of Alzheimer's disease. The cells were separately pre-treated with TPG and DAG at various concentrations ranging from 6.26 μg/ml–200 μg/ml, followed by co-incubation with 20 μM $A\beta_{25–35}$ for different duration. Cell viability, mitochondrial membrane potential (MMP) and ultrastructure, intracellular ATP, reactive oxygen species (ROS) and calcium ($Ca^{2+}$) level, the expression of mitochondrial dynamic proteins and biomarkers of apoptosis were measured. Pretreatment with TPG and DAG reversed the Aβ-induced reduction of cell viability in a dose-dependent manner. Both TPG and DAG significantly increased MMP and ATP, alleviated the accumulation of damaged mitochondrial fragments, and normalized the aberrant expression of multiple mitochondrial dynamic proteins of the Aβ-exposed cells. Both gelatins also suppressed intracellular ROS overproduction and $Ca^{2+}$ overload, overexpression of cytochrome c and pro-apoptosis biomarkers induced by the Aβ exposure. These results suggest that TPG

**Abbreviations:** TPG, Tortoise plastron gelatin; DAG, deer antler gelatin; AD, Alzheimer's disease; MMP; mPTP, mitochondrial membrane permeability transition pores; Drp1, dynamin-related protein 1; Fis1, fission 1; Mfn1, mitofusin l; Opa 1, optic atrophy 1; TCM, traditional Chinese medicine; GMP, Good Manufacturing Practice; ChP, Pharmacopoeia of the People's Republic of China; PBS, phosphate-buffered saline; DMEM, Dulbecco's Modified Eagle Media; FBS, Fetal bovine serum; CCK-8, Cell Counting Kit; TEM, Transmission electron microscope; HBSS, Hank's Balanced Salt Solution; DCF, 2,7-dichloro-fluorescein; RIPA, radioimmunoprecipitation assay; SDS-PAGE, sodium dodecyl sulfate-polyacrylamide gel electrophoresis; PVDF, polyvinylidene difluoride; TBST, Tris-buffered saline containing Tween 20; CaMKII, calmodulin-dependent protein kinase II; CaSR, calcium-sensing receptor.

and DAG may have the anti-dementia potential by preventing neuronal mitochondria from oxidative damage.

**Keywords: deer antler gelatin, tortoise plastron gelatin, Alzheimer's disease, oxidative damage, mitochondrial dysfunction**

## INTRODUCTION

Alzheimer's disease (AD) is a progressive neurodegeneration disorder that affects millions of people worldwide. The most apparent pathological feature of AD is the accumulation of amyloid β (Aβ) peptide in the neocortex, hippocampus, and other brain regions essential for cognitive function (Eckert et al., 2010). Aβ is a neurotoxin that impairs subcellular components of cerebral neurons, including mitochondria, leading to neuron degeneration and death (Coleman and Yao, 2003). Due to the fact that the development of multiple drugs directly targeting Aβ has failed to achieve the expected success (Huang et al., 2020), neuronal oxidative hypometabolism has been considered as an alternative therapeutic target in a search of novel therapy for AD (Costantini et al., 2008; Struble et al., 2010).

Mitochondria is the primary site of energy metabolism that plays the fundamental roles in the pathogenesis of AD (Mcbride et al., 2006; Lim et al., 2010). During the evolution of AD, mitochondria suffer profound alterations, manifesting as morphological damage, decreased ATP generation, and increased production of reactive oxygen species (ROS) (Lin and Beal, 2006). An excessive ROS production, in turn, exacerbates mitochondrial dysfunction with decreased mitochondrial membrane potential (MMP) and intracellular calcium ($Ca^{2+}$) overflow (Manczak et al., 2010; Tönnies and Trushina, 2017), resulting in the release of apoptotic factors, such as cytochrome c, an apoptotic mediator in the organelles and procaspase-9 and caspase-3, the two pro-apoptotic factors in response to apoptotic signals (Hengartner, 2000; Giorgi et al., 2012). Neuronal calcium influx further disturbs the maintenance of mitochondrial dynamics with an imbalance in mitochondrial fission and fusion, leading to aberrant expression of fission-mediated proteins, such as fission1 (fis1) and dynamin-related protein 1 (Drp1), and fusion-associated proteins, such as Mitofusin 1 (Mfn1), Mitofusin 2 (Mfn2), and Optic atrophy 1 (Opa1) (Ishihara et al., 2004; Losón et al., 2013).

In traditional Chinese medicine (TCM) practice, animal tissue-derived gelatins are often empirically used as nootropic and brain function-enhancing agents to treat cognitive deterioration and senile dementia (Kong, 2007; Chen et al., 2016; Zhan et al., 2018; Li and Ms, 2019; Tang et al., 2019). Tortoise plastron gelatin (TPG) and deer antler gelatin (DAG) are the two most commonly prescribed gelatins for this purpose (Li and Ms, 2019; Tang et al., 2019). Previous studies have revealed that TPG and DAG contain multiple amino acids and trace minerals, and possess the effects in modulating energy metabolism and improving memory and other cognitive symptoms (**Table 1**; Shi et al., 2012; Jiang et al., 2015; Guo et al., 2016; Wang et al., 2018; Long et al., 2019). These have led to the hypothesis that the anti-dementia effects of the two gelatins were perhaps achieved by preventing neuronal mitochondria from oxidative damage. To test this hypothesis, the effects of TPG and DAG were examined in $A\beta_{25-35}$-exposed PC12 cells, a cell line derived from a rat pheochromocytoma, that served as an *in vitro* model of Alzheimer's disease. It is well documented that PC12 is an appropriate model that has been widely used to investigate mitochondria-and Alzheimer's disease-related pathological profiles (Dubey et al., 2019). Cell viability, mitochondrial ultrastructure and MMP, intracellular ATP, ROS and $Ca^{2+}$ level, the expression of mitochondrial dynamic- and apoptosis-related biomarkers were measured.

## MATERIALS AND METHODS

### Drug Preparations

Tortoise plastron gelatin (TPG) and deer antler gelatin (DAG) were generously provided by Hongxing pharmaceutical Co. Ltd (Shantou, Guangdong, China). TPG-and DAG-contained products have been approved by National Medical Products Administration for marketing (Approved code: Z44021133) (http://gdhxjtgfyxgshxzyc.liangyi360.com/yaopin/818003604.

**TABLE 1** | Amino acids and trace mineral elements contained in the gelatins[a].

| Components | Tortoise plastron gelatin | Deer antler gelatin |
|---|---|---|
| Amino acids (%) | | |
| Alanine | 4.5–8.2 | 6.8–9.8 |
| Arginine | 2.4–5.7 | 2.4–15.0 |
| L-Aspartic acid | 2.1–2.3 | 2.2–7.2 |
| L-Cystine | 0.2–0.3 | 0.2–1.0 |
| Glutamic acid | 3.5–7.6 | 3.1–12.4 |
| Glycine | 14.3–18.2 | 17.1–55.9 |
| Histidine | 0.2–0.4 | 0.4–1.3 |
| Hydroxyproline | 7.6–7.9 | 8.8–11.9 |
| Isoleucine | 0.7–1.8 | 1.3–3.0 |
| Leucine | 1.5–2.8 | 2.7–5.3 |
| Lysine | 1.4 | 1.5–5.8 |
| Phenprobamate | 1.4–1.9 | 2.0–3.9 |
| Proline | 6.7–11.8 | 8.5–19.2 |
| Serine | 2.4–3.0 | 2.5–2.6 |
| Threonine | 1.0–1.6 | 1.1–2.5 |
| Tyrosine | 0.5–0.8 | 0.6 |
| Valine | 0.9–1.6 | 1.6–4.5 |
| Trace mineral elements (mg/kg) | | |
| Calcium (Ca) | 150–961 | |
| Magnesium (Mg) | 115–760 | |
| Zinc (Zn) | 0.3–06 | |
| Iron (Fe) | 36–122 | |
| Strontium (Sr) | 0.1–34.3 | |

[a]*Data are generated from Refs [Guo et al. (2016), Long et al. (2019), Wang et al. (2018), Jiang et al. (2015), Shi et al. (2012)].*

html). The detailed manufacturing procedure of the two gelatins was carried out in strict compliance with Pharmacopoeia of the People's Republic of China (2020) and Good Manufacturing Practice (GMP). The quality control of both gelatins adhered to the specifications and test procedures according to the internal standard. The gelatins were dissolved into phosphate buffered saline (PBS) to form a 20 mg/ml stock solution and stored at 4°C for later use.

$A\beta_{25-35}$ fragments (Sigma-Aldrich) were generated as described in a previous method (Kim et al., 2010). Briefly, $A\beta_{25-35}$ monomer was dissolved in distilled water to a stock concentration of 1 mmol/L, incubated at 37°C for seven days, and then stored $A\beta_{25-35}$ plaques at-20°C for later use.

## Cell Culture and Treatment

PC12 cells were cultured in Dulbecco's Modified Eagle Media (DMEM, Gibco, America) supplemented with 10% fetal bovine serum (FBS, Gibco, United States) and 1% Penicillin-Streptomycin Solution (Invitrogen, Unites States) at 37°C in a 5% $CO_2$ incubator.

The cells were seeded into 96-well plates at a density of $5 \times 10^3$ cells/well for cell viability analysis, 10 cm cell culture dish for transmission electron microscopy and 6-well plates at a density of $1.25 \times 10^5$ cell/ml for other experiments. Seeded cells were allowed to grow for 24 h. After then, for most experiments, the cells were treated respectively with multiple concentrations of TPG and DAG, ranging from 6.26 μg/ml–200 μg/ml, for 1 h; 20 μM $A\beta_{25-35}$ was subsequently added for co-incubation for additional 23 h, such that the preventive effects of the gelatins against Aβ neurotoxicity was tested. Following the completion of treatment, various experimental procedures were further performed.

A separate experiment was conducted to examine the acute effects on MMP (see below) by adding 20 μM $A\beta_{25-35}$ at 20 h after gelatin treatment and co-incubating for additional 4 h. To determine the optimal time point at which the production of Aβ-induced intracellular (ROS) reached the peak level, the cells were exposed to 20 μM $A\beta_{25-35}$ for 1, 6, 12, and 24 h, respectively. The highest ROS level was observed at 1 h (**Supplementary Figure S2**). The ROS experiment was then conducted by adding 20 μM $A\beta_{25-35}$ at 23 h after gelatin treatment and co-incubating for additional 1 h (see below).

## Cell Viability Assay

Cell viability was measured using a Cell Counting Kit-8 (CCK-8) assay (ApeBio, United States). Briefly, following the completion of treatment, 10 μl CCK-8 solution was added to each well and incubated for 2 h. The absorbance for optical density (OD) in each well was read at 450 nm on a Microplate reader (Bio-Rad, United States). Cell viability was calculated using the following equation: Cell viability (%) = (mean OD of drug-treated cells-mean OD blank)/(mean OD of untreated cells-mean OD blank) × 100%.

## Transmission Electron Microscopy

The cells were collected into the trypsin-EDTA solution, centrifuged at 1,000 rpm for 5 min, washed for three times in PBS, and fixed in a 2.5% glutaraldehyde solution at 4°C overnight. After then, glutaraldehyde solution was removed. The cells were washed for three times in PBS, post-fixed in 1% osmium tetroxide for 3 h and stained with 2% uranyl acetate at 4°C. The cells were further dehydrated in a gradient ethanol concentration from 50 to 100% and embedded in spur resin. Ultrathin (60 nm) sections were stained in a combination of 3% uranyl acetate and lead citrate, and then examined under TEM (Philips CM100).

## Flow Cytometry Analysis

Flow cytometry was used to analyze MMP and cell apoptosis.

MMP was examined using a JC-1 mitochondrial assay kit (Beyotime, Beijing, China) with flow cytometry (BD, United States). JC-1 forms aggregates that emit red fluorescence at high MMP while forms monomers that emit green fluorescence at low MMP (Berlepsch and Böttcher, 2013). PC12 cells were washed twice in PBS and incubated at 37°C for 30 min at the final concentration of JC-1 (1×) dissolved in the staining buffer and distilled water. The cells were washed three times in PBS and re-suspended in the same buffer in the culture tube for flow cytometry detection.

Cell apoptosis was analyzed using PE Annexin V Apoptosis detection kit (BD Pharmingen, United States), in which Annexin V was conjugated to the fluorochrome phycoerythrin (PE), to detect the phosphatidylserine (PS) on the outer membrane of the apoptosis cells (Leventis and Grinstein, 2010). PC12 cells were washed twice with cold PBS and then re-suspended in 1× binding buffer at a concentration of $1 \times 10^6$ cell/mL. After that, 100 μL of cells were transferred to the culture tube and incubated with a mixture of 10 μl PE Annexin V and 7-AAD at room temperature for 20 min in the dark. Cells were subjected to flow cytometric analysis.

## Fluorescence Spectrophotometry of ATP

The intracellular ATP level was measured using a luminescent ATP detection assay kit (Beyotime, Beijing China). Following the treatment as described above, the medium was discarded and the cells were washed for three times in PBS. Then, 200 μl lysis buffer of luminescent ATP assay was added to each well and incubated for 30 min. The cells were collected and centrifuged at 12,000 g for 5 min; the supernatant was aspirated for cell lysate. Finally, 90 μl ATP assay kit was added to 10 μl of cell lysate or the ATP standard solution in the 96-well plates. Luminescence was measured with fluorospectrometer.

## Fluorescence Analysis of Intracellular $Ca^{2+}$and ROS Levels

The intracellular $Ca^{2+}$ level was measured using the Fluo-4-AM (Invitrogen, United States) dye. PC12 cells were stained with 2.5 μM of Fluo-4-AM solution for 30 min in darkness at 37°C and then washed for three times in Hank's Balanced Salt Solution (HBSS) (Corning, United States). Green fluorescence, which reflects the intracellular $Ca^{2+}$ level, was recorded with a fluorescence microscope (Carl Zeiss, Germany).

Intracellular ROS levels were detected using fluorescence microscopy with DCFH-DA (Beyotime Biotechnology, Beijing,

China). The DCFH-DA was intracellularly deacetylated by a nonspecific esterase, further oxidized by ROS to produce the fluorescent compound 2,7-dichlorofluorescein (DCF) (An et al., 2017). The analysis was performed with the assay kit protocol. Briefly, PC12 cells were washed twice in DMEM without FBS and incubated with DCFH-DA at 37°C for 25 min. The cells were then washed twice with PBS and analyzed in a fluorescence microscope (Carl Zeiss, Germany).

The intensity of $Ca^{2+}$ and ROS-labelled cells was further quantified. The labeled cells were counted from five areas under × 20 field or × 40 field randomly chosen from each well using ImageJ software.

## Western Blot Analysis

PC12 cells were lyzed in radioimmunoprecipitation assay (RIPA) buffer (Sigma-Aldrich, United States) supplemented with a protease inhibitor cocktail (Cell Signaling Technology, United States). The total protein quantification and western blot procedures were performed routinely (Bass et al., 2017). Equal amounts of proteins were resolved by sodium dodecyl sulfate-polyacrylamide gel electrophoresis (SDS-PAGE) and transferred onto polyvinylidene difluoride (PVDF) membranes. The membranes were incubated with blocking buffer (5% BSA) for 1.5 h at first and then incubated with the primary antibodies against mitochondrial dynamic-related proteins, Drp-1, Mfn1, Mfn2, Fis1, p-Drp1 (ser616), and Opa1 (Proteintech, Wuhan, China); the antibodies against apoptosis-related biomarkers, caspase-9, cleaved caspase-3, cytochrome c (CST, United States), caspase-3 (Santa-Cruz Biotechnology, Unites States), Bax (Abclonal), and Bcl-2 (Abcam, USA); the $Ca^{2+}$/calmodulin-dependent protein kinases, CaMKII, p-CaMKII (Santa-Cruz Biotechnology, USA). After that, the corresponding secondary antibodies were added on PVDF membrane for additional incubation for 1.5 h at room temperature. Finally, the proteins were detected using an ECL select western blotting detection reagent (GE Healthcare, United States) and quantified in ChemiDoc XRS + imaging system (Bio-Rad, Unites States).

## Statistical Analysis

All data were expressed as mean ± standard error (SE). One-way analysis of variance (ANOVA) was used to detect statistical significance, followed by Tukey's HSD post hoc test to determine between-group differences. $p < 0.05$ was defined as statistical significance. Statistical analyses were performed using the GraphPad prism 6 (Graphpad software Inc., Califonia, United States).

# RESULTS

## Cell Viability

The viability of the $A\beta_{25-35}$-exposed cells was pronouncedly lower than that of the unexposed cells ($p = 0.0078$). TPG-and DAG-pretreated cells at concentration of 12.5–100 μg/ml exhibited significantly greater viability than the $A\beta_{25-35}$-exposed cells ($p < 0.05$). The peak effects of the two gelatins was present consistently at 25 μg/ml. This concentration was then selected for further experiments (**Figure 1**). $IC_{50}$, the concentration that produces a 50% reduction of cell viability, was 2,173 μg/ml with TPG and 2,430 μg/ml with DAG, which were 87- to 97-fold higher than that of the peak effects.

## The Effects on Mitochondrial Ultrastructure

The Aβ exposure caused a large accumulation of damaged mitochondrial fragments with excessive fission and fusion, unclearly arranged crests, and defective organelle morphology. The cells pre-treated with TPG and DAG displayed the neatly arranged lamellar mitochondrial crests (**Figure 2**).

## The Effects on Intracellular ATP Level

Intracellular ATP level of the $A\beta_{25-35}$-exposed cells was 4.5 ± 0.6 μM. This was markedly lower than 9.4 ± 1.7 μM of the untreated cells ($p = 0.0214$), 9.5 ± 1.1 μM of the TPG-treated cells ($p = 0.0203$), and 8.9 ± 1.3 μM of the DAG-treated cells ($p = 0.0345$). The levels of the latter three groups were not significantly different (**Figure 3**).

## The Effects on Mitochondrial Membrane Potential

The $A\beta_{25-35}$ exposure for 4 and 23 h caused an approximately two-and six-fold decrease of MPP, respectively, as compared with the unexposed cells ($p < 0.01$) (**Figure 4**). MPP value of both TPG-and DAG-pretreated cells was strikingly greater than that of the cells co-incubated with $A\beta_{25-35}$ for 4 h ($p < 0.05$) (**Figure 4A**), but similar to that co-incubated for 23 h (**Figure 4B**).

## The Effects on Reactive Oxygen Species

The intracellular ROS level was measured at 1, 6, 12, and 24 h after $A\beta_{25-35}$ exposure. The production of intracellular ROS reached the peak level at 1 h post-exposure, but gradually decreased with increasing exposure time (**Supplementary Figure S2**). The effects of TPG and DAG on ROS were thus examined in the 1 h exposed cells. The intracellular ROS level of TPG-and DAG-treated cells was strikingly lower than that of the unexposed and $A\beta_{25-35}$-exposed cells ($p < 0.005$) (**Figure 5**).

## The Effects of on Intracellular $Ca^{2+}$ and CaMKII

Intracellular $Ca^{2+}$ level of the $A\beta_{25-35}$-exposed cells was significantly higher than that of the unexposed cells ($p = 0.0051$). Pre-treatment with TPG and DAG remarkably lowered the Aβ-induced increase of $Ca^{2+}$ ($p < 0.01$) (**Figure 6A**).

The expression of CaMKII, a downstream calcium protein, and its phosphorylation (p-CaMKII), was examined using western blot. The ratio of p-CaMKII/CaMKII was calculated. The $A\beta_{25-35}$ exposure caused a significant increase of the ratio compared to the unexposed cells ($p = 0.0378$). The cells pre-treated with TPG and DAG markedly reduced the increased ratio to control value ($p < 0.01$) (**Figure 6B**).

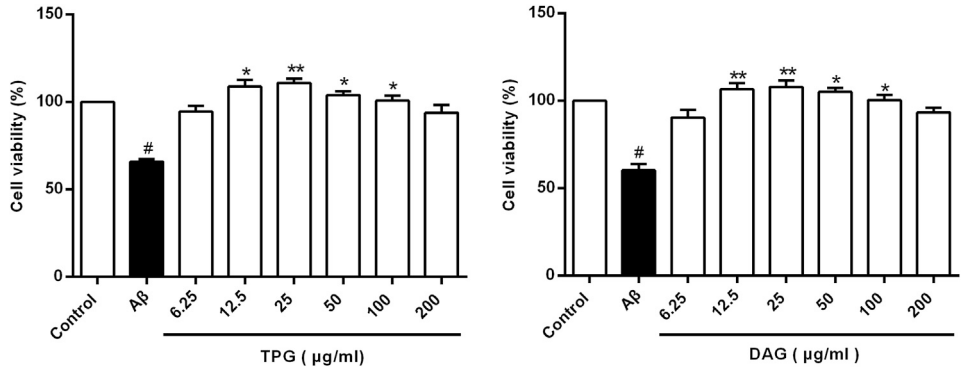


**FIGURE 1 |** Cells viability of the $A\beta_{25-35}$-exposed cells being treated with TPG and DAG. Statistical analyses were performed using one-way ANOVA and Tukey-HSD post hoc comparisons. All values were shown as mean ± SEM from three independent studies. #$p < 0.05$, vs. control group; *$p < 0.05$, vs. $A\beta_{25-35}$ models; **$p < 0.01$, vs. models. TPG, tortoise plastron gelatin; DAG, deer antler gelatin.

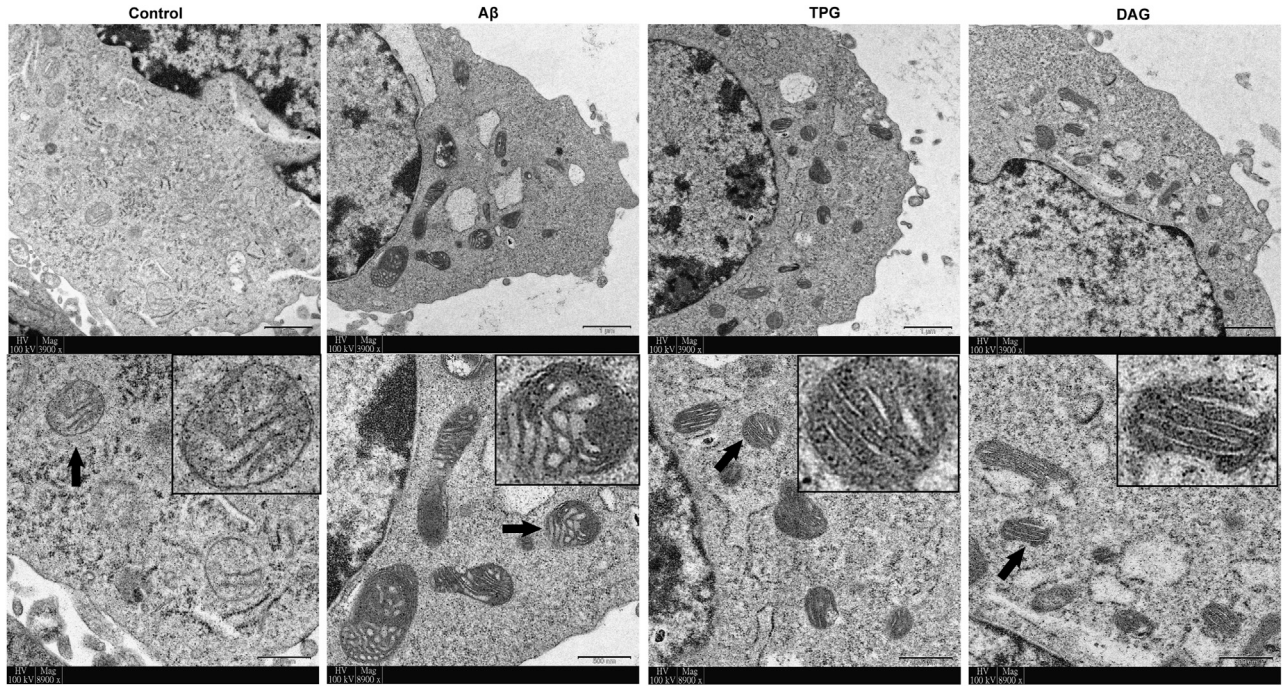


**FIGURE 2 |** The improvement of TPG and DAG on mitochondrial ultrastructure in the $A\beta_{25-35}$-exposed cells. The transmission electron microscope (TEM) was used to examine ultrathin slices or in different groups. The images below each group were the enlarged representative mitochondria. The representative mitochondria marked by black arrow in each group were magnified in the black box. Magnification: ×3,900 and ×8,900, respectively. Scale bars: 1 μm and 500 nm, respectively. TPG, tortoise plastron gelatin; DAG, deer antler gelatin.

## The Effects on the Expression of Mitochondrial Dynamic-Related Proteins

The expression of Drp1 and Fis1, the two proteins that regulate the mitochondrial fission, and the phosphorylation of Drp1 at ser616 [p-Drp1 (ser616)] was detected. The $A\beta_{25-35}$ exposure induced significant increase of the expression of the three fission proteins compared to the unexposed cells ($p < 0.05$). Pre-treatment with TPG reversed the $A\beta_{25-35}$-induced increase of the Drp1 and p-Drp1 (ser616) expression ($p < 0.05$), but had no effects on Fis1. Pre-treatment with DAG markedly suppressed the overexpression of Drp1 (ser616) and Fis1 ($p < 0.05$), but did not change the overexpression of Drp1 (**Figure 7**).

The three mitochondrial fusion-related proteins, Mfn1, Mfn2, and Opal, was also evaluated. The expression level of the three proteins of the $A\beta_{25-35}$-exposed cells was markedly lower than that of the unexposed cells ($p < 0.05$). The TPG-pretreated cells had significantly higher level of Mfn1 and Opa1 than the $A\beta_{25-35}$-exposed cells ($p < 0.05$). DAG had no effects on the $A\beta_{25-35}$-induced decrease of the three fusion protein expression (**Figure 7**).

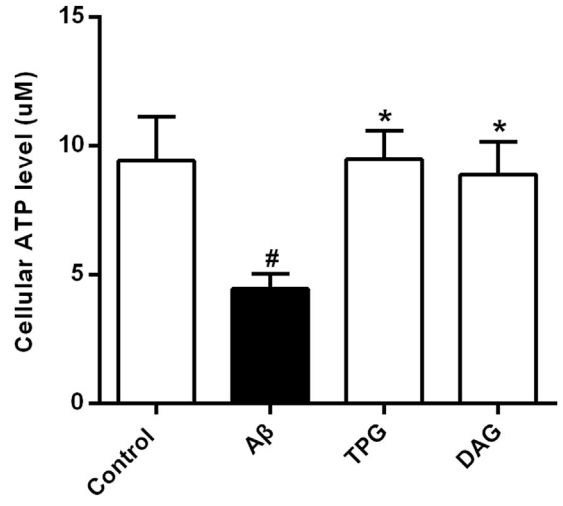


**FIGURE 3 |** The improvement of TPG and DAG on the intracellular ATP level in $A\beta_{25-35}$-exposed cells. The concentrations of intracellular ATP level in different groups. All values were shown as mean ± SEM from three independent studies. Statistical analyses were performed using one-way ANOVA and Tukey-HSD post hoc comparisons. $^{\#}p < 0.05$, vs. control group; $^{*}p < 0.05$, vs. $A\beta_{25-35}$ models. TPG, tortoise plastron gelatin; DAG, deer antler gelatin.

## The Effects on Cell Apoptosis and Related Biomarkers

Cell apoptosis was examined using flow cytometry. Percent of late apoptotic cells was strikingly increased in the $A\beta_{25-35}$-exposed cells ($p = 0.0018$). Pretreatment with TPG and DAG prominently reduced percent of the late apoptosis cells ($p < 0.05$) (**Figure 8A**).

The expression of the pro-apoptotic proteins, cleaved-caspase-9, caspase-9, cleaved-caspase-3, caspase-3, and cytochrome c, and the apoptosis regulators, Bax and Bcl-2, was evaluated with western blot. The ratios of cleaved-caspase-9/caspase-9, cleaved-caspase-3/caspase-3, and Bax/Bcl-2 were obtained. The $A\beta_{25-35}$-exposed cells exhibited the overexpression of cytochrome c ($p = 0.0377$) and significant increases of the three ratios ($p< 0.05$). Pretreatment with both gelatins significantly decreased the ratio of Bax/Bcl-2 and the expression of cytochrome c ($P < 0.05$). DAG further significantly reduced the ratios of cleaved-caspase-9/caspase-9 and cleaved-caspase-3/caspase-3 ($p < 0.05$) (**Figure 8B**).

## DISCUSSION

This study represents the first to explore novel anti-dementia agents from animal tissue-derived gelatins that may have the

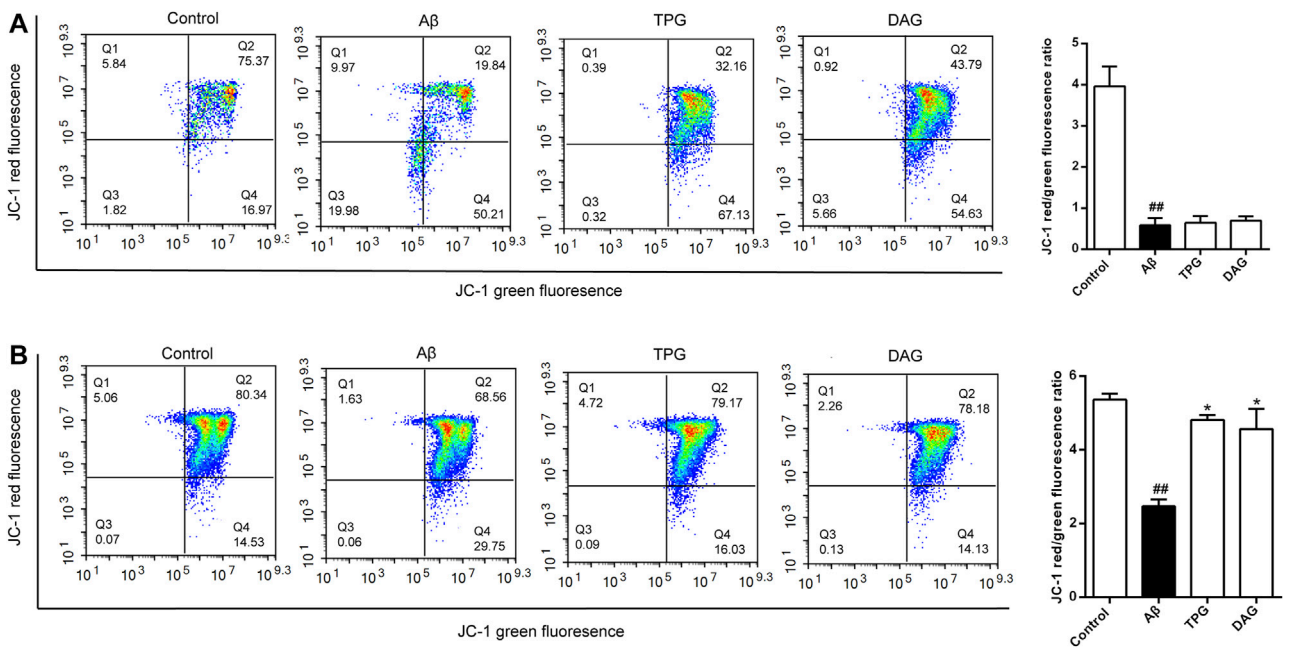


**FIGURE 4 |** The improvement of TPG and DAG on mitochondrial membrane potential in $A\beta_{25-35}$-exposed cells. Cells with high MMP promote the formation of dye aggregates and fluoresce red, while cells with low potential contain monomeric JC-1 and fluoresce green. The ratio of red/green fluorescence indicated MMP level in each group **(A)** The ratio of red/green fluorescence in different groups after 24 h of $A\beta_{25-35}$-exposed cells **(B)** The ratio of red/green fluorescence in different groups after 4 h of $A\beta_{25-35}$-exposed cells. All values were shown as mean ± SEM from three independent studies. Statistical analyses were performed using one-way ANOVA and Tukey-HSD post hoc comparisons. $^{\#}p < 0.05$, vs. control group; $^{\#\#}p < 0.01$, vs. control group; $^{*}p < 0.05$, vs. $A\beta_{25-35}$ models. TPG, tortoise plastron gelatin; DAG, deer antler gelatin.

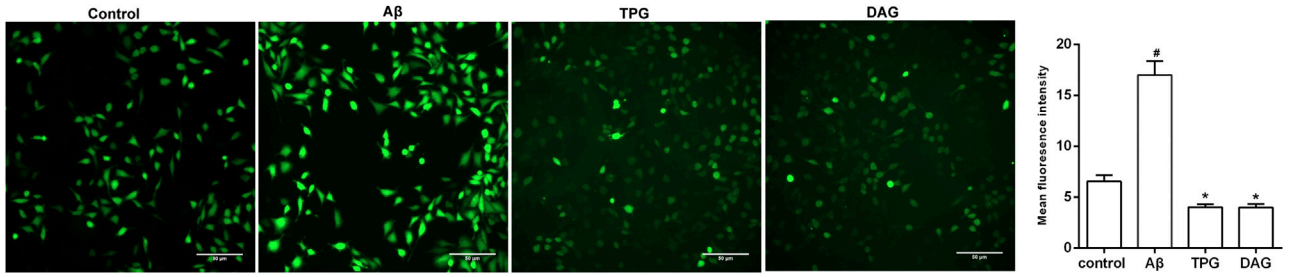


**FIGURE 5 |** The regulation of TPG and DAG on the intracellular ROS in $A\beta_{25-35}$-exposed cells. The intracellular ROS level was recorded by fluorescence microscope with DCFH-DA. The intracellular ROS level in different groups after being induced with $A\beta_{25-35}$ or treated with the two gelatins. Scale bars: 50 μm. All values were shown as mean ± SEM. #$p < 0.05$, vs. control group; *$p < 0.05$, vs. $A\beta_{25-35}$ models. TPG, tortoise plastron gelatin; DAG, deer antler gelatin.

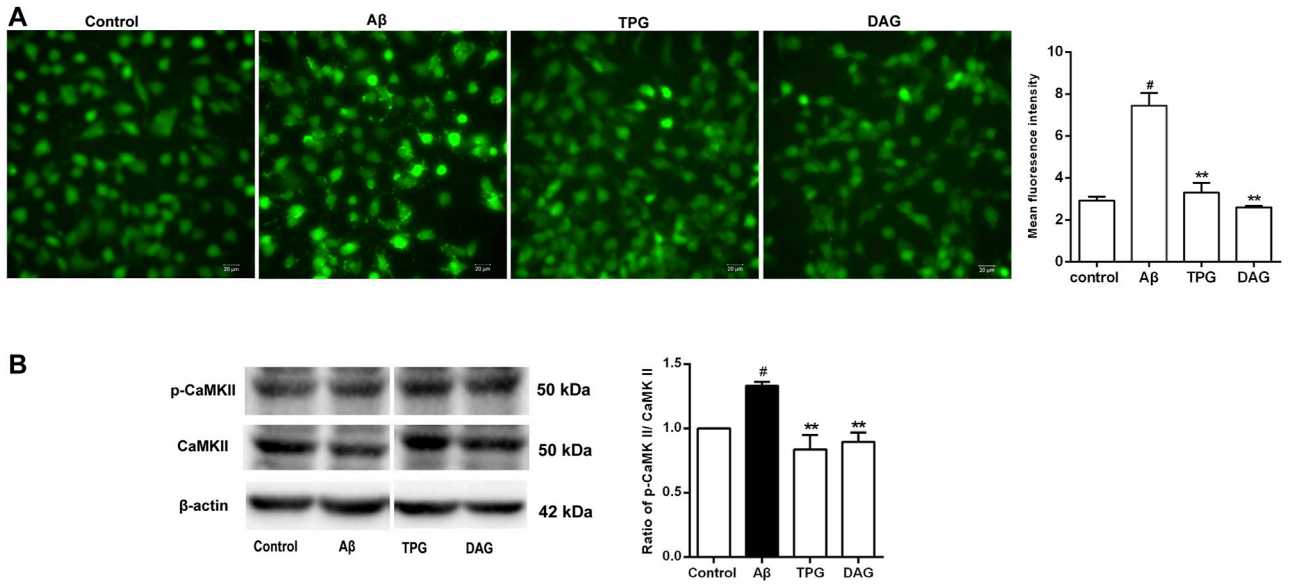


**FIGURE 6 |** The regulation of TPG and DAG on the calcium overload in the $A\beta_{25-35}$-exposed cells **(A)** The image of intracellular calcium in different groups recorded by a fluorescence microscope. Scale bars: 20 μm **(B)** The expression level of CaMKII and its phosphorylation in different groups were measured by western blot. All values were shown as mean ± SEM from three independent studies. Statistical analyses were performed using one-way ANOVA and Tukey-HSD post hoc comparisons. #$p < 0.05$, vs. control group; *$p < 0.05$, vs. $A\beta_{25-35}$ models; **$p < 0.01$, vs. $A\beta_{25-35}$ models. TPG, tortoise plastron gelatin; DAG, deer antler gelatin.

potential in preventing against neuronal mitochondrial dysfunction. Previous studies have confirmed that Aβ toxicity-induced multiple molecular and subcellular pathological events were initially triggered by the impairment of mitochondrial $Ca^{2+}$ buffering capacity, leading to an intracellular overflow of $Ca^{2+}$, damaged mitochondrial respiratory chain, and excessive production of ROS (Orrenius et al., 2003; Manczak et al., 2011; Pallo and Johnson, 2015). This study revealed that the $A\beta_{25-35}$ exposure resulted in a dramatic increase of intracellular $Ca^{2+}$ level, rapid overproduction of ROS and cellular and mitochondrial damage, manifesting as reduced cell viability, mitochondrial fragmentation, increased cytochrome c level, and decreased MMP. The neurotoxin also largely inhibited mitochondrial ATP production. These results well validated the $A\beta_{25-35}$-exposed PC12 cells as an *in vitro* model in mimicking Alzheimer's disease in association with mitochondria dysfunction.

We further found that the intracellular ROS level reached the peak in an hour, but gradually decreased to a minimum level in 24 h following the $A\beta_{25-35}$ exposure. Likewise, MMP decreased from 2-fold at 4 h to 6-fold at 24 h. Similar phenomena were also observed in previous studies, confirming that oxidative stress occurred in the early stage of Alzheimer's disease could mediate oxygen-containing substances and generate ROS (Sancar et al., 2004; Fan et al., 2017). It thus appears that the Aβ-induced excessive production of ROS is an early, short-term, but irreversible event that subsequently causes the disruption of MMP, leading to mitochondrial DNA damage and functional defects (Wang et al., 2008).

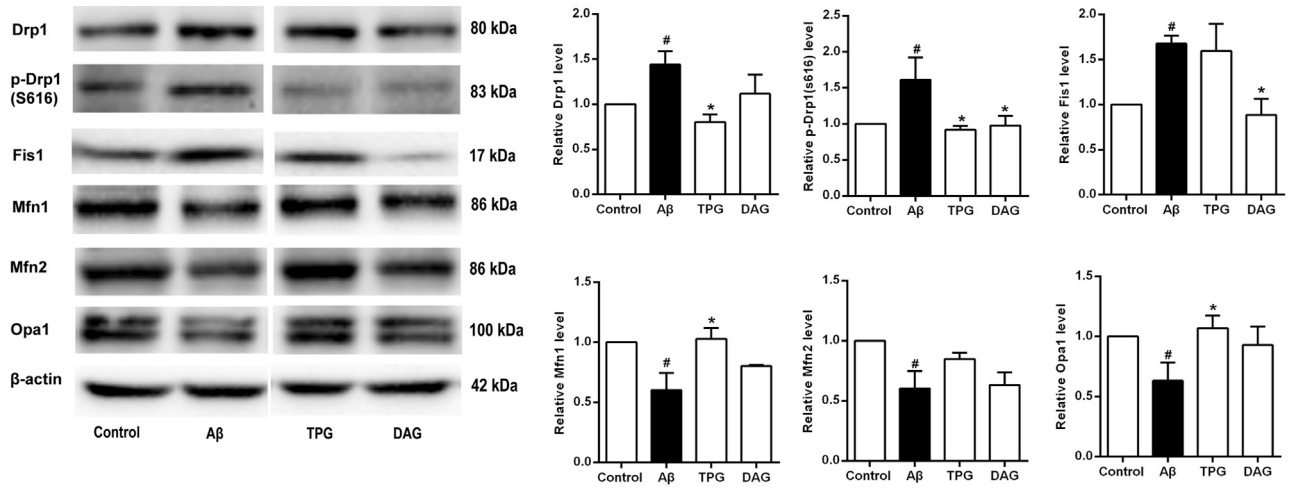


**FIGURE 7 |** The regulation of TPG and DAG on the expression level of mitochondrial dynamics-related proteins in $A\beta_{25-35}$-exposed cells. The expression level of the proteins in each group was relative to the control group. All values were shown as mean ± SEM from three independent studies. Statistical analyses were performed using one-way ANOVA and Tukey-HSD post hoc comparisons. $^{\#}p < 0.05$, vs. control group; $^{*}p < 0.05$, vs. $A\beta_{25-35}$ models. TPG, tortoise plastron gelatin; DAG, deer antler gelatin.

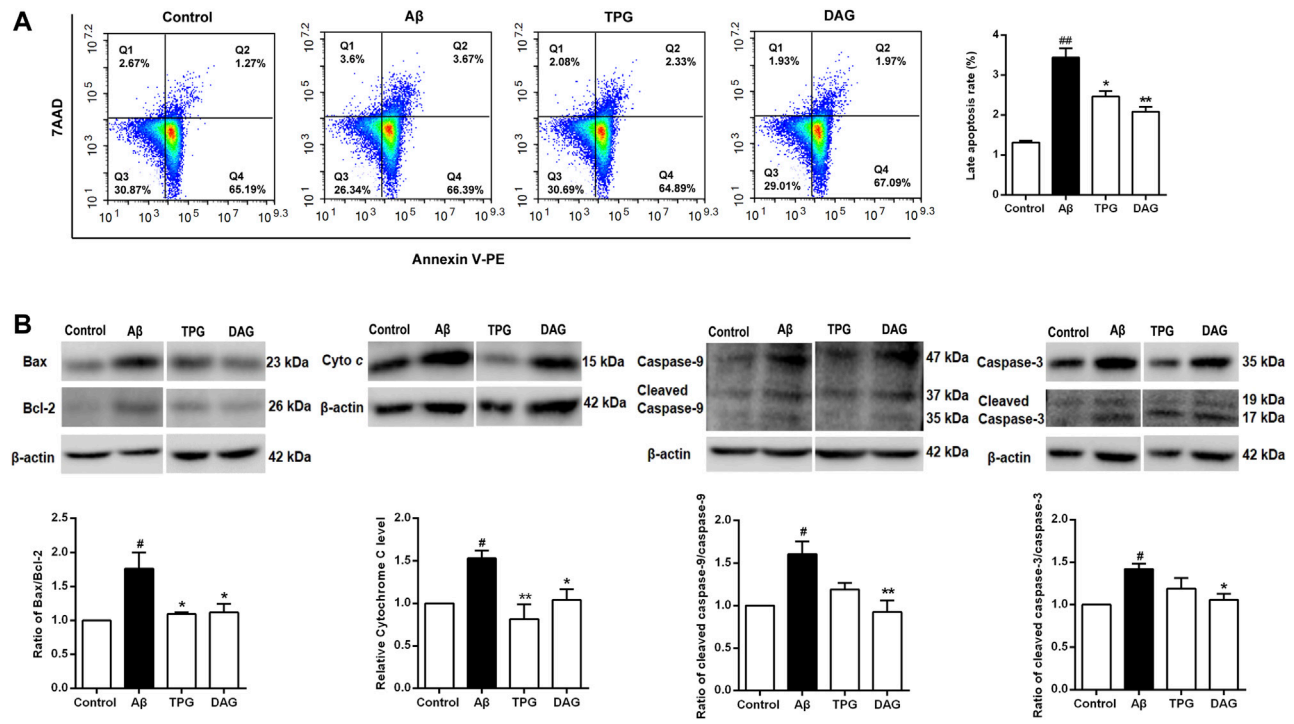


**FIGURE 8 |** The regulation of TPG and DAG on the cell apoptosis **(A)** The apoptotic cell was measured by flow cytometry. Late apoptotic cell rate was detected in different groups after 20 h pre-treatment with the four drugs and a subsequent 4 h incubated with $A\beta_{25-35}$ **(B)** The expression levels of pro-apoptosis proteins were detected using western blot. All values were shown as mean ± SEM from three independent studies. Statistical analyses were performed using one-way ANOVA and Tukey-HSD post hoc comparisons. $p^{\#} < 0.05$, vs. control group; $^{*}p < 0.05$, vs. $A\beta_{25-35}$ models; $^{**}p < 0.01$, vs. $A\beta_{25-35}$ models. Cyto c, Cytochrome c; TPG, tortoise plastron gelatin; DAG, deer antler gelatin.

Pretreatment with TPG and DAG suppressed the $A\beta_{25-35}$-induced increase of $Ca^{2+}$ and cytochrome c, and prevented cell viability and mitochondrial ultrastructure from Aβ toxicity. The two gelatins completely resumed decreased ATP production to the control level. Both TPG and DAG also reversed MMP to the control values in the short-term $A\beta_{25-35}$ exposure, although they had no effects in preventing MMP from the long-term $A\beta_{25-35}$ exposure. Both gelatins further inhibited the rapid overproduction of ROS. These results suggest that TPG and DAG could protect mitochondrial structure and functions by blocking intracellular $Ca^{2+}$ overflow and early excessive production of ROS. Additionally, this study also indicated the least cytotoxic effects of the two gelatins, as evidenced by the fact that $IC_{50}$ values were average 92-fold higher than the concentration of the peak effects.

One apparent molecular pathology of mitochondria caused by Aβ is the disturbance of mitochondrial dynamics, manifesting as an imbalance in the expression of mitochondrial fission and fusion proteins that are involved in the mitochondrial division and maintenance of mitochondrial morphology (Taguchi et al., 2007; Manczak et al., 2011; Itoh et al., 2013; Kim et al., 2016; Pernas and Scorrano, 2016; Jiang et al., 2018). In particular, the phosphorylation of Drp1-serine 616 is essential in the mitochondrial division (Taguchi et al., 2007). In this study, we observed that the expression of Drp1, p-Drp1 (s616), and Fis1 was increased, but the expression of Mfn1, Mfn2, and Opal was decreased in the $A\beta_{25-35}$-exposed cells. These results proved the effects of the neurotoxin in causing aberrant expression of mitochondrial fission and fusion proteins. While both TPG and DAG equivalently inhibited the phosphorylation of Drp1-serine 616 and had no effects on Mfn2, TPG displayed stronger effects in normalizing the aberrant expression of Drp1, Mfn1, and Opa1, whereas DAG only had a significant effect in suppressing Fis1. It seems to suggest that TPG and DAG may differentially mediate mitochondrial dynamic proteins, i.e., in addition to fission proteins, TPG also had significant effects in mediating fusion proteins, but DAG did not. Whether a combination of the two gelatins with the differential effects on the dynamic proteins could produce additive or even synergistic actions in preventing mitochondrial functions deserves for further investigations.

Mitochondria dynamic proteins interact with apoptosis and $Ca^{2+}$ homeostasis. The downregulation of Drp1 and Fis1 attenuated the release of cytochrome c and delayed apoptosis (Iwasawa et al., 2011; Clerc et al., 2014). Mfn2 plays a crucial role in the conduction of calcium signals (Wang et al., 2015). On the other hand, the Aβ-induced intracellular $Ca^{2+}$ overload activated the downstream proteins, calmodulin-dependent protein kinase II (CaMKII), then upregulated the phosphorylation of Drp1-serine 616, and increased the fission event rates (Xu et al., 2016; Divakaruni et al., 2018). In this study, while the two gelatins exerted differential effects on the dynamic proteins, they inhibited intracellular $Ca^{2+}$ overflow and the phosphorylation of CaMKII induced by Aβ. It appears that the effects of the gelatins in protecting mitochondria function may be associated with their mediation of the interaction between mitochondrial dynamic proteins and calcium-dependent pathways.

Aβ-induced mitochondrial $Ca^{2+}$ overload further triggered mitochondrial $Ca^{2+}$-dependent apoptosis by opening the mitochondrial permeability transition pore (mPTP) and releasing cytochrome c and pro-apoptotic factors, such as caspase-9 and caspase-3 (Joza et al., 2001; Orrenius et al., 2003; Abramov et al., 2007; Chen et al., 2011; Calvo Rodriguez et al., 2020). Bax is a pro-apoptotic protein that causes the loss of MMP and eventually lead to the release of apoptotic factors into the cytoplasm, while Bcl-2 inhibits cell apoptosis (Glantz et al., 2006; Ola et al., 2011). The relative level of Bax and Bcl-2 is thus essential for determining whether cells undergo cell apoptosis (Khodapasand et al., 2015). This study revealed that the $A\beta_{25-35}$-exposed cells had a much higher proportion of late apoptotic cells, increased ratio of Bax/Bcl-2, cleaved-caspase-9/caspase-9, and cleaved-caspase-3/caspase-3. $A\beta_{25-35}$ also induced the overexpression of cytochrome c. These results confirm the effects of $A\beta_{25-35}$ in inducing apoptosis *via* the mitochondrial pathway. Pretreatment with TPG and DAG, however, decreased the proportion of late apoptotic cells, the ratio of Bax/Bcl-2 and the expression level of cytochrome c. DAG further suppressed the $A\beta_{25-35}$-induced increase of ratios of cleaved-caspase-9/caspase-9 and cleaved-caspase-3/caspase-3. The preventive effects of the two gelatins appear to be, at least partly, derived from their inhibition of mitochondrial apoptosis pathway.

Given that $Ca^{2+}$ dyshomeostasis is heavily involved in the pathogenesis of Alzheimer's disease, agents that regulate $Ca^{2+}$ homeostasis and protect mitochondrial function may possess anti-dementia potential (Calvo Rodriguez and Bacskai, 2020). It has been reported that endogenous and exogenous cations and amino acids indirectly regulates the calcium-sensing receptor (CaSR), a classic G protein-coupled receptor, and maintain $Ca^{2+}$ homeostasis in the body. In this process, amino acids act as pure positive allosteric modulators to enhance calcium-active receptor function (Liu et al., 2020). As shown in **Table 1**, TPG and DAG contain an abundance of various amino acids and trace mineral elements (Shi et al., 2012; Jiang et al., 2015; Guo et al., 2016; Wang et al., 2018; Long et al., 2019). It seems that the two gelatins act as positive allosteric regulators to enhance the efficiency of the calcium-active receptor, thereby activating CaSR, maintaining intracellular calcium homeostasis, and protecting mitochondrial function. On the other hand, glycine, the most abundant amino acid of the two gelatins, could protect against brain injury by regulating mitochondria-mediated autophagy (Cai et al., 2019). Lower level of iron, manganese, and zinc have been observed in patients with Alzheimer's disease (Basun et al., 1991). Iron, zinc, calcium, manganese, and strontium level correlated with memory and cognitive functions in patients with Alzheimer's disease (Basun et al., 1991; Veronese et al., 2016; Lei et al., 2021). It is suggested that TPG and DAG could serve as specific supplements for the treatment of Alzheimer's disease.

There are three apparent limitations in this study. First, this was a preliminary *in vitro* study. Behavioral, pharmacological, and *in vivo* imaging approaches in animal models should be further considered to determine the anti-dementia or nootropic effects. Second, although the batch of TPD and DAG used in this study was not examined, it was manufactured in compliance with Pharmacopoeia of the People's Republic of China (2020) and

Good Manufacturing Practice (GMP). The contents of major components have been well identified with high consistency as shown in **Table 1** (Shi et al., 2012; Jiang et al., 2015; Guo et al., 2016; Wang et al., 2018; Long et al., 2019). Despite this, there is no global standard available for the preparation of the two gelatins. Caution should nevertheless be taken when other TPD and DAG products are used. Third, various amino acids and trace mineral elements are contained in the two gelatins. As these small-molecule compounds are more accessible to the blood–brain barrier (BBB), they could exert greater pharmacokinetic and pharmacodynamic effects in the central nervous system compared with the macromolecular natural compounds, such as ginsenosides. Further experiments should be considered to identify major components that may play the principal roles in the therapeutic effects of the two gelatins.

## CONCLUSION

Pretreatment with TPG and DAG reversed the $A\beta_{25-35}$-induced decrease in cell viability, MMP and ATP, alleviated the accumulation of damaged mitochondrial fragments, and normalized the aberrant expression of multiple mitochondrial dynamic proteins of the $A\beta_{25-35}$-exposed cells. Both gelatins also suppressed intracellular ROS overproduction and $Ca^{2+}$ overload, overexpression of cytochrome c and pro-apoptosis biomarkers induced by the $A\beta_{25-35}$ exposure. This study suggests that TPG and DAG may possess the anti-dementia potential and could serve as specific supplements for the treatment of Alzheimer's disease.

## DATA AVAILABILITY STATEMENT

The original contributions presented in the study are included in the article/**Supplementary Material**, further inquiries can be directed to the corresponding author.

## AUTHOR CONTRIBUTIONS

DC and Z-JZ designed the studies, DC analyzed the data, performed the experiments, wrote and revised the manuscript. X-JY, LZ, Z-SQ, W-QL, and H-CX, performed some of the experiments. Z-JZ supervised the project, generated resources, reviewed, revised and finally approved the manuscript.

## FUNDING

This study was supported by General Research Fund (GRF) of Research Grant Council of HKSAR (17115017), and National Key R&D Program of China (2018YFC1705801). All sources of funding received for the research being submitted.

## SUPPLEMENTARY MATERIAL

The Supplementary Material for this article can be found online at: https://www.frontiersin.org/articles/10.3389/fphar.2021.690256/full#supplementary-material

## REFERENCES

Abramov, A. Y., Fraley, C., Diao, C. T., Winkfein, R., Colicos, M. A., Duchen, M. R., et al. (2007). Targeted Polyphosphatase Expression Alters Mitochondrial Metabolism and Inhibits Calcium-Dependent Cell Death. *Proc. Natl. Acad. Sci.* 104, 18091–18096. doi:10.1073/pnas.0708959104

An, S. Y., Youn, G. S., Kim, H., Choi, S. Y., and Park, J. (2017). Celastrol Suppresses Expression of Adhesion Molecules and Chemokines by Inhibiting JNK-Stat1/nf-Kb Activation in Poly(I:C)-Stimulated Astrocytes. *BMB Rep.* 50, 25–30. doi:10.5483/bmbrep.2017.50.1.114

Bass, J. J., Wilkinson, D. J., Rankin, D., Phillips, B. E., Szewczyk, N. J., Smith, K., et al. (2017). An Overview of Technical Considerations for Western Blotting Applications to Physiological Research. *Scand. J. Med. Sci. Sports* 27, 4–25. doi:10.1111/sms.12702

Basun, H., Forssell, L. G., Wetterberg, L., and Winblad, B. (1991). Metals and Trace Elements in Plasma and Cerebrospinal Fluid in Normal Aging and Alzheimer's Disease. *J. Neural Transm. Park Dis. Dement Sect.* 3, 231–258.

Berlepsch, H. V., and Böttcher, C. (2013). Supramolecular Structure of TTBC J-Aggregates in Solution and on Surface. *Langmuir* 29, 4948–4958. doi:10.1021/la400417d

Cai, C. C., Zhu, J. H., Ye, L. X., Dai, Y. Y., Fang, M. C., Hu, Y. Y., et al. (2019). *Glycine* Protects Against Hypoxic-Ischemic Brain Injury by Regulating Mitochondria-Mediated Autophagy via the AMPK Pathway. *Oxid. Med. Cell. longev.* 2019, 4248529. doi:10.1155/2019/4248529

Calvo Rodriguez, M., and Bacskai, B. J. (2020). Mitochondria and Calcium in Alzheimer's Disease: From Cell Signaling to Neuronal Cell Death. *Trends Neurosci.* 44, 136–151. doi:10.1016/j.tins.2020.10.004

Calvo Rodriguez, M., Hou, S. S., Snyder, A. C., Kharitonova, E. K., Russ, A. N., Das, S., et al. (2020). Increased Mitochondrial Calcium Levels Associated with Neuronal Death in a Mouse Model of Alzheimer's Disease. *Nat. Commun.* 11, 1–17. doi:10.1038/s41467-020-16074-2

Chen, H. Y., Chen, F. L., Lin, Z. M., and Yang, Z. Q. (2016). The Influence of Huanglian Ejiao Decoction on the Hypnotic Effect of Pentobarbital Sodium in Mice. *Guangdong Med. J.* 37, 3165–3168. doi:10.13820/j.cnki.gdyx.20161124.016

Chen, Y.-C., Chen, C.-H., Hsu, Y.-H., Chen, T.-H., Sue, Y.-M., Cheng, C.-Y., et al. (2011). Leptin Reduces Gentamicin-Induced Apoptosis in Rat Renal Tubular Cells via the PI3K-Akt Signaling Pathway. *Eur. J. Pharmacol.* 658, 213–218. doi:10.1016/j.ejphar.2011.02.025

Clerc, P., Ge, S. X., Hwang, H., Waddell, J., Roelofs, B. A., Karbowski, M., et al. (2014). Drp1 Is Dispensable for Apoptotic Cytochromecrelease in Primed MCF10A and Fibroblast Cells but Affects Bcl-2 Antagonist-Induced Respiratory Changes. *Br. J. Pharmacol.* 171, 1988–1999. doi:10.1111/bph.12515

Coleman, P., and Yao, P. J. (2003). Synaptic Slaughter in Alzheimer's Disease. *Neurobiol. Aging* 24, 1023–1027. doi:10.1016/j.neurobiolaging.2003.09.001

Costantini, L. C., Barr, L. J., Vogel, J. L., and Henderson, S. T. (2008). Hypometabolism as a Therapeutic Target in Alzheimer's Disease. *BMC Neurosci.* 9, 1–9. doi:10.1186/1471-2202-9-s2-s16

Divakaruni, S. S., Van Dyke, A. M., Chandra, R., Legates, T. A., Contreras, M., Dharmasri, P. A., et al. (2018). Long-Term Potentiation Requires a Rapid Burst of Dendritic Mitochondrial Fission during Induction. *Neuron* 100, 860–875. doi:10.1016/j.neuron.2018.09.025

Dubey, S. K., Ram, M. S., Krishna, K. V., Saha, R. N., Singhvi, G., Agrawal, M., et al. (2019). Recent Expansions on Cellular Models to Uncover the Scientific Barriers Towards Drug Development for Alzheimer's Disease. *Cell Mol. Neurobiol.* 39, 181–209. doi:10.1007/s10571-019-00653-z

Eckert, A., Schulz, K. L., Rhein, V., and Götz, J. (2010). Convergence of Amyloid-β and Tau Pathologies on Mitochondria *In Vivo*. *Mol. Neurobiol.* 41, 107–114. doi:10.1007/s12035-010-8109-5

Fan, C-d., Li, Y., Fu, X-t., Wu, Q-j., Hou, Y-j., Yang, M-f., et al. (2017). Reversal of Beta-Amyloid-Induced Neurotoxicity in PC12 Cells by Curcumin, the Important Role of ROS-Mediated Signaling and ERK Pathway. *Cell Mol. Neurobiol.* 37, 211–222. doi:10.1007/s10571-016-0362-3

Giorgi, C., Baldassari, F., Bononi, A., Bonora, M., De Marchi, E., Marchi, S., et al. (2012). Mitochondrial Ca2+ and Apoptosis. *Cell calcium.* 52, 36–43. doi:10.1016/j.ceca.2012.02.008

Glantz, L. A., Gilmore, J. H., Lieberman, J. A., and Jarskog, L. F. (2006). Apoptotic Mechanisms and the Synaptic Pathology of Schizophrenia. *Schizophrenia Res.* 81, 47–63. doi:10.1016/j.schres.2005.08.014

Guo, S., Zhou, X., Ji, C., Duan, X., Zhang, Y., and Xu, Y. (2016). The Analysis of 17 Amino Acids in Colla Corii Asini,Colla Carapacis et Plastri Testudinis,and Colla Cornus Cervi by Liquid Chromatography Tandem Mass Spectrometry. *Sci. Tech. Gelatin* 36, 86–91 .

Hengartner, M. O. (2000). The Biochemistry of Apoptosis. *Nature* 407, 770–776. doi:10.1038/35037710

Huang, L. K., Chao, S. P., and Hu, C. J. (2020). Clinical Trials of New Drugs for Alzheimer Disease. *J. Biomed. Sci.* 27, 1–13. doi:10.1186/s12929-019-0609-7

Ishihara, N., Eura, Y., and Mihara, K. (2004). Mitofusin 1 and 2 Play Distinct Roles in Mitochondrial Fusion Reactions via GTPase Activity. *J. Cel. Sci.* 117, 6535–6546. doi:10.1242/jcs.01565

Itoh, K., Nakamura, K., Iijima, M., and Sesaki, H. (2013). Mitochondrial Dynamics in Neurodegeneration. *Trends Cell Biology* 23, 64–71. doi:10.1016/j.tcb.2012.10.006

Iwasawa, R., Mahul-Mellier, A-L., Datler, C., Pazarentzos, E., and Grimm, S. (2011). Fis1 and Bap31 Bridge the Mitochondria-ER Interface to Establish a Platform for Apoptosis Induction. *EMBO J.* 30, 556–568. doi:10.1038/emboj.2010.346

Jiang, S., Chen, F., Xiong, D. N., and Lu, J. Z. (2015). Pre-Column Derivatization HPLC for Simultaneous Determination of 14 Hydrolytic Amino Acids in Tortoise Plastron Glue. *Chin. J. Pharm. Anal.* 35, 1790–1795. doi:10.16155/j.0254-1793.2015.10.16

Jiang, S., Nandy, P., Wang, W., Ma, X., Hsia, J., Wang, C., et al. (2018). Mfn2 Ablation Causes an Oxidative Stress Response and Eventual Neuronal Death in the hippocampus and Cortex. *Mol. neurodegen.* 13, 1–15. doi:10.1186/s13024-018-0238-8

Joza, N., Susin, S. A., Daugas, E., Stanford, W. L., Cho, S. K., Li, C. Y. J., et al. (2001). Essential Role of the Mitochondrial Apoptosis-Inducing Factor in Programmed Cell Death. *Nature* 410, 549–554. doi:10.1038/35069004

Khodapasand, E., Jafarzadeh, N., Farrokhi, F., Kamalidehghan, B., and Houshmand, M. (2015). IS Bax/Bcl-2 Ratio Considered as a Prognostic Marker With Age and Tumor Location in Colorectal Cancer? *Iran Biomed. J.* 19, 69–75. doi:10.6091/ibj.1366.2015

Kim, H. G., Ju, M. S., Ju, H., Seo, Y., Jang, Y. P., Hong, J., et al. (2010). Evaluation of Samjunghwan, a Traditional Medicine, for Neuroprotection against Damage by Amyloid-Beta in Rat Cortical Neurons. *J. ethnopharmacol.* 130, 625–630. doi:10.1016/j.jep.2010.05.040

Kim, D. I., Lee, K. H., Lee, A. A., Choi, G. E., Kim, J. S., Ko, S. H., et al. (2016). Aβ-Induced Drp1 Phosphorylation through Akt Activation Promotes Excessive Mitochondrial Fission Leading to Neuronal Apoptosis. *Biochim. Biophys. Acta (Bba) - Mol. Cel Res.* 1863, 2820–2834. doi:10.1016/j.bbamcr.2016.09.003

Kong, D. (2007). 60 Cases of Senile Dementia Treated With Guilu Erxianjiao. *TCM Res.* 10, 33–34.

Lei, P., Ayton, S., and Bush, A. I. (2021). The Essential Elements of Alzheimer's Disease. *J. Biol. Chem.* 296, 100105. doi:10.1074/jbc.rev120.008207

Leventis, P. A., and Grinstein, S. (2010). The Distribution and Function of Phosphatidylserine in Cellular Membranes. *Annu. Rev. Biophys.* 39, 407–427. doi:10.1146/annurev.biophys.093008.131234

Li, M. M., and Ms (2019). Changes in the Properties of Antler Gum, Tortoise Shell Gum and Oxhide Gelatin and Modern Research. *J. Hunan Univ. Chin. Med.* 39, 1044–1046.

Lim, Y.-A., Rhein, V., Baysang, G., Meier, F., Poljak, A., J. Raftery, M. M., et al. (2010). Aβ and Human Amylin Share a Common Toxicity Pathway *via* Mitochondrial Dysfunction. *Proteomics* 10, 1621–1633. doi:10.1002/pmic.200900651

Lin, M. T., and Beal, M. F. (2006). Mitochondrial Dysfunction and Oxidative Stress in Neurodegenerative Diseases. *Nature* 443, 787–795. doi:10.1038/nature05292

Liu, H., Yi, P., Zhao, W., Wu, Y., Acher, F., Pin, J.-P., et al. (2020). Illuminating the Allosteric Modulation of the Calcium-Sensing Receptor. *Proc. Natl. Acad. Sci. USA* 117, 21711–21722. doi:10.1073/pnas.1922231117

Long, X., Chen, Y., Qin, Fei. Yi., Xiao, Ling., Nie, Jing., and Huang, Zhi. (2019). Determination and Risk Evaluation of 25 Metals and Harmful Elements in Testudinis Carapax Et Plastrum and Testudinis Carapax Et Plastri Colla. *Chin. J. Pharm. Anal.* 39, 870–880. doi:10.16155/j.0254-1793.2019.05.15

Losón, O. C., Song, Z., Chen, H., and Chan, D. C. (2013). Fis1, Mff, MiD49, and MiD51 Mediate Drp1 Recruitment in Mitochondrial Fission. *MBoC* 24, 659–667. doi:10.1091/mbc.e12-10-0721

Manczak, M., Mao, P., Calkins, M. J., Cornea, A., Reddy, A. P., Murphy, M. P., et al. (2010). Mitochondria-Targeted Antioxidants Protect Against Amyloid-β Toxicity in Alzheimer's Disease Neurons. *Jad* 20, S609–S631. doi:10.3233/jad-2010-100564

Manczak, M., Calkins, M. J., and Reddy, P. H. (2011). Impaired Mitochondrial Dynamics and Abnormal Interaction of Amyloid Beta With Mitochondrial Protein Drp1 in Neurons From Patients With Alzheimer's Disease: Implications for Neuronal Damage. *Hum. Mol. Genet.* 20, 2495–2509. doi:10.1093/hmg/ddr139

Mcbride, H. M., Neuspiel, M., and Wasiak, S. (2006). Mitochondria: More Than Just a Powerhouse. *Curr. Biol.* 16, R551–R560. doi:10.1016/j.cub.2006.06.054

Ola, M. S., Nawaz, M., and Ahsan, H. (2011). Role of Bcl-2 Family Proteins and Caspases in the Regulation of Apoptosis. *Mol. Cell Biochem.* 351, 41–58. doi:10.1007/s11010-010-0709-x

Orrenius, S., Zhivotovsky, B., and Nicotera, P. (2003). Regulation of Cell Death: the Calcium-Apoptosis Link. *Nat. Rev. Mol. Cell Biol.* 4, 552–565. doi:10.1038/nrm1150

Pallo, S. P., and Johnson, G. V. W. (2015). Tau Facilitates Aβ-Induced Loss of Mitochondrial Membrane Potential Independent of Cytosolic Calcium Fluxes in Mouse Cortical Neurons. *Neurosci. Lett.* 597, 32–37. doi:10.1016/j.neulet.2015.04.021

Pernas, L., and Scorrano, L. (2016). Mito-Morphosis: Mitochondrial Fusion, Fission, and Cristae Remodeling as Key Mediators of Cellular Function. *Annu. Rev. Physiol.* 78, 505–531. doi:10.1146/annurev-physiol-021115-105011

Pharmacopoeia of the People's Republic of China (2020). *Pharmacopoeia of the People's Republic of China, Part I*. Beijing, China: China Medical Science and Technology Press.

Sancar, A., Lindsey-Boltz, L. A., Ünsal-Kaçmaz, K., and Linn, S. (2004). Molecular Mechanisms of Mammalian DNA Repair and the DNA Damage Checkpoints. *Annu. Rev. Biochem.* 73, 39–85. doi:10.1146/annurev.biochem.73.011303.073723

Shi, Y., Fan, X. L., and Xiao, X. Y. (2012). Research on Determination of 4 Main Amino Acids in Deerhorn Glue. *Chin. J. Pharm. Anal.* 32, 783–787. doi:10.16155/j.0254-1793.2012.05.013

Struble, R. G., Ala, T., Patrylo, P. R., Brewer, G. J., and Yan, X.-X. (2010). IS Brain Amyloid Production a Cause or a Result of Dementia of the Alzheimer's Type? *Jad* 22, 393–399. doi:10.3233/jad-2010-100846

Taguchi, N., Ishihara, N., Jofuku, A., Oka, T., and Mihara, K. (2007). Mitotic Phosphorylation of Dynamin-Related GTPase Drp1 Participates in Mitochondrial Fission. *J. Biol. Chem.* 282, 11521–11529. doi:10.1074/jbc.m607279200

Tang, Y., Xiao, D., Liu, Z. Y., Wang, L., Luo, L. Y., and Qing-Hu, H. E. (2019). Research Status and Prospect of Testudinis Carapacis Et Plastri Colla. *China J. Traditional Chin. Med. Pharm.* 34, 2593–2598.

Tönnies, E., and Trushina, E. (2017). Oxidative Stress, Synaptic Dysfunction, and Alzheimer's Disease. *Jad* 57, 1105–1121. doi:10.3233/jad-161088

Veronese, N., Zurlo, A., Solmi, M., Luchini, C., Trevisan, C., Bano, G., et al. (2016). Magnesium Status in Alzheimer's Disease. *Am. J. Alzheimers Dis. Other Demen.* 31, 208–213. doi:10.1177/1533317515602674

Wang, X., Su, B., Siedlak, S. L., Moreira, P. I., Fujioka, H., Wang, Y., et al. (2008). Amyloid-Overproduction Causes Abnormal Mitochondrial Dynamics *via* Differential Modulation of Mitochondrial Fission/fusion Proteins. *Proc. Natl. Acad. Sci.* 105, 19318–19323. doi:10.1073/pnas.0804871105

Wang, W., Xie, Q., Zhou, X., Yao, J., Zhu, X., Huang, P., et al. (2015). Mitofusin-2 Triggers Mitochondria Ca2+ Influx From the Endoplasmic Reticulum to

Induce Apoptosis in Hepatocellular Carcinoma Cells. *Cancer Lett.* 358, 47–58. doi:10.1016/j.canlet.2014.12.025

Wang, J., Wang, Y. J., Tian, S. S., Zhou, X. S., Zhao, T. T., Shi, Y. J., et al. (2018). Determination of Ca, Mg, Fe, Zn and Other Eight Trace Elements in Tortoise-Shell Glue and Antler Glue by ICP-MS. *Res. Pract. Chin. Medicines* 32, 42–45. doi:10.13728/j.1673-6427.2018.06.012

Xu, S., Wang, P., Zhang, H., Gong, G., Cortes, N. G., Zhu, W., et al. (2016). CaMKII Induces Permeability Transition through Drp1 Phosphorylation During Chronic β-AR Stimulation. *Nat. Commun.* 7, 1–13. doi:10.1038/ncomms13189

Zhan, Z. L., Cheng, Z. G., Jiang-Ping, A. I., Wang, J. B., and Hospital, S. P. (2018). Effect of Modified Shenfutang Combined With Huanglian Ejiao Tang on Postoperative Cognitive Dysfunction of Patients with Postoperative Delirium After Orthopedics Operation. *Chin. J. Exp. Traditional Med. Formulae* 24, 188–193. doi:10.13422/j.cnki.syfjx.20181219

**Conflict of Interest:** The authors declare that the research was conducted in the absence of any commercial or financial relationships that could be construed as a potential conflict of interest.

frontiers in Pharmacology

ORIGINAL RESEARCH
published: 24 June 2021
doi: 10.3389/fphar.2021.706225

# Cytisine Exerts an Anti-Epileptic Effect via α7nAChRs in a Rat Model of Temporal Lobe Epilepsy

*Jing-jun Zheng[1,2†], Teng-yue Zhang[1†], Hong-tao Liu[1], Ze-xin Huang[1], Jing-mei Teng[1], Jing-xian Deng[1], Jia-gui Zhong[3], Xu Qian[1], Xin-wen Sheng[1], Ji-qiang Ding[3], Shu-qiao He[4], Xin Zhao[1], Wei-dong Ji[5], De-feng Qi[6], Wei Li[3]* and Mei Zhang[1]**

[1]Key Laboratory of Molecular Target and Clinical Pharmacology, Department of Clinical Pharmacology, School of Pharmaceutical Sciences and the Fifth Affiliated Hospital, Guangzhou Medical University, Guangzhou, China, [2]Department of Pharmacy, Shenzhen Kangning Hospital, Shenzhen Mental Health Center, Shenzhen, China, [3]Department of Neurosurgery, The First Affiliated Hospital of Jinan University, Guangzhou, China, [4]Department of Pharmacy, Maoming People's Hospital, Maoming, China, [5]Center for Translational Medicine, The First Affiliated Hospital, Sun Yat-sen University, Guangzhou, China, [6]Department of Urology, Minimally Invasive Surgery Center, The First Affiliated Hop-ital of Guangzhou Medical University, Guangdong Key Laboratory of Urology, Guangzhou, China

OPEN ACCESS

**Edited by:**
Fushun Wang,
Nanjing University of Chinese Medicine, China

**Reviewed by:**
Wei Liu,
Guangzhou University of Chinese Medicine, China
Damanpreet Singh,
Institute of Himalayan Bioresource Technology, India

***Correspondence:**
Mei Zhang
zhmeic@gzhmu.edu.cn
Wei Li
tliwei@jnu.edu.cn

[†]These authors contributed equally to this work

**Received:** 07 May 2021
**Accepted:** 09 June 2021
**Published:** 24 June 2021

**Citation:**
Zheng J, Zhang T, Liu H, Huang Z, Teng J, Deng J, Zhong J, Qian X, Sheng X, Ding J, He S, Zhao X, Ji W, Qi D, Li W and Zhang M (2021) Cytisine Exerts an Anti-Epileptic Effect via α7nAChRs in a Rat Model of Temporal Lobe Epilepsy. Front. Pharmacol. 12:706225. doi: 10.3389/fphar.2021.706225

**Background and Purpose:** Temporal lobe epilepsy (TLE) is a common chronic neurological disease that is often invulnerable to anti-epileptic drugs. Increasing data have demonstrated that acetylcholine (ACh) and cholinergic neurotransmission are involved in the pathophysiology of epilepsy. Cytisine, a full agonist of α7 nicotinic acetylcholine receptors (α7nAChRs) and a partial agonist of α4β2nAChRs, has been widely applied for smoking cessation and has shown neuroprotection in neurological diseases. However, whether cytisine plays a role in treating TLE has not yet been determined.

**Experimental Approach:** In this study, cytisine was injected intraperitoneally into pilocarpine-induced epileptic rats for three weeks. Alpha-bungarotoxin (α-bgt), a specific α7nAChR antagonist, was used to evaluate the mechanism of action of cytisine. Rats were assayed for the occurrence of seizures and cognitive function by video surveillance and Morris water maze. Hippocampal injuries and synaptic structure were assessed by Nissl staining and Golgi staining. Furthermore, levels of glutamate, γ-aminobutyric acid (GABA), ACh, and α7nAChRs were measured.

**Results:** Cytisine significantly reduced seizures and hippocampal damage while improving cognition and inhibiting synaptic remodeling in TLE rats. Additionally, cytisine decreased glutamate levels without altering GABA levels, and increased ACh levels and α7nAChR expression in the hippocampi of TLE rats. α-bgt antagonized the above-mentioned effects of cytisine treatment.

**Abbreviations:** TLE, temporal lobe epilepsy; SRS, spontaneous recurrent seizures; SE, status epilepticus; AEDs, anti-epileptic drugs; CNS, central nervous system; ACh, acetylcholine; α7nAChRs, α7 nicotinic acetylcholine receptors; GABA, γ-aminobutyric acid; α-bgt, alpha-bungarotoxin; JME, juvenile myoclonic epilepsy; ADNFLE, autosomal-dominant nocturnal frontal lobe epilepsy; PFA, paraformaldehyde; GLT-1, glutamate transporter-1.

**Conclusion and Implications:** Taken together, these findings indicate that cytisine exerted an anti-epileptic and neuroprotective effect in TLE rats via activation of α7nAChRs, which was associated with a decrease in glutamate levels, inhibition of synaptic remodeling, and improvement of cholinergic transmission in the hippocampus. Hence, our findings not only suggest that cytisine represents a promising anti-epileptic drug, but provides evidence of α7nAChRs as a novel therapeutic target for TLE.

**Keywords: cytisine, temporal lobe epilepsy, neuroprotection, synaptic remodeling, cholinergic transmission, α7nAChRs**

## INTRODUCTION

Epilepsy is characterized by spontaneous seizures and is the second-most-prevalent neurological disease. Approximately 70 million people worldwide suffer from epilepsy (Singh and Trevick, 2016; Asadi-Pooya et al., 2017; Song et al., 2017). Anti-epileptic drugs (AEDs) remain as the primary treatment for epilepsy. Despite there being approximately 30 AEDs available with diverse molecular targets, one-third of patients still develop drug-resistant epilepsy, among which the most common type is temporal lobe epilepsy (TLE) (Asadi-Pooya et al., 2017; Wang and Chen, 2019). Most TLE patients not only exhibit the typical sign of spontaneous recurrent seizures (SRS), but also suffer from cognitive and memory impairments (Asadi-Pooya et al., 2017). In addition to psychological and physical stress, as well as exacerbation of mental disorders, the lives of epileptic patients are seriously affected by a much higher risk of disability and death (Robertson et al., 2015; Devinsky et al., 2018). Therefore, continued discovery of novel drug targets and promising drugs is imperative for improving TLE treatments.

The pathological mechanisms of epilepsy involve abnormal ion channels, inflammation, neuronal death, gliosis, and synaptic structural changes (Pitkänen and Lukasiuk, 2011; Pitkanen et al., 2015). It has long been considered that epilepsy is due to hyper-synchronous neuronal activity, during which the balance between excitation and inhibition is disrupted. Glutamate and $\gamma$-aminobutyric acid (GABA) are the most prevalent excitatory and inhibitory neurotransmitters, respectively, in the central nervous system (CNS), and play a pivotal role in epileptogenesis (Khazipov, 2016; Albrecht and Zielińska, 2017). Recently, increasing data have suggested that acetylcholine (ACh) and cholinergic neurotransmission participate in the pathophysiology of epilepsy (Ghasemi and Hadipour-Niktarash, 2015; Biagioni et al., 2019; Meller et al., 2019). Genetic studies have also demonstrated that mutations in neuronal nicotinic ACh receptors (nAChRs) are responsible for some specific forms of epileptic disorders, such as juvenile myoclonic epilepsy (JME) and autosomal-dominant nocturnal frontal lobe epilepsy (ADNFLE) (Rozycka et al., 2009; Rozycka et al., 2013; Weltzin et al., 2016; Villa et al., 2019). Neural nAChRs are extensively distributed in the CNS and represent a large family of ligand-gated ion channels constructed from combinations of α (α2–α10) and β (β2–β4) subunits (Gotti et al., 2006). Among them, homomeric α7 and heteromeric α4β2 pentameric nAChRs are predominant subtypes in the brain (Gotti et al., 2006). It has been reported that α7 and α4β2 subtypes of nAChRs might be linked to some idiopathic types of epilepsy, including JME and ADNFLE (Rozycka et al., 2009; Rozycka et al., 2013; Weltzin et al., 2016; Villa et al., 2019). Therefore, nAChR abnormalities may serve as a biomarker in epilepsy with a genetic background (Garibotto et al., 2019), suggesting that nAChRs may also be a potential target for the treatment of epilepsy.

Cytisine ($C_{11}H_{14}N_2O$), a quinolizidine alkaloid extracted from the seeds of Cytisus laburnum, a natural plant of the Leguminosae family, is a full agonist of α7nAChRs and a partial agonist of α4β2nAChRs (Rouden et al., 2014). Historically, cytisine was initially used as an emetic, purgative, respiratory, analeptic, and diuretic agent in both Europe and North America (Paduszynska et al., 2018; Tutka et al., 2019). Presently, cytisine is widely applied for smoking cessation in Central and Eastern Europe (trade names: Tabex and Desmoxan) (Paduszynska et al., 2018; Tutka et al., 2019). There is a high systemic bioavailability of cytisine in healthy smokers taking this drug for smoking cessation, albeit with mild adverse reactions (Hajek et al., 2013). Accumulating evidence has shown that cytisine has neuroprotective effects in some neurological diseases such as Parkinson's disease, depression, and cerebral injury induced by ischemia-reperfusion in animal models (Abin-Carriquiry et al., 2008; Han et al., 2016; Zhao et al., 2018). However, whether cytisine plays a role in the treatment of chronic spontaneous epilepsy remains unknown. Therefore, the present study investigated the effects and underlying mechanisms of cytisine in a rat model of TLE. Our results not only provide novel evidence of the use of cytisine as an efficacious drug for treating TLE, but further verify that nAChRs may serve as a therapeutic target for ameliorating epilepsy.

## RESULTS

### Cytisine Reduces the Occurrence of SRS in Epileptic Rats

SRS emerged at an average of 12 days after SE induction in rats, which is consistent with our previous research (Qian et al., 2019). Cytisine treatment for three weeks after the onset

**TABLE 1 |** Cytisine reduces the frequency of SRS in epileptic rats.

| Groups | Seizurs/week (times) | Seizurs score | Seizure durations(s) |
|---|---|---|---|
| Normal | 0 | — | 0 |
| Epilepsy | 5.17 ± 0.48 | IV/V | 23.56 ± 4.22 |
| Ep + Cyt | 2.33 ± 0.56$^{\#}$ | IV/V | 21.38 ± 3.91 |
| Ep + Cyt + α-bgt | 4.83 ± 0.91 $^{\$}$ | IV/V | 20.31 ± 3.72 |
| Ep + α-bgt | 5.83 ± 0.40 | IV/V | 26.73 ± 5.65 |
| Norm + α-bgt | 0 | — | 0 |

*Experimental rats received cytisine (2 mg/kg/d) and α-bgt (1 μg/kg/d) by i.p injection for three weeks. The numbers and durations of SRS were recorded. Cyt is the abbreviation of cytisine, Ep is the abbreviation of epilepsy, and Norm is the abbreviation of normal. Normal and Norm + α-bgt rats did not have any seizures. The statistical results of the remaining four groups are as follows (seizures/week): F (3,36) = 15.422, n = 10, epilepsy vs. epilepsy + Cyt, $^{\#}p < 0.05$, epilepsy + Cyt vs. epilepsy + Cyt + α-bgt, $^{\$}p < 0.05$.*

of SRS significantly reduced the frequency of SRS without influencing seizure durations (**Table 1**). However, α-bgt inhibited this effect in cytisine-treated epileptic rats, which suggests that cytisine's anti-epileptic effect involved α7nAChR signaling. Importantly, α-bgt administration alone did not affect SRS frequency in epileptic rats, nor did it induce any adverse reactions in normal rats.

## Cytisine ameliorates Cognitive Dysfunction in Epileptic Rats

Learning and memory were assessed using the Morris water maze. The path length, latency to reach the target platform, and average swimming speed were recorded during all 5 days of training (**Figures 1A–C**). Epileptic rats showed decreased learning in searching for the underwater platform as compared to that of the normal group, which was manifested as an increased travel distance and latency to reach the target platform during the training trials (**Figures 1A,B**). There was no significant difference in swimming speed among the groups during the 5 days of training (**Figure 1C**). Epileptic rats spent more time searching for the target quadrant and had a reduced number of crossing over the platform area during the probe trial compared with these parameters in normal rats (**Figures 1D,E**). Cytisine treatment significantly shortened both the distance and latency to reach the target platform (**Figures 1A,B**), and increased the number of crossing over the target platform in epileptic rats compared to those treated with vehicle (**Figures 1D,E**). These results indicated that impaired learning abilities in epileptic rats were rescued by cytisine treatment. Furthermore, α-bgt antagonized cytisine's effect on cognitive deficits in TLE rats. Importantly, α-bgt used alone did not influence learning and memory in either epileptic rats or normal rats.

## Cytisine attenuates Hippocampal Injuries in Epileptic Rats

Neuronal damage in the hippocampus was examined via Nissl staining. Our results showed that pyramidal neurons were aligned regularly and exhibited intact structures with clear nucleoli in hippocampal CA1 and CA3 regions of normal rats (**Figure 2A**). CA1 regions exhibited destruction of the layered structure of pyramidal neurons with an evident neuronal loss, and CA3 regions exhibited a disordered arrangement of pyramidal neurons with an atactic shape, opaque cytoplasm, and shrinking nuclei in the hippocampi of epileptic rats (**Figure 2A**). Cytisine treatment significantly attenuated the epileptic-induced loss of pyramidal neurons and mitigated these pathological changes in both CA1 and CA3 regions of the hippocampus (**Figures 2B,C**). Furthermore, α-bgt partially abolished cytisine's neuroprotective effect on hippocampal neurons. Importantly, α-bgt used alone did not influence hippocampal structures in either normal or epileptic rats.

## Influences of Cytisine on Neurotransmitters in the Hippocampus of Epileptic Rats

Glutamate and GABA are essential for maintaining a balance of neuronal excitation and inhibition within the brain. Our results demonstrated that glutamate levels were increased and GABA levels were decreased in the hippocampi of epileptic rats. Cytisine treatment remarkably decreased glutamate levels without altering GABA levels obviously (**Figures 3A,B**). GLT-1 is a glutamate transporter that is responsible for reuptake of excess glutamate from the synaptic cleft. To further determine changes related to epileptic-induced alterations in glutamate levels, the expression of GLT-1 in the hippocampus was assessed. We found that the expression of hippocampal GLT-1 was decreased in epileptic rats and that this decrease was reversed by cytisine compared to that of vehicle treatment, the effect of which may have accelerated reuptake of glutamate (**Figures 3C,D**). Furthermore, α-bgt inhibited cytisine's effects on glutamate level and GLT-1 expression, but GABA levels were not changed. However, α-bgt used alone did not influence neurotransmitters levels or GLT-1 expression in either normal or epileptic rats.

## Cytisine inhibits Synapse Remodeling in the Hippocampi of Epileptic Rats

Synapse remodeling occurs as a result of epileptogenesis. Hence, synaptic structures were assessed to investigate whether cytisine's anti-epileptic effect involved synaptic remodeling. The densities of dendritic spines in epileptic rats were increased significantly compared to those in normal rats, suggesting synaptic remodeling in the hippocampus of epileptic rats. Cytisine treatment reversed

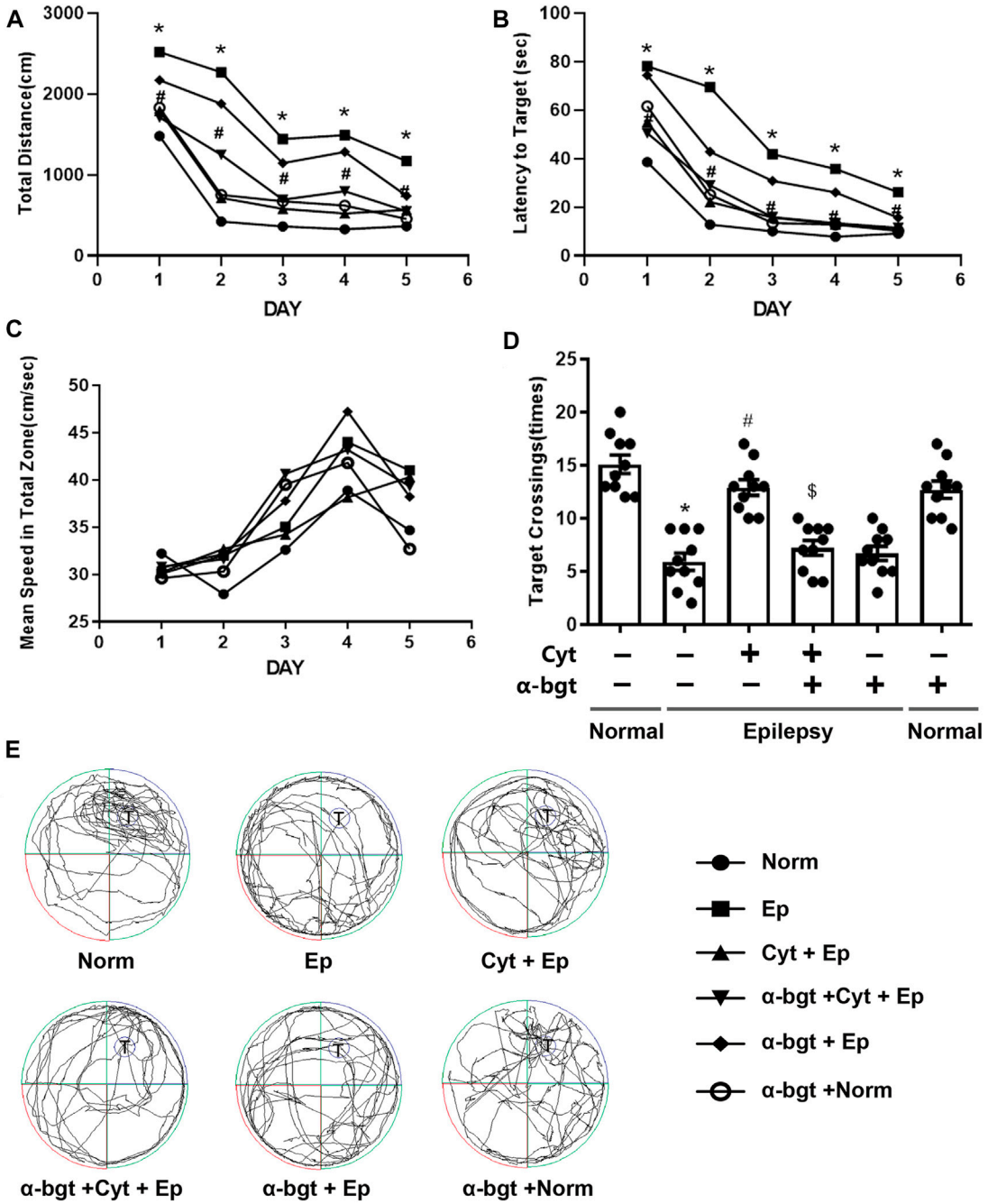


**FIGURE 1 |** *Cytisine ameliorates deficits in learning and memory in TLE rats*. The effects of cytisine on learning and memory in rats were evaluated using the Morris water maze. **A–C:** Acquisition training. **A:** Swim path distance. **B:** Latency to reach underwater platform. **C:** Mean swim speed. **D–E:** Probe trial. **D:** The number of crossing over the target quadrant. **E:** Searching trajectories for the target quadrant (T: target). Statistical results are as follows: $F(5,54) = 26.017$, $n = 10$; normal vs. epilepsy, $^{*}p < 0.05$; epilepsy vs. epilepsy + Cyt, $^{\#}p < 0.05$; epilepsy + Cyt vs. epilepsy + Cyt + α-bgt, $^{\$}p < 0.05$.

this alteration by reducing the number of dendritic spines (**Figures 4A,B**). Synaptophysin, a synapse-associated protein, participates in synaptic remodeling. Our results showed that synaptophysin expression was increased in the hippocampi of epileptic rats, and we found that cytisine treatment suppressed this change (**Figures 4C,D**). Furthermore, α-bgt antagonized cytistine-induced inhibition in the numbers of dendritic spines, and simultaneously abolished cytisine-induced suppression of synaptophysin expression. However, α-bgt used alone did not have any impact on the density of dendritic spines or synaptophysin expression in either normal or epileptic rats.

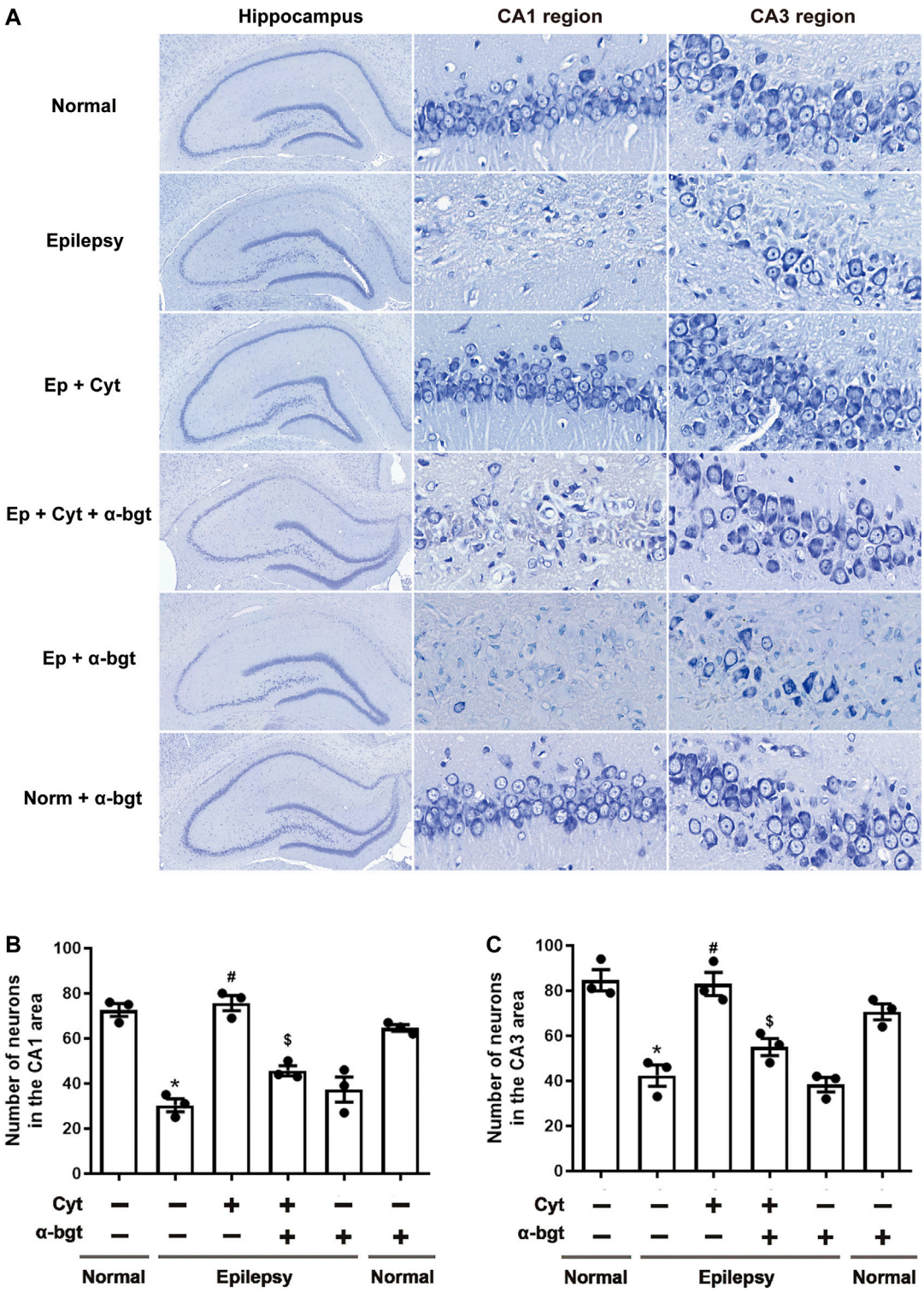


**FIGURE 2 |** *Cytisine attenuates hippocampal damage in epileptic rats.* Nissl staining was used to assess neuronal damage in hippocampal regions. **A:** Nissl staining of the entire hippocampus (5×). CA1 and CA3 regions of the hippocampus (90×). **B:** Quantitative analysis of pyramidal neurons in CA1 regions. Statistical results are as follows: **F** (5,12) = 33.59, $p < 0.05$, $n = 3$; normal vs. epilepsy, $^{*}p < 0.05$; epilepsy vs. epilepsy + Cyt, $^{\#}p < 0.05$; epilepsy + Cyt vs. epilepsy + Cyt + α-bgt, $^{\$}p < 0.05$. **C:** Quantitative analysis of pyramidal neurons in CA3 regions. Statistical results are as follows: **F** (5,12) = 22.618, $p < 0.05$, $n = 3$; normal vs. epilepsy, $^{*}p < 0.05$; epilepsy vs. epilepsy + Cyt, $^{\#}p < 0.05$; epilepsy + Cyt vs. epilepsy + Cyt + α-bgt, $^{\$}p < 0.05$.

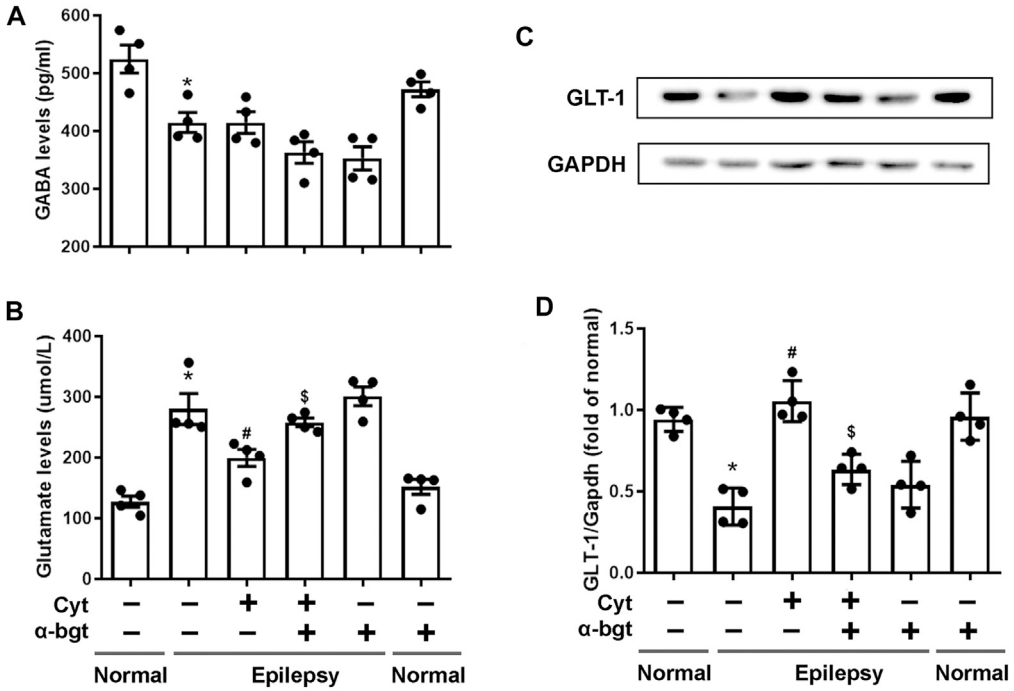


**FIGURE 3 |** *Influences of cytisine treatment on neurotransmitter levels in the hippocampi of epileptic rats.* **A–B:** GABA and glutamate levels in the hippocampus were measured by colorimetry. Statistical results are as follows: GABA: **F** (5,18) = 11.924, $p < 0.05$, $n = 4$; normal vs. epilepsy, $^{*}p < 0.05$; epilepsy vs. epilepsy + Cyt, $p > 0.05$; epilepsy + Cyt vs. epilepsy + Cyt + α-bgt, $p > 0.05$; Glu: **F** (5,18) = 21.889, $p < 0.05$, $n = 4$; normal vs. epilepsy, $^{*}p < 0.05$; epilepsy vs. epilepsy + Cyt, $^{\#}p < 0.05$; epilepsy + Cyt vs. epilepsy + Cyt + α-bgt, $^{\$}p < 0.05$. **C–D:** GLT-1 expression in the hippocampus was analyzed by Western blotting.Statistical results are as follows: GLT-1:F (5,18) = 19.741,$p < 0.05$, $n = 4$; normal vs. epilepsy, $^{*}p < 0.05$; epilepsy vs. epilepsy + Cyt, $^{\#}p < 0.05$; epilepsy + Cyt vs. epilepsy + Cyt + α-bgt, $^{\$}p < 0.05$.

## Cytisine Strengthens Cholinergic Transmission in the Hippocampi of Epileptic Rats

Cholinergic transmission is altered as a result of epileptogenesis. Thus, ACh levels and α7nAChR expression were measured in order to investigate whether cytisine's therapeutic amelioration of epilepsy was associated with cholinergic transmission. Our experiments showed that ACh levels were significantly decreased in the hippocampi of epileptic rats (**Figure 5F**). Accordingly, both hippocampal slices and tissue homogenates from epileptic rats showed decreased expression of α7nAChRs (**Figures 5A–E**). Moreover, cytisine treatment increased ACh levels and α7nAChR expression. α-bgt partly blocked cytisine's effects on ACh levels or α7nAChR expression, but showing no significance. However, α-bgt used alone increased ACh levels without affecting α7nAChR expression in epileptic rats, and did not influence either of these parameters in normal rats.

## DISCUSSION

Our present study demonstrated that cytisine treatment for three weeks after the onset of spontaneous seizures in TLE rats significantly reduced the frequency of SRS, mitigated deficits in learning and memory, ameliorated hippocampal damage, and inhibited synaptic remodeling. These findings indicate that cytisine exerted anti-epileptic and neuroprotective effects in TLE rats. Moreover, these findings represent the first demonstration that cytisine mitigates TLE in rats.

Hyperactivity of glutamatergic function and insufficient GABAergic neurotransmission has been regarded as the most important mechanisms in epileptic seizures (Khazipov, 2016; Albrecht and Zielińska, 2017). Based on this canonical perspective, current AEDs play a therapeutic role via either inhibiting excitatory drive or strengthening inhibitory drive. Some conventional antiepileptic drugs such as sodium valproate, carbamazepine, and oxcarbazepine work in this manner. The present study showed that the occurrences of spontaneous seizures in TLE rats were decreased following cytisine treatment. Further investigation indicated that cytisine significantly reduced glutamate levels in hippocampus of TLE rats, which may have accounted for the concomitant reduction in SRS following cytisine treatment. However, it has been shown that activation of α7nAChRs by nicotine enhanced glutamate release in hippocampal pyramidal neurons (Cheng and Yakel, 2015). As an agonist of α7nAChRs, present study demonstrated that cytisine reduced glutamate levels in hippocampus of TLE rats. For this inconsistency, we speculated that it may be due to the effect of cytisine on neuroglial cells. Besides neuronal expression, α7nAChRs are also expressed on non-neuronal cells such as astrocytes in the hippocampal CA1 region (Shen and Yakel, 2012). The clearance of glutamate from synapse is

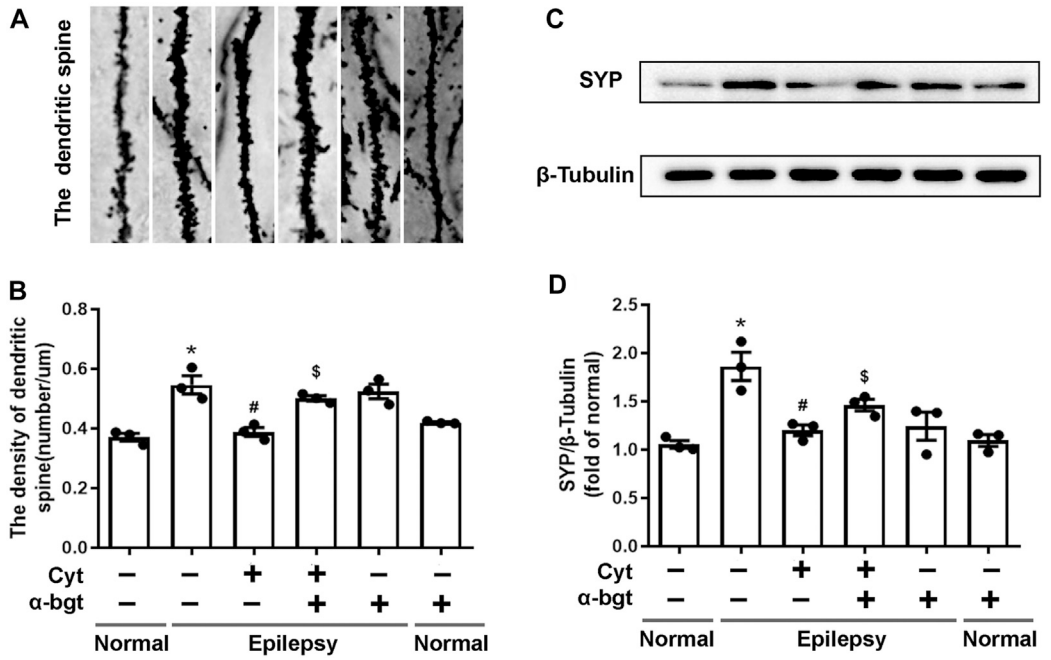


**FIGURE 4 |** *Cytisine inhibits synaptic remodeling in the hippocampi of epileptic rats.* **A:** Dendritic spines dyed by Golgi staining in the dentate gyrus of the hippocampus. **B:** Quantitative analysis of the densities of dendritic spines. Statistical results are as follows: **F** (5,12) = 16.685, $p < 0.05$, $n = 3$; normal vs. epilepsy, $^{*}p < 0.05$; epilepsy vs. epilepsy + Cyt, $^{\#}p < 0.05$; epilepsy + Cyt vs. epilepsy + Cyt + α-bgt, $^{\$}p < 0.05$. **C–D:** The expression of synaptophysin in the hippocampus was analyzed by Western blotting. Statistical results are as follows: **F** (5,12) = 10.802, $p < 0.05$, $n = 3$; normal vs. epilepsy, $^{*}p < 0.05$; epilepsy vs. epilepsy + Cyt, $^{\#}p < 0.05$; epilepsy + Cyt vs. epilepsy + Cyt + α-bgt, $^{\$}p < 0.05$.

performed by neuroglia via glutamate transporters, which is mediated by activation of α7nAChRs (Morioka et al., 2014). Compared to neuroglial cells, hippocampal pyramidal neurons are more vulnerable to insults under pathological conditions, which also has been shown in our present study. Epileptic seizures initially result in damages to hippocampal neurons, accompanied by a decrease of α7nAChRs that weakened its role in modulating neurotransmitters release. Under this circumstance, neuroglial cells may play a more important role in glutamate metabolism. Glutamate reuptake at the synaptic cleft is mainly mediated by GLT-1 (Rimmele and Rosenberg, 2016). Our present study showed that cytisine increased the expression of GLT-1 in the hippocampus of TLE rats. Accordingly, this may result in accelerated glutamate clearance and decreased synaptic glutamate levels. Although cytisine activates both α7 and α4β2 subtypes of nAChRs, it is a full agonist of α7nAChRs, suggesting that high-efficacy activation of α7nAChRs may be more important for cytisine's therapeutic effects (Rouden et al., 2014; Tutka et al., 2019). Hence, in our present study, the α7nAChR-specific blocker, α-bgt, was used to determine its influence on cytisine's effects. In our experiments, methyllcaconitine (MLA), a reversible antagonist of α7nAChR, has not been selected as the α7nAChR blocker for its affinity, albeit low, to α3β4 and α4β2 subtypes (Drasdo et al., 1992). We found that α-bgt antagonized not only anti-epileptic effects, but also effects on glutamate reuptake, induced by cytisine treatment, indicating that α7nAChR signaling is involved in cytisine's anti-epileptic effects. It should be mentioned that α-bgt administration alone did not affect SRS frequency in epileptic rats, nor did it induce any adverse reactions in normal rats. In our present study, a dose of 1 μg/kg α-bgt was selected for treatment, and this dose was also used for other previous studies (Gao et al., 2010; Du et al., 2013). A higher dose of α-bgt (3–5 μg/kg) was often used to induce animal model for myasthenia gravis in which the main symptoms manifested as facial muscle weakness, showing no obvious toxic effects (Plomp et al., 1994). It should be noted that cytisine did not alter GABA levels in the hippocampus of TLE rats at present study. Although α7nAChRs are also involved in the functional modulation of GABAergic neurons, cholinergic neuromodulation in GABAergic interneurons is extremely complicated, involving in multiple factors such as network oscillation, et al. (Lawrence, 2008). In addition, damages of hippocampal GABAergic neurons during epileptogenesis may partly abolished the modulation of α7nAChRs activation on neurotransmitter release. Therefore, the exact effects of cytisine on GABAergic transmission require further investigation.

The hippocampus is an essential region in the brain that is closely associated with cognition and memory. Hippocampal neuronal injury is the primary neuropathological feature of TLE that contributes to cognitive and memory impairments (Titiz et al., 2014). Our previous study showed that lithium- and pilocarpine-induced epileptic rats exhibited typical traits of TLE accompanied by cognitive deficits (Qian et al., 2019). Our present study indicated that cytisine treatment reduced epileptic-mediated loss of pyramidal neurons in the CA1 and CA3 regions

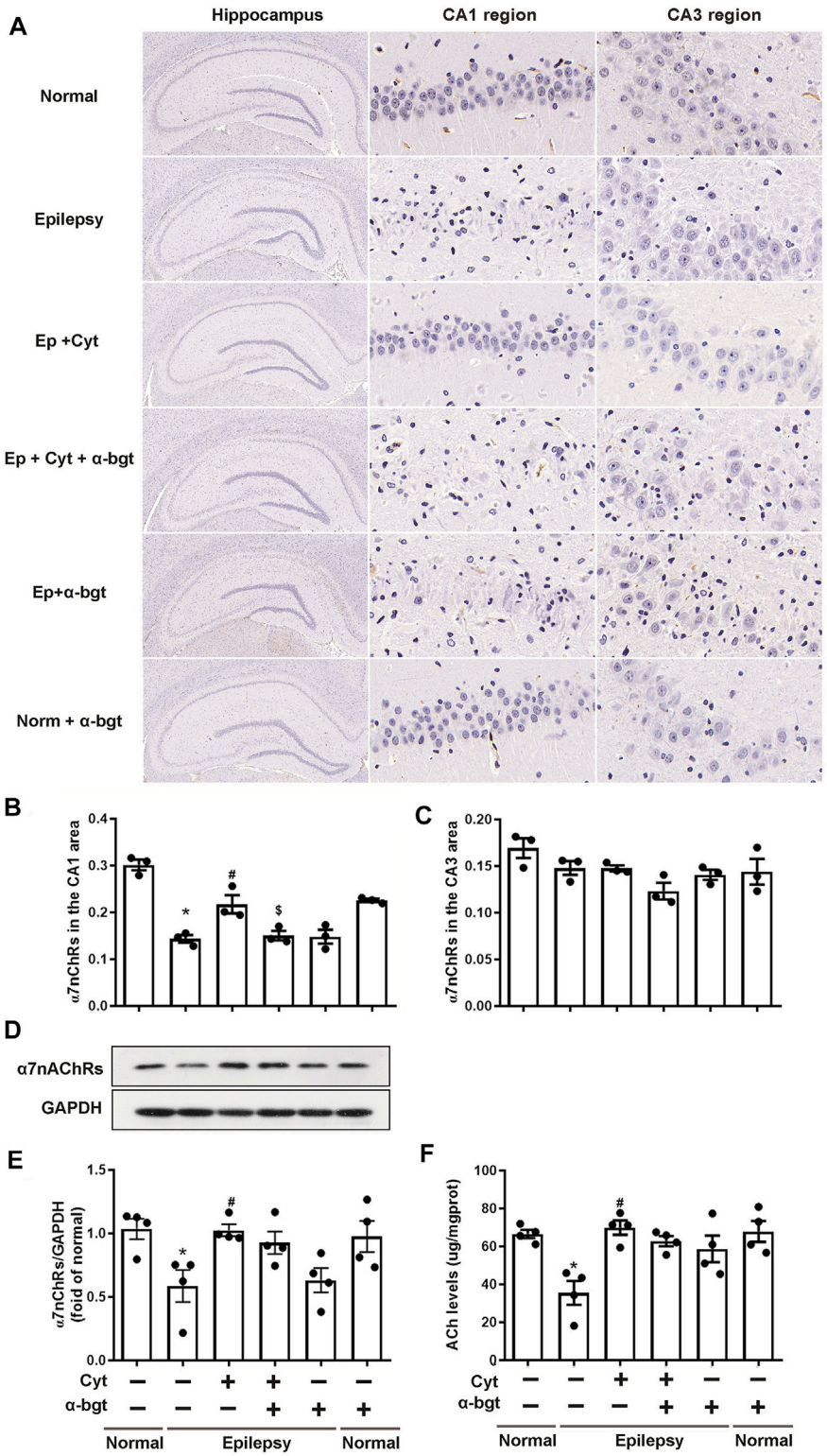


**FIGURE 5 |** *Cytisine enhances cholinergic transmission in the hippocampi of epileptic rats.* **A–C:** The expression of α7nAChRs in the hippocampus was stained by immunohistochemistry. Statistical results are as follows: **F** (5,12) = 26.033, $p < 0.05$, $n = 3$; normal vs. epilepsy, $^{*}p < 0.05$; epilepsy vs. epilepsy + Cyt, $^{\#}p < 0.05$; epilepsy + Cyt vs. epilepsy + Cyt + α-bgt, $^{\$}p < 0.05$. **D–E:** The expression of α7nAChRs in the hippocampus was analyzed by Western blotting. Statistical results are as follows: F (5,18) = 4.271, $p < 0.05$, $n = 4$; normal vs. epilepsy, $^{*}p < 0.05$; epilepsy vs. epilepsy + Cyt, $^{\#}p < 0.05$. **F:** ACh levels in the hippocampus were measured by colorimetry. Statistical results are as follows: **F** (5,18) = 6.705, $p < 0.05$, $n = 4$; normal vs. epilepsy, $^{*}p < 0.05$; epilepsy vs. epilepsy + Cyt, $^{\#}p < 0.05$.

of the hippocampus and mitigated deficits in learning and memory in TLE rats. Several other studies have demonstrated that cytisine confers neuroprotection against cytotoxicity induced by beta amyloid and N-methyl-D-aspartate in both cortical neurons *in vitro* and in a mouse model of cerebral ischemia-reperfusion injury (Kihara et al., 1998; Li et al., 2013; Zhao et al., 2018). Similarly, cytisine has been shown to exhibit neuroprotection of dopaminergic neurons in a mouse model of Parkinson's disease (Ferger et al., 1998; Abin-Carriquiry et al., 2008). Consistent with these previous findings, our present study revealed that cytisine also exerted neuroprotection in TLE rats. In inconsistent to our present results, in previous studies cytisine attenuated neuroprotection and anticonvulsive activity when combined with antiepileptic drugs in electroshock and 6-Hz stimulation-induced mouse model (Tutka et al., 2013; Tutka et al., 2017). This discrepancy may be due to differences in the types of epileptic models and the manner of cytisine treatments. In our present study, we found that α-bgt antagonized cytisine's neuroprotective effects in TLE rats, suggesting a role for α7nAChR signaling.

Synaptic remodeling occurs during the development of the brain and shares common features with epileptogenesis (Bozzi et al., 2012). Neuronal loss and abnormal synaptic contacts induced by seizures result in aberrant neuronal network in both animal models of epilepsy and in human TLE, which may be associated with enhancement of synaptic efficiency and may play an important role in epileptogenesis (Leite et al., 2005; Lillis et al., 2015). Dendritic spines, the dendritic arborizations of neurons, are key synaptic structures and postsynaptic targets of excitatory synapses in the CNS. Abnormally-high numbers of dendritic spines strengthen synaptic transmission and are attributed to neuronal hyperexcitability in epilepsy (Ma et al., 2013; Janz et al., 2018). Our present study demonstrated that numbers and densities of dendritic spines were significantly increased in the hippocampi of TLE rats, and cytisine treatment reduced this epileptic-induced augmentation of dendritic spines. Therefore, cytisine treatment may have inhibited epileptic-mediated formation of abnormal excitability in the hippocampus, which may have resulted in reducing SRS in TLE rats. Synaptophysin is a vesicular protein that is widely expressed in axonal terminals and is closely related to synaptic structure and function (Thiel, 1993). As an important marker for synaptic activity, synaptophysin participates in synaptogenesis and synaptic remodeling (Masliah et al., 1991; Thiel, 1993). In our present study, we found that cytisine reduced epileptic-induced upregulation of synaptophysin in the hippocampi of TLE rats, suggesting that inhibition of synaptic reorganization may represent one of the mechanisms underlying cytisine's anti-epileptic effects. In line with the above results, we found that α-bgt antagonized cytisine's reduction of synaptic remodeling in TLE rats.

Accumulating evidence suggests that abnormal central cholinergic signaling is involved in the pathophysiology of epilepsy (Hamilton et al., 1997; Ferencz et al., 2001; Ghasemi and Hadipour-Niktarash, 2015; Biagioni et al., 2019; Meller et al., 2019). Cholinergic neurons serve as an important part of the CNS in terms of regulating neuronal excitability, modulating synaptic transmission, and inducing synaptic plasticity (Picciotto et al., 2012). Recently, a number of studies have demonstrated that ACh and cholinergic neurotransmission are involved in epileptogenesis (Ghasemi and Hadipour-Niktarash, 2015; Biagioni et al., 2019; Meller et al., 2019). Genetic studies have shown that mutations in neuronal nAChRs are responsible for some forms of idiopathic epilepsy (Rozycka et al., 2013; Weltzin et al., 2016; Garibotto et al., 2019; Villa et al., 2019). In our present study, we found that both ACh levels and α7nAChR expression were decreased in the hippocampi of TLE rats, while treatment with cytisine reversed these alterations, indicating that cytisine ameliorated epileptic-induced deficits in cholinergic transmission in TLE rats. A number of studies have shown that cholinergic transmission plays a role in epilepsy. The cholinergic system exerts powerful antiepileptic effects in hippocampal-kindling epileptogenesis (Ferencz et al., 2001). Additionally, degeneration of cholinergic nuclei in the basal forebrain is associated with focally-induced seizures (Biagioni et al., 2019). A few conventional antiepileptic drugs, such as carbamazepine and zonisamide, increase basal ACh levels via facilitating release in various brain regions (Mizuno et al., 2000; Zhu et al., 2002). The recent study has shown that ACh levels are decreased in the hippocampi of two rat models of TLE during chronic epileptic states (Meller et al., 2019). Similarly, our present study not only further confirmed that cholinergic transmission was involved in epilepsy, but also suggests that cytisine exerted antiepileptic effects by compensating for cholinergic deficiency in epileptic rats. Previous studies have shown that nAChR agonists induce up-regulation of nAChR and facilitate the release of ACh (Beani et al., 1985; Nordberg et al., 1989; Madhok et al., 1995; Doura et al., 2008), which are coincide with our data that the effects of cytisine on nAChR expression and ACh level in epileptic rats in present study. Despite its role as the primary excitatory neurotransmitter in periphery, ACh mainly plays a neuromodulatory role in the brain (Picciotto et al., 2012). As a result, it has been determined that ACh does not exert merely an excitatory or inhibitory action in epilepsy. Therefore, we speculated that decreased ACh and α7nAChRs in the brains of epileptic rats may weaken its neuroregulation, leading to an imbalance of excitation and inhibition, while cytisine produce an antiepileptic effect by restoring abnormal cholinergic regulation. However, in our present study, we found that α-bgt did not significantly block cytisine's effects on ACh levels and α-bgt used alone increased ACh levels in brain of epileptic rats. Some previous studies have shown that chronic α-bgt treatment facilitates ACh release in motor nerve endings (Miledi et al., 1978; Plomp et al., 1994; Plomp and Molenaar, 1996). Consequently, α-bgt-induced the elevation of ACh levels partly counteracted its effect on cytisine's action as an antagonist of α7nAChRs in brains of TLE rats.

In light of its involvement in epilepsy, neuronal nAChRs represent a novel target for therapy of epilepsy (Löscher et al., 2003; Ghasemi and Hadipour-Niktarash, 2015). A pre-clinical study has demonstrated that nAChR antagonists are beneficial in different epileptic animal models (Ghasemi and Hadipour-Niktarash, 2015). Conventional antiepileptic drugs, such as carbamazepine, zonisamide, and lamotrigine, exert

anticonvulsive effects via blockade of α4β2nAChRs in some genetic models of epilepsy (Picard et al., 1999; Provini et al., 1999; Zheng et al., 2010). Our present study showed that cytisine exerted an antiepileptic effect by activating α7nAChRs in TLE rats. This result is contrary to the conventional understanding of how nAChRs antagonists work as antiepileptic agents. The use of nAChR antagonists for antiepileptic drug development has been controversial because such agents exhibit disparate antiepileptic effects across different animal models (Löscher et al., 2003). For instance, neuronal nAChR antagonists exert potent anticonvulsive effects on generalized epileptic seizures but show less robust effects on complex partial seizures (Löscher et al., 2003). Our present study was conducted in TLE rats, which is a complex partial-seizure model, and we investigated the role of α7nAChRs in the treatment of epilepsy. Thus, differences in epilepsy models and nAChR subtypes may partly account for the inconsistent results between our present study and some previous studies. Furthermore, in line with our present findings a recent study has demonstrated that the α7nAChR agonist, choline chloride, ameliorates seizure severity, memory impairment, and depression in a pentylenetetrazole-kindled mouse model of epilepsy (Sharma et al., 2020).

α7nAChRs are non-selective cation channels, but have a high $Ca^{2+}$ permeability (Fucile et al., 2003). Intracellular $Ca^{2+}$ signals contribute to the regulation of neurotransmitter release and neuronal plasticity (Role and Berg, 1996; Broide and Leslie, 1999). As a result, α7nAChRs may serve a distinct role in modulating these events. Our present results demonstrated that α7nAChR activation may be an important mechanism of cytisine's anti-epileptic actions by affecting neurotransmitter release and synaptic remodeling. In its use as a medicine for smoking cessation, cytisine possesses good pharmacokinetics and mild adverse reactions such as nausea, vomiting, and dry mouth (Jeong et al., 2015; Paduszynska et al., 2018; Tutka et al., 2019). Moreover, cytisine has advantages in terms of its low cost and high tolerability, making it a promising agent in clinical applications (Rouden et al., 2014; Paduszynska et al., 2018). However, our present study only focused on the involvement of α7nAChRs in cytisine's antiepileptic effects, as we did not investigate any potential role of the α4β2 subtype in our study. Hence, further studies are required to determine whether α4β2 nAChRs also play a role in cytisine's antiepileptic effects. Additionally, the specific molecular mechanisms by which cytisine interacts with α7nAChRs requires elucidation in future studies *in vitro*.

# MATERIALS AND METHODS

## Experimental Animals

### Animals

Male Sprague-Dawley (200 ± 20 g) rats were purchased from the Experimental Animal Centre of Guangzhou University of Chinese Medicine (SCXK YUE 2013–0,034). Rats were bred under standard laboratory conditions under a 12 h light/dark cycle at 22 ± 2°C, with food and water provided ad libitum. Rats were fed habitually for one week before experiments. All procedures were conducted according to the National Institutes of Health Guidelines for Animal Research and were approved by the Ethics Committee for Animal Research at Guangzhou Medical University.

## Rat Model of Temporal Lobe Epilepsy

We established a pilocarpine-induced epileptic rat model in our present study according to a previous protocol (Qian et al., 2019). A total of 60 male rats were first treated with lithium chloride (127 mg/kg, Sigma-Aldrich, St. Louis, MO, United States ) and were then subsequently administered pilocarpine hydrochloride 18–20 h later (30 mg/kg, Sigma-Aldrich) via intraperitoneal injection. Atropine sulfate (1 mg/kg, King York, China) was used to reduce peripheral cholinergic side effects at 30 min before pilocarpine injection. Additional pilocarpine hydrochloride (10 mg/kg) was administered every 30 min until the development of status epilepticus (SE) for rats showing no occurrence following the first injection. The evoked seizures were scored according to the Racine scale. Seizures were classified as following: stage I, mouth and facial automatism; stage II, nodding or wet dog shaking; stage III, forelimb clonus; stage IV, standing and bilateral forelimb clonus; stage V, generalized clonic seizures and falls. Only rats with stage IV or stage V seizures were included in our experiment. 54 rats developed to status epilepticus. Control rats received the same treatment with vehicle. Rats sustained with SE for 60 min were then administered diazepam (10 mg/kg, King York, China) to terminate seizures. Intensive care including warming and oral injections of sugar saline to reduce the mortality rates of rats. Among 54 rats with epileptic seizures, 13 rats died in the acute phase. Survived animals were used in the following experiment and survival rate of rats were about 76%. The occurrence of SRS began approximately two weeks after SE.

## Animal Groupings and Drug Treatments

A total of 20 normal rats were randomly divided into two groups (10 rats per group): normal group and normal + α-bgt group. A total of 40 epileptic rats were randomly divided into four groups (10 rats per group): epilepsy group; epilepsy + cytisine group; epilepsy + cytisine + α-bgt group; epilepsy + α-bgt group. The α7nAChR-specific blocker, α-bgt, was employed to investigate the mechanism of action of cytisine. Because of its biotoxicity, α-bgt was administered alone to observe any possible adverse reactions in control and epileptic rats. Cytisine (Macklin, China) and α-bgt (Cayman, United States ) were dissolved in saline. Cytisine was administered daily via intraperitoneal injection at 2 mg/kg/d for three weeks after the onset of SRS, and α-bgt was injected intraperitoneally at a dose of 1 μg/kg/d at 30 min before cytisine injection.

Other rats received saline as a control. On accounting of its wide using, cytisine has not been administered alone to control rats in present experiment. All 10 rats received video monitoring and Morris water maze test. For Nissl staining and immunohistochemistry analysis, three rats were included, and three rats were used for Golgi staining. The remaining four rats were applied for measurement of neurotransmitters and western blotting assay.

## Monitoring of Spontaneous Recurrent Seizures

Rats were continuously video-monitored in transparent cages via a four-camera system (Hikvision, China). The occurrence, severity, and duration of spontaneous seizures were evaluated blindly by an observer, and stage IV seizures or above (as determined by the Racine scale) were recorded. Seizure-like activities in rats were confirmed by another observer in order to avoid bias.

## Morris Water Maze

The Morris water maze was carried out to evaluate learning and memory in rats. This test assesses place-mediated navigation and spatial exploration. The system consisted of a circular pool (150 cm diameter and 50 cm depth) and pool was filled with 30 cm depth of water (22–24°C) made opaque by the addition of non-toxic white paint. The pool was divided into four quadrants and a hidden platform with a diameter of 12 cm was located in a fixed target quadrant 2 cm beneath the water surface. Experimental rats were trained with four trials daily for 5 days during the acquisition phase. Rats facing a wall were put randomly placed into one of four different quadrants in the water maze and were allowed to swim to search for the underwater platform during acquisition training. Rats were permitted to stay for 10 s on the platform to survey the spatial cues in the environment before being returned to their cages. The path length, latency to reach the underwater platform, and mean swimming speed was recorded using a computerized video-tracking system. The underwater platform was removed after 5 days of acquisition and a spatial probe trial was performed at the sixth day. The time spent in the objective quadrant that previously contained the underwater platform during the spatial probe trial was calculated for 120 s.

## Nissl Staining

Rats were deeply anaesthetized with chloral hydrate (350 mg/kg, i.p.) and the thoracic cavity was cut rapidly to expose the heart. A catheter was inserted into the ascending aorta. Rats were perfused with 4% paraformaldehyde (PFA, pH7.4) in phosphate-buffered saline following systemic blood clearance by heparin saline. The brains were removed and fixed in 4% PFA overnight at 4°C, and were then dehydrated, transparentized, and embedded in paraffin. Serial coronal sections were gained by a rotary microtome (RM 2016; Shanghai Leica). All hippocampal sections were gathered in sequence. Nissl staining was employed to assess hippocampal structure. Briefly, hippocampal sections were deparaffinized, rehydrated, and stained with 1% toluidine blue. Every 15th stained section was chosen for quantitative analysis (n = 3 rats per group, five sections per rat). Images of CA1 and CA3 in hippocampal sections were acquired with 90× magnification. Neurons were measured and quantified using ImageJ software.

## Immunohistochemistry

Paraffin sections were used for immunohistochemistry. Serial coronal sections of brain were gained and hippocampal sections were gathered in sequence. Every 15th staining section was chosen for quantitative analysis (five sections per rat). After being dewaxed in xylene, hippocampal sections were hydrated in a graded series of alcohols. Then the sections placed into 0.01 M citrate buffer (pH6.0) were heated for 8 min in microwave oven to complete antigen retrieval, subsequently were blocked for endogenous peroxidases. The treated hippocampal sections were sealed using 3% BSA for 30 min at room temperature, and were then incubated with an anti-α7nAChR antibody (0.5 mg/ml, Abcam, Cat. ab110851, United States ) overnight at 4°C. After washing three times, the sections were incubated with a biotinylated anti-rabbit IgG (1:1,000, Abcam, Cat.150,077, United States ) for 1 h at 37°C and were then developed via DAB reagent. Subsequently, the sections were counterstained with hematoxylin, dehydrated, and mounted on gelatin-coated slides. Images of CA1 and CA3 regions were obtained with 90× magnification. Three fields in one section were chosen for calculating the numbers of positive neurons. Positively-labeled neurons were quantified using ImageJ software.

## Golgi Staining

The brains were removed and fixed in 4% PFA for 48 h, and were then cut into 2-3-mm-thick sections, after which they were immersed in Golgi dye solution for 14 days in a cool and ventilated condition. During this period, Golgi dye solution was changed every 3 days. The brain sections were dehydrated with a gradient sucrose solution in the dark at 4°C for 3 days. Subsequently, the brain sections were developed with strong ammonia water for 45 min and were immersed into acid-hardening fixative for 45 min. The brain sections were dehydrated once again with 30% sucrose in the dark at 4°C for 2–3 days. After embedding in OCT, the brain sections were cut into frozen sections (100 μm thick) and mounted with glycerin gelatin. Images of hippocampal sections were obtained via a digital slice scanner. There is evidence that terminal branches are more plastic than non-terminal branches, so numbers of terminal branches of dendrite were used to evaluated localized dendritic remodeling (Wellman, 2017). Dendritic segments (25 μm in length each) of 10 neurons per animal were selected in the region of the dentate gyrus for counting numbers of dendritic spines. Densities of dendritic spines were expressed as spines per unit length.

## Measurement of Neurotransmitters

Hippocampus tissues were homogenized with ice-cold phosphate-buffered saline and centrifuged at 12,000 rpm for 10 min at 4°C to obtain supernatants. Glutamate and ACh levels were measured using colorimetry according to the manufacturer's instructions (Nanjing Jian Cheng Bioengineering Institute, China). For the determination of glutamate levels, supernatants were catalyzed by glutamate dehydrogenase, which produced α-ketoglutarate and reduced NADH, which have high absorption peaks. Sample absorbance was read at 340 nm. Measurement of ACh was accomplished via the hydroxylamine method. Briefly, supernatants were incubated with hydroxylamine and then reacted to ferric ion, which produced a red-purple complex. The absorbance was measured at 550 nm. The contents of GABA were assessed using commercial ELISA kits according to the manufacturer's instructions (Cloud-Clone Corp, United States ). Briefly, the sample was incubated with Reagent A for 1 h at 37°C. After washing, Reagent B was added and incubated for 30 min at 37°C, after which the sample was developed with substrate

solution. Absorbance was measured at 450 nm using a microplate reader.

### Western Blotting

Hippocampi were separated, homogenized with ice-cold RIPA buffer containing 1% PMSF, and centrifuged at 12,000 g for 10 min at 4°C. The supernatant was collected and the protein concentration was measured using a BCA kit (Beyotime, Shanghai, China). Protein samples (30 μg each) were isolated by 10% SDS-PAGE and transferred to PVDF membranes (Millipore, United States ). After blocking with 5% nonfat milk in Tris-buffered saline containing Tween 20 (TBST) at room temperature for 1 h, membranes were incubated with anti-α7nAChR (1:500, Abcam, Cat.10096, United States), anti-GLT-1 (1:1,000, Invitrogen, Cat.701,988, United States), and anti-SYP (1:1,000, Servicebio, Cat.11553, China) antibodies overnight at 4°C. The membranes were washed three times with TBST and were then subsequently incubated with HRP-conjugated secondary antibodies in TBST at room temperature for 1 h. The membrane was dyed with ECL reagent and developed using autoradiography film. Protein-band intensities were quantified using Quantity One software (Bio-Rad).

### Statistical Analyses

The experimental data were analyzed by GraphPad Prism and are expressed as the mean ± standard error of the mean (SEM). Homogeneity of variances among groups was evaluated using one-way analysis of variance (ANOVA). The Bonferroni method was applied for multiple comparisons of means between two groups. Differences were considered statistically significant at $p < 0.05$.

## DATA AVAILABILITY STATEMENT

The original contributions presented in the study are included in the article/**Supplementary Material**, further inquiries can be directed to the corresponding authors.

## ETHICS STATEMENT

The animal study was reviewed and approved by the Animal Research Committee of Guangzhou Medical University.

## AUTHOR CONTRIBUTIONS

MZ, WL, JZ and TZ conceived and designed the research. JZ, TZ, HL, ZH, JT, JD, XQ, XZ, DQ and XS performed experiments and analysed and interpreted the data. JZ, TZ, SH, WJ and JD performed the statistical analysis. MZ, JZ and TZ wrote the manuscript. MZ and WL supervised the project.

## FUNDING

This work was supported by the Natural Science Project of the Department of Education of Guangdong Province (No. 2019KTSCX138), the Key Project of Science and Technology Program of Guangzhou (No. 201804020023), the National Natural Science Foundation of China (No 81772699, 82073047), the Science and Technology Programs of Guangdong Province (No. 2017B030301009), the Shenzhen Fund for Guangdong Provincial High-level Clinical Key Specialties (No. SZGSP013), the College Student's Science and Technology Innovation Project of Guangzhou Medical University (No. 2019A031), and the College student's Innovation and Entrepreneurship Training Program of Guangdong Province (No. S202010570068, No. S202010570026).

## SUPPLEMENTARY MATERIAL

The Supplementary Material for this article can be found online at: https://www.frontiersin.org/articles/10.3389/fphar.2021.706225/full#supplementary-material

## REFERENCES

Abin-Carriquiry, J. A., Costa, G., Urbanavicius, J., Cassels, B. K., Rebolledo-Fuentes, M., Wonnacott, S., et al. (2008). *In Vivo* modulation of Dopaminergic Nigrostriatal Pathways by Cytisine Derivatives: Implications for Parkinson's Disease. *Eur. J. Pharmacol.* 589, 80–84. doi:10.1016/j.ejphar.2008.05.013

Albrecht, J., and Zielińska, M. (2017). Mechanisms of Excessive Extracellular Glutamate Accumulation in Temporal Lobe Epilepsy. *Neurochem. Res.* 42, 1724–1734. doi:10.1007/s11064-016-2105-8

Asadi-Pooya, A. A., Stewart, G. R., Abrams, D. J., and Sharan, A. (2017). Prevalence and Incidence of Drug-Resistant Mesial Temporal Lobe Epilepsy in the United States. *World Neurosurg.* 99, 662–666. doi:10.1016/j.wneu.2016.12.074

Beani, L., Bianchi, C., Nilsson, L., Nordberg, A., Romanelli, L., and Sivilotti, L. (1985). The Effect of Nicotine and Cytisine on3H-Acetylcholine Release from Cortical Slices of guinea-pig Brain. *Naunyn-schmiedeberg's Arch. Pharmacol.* 331, 293–296. doi:10.1007/bf00634252

Biagioni, F., Gaglione, A., Giorgi, F. S., Bucci, D., Moyanova, S., De Fusco, A., et al. (2019). Degeneration of Cholinergic Basal Forebrain Nuclei after Focally Evoked Status Epilepticus. *Neurobiol. Dis.* 121, 76–94. doi:10.1016/j.nbd.2018.09.019

Bozzi, Y., Casarosa, S., and Caleo, M. (2012). Epilepsy as a Neurodevelopmental Disorder. *Front. Psychiatry* 3, 19. doi:10.3389/fpsyt.2012.00019

Broide, R. S., and Leslie, F. M. (1999). The α7 Nicotinic Acetylcholine Receptor in Neuronal Plasticity. *Mol. Neurobiol.* 20, 1–16. doi:10.1007/bf02741361

Cheng, Q., and Yakel, J. L. (2015). The Effect of α7 Nicotinic Receptor Activation on Glutamatergic Transmission in the hippocampus. *Biochem. Pharmacol.* 97, 439–444. doi:10.1016/j.bcp.2015.07.015

Devinsky, O., Vezzani, A., O'Brien, T. J., Jette, N., Scheffer, I. E., de Curtis, M., et al. (2018). Epilepsy. *Nat. Rev. Dis. Primers.* 4, 18024. doi:10.1038/nrdp.2018.24

Doura, M. B., Gold, A. B., Keller, A. B., and Perry, D. C. (2008). Adult and Periadolescent Rats Differ in Expression of Nicotinic Cholinergic Receptor Subtypes and in the Response of These Subtypes to Chronic Nicotine Exposure. *Brain Res.* 1215, 40–52. doi:10.1016/j.brainres.2008.03.056

Drasdo, A., Caulfield, M., Bertrand, D., Bertrand, S., and Wonnacott, S. (1992). Methyl Lycaconitine: A Novel Nicotinic Antagonist. *Mol. Cell Neurosci.* 3, 237–243. doi:10.1016/1044-7431(92)90043-2

Du, M.-H., Luo, H. M., Hu, S., Lv, Y., Lin, Z. L., and Ma, L. (2013). Electroacupuncture Improves Gut Barrier Dysfunction in Prolonged Hemorrhagic Shock Rats through Vagus Anti-inflammatory Mechanism. *Wjg* 19, 5988–5999. doi:10.3748/wjg.v19.i36.5988

Ferencz, I., Leanza, G., Nanobashvili, A., Kokaia, Z., Kokaia, M., and Lindvall, O. (2001). Septal Cholinergic Neurons Suppress Seizure Development in

Hippocampal Kindling in Rats: Comparison with Noradrenergic Neurons. *Neuroscience* 102, 819–832. doi:10.1016/s0306-4522(00)00499-1

Ferger, B., Spratt, C., Teismann, P., Seitz, G., and Kuschinsky, K. (1998). Effects of Cytisine on Hydroxyl Radicals *In Vitro* and MPTP-Induced Dopamine Depletion *In Vivo*. *Eur. J. Pharmacol.* 360, 155–163. doi:10.1016/s0014-2999(98)00696-7

Fucile, S., Renzi, M., Lax, P., and Eusebi, F. (2003). Fractional Ca 2+ Current through Human Neuronal α7 Nicotinic Acetylcholine Receptors. *Cell Calcium* 34, 205–209. doi:10.1016/s0143-4160(03)00071-x

Gao, Z., Müller, M. H., Karpitschka, M., Mittler, S., Kasparek, M. S., Renz, B., et al. (2010). Role of the Vagus Nerve on the Development of Postoperative Ileus. *Langenbecks Arch. Surg.* 395, 407–411. doi:10.1007/s00423-010-0594-5

Garibotto, V., Wissmeyer, M., Giavri, Z., Goldstein, R., Seimbille, Y., Seeck, M., et al. (2019). Nicotinic Receptor Abnormalities as a Biomarker in Idiopathic Generalized Epilepsy. *Eur. J. Nucl. Med. Mol. Imaging* 46, 385–395. doi:10.1007/s00259-018-4175-0

Ghasemi, M., and Hadipour-Niktarash, A. (2015). Pathologic Role of Neuronal Nicotinic Acetylcholine Receptors in Epileptic Disorders: Implication for Pharmacological Interventions. *Rev. Neurosci.* 26, 199–223. doi:10.1515/revneuro-2014-0044

Gotti, C., Zoli, M., and Clementi, F. (2006). Brain Nicotinic Acetylcholine Receptors: Native Subtypes and Their Relevance. *Trends Pharmacol. Sci.* 27, 482–491. doi:10.1016/j.tips.2006.07.004

Hajek, P., McRobbie, H., and Myers, K. (2013). Efficacy of Cytisine in Helping Smokers Quit: Systematic Review and Meta-Analysis. *Thorax* 68, 1037–1042. doi:10.1136/thoraxjnl-2012-203035

Hamilton, S. E., Loose, M. D., Qi, M., Levey, A. I., Hille, B., McKnight, G. S., et al. (1997). Disruption of the M1 Receptor Gene Ablates Muscarinic Receptor-dependent M Current Regulation and Seizure Activity in Mice. *Proc. Natl. Acad. Sci.* 94, 13311–13316. doi:10.1073/pnas.94.24.13311

Han, J., Wang, D.-S., Liu, S.-B., and Zhao, M.-G. (2016). Cytisine, a Partial Agonist of α4β2 Nicotinic Acetylcholine Receptors, Reduced Unpredictable Chronic Mild Stress-Induced Depression-like Behaviors. *Biomolecules Ther.* 24, 291–297. doi:10.4062/biomolther.2015.113

Janz, P., Hauser, P., Heining, K., Nestel, S., Kirsch, M., Egert, U., et al. (2018). Position- and Time-dependent Arc Expression Links Neuronal Activity to Synaptic Plasticity during Epileptogenesis. *Front Cel Neurosci* 12, 244. doi:10.3389/fncel.2018.00244

Jeong, S. H., Newcombe, D., Sheridan, J., and Tingle, M. (2015). Pharmacokinetics of Cytisine, an α 4 β 2 Nicotinic Receptor Partial Agonist, in Healthy Smokers Following a Single Dose. *Drug Test. Anal.* 7, 475–482. doi:10.1002/dta.1707

Khazipov, R. (2016). GABAergic Synchronization in Epilepsy. *Cold Spring Harb Perspect. Med.* 6, a022764. doi:10.1101/cshperspect.a022764

Kihara, T., Shimohama, S., Urushitani, M., Sawada, H., Kimura, J., Kume, T., et al. (1998). Stimulation of α4β2 Nicotinic Acetylcholine Receptors Inhibits β-amyloid Toxicity. *Brain Res.* 792, 331–334. doi:10.1016/s0006-8993(98)00138-3

Lawrence, J. J. (2008). Cholinergic Control of GABA Release: Emerging Parallels between Neocortex and hippocampus. *Trends Neurosciences* 31, 317–327. doi:10.1016/j.tins.2008.03.008

Leite, J. P., Neder, L., Arisi, G. M., Carlotti, C. G., Jr., Assirati, J. A., and Moreira, J. E. (2005). Plasticity, Synaptic Strength, and Epilepsy: what Can We Learn from Ultrastructural Data? *Epilepsia* 46 (Suppl. 5), 134–141. doi:10.1111/j.1528-1167.2005.01021.x

Li, Y.-J., Yang, Q., Zhang, K., Guo, Y.-Y., Li, X.-B., Yang, L., et al. (2013). Cytisine Confers Neuronal protection against Excitotoxic Injury by Down-Regulating GluN2B-Containing NMDA Receptors. *Neurotoxicology* 34, 219–225. doi:10.1016/j.neuro.2012.09.009

Lillis, K. P., Wang, Z., Mail, M., Zhao, G. Q., Berdichevsky, Y., Bacskai, B., et al. (2015). Evolution of Network Synchronization during Early Epileptogenesis Parallels Synaptic Circuit Alterations. *J. Neurosci.* 35, 9920–9934. doi:10.1523/jneurosci.4007-14.2015

Löscher, W., Potschka, H., Wlaź, P., Danysz, W., and Parsons, C. G. (2003). Are Neuronal Nicotinic Receptors a Target for Antiepileptic Drug Development? Studies in Different Seizure Models in Mice and Rats. *Eur. J. Pharmacol.* 466, 99–111. doi:10.1016/s0014-2999(03)01542-5

Ma, Y., Ramachandran, A., Ford, N., Parada, I., and Prince, D. A. (2013). Remodeling of Dendrites and Spines in theC1qknockout Model of Genetic Epilepsy. *Epilepsia* 54, 1232–1239. doi:10.1111/epi.12195

Madhok, T. C., Matta, S. G., and Sharp, B. M. (1995). Nicotine Regulates Nicotinic Cholinergic Receptors and Subunit rnRNAs in PC 12 Cells through Protein Kinase A. *Mol. Brain Res.* 32, 143–150. doi:10.1016/0169-328x(95)00073-2

Masliah, E., Fagan, A. M., Terry, R. D., DeTeresa, R., Mallory, M., and Gage, F. H. (1991). Reactive Synaptogenesis Assessed by Synaptophysin Immunoreactivity Is Associated with GAP-43 in the Dentate Gyrus of the Adult Rat. *Exp. Neurol.* 113, 131–142. doi:10.1016/0014-4886(91)90169-d

Meller, S., Brandt, C., Theilmann, W., Klein, J., and Löscher, W. (2019). Commonalities and Differences in Extracellular Levels of Hippocampal Acetylcholine and Amino Acid Neurotransmitters during Status Epilepticus and Subsequent Epileptogenesis in Two Rat Models of Temporal Lobe Epilepsy. *Brain Res.* 1712, 109–123. doi:10.1016/j.brainres.2019.01.034

Miledi, R., Molenaar, P. C., and Polak, R. L. (1978). α-Bungarotoxin Enhances Transmitter 'released' at the Neuromuscular junction. *Nature* 272, 641–643. doi:10.1038/272641a0

Mizuno, K., Okada, M., Murakami, T., Kamata, A., Zhu, G., Kawata, Y., et al. (2000). Effects of Carbamazepine on Acetylcholine Release and Metabolism. *Epilepsy Res.* 40, 187–195. doi:10.1016/s0920-1211(00)00129-7

Morioka, N., Tokuhara, M., Nakamura, Y., Idenoshita, Y., Harano, S., Zhang, F. F., et al. (2014). Primary Cultures of Rat Cortical Microglia Treated with Nicotine Increases in the Expression of Excitatory Amino Acid Transporter 1 (GLAST) via the Activation of the α7 Nicotinic Acetylcholine Receptor. *Neuroscience* 258, 374–384. doi:10.1016/j.neuroscience.2013.11.044

Nordberg, A., Romanelli, L., Sundwall, A., Bianchi, C., and Beani, L. (1989). Effect of Acute and Subchronic Nicotine Treatment on Cortical Acetylcholine Release and on Nicotinic Receptors in Rats and guinea-pigs. *Br. J. Pharmacol.* 98, 71–78. doi:10.1111/j.1476-5381.1989.tb16864.x

Paduszynska, A., Banach, M., Rysz, J., Dabrowa, M., Gasiorek, P., and Bielecka-Dabrowa, A. (2018). Cytisine - from the Past to the Future. *Curr. Pharm. Des.* 24, 4413–4423. doi:10.2174/1381612825666181123124733

Picard, F., Bertrand, S., Steinlein, O. K., and Bertrand, D. (1999). Mutated Nicotinic Receptors Responsible for Autosomal Dominant Nocturnal Frontal Lobe Epilepsy Are More Sensitive to Carbamazepine. *Epilepsia* 40, 1198–1209. doi:10.1111/j.1528-1157.1999.tb00848.x

Picciotto, M. R., Higley, M. J., and Mineur, Y. S. (2012). Acetylcholine as a Neuromodulator: Cholinergic Signaling Shapes Nervous System Function and Behavior. *Neuron* 76, 116–129. doi:10.1016/j.neuron.2012.08.036

Pitkanen, A., Lukasiuk, K., Dudek, F. E., and Staley, K. J. (2015). Epileptogenesis. *Cold Spring Harb Perspect. Med.* 5, a022822. doi:10.1101/cshperspect.a022822

Pitkänen, A., and Lukasiuk, K. (2011). Mechanisms of Epileptogenesis and Potential Treatment Targets. *Lancet Neurol.* 10, 173–186. doi:10.1016/s1474-4422(10)70310-0

Plomp, J. J., and Molenaar, P. C. (1996). Involvement of Protein Kinases in the Upregulation of Acetylcholine Release at Endplates of Alpha-Bungarotoxin-Treated Rats. *J. Physiol.* 493 (Pt 1), 175–186. doi:10.1113/jphysiol.1996.sp021373

Plomp, J. J., van Kempen, G. T., and Molenaar, P. C. (1994). The Upregulation of Acetylcholine Release at Endplates of Alpha-Bungarotoxin-Treated Rats: its Dependency on Calcium. *J. Physiol.* 478 (Pt 1), 125–136. doi:10.1113/jphysiol.1994.sp020236

Provini, F., Plazzi, G., Tinuper, P., Vandi, S., Lugaresi, E., and Montagna, P. (1999). Nocturnal Frontal Lobe Epilepsy. A Clinical and Polygraphic Overview of 100 Consecutive Cases. *Brain* 122 (Pt 6), 1017–1031. doi:10.1093/brain/122.6.1017

Qian, X., Wang, Z.-R., Zheng, J.-J., Ding, J.-Q., Zhong, J.-G., Zhang, T.-Y., et al. (2019). Baicalein Improves Cognitive Deficits and hippocampus Impairments in Temporal Lobe Epilepsy Rats. *Brain Res.* 1714, 111–118. doi:10.1016/j.brainres.2019.02.028

Rimmele, T. S., and Rosenberg, P. A. (2016). GLT-1: The Elusive Presynaptic Glutamate Transporter. *Neurochem. Int.* 98, 19–28. doi:10.1016/j.neuint.2016.04.010

Robertson, J., Hatton, C., Emerson, E., and Baines, S. (2015). Mortality in People with Intellectual Disabilities and Epilepsy: A Systematic Review. *Seizure* 29, 123–133. doi:10.1016/j.seizure.2015.04.004

Role, L. W., and Berg, D. K. (1996). Nicotinic Receptors in the Development and Modulation of CNS Synapses. *Neuron* 16, 1077–1085. doi:10.1016/s0896-6273(00)80134-8

Rouden, J., Lasne, M.-C., Blanchet, J., and Baudoux, J. (2014). (−)-Cytisine and Derivatives: Synthesis, Reactivity, and Applications. *Chem. Rev.* 114, 712–778. doi:10.1021/cr400307e

Rozycka, A., Dorszewska, J., Steinborn, B., Kempisty, B., Lianeri, M., Wisniewska, K., et al. (2013). Original Article A Transcript Coding for a Partially Duplicated Form of α7 Nicotinic Acetylcholine Receptor Is Absent from the CD4 + T-Lymphocytes of Patients with Autosomal Dominant Nocturnal Frontal Lobe Epilepsy (ADNFLE). *Folia Neuropathol* 1, 65–75. doi:10.5114/fn.2013.34198

Rozycka, A., Steinborn, B., and Trzeciak, W. H. (2009). The 1674+11C>T Polymorphism of CHRNA4 Is Associated with Juvenile Myoclonic Epilepsy. *Seizure* 18, 601–603. doi:10.1016/j.seizure.2009.06.007

Sharma, N. K., Kaur, S., and Goel, R. K. (2020). Exploring the Ameliorative Role of α7 Neuronal Nicotinic Acetylcholine Receptor Modulation in Epilepsy and Associated Comorbidities in post-PTZ-kindled Mice. *Epilepsy Behav.* 103, 106862. doi:10.1016/j.yebeh.2019.106862

Shen, J.-x., and Yakel, J. L. (2012). Functional α7 Nicotinic ACh Receptors on Astrocytes in Rat Hippocampal CA1 Slices. *J. Mol. Neurosci.* 48, 14–21. doi:10.1007/s12031-012-9719-3

Singh, A., and Trevick, S. (2016). The Epidemiology of Global Epilepsy. *Neurol. Clin.* 34, 837–847. doi:10.1016/j.ncl.2016.06.015

Song, P., Liu, Y., Yu, X., Wu, J., Poon, A. N., Demaio, A., et al. (2017). Prevalence of Epilepsy in China between 1990 and 2015: A Systematic Review and Meta-Analysis. *J. Glob. Health* 7, 020706. doi:10.7189/jogh.07.020706

Thiel, G. (1993). Synapsin I, Synapsin II, and Synaptophysin: Marker Proteins of Synaptic Vesicles. *Brain Pathol.* 3, 87–95. doi:10.1111/j.1750-3639.1993.tb00729.x

Titiz, A. S., Mahoney, J. M., Testorf, M. E., Holmes, G. L., and Scott, R. C. (2014). Cognitive Impairment in Temporal Lobe Epilepsy: Role of Online and Offline Processing of Single Cell Information. *Hippocampus* 24, 1129–1145. doi:10.1002/hipo.22297

Tutka, P., Kondrat-Wróbel, M. W., Zaluska, K., Żółkowska, D., Florek-Łuszczki, M., and Łuszczki, J. J. (2017). Cytisine Inhibits the Protective Activity of Various Classical and Novel Antiepileptic Drugs against 6 Hz-Induced Psychomotor Seizures in Mice. *Psychopharmacology* 234, 281–291. doi:10.1007/s00213-016-4461-0

Tutka, P., Mróz, T., Bednarski, J., Styk, A., Ognik, J., Mosiewicz, J., et al. (2013). Cytisine Inhibits the Anticonvulsant Activity of Phenytoin and Lamotrigine in Mice. *Pharmacol. Rep.* 65, 195–200. doi:10.1016/s1734-1140(13)70978-2

Tutka, P., Vinnikov, D., Courtney, R. J., and Benowitz, N. L. (2019). Cytisine for Nicotine Addiction Treatment: a Review of Pharmacology, Therapeutics and an Update of Clinical Trial Evidence for Smoking Cessation. *Addiction* 114, 1951–1969. doi:10.1111/add.14721

Villa, C., Colombo, G., Meneghini, S., Gotti, C., Moretti, M., Ferini-Strambi, L., et al. (2019). CHRNA2 and Nocturnal Frontal Lobe Epilepsy: Identification and Characterization of a Novel Loss of Function Mutation. *Front. Mol. Neurosci.* 12, 17. doi:10.3389/fnmol.2019.00017

Wang, Y., and Chen, Z. (2019). An Update for Epilepsy Research and Antiepileptic Drug Development: Toward Precise Circuit Therapy. *Pharmacol. Ther.* 201, 77–93. doi:10.1016/j.pharmthera.2019.05.010

Wellman, C. L. (2017). Visualizing Changes in Neuronal Dendritic Morphology in Response to Stress and Pharmacological Challenge. *Curr. Protoc. Neurosci.* 78, 8381–83818. doi:10.1002/cpns.18

Weltzin, M. M., Lindstrom, J. M., Lukas, R. J., and Whiteaker, P. (2016). Distinctive Effects of Nicotinic Receptor Intracellular-Loop Mutations Associated with Nocturnal Frontal Lobe Epilepsy. *Neuropharmacology* 102, 158–173. doi:10.1016/j.neuropharm.2015.11.004

Zhao, P., Yang, J.-M., Wang, Y.-S., Hao, Y.-J., Li, Y.-X., Li, N., et al. (2018). Neuroprotection of Cytisine against Cerebral Ischemia-Reperfusion Injury in Mice by Regulating NR2B-ERK/CREB Signal Pathway. *Neurochem. Res.* 43, 1575–1586. doi:10.1007/s11064-018-2572-1

Zheng, C., Yang, K., Liu, Q., Wang, M.-Y., Shen, J., Vallés, A. S., et al. (2010). The Anticonvulsive Drug Lamotrigine Blocks Neuronal α4β2 Nicotinic Acetylcholine Receptors. *J. Pharmacol. Exp. Ther.* 335, 401–408. doi:10.1124/jpet.110.171108

Zhu, G., Okada, M., Murakami, T., Kawata, Y., Kamata, A., and Kaneko, S. (2002). Interaction between Carbamazepine, Zonisamide and Voltage-Sensitive Ca2+ Channel on Acetylcholine Release in Rat Frontal Cortex. *Epilepsy Res.* 49, 49–60. doi:10.1016/s0920-1211(02)00015-3

**Conflict of Interest:** The authors declare that the research was conducted in the absence of any commercial or financial relationships that could be construed as a potential conflict of interest.

frontiers in Pharmacology

CLINICAL TRIAL
published: 03 August 2021
doi: 10.3389/fphar.2021.721216

# Ginkgo Biloba Extract Is Comparable With Donepezil in Improving Functional Recovery in Alzheimer's Disease: Results From a Multilevel Characterized Study Based on Clinical Features and Resting-State Functional Magnetic Resonance Imaging

*Yu Zheng[1†], Yi Xie[2†], Ming Qi[3†], Ling Zhang[3], Wei Wang[2], Wanrong Zhang[2], Liju Sha[2], Jiawen Wu[2], Wanting Li[2] and Ting Wu[2,4]**

[1]Department of Rehabilitation Medicine, The First Affiliated Hospital of Nanjing Medical University, Nanjing, China, [2]Division of Brain Rehabilitation, Department of Neurology, The First Affiliated Hospital of Nanjing Medical University, Nanjing, China, [3]Departments of Radiology, The First Affiliated Hospital of Nanjing Medical University, Nanjing, China, [4]Department of Neurology, The First Affiliated Hospital of Nanjing Medical University, Nanjing, China

OPEN ACCESS

**Edited by:**
Fang Pan,
Shandong University, China

**Reviewed by:**
Zhongkuan Lyu,
Fudan University, China
Yafei Shi,
Guangzhou Hospital of Traditional Chinese Medicine, China
Xiao-Qing Tang,
University of South China, China

***Correspondence:**
Ting Wu
wuting80000@126.com

[†]These authors contributed equally to this work

**Specialty section:**
This article was submitted to Neuropharmacology, a section of the journal Frontiers in Pharmacology

**Received:** 06 June 2021
**Accepted:** 01 July 2021
**Published:** 03 August 2021

**Citation:**
Zheng Y, Xie Y, Qi M, Zhang L, Wang W, Zhang W, Sha L, Wu J, Li W and Wu T (2021) Ginkgo Biloba Extract Is Comparable With Donepezil in Improving Functional Recovery in Alzheimer's Disease: Results From a Multilevel Characterized Study Based on Clinical Features and Resting-State Functional Magnetic Resonance Imaging. Front. Pharmacol. 12:721216. doi: 10.3389/fphar.2021.721216

**Background:** Ginkgo biloba extract (GBE) and donepezil have been reported to be effective in patients with Alzheimer's disease (AD). Nonetheless, how these drugs impact spontaneous brain activities and how they consequently improve functional recovery are currently unclear.

**Objectives:** This study was to explore the efficacy of GBE vs. donepezil and their add-on efficacy on functional recovery and the adaption of spontaneous brain activities following pharmacologic treatment in patients with AD.

**Methods:** Patients with AD were enrolled and assigned to the GBE group ($n$ = 50), the donepezil group ($n$ = 50), or the combined group ($n$ = 50). Neuropsychological assessments, including minimum mental state examination (MMSE), Alzheimer's disease assessment scale-cognition (ADAS-Cog), instrumental activity of daily living (IADL), geriatric depression scale (GDS), neuropsychiatric inventory (NPI), and quality of life in Alzheimer's disease (QOL-AD), were conducted at baseline, 1 month, 3 months, and 6 months. Resting-state functional magnetic resonance imaging (rs-fMRI) was collected to compare the amplitude of low-frequency fluctuation (ALFF), percent amplitude of fluctuation (PerAF), regional homogeneity (ReHo), and degree centrality (DC) at baseline and 6 months.

**Results:** No major significant differences were detected in all comparisons between groups across all follow-up time points. For intragroup comparison, MMSE and ADAS-Cog scores differed significantly across all follow-ups in three groups. The combined group showed significant improvement of GDS scores between baseline and 6 months ($p$ = 0.007). The GBE group ($p$ = 0.044) and donepezil group ($p$ = 0.012) demonstrated

significant improvement of NPI scores between baseline and 6 months. Significant correlations were observed between IADL and ALFF in the right gyrus rectus ($p$ = 0.03) and in the left superior cerebellum gyrus ($p$ = 0.01), between GDS and ALFF in the right middle temporal gyrus ($p$ = 0.01), between NPI and PerAF in the left fusiform gyrus ($p$ = 0.03), and between MMSE and ReHo in right superior frontal gyrus ($p$ = 0.04).

**Conclusion:** GBE was comparable with donepezil in the improvement of functional recovery in patients with AD while the combined application of GBE and donepezil seems unnecessary. GBE-mediated improvement of functional recovery was characterized by decreased ALFF values in the right gyrus rectus and decreased PerAF values in the left fusiform gyrus. These featured variations of imaging metrics in specific brain regions may serve as biomarkers in the monitoring of the therapeutic efficacy of GBE.

**Keywords: ginkgo biloba extract, donepezil, Alzheimer's disease, resting-state functional magnetic resonance imaging, functional recovery**

## INTRODUCTION

As one of the most prevalent causes of dementia, Alzheimer's disease (AD) is an irreversible neurodegenerative disorder and is characterized by progressive cognitive and intellectual deficits (Reitz et al., 2011). Currently, approximately 47 million people suffer from AD worldwide, and it is expected to increase to more than 130 million by 2050 (Alzheimer's Disease International, 2015). The residual effect of AD may have a devastating personal and financial impact on individuals, families, and society.

Due to the difficulties in participating in physical and psychological interventions, patients with moderate-to-severe AD are more likely to be treated with pharmacologic strategies. Unfortunately, only several pharmacological agents, either preclinical or licensed, are currently available for the treatment of AD (Arvanitakis et al., 2019). The acetylcholinesterase inhibitors (e.g., donepezil) can specifically inhibit the acetylcholinesterase enzyme in the central nervous system, thereby promoting increases in acetylcholine abundance at the synaptic cleft for cholinergic neurotransmission. Based on a recently published Cochrane review, donepezil was proved to be a promising agent that has benefits on cognitive function, activities of daily living, and global impression scales (Birks and Harvey, 2018). Differentiated from acetylcholinesterase inhibitors, the Ginkgo biloba extract (GBE) is hypothesized to act on amyloid $\beta$-induced hippocampal neuron dysfunction and death, amyloid $\beta$ aggregation, and neurogenesis (Bastianetto et al., 2000; Luo et al., 2002; Tchantchou et al., 2007). Recently, GBE has been extensively tested for treating cognitive impairment in patients with AD, while only limited clinical efficacy was demonstrated (Canter and Ernst, 2007; DeKosky et al., 2008; Vellas et al., 2012). Based on this condition, well-designed and executed clinical trials are warranted. Its efficacy needs to be further clarified when comparing its effects with conventional pharmacologic therapy. Furthermore, the question that, whether GBE adds benefit for patients already taking conventional drugs, is hopefully to be answered.

Afterward, the upcoming question is that how these agents interact with the brain. Specifically, it remains unknown whether the local spontaneous brain activities after pharmacologic treatment capture the neural recovery underlying global functional recovery as assessed by standardized measures used in AD clinical practice. The answers may further assist clinicians to understand which agents are effective overall and the relative efficacy of different agents. Therefore, there is an urgent need for sensitive biomarkers to detect a signal of pharmacologic efficacy. A number of major reviews on brain region disruption as assessed with functional magnetic resonance imaging (fMRI) have shown distinct patterns of brain region disruption across the major neurodegenerative diseases (Bozzali et al., 2011; Di Perri et al., 2016; Guo et al., 2016; Yang et al., 2020). It has been achieved consensus that the progression of AD induced symptoms follows a relatively stereotyped order: episodic memory loss occurs first, followed by semantic memory loss, aphasic, apraxic, and visuospatial symptoms, and finally motor and visual deficits (Dubois et al., 2007). The role of fMRI in this aspect is to link the functional impairment to the specific brain region. In a similar way, it can also demonstrate the functional adaption following pharmacologic treatment based on the featured fluctuations of blood oxygen level dependent (BOLD) signaling. With this advanced neurophysiological technique, the impact of pharmacologic treatment on spontaneous brain activities can be investigated noninvasively and then spread to functional recovery.

Based on the above perspectives, the aim of the current trial is 1) to compare the efficacy of GBE vs. donepezil on cognition, behavioral function, psychological function, and quality of life (QoL); 2) to explore the add-on efficacy of GBE with donepezil; and 3) to provide an overview of findings on adaption of spontaneous brain activities following pharmacologic treatment in patients with AD.

## MATERIALS AND METHODS

### Study Design and Participants

This cohort study was a secondary analysis of data collected by an ongoing pragmatic, controlled, three-arm, parallel group,

randomized controlled clinical trial, which was prospectively registered at the Clinical Trial Registry (https://clinicaltrials.gov): NCT03090516, August 5, 2019. The trial protocol was developed according to the Consolidated Standards of Reporting Trials (CONSORT) statements for pragmatic trials and has been reviewed and approved by the Research Ethics Committee at the First Affiliated Hospital of Nanjing Medical University (Reference number: 2016-SR-134). In accordance with the Declaration of Helsinki of 1964 as revised in 2013, the International Conference of Harmonization Guidelines for Good Clinical Practice and the requirement of the local ethics committees, written informed consent was obtained from all enrolled participants.

The target population for this study were those who met the consolidated inclusion criteria: 1) aged 50–85 years and right-handed; 2) diagnosed with AD or MCI according to the NINCDS/ADRDA guidelines (Dubois et al., 2007); 3) CT or MRI performed within 1 year potentially indicating AD or MCI (Planche et al., 2020); 4) MMSE score of 27 or less (Cummings, 1993); 5) able to follow medical instruction or assessment requirement; and 6) signed informed consent. The exclusion criteria were as follows: 1) diagnosed with vascular dementia according to the NINDS-AIREN criteria (Roman et al., 1993); 2) modified Hachinski ischemic score of 4 or more (Rosen et al., 1980); and 3) with major depression, schizophrenia, cerebrovascular diseases, Parkinson's disease, or other systemic and neurodegenerative diseases.

One hundred and fifty eligible patients were enrolled and assigned into: 1) the Ginkgo biloba extract (GBE) group ($n = 50$), orally received 150 mg GBE three times daily for 6 months; 2) the donepezil group ($n = 50$), orally received 5 mg donepezil once daily for 6 months; and 3) the combined group ($n = 50$), orally received both GBE (150 mg three times daily) and donepezil (5 mg once daily) for 6 months.

## Assessments

Baseline demographics and clinical characteristics, collected directly from the patients or the medical documents, are as follows: gender, age, education length, disease subtype, AD/MCI history, family history of AD/MCI; comorbidity, ApoE genotype, modified Hachinski score (MHIS), Hamilton anxiety scale (HAMA) score, and clinical dementia rating (CDR) score (Thompson, 2015; Woolf et al., 2016).

Apart from the above variables, data in terms of minimum mental state examination (MMSE), Alzheimer's disease assessment scale-cognition (ADAS-Cog), instrumental activity of daily living (IADL), geriatric depression scale (GDS), neuropsychiatric inventory (NPI), and quality of life in Alzheimer's disease (QOL-AD) were collected at baseline, 1 month, 3 months, and 6 months. In addition, images and data of resting-state functional magnetic resonance imaging (rs-fMRI) were collected at baseline and 6 months. Detailed information of the above assessments is provided as follows.

## Minimum Mental State Examination

MMSE contains items assessing a wide range of cognitive functions, including orientation to time and place, concentration, language functions (following a three-step command, repeating a difficult phrase, naming high-frequency items, following a written command), construction, verbal learning, and short-delay recall. MMSE ranges from 0 to 30 with a higher score indicating better cognitive function. The cutoffs for AD and MCI are 24 and 27, respectively (Malloy et al., 1997).

## Alzheimer's Disease Assessment Scale-Cognition

ADAS-Cog is consisted of the following 11 items: orientation (0–8), word recall (0–10), word recognition (0–12), commands (0–5), naming objects and fingers (0–5), ideational praxis (0–5), constructional praxis (0–5), ability of remembering (0–5), expressing (0–5), comprehension (0–5), and word finding (0–5). It is scored 0–70, and a higher score indicates poor performance (Doraiswamy et al., 2001).

## Instrumental Activity of Daily Living

IADL contains 14 items of instrumental activity of daily living: laundry, shopping, bathing, brushing hair and teeth, light housework, meals, walking, managing money, managing medications, dressing, transferring, using the phone, toileting, and eating. They are rated as follows: 1: can do, 2: some difficulty but can do, 3: need some help, and 4: cannot do on their own. A higher single score indicates poor ability of daily living, and a total score of higher than 16 indicates different degrees of functional decline (LaPlante, 2010).

## Geriatric Depression Scale

Thirty questions are included in the GDS and answered with yes or no. Positive answers in 20 out of 30 questions indicate presence of depression (e.g., Have you given up many of your activities and interests?), while other 10 questions with negative answers indicate presence of depression (e.g., Are you generally satisfied with your life?). The cumulative score is rated and classified with 0–9 as normal, 10–19 as mildly depressed, and 20–30 as severely depressed (Defrancesco et al., 2018).

## Neuropsychiatric Inventory

NPI is used to assess 12 symptoms reflecting behavioral function including delusions, hallucinations, agitation/aggression, dysphoria, anxiety, euphoria, apathy, disinhibition, irritability/lability, and aberrant motor activity. The absence of symptom is scored as 0. Both the frequency (1: occasionally, 2: often, 3: frequently, and 4: very frequently) and the severity of each symptom (1: mild, 2: moderate, and 3: severe) are rated. A total NPI score is calculated with the frequency*severity as a multiplied score (0–144). A higher score indicates severer psychobehavioral dysfunction and the cut off of 24 or more indicates a clinically significant psychobehavioral dysfunction (Vik-Mo et al., 2020).

## Quality of Life in Alzheimer's Disease

The score of QOL-AD is computed by adding the following 13 items with each item scored 1–4: physical health, energy, mood,

living situation, memory, family, marriage, friends, self as a whole, ability to do chores around the house, ability to do things for fun, money, and life as a whole. It is scored 13–52, and a higher score indicates higher QOL (Logsdon et al., 2002).

## Resting-State Functional Magnetic Resonance Imaging

### Data Acquisition

rs-fMRI data were collected at baseline and 6 months. Scanning was performed on a Siemens Magnetom Trio 3.0T MRI System (Siemens AG, Erlangen, Germany) using a standard birdcage head transmit and receive coil. Functional images were acquired using a single-shot, gradient-recalled echo planar imaging sequence [repetition time (TR) = 2,000 ms; echo time (TE) = 30 ms; flip angle (FA) = 90°]. A total of 33 transverse slices [field of view (FOV) = 256 × 256 $mm^2$; in-plane matrix = 64 × 64; slice thickness = 4 mm; inter-slice gap = 1 mm; voxel size = 4 × 4 × 4 $mm^3$] aligned along the anterior-posterior commissure line. For each patient, a total of 240 volumes were acquired, resulting in a total scan time of 480 s. Patients were instructed to simply rest with their eyes closed. The high-resolution 3D T1-weighted anatomical images were collected in a sagittal orientation using a magnetization-prepared rapid gradient-echo sequence (TR = 1,900 ms; TE = 2.52 ms; FA = 9°; FOV = 256 × 256 $mm^2$; matrix size = 256 × 256; slice thickness = 1 mm; inter-slice gap = 0.5 mm; voxel size = 1 × 1 × 1 $mm^3$; 176 slices).

### Processing

Data processing was based on MATLAB R2014a platform, using DPABI software and SPM12 software to process the scanning data (http://www.fil.ion.ucl.ac.uk/spm/software/spm12) (Chao-Gan and Yu-Feng, 2010). The data analysis toolkit converted the original image in the DICOM format to NIFTI format, and then performed image preprocessing. The detailed preprocessing steps are as follows. The first 10 time points were removed to avoid nonequilibrium effects of magnetization allowing patients to adjust to the scanner noise. Slice timing and correction of head motion were then performed. Twenty-one patients were excluded due to their head movement exceeded 3° rotation or 3 mm translocation in any direction during scanning. The individual structural images were then coregistered to the mean functional image after motion correction by using a linear transformation. The transformed structural images were segmented into gray matter, white matter, and cerebrospinal fluid by using a unified segmentation algorithm. The motion-corrected functional volumes were spatially normalized to Montreal Neurologic Institute space and resampled to 3 mm*3 mm*3 mm voxels by using normalization parameters estimated during unified segmentation. Linear detrending processing was conducted to remove the linear signal drift. The individual-level regression analysis was conducted to minimize the influence of head motion (Friston-24 model) (Friston et al., 1996), whiter matter signal noise, and cerebrospinal fluid signal noise. A band-pass filter (0.01–0.08 Hz) was applied in percent amplitude of fluctuation (PerAF), regional homogeneity (ReHo) and degree centrality (DC) calculation but not in amplitude of low-frequency fluctuation (ALFF).

### Calculation of Amplitude of Low-Frequency Fluctuation, Percent Amplitude of Fluctuation, Regional Homogeneity and Degree Centrality

ALFF was estimated based on Fast Fourier transform (FFT) using DPABI v4.0 (Chao-Gan and Yu-Feng, 2010). Each time course was then converted to frequency domain without band-pass filtering. Then, the square root of the power spectrum at each frequency was averaged across the filtered band (0.01–0.08 Hz). The ALFF of each voxel was then divided by the global mean of ALFF values (mALFF) for standardization.

PerAF of each voxel was estimated with the following equations:

$$PerAF = \frac{1}{n}\sum_{i=1}^{n}\left|\frac{X_i - \mu}{\mu}\right| \times 100\%,$$

$$\mu = \frac{1}{n}\sum_{i=1}^{n} X_i.$$

Here, "$X$" represents the signal intensity of the time point, "$n$" refers to the total number of time points of time course, and "$\mu$" is the mean value of the time course.

With DPABI v4.0, the Kendall's coefficient of concordance (KCC) of time course of every 27 nearest neighboring voxels was calculated to account for ReHo. To reduce the influence of individual variations, ReHo map normalizations were performed by dividing KCC across each voxel with the averaged KCC of the whole brain.

DC represents the sum of weights that shows node strength with a given voxel in weighted graphs. For each voxel, the BOLD time course was extracted, and the Pearson correlation coefficients with every other voxel in the brain were calculated. A matrix of Pearson correlation coefficients between a given voxel and all other voxels was generated to show the whole-brain functional connectivity matrix for each voxel. An undirected adjacency matrix was then generated by setting a threshold to each correlation at an $r$ value more than 0.25 (Buckner et al., 2009; Wang et al., 2018; Wang et al., 2020). DC is defined as the sum of weights (r-values) of significant functional connections ($r > 0.25$) for each voxel. The DC value of each voxel was divided by the global mean of the DC values for standardization.

The standardized ALFF, PerAF and ReHo maps, and DC matrices were smoothed with Gaussian kernel (full width at half maximum FWHM = 6 mm).

## Statistical Analysis

Analyses for clinical data were performed using SPSS 20.0 (IBM Corporation, United States). Descriptive statistics (mean, standard deviation, and proportion) were utilized to demonstrate the distribution of the results with respect to statistical quantitative features. After testing the normality, the demographic data of the two experimental groups were compared with independent samples $t$-test and chi-square test. For the intergroup comparison, the continuous data, including MMSE, ADAS-Cog, IADL, GDS, NPI, and QOL-AD, were compared with repeated one-way ANOVA. For the intragroup comparison, repeated one-way ANOVA was applied for the comparison of

**TABLE 1 |** Clinical characteristics of the sample.

| | GBE group ($n$ = 50) | Donepezil group ($n$ = 50) | Combined group ($n$ = 50) | $p$ value |
|---|---|---|---|---|
| Male, % | 19 (38) | 21 (42) | 18 (36) | 0.821 |
| Age, mean (SD) | 71.06 (7.65) | 71.34 (8.23) | 70.98 (6.71) | 0.969 |
| Education length in year, mean (SD) | 12.92 (2.59) | 12.39 (3.00) | 12.58 (3.05) | 0.650 |
| Disease stage (MCI/AD), % | 24/26 | 16/34 | 17/33 | 0.199 |
| Disease duration in year, mean (SD) | 2.39 (1.71) | 2.31 (1.68) | 2.57 (1.66) | 0.746 |
| Family history of AD, % | 11 (22) | 10 (20) | 14 (28) | 0.616 |
| Complications, % | | | | |
| Stroke or TIA history | 8 (16) | 5 (10) | 6 (12) | 0.656 |
| Hypertension | 9 (18) | 17 (34) | 9 (18) | 0.092 |
| Diabetes | 3 (6) | 8 (16) | 3 (6) | 0.140 |
| Coronary atherosclerosis | 1 (2) | 2 (4) | 2 (4) | 0.813 |
| Hypothyroidism | 0 (0) | 1 (2) | 1 (2) | 0.602 |
| Asthma | 0 (0) | 2 (4) | 0 (0) | 0.132 |
| APOE ε4+, % | 6 (25) | 3 (19) | 5 (21) | 0.898 |
| MHIS, mean (SD) | 0.96 (0.81) | 0.78 (0.71) | 0.86 (0.83) | 0.518 |
| HAMA, mean (SD) | 2.48 (2.60) | 1.72 (2.12) | 2.00 (1.99) | 0.237 |
| CDR, mean (SD) | 1.08 (0.27) | 1.24 (0.43) | 1.22 (0.42) | 0.077 |

*GBE: Ginkgo biloba extract; SD: standard deviation; MHIS: modified Hachinski score; MCI: mild cognitive impaired; AD: Alzheimer's disease; TIA: transient ischemic attacks; HAMA: Hamilton anxiety scale; CDR: clinical dementia rating.*

differences between individual time points (baseline vs. 1 month, baseline vs. 3 months and baseline vs. 6 months). Post-hoc tests were conducted with the Bonferroni method. The statistical significance was determined with adjusted $p$ value less than 0.05.

To examine differences of ALFF, PerAF, ReHo, and DC between baseline and 6 months, paired $t$-test was conducted using DPABI v4.0. To reduce the impact of confounding variables in the analysis, we performed paired $t$-tests with the mean framewise displacement as covariates (Jenkinson et al., 2002). Multiple comparison correction was performed based on the Gaussian random field theory (GRF, voxel-wise $p < 0.005$, cluster-wise $p < 0.05$, and two-tailed). For any measure (ALFF, PerAF, ReHo, or DC) showing post-intervention alterations, the Pearson correlation was used to predict associations between the value changes of the sphere, the peak coordinate of the significant discriminative cluster with a radius of 6 mm, with clinical neuropsychological changes. The correlations were considered significant at a threshold of $p < 0.05$.

# RESULTS

## Sample Characteristics

A total of 191 patients were enrolled while 41 of them were excluded according to the results of eligibility assessment. Therefore, a total of 150 eligible patients participated the current study and received several follow-up assessments. Demographic and clinical characteristics of the sample were presented in **Table 1**. No significant differences were detected in all variables across three groups. Based on the results of quality check, 20 cases from the GBE group, 17 cases from the donepezil group, and 20 cases from the combined group provided sufficiently qualified fMRI data for further multi-model analysis. The study logistics of recruitment, assignment, intervention, and assessment were demonstrated in **Figure 1**.

## Changes of Neuropsychological Function Following Pharmacologic Treatment

**Table 2** shows the intergroup comparison across baseline, 1 month, 3 months, and 6 months. Unfortunately, no significant differences were detected in all comparisons between groups across all follow-up time points except MMSE between the GBE group and donepezil group at 1 month ($p$ = 0.019). For the intragroup comparison, MMSE and ADAS-Cog scores differed significantly in all three groups. Compared to the status at baseline, a gradual improvement of cognitive function was observed as time went by (**Tables 3**–**5**). IADL and QOL-AD scores changed marginally across four visits in all three groups although occasional significant differences were presented between baseline and 3-month evaluation of IADL in the GBE group and combined group (**Tables 3**, **5**), and between baseline and 3-month evaluation of QOL-AD in the combined group (**Table 5**). Regarding the comparison of GDS scores between baseline and 6 months, only the combined group showed a significant difference ($p$ = 0.007, **Table 5**). In addition, the GBE group ($p$ = 0.044) and donepezil group ($p$ = 0.012) demonstrated significant improvement between baseline and 6-month evaluation in terms of NPI scores (**Tables 3**, **4**).

## Changes of Local Spontaneous Brain Activity Following Pharmacologic Treatment

As shown in **Figure 2**; **Table 6**, significant discriminative brain regions, reflected by changes of four metrics, including ALFF, PerAF, ReHo, and DC before and after treatment, were presented according to different treatment strategies.

Patients in the GBE group showed a significant decrease of ALFF in the left parahippocampal gyrus, left fusiform gyrus, right gyrus rectus, and right superior frontal gyrus while an increase of ALFF in the right middle temporal gyrus. As compared to the

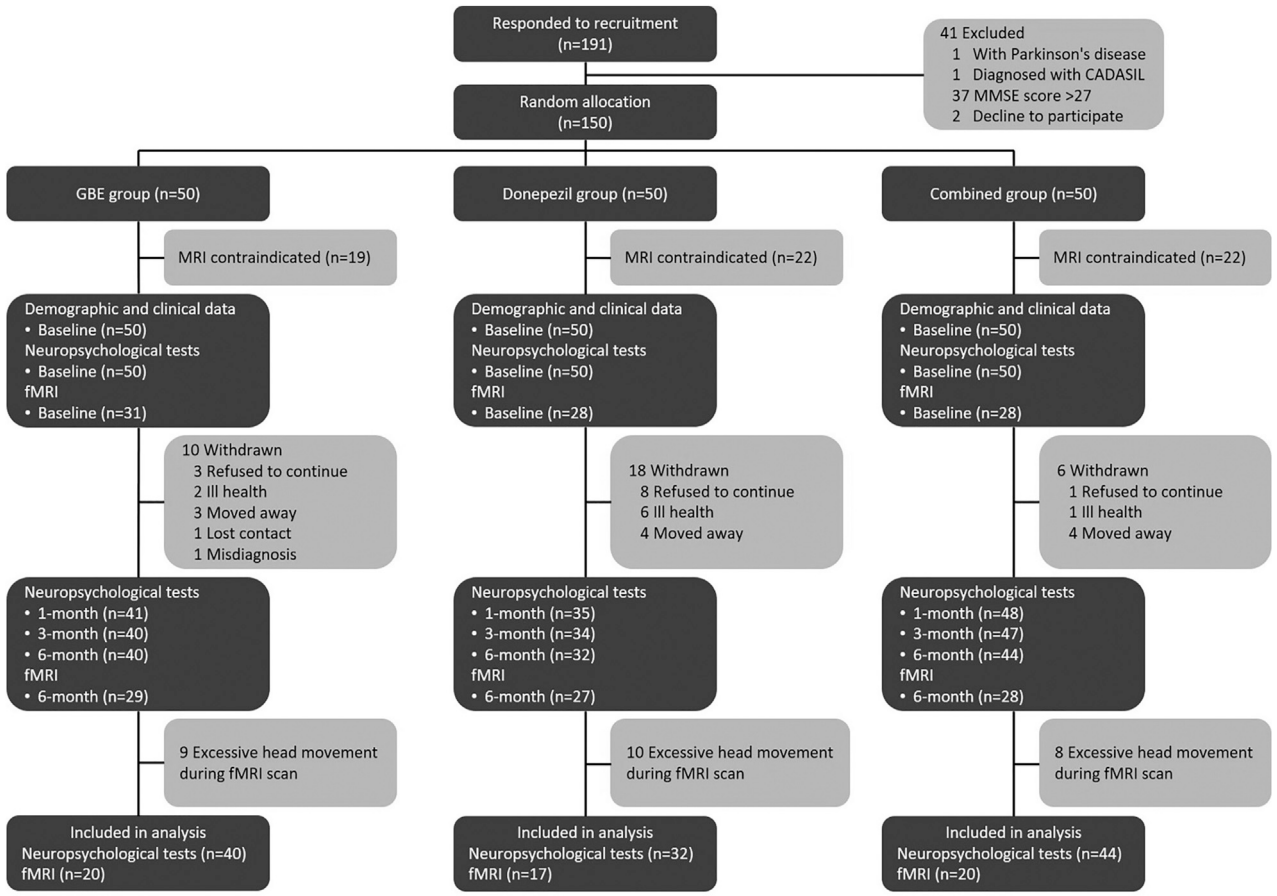


**FIGURE 1 |** Study logistics of recruitment, assignment, intervention, and assessment. CADASIL: cerebral autosomal dominant with subcortical infarcts and leukoencephalopathy; MMSE: minimum mental state examination; GBE: Ginkgo biloba extract; MRI: magnetic resonance imaging; fMRI: functional magnetic resonance imaging.

GBE group, the discriminative brain regions in the donepezil group were quite different including the right inferior cerebellum gyrus, left superior cerebellum gyrus, right middle frontal gyrus, right caudate nucleus, and right lenticular nucleus. The combined group also showed significant changes in right anterior cingulate and paracingulate gyri. Interestingly, the three groups shared one same significantly discriminative brain regions, the right superior frontal gyrus.

In terms of PerAF, several brain regions in the GBE group showed significant discriminative including the left inferior and superior cerebellum gyrus, left inferior temporal gyrus, left fusiform gyrus, right gyrus rectus, right superior frontal gyrus, left inferior frontal gyrus, right precental gyrus, and right middle frontal gyrus. In addition, brain regions, including the bilateral inferior cerebellum gyrus, left inferior frontal gyrus, left superior frontal gyrus in the donepezil group and inferior and middle temporal gyrus in the combined group, showed a significant increase of PerAF values.

Due to the sensitivity issue, sufficiently changed signaling was only observed in the GBE group and the combined group for both ReHo and DC. A significantly increased ReHo signaling was detected in the right superior frontal gyrus and right supplementary motor area in the GBE group and the left inferior and superior cerebellum gyrus in the combined group. However, a decreased signaling was detected in the bilateral anterior cingulate and paracingulate gyri in the combined group. Furthermore, significant DC changes were presented in the left cuneus in the GBE group and left inferior and superior cerebellum gyrus in the combined group.

## Correlations Between Changes of Neuropsychological Function and Functional Magnetic Resonance Imaging Metrics

**Figure 3** and **Supplementary Tables S1–S4** show the correlations between changes of neuropsychological function and fMRI metrics. Significant positive correlations were observed between IADL changes and ALFF changes in the right gyrus rectus in the GBE group ($p$ = 0.03) and negative in the left superior cerebellum gyrus in the donepezil group ($p$ = 0.01).

**TABLE 2 |** Intergroup outcome comparison across four visits.

| | GBE group (I) | | Donepezil group (II) | | Combined group (III) | | *p* value† | | |
|---|---|---|---|---|---|---|---|---|---|
| | Mean | SD | Mean | SD | Mean | SD | I vs. II | I vs. III | II vs. III |
| Baseline | | | | | | | | | |
| MMSE | 23.72 | 2.86 | 22.32 | 3.40 | 22.10 | 4.35 | 0.159 | 0.077 | 1.000 |
| ADAS-Cog | 17.65 | 8.00 | 21.05 | 8.57 | 21.99 | 10.90 | 0.213 | 0.066 | 1.000 |
| IADL | 15.16 | 2.68 | 15.44 | 1.77 | 16.08 | 3.58 | 1.000 | 0.300 | 0.754 |
| GDS | 5.43 | 5.64 | 4.42 | 4.76 | 5.58 | 5.49 | 1.000 | 1.000 | 0.829 |
| NPI | 2.34 | 5.77 | 1.44 | 2.93 | 1.82 | 8.32 | 1.000 | 1.000 | 1.000 |
| QOL-AD | 31.06 | 6.85 | 32.90 | 6.05 | 33.14 | 6.85 | 0.502 | 0.357 | 1.000 |
| 1 month | | | | | | | | | |
| MMSE | 26.20 | 2.65 | 23.54 | 4.45 | 24.16 | 4.87 | 0.019* | 0.066 | 1.000 |
| ADAS-Cog | 14.41 | 6.13 | 19.19 | 9.44 | 18.13 | 11.04 | 0.078 | 0.177 | 1.000 |
| IADL | 14.83 | 1.88 | 15.63 | 1.96 | 16.69 | 3.09 | 0.475 | 0.293 | 1.000 |
| GDS | 3.10 | 3.13 | 3.69 | 3.50 | 3.86 | 3.81 | 1.000 | 0.927 | 1.000 |
| NPI | 0.78 | 2.23 | 0.37 | 1.03 | 0.82 | 2.73 | 1.000 | 1.000 | 1.000 |
| QOL-AD | 32.32 | 6.49 | 31.60 | 5.25 | 33.63 | 5.48 | 1.000 | 0.851 | 0.342 |
| 3 months | | | | | | | | | |
| MMSE | 26.43 | 2.68 | 24.00 | 4.75 | 24.31 | 5.24 | 0.060 | 0.082 | 1.000 |
| ADAS-Cog | 12.73 | 6.05 | 17.07 | 9.73 | 17.16 | 11.37 | 0.153 | 0.091 | 1.000 |
| IADL | 14.63 | 1.56 | 15.32 | 1.98 | 15.65 | 3.21 | 0.668 | 0.160 | 1.000 |
| GDS | 3.40 | 4.58 | 4.29 | 5.17 | 3.33 | 3.60 | 1.000 | 1.000 | 0.997 |
| NPI | 0.83 | 2.25 | 0.47 | 1.85 | 1.16 | 3.24 | 1.000 | 1.000 | 0.703 |
| QOL-AD | 32.43 | 6.49 | 32.50 | 6.12 | 34.60 | 5.82 | 1.000 | 0.298 | 0.384 |
| 6 months | | | | | | | | | |
| MMSE | 26.71 | 2.46 | 23.85 | 4.86 | 24.70 | 5.25 | 0.972 | 0.943 | 0.962 |
| ADAS-Cog | 12.31 | 5.43 | 16.36 | 9.09 | 16.54 | 10.76 | 0.119 | 0.081 | 1.000 |
| IADL | 14.64 | 1.82 | 15.26 | 2.22 | 15.50 | 2.89 | 0.737 | 0.286 | 1.000 |
| GDS | 4.20 | 5.32 | 4.67 | 5.65 | 3.43 | 5.00 | 1.000 | 1.000 | 0.795 |
| NPI | 0.52 | 1.52 | 0.21 | 0.77 | 0.52 | 1.56 | 0.870 | 1.000 | 0.859 |
| QOL-AD | 32.38 | 6.62 | 33.51 | 6.50 | 33.91 | 6.29 | 1.000 | 0.827 | 1.000 |

*GBE: Ginkgo biloba extract; SD: standard deviation; MMSE: minimum mental state examination; ADAS-Cog: Alzheimer's disease assessment scale-cognition; IADL: instrumental activity of daily living; GDS: geriatric depression scale; NPI: neuropsychiatric inventory; QOL-AD: quality of life in Alzheimer's disease. †: Bonferroni pairwise comparison. *p < 0.05.*

**TABLE 3 |** Intragroup outcome comparison in the GBE group.

| | Baseline | | 1 month | | 3 months | | 6 months | | *p* value | | |
|---|---|---|---|---|---|---|---|---|---|---|---|
| | Mean | SD | Mean | SD | Mean | SD | Mean | SD | 1 m vs. BL | 3 m vs. BL | 6 m vs. BL |
| MMSE | 23.72 | 2.86 | 26.20 | 2.65 | 26.43 | 2.68 | 26.71 | 2.46 | <0.001* | <0.001* | <0.001* |
| ADAS-Cog | 17.65 | 8.00 | 14.41 | 6.13 | 12.73 | 6.05 | 12.31 | 5.43 | <0.001* | <0.001* | <0.001* |
| IADL | 15.16 | 2.68 | 14.83 | 1.88 | 14.63 | 1.56 | 14.64 | 1.82 | 0.181 | 0.017* | 0.194 |
| GDS | 5.43 | 5.64 | 3.10 | 3.13 | 3.40 | 4.58 | 4.20 | 5.32 | 0.001* | 0.007* | 0.184 |
| NPI | 2.34 | 5.77 | 0.78 | 2.23 | 0.83 | 2.25 | 0.52 | 1.52 | 0.056 | 0.057 | 0.044* |
| QOL-AD | 31.06 | 6.85 | 32.32 | 6.49 | 32.43 | 6.49 | 32.38 | 6.62 | 0.197 | 0.105 | 0.138 |

*GBE: Ginkgo biloba extract; SD: standard deviation; BL: baseline; 1 m: 1 month; 3 m: 3 months; 6 m: 6 months; MMSE: minimum mental state examination; ADAS-Cog: Alzheimer's disease assessment scale-cognition; IADL: instrumental activity of daily living; GDS: geriatric depression scale; NPI: neuropsychiatric inventory; QOL-AD: quality of life in Alzheimer's disease. *p < 0.05.*

However, GDS changes was negatively correlated with ALFF changes in right middle temporal gyrus in the GBE group ($p$ = 0.01). A negative correlation between NPI changes and PerAF changes in the left fusiform gyrus in the GBE group was also detected ($p$ = 0.03). In addition, MMSE changes correlated negatively with ReHo changes in the right superior frontal gyrus in the GBE group ($p$ = 0.04). Unfortunately, no significant correlation was found between DC changes and any neuropsychological function assessments.

## DISCUSSION

Our results demonstrated that GBE was not superior to donepezil in terms of efficacy on AD patients' functional recovery reflected with MMSE, ADAS-Cog, IADL, GDS, NPI, and QOL-AD across all three follow-ups. We also failed to demonstrate the superimposed efficacy when provided AD patients with both GBE and donepezil. Nonetheless, longitudinal improvement of functional impairment was observed in all three groups.

**TABLE 4 |** Intragroup comparison of clinical scales in the donepezil group.

| | Baseline | | 1 month | | 3 months | | 6 months | | *p* value | | |
|---|---|---|---|---|---|---|---|---|---|---|---|
| | Mean | SD | Mean | SD | Mean | SD | Mean | SD | 1 m vs. BL | 3 m vs. BL | 6 m vs. BL |
| MMSE | 22.32 | 3.40 | 23.54 | 4.45 | 24.00 | 4.75 | 23.85 | 4.86 | 0.007* | <0.001* | 0.002* |
| ADAS-Cog | 21.05 | 8.57 | 19.19 | 9.44 | 17.07 | 9.73 | 16.36 | 9.09 | 0.001* | <0.001* | <0.001* |
| IADL | 15.44 | 1.77 | 15.63 | 1.96 | 15.32 | 1.98 | 15.26 | 2.22 | 0.360 | 0.099 | 0.539 |
| GDS | 4.42 | 4.76 | 3.69 | 3.50 | 4.29 | 5.17 | 4.67 | 5.65 | 0.048* | 0.611 | 0.795 |
| NPI | 1.44 | 2.93 | 0.37 | 1.03 | 0.47 | 1.85 | 0.21 | 0.77 | 0.041 | 0.141 | 0.012* |
| QOL-AD | 32.90 | 6.05 | 31.60 | 5.25 | 32.50 | 6.12 | 33.51 | 6.50 | 0.720 | 0.532 | 0.413 |

*SD: standard deviation; BL: baseline; 1 m: 1 month; 3 m: 3 months; 6 m: 6 months; MMSE: minimum mental state examination; ADAS-Cog: Alzheimer's disease assessment scale-cognition; IADL: instrumental activity of daily living; GDS: geriatric depression scale; NPI: neuropsychiatric inventory; QOL-AD: quality of life in Alzheimer's disease.* *p < 0.05.

**TABLE 5 |** Intragroup comparison of clinical scales in the combined group.

| | Baseline | | 1 month | | 3 months | | 6 months | | *p* value | | |
|---|---|---|---|---|---|---|---|---|---|---|---|
| | Mean | SD | Mean | SD | Mean | SD | Mean | SD | 1 m vs. BL | 3 m vs. BL | 6 m vs. BL |
| MMSE | 22.10 | 4.35 | 24.16 | 4.87 | 24.31 | 5.24 | 24.70 | 5.25 | <0.001* | <0.001* | <0.001* |
| ADAS-Cog | 21.99 | 10.90 | 18.13 | 11.04 | 17.16 | 11.37 | 16.54 | 10.76 | <0.001* | <0.001* | <0.001* |
| IADL | 16.08 | 3.58 | 15.69 | 3.09 | 15.65 | 3.21 | 15.50 | 2.89 | 0.098 | 0.041* | 0.223 |
| GDS | 5.58 | 5.49 | 3.86 | 3.91 | 3.33 | 3.60 | 3.43 | 4.01 | 0.002* | <0.001* | 0.007* |
| NPI | 1.82 | 8.32 | 0.82 | 2.73 | 1.17 | 3.24 | 0.52 | 1.56 | 0.291 | 0.441 | 0.328 |
| QOL-AD | 33.14 | 6.85 | 33.63 | 5.48 | 34.60 | 5.82 | 33.91 | 6.29 | 0.413 | 0.022* | 0.226 |

*SD: standard deviation; BL: baseline; 1 m: 1 month; 3 m: 3 months; 6 m: 6 months; MMSE: minimum mental state examination; ADAS-Cog: Alzheimer's disease assessment scale-cognition; IADL: instrumental activity of daily living; GDS: geriatric depression scale; NPI: neuropsychiatric inventory; QOL-AD: quality of life in Alzheimer's disease.* *p < 0.05.

Specifically, MMSE and ADAS-Cog scores increased significantly while only marginal changes were detected for IADL and QOL-AD scores. A baseline and 6-month comparison revealed a significant increase of GDS scores only in those receiving both GBE and donepezil while improvement of NPI scores were observed in patients treated with GBE or donepezil. The potential longitudinal impacts on specific adaption of the brain launched by these agents were further explored with rs-fMRI scanning and the spontaneous brain activities responded to the treatment was evaluated with four amplitude methods including ALFF, PerAF, ReHo, and DC. In addition to the adaptive changes in specific brain regions, several significant correlations should be emphasized including 1) positive correlations between IADL and ALFF changes in the right precentral gyrus right gyrus rectus in the GBE group and negative in the left superior cerebellum gyrus in the donepezil group; 2) negative correlation between GDS and ALFF changes in the right middle temporal gyrus in the GBE group; 3) negative correlation between NPI and PerAF changes in the left fusiform gyrus in the GBE group; and 4) negative correlations between MMSE and ReHo changes in the right superior frontal gyrus in the GBE group.

In the current study, we examined cognitive, behavioral, psychological, and global outcomes across three different pharmacologic strategies. As the second-generation acetylcholinesterase inhibitors, donepezil has been licensed for use in more than 90 countries after the completion of large multicenter studies (Cacabelos, 2007). Dose-dependent trials reported that a higher dose (10 mg/day) of donepezil was effective to show certain improvement of cognitive function, however benefits on a higher dose were only marginally larger than that on a lower dose (5 mg/day) in terms of ADL and clinician-related global impression (Homma et al., 2008). In addition, patients treated with a higher dose were more likely to experience adverse events or to withdraw from the trial (Birks and Harvey, 2018). For these reasons, we adopted the lower dose with which the efficacy was compared with GBE on multiple outcomes. As a preclinical drug for AD, GBE is still in the development phase and substantial efforts have been taken to verify its efficacy. Unfortunately, two randomized, double-blind, placebo-controlled trials failed to show adequate efficacy (Schneider et al., 2005; McCarney et al., 2008). The Cochrane review summarized that the evidence was not sufficient to support its benefits on cognitive impairment (Birks and Grimley Evans, 2009). Nonetheless, the current study showed non-inferiority results of GBE vs. donepezil across all comparisons at each follow-up. In addition to QoL, the longitudinal analysis also showed promising results supporting the efficacy of GBE. Taken together, GBE might be anticipated to present superimposed efficacy with the use of donepezil. However, the combined group showed no significant improvement according to the results of multiple comparisons. Therefore, the combined application of GBE and donepezil seems to be unnecessary. Our attention was then shifted to the observed discrepancies of multiple outcomes between GBE vs. donepezil. The upcoming challenge becomes the clinical selection of these two drugs with which different brain regions may be impacted and then spread into improvement of specific functional recovery.

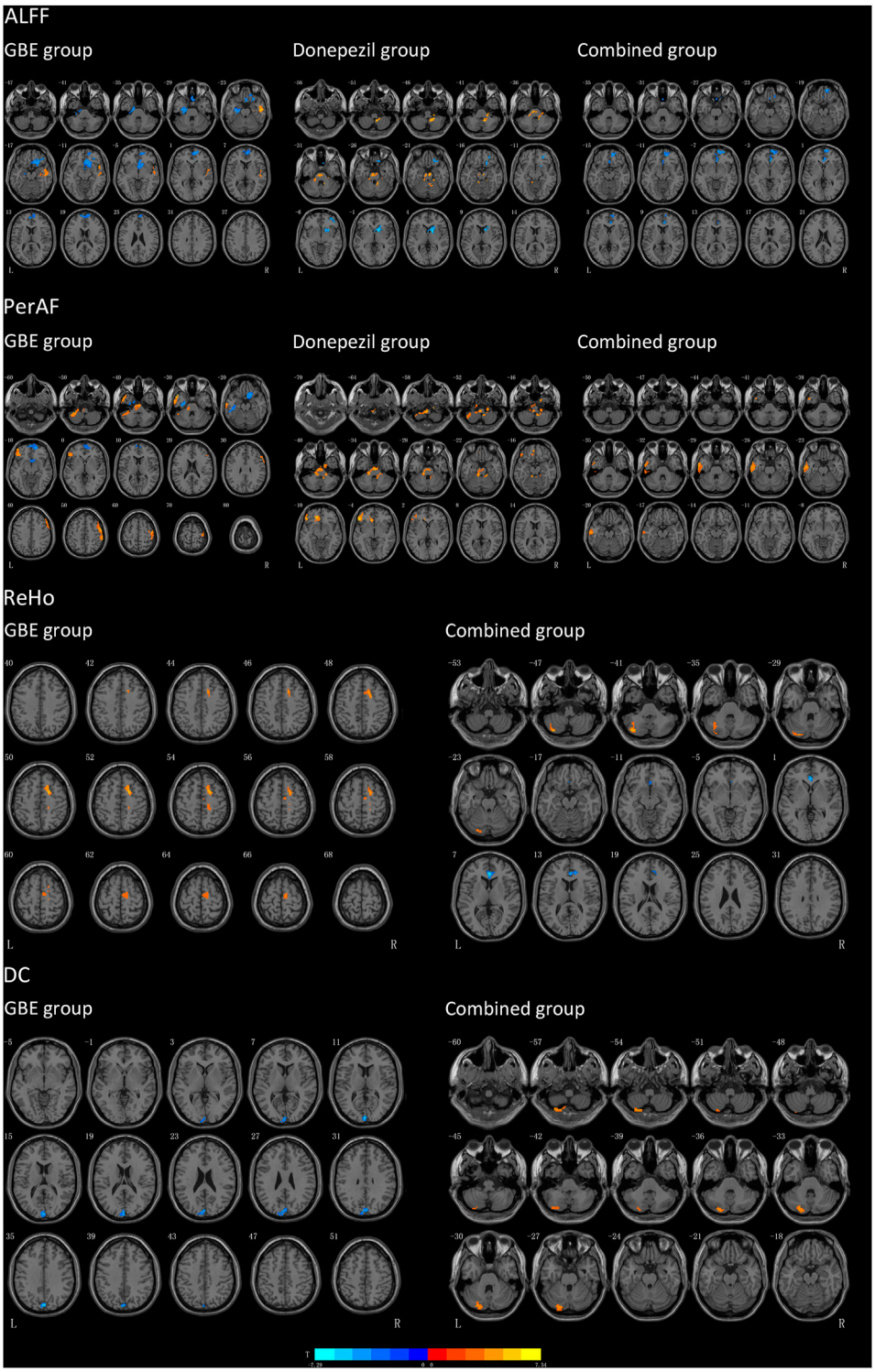


**FIGURE 2 |** Results of brain regions demonstrate significant differences in three groups pre-and post-intervention. The pseudo-color map revealed increases in ALFF, PerAF, ReHo and DC following the intervention. Results are displayed at $p < 0.005$ corrected by GRF. T value obtained from paired *t*-test of the group. GBE: Ginkgo biloba extract; ALFF: amplitude of low-frequency fluctuation; PerAF: percent amplitude of fluctuation; DC: degree centrality; ReHo: reginal homogeneity; R: right; L: left.

**TABLE 6 |** Brain regions with significant different values of ALFF, PerAF, ReHo, and DC of three groups before and after pharmacologic treatment.

| | Clusters | MNI coordinates | | | Brain regions | Voxels | T values |
|---|---|---|---|---|---|---|---|
| | | X | Y | Z | | | |
| ALFF | GBE group | | | | | | |
| | Cluster 1 | −24 | −18 | −27 | Parahippocampal gyrus (L) | 55 | −5.03 |
| | | — | | | Fusiform gyrus (L) | 55 | −5.03 |
| | Cluster 2 | 3 | 18 | −27 | Gyrus rectus (R) | 69 | −4.75 |
| | Cluster 3 | 54 | −15 | −24 | Middle temporal gyrus (R) | 63 | 6.22 |
| | Cluster 4 | 9 | 54 | 3 | Superior frontal gyrus, medial (R) | 136 | −4.60 |
| | Donepezil group | | | | | | |
| | Cluster 1 | 18 | −45 | −45 | Inferior cerebellum gyrus (R) | 78 | 7.08 |
| | Cluster 2 | −21 | −33 | −33 | Superior cerebellum gyrus (L) | 22 | 5.93 |
| | Cluster 3 | 9 | 21 | −33 | Superior frontal gyrus, orbital part (R) | 42 | -4.46 |
| | | — | | | Middle frontal gyrus, orbital part (R) | 38 | −4.46 |
| | Cluster 4 | 15 | 9 | 3 | Caudate nucleus (R) | 77 | −6.24 |
| | | — | | | Lenticular nucleus, putamen (R) | 36 | −6.24 |
| | Combined group | | | | | | |
| | Cluster 1 | 3 | 33 | −3 | Anterior cingulate and paracingulate gyri (R) | 47 | −5.3 |
| | Cluster 2 | 9 | 51 | −21 | Superior frontal gyrus, orbital part (R) | 73 | −5.19 |
| PerAF | GBE group | | | | | | |
| | Cluster 1 | −33 | −42 | −45 | Inferior cerebellum gyrus (L) | 100 | 5.36 |
| | | — | | | Superior cerebellum gyrus (L) | 57 | 5.36 |
| | Cluster 2 | 6 | −15 | −36 | Superior cerebellum gyrus (L) | 1 | 5.11 |
| | Cluster 3 | −51 | 12 | −33 | Inferior temporal gyrus (L) | 69 | 5.42 |
| | Cluster 4 | −27 | −12 | −30 | Fusiform gyrus (L) | 66 | −4.74 |
| | Cluster 5 | 12 | 18 | −18 | Gyrus rectus (R) | 45 | −4.8 |
| | Cluster 6 | 15 | 57 | −12 | Superior frontal gyrus, medial orbital (R) | 69 | −4.23 |
| | Cluster 7 | −45 | 30 | −3 | Inferior frontal gyrus, orbital part (L) | 97 | 5.14 |
| | Cluster 8 | 54 | −3 | 51 | Precental gyrus (R) | 147 | 5.75 |
| | | — | | | Middle frontal gyrus (R) | 101 | 5.75 |
| | Donepezil group | | | | | | |
| | Cluster 1 | −12 | −33 | −24 | Inferior cerebellum gyrus (L) | 42 | 5.67 |
| | Cluster 2 | 21 | −30 | −54 | Inferior cerebellum gyrus (R) | 50 | 5.45 |
| | Cluster 3 | −48 | 33 | −3 | Inferior frontal gyrus, orbital part (L) | 87 | 7.54 |
| | | — | | | Inferior frontal gyrus, triangular part (L) | 40 | 7.54 |
| | Cluster 4 | −15 | 39 | −9 | Superior frontal gyrus, medial orbital (L) | 37 | 5.98 |
| | Combined group | | | | | | |
| | Cluster 1 | −57 | −6 | −27 | Inferior temporal gyrus (L) | 100 | 4.64 |
| | | — | | | Middle temporal gyrus (L) | 74 | 4.64 |
| ReHo | GBE group | | | | | | |
| | Cluster 1 | 21 | 3 | 51 | Superior frontal gyrus, dorsolateral (R) | 69 | 5.63 |
| | | — | | | Supplementary motor area (R) | 51 | 5.63 |
| | Combined group | | | | | | |
| | Cluster 1 | −39 | −75 | −42 | Inferior cerebellum gyrus (L) | 87 | 5.45 |
| | | | | | Superior cerebellum gyrus (L) | 43 | 5.45 |
| | Cluster 2 | 3 | 36 | 6 | Anterior cingulate and paracingulate gyri (R) | 53 | −7.29 |
| | | — | | | Anterior cingulate and paracingulate gyri (L) | 28 | −7.29 |
| DC | GBE group | | | | | | |
| | Cluster 1 | 0 | −81 | 36 | Cuneus (L) | 104 | −6.11 |
| | Combined group | | | | | | |
| | Cluster 1 | −30 | −75 | −54 | Inferior cerebellum gyrus (L) | 54 | 5.33 |
| | | — | | | Superior cerebellum gyrus (L) | 35 | 5.33 |

*GBE: Ginkgo biloba extract; ALFF: amplitude of low frequency fluctuation; PerAF: percent amplitude of fluctuation; ReHo: reginal homogeneity; DC: degree centrality; MNI: Montreal Neurological Institute; L: left, R: right.*

The gyrus rectus is located at the medial margin of the inferior surface of the frontal lobe and is associated with memory and behavioral function (Joo et al., 2016; Destrieux et al., 2017). Impaired gyrus rectus function with decreased spontaneous brain activities was previously demonstrated in patients with AD as compared to the healthy controls, which might reflect a common pathological condition in patients with AD (Sheline et al., 2010; Cheng et al., 2019). However, its linkage to the neurotoxicity of the amyloid $\beta$ protein proposed a possible treatment hallmark that this condition might be reversed through GBE treatment (Sheline et al., 2010). Our results were consistent with these findings and hypotheses. Specifically, we observed decreased ALFF values in the right gyrus rectus which was positively correlated with improved IADL scores after GBE treatment, indicating that benefits in IADL may be partially attributed to the GBE-induced compromise of ALFF reduction.

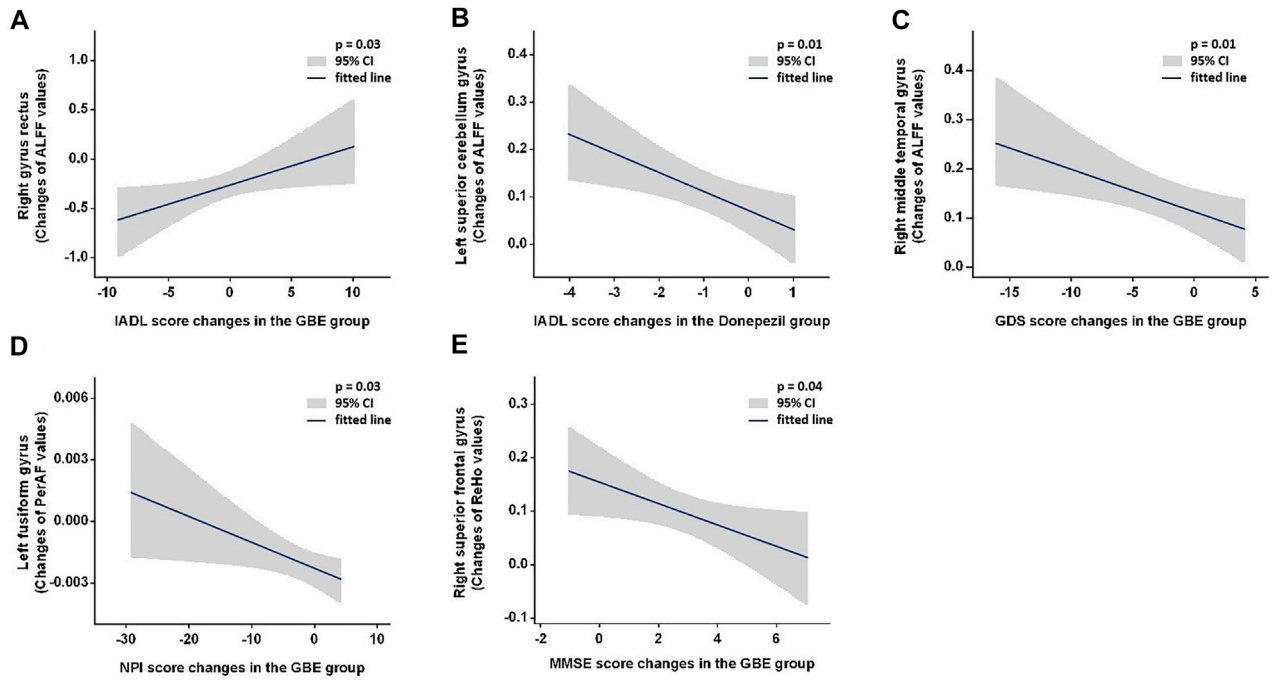


**FIGURE 3 |** Demonstration of significant correlations between changes of neuropsychological function and fMRI metrics. GBE: Ginkgo biloba extract; ALFF: amplitude of low frequency fluctuation; PerAF: percent amplitude of fluctuation; ReHo: reginal homogeneity; IADL: instrumental activity of daily living; GDS: geriatric depression scale; NPI: neuropsychiatric inventory; MMSE: minimum mental state examination.

According to the literature review, few studies investigated the adaptive changes in the middle temporal gyrus after AD. Abnormal ALFF values in AD patients, either increased or decreased, were observed in a recent study (Liu et al., 2014). The authors hypothesized that abnormalities may be associated with specific frequency bands in ALFF measurements. Therefore, they divided the low frequency range into several distinct bands and found decreased ALFF value in the slow-5 band (0.01–0.027 Hz) and increased ALFF value in the slow-4 band (0.027–0.073 Hz). They concluded that a specific frequency band would contribute to sensitive detection of spontaneous brain activity abnormalities. Although the current study observed increased ALFF values in the right middle temporal gyrus after GBE treatment, it is unlikely to draw a conclusion because our ALFF measurement was performed in a standardized way (frequency band of 0.01–0.08 Hz). Although a significant correlation was detected, the improvement of GDS score was difficult to be explained by the change of right middle temporal gyrus function since this specific brain region was previously reported to be involved in verbal or semantic cognition and associated with oral short-term memory (Vandenberghe et al., 1996). Both change of spontaneous brain activity in the middle temporal gyrus and its interaction with depression status following pharmacologic treatment need to be further clarified with well-designed clinical studies.

As a newly developed metric, PerAF is an analog to the percent signal change and a straightforward measurement of BOLD signal fluctuations during the resting state (Jia et al., 2020). It has been proven to be more reliable and sensitive than ALFF and fractional ALFF (fALFF) in a test-retest reliability analysis. Nonetheless, it has not been widely used in fMRI studies. Therefore, as compared to the healthy controls increased values in the fusiform gyrus of AD patients were only reported in the ALFF and ReHo measurement (Dai et al., 2012). We presented decreased PerAF values indicating that GBE was effective in compromising left fusiform gyrus function to some extent. Additionally, the fusiform gyrus was reported to be linked to various neurological phenomena including synesthesia, dyslexia, and prosopagnosia. Along with the results of correlation analysis, it is reasonable to document a positive interaction between reversed PerAF values in the left fusiform gyrus and improved neuropsychiatric status following GBE treatment.

We only observed one significant correlation in the donepezil group. As documented in previous studies, the cerebellum is involved in motor and balance as well as cognitive functions. The spontaneous brain activities in this region were reported to present decreased trends in patients with AD (Gottwald et al., 2003; Yang et al., 2018). Although the current study showed an increased trend of ALFF values in the left superior cerebellum gyrus after the treatment of donepezil, its negative correlation with improved IADL ability suggested that the functional improvement might not be directly subject to the recovery of cerebellum function while a potential effect inferred by the altered functional connection of salience network to the whole brain induced by donepezil (Cai et al., 2020). Similar situations can be casted to the observed negative correlations between increased ReHo values in the right superior frontal gyrus and improved MMSE scores. Further studies are warranted to clarify how this drug improves the IADL ability.

This study is not without limitations. Subsequent efforts had been donated during the enrollment period, for example, to minimize dropouts dosage selection of donepezil had been carefully considered according to both literature evidence and clinical experience. However, the dropout rate in the donepezil group was relatively high. Such attrition could have biased the results of multiple comparisons. In addition, the variation of cognitive impairment severity may lead to confounding bias although the average baseline MMSE values were comparable and the SDs were small across the three groups. Nonetheless, this limitation may be balanced with the application of multilevel imaging metrics including ALFF, PerAF, ReHo, and DC. Their discriminative sensitive features allowed the capture of potential significant changes of BOLD signaling in specific brain regions. Indeed, without healthy controls the compromised reduction or increase of fMRI metrics cannot be clearly defined and the impact of natural history of AD cannot be totally ruled out. Finally, due to the heterogeneity of pharmacological (e.g., type, dosage and duration) and analytic strategies, a generalization of the results is challenging.

## CONCLUSION

In conclusion, based on the results of inter-and intragroup comparison, GBE was comparable with donepezil in the improvement of cognitive, behavioral, psychological, and global functions in patients with AD while the combined application of GBE and donepezil seems unnecessary. Nonetheless, the acting mechanisms of these two drugs were discriminative. Although the IADL improvement might not be directly revealed with the recovery of cerebellum function following donepezil treatment, GBE-mediated improvement of functional recovery was potentially linked to the decreased ALFF values in the right gyrus rectus and decreased PerAF values in the left fusiform gyrus. These featured variations of imaging metrics in specific brain regions may serve as potential biomarkers in the monitoring of the therapeutic efficacy of GBE. Well-designed studies are warranted to fully investigate the efficacy and mechanisms of pharmacologic treatment on functional recovery in patients with AD.

## DATA AVAILABILITY STATEMENT

The original contributions presented in the study are included in the article **Supplementary Material**; further inquiries can be directed to the corresponding author.

## ETHICS STATEMENT

The trial protocol has been reviewed and approved by the Research Ethics Committee at the First Affiliated Hospital of Nanjing Medical University (Reference number: 2016-SR-134). The patients/participants provided their written informed consent to participate in this study. Written informed consent was obtained from the individual(s) for the publication of any potentially identifiable images or data included in this article.

## AUTHOR CONTRIBUTIONS

YZ contributed to the resources, methodology, visualization, writing original draft and supervision. YX contributed to the investigation and writing original draft. MQ contributed to the resources, methodology, visualization, supervision and writing—review and editing. LZ contributed to the resources, investigation and methodology. WW, WZ, LS, JW, and WL contributed to the resources and investigation. TW contributed to the conceptualization, data curation, funding acquisition and supervision. All authors read and approved the final manuscript.

## FUNDING

This trial was funded by the National Natural Science Foundation of China (Grant number: 81772454 and 81971237), the Jiangsu Municipal Science and Technology Bureau (Grant number: BE2017734) and the Nanjing Municipal Science and Technology Bureau (Grant number: 2019060002). The funding bodies had no role in the study design, data collection, analysis, and interpretation of data.

## ACKNOWLEDGMENTS

The authors are grateful for the support of the medical and research staff of this study. The authors particularly appreciate the patients and families for their participation in this study.

## SUPPLEMENTARY MATERIAL

The Supplementary Material for this article can be found online at: https://www.frontiersin.org/articles/10.3389/fphar.2021.721216/full#supplementary-material

## REFERENCES

Alzheimer's Disease International (2015). *World Alzheimer Report 2015: The Global Impact of Dementia: An Analysis of Prevalence, Incidence, Cost and Trends*. London: ADI website, 1–82.

Arvanitakis, Z., Shah, R. C., and Bennett, D. A. (2019). Diagnosis and Management of Dementia: Review. *Jama* 322 (16), 1589–1599. doi:10.1001/jama.2019.4782

Bastianetto, S., Ramassamy, C., Doré, S., Christen, Y., Poirier, J., and Quirion, R. (2000). The Ginkgo Biloba Extract (EGb 761) Protects Hippocampal Neurons against Cell Death Induced by β-amyloid. *Eur. J. Neurosci.* 12 (6), 1882–1890. doi:10.1046/j.1460-9568.2000.00069.x

Birks, J., and Grimley Evans, J. (2009). Ginkgo Biloba for Cognitive Impairment and Dementia. *Cochrane Database Syst. Rev.* 1, Cd003120. doi:10.1002/14651858.CD003120.pub2

Birks, J. S., and Harvey, R. J. (2018). Donepezil for Dementia Due to Alzheimer's Disease. *Cochrane Database Syst. Rev.* 6, CD001190. doi:10.1002/14651858.CD001190.pub3

Bozzali, M., Padovani, A., Caltagirone, C., and Borroni, B. (2011). Regional Grey Matter Loss and Brain Disconnection across Alzheimer Disease Evolution. *Cmc* 18 (16), 2452–2458. doi:10.2174/092986711795843263

Buckner, R. L., Sepulcre, J., Talukdar, T., Krienen, F. M., Liu, H., Hedden, T., et al. (2009). Cortical Hubs Revealed by Intrinsic Functional Connectivity: Mapping, Assessment of Stability, and Relation to Alzheimer's Disease. *J. Neurosci.* 29 (6), 1860–1873. doi:10.1523/jneurosci.5062-08.2009

Cacabelos, R. (2007). Donepezil in Alzheimer's Disease: From Conventional Trials to Pharmacogenetics. *Neuropsychiatr. Dis. Treat.* 3 (3), 303–333.

Cai, C., Huang, C., Yang, C., Lu, H., Hong, X., Ren, F., et al. (2020). Altered Patterns of Functional Connectivity and Causal Connectivity in Salience Subnetwork of Subjective Cognitive Decline and Amnestic Mild Cognitive Impairment. *Front. Neurosci.* 14, 288. doi:10.3389/fnins.2020.00288

Canter, P., and Ernst, E. (2007). Ginkgo Biloba Is Not a Smart Drug: an Updated Systematic Review of Randomised Clinical Trials Testing the Nootropic Effects ofG. Biloba Extracts in Healthy People. *Hum. Psychopharmacol. Clin. Exp.* 22 (5), 265–278. doi:10.1002/hup.843

Chao-Gan, Y., and Yu-Feng, Z. (2010). DPARSF: A MATLAB Toolbox for "Pipeline" Data Analysis of Resting-State fMRI. *Front. Syst. Neurosci.* 4 (13), 13. doi:10.3389/fnsys.2010.00013

Cheng, J., Yang, H., and Zhang, J. (2019). Donepezil's Effects on Brain Functions of Patients with Alzheimer Disease: A Regional Homogeneity Study Based on Resting-State Functional Magnetic Resonance Imaging. *Clin. Neuropharm* 42 (2), 42–48. doi:10.1097/wnf.0000000000000324

Cummings, J. L. (1993). Mini-Mental State Examination. *Jama* 269 (18), 2420–2421. doi:10.1001/jama.1993.03500180112046

Dai, Z., Yan, C., Wang, Z., Wang, J., Xia, M., Li, K., et al. (2012). Discriminative Analysis of Early Alzheimer's Disease Using Multi-Modal Imaging and Multi-Level Characterization with Multi-Classifier (M3). *Neuroimage* 59 (3), 2187–2195. doi:10.1016/j.neuroimage.2011.10.003

Defrancesco, M., Pechlaner, R., Kiechl, S., Willeit, J., Deisenhammer, E., Hinterhuber, H., et al. (2018). What Characterizes Depression in Old Age? Results from the Bruneck Study. *Pharmacopsychiatry* 51 (4), 153–160. doi:10.1055/s-0043-119417

DeKosky, S. T., Williamson, J. D., Fitzpatrick, A. L., Kronmal, R. A., Ives, D. G., Saxton, J. A., et al. (2008). Ginkgo Biloba for Prevention of DementiaA Randomized Controlled Trial. *Jama* 300 (19), 2253–2262. doi:10.1001/jama.2008.683

Destrieux, C., Terrier, L. M., Andersson, F., Love, S. A., Cottier, J.-P., Duvernoy, H., et al. (2017). A Practical Guide for the Identification of Major Sulcogyral Structures of the Human Cortex. *Brain Struct. Funct.* 222 (4), 2001–2015. doi:10.1007/s00429-016-1320-z

Di Perri, C., Bahri, M. A., Amico, E., Thibaut, A., Heine, L., Antonopoulos, G., et al. (2016). Neural Correlates of Consciousness in Patients Who Have Emerged from a Minimally Conscious State: a Cross-Sectional Multimodal Imaging Study. *Lancet Neurol.* 15 (8), 830–842. doi:10.1016/s1474-4422(16)00111-3

Doraiswamy, P. M., Kaiser, L., Bieber, F., and Garman, R. L. (2001). The Alzheimer's Disease Assessment Scale: Evaluation of Psychometric Properties and Patterns of Cognitive Decline in Multicenter Clinical Trials of Mild to Moderate Alzheimer's Disease. *Alzheimer Dis. Associated Disord.* 15 (4), 174–183. doi:10.1097/00002093-200110000-00003

Dubois, B., Feldman, H. H., Jacova, C., Dekosky, S. T., Barberger-Gateau, P., Cummings, J., et al. (2007). Research Criteria for the Diagnosis of Alzheimer's Disease: Revising the NINCDS-ADRDA Criteria. *Lancet Neurol.* 6 (8), 734–746. doi:10.1016/s1474-4422(07)70178-3

Friston, K. J., Williams, S., Howard, R., Frackowiak, R. S. J., and Turner, R. (1996). Movement-related Effects in fMRI Time-Series. *Magn. Reson. Med.* 35 (3), 346–355. doi:10.1002/mrm.1910350312

Gottwald, B., Mihajlovic, Z., Wilde, B., and Mehdorn, H. M. (2003). Does the Cerebellum Contribute to Specific Aspects of Attention?. *Neuropsychologia* 41 (11), 1452–1460. doi:10.1016/s0028-3932(03)00090-3

Guo, J. N., Kim, R., Chen, Y., Negishi, M., Jhun, S., Weiss, S., et al. (2016). Impaired Consciousness in Patients with Absence Seizures Investigated by Functional MRI, EEG, and Behavioural Measures: a Cross-Sectional Study. *Lancet Neurol.* 15 (13), 1336–1345. doi:10.1016/s1474-4422(16)30295-2

Homma, A., Imai, Y., Tago, H., Asada, T., Shigeta, M., Iwamoto, T., et al. (2008). Donepezil Treatment of Patients with Severe Alzheimer's Disease in a Japanese Population: Results from a 24-Week, Double-Blind, Placebo-Controlled, Randomized Trial. *Dement Geriatr. Cogn. Disord.* 25 (5), 399–407. doi:10.1159/000122961

Jenkinson, M., Bannister, P., Brady, M., and Smith, S. (2002). Improved Optimization for the Robust and Accurate Linear Registration and Motion Correction of Brain Images. *Neuroimage* 17 (2), 825–841. doi:10.1006/nimg.2002.1132

Jia, X. Z., Sun, J. W., Ji, G. J., Liao, W., Lv, Y. T., Wang, J., et al. (2020). Percent Amplitude of Fluctuation: A Simple Measure for Resting-State fMRI Signal at Single Voxel Level. *PLoS One* 15 (1), e0227021. doi:10.1371/journal.pone.0227021

Joo, M. S., Park, D. S., Moon, C. T., Chun, Y. I., Song, S. W., and Roh, H. G. (2016). Relationship between Gyrus Rectus Resection and Cognitive Impairment after Surgery for Ruptured Anterior Communicating Artery Aneurysms. *J. Cerebrovasc. Endovasc Neurosurg.* 18 (3), 223–228. doi:10.7461/jcen.2016.18.3.223

LaPlante, M. P. (2010). The Classic Measure of Disability in Activities of Daily Living Is Biased by Age but an Expanded IADL/ADL Measure Is Not. *Journals Gerontol. Ser. B: Psychol. Sci. Soc. Sci.* 65B (6), 720–732. doi:10.1093/geronb/gbp129

Liu, X., Wang, S., Zhang, X., Wang, Z., Tian, X., and He, Y. (2014). Abnormal Amplitude of Low-Frequency Fluctuations of Intrinsic Brain Activity in Alzheimer's Disease. *Jad* 40 (2), 387–397. doi:10.3233/jad-131322

Logsdon, R. G., Gibbons, L. E., McCurry, S. M., and Teri, L. (2002). Assessing Quality of Life in Older Adults with Cognitive Impairment. *Psychosomatic Med.* 64 (3), 510–519. doi:10.1097/00006842-200205000-00016

Luo, Y., Smith, J. V., Paramasivam, V., Burdick, A., Curry, K. J., Buford, J. P., et al. (2002). Inhibition of Amyloid- Aggregation and Caspase-3 Activation by the Ginkgo Biloba Extract EGb761. *Proc. Natl. Acad. Sci.* 99 (19), 12197–12202. doi:10.1073/pnas.182425199

Malloy, P. F., Cummings, J. L., Coffey, C. E., Duffy, J., Fink, M., Lauterbach, E. C., et al. (1997). Cognitive Screening Instruments in Neuropsychiatry: a Report of the Committee on Research of the American Neuropsychiatric Association. *J. Neuropsychiatry Clin. Neurosci.* 9 (2), 189–197. doi:10.1176/jnp.9.2.189

McCarney, R., Fisher, P., Iliffe, S., van Haselen, R., Griffin, M., van der Meulen, J., et al. (2008). Ginkgo Biloba for Mild to Moderate Dementia in a Community Setting: a Pragmatic, Randomised, Parallel-Group, Double-Blind, Placebo-Controlled Trial. *Int. J. Geriat. Psychiatry* 23 (12), 1222–1230. doi:10.1002/gps.2055

Planche, V., Bouteloup, V., Mangin, J. F., Dubois, B., Delrieu, J., Pasquier, F., et al. (2020). Clinical Relevance of Brain Atrophy Subtypes Categorization in Memory Clinics. *Alzheimers Dement.* 17 (4), 641–652. doi:10.1002/alz.12231

Reitz, C., Brayne, C., and Mayeux, R. (2011). Epidemiology of Alzheimer Disease. *Nat. Rev. Neurol.* 7 (3), 137–152. doi:10.1038/nrneurol.2011.2

Roman, G. C., Tatemichi, T. K., Erkinjuntti, T., Cummings, J. L., Masdeu, J. C., Garcia, J. H., et al. (1993). Vascular Dementia: Diagnostic Criteria for Research Studies: Report of the NINDS-AIREN International Workshop. *Neurology* 43 (2), 250. doi:10.1212/wnl.43.2.250

Rosen, W. G., Terry, R. D., Fuld, P. A., Katzman, R., and Peck, A. (1980). Pathological Verification of Ischemic Score in Differentiation of Dementias. *Ann. Neurol.* 7 (5), 486–488. doi:10.1002/ana.410070516

Schneider, L., DeKosky, S., Farlow, M., Tariot, P., Hoerr, R., and Kieser, M. (2005). A Randomized, Double-Blind, Placebo-Controlled Trial of Two Doses of Ginkgo Biloba Extract in Dementia of the Alzheimers Type. *Car* 2 (5), 541–551. doi:10.2174/156720505774932287

Sheline, Y. I., Raichle, M. E., Snyder, A. Z., Morris, J. C., Head, D., Wang, S., et al. (2010). Amyloid Plaques Disrupt Resting State Default Mode Network Connectivity in Cognitively normal Elderly. *Biol. Psychiatry* 67 (6), 584–587. doi:10.1016/j.biopsych.2009.08.024

Tchantchou, F., Xu, Y., Wu, Y., Christen, Y., and Luo, Y. (2007). EGb 761 Enhances Adult Hippocampal Neurogenesis and Phosphorylation of CREB in Transgenic Mouse Model of Alzheimer's Disease. *FASEB j.* 21 (10), 2400–2408. doi:10.1096/fj.06-7649com

Thompson, E. (2015). Hamilton Rating Scale for Anxiety (HAM-A). *Occmed* 65 (7), 601. doi:10.1093/occmed/kqv054

Vandenberghe, R., Price, C., Wise, R., Josephs, O., and Frackowiak, R. S. J. (1996). Functional Anatomy of a Common Semantic System for Words and Pictures. *Nature* 383 (6597), 254–256. doi:10.1038/383254a0

Vellas, B., Coley, N., Ousset, P. J., Berrut, G., Dartigues, J. F., Dubois, B., et al. (2012). Long-term Use of Standardised Ginkgo Biloba Extract for the Prevention of Alzheimer's Disease (GuidAge): a Randomised Placebo-Controlled Trial. *Lancet Neurol.* 11 (10), 851–859. doi:10.1016/s1474-4422(12)70206-5

Vik-Mo, A. O., Giil, L. M., Borda, M. G., Ballard, C., and Aarsland, D. (2020). The Individual Course of Neuropsychiatric Symptoms in People with Alzheimer's and Lewy Body Dementia: 12-year Longitudinal Cohort Study. *Br. J. Psychiatry* 216 (1), 43–48. doi:10.1192/bjp.2019.195

Wang, H., Chen, H., Wu, J., Tao, L., Pang, Y., Gu, M., et al. (2018). Altered Resting-State Voxel-Level Whole-Brain Functional Connectivity in Depressed Parkinson's Disease. *Parkinsonism Relat. Disord.* 50, 74–80. doi:10.1016/j.parkreldis.2018.02.019

Wang, T., Liao, H., Zi, Y., Wang, M., Mao, Z., Xiang, Y., et al. (2020). Distinct Changes in Global Brain Synchronization in Early-Onset vs. Late-Onset Parkinson Disease. *Front. Aging Neurosci.* 12, 604995. doi:10.3389/fnagi.2020.604995

Woolf, C., Slavin, M. J., Draper, B., Thomassen, F., Kochan, N. A., Reppermund, S., et al. (2016). Can the Clinical Dementia Rating Scale Identify Mild Cognitive Impairment and Predict Cognitive and Functional Decline?. *Dement Geriatr. Cogn. Disord.* 41 (5-6), 292–302. doi:10.1159/000447057

Yang, J., Gohel, S., and Vachha, B. (2020). Current Methods and New Directions in Resting State fMRI. *Clin. Imaging* 65, 47–53. doi:10.1016/j.clinimag.2020.04.004

Yang, L., Yan, Y., Wang, Y., Hu, X., Lu, J., Chan, P., et al. (2018). Gradual Disturbances of the Amplitude of Low-Frequency Fluctuations (ALFF) and Fractional ALFF in Alzheimer Spectrum. *Front. Neurosci.* 12, 975. doi:10.3389/fnins.2018.00975

**Conflict of Interest:** The authors declare that the research was conducted in the absence of any commercial or financial relationships that could be construed as a potential conflict of interest.

**Publisher's Note:** All claims expressed in this article are solely those of the authors and do not necessarily represent those of their affiliated organizations, or those of the publisher, the editors and the reviewers. Any product that may be evaluated in this article, or claim that may be made by its manufacturer, is not guaranteed or endorsed by the publisher.

frontiers in Pharmacology

ORIGINAL RESEARCH
published: 10 September 2021
doi: 10.3389/fphar.2021.746711

# Rhein Relieves Oxidative Stress in an $A\beta_{1-42}$ Oligomer-Burdened Neuron Model by Activating the SIRT1/PGC-1α-Regulated Mitochondrial Biogenesis

*Zhihui Yin, Xinyue Geng, Zhengyi Zhang, Ying Wang* and Xiaoyan Gao**

*School of Chinese Materia Medica, Beijing University of Chinese Medicine, Beijing, China*

OPEN ACCESS

**Edited by:**
*Fushun Wang,*
*Nanjing University of Chinese Medicine, China*

**Reviewed by:**
*Ke-Wu Zeng,*
*Peking University Health Science Centre, China*
*Miao Qu,*
*Capital Medical University, China*

***Correspondence:**
*Ying Wang*
*wangy174@126.com*
*Xiaoyan Gao*
*gaoxiaoyan@bucm.edu.cn*

**Specialty section:**
*This article was submitted to Neuropharmacology, a section of the journal Frontiers in Pharmacology*

**Received:** *24 July 2021*
**Accepted:** *31 August 2021*
**Published:** *10 September 2021*

**Citation:**
*Yin Z, Geng X, Zhang Z, Wang Y and Gao X (2021) Rhein Relieves Oxidative Stress in an $A\beta_{1-42}$ Oligomer-Burdened Neuron Model by Activating the SIRT1/PGC-1α-Regulated Mitochondrial Biogenesis. Front. Pharmacol. 12:746711. doi: 10.3389/fphar.2021.746711*

Neuronal mitochondrial oxidative stress induced by β-amyloid (Aβ) is an early event of Alzheimer's disease (AD). Emerging evidence has shown that antioxidant therapy represents a promising therapeutic strategy for the treatment of AD. In this study, we investigated the antioxidant activity of rhein against $A\beta_{1-42}$ oligomer-induced mitochondrial oxidative stress in primary neurons and proposed a potential antioxidant pathway involved. The results suggested that rhein significantly reduced reactive oxygen species (ROS) level, reversed the depletion of mitochondrial membrane potential, and protected neurons from oxidative stress-associated apoptosis. Moreover, further study indicated that rhein activated mitochondrial biogenesis accompanied by increased cytochrome C oxidase (CytOx) and superoxide dismutase (SOD) activities. CytOx on the respiratory chain inhibited the production of ROS from electron leakage and SOD helped to eliminate excess ROS. Finally, western blot analysis confirmed that rhein remarkedly increased the protein expression of peroxisome proliferator-activated receptor gamma coactivator 1-alpha (PGC-1α) together with its upstream deacetylase sirtuin 1 (SIRT1), and activated downstream transcription factor nuclear respiratory factor 1, promoting mitochondrial biogenesis. In conclusion, our results demonstrate that rhein activates mitochondrial biogenesis regulated by the SIRT1/PGC-1α pathway as an antioxidant defense system against $A\beta_{1-42}$ oligomer-induced oxidative stress. These findings broaden our knowledge of improving mitochondrial biogenesis as an approach for relieving neuronal oxidative stress in AD.

**Keywords: β-amyloid, oxidative stress, rhein, mitochondrial biogenesis, sirtuin 1, peroxisome proliferator-activated receptor gamma coactivator 1-alpha**

**Abbreviations:** ΔΨm, mitochondrial membrane potential; Aβ, β-amyloid; AD, Alzheimer's disease; BCA, bicinchoninic acid; CD, circular dichroism; CytOx, cytochrome C oxidase; cyto c, cytochrome c; H2O2, hydrogen peroxide; mPTP, mitochondrial permeability transition pore; mtDNA, mitochondrial DNA; MTT, 3-(4,5-dimethylthiazol-2-yl)-2,5-diphenyltetrazolium bromide; NO, nitric oxide; NRF1, nuclear respiratory factor 1; PD, pharmacodynamic; PDB, Protein Data Bank; PGC-1α, peroxisome proliferator-activated receptor gamma coactivator 1-alpha; PI: propidium iodide; ROS, reactive oxygen species; SIRT1, sirtuin 1; SOD, superoxide dismutase; TEM, transmission electron microscopy; TFAM, transcription factor A; ThT, thioflavin T.

## INTRODUCTION

Alzheimer's disease (AD), the most common neurodegenerative disease, is characterized by memory loss and cognitive dysfunction (Alzheimer's Association, 2021). Mounting evidence indicates neuronal oxidative stress induced by β-amyloid (Aβ) is considered to be a critical pathological event in AD, although the etiology of AD has not been fully elucidated (Lin and Beal, 2006; Borger et al., 2011; Swerdlow, 2018). Aβ destroys the electron respiratory chain in the mitochondrial inner membrane by reducing the activities of enzymes in mitochondrial respiratory chain complexes, especially cytochrome C oxidase (CytOx) in complex IV, leading to electron leakage and excess production of reactive oxygen species (ROS) (Atamna and Frey, 2004; Battogtokh et al., 2018; Misrani et al., 2021). Excess ROS aggravates mitochondrial dysfunction, which opens the mitochondrial permeability transition pore (mPTP), accelerates the release of cytochrome c (cyto c) into the cytosol, and subsequently induces the caspase-related apoptosis cascade, triggering the apoptosis of neurons (Mehan et al., 2011; Xiao et al., 2019). Meanwhile, ROS upregulates the expression of amyloid precursor protein and β-site APP-cleaving enzyme 1 by activating the c-Jun N-terminal kinase pathway, facilitates the generation and accumulation of Aβ, and finally accelerates the progression of AD (Chami and Checler, 2012; Tamagno et al., 2012; Zhao and Zhao, 2013; Ganguly et al., 2017). Therefore, relieving oxidative stress is an effective therapeutic strategy for AD.

Mitochondrial biogenesis as a cellular endogenous antioxidant defense system is actively mobilized under pathological conditions to overcome intracellular oxidative stress (Du et al., 2017; Panes et al., 2020). The sirtuin 1 (SIRT1)/peroxisome proliferator-activated receptor-γ coactivator 1-α (PGC-1α) pathway is pivotal for mitochondrial biogenesis (Menzies et al., 2013). SIRT1 is a nicotinamide adenine dinucleotide-dependent deacetylase, which is responsible for deacetylation and activation of the mitochondrial regulatory factor PGC-1α. Activated PGC-1α targets downstream transcription factors, such as nuclear respiratory factor 1 (NRF1) and NRF-2, which upregulate mitochondrial transcription factor A (TFAM). TFAM initiates the transcription and replication of mitochondrial DNA (mtDNA), and ultimately, newly healthy mitochondria are generated for the self-repair of mitochondria and synthesis of antioxidant enzymes (Canto et al., 2009; Kume et al., 2010; Aquilano et al., 2013). The newly generated healthy mitochondria can repair the damaged mitochondrial respiratory chain via mitochondrial fusion through mitochondrial dynamics, inhibiting the production of mitochondria-derived ROS (Liao et al., 2020; Zeng et al., 2021). In addition, synthesis of the mitochondrial antioxidant enzymes, mainly superoxide dismutase (SOD), is increased by generating new mitochondria, thus reducing ROS (St-Pierre et al., 2006; Dhar et al., 2008; Piantadosi and Suliman, 2008; Yan et al., 2016). Unfortunately, under the oxidative stress induced by Aβ, the SIRT1/PGC-1α pathway is suppressed (Gao et al., 2011; Shaerzadeh et al., 2014). Therefore, the activation of SIRT1/PGC-1α-regulated mitochondrial biogenesis as an antioxidant defense system to maintain intracellular mitochondrial homeostasis is essential for relieving the oxidative stress of neurons (Katsouri et al., 2016).

1,8-dihydroxyanthraquinone derivatives are a class of natural compounds with antioxidant activity (Wang et al., 2012; Lu et al., 2015; Markovic et al., 2016; Wang et al., 2016). Representative compounds including rhein, emodin, aloe-emodin, chrysophanol, and physcion are considered candidate compounds for antioxidant therapy. Rhein can protect IEC-6 cells from oxidative damage by inhibiting hydrogen peroxide ($H_2O_2$)-induced ROS, caspase 3, and even apoptosis (Zhuang et al., 2019). Aloe-emodin improves cell viability by reducing the levels of nitric oxide (NO) and ROS in PC12 cells induced by $H_2O_2$ (Tao et al., 2014). Physcion exhibits neuroprotection effect in SH-SY5Y cells by reducing Aβ-induced oxidative stress and the influx of $Ca^{2+}$ (Ho et al., 2015). *In vivo* studies showed that chrysophanol enhanced the activities of SOD and manganese SOD, and inhibited the production of ROS, ultimately relieving oxidative stress injury in the brain of a focal cerebral ischemia/reperfusion mouse model (Zhao et al., 2018). Emodin downregulated 4-hydroxynonenal, a cerebral oxidative damage indicator, increased the expression levels of SOD1 and catalase, and improved the antioxidant capacity of APP/PS1 mice (Li et al., 2021). Therefore, screening of natural compounds with antioxidant activity from anthraquinones is of great clinical significance for relieving oxidative stress and protecting neurons in AD.

As one of the *in vitro* evaluation methods for AD, the cell model is very important for the screening of pharmacodynamic (PD) activity. To date, the screening platform for the evaluation of antioxidants against oxidative stress in AD is still dominated by immortalized cell lines, such as PC12 and SH-SY5Y cells (Lopes et al., 2017; Wang and Xu, 2019; Sotolongo et al., 2020). Nevertheless, after multiple rounds of proliferation and passaging, some traits of immortalized cell lines are quite different from those of living cells *in vivo*. As a consequence, the positive PD results screened from a cell model cannot be replicated when applied to an *in vivo* model. In contrast, the primary neurons obtained from living organisms are closer to the neurons *in vivo*. In addition, recent studies have suggested that $A\beta_{1\text{-}42}$ oligomers are the pathogens of early AD (Haass and Selkoe, 2007; Zahs and Ashe, 2013; Fontana et al., 2020). Thus, establishing an $A\beta_{1\text{-}42}$ oligomer-induced primary neuron model similar to the pathological environment of AD will greatly improve the screening effectiveness of candidate compounds.

In this study, an AD-like neuronal oxidative stress model was established on primary neurons by optimizing the aggregation states of $A\beta_{1\text{-}42}$. Thereafter, the antioxidant activities of five anthraquinones were evaluated by intracellular ROS and mitochondrial membrane potential. As a result, rhein exhibited excellent antioxidant activity and inhibited neuronal apoptosis. Further study was to explore the antioxidant mechanism of rhein. Finally, our results demonstrate that rhein activates mitochondrial biogenesis regulated by the SIRT1/PGC-1α pathway against $A\beta_{1\text{-}42}$ oligomer-induced mitochondrial oxidative stress. Taken together, rhein may present a promising candidate molecule for relieving neuronal

oxidative stress as well as oxidative stress-associated neurodegenerative disorders.

# MATERIALS AND METHODS

## Materials and Reagents

$A\beta_{1\text{-}42}$ (CAS: 107761-42-2 for lyophilized $A\beta_{1\text{-}42}$) was obtained from Nanjing Peptide Biotech Co., Ltd. (Nanjing, China). Rhein (MW 284.22 of purity >98%, CAS: 478-43-3), 1,1,1,3,3,3-hexafluoro-2-propanol (HFIP, CAS: 920-66-1), thioflavin T (ThT, CAS: 2390-54-7), and phosphotungstic acid (CAS: 12501-23-4) were obtained from Shanghai Aladdin Biochemical Technology Co., Ltd. (Shanghai, China). Emodin (MW 270.24 of purity >98%, CAS: 518-82-1), aloe-emodin (MW 270.24 of purity >97%, CAS: 481-72-1), chrysophanol (MW 254.24 of purity >98%, CAS: 481-74-3), and physcion (MW 284.26 of purity >98%, CAS: 521-61-9) were obtained from Shanghai yuanye Bio-Technology Co., Ltd. (Shanghai, China). B27 (Cat: 17504044) and penicillin-streptomycin (PS, Cat: 10378016) were purchased from Gibco Corporation (Grand Island, NY, USA). Dulbecco's modified Eagle medium (DMEM, Cat: C11995500), Neurobasal medium (Cat: 21103049), and L-glutamine (Cat: A2916801) were purchased from Invitrogen Corporation (Carlsbad, CA, USA). Poly-L-lysine (Cat: P2100), 3-(4,5-dimethylthiazol-2-yl)-2,5-diphenyltetrazolium bromide (MTT, Cat: M8180), and CytOx activity detection kit (Cat: BC0945) were obtained from Beijing Solarbio Science & Technology Co., Ltd. (Beijing, China). Bicinchoninic acid (BCA) protein quantification kit (Cat: P0010), ROS assay kit (Cat: S0033), Mitochondrial membrane potential detection kit (Cat: C2006), SOD activity detection kit (Cat: S0101), Annexin V-FITC apoptosis detection kit (Cat: C1062), and cytosol/mitochondria fraction isolation kit (Cat: C3601) were obtained from Beyotime Biotechnology (Shanghai, China). Primary antibodies, MAP2 rabbit polyclonal antibody (Cat: 17490-1-AP), PGC-1α monoclonal antibody (Cat: 66369-1-Ig), NRF1 polyclonal antibody (Cat: 12482-1-AP), caspase 3 polyclonal antibody (Cat: 19677-1-AP), cyto c polyclonal antibody (Cat: 10993-1-AP), and β-Actin monoclonal antibody (Cat: 66009-1-Ig) were obtained from Proteintech Group, Inc. (Rosemont, IL, USA). SIRT1 monoclonal antibody (Cat: 9475S) was purchased from Cell Signaling Technology Inc. (Danvers, MA, USA). Secondary antibodies, goat anti-mouse IgG (Cat: SA00001-1) and goat anti-rabbit IgG (Cat: SA00001-2) were obtained from Proteintech Group, Inc. All other chemicals used were of the highest grade commercially available.

## $A\beta_{1\text{-}42}$ Preparation

$A\beta_{1\text{-}42}$ monomers were prepared as described previously (Sinha et al., 2011). The lyophilized $A\beta_{1\text{-}42}$ peptides were dissolved in HFIP at a concentration of 1 mg/ml and sonicated for 10 min in an ice-bath, followed by incubation with shaking at 4°C for 3 h. Subsequently, the resulting solution was evaporated under a gentle stream of $N_2$ gas to remove HFIP, and peptide films were formed. Thereafter, the peptide films were dissolved in 10 mM sodium hydroxide alone with sonication for 1 min and centrifuged at 4°C (16000 × g, 10 min). Finally, the supernatant was collected and quantified using a NanoDrop One spectrometer (Thermo Fisher Scientific, Waltham, MA, United States) at 280 nm using an extinction coefficient of 1490 $M^{-1}$ $cm^{-1}$.

To prepare different aggregation stages of $A\beta_{1\text{-}42}$, $A\beta_{1\text{-}42}$ monomers were diluted in phosphate-buffered solution (PBS, 10 mM, pH 7.4) at a final peptide concentration of 50 μM and incubated with continuous orbital shaking at 150 rpm. At different incubation time points, $A\beta_{1\text{-}42}$ solution was collected for corresponding experiments.

## Circular Dichroism Spectra Assay

The prepared $A\beta_{1\text{-}42}$ was diluted in PBS at a final concentration of 25 μM. 100 μL sample was added to a 0.5 mm path length quartz cell. The spectrum was collected with an average of three scans at a speed of 1 nm/s over the wavelength range from 195 to 260 nm using a Chirascan spectrometer (Applied Photophysics Ltd., Surrey, BA, United Kingdom).

## ThT Fluorescence Assay

The kinetic process of $A\beta_{1\text{-}42}$ aggregation was monitored by ThT, the fluorescence intensity of which is dependent on the formation of β-sheet. At different incubation times, $A\beta_{1\text{-}42}$ solution was taken for fluorescence assay at the concentration of 1 μM for $A\beta_{1\text{-}42}$ and 10 μM for ThT, respectively. The fluorescence was measured using a LS45 fluorescence spectrometer (PerkinElmer Inc., Waltham, MA, United States). The excitation wavelength and emission wavelength were set at 440 and 480 nm, respectively.

## Transmission Electron Microscopy

The prepared $A\beta_{1\text{-}42}$ (20 μL) was dropped on a carbon-coated copper grid. After 1 h, the redundant solution was removed with filter paper, and prepared $A\beta_{1\text{-}42}$ was stained with 20 μL of 1% phosphotungstic acid for 90 s. Then, the transmission electron microscopy (TEM) images were taken using a JEM-1230 transmission electron microscope (JEOL Ltd., Akishima-shi, Japan) with an acceleration voltage of 100 kV.

## Primary Neuron Cultures

Primary neurons were extracted and isolated from neonatal SD rats as described previously (Dong et al., 2018). Neonatal SD rats were obtained from SPF Biotechnology Co., Ltd. (Beijing, China). Primary neurons were seeding in poly-L-lysine precoated 96-well plates or 24-well plates with a cell density at $5 \times 10^5$ cells/mL and cultured in neurobasal medium supplemented with 2% B27 supplements, 1% L-glutamine, and 1% PS at 37°C in a humidified atmosphere containing 5% $CO_2$. After culture for 7 days, the primary neurons can be used for experiments.

As illustrated in **Supplementary Figure 1**, the purity of primary neurons was identified to be above 95% by the immunofluorescence assay labelled with anti-MAP2 antibodies, and the purity of the primary neurons met the requirements for subsequent experiments.

## Cell Treatments

To examine the cytotoxicity of $A\beta_{1-42}$ in different aggregation, primary neurons were incubated with DMEM containing 5 μM $A\beta_{1-42}$ aggregates. After incubation for 24 h, the cell viability was measured. To examine the antioxidant effects of the five anthraquinones against $A\beta_{1-42}$ oligomer-induced oxidative stress, primary neurons which were incubated with DMEM containing 5 μM $A\beta_{1-42}$ and different concentrations of anthraquinones (1, 5 and 10 μM as low, medium, and high doses, respectively) were the treated groups. After incubation for 24 h, treated groups were used for further experiments. Meanwhile, untreated primary neurons were the control group, and primary neurons treated with 5 μM $A\beta_{1-42}$ oligomers alone were the $A\beta_{1-42}$ group.

## Cell Viability Assay

Cell viability was measured by the MTT assay. After the cell treatment, the medium in 96-well plates was discarded. Then, 100 μL DMEM containing MTT at a final concentration of 0.5 mg/ml was added into 96-well plates. After incubation for another 4 h, the solution was discarded followed by adding 100 μL DMSO. Finally, the absorbance at 490 nm was measured using an Epoch Microplate Spectrophotometer (BioTek Instruments Inc., Winooski, VT, United States).

## Intracellular ROS Measurement

ROS in primary neurons was detected using a DCFH-DA probe. DCFH-DA at a concentration of 10 μM was added to 96-well plates. After incubation for 20 min at 37°C, primary neurons were washed three times to fully remove excessive DCFH-DA. Finally, fresh culture medium was added and fluorescence images were taken under a fluorescence microscope (Nikon Instruments Inc., Melville, NY, United States).

## Mitochondrial Membrane Potential (ΔΨm) Measurement

ΔΨm in primary neurons was detected using a JC-1 probe. Mitochondria were stained with a JC-1 staining kit according to the manufacturer's instructions. Briefly, JC-1 staining solution was added to 24-well plates. After incubation for 20 min at 37°C, primary neurons were washed twice to fully remove excessive JC-1. Finally, fresh culture medium was added and fluorescence images were taken under a fluorescence microscope.

## Molecular Docking

To study the structure-activity relationship of the five anthraquinones, rhein, emodin, aloe-emodin, chrysophanol, and physcion were selected as ligand molecules, and docked with the receptor of SIRT1 (PDB code: 4I5I), respectively. The 3D structures of the five ligand molecules were acquired from the Pubchem Compound database (https://pubchem.ncbi.nlm.nih.gov/). The X-ray crystal structure of human Sirt1 was obtained from the Protein Data Bank (https://www.rcsb.org/). Molecular docking was performed by AutoDock Vina 1.1.2 and AutoDock Tools (The Scripps Research Institute, La Jolla, CA, United States). The size of the grid box in AutoDock Vina was kept as 40 × 40 × 40 for X, Y, and Z. The final model was determined based on the binding energy and molecular interaction. Docked complexes were analyzed and figures were exported using PyMOL 2.3.4 (Schrödinger, Inc., New York, NY, United States).

## Measurement of CytOx Activity

CytOx activity was measured using a CytOx activity detection kit according to the manufacturer's instructions. Briefly, primary neurons after treatment were washed once with cold PBS and lysed in an extracting solution. The lysate was centrifuged at 4°C (600 × g, 10 min), and the supernatant was transferred to another tube for centrifugation at 4°C (11000 × g, 15 min). Then, the sediment was collected and extracted by extracting solution. After sufficient ultrasonication, each sample was quantified by a BCA protein quantification kit. Finally, 20 μL sample, and 200 μL working solution were added to 96-well plates and the absorbance at 550 nm was measured using an Epoch Microplate Spectrophotometer.

## Measurement of SOD Activity

SOD activity was measured using a SOD activity detection kit according to the manufacturer's instructions. Briefly, primary neurons after treatment were washed once with cold PBS and lysed in a SOD preparation solution. The lysate was centrifuged at 4°C (16000 × g, 5 min), and the supernatant was collected. Each sample was quantified by a BCA protein quantification kit. Then, 20 μL protein sample, 160 μL working solution, and 20 μL reaction working solution were added to 96-well plates. After incubation for 30 min at 37°C, the absorbance at 450 nm was measured using an Epoch Microplate Spectrophotometer.

## Annexin V-FITC/Propidium Iodide Staining Assay

Apoptosis was evaluated using an Annexin V-FITC apoptosis detection kit according to the manufacturer's instructions. In brief, primary neurons after treatment were washed once with cold PBS. Then, 195 μL Annexin V-FITC binding buffer, 5 μL Annexin V- FITC, and 10 μL propidium iodide (PI) were sequentially added to 96-well plates. After incubation for 15 min in the dark, fresh culture medium was added and fluorescence images were taken under a fluorescence microscope.

## Western Blot

Primary neurons after treatment were washed once with cold PBS and lysed in an ice-cold lysis buffer containing 20 mM Tris-HCl pH 7.5, 150 mM NaCl, 1% Triton X-100, 1 mM PMSF and other inhibitors including sodium pyrophosphate, β-glycerophosphate, EDTA, $Na_3VO_4$ and leupeptin. The lysate was centrifuged at 4°C (16000 × g, 5 min), and the supernatant was collected. Cytosolic fraction for cytosolic cyto c was prepared using a cytosol/mitochondria fraction isolation kit. After quantification of protein concentration, equivalent amounts of sample were separated by an SDS-PAGE and then transferred onto polyvinylidene fluoride membranes. After being blocked with 5% non-fat milk for 2 h at room temperature, the membranes were incubated with primary antibodies of interest overnight at 4°C and followed by the incubation

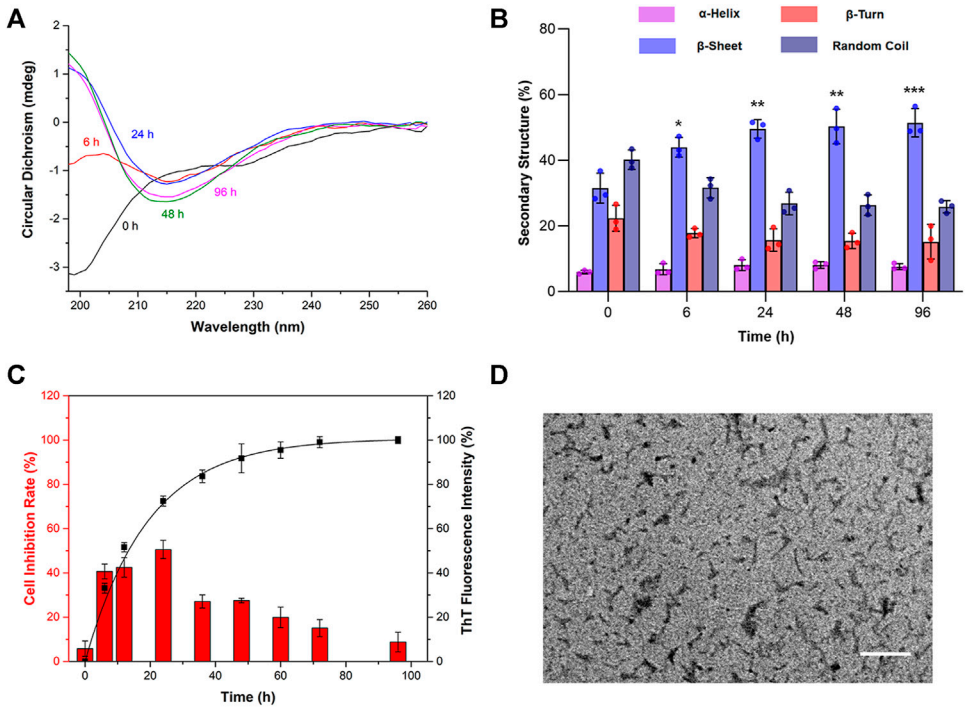


**FIGURE 1 |** The cytotoxicity of $A\beta_{1-42}$ in different aggregation stages in primary neurons. $A\beta_{1-42}$ monomers were incubated by continuous orbital shaking at 150 rpm and 37°C. **(A)** The changes in the secondary structure of prepared $A\beta_{1-42}$ in different aggregation stages were detected by circular dichroism (CD) spectra. **(B)** The proportions of the secondary structure were further analyzed. **(C)** The aggregation process of $A\beta_{1-42}$ was investigated by the thioflavin T (ThT) assay ($n = 4$) and the cytotoxicity of $A\beta_{1-42}$ in different aggregation stages in primary neurons was determined by the MTT assay ($n = 5$). **(D)** Representative transmission electron microscope image of $A\beta_{1-42}$ incubated for 24 h at 37°C. Scale bars: 200 nm. Data are presented as the mean ± standard deviation (SD). $^{*}p < 0.05$, $^{**}p < 0.01$ and $^{***}p < 0.001$ compared with the proportions of β-sheets at 0 h (one-way ANOVA).

with secondary antibodies for 2 h at room temperature. The immunoblots were developed with ECL reagents and visualized by a ChemiDoc™ MP Imaging System (Bio-Rad Laboratories, Inc., Hercules, CA, United States). The results were normalized to β-Actin and analyzed using ImageJ software (National Institutes of Health, Bethesda, MD, United States).

## Statistical Analysis

All data were presented as means ± standard deviation (SD) for at least three independent experiments. Statistical significance was analyzed using one-way analysis of variance (ANOVA), followed by the least significant difference (LSD) test for multiple comparisons. Levels of significance were indicated as follows: $^{*}p < 0.05$; $^{**}p < 0.01$; $^{***}p < 0.001$. All statistical analyses were performed using SPSS Statistics 25.0 software (IBM Corporation, Armonk, NY, United States).

# RESULTS

## $A\beta_{1-42}$ Oligomer-Induced Oxidative Stress Model Established Based on Primary Neurons

To establish an *in vitro* model of AD-like oxidative stress, the preparation of $A\beta_{1-42}$ was optimized. First of all, the changes in the secondary structure of prepared $A\beta_{1-42}$ with different incubation times were detected by circular dichroism (CD) spectra. As shown in **Figure 1A**, Aβ was in a monomeric state at 0 h and was structured as a random coil with a negative absorption peak at 198 nm. With the extension of incubation time, the absorption at 198 nm gradually weakened, and a new absorption peak appeared at 215 nm at 6 h. Its characteristic β-sheet structure at 215 nm revealed that Aβ changed from random coil in the monomer state to β-sheet (i.e., gradually aggregated). With increasing incubation times of 24, 48, and 96 h, the absorption at 215 nm gradually enhanced as well. As shown in **Figure 1B**, the secondary structure illustrated that the proportions of β-sheets at 6, 24, 48, and 96 h were 32, 44, 50, and 51%, respectively, implying that Aβ gradually aggregated and tended to be stable. The aggregation process of $A\beta_{1-42}$ was further investigated by ThT fluorescence assay. As shown in **Figure 1C**, the fluorescence intensity of ThT rapidly increased from 6 to 36 h, indicating that $A\beta_{1-42}$ was in the exponential growth phase. After 48 h, the curve grew slowly and gradually reached the plateau phase. These results demonstrated that the prepared $A\beta_{1-42}$ depicted the typical aggregation kinetic process of monomer-oligomer-protofibril-fibril.

To examine the cytotoxicity of $A\beta_{1-42}$ in different aggregation stages in primary neurons, $A\beta_{1-42}$ aggregates prepared at different incubation times in the final concentration of 5 μM were used to

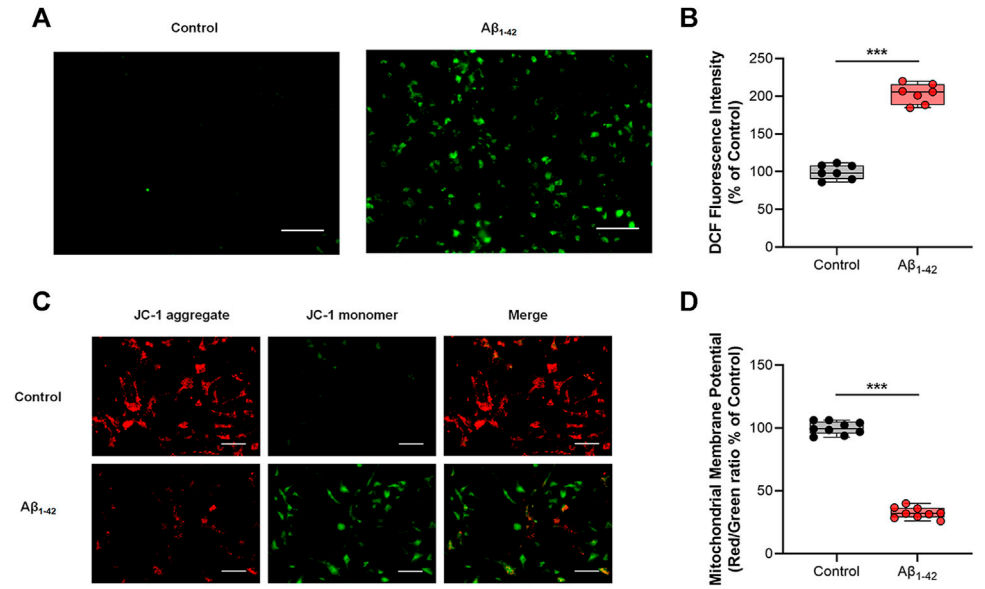


**FIGURE 2 |** $A\beta_{1\text{-}42}$ oligomer-induced oxidative stress model on primary neurons. Untreated primary neurons were the control group, and primary neurons treated with 5 μM $A\beta_{1\text{-}42}$ oligomers alone were the $A\beta_{1\text{-}42}$ group. **(A)** Representative fluorescence images of intracellular ROS. **(B)** Quantification of intracellular ROS by the fluorescence intensity of DCF and normalization to the control group ($n$ = 7). **(C)** Representative fluorescence images of ΔΨm. **(D)** Quantification analysis of ΔΨm by the fluorescence intensity of red/green ratio with JC-1 and normalization to the control group ($n$ = 9). Scale bars: 50 μm. Data are presented as the mean ± standard deviation (SD). ***$p$ < 0.001 compared with the $A\beta_{1\text{-}42}$ group (one-way ANOVA).

evaluate the cell inhibition rate by the MTT assay. The results are shown in **Figure 1C**. The $A\beta_{1\text{-}42}$ monomer did not cause distinct toxicity, and the cell inhibition rate was lower than 10%. With the extension of incubation time, the toxicity of $A\beta_{1\text{-}42}$ significantly increased. After incubation for 6, 12, and 24 h, the toxicity of $A\beta_{1\text{-}42}$ continued to increase, with inhibition rates of 41, 42, and 51%, respectively. At the plateau phase, the toxicity began to decrease. At 48, 60, 72, and 96 h, the inhibition rates of neurons were 27, 20, 15, and 9%, respectively. According to the abovementioned results, $A\beta_{1\text{-}42}$ at 24 h caused maximum damage to the neurons. The morphology of the $A\beta_{1\text{-}42}$ aggregates at 24 h was further characterized by TEM. After phosphotungstic acid staining, $A\beta_{1\text{-}42}$ had a width of ~5 nm and a length of <200 nm in the TEM image, suggesting that it was in the oligomeric form (**Figure 1D**). Taken together, the $A\beta_{1\text{-}42}$ oligomers obtained by incubation for 24 h were the most toxic, which could be used to establish an AD oxidative stress cell model.

After determining the preparation method for toxic Aβ, primary neurons were stimulated by $A\beta_{1\text{-}42}$ oligomers to induce oxidative stress. The intracellular ROS level was detected by the DCFH-DA probe. After being oxidized by ROS, DCFH-DA transformed to DCF, a fluorescent substance, and the fluorescence intensity of DCF was used to evaluate intracellular oxidative stress. As illustrated in **Figures 2A,B**, compared with the control group, the fluorescence intensity of DCF in the $A\beta_{1\text{-}42}$ group increased to 203%, indicating that $A\beta_{1\text{-}42}$ oligomers induced high ROS levels in primary neurons. Because intracellular ROS was derived from mitochondrial dysfunction, the intracellular ΔΨm was detected with a JC-1 probe to evaluate mitochondrial function. As shown in **Figures 2C,D**, the $A\beta_{1\text{-}42}$ group exhibited more JC-1 monomers (green fluorescence) and fewer JC-1 aggregates (red fluorescence) than the control group. The fluorescence intensity of the red/green ratio decreased to 32% after being normalized to the control group, suggesting that a lower ΔΨm was due to mitochondrial damage. These results demonstrated that $A\beta_{1\text{-}42}$ oligomers damaged mitochondrial function and caused oxidative stress in primary neurons.

## Evaluation of the Antioxidative Activities of the Five Anthraquinones in Alleviating $A\beta_{1\text{-}42}$ Oligomer-Induced Oxidative Stress in Primary Neurons

After establishing an oxidative stress neuron model induced by $A\beta_{1\text{-}42}$ oligomers, we used this model to investigate the antioxidant activities of five anthraquinones. The chemical structures of the five anthraquinones are displayed in **Figure 3A**. They shared 1,8-dihydroxy anthraquinone as the same structure, yet they were substituted with different functional groups at the 3- or 6-position. Thereafter, the effects of the five anthraquinones on intracellular ROS level were determined. As shown in **Figure 3B** and **Supplementary Figure 2**, compared with the $A\beta_{1\text{-}42}$ group, rhein treatment at doses of 1, 5, and 10 μM inhibited intracellular ROS levels by 182, 145, and 122%, respectively, manifesting an obvious dose dependency. The 5 μM rhein was sufficient to produce a significant difference, while the 10 μM rhein reduced ROS to the level of the control group. Emodin was also able to lower intracellular ROS levels. Emodin treatment at doses of 1, 5, and 10 μM reduced ROS levels by 189, 172, and 149%, respectively. Nevertheless, a significant difference was only found in the

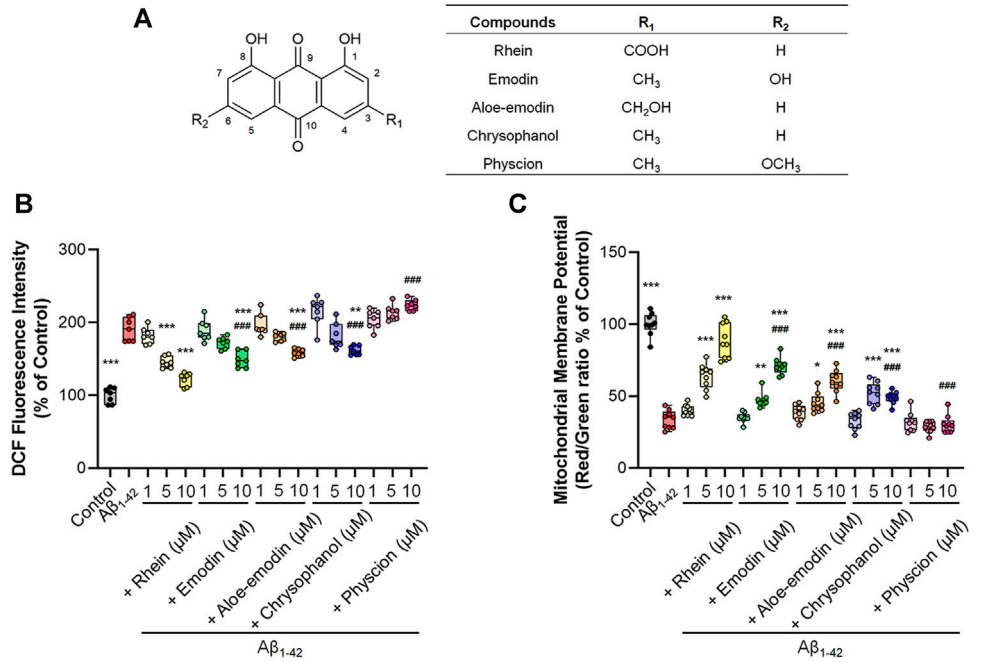


**FIGURE 3 |** The antioxidant effects of the five anthraquinones on primary neurons. Primary neurons were incubated with 5 μM $A\beta_{1-42}$ oligomers and different concentrations of anthraquinones (1, 5 and 10 μM) for 24 h at 37°C, respectively. Untreated primary neurons were the control group, and primary neurons treated with 5 μM $A\beta_{1-42}$ oligomers alone were the $A\beta_{1-42}$ group. **(A)** The chemical structures of rhein, emodin, aloe-emodin, chrysophanol, and physcion. **(B)** Quantification of intracellular ROS by the fluorescence intensity of DCF and normalization to the control group ($n = 7$). **(C)** Quantification analysis of ΔΨm by the fluorescence intensity of red/green ratio with JC-1 and normalization to the control group ($n = 9$). Data are presented as the mean ± standard deviation (SD). $^{*}p < 0.05$, $^{**}p < 0.01$, $^{***}p < 0.001$ compared with the $A\beta_{1-42}$ group; $^{###}p < 0.001$, compared with the 10 μM rhein group (one-way ANOVA).

10 μM emodin group. Aloe-emodin treatment at doses of 1, 5, and 10 μM reduced intracellular ROS levels by 196, 180, and 159%, respectively. Similar to aloe-emodin, the ROS scavenging effects of chrysophanol at doses of 1, 5, and 10 μM were 215, 181, and 162%, respectively. However, none of the three doses of physcion were able to effectively reduce intracellular ROS levels. The abovementioned results manifested that rhein, emodin, aloe-emodin, and chrysophanol could alleviate intracellular oxidative stress to varying degrees, with the exception of physcion.

The difference in antioxidant activity among the five anthraquinones was analyzed under the same condition, by comparing emodin, aloe-emodin, chrysophanol, and physcion with rhein at the same dose of 10 μM. Statistical analyses and the tendency of ROS to alleviate oxidative stress showed that the comparison for antioxidant activities of the five anthraquinones was rhein > emodin > aloe-emodin > chrysophanol > physcion.

JC-1 was used as an indicator to detect the intracellular ΔΨm. **Figure 3C** and **Supplementary Figure 3** illustrated the results of ΔΨm. With the exception of physcion, which did not alleviate oxidative stress, the other four anthraquinones restored ΔΨm to varying degrees. The 1 μM rhein slightly increased the ΔΨm and the difference was insignificant. The 10 μM rhein increased the ΔΨm to 89%, and different doses presented a distinct dose-dependent increase. The effects of emodin and aloe-emodin were similar, also manifesting a dose-dependent increase with the strongest effects occurring at the dose of 10 μM (71 and 60%, respectively). The effect of the 5 μM chrysophanol on ΔΨm was stronger than that of 1 μM but was not significantly different from that of 10 μM.

Likewise, the intensity difference of the recovery effect among the five anthraquinones on ΔΨm was analyzed by comparing emodin, aloe-emodin, chrysophanol, and physcion with rhein at the same dose of 10 μM. Statistical analyses showed that the comparison for the effects of the five anthraquinones was rhein > emodin > aloe-emodin > chrysophanol > physcion.

## Molecular Docking Simulation and Structure-activity Relationship Analysis

SIRT1-dependent deacetylation of PGC-1α promotes mitochondrial biogenesis, which can repair the function of the neuronal mitochondrial respiratory chain and increase the level of antioxidant enzymes, thereby synergically alleviating Aβ-induced oxidative stress (Lagouge et al., 2006; Li et al., 2020; Lu et al., 2020). Under the oxidative stress in AD, the expression levels of both SIRT1 and PGC-1α are reduced, leading to impaired mitochondrial biogenesis. Hence, oxidative stress in neurons cannot be alleviated (Qin et al., 2009; Sheng et al., 2012). Here, to compare the impact of the structural differences of the five anthraquinones on their antioxidant activity, SIRT1 was selected as the potential receptor protein to study the structure-activity relationship by molecular docking.

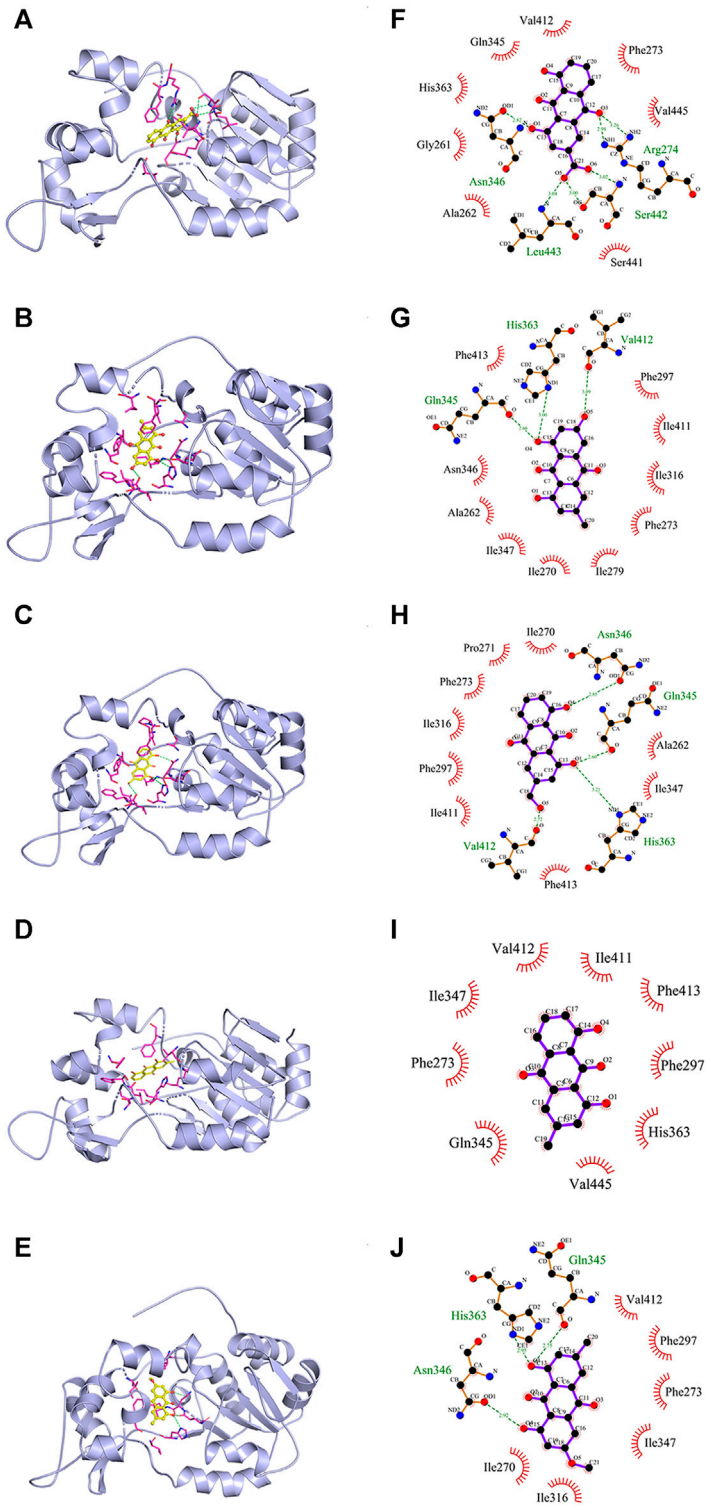


**FIGURE 4 |** The molecular simulation between five anthraquinones and SIRT1 (PDB code: 4I5I). **(A-E)** Rhein, emodin, aloe-emodin, chrysophanol, and physcion in the active site of SIRT1. **(F-J)** The binding modes of the five ligands with receptor SIRT1. Green dotted line: H-bonds; red arc: hydrophobic interaction.

**TABLE 1 |** Binding affinity of the five anthraquinones with SIRT1.

| Ligands | Binding energy (kcal/mol) | H-bonds | | Hydrophobic interaction | |
|---|---|---|---|---|---|
| | | Number | Interacting residues | Number | Interacting residues |
| Rhein | −9.4 | 6 | Arg274, Ser442, Asn346, Leu443 | 8 | His363, Gly261, Ala262, Ser441, Val445, Phe273, Val412, Gln345 |
| Emodin | −9.1 | 3 | His363, Gln345, Val412 | 10 | Phe413, Phe297, Ile411, Ile316, Phe273, Ile279, Ile270, Ile347, Ala262, Asn346 |
| Aloe-emodin | −8.8 | 4 | Asn346, Gln345, His363, Val412 | 9 | Ile270, Pro271, Phe273, Ile316, Phe297, Ile411, Phe413, Ile347, Ala262 |
| Chrysophanol | −9.0 | — | — | 9 | Val412, Ile347, Phe273, Gln345, Val445, His363, Phe297, Phe413, Ile411 |
| Physcion | −8.8 | 3 | Gln345, His363, Asn346 | 6 | Val412, Phe297, Phe273, Ile347, Ile316, Ile270 |

First of all, SIRT1 was taken as the receptor protein (PDB code: 4I5I) to analyze its binding capacity to anthraquinones. As shown in **Figures 4A–E**, all the five anthraquinones were directly bound to SIRT1 and occupied its active site, indicating that anthraquinones could interact with SIRT1. As shown in **Table 1**, the binding energy between rhein, emodin, aloe-emodin, chrysophanol, and physcion and SIRT1 was −9.4, −9.1, −8.8, −9.0, and −8.8 kcal/mol, respectively. Among them, the binding capacity between rhein and SIRT1 was the strongest, followed by emodin and chrysophanol, while the binding capacity of aloe-emodin was relatively weaker and equivalent to that of physcion.

Subsequently, the effect of substituents of anthraquinones on the binding capacity to SIRT1 was further compared by analyzing the binding mode. As shown in **Figures 4F–J** and **Table 1**, hydrogen bonds and hydrophobic interactions existed between SIRT1 and the five anthraquinones, which jointly determined the binding stability of the receptor-ligand. In terms of hydrophobicity, since the five anthraquinones shared the same hydrophobic structure of 1,8-dihydroxyanthraquinone, they all formed corresponding hydrophobic interactions with different amino acid residues on SIRT1, and different substituents had little effect on the number of residues of hydrophobic interactions. In contrast, the substituents had a noticeable effect on the number of hydrogen bonds. Rhein formed six hydrogen bonds with residues Arg274, Ser442, Asn346, and Leu443 in the active site of SIRT1. Among them, the carboxyl group at position-3 contributed three hydrogen bonds. Emodin formed three hydrogen bonds with His363, Gln345, and Val412, and the phenolic hydroxyl group at position-6 contributed one hydrogen bond. Aloe-emodin formed four hydrogen bonds with Asn346, Gln345, His363, and Val412. Among them, the hydroxymethyl group at position-3 contributed one hydrogen bond. Due to the lack of hydrogen bond donor or acceptor on the methyl group at position-3, chrysophanol did not form a stable hydrogen bond with SIRT1. Thus, chrysophanol was bound to SIRT1 only through the hydrophobic interactions. The electron distribution in the oxygen atom environment of methoxyl group at position-6 in physcion was in the homogeneous distribution, which impeded the formation of hydrogen bonds with residues in the active site; so, it did not contribute any hydrogen bonds.

The abovementioned results suggested that the polar substituents of anthraquinones (i.e., carboxyl, phenolic hydroxyl, and hydroxymethyl) were dominant groups and enhanced the binding capacity or binding stability with SIRT1. This finding was consistent with the experimental results on antioxidant activity.

## Rhein Inhibited Cell Apoptosis Induced by Mitochondrial Oxidative Stress

Mitochondrial oxidative stress can induce neuronal oxidative damage and apoptosis. Encouraged by the excellent antioxidant activity of rhein, we further confirmed the role of rhein in neuroprotection by alleviating mitochondrial oxidative stress. Annexin V-FITC/PI double staining assay was performed to evaluate the effect of rhein on neuronal apoptosis. As shown in **Figure 5A**, compared with the control group, the green and red fluorescence intensity in the $A\beta_{1\text{-}42}$ group was greatly enhanced, indicating that the neuronal cells were undergoing early and late apoptosis, respectively. Interestingly, compared with the $A\beta_{1\text{-}42}$ group, rhein reversed apoptosis. The 10 μM rhein significantly reduced the intracellular green and red fluorescence intensity. The abovementioned results proved that rhein could inhibit the apoptosis of primary neurons by relieving oxidative stress.

Oxidative stress can damage the ultrastructural integrity of mitochondria. Cyto c, an apoptotic factor, is released from the inner mitochondrial membrane to activate procaspase 3 into cleaved caspase 3, which induces the apoptosis cascade. This is a critical pathological process for the loss of neuronal synapses (Ye et al., 2013). To investigate the mechanism underlying anti-apoptosis by rhein, the expression levels of cyto c in the cytosol and cleaved caspase 3 in primary neurons were evaluated by western blotting. The results are shown in **Figures 5B,C**. Because $A\beta_{1\text{-}42}$ induced oxidative damage in mitochondria, the expression of cytosolic cyto c in the $A\beta_{1\text{-}42}$ group significantly increased. Impressively, after treatment with rhein, the level of overexpressed cytosolic cyto c decreased, indicating that rhein reduced the release of cyto c from mitochondria. The expression level of cleaved caspase 3 is shown in **Figures 5D,E**. Compared with the control group, the level of cleaved caspase 3 in the $A\beta_{1\text{-}42}$ group was significantly increased, suggesting that the apoptosis cascade was activated. By contrast, rhein inhibited the level of overexpressed cleaved caspase 3. As shown by the above results, rhein inhibited the release of cyto c from mitochondria by relieving oxidative damage in mitochondria to prevent the

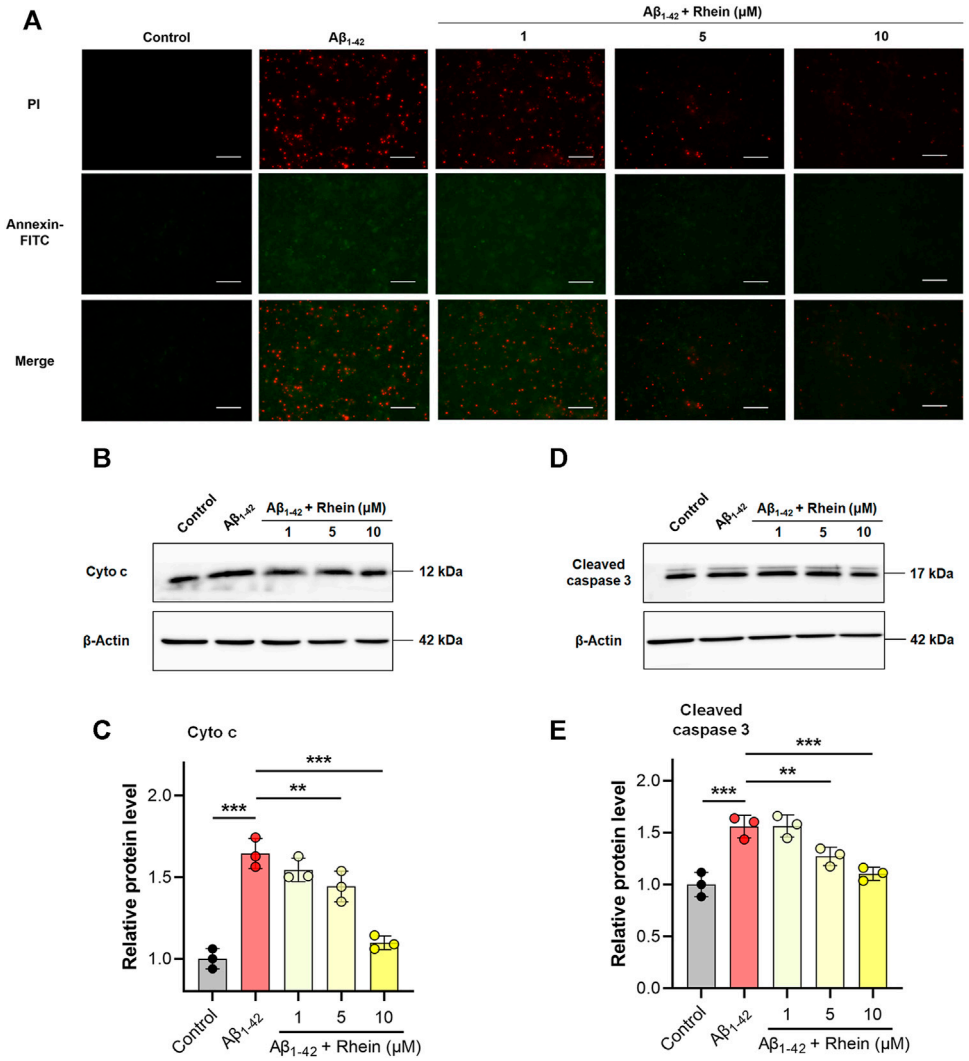


**FIGURE 5 |** Rhein inhibited mitochondrial oxidative stress-associated apoptosis in primary neurons induced by $A\beta_{1\text{-}42}$ oligomers. Primary neurons were incubated with 5 μM $A\beta_{1\text{-}42}$ oligomers and rhein at different doses (1, 5 and 10 μM) for 24 h at 37°C, respectively. Untreated primary neurons were the control group, and primary neurons treated with 5 μM $A\beta_{1\text{-}42}$ oligomers alone were the $A\beta_{1\text{-}42}$ group. **(A)** Representative images of Annexin V-FITC/propidium iodide (PI) double staining. Annexin V-FITC stains early apoptotic cells; PI stains late apoptotic cells. Scale bars: 50 μm. **(B)** Representative western blot images of cytosolic cytochrome c (cyto c). **(C)** Relative expression level of cytosolic Cyto c and normalization to β-Actin ($n = 3$). **(D)** Representative western blot images of cleaved caspase 3. **(E)** Relative expression level of cleaved caspase 3 and normalization to β-Actin ($n = 3$). Data are presented as the mean ± standard deviation (SD). $^{**}p < 0.01$ and $^{***}p < 0.001$ compared with the $A\beta_{1\text{-}42}$ group (one-way ANOVA).

activation of the apoptosis cascade and ultimately avoid neuronal apoptosis.

## Rhein Increased the Activities of Mitochondrial CytOx and SOD

Considering that oxidative stress can be effectively alleviated through mitochondrial biogenesis, we focused on the effects of rhein on enzymes related to mitochondrial biogenesis, such as CytOx in the mitochondrial respiratory complex IV and antioxidant enzyme SOD. First, the activity of CytOx was evaluated. As shown in **Figure 6A**, compared with the control group, $A\beta_{1\text{-}42}$ damaged the mitochondrial electron transport chain and diminished the activity of CytOx. After treatment with rhein, the activity of CytOx increased. The effect of the 10 μM rhein group was close to that of the control group. Then, the antioxidant capacity of mitochondria was evaluated by detecting SOD activity, a mitochondria-related antioxidant enzyme. As shown in **Figure 6B**, the activity of SOD decreased in the $A\beta_{1\text{-}42}$ group; thus, the antioxidant capacity of primary neurons was reduced as well. Notably, rhein improved the activity of SOD. These results revealed that rhein not only repaired the mitochondrial electron transport chain to inhibit the production of ROS but also improved the activity of mitochondrial antioxidant enzymes by activating the mitochondrial antioxidant defense system, thus enhancing

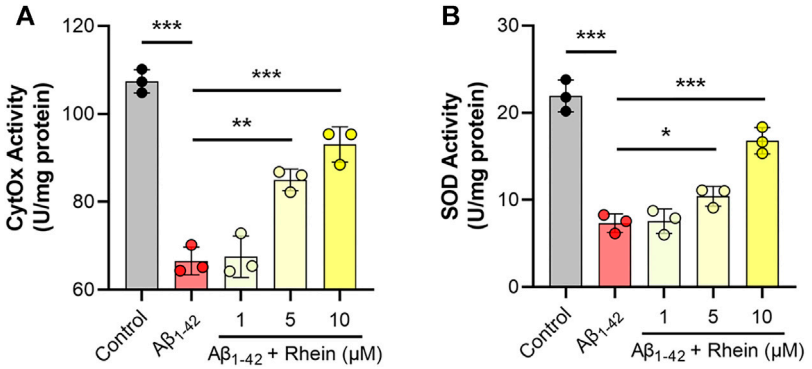


**FIGURE 6 |** Rhein increased the activities of mitochondrial cytochrome C oxidase (CytOx) and superoxide dismutase (SOD). Primary neurons were incubated with 5 μM $A\beta_{1\text{-}42}$ oligomers and rhein at different doses (1, 5 and 10 μM) for 24 h at 37°C, respectively. Untreated primary neurons were the control group, and primary neurons treated with 5 μM $A\beta_{1\text{-}42}$ oligomers alone were the $A\beta_{1\text{-}42}$ group. The effects of rhein on the activities of **(A)** CytOx and **(B)** SOD ($n = 3$). Data are presented as the mean ± standard deviation (SD). $^{*}p < 0.05$, $^{**}p < 0.01$ and $^{***}p < 0.001$ compared with the $A\beta_{1\text{-}42}$ group (one-way ANOVA).

the elimination of intracellular ROS, which might be related to the improvement of mitochondrial biogenesis.

## Rhein Improved Mitochondrial Biogenesis by Activating the SIRT1/PGC-1α Pathway

The SIRT1/PGC-1α pathway is critical for mitochondrial biogenesis. To further validate the regulatory mechanism of rhein for mitochondrial biogenesis, the expression levels of SIRT1 and PGC-1α were detected by western blotting. Compared with the control group, the expression level of SIRT1 was significantly decreased in the $A\beta_{1\text{-}42}$ group. As expected, rhein effectively reversed the decreased expression of SIRT1 (**Figures 7A,B**). Also, $A\beta_{1\text{-}42}$ reduced the expression of PGC-1α, indicating that SIRT1/PGC-1α was inhibited in the Aβ-burdened neuronal model (**Figures 7C,D**). After treatment with rhein, the expression level of PGC-1α was significantly increased. Hence, rhein was able to activate the SIRT1/PGC-1α pathway. In addition, the expression level of NRF1, a downstream transcription factor related to mitochondrial biogenesis, was also detected. The results are shown in **Figures 7C,E**. In the $A\beta_{1\text{-}42}$ group, because of the dysfunction of mitochondrial biogenesis, the expression level of NRF1 decreased. Rhein induced the expression of NRF1 by activating the SIRT1/PGC-1α pathway. It could be concluded that rhein could restore the function of mitochondrial biogenesis to alleviate oxidative stress in primary neurons by increasing the expression of SIRT1, PGC-1α, and NRF1.

# DISCUSSION

Neuronal oxidative stress induced by Aβ is an important pathological feature of AD. High ROS level derived from mitochondrial induces neuronal apoptosis (Lustbader et al., 2004; Petersen et al., 2008). Meanwhile, ROS accelerates the progression of AD by increasing the production and accumulation of Aβ (Takuma et al., 2009; Borger et al., 2013). Thus, introducing antioxidants to relieve oxidative stress is an effective therapeutic strategy for AD. 1,8-dihydroxyanthraquinone derivatives including rhein, emodin, aloe-emodin, chrysophanol, and physcion have garnered widespread attention as antioxidative components. Thus, screening of antioxidants from anthraquinones is extremely promising for the antioxidant therapy of AD. Herein, a comparative analysis of the antioxidant activity of the five anthraquinones was carried out using an $A\beta_{1\text{-}42}$ oligomer-induced oxidative stress model based on primary cultured neurons. Among all the five anthraquinones, rhein possessed excellent antioxidant activity and was selected to explore its mechanism of alleviating oxidative stress.

With the progression of AD, accumulated Aβ monomers gradually aggregate and form oligomers, protofibrils, fibrils, and finally senile plaques (Kung, 2012; Wang et al., 2015). The latest β-amyloid cascade hypothesis suggests that Aβ in the oligomeric form is the earliest culprit of AD (Lacor et al., 2004; Staderini et al., 2015; Lee et al., 2017). To establish a drug screening platform that is similar to the *in vivo* pathological environment of oxidative stress in AD, the preparation of toxic Aβ was examined firstly on primary neurons. By combining CD with the ThT assay, the kinetic process of Aβ aggregation was described with β-sheets as the characteristic structure. Then, the correlation between the aggregation form of Aβ and cytotoxicity was analyzed. The results indicated Aβ oligomers incubated for 24 h caused the most damage to the primary neurons, while Aβ monomers or fibrils prepared *in vitro* were less toxic. TEM analysis further confirmed the formation of Aβ oligomers. These findings are consistent with recent researches (Wang-Dietrich et al., 2013; Shea et al., 2019). After incubation with $A\beta_{1\text{-}42}$ oligomers, the primary neurons exhibited high ROS level and depletion of $\Delta\Psi m$, verifying that a mitochondrial oxidative stress cell model was successfully established.

For comparative analysis of antioxidant activities of five anthraquinones, we used aforementioned $A\beta_{1\text{-}42}$ oligomer-induced primary neurons as an *in vitro* oxidative stress model.

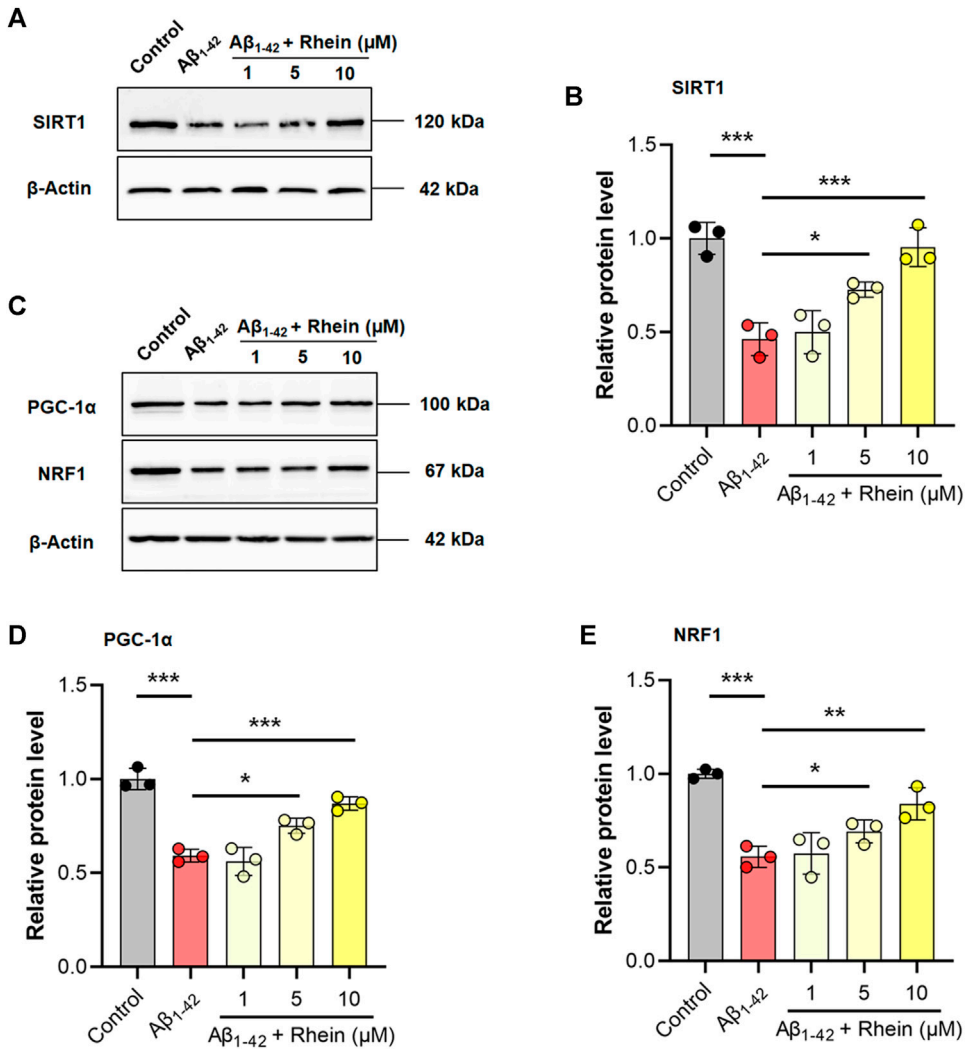


**FIGURE 7 |** Rhein enhanced mitochondrial biogenesis by activating the SIRT1/PGC-1α pathway. Primary neurons were incubated with 5 μM $A\beta_{1\text{-}42}$ oligomers and rhein at different doses (1, 5 and 10 μM) for 24 h at 37°C, respectively. Untreated primary neurons were the control group, and primary neurons treated with 5 μM $A\beta_{1\text{-}42}$ oligomers alone were the $A\beta_{1\text{-}42}$ group. **(A)** Representative western blot images of SIRT1. **(B)** Relative expression level of SIRT1 and normalization to β-Actin ($n = 3$). **(C)** Representative western blotting images of PGC-1α and NRF1. **(D)** Relative expression level of PGC-1α and normalization to β-Actin ($n = 3$). **(E)** Relative expression level of NRF1 and normalization to β-Actin ($n = 3$). Data are presented as the group mean ± standard deviation (SD). $^*p < 0.05$, $^{**}p < 0.01$ and $^{***}p < 0.001$ compared with the $A\beta_{1\text{-}42}$ group (one-way ANOVA).

The results suggested that rhein, emodin, aloe-emodin, and chrysophanol reduced intracellular ROS levels to varying degrees in a dose-dependent manner, with the exception of physcion. As expected, rhein, emodin, aloe-emodin, and chrysophanol effectively restored ΔΨm, except physcion. These results indicate that the comparison for antioxidant activities of the five anthraquinones is: rhein > emodin > aloe-emodin > chrysophanol > physcion. To theoretically elucidate the effects of the structural differences of the five anthraquinones on the antioxidant activity, molecular docking was performed to compare the binding mode between anthraquinones and the receptor protein SIRT1. The results showed that rhein, emodin, aloe-emodin, chrysophanol, and physcion were directly bound to the active site of SIRT1. Among them, rhein showed the relatively lower binding energy of −9.4, indicating a better binding capacity with SIRT1. Furthermore, the binding mode showed that the carboxyl group on rhein formed more hydrogen bonds with amino acid residues and increased the stability of the rhein-SIRT1 complex. These findings might partly explain why rhein exhibited excellent antioxidant activity against oxidative stress induced by $A\beta_{1\text{-}42}$ oligomers.

Ongoing oxidative stress can trigger apoptosis cascade and induce neuronal apoptosis. When neuronal mitochondria undergo oxidative damage, the apoptosis factor, cyto c, is released from the opened mPTP into the cytosol. Then, procaspase 3 is activated into cleaved caspase 3 by cyto c, which induces the downstream apoptosis cascade and

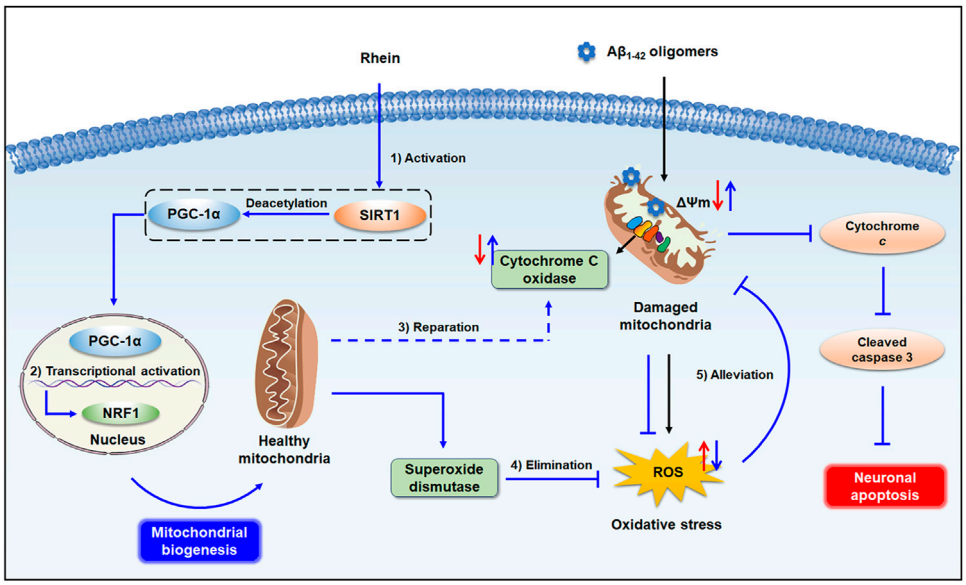


**FIGURE 8 |** Schematic illustration of mitochondrial endogenous antioxidant defense system triggered by rhein. 1). Rhein activated the SIRT1/PGC-1α pathway by increasing the expression levels of SIRT1 and PGC-1α. 2). The PGC-1α in the nucleus activated the downstream transcription factor NRF1, and healthy mitochondria were generated by promoted mitochondrial biogenesis. 3). Newly generated healthy mitochondria restored the decreased activity of CytOx in mitochondrial respiratory chain complex IV induced by $A\beta_{1\text{-}42}$ oligomers, inhibiting the production of ROS. 4). mitochondrial SOD effectively facilitated the elimination of excess ROS. 5). Rhein alleviated the mitochondrial oxidative damage, inhibited the caspase 3-related apoptosis cascade by reducing the release of cyto c from mitochondria, and ultimately, protected neurons from apoptosis.

neuronal apoptosis irreversibly (Bonda et al., 2014). Annexin V-FITC/PI staining showed that the number of neuronal cells with early apoptosis (green fluorescence) and late apoptosis (red fluorescence) was significantly increased in the $A\beta_{1\text{-}42}$ group, indicating neuronal apoptosis occurred (**Figure 5A**). After treatment with rhein, the number of apoptotic neurons was effectively reduced. According to the western blot analysis, there was the overexpression of cytosolic cyto c and cleaved caspase 3 in the $A\beta_{1\text{-}42}$ group. Interestingly, the levels of cytosolic cyto c and cleaved caspase 3 were reversed after rhein treatment. Thus, rhein reduced the release of cyto c from mitochondria, inhibiting the apoptosis cascade and ultimately protecting neurons from apoptosis.

Neuronal oxidative stress is closely related to mitochondrial dysfunction. Mitochondrial biogenesis is an intracellular antioxidative defense system, in which cells maintain healthy mitochondrial function by producing new mitochondria. Newly generated mitochondria repair the respiratory chain complexes by mitochondrial fusion and further prevent electron leakage, thereby inhibiting the continuous production of ROS. In addition, the increased synthesis of antioxidant enzymes in mitochondria can effectively remove the accumulated ROS to maintain mitochondrial redox homeostasis (Venditti et al., 2013). Under the oxidative stress induced by Aβ, mitochondrial biogenesis is blocked. The activities of enzymes in mitochondrial respiratory chain complexes and antioxidant enzymes decrease, and the antioxidant defense system is also destroyed. Indeed, in this study, it was found that the activity of CytOx, an enzyme in respiratory chain complex IV, was significantly reduced in the mitochondria of primary neurons damaged by $A\beta_{1\text{-}42}$ oligomers (Atamna and Frey, 2004; Atamna et al., 2009). However, the activity of CytOx increased after treatment with rhein, indicating that the activity of enzymes in the respiratory chain was improved, which helped to reduce ROS production. Due to the impairment of mitochondrial function caused by $A\beta_{1\text{-}42}$ oligomers, the activity of SOD, the main enzyme of mitochondrial antioxidants, was greatly reduced, making mitochondria unable to resist the existing oxidative stress. By contrast, SOD activity was significantly increased under the treatment of rhein, so that mitochondria could effectively remove the existing ROS. The results showed that rhein played a positive role in regulating both the enzymes in mitochondrial respiratory chain complexes and antioxidant enzymes, suggesting that it may be beneficial to improve mitochondrial biogenesis.

The SIRT1/PGC-1α pathway plays a crucial role in mitochondrial biogenesis. SIRT1, a deacetylase, is responsible for the deacetylation and activation of PGC-1α. PGC-1α, an important regulator of mitochondrial biogenesis, activates the downstream transcription factors NRF-1, NRF-2, and TFAM, and initiates the transcription and replication of mtDNA. Therefore, the expression of SIRT1 and PGC-1α is closely related to the self-repair of mitochondria and synthesis of antioxidant enzymes (St-Pierre et al., 2006; Kang et al., 2017). To explore the mechanism underlying the activation of mitochondrial biogenesis by rhein, the expression of related

proteins was evaluated by western blot analysis. The results confirmed that mitochondrial biogenesis was impaired by $A\beta_{1-42}$ oligomers accompanied by the reduced expression levels of SIRT1, PGC-1α, and downstream transcription factor NRF1. As a result, after treatment with rhein, the expression levels of SIRT1 and PGC-1α were significantly increased, indicating that the SIRT1/PGC-1α pathway was activated. Meanwhile, the increased expression of NRF1 confirmed that rhein was involved in the regulation of mitochondrial biogenesis. Hence, the activation of SIRT1/PGC-1α-mediated mitochondrial biogenesis by rhein might be a key mechanism for triggering the mitochondrial antioxidant defense system (**Figure 8**).

In summary, we used an AD-like neuronal oxidative stress model induced by $A\beta_{1-42}$ oligomers to screen the antioxidant activities of the five anthraquinones, including rhein, emodin, aloe-emodin, chrysophanol, and physcion. According to the results of intracellular ROS and ΔΨm, rhein exhibited outstanding antioxidant activity and inhibited oxidative stress-associated neuronal apoptosis. More importantly, rhein activated mitochondrial biogenesis as an endogenous antioxidant defense system against $A\beta_{1-42}$ oligomer-induced oxidative stress. That is to say, CytOx in the respiratory chain complex IV inhibited the production of ROS from electron leakage and SOD helped to eliminate superfluous ROS by promoted mitochondrial biogenesis. Western blot analysis further confirmed that the SIRT1/PGC-1α pathway activated by rhein was a potential antioxidant pathway involved. Taken together, our results provide evidence that rhein activates mitochondrial biogenesis regulated by the SIRT1/PGC-1α pathway as an antioxidant defense system against $A\beta_{1-42}$ oligomer-induced oxidative stress. This study contributes to the fundamental research for the antioxidant therapy of AD.

## DATA AVAILABILITY STATEMENT

The original contributions presented in the study are included in the article/**Supplementary Material**, further inquiries can be directed to the corresponding authors.

## AUTHOR CONTRIBUTIONS

XGa designed the research. ZY and XGe performed the experiments. XGe and ZZ analysed the data. ZY and YW wrote the paper. XGa and YW reviewed and edited the draft.

## FUNDING

This work was supported by the National Natural Science Foundation of China (81973467/H2803) and the Fundamental Research Funds for the Central Universities (2020-JYB-ZDGG-033).

## SUPPLEMENTARY MATERIAL

The Supplementary Material for this article can be found online at: https://www.frontiersin.org/articles/10.3389/fphar.2021.746711/full#supplementary-material

## REFERENCES

Alzheimer's Association (2021). 2021 Alzheimer's Disease Facts and Figures. *Alzheimers Dement* 17 (3), 327–406. doi:10.1002/alz.12328

Aquilano, K., Baldelli, S., Pagliei, B., and Ciriolo, M. R. (2013). Extranuclear Localization of SIRT1 and PGC-1α: an Insight into Possible Roles in Diseases Associated with Mitochondrial Dysfunction. *Curr. Mol. Med.* 13 (1), 140–154. doi:10.2174/156652413804486241

Atamna, H., and Frey, W. H. (2004). A Role for Heme in Alzheimer's Disease: Heme Binds Amyloid Beta and Has Altered Metabolism. *Proc. Natl. Acad. Sci. U. S. A.* 101 (30), 11153–11158. doi:10.1073/pnas.0404349101

Atamna, H., Frey, W. H., and Ko, N. (2009). Human and Rodent Amyloid-Beta Peptides Differentially Bind Heme: Relevance to the Human Susceptibility to Alzheimer's Disease. *Arch. Biochem. Biophys.* 487 (1), 59–65. doi:10.1016/j.abb.2009.05.003

Battogtokh, G., Choi, Y. S., Kang, D. S., Park, S. J., Shim, M. S., Huh, K. M., et al. (2018). Mitochondria-targeting Drug Conjugates for Cytotoxic, Anti-oxidizing and Sensing Purposes: Current Strategies and Future Perspectives. *Acta Pharm. Sin. B* 8 (6), 862–880. doi:10.1016/j.apsb.2018.05.006

Bonda, D. J., Wang, X., Lee, H. G., Smith, M. A., Perry, G., and Zhu, X. (2014). Neuronal Failure in Alzheimer's Disease: A View through the Oxidative Stress Looking-Glass. *Neurosci. Bull.* 30 (2), 243–252. doi:10.1007/s12264-013-1424-x

Borger, E., Aitken, L., Muirhead, K. E., Allen, Z. E., Ainge, J. A., Conway, S. J., et al. (2011). Mitochondrial β-amyloid in Alzheimer's Disease. *Biochem. Soc. Trans.* 39, 868–873. doi:10.1042/bst0390868

Borger, E., Aitken, L., Du, H., Zhang, W., Gunn-Moore, F. J., and Yan, S. S. (2013). Is Amyloid Binding Alcohol Dehydrogenase a Drug Target for Treating Alzheimer's Disease? *Curr. Alzheimer Res.* 10 (1), 21–29. doi:10.2174/156720513804871381

Cantó, C., Gerhart-Hines, Z., Feige, J. N., Lagouge, M., Noriega, L., Milne, J. C., et al. (2009). AMPK Regulates Energy Expenditure by Modulating NAD+ Metabolism and SIRT1 Activity. *Nature* 458 (7241), 1056–1060. doi:10.1038/nature07813

Chami, L., and Checler, F. (2012). BACE1 Is at the Crossroad of a Toxic Vicious Cycle Involving Cellular Stress and β-amyloid Production in Alzheimer's Disease. *Mol. Neurodegener.* 7, 52. doi:10.1186/1750-1326-7-52

Dhar, S. S., Ongwijitwat, S., and Wong-Riley, M. T. (2008). Nuclear Respiratory Factor 1 Regulates All Ten Nuclear-Encoded Subunits of Cytochrome C Oxidase in Neurons. *J. Biol. Chem.* 283 (6), 3120–3129. doi:10.1074/jbc.M707587200

Dong, Y. T., Cao, K., Tan, L. C., Wang, X. L., Qi, X. L., Xiao, Y., et al. (2018). Stimulation of SIRT1 Attenuates the Level of Oxidative Stress in the Brains of APP/PS1 Double Transgenic Mice and in Primary Neurons Exposed to Oligomers of the Amyloid-β Peptide. *J. Alzheimers Dis.* 63 (1), 283–301. doi:10.3233/jad-171020

Du, F., Yu, Q., Yan, S., Hu, G., Lue, L. F., Walker, D. G., et al. (2017). PINK1 Signalling Rescues Amyloid Pathology and Mitochondrial Dysfunction in Alzheimer's Disease. *Brain* 140, 3233–3251. doi:10.1093/brain/awx258

Fontana, I. C., Zimmer, A. R., Rocha, A. S., Gosmann, G., Souza, D. O., Lourenco, M. V., et al. (2020). Amyloid-β Oligomers in Cellular Models of Alzheimer's Disease. *J. Neurochem.* 155 (4), 348–369. doi:10.1111/jnc.15030

Ganguly, G., Chakrabarti, S., Chatterjee, U., and Saso, L. (2017). Proteinopathy, Oxidative Stress and Mitochondrial Dysfunction: Cross Talk in Alzheimer's Disease and Parkinson's Disease. *Drug Des. Devel Ther.* 11, 797–810. doi:10.2147/dddt.S130514

Gao, Z., Zhang, J., Kheterpal, I., Kennedy, N., Davis, R. J., and Ye, J. (2011). Sirtuin 1 (SIRT1) Protein Degradation in Response to Persistent C-Jun N-Terminal Kinase 1 (JNK1) Activation Contributes to Hepatic Steatosis in Obesity. *J. Biol. Chem.* 286 (25), 22227–22234. doi:10.1074/jbc.M111.228874

Haass, C., and Selkoe, D. J. (2007). Soluble Protein Oligomers in Neurodegeneration: Lessons from the Alzheimer's Amyloid Beta-Peptide. *Nat. Rev. Mol. Cel Biol.* 8 (2), 101–112. doi:10.1038/nrm2101

Ho, S.-L., Poon, C.-Y., Lin, C., Yan, T., Kwong, D., Yung, K., et al. (2015). Inhibition of β-Amyloid Aggregation by Albiflorin, Aloeemodin and Neohesperidin and Their Neuroprotective Effect on Primary Hippocampal Cells against β-Amyloid Induced Toxicity. *Car* 12 (5), 424–433. doi:10.2174/1567205012666150504144919

Kang, H., Khang, R., Ham, S., Jeong, G. R., Kim, H., Jo, M., et al. (2017). Activation of the ATF2/CREB-PGC-1α Pathway by Metformin Leads to Dopaminergic Neuroprotection. *Oncotarget* 8 (30), 48603–48618. doi:10.18632/oncotarget.18122

Katsouri, L., Lim, Y. M., Blondrath, K., Eleftheriadou, I., Lombardero, L., Birch, A. M., et al. (2016). PPARγ-coactivator-1α Gene Transfer Reduces Neuronal Loss and Amyloid-β Generation by Reducing β-secretase in an Alzheimer's Disease Model. *Proc. Natl. Acad. Sci. USA* 113 (43), 12292–12297. doi:10.1073/pnas.1606171113

Kume, S., Uzu, T., Horiike, K., Chin-Kanasaki, M., Isshiki, K., Araki, S., et al. (2010). Calorie Restriction Enhances Cell Adaptation to Hypoxia through Sirt1-dependent Mitochondrial Autophagy in Mouse Aged Kidney. *J. Clin. Invest.* 120 (4), 1043–1055. doi:10.1172/jci41376

Kung, H. F. (2012). The β-Amyloid Hypothesis in Alzheimer's Disease: Seeing Is Believing. *ACS Med. Chem. Lett.* 3 (4), 265–267. doi:10.1021/ml300058m

Lacor, P. N., Buniel, M. C., Chang, L., Fernandez, S. J., Gong, Y., Viola, K. L., et al. (2004). Synaptic Targeting by Alzheimer's-Related Amyloid Beta Oligomers. *J. Neurosci.* 24 (45), 10191–10200. doi:10.1523/jneurosci.3432-04.2004

Lagouge, M., Argmann, C., Gerhart-Hines, Z., Meziane, H., Lerin, C., Daussin, F., et al. (2006). Resveratrol Improves Mitochondrial Function and Protects against Metabolic Disease by Activating SIRT1 and PGC-1alpha. *Cell* 127 (6), 1109–1122. doi:10.1016/j.cell.2006.11.013

Lee, S. J., Nam, E., Lee, H. J., Savelieff, M. G., and Lim, M. H. (2017). Towards an Understanding of Amyloid-β Oligomers: Characterization, Toxicity Mechanisms, and Inhibitors. *Chem. Soc. Rev.* 46 (2), 310–323. doi:10.1039/c6cs00731g

Li, B., Liu, J., Gu, G., Han, X., Zhang, Q., and Zhang, W. (2020). Impact of Neural Stem Cell-Derived Extracellular Vesicles on Mitochondrial Dysfunction, Sirtuin 1 Level, and Synaptic Deficits in Alzheimer's Disease. *J. Neurochem.* 154 (5), 502–518. doi:10.1111/jnc.15001

Li, Z., Bi, H., Jiang, H., Song, J., Meng, Q., Zhang, Y., et al. (2021). Neuroprotective Effect of Emodin against Alzheimer's Disease via Nrf2 Signaling in U251 Cells and APP/PS1 Mice. *Mol. Med. Rep.* 23 (2), 108. doi:10.3892/mmr.2020.11747

Liao, L. X., Wang, J. K., Wan, Y. J., Liu, Y., Dong, X., Tu, P. F., et al. (2020). Protosappanin A Maintains Neuronal Mitochondrial Homeostasis through Promoting Autophagic Degradation of Bax. *ACS Chem. Neurosci.* 11 (24), 4223–4230. doi:10.1021/acschemneuro.0c00488

Lin, M. T., and Beal, M. F. (2006). Mitochondrial Dysfunction and Oxidative Stress in Neurodegenerative Diseases. *Nature* 443 (7113), 787–795. doi:10.1038/nature05292

Lopes, F. M., da Motta, L. L., De Bastiani, M. A., Pfaffenseller, B., Aguiar, B. W., de Souza, L. F., et al. (2017). RA Differentiation Enhances Dopaminergic Features, Changes Redox Parameters, and Increases Dopamine Transporter Dependency in 6-Hydroxydopamine-Induced Neurotoxicity in SH-SY5Y Cells. *Neurotox. Res.* 31 (4), 545–559. doi:10.1007/s12640-016-9699-0

Lu, K., Zhang, C., Wu, W., Zhou, M., Tang, Y., and Peng, Y. (2015). Rhubarb Extract Has a Protective Role against Radiation-Induced Brain Injury and Neuronal Cell Apoptosis. *Mol. Med. Rep.* 12 (2), 2689–2694. doi:10.3892/mmr.2015.3693

Lu, J., Huang, Q., Zhang, D., Lan, T., Zhang, Y., Tang, X., et al. (2020). The Protective Effect of DiDang Tang against AlCl3-Induced Oxidative Stress and Apoptosis in PC12 Cells through the Activation of SIRT1-Mediated Akt/Nrf2/HO-1 Pathway. *Front. Pharmacol.* 11, 466. doi:10.3389/fphar.2020.00466

Lustbader, J. W., Cirilli, M., Lin, C., Xu, H. W., Takuma, K., Wang, N., et al. (2004). ABAD Directly Links Abeta to Mitochondrial Toxicity in Alzheimer's Disease. *Science* 304 (5669), 448–452. doi:10.1126/science.1091230

Marković, Z., Jeremić, S., Dimitrić Marković, J., Stanojević Pirković, M., and Amić, D. (2016). Influence of Structural Characteristics of Substituents on the Antioxidant Activity of Some Anthraquinone Derivatives. *Comput. Theor. Chem.* 1077, 25–31. doi:10.1016/j.comptc.2015.10.004

Mehan, S., Meena, H., Sharma, D., and Sankhla, R. (2011). JNK: a Stress-Activated Protein Kinase Therapeutic Strategies and Involvement in Alzheimer's and Various Neurodegenerative Abnormalities. *J. Mol. Neurosci.* 43 (3), 376–390. doi:10.1007/s12031-010-9454-6

Menzies, K. J., Singh, K., Saleem, A., and Hood, D. A. (2013). Sirtuin 1-mediated Effects of Exercise and Resveratrol on Mitochondrial Biogenesis. *J. Biol. Chem.* 288 (10), 6968–6979. doi:10.1074/jbc.M112.431155

Misrani, A., Tabassum, S., and Yang, L. (2021). Mitochondrial Dysfunction and Oxidative Stress in Alzheimer's Disease. *Front. Aging Neurosci.* 13, 617588. doi:10.3389/fnagi.2021.617588

Panes, J. D., Godoy, P. A., Silva-Grecchi, T., Celis, M. T., Ramirez-Molina, O., Gavilan, J., et al. (2020). Changes in PGC-1α/SIRT1 Signaling Impact on Mitochondrial Homeostasis in Amyloid-Beta Peptide Toxicity Model. *Front. Pharmacol.* 11, 709. doi:10.3389/fphar.2020.00709

Hansson Petersen, C. A., Alikhani, N., Behbahani, H., Wiehager, B., Pavlov, P. F., Alafuzoff, I., et al. (2008). The Amyloid Beta-Peptide Is Imported into Mitochondria via the TOM Import Machinery and Localized to Mitochondrial Cristae. *Proc. Natl. Acad. Sci. U. S. A.* 105 (35), 13145–13150. doi:10.1073/pnas.0806192105

Piantadosi, C. A., and Suliman, H. B. (2008). Transcriptional Regulation of SDHa Flavoprotein by Nuclear Respiratory Factor-1 Prevents Pseudo-hypoxia in Aerobic Cardiac Cells. *J. Biol. Chem.* 283 (16), 10967–10977. doi:10.1074/jbc.M709741200

Qin, W., Haroutunian, V., Katsel, P., Cardozo, C. P., Ho, L., Buxbaum, J. D., et al. (2009). PGC-1alpha Expression Decreases in the Alzheimer Disease Brain as a Function of Dementia. *Arch. Neurol.* 66 (3), 352–361. doi:10.1001/archneurol.2008.588

Shaerzadeh, F., Motamedi, F., and Khodagholi, F. (2014). Inhibition of Akt Phosphorylation Diminishes Mitochondrial Biogenesis Regulators, Tricarboxylic Acid Cycle Activity and Exacerbates Recognition Memory Deficit in Rat Model of Alzheimer's Disease. *Cell. Mol. Neurobiol.* 34 (8), 1223–1233. doi:10.1007/s10571-014-0099-9

Shea, D., Hsu, C. C., Bi, T. M., Paranjapye, N., Childers, M. C., Cochran, J., et al. (2019). α-Sheet Secondary Structure in Amyloid β-peptide Drives Aggregation and Toxicity in Alzheimer's Disease. *Proc. Natl. Acad. Sci. U. S. A.* 116 (18), 8895–8900. doi:10.1073/pnas.1820585116

Sheng, B., Wang, X., Su, B., Lee, H. G., Casadesus, G., Perry, G., et al. (2012). Impaired Mitochondrial Biogenesis Contributes to Mitochondrial Dysfunction in Alzheimer's Disease. *J. Neurochem.* 120 (3), 419–429. doi:10.1111/j.1471-4159.2011.07581.x

Sinha, S., Lopes, D. H., Du, Z., Pang, E. S., Shanmugam, A., Lomakin, A., et al. (2011). Lysine-specific Molecular Tweezers Are Broad-Spectrum Inhibitors of Assembly and Toxicity of Amyloid Proteins. *J. Am. Chem. Soc.* 133 (42), 16958–16969. doi:10.1021/ja206279b

Sotolongo, K., Ghiso, J., and Rostagno, A. (2020). Nrf2 Activation through the PI3K/GSK-3 axis Protects Neuronal Cells from Aβ-Mediated Oxidative and Metabolic Damage. *Alzheimers Res. Ther.* 12 (1), 13. doi:10.1186/s13195-019-0578-9

Staderini, M., Martín, M. A., Bolognesi, M. L., and Menéndez, J. C. (2015). Imaging of β-amyloid Plaques by Near Infrared Fluorescent Tracers: a New Frontier for Chemical Neuroscience. *Chem. Soc. Rev.* 44 (7), 1807–1819. doi:10.1039/c4cs00337c

St-Pierre, J., Drori, S., Uldry, M., Silvaggi, J. M., Rhee, J., Jäger, S., et al. (2006). Suppression of Reactive Oxygen Species and Neurodegeneration by the PGC-1 Transcriptional Coactivators. *Cell* 127 (2), 397–408. doi:10.1016/j.cell.2006.09.024

Swerdlow, R. H. (2018). Mitochondria and Mitochondrial Cascades in Alzheimer's Disease. *J. Alzheimers Dis.* 62 (3), 1403–1416. doi:10.3233/JAD-170585

Takuma, K., Fang, F., Zhang, W., Yan, S., Fukuzaki, E., Du, H., et al. (2009). RAGE-mediated Signaling Contributes to Intraneuronal Transport of Amyloid-Beta and Neuronal Dysfunction. *Proc. Natl. Acad. Sci. U. S. A.* 106 (47), 20021–20026. doi:10.1073/pnas.0905686106

Tamagno, E., Guglielmotto, M., Monteleone, D., and Tabaton, M. (2012). Amyloid-β Production: Major Link between Oxidative Stress and BACE1. *Neurotox. Res.* 22 (3), 208–219. doi:10.1007/s12640-011-9283-6

Tao, L., Xie, J., Wang, Y., Wang, S., Wu, S., Wang, Q., et al. (2014). Protective Effects of Aloe-Emodin on Scopolamine-Induced Memory Impairment in Mice and $H_2O_2$-induced Cytotoxicity in PC12 Cells. *Bioorg. Med. Chem. Lett.* 24 (23), 5385–5389. doi:10.1016/j.bmcl.2014.10.049

Venditti, P., Di Stefano, L., and Di Meo, S. (2013). Mitochondrial Metabolism of Reactive Oxygen Species. *Mitochondrion* 13 (2), 71–82. doi:10.1016/j.mito.2013.01.008

Wang, M., and Xu, T. (2019). Methyl B12 Protects PC12 Cells against Cytotoxicity Induced by Aβ25-35. *J. Cel. Biochem.* 120 (7), 11921–11930. doi:10.1002/jcb.28475

Wang, Y., Huang, X., Liang, Q. H., Fan, R., Qin, F., Guo, Y., et al. (2012). A Strategy for Detecting Absorbed Bioactive Compounds for Quality Control in the Water Extract of Rhubarb by Ultra Performance Liquid Chromatography with Photodiode Array Detector. *Chin. J. Integr. Med.* 18 (9), 690–698. doi:10.1007/s11655-012-1053-7

Wang, J., Zhao, C., Zhao, A., Li, M., Ren, J., and Qu, X. (2015). New Insights in Amyloid Beta Interactions with Human Telomerase. *J. Am. Chem. Soc.* 137 (3), 1213–1219. doi:10.1021/ja511030s

Wang, Y., Fan, X., Tang, T., Fan, R., Zhang, C., Huang, Z., et al. (2016). Rhein and Rhubarb Similarly Protect the Blood-Brain Barrier after Experimental Traumatic Brain Injury via Gp91phox Subunit of NADPH oxidase/ROS/ERK/MMP-9 Signaling Pathway. *Sci. Rep.* 6, 37098. doi:10.1038/srep37098

Wang-Dietrich, L., Funke, S. A., Kühbach, K., Wang, K., Besmehn, A., Willbold, S., et al. (2013). The Amyloid-β Oligomer Count in Cerebrospinal Fluid Is a Biomarker for Alzheimer's Disease. *J. Alzheimers Dis.* 34 (4), 985–994. doi:10.3233/jad-122047

Xiao, X., Chen, Q., Zhu, X., and Wang, Y. (2019). ABAD/17β-HSD10 Reduction Contributes to the Protective Mechanism of Huperzine a on the Cerebral Mitochondrial Function in APP/PS1 Mice. *Neurobiol. Aging* 81, 77–87. doi:10.1016/j.neurobiolaging.2019.05.016

Yan, S., Du, F., Wu, L., Zhang, Z., Zhong, C., Yu, Q., et al. (2016). F1F0 ATP Synthase-Cyclophilin D Interaction Contributes to Diabetes-Induced Synaptic Dysfunction and Cognitive Decline. *Diabetes* 65 (11), 3482–3494. doi:10.2337/db16-0556

Ye, J., Liu, Z., Wei, J., Lu, L., Huang, Y., Luo, L., et al. (2013). Protective Effect of SIRT1 on Toxicity of Microglial-Derived Factors Induced by LPS to PC12 Cells via the P53-caspase-3-dependent Apoptotic Pathway. *Neurosci. Lett.* 553, 72–77. doi:10.1016/j.neulet.2013.08.020

Zahs, K. R., and Ashe, K. H. (2013). β-Amyloid Oligomers in Aging and Alzheimer's Disease. *Front. Aging Neurosci.* 5, 28. doi:10.3389/fnagi.2013.00028

Zeng, K.-W., Wang, J.-K., Wang, L.-C., Guo, Q., Liu, T.-T., Wang, F.-J., et al. (2021). Small Molecule Induces Mitochondrial Fusion for Neuroprotection via Targeting CK2 without Affecting its Conventional Kinase Activity. *Sig Transduct Target. Ther.* 6 (1), 71. doi:10.1038/s41392-020-00447-6

Zhao, Y., and Zhao, B. (2013). Oxidative Stress and the Pathogenesis of Alzheimer's Disease. *Oxid. Med. Cell Longev.* 2013, 1–10. doi:10.1155/2013/316523

Zhao, Y., Huang, Y., Fang, Y., Zhao, H., Shi, W., Li, J., et al. (2018). Chrysophanol Attenuates Nitrosative/oxidative Stress Injury in a Mouse Model of Focal Cerebral Ischemia/reperfusion. *J. Pharmacol. Sci.* 138 (1), 16–22. doi:10.1016/j.jphs.2018.08.002

Zhuang, S., Yu, R., Zhong, J., Liu, P., and Liu, Z. (2019). Rhein from Rheum Rhabarbarum Inhibits Hydrogen-Peroxide-Induced Oxidative Stress in Intestinal Epithelial Cells Partly through PI3K/Akt-Mediated Nrf2/HO-1 Pathways. *J. Agric. Food Chem.* 67 (9), 2519–2529. doi:10.1021/acs.jafc.9b00037

**Conflict of Interest:** The authors declare that the research was conducted in the absence of any commercial or financial relationships that could be construed as a potential conflict of interest.

**Publisher's Note:** All claims expressed in this article are solely those of the authors and do not necessarily represent those of their affiliated organizations, or those of the publisher, the editors and the reviewers. Any product that may be evaluated in this article, or claim that may be made by its manufacturer, is not guaranteed or endorsed by the publisher.

frontiers in Pharmacology

ORIGINAL RESEARCH
published: 23 September 2021
doi: 10.3389/fphar.2021.735812

# Qiangji Decoction Alleviates Neurodegenerative Changes and Hippocampal Neuron Apoptosis Induced by D-Galactose *via* Regulating AMPK/SIRT1/NF-κB Signaling Pathway

*Li-Ling He[1†], Yun-Cui Wang[2†], Ya-Ting Ai[2†], Ling Wang[2], Si-Meng Gu[3], Ping Wang[1], Qing-Hua Long[1]* and Hui Hu[1,2]**

[1]School of Basic Medicine, Hubei University of Chinese Medicine, Wuhan, China, [2]School of Nursing, Hubei University of Chinese Medicine, Wuhan, China, [3]Department of Psychology, Jiangsu University Medical School, Zhenjiang, China

OPEN ACCESS

**Edited by:**
*Fang Pan,*
*Shandong University, China*

**Reviewed by:**
*Jian Xu,*
*China Pharmaceutical University, China*
*Dongfeng Wei,*
*China Academy of Chinese Medical Sciences, China*

***Correspondence:**
*Qing-Hua Long*
*287201413@qq.com*
*Hui Hu*
*zhongyi90@163.com*

*†These authors have contributed equally to this work and share first authorship*

**Received:** *03 July 2021*
**Accepted:** *03 August 2021*
**Published:** *23 September 2021*

**Citation:**
*He L-L, Wang Y-C, Ai Y-T, Wang L, Gu S-M, Wang P, Long Q-H and Hu H (2021) Qiangji Decoction Alleviates Neurodegenerative Changes and Hippocampal Neuron Apoptosis Induced by D-Galactose via Regulating AMPK/SIRT1/NF-κB Signaling Pathway. Front. Pharmacol. 12:735812. doi: 10.3389/fphar.2021.735812*

Qiangji Decoction (QJD), a classic formula, has been widely used to treat brain aging–related neurodegenerative diseases. However, the mechanisms underlying QJD's improvement in cognitive impairment of neurodegenerative diseases remain unclear. In this study, we employed D-galactose to establish the model of brain aging by long-term D-galactose subcutaneous injection. Next, we investigated QJD's effect on cognitive function of the model of brain aging and the mechanisms that QJD suppressing neuroinflammation as well as improving neurodegenerative changes and hippocampal neuron apoptosis. The mice of brain aging were treated with three different dosages of QJD (12.48, 24.96, and 49.92 g/kg/d, respectively) for 4 weeks. Morris water maze was used to determine the learning and memory ability of the mice. HE staining and FJB staining were used to detect the neurodegenerative changes. Nissl staining and TUNEL staining were employed to detect the hippocampal neuron apoptosis. The contents of TNF-α, IL-1β, and IL-6 in the hippocampus were detected by using ELISA. Meanwhile, we employed immunofluorescence staining to examine the levels of GFAP and IBA1 in the hippocampus. Besides, the protein expression levels of Bcl-2, Bax, caspase-3, cleaved caspase-3, AMPKα, p-AMPKα-Thr172, SIRT1, IκBα, NF-κB p65, p-IκBα-Ser32, and p-NF-κB p65-Ser536 in the hippocampus of different groups were detected by Western blot (WB). Our findings showed that the QJD-treated groups, especially the M-QJD group, mitigated learning and memory impairments of the model of brain aging as well as the improvement of neurodegenerative changes and hippocampal

**Abbreviation:** AMPK, mammalian 5′-AMP-activated protein kinase; Bax, BCL-2–associated X protein; Bcl-2, B-cell lymphoma 2; DAPI, 4′ 6-diamidino-2-phenylindole; D-gal, D-galactose; FJB, Fluoro-Jade B; GFAP, glial fibrillary acid protein; HE, hematoxylin-eosin; IBAl, ionized calcium-binding adaptor molecule 1; IL-6, interleukin-6; IL-lβ, interleukin-l beta; IκBα, nuclear factor of kappa light polypeptide gene enhancer in B-cell inhibitor; MWM, Morris water maze; NF-κB, nuclear factor-kappa beta; PBS, phosphate-buffered saline; PVDF, polyvinylidene difluoride; QJD, Qiangji Decoction; SDS-PAGE, sodium dodecyl sulfate-polyacrylamide gel electrophoresis; SIRT1, silent information regulator of transcription 1; TNF-α, tumor necrosis factor-alpha; TUNEL, terminal deoxynucleotidyl transferase-mediated dUTP-biotin nick end labeling; WB, Western blot.

neuron apoptosis. Moreover, the M-QJD markedly attenuated the neuroinflammation by regulating the AMPK/SIRT1/NF-κB signaling pathway. Taken together, QJD alleviated neurodegenerative changes and hippocampal neuron apoptosis in the model of brain aging via regulating the AMPK/SIRT1/NF-κB signaling pathway.

**Keywords: Qiangji Decoction, brain aging, D-galactose, AMPK/SIRT1/NF-κB signaling pathway, neuroinflammation, neurodegenerative changes**

## INTRODUCTION

Brain aging is the main factor inducing aging-related neurodegenerative diseases (Fung et al., 2020). With the rapid escalation of the aging population all over the world, the prevalence of chronic neurodegenerative diseases including mild cognitive impairment (MCI) and Alzheimer's disease (AD) is increasing rapidly. Although we have made encouraging progress in the research of MCI and AD, its high prevalence has resulted in a heavy burden on the economy and society of the world. To date, we have no effective therapies against MCI and AD, and current drugs cannot fundamentally reverse the pathological process of MCI and AD (Yiannopoulou and Papageorgiou, 2020; Trevisan et al., 2021). Thus, the delay of brain aging has been recognized as a key to prevent the onset of MCI and AD.

The causes resulting in brain aging are complex, of which neuroinflammation is considered as the crucial culprit. The increasing researches have confirmed that neuroinflammation can damage the structure and function of the brain and finally result in hippocampal-dependent learning and memory impairment (Lima Giacobbo et al., 2019; Yahfoufi et al., 2020; Salami et al., 2021). Therefore, the inhibition of neuroinflammation has been regarded as an effective therapeutic intervention to alleviate the progression of chronic neurodegenerative diseases.

D-galactose (D-gal), a type of reducing sugar, has been commonly found to present as the lactose in the milk of mammals (Shwe et al., 2018). In general, the low dose of D-gal can be metabolized into galactose-1-phosphate. But at higher concentrations, D-gal can be converted to aldose and hydrogen peroxide, causing the disposition of superoxide anion and oxygen-derived free radicals in the brain, and finally lead to brain damage (Sun et al., 2018). Mounting studies have confirmed that chronic D-gal administration leads to the cognitive impairment of rodents by the accumulated oxidative stress, mitochondrial deficits, and neuroinflammation (Chen et al., 2019; Jeong et al., 2021; Oskouei et al., 2021). For these reasons, chronic administration of D-gal is well-established in the experimental rodent models of aging-related cognitive impairment and investigating the anti-aging pharmacological studies. Chronic D-gal administration can not only induce oxidative stress but also lead to neuroinflammation. Previous researches have pointed out that neuroinflammation acts as a contributor in accelerating and deteriorating the pathological process of brain aging. Cumulative reports have showed that chronic D-gal administration can suppress the AMPK/SIRT1 signaling pathway, thereby activating the NF-κB signaling pathway (Wang et al., 2020a; Lin et al., 2020; Wang et al., 2021). When the NF-κB signaling pathway is activated, it can induce neuroinflammation (Wang et al., 2020b; El-Far et al., 2020). However, once the AMPK/SIRT1 signaling pathway is activated, NF-κB is also inhibited accordingly, and finally alleviating cognitive impairment and neurodegenerative changes induced by D-gal.

From the view of traditional Chinese medicine, kidney deficiency is considered as an important factor causing brain aging, and tonifying kidney is a critical treatment method for anti–brain aging. Qiangji Decoction (QJD) is a classic formula created by Chen Shiduo in Qing Dynasty and can nourish kidneys to delay the process of brain aging. QJD comprised four raw herbs, namely, wine-steamed roots of *Rehmannia glutinosa* Libosch. (family: Scrophulariaceae, Shudihuang in Chinese), air-dried mature seeds of *Ziziphus jujuba* Mill. var. *spinosa* (Bunge) Hu ex H. F. Chou (family: Rhamanaceae, Suanzaoren in Chinese), air-dried tuberous roots of *Ophiopogon japonicus* (L. f) Ker-Gawl. (family: Liliaceae, Maidong in Chinese), air-dried roots and rhizomes of *Polygala tenuifolia* Wild., or *Polygala sibirica* L. (family: Polygalaceae, Yuanzhi in Chinese). Since the Qing Dynasty, QJD has been demonstrated to have a positive therapeutic effect on chronic neurodegenerative diseases including MCI and AD. A large body of clinical practice has confirmed that QJD can alleviate the aging-related cognitive impairment. At the same time, animal experiments have also verified that QJD can alleviate the cognitive impairment and neurodegenerative changes induced by D-gal and scopolamine (Gu., et al., 2008; Li., et al., 2008). However, the molecular mechanism underlying QJD's anti–brain aging is still unclear, so the present study was designed to evaluate whether QJD could mitigate the cognitive impairment induced by D-gal and then the molecular mechanisms that QJD inhibited neurodegenerative changes through anti-neuroinflammation were explored.

## MATERIALS AND METHODS

### Animals

A total of 60 eight-week-old male C57BL/6 mice with specific pathogen free (SPF) were used in this study, weighing about 25 ± 2 g, which were obtained from Liaoning Changsheng Biotechnology Co., Ltd. (Benxi, Liaoning, China; Certification number: SCXK 2020-0001). The experimental animals used in this study were housed in the Center Laboratory of Chinese Medicine of Hubei University of Chinese Medicine. The standard laboratory was controlled at the temperature of 23 ± 2°C, 60% relative humidity, and 12:12 h lightdark cycle. During the experiment, the animals had free access to a standard diet and water. The approval of animal feeding and experiment protocol were obtained from the Animal Ethics Review Committee of

Hubei University of Chinese Medicine (No. 8217150845) and conducted in accordance with the ethical guidelines.

## Drugs

Qiangji Decoction (QJD) comprised four raw herbs, including wine-steamed roots of *Rehmannia glutinosa* Libosch. (30 g), air-dried mature seeds of *Ziziphus jujuba* Mill. var. *spinosa* (Bunge) Hu ex H. F. Chou (30 g), air-dried tuberous roots of Ophiopogon japonicus (L. f) Ker-Gawl. (30 g), air-dried roots and rhizomes of *Polygala tenuifolia* Wild. or *Polygala sibirica* L. (6 g), which were provided by Jinpai Chizhengtang Pharmaceutical Co., Ltd. (Huangshi, Hubei, China). All raw herbs were authenticated by Prof. Qiu-yun You, a pharmacologist from Hubei University of Chinese Medicine, and identified in accordance with the Chinese Pharmacopoeia. Metformin hydrochloride extended-release tablets (0.5 g/tablet, batch number: ABU7707) were obtained from Sino-American Shanghai Squibb Pharmaceutical Co., Ltd. (Shanghai, China).

## Preparation of QJD Extract and Metformin

According to the methods described in our previous report with minor modifications, the stock solution of QJD was prepared (Long et al., 2021). In general, the raw herbs were crushed into pieces, and the mixtures of raw herbs were soaked in water (1:8, w/v) for 30 min. Subsequently, the mixed herbs were decocted for 30 min. After filtration, the residue was decocted for 20 min (1:6, w/v). The two filtrates were mixed and refluxed in the rotary evaporators (QYMD-60, Qi yu industry co., LTD., Shanghai, China) for 1.5 h, and finally concentrated into a stock solution. Metformin was dissolved in saline and prepared as a 0.01 g/ml stock solution.

## Reagents and Antibodies

D-galactose (D-gal), purity>99.0%, was supplied by Solarbio Science and Technology Co., Ltd. (Beijing, China; D8310). HE staining solution, Nissl staining solution, and Fluorescein (FITC) TUNEL Cell Apoptosis Detection Kit were obtained from Servicebio Technology Co., Ltd. (Wuhan, Hubei, China; G1005, G1036, and G1501, respectively). Fluoro-Jade B (FJB) staining kit was obtained from Merck-Millipore (Darmstadt, Germany; AG310). ELISA Kits for the detection of TNF-α, IL-1β, and IL-6 were supplied by ABclonal technology (Wuhan, Hubei, China; RK00027, RK00006, and RK00008, respectively). Rabbit monoclonal anti–Bcl-2, rabbit monoclonal anti-Bax, rabbit monoclonal anti–caspase-3, rabbit polyclonal anti–cleaved caspase-3, rabbit monoclonal anti–total-AMPKα, rabbit monoclonal anti–phospho-AMPKα (Thr172), rabbit monoclonal anti-SIRT1, rabbit monoclonal anti–*β*-actin, and HRP-linked goat anti-rabbit IgG were purchased from ABcam (Cambridge, MA, USA; ab32124, ab32503, ab32351,ab2302, ab32047, ab133448, ab110304, ab8227, and ab6721, respectively). Rabbit polyclonal anti-GFAP, rabbit monoclonal anti-IBA1, and Cy3-conjugated goat anti-rabbit IgG were purchased from ABclonal technology (Wuhan, Hubei, China; A0237, A1527, and AS007, respectively). Rabbit monoclonal anti–total-IκBα, rabbit monoclonal anti–phospho-IκBα (Ser32), rabbit monoclonal anti–total-NF-κB p65, and rabbit monoclonal anti–phospho-NF-κB p65 (Ser536) were purchased from Cell Signaling Technology (Beverly, MA, USA; #4812, #2859, #8242, and #3033, respectively).

## Experimental Model and QJD Administration

After the acclimation, the mice were randomly assigned to the following six different groups of 10 animals each, namely, negative control group (NC), D-gal group (D-gal), metformin group (Met), low dose of QJD group (L-QJD), middle dose of QJD group (M-QJD), and high dose of QJD group (H-QJD). With reference to the previous reports (Baeta-Corral et al., 2018; Ullah et al., 2020; Ahmad et al., 2021), the mice in the negative control group were administered with 0.9% saline by subcutaneous injection for 8 weeks, while the other groups were administered with D-gal (100 mg/kg/d). Based on the previous reports and clinical equivalent doses (Farr et al., 2019; Li et al., 2019), the therapeutic dose of the metformin group and QJD-treated group was confirmed accordingly. From the fifth to the eighth week, the NC group and the D-gal group received the same amount of normal saline by oral administration, the metformin group was given metformin (200 mg/kg/d), and the QJD-treated groups were treated with three different doses of QJD extract (L-QJD: 12.48 g/kg/d, M-QJD: 24.96 g/kg/d, H-QJD: 49.92 g/kg/d). As shown in **Figure 1A**, the study design of this research has been illustrated.

## Morris Water Maze

After the treatment was completed, the hippocampus-dependent learning and memory ability of mice in each group were evaluated by the Morris water maze (MWM) test. The equipment of the MWM test was given in our previous report, and it was performed with minor modifications (Long et al., 2021). Briefly, the MWM test contains two tests, namely, the navigation and spatial probe test. During the navigation test, every trained animal was given 60 s to search for the platform, and the escape latency was documented by the MWM software (version YH-MWM, Wuhan Yihong Technology Co., Ltd., China). If the experimental animals did not locate the platform within the allocated 60 s, they were manually led to the platform and allowed to remain on the platform for at least 15 s. After the completion of the navigation test, the hidden platform was retracted manually, and then the spatial probe test was executed. MWM software automatically recorded and analyzed the number of crossing the hidden platform in the spatial probe test. In addition, we also analyzed and counted the time of staying on the target quadrant and the mean swimming speed in each group.

## Hippocampal Tissue Collections

After the completion of MWM, four animals in each group were sacrificed, and then the brain tissues were collected to fix in 4% paraformaldehyde for HE staining, FJB staining, Nissl staining, TUNEL staining, and immunofluorescence staining. The remaining mice were anesthetized in the same way, and the hippocampal tissue was separated and split into two parts on a

cold plate. One portion of the hippocampal tissue was used for ELISA, and another part was used for Western blot. After separation, the hippocampal tissue was in a cryopreservation tube and stored in liquid nitrogen for 30 min, finally kept at −80°C until further processing.

## HE Staining

The brain tissues were immersed in 4% paraformaldehyde at 4°C for 24 h and then processed into paraffin-embedded tissues. Subsequently, a microtome (CM 2016, Leica, Germany) was employed to cut the paraffin-embedded tissues into 5-μm-thick slices. The slices were dewaxed with xylene and dehydrated with gradient ethanol (100–75%). After being rinsed with double distilled water, the slices were placed in a solution of hematoxylin for 3–5 min and then stained with a solution of eosin for 5 min. Finally, neutral gum was used to mount the slices. The stained slices were photographed and analyzed with an upright optical microscope (ECLIPSE Ni-E, Nikon, Japan).

## Fluoro-Jade B Staining

Based on the manufacturer's protocol and a previously described report, the FJB staining was carried out (Xie et al., 2019). Briefly, the prepared sections were immersed in xylene for 15 min. Subsequently, the slices were placed in a gradient ethanol of 85 and 75% for dehydration for 5 min each. The slices were rinsed in 0.1 M PBS for 1–2 min and then incubated to a solution of final working concentration of FJB for 10 min. The cell nuclei were labeled by 4 ′6-diamidino-2-phenylindole (DAPI). After FJB staining, the slices were visualized and photographed under an upright fluorescence microscope (DP72, Olympus, Japan), and then the number of FJB-positive cells were measured by using Image-Pro Plus 7.0 software (Media Cybernetics, Inc., Rockville, MD, USA).

## Nissl Staining

The paraffin-embedded slices were dewaxed with xylene for 5 min. Later, the dewaxed slices were dehydrated in a gradient ethanol series with decreasing concentration for 5 min (100–75%). After being dehydrated, the slices were treated with Nissl staining solution at 37°C for 30 min and then washed in 0.1 M PBS for 5 min. Subsequently, the paraffinized slices were incubated in 70% alcohol differentiation at 37°C for 15 s. The sections were dehydrated with gradient alcohol (70–95%) for 2 min and finally covered with neutral gum. The images were photographed and analyzed with an imaging system (BX50, Olympus, Japan). Subsequently, the number of neurons in the hippocampus was analyzed by Image-Pro Plus 7.0 software.

## TUNEL Staining

The TUNEL staining was employed to assess the level of hippocampal neuron apoptosis in each group, and it performed as described previously (Li et al., 2021). After being dewaxed and rehydrated, the paraffin-embedded slices were incubated with proteinase K at room temperature for 25 min. After incubation, the sections were washed in 0.1 M PBS for 5 min and then incubated in permeabilize working solution at room temperature for 20 min. The slices are slightly dried and then incubated with TUNEL mixture at room temperature for 2 h. Subsequently, the cell nuclei were counterstained by using 4′ 6-diamidino-2-phenylindole (DAPI), and the slices were finally mounted with anti-fade mounting medium. The slices were observed under an upright fluorescence microscope (DP72, Olympus, Japan). In this study, we used Image-Pro Plus 7.0 software to measure the number of TUNEL-positive cells, so as to assess whether QJD could improve the hippocampal neuronal apoptosis.

## Immunofluorescence Staining

Based on the previous report, the immunofluorescence staining was conducted with minor modifications (Rong et al., 2019). In brief, the slices were dewaxed with xylene and dehydrated with gradient ethanol (100–75%), and then washed in 0.1 M PBS for 5 min. Next, the dehydrated slices were placed in EDTA antigen retrieval buffer for 8 min at a sub-boiling temperature. Subsequently, the slices were blocked in 3% bovine serum albumin (BAS). After washing three times using 0.1 M PBS 3 min, the primary antibody (IBA1, 1:100; GFAP, 1:200) was selected to incubate the slices overnight at 4°C. The following day, the Cy3-conjugated secondary antibody (1:200) was added to incubate at 37°C for 50 min. DAPI was employed to label the cell nuclei, and the slices were finally mounted with anti-fade mounting medium. In this study, we used Image-Pro Plus 7.0 software to calculate the mean fluorescence intensity of images.

## Enzyme-Linked Immunosorbent Assay

To evaluate whether QJD could inhibit the neuroinflammation, we employed enzyme-linked immunosorbent assay (ELISA) kits to estimate the contents of pro-inflammatory factors in hippocampal tissue, such as TNF-α, IL-1β, and IL-6. In brief, the separated hippocampus was immersed in PBS (1:8, w/v), homogenized in a cold tissue homogenizer (JXFSTPRP-CL-24, Tuohe Electromechanical Technology Co., Ltd., Shanghai, China), followed by centrifugation (12,000 rpm) at 4°C for 10 min. The supernatant was then collected. Subsequently, the level of protein was quantified using the BCA Protein Assay kit. Finally, the contents of TNF-α, IL-1β, and IL-6 in hippocampus were detected using ELISA kits, following the manufacturer's protocol.

## Western Blot

In brief, the separated hippocampus was lysed in RIPA lysis buffer (1:8, w/v) containing phenylmethylsulfonyl fluoride (PMSF) and phosphatase inhibitors to extract the total proteins of hippocampus. After homogenizing, the hippocampal homogenates were subjected to centrifugation (12,000 rpm) at 4°C for 30 min, and the supernatants were collected. Subsequently, BCA Protein Assay kit was used to calculate the protein concentration of each sample. After that, the 10–12% separation gel buffer and 5% stacking gel buffer were prepared, and the protein of each sample (30 μg) was separated with SDS-PAGE. The protein was then transferred to the PVDF membranes (Millipore, Darmstadt, Germany). After blocked in 5% nonfat milk at room temperature for 30 min, the membranes

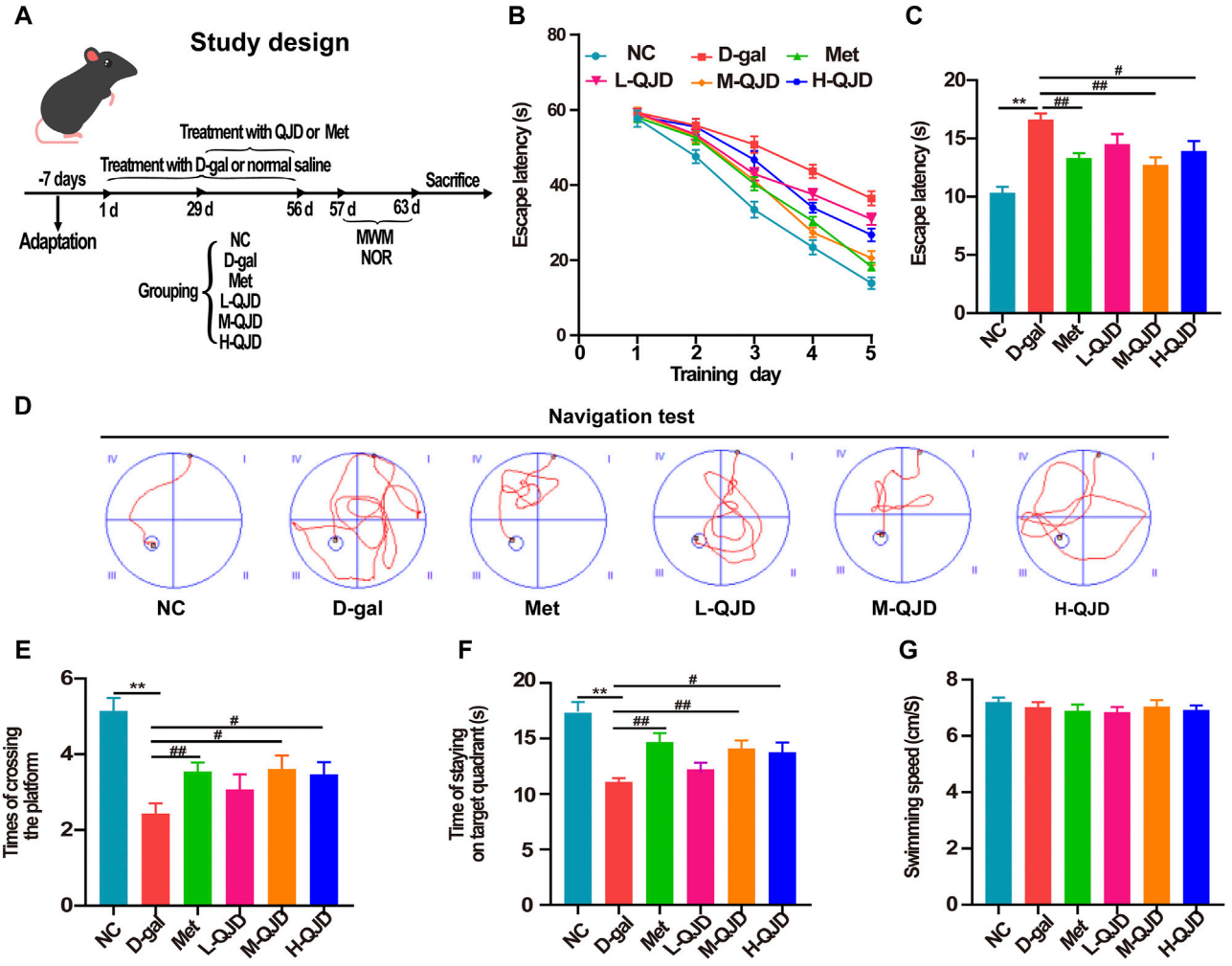


**FIGURE 1 |** QJD alleviated learning and memory impairments in D-gal–induced mice. **(A)** Study design. **(B)** Mean escape latency to the platform of each group during the training session of five consecutive days. **(C)** Escape latency to the platform of each group in the navigation test. **(D)** Representative path tracings of each group in the navigation test. **(E)** The number of crossing platform in the permitted 60 s. **(F)** Time of staying on the target quadrant in the permitted 60 s. **(G)** The mean swimming speed of mice in all groups. All data were presented as mean ± SEM ($n$ = 10/group). $^{**}p < 0.01$ vs. NC group; $^{\#}p < 0.05$ and $^{\#\#}p < 0.01$ vs. D-gal group.

were incubated with primary antibodies including anti–Bcl-2 (1:1,000), anti-Bax (1:1,000), anti–cleaved caspase-3 (1:1,000), anti-AMPKα (1:1,000), anti–*p*-AMPKα-Thr172 (1:1,000), anti-SIRT1 (1:1,000), anti-IκBα (1:1,000), anti–*p*-IκBα-Ser32 (1:1,000), anti–NF-κB p65 (1:1,000), anti–p-NF-κB p65-Ser536 (1:1,000), and anti–β-actin (1:1,000) at 4°C overnight. The next day, the membranes were incubated with HRP-linked secondary antibody (1:10,000) at room temperature for 30 min. After washing three times with TBST, ECL kit was used to capture the blots, and the band intensity of each sample was quantified by using the Image J software (Bethesda, United States).

## Statistical Analysis

All experimental data were dealt by using Statistical Analysis System software (SAS, version 9.4, SAS Institute Inc., Cary, NC, USA), and the results were expressed as mean ± standard error of the mean (SEM). The two-way analysis of variance (ANOVA) with repeated measures was used to analyze the escape latency, and the remaining data were analyzed by one-way ANOVA. If the variance was homogeneous, the Bonferroni post hoc test was adopted. If not, the Tamhane T2 test was used. When the *p*-value was less than 0.05, values were considered statistically significant.

# RESULTS

## QJD Alleviates Learning and Memory Impairments in D-Gal–Induced Mice

MWM is one of the most widely used behavioral testing methods, which has been commonly used to evaluate the learning and memory ability of brain aging–related neurodegenerative diseases (Garthe and Kempermann, 2013; Wahl et al., 2017). Accordingly, we assessed the mice's spatial learning ability in each group by using the navigation test. During the navigation test, there was no

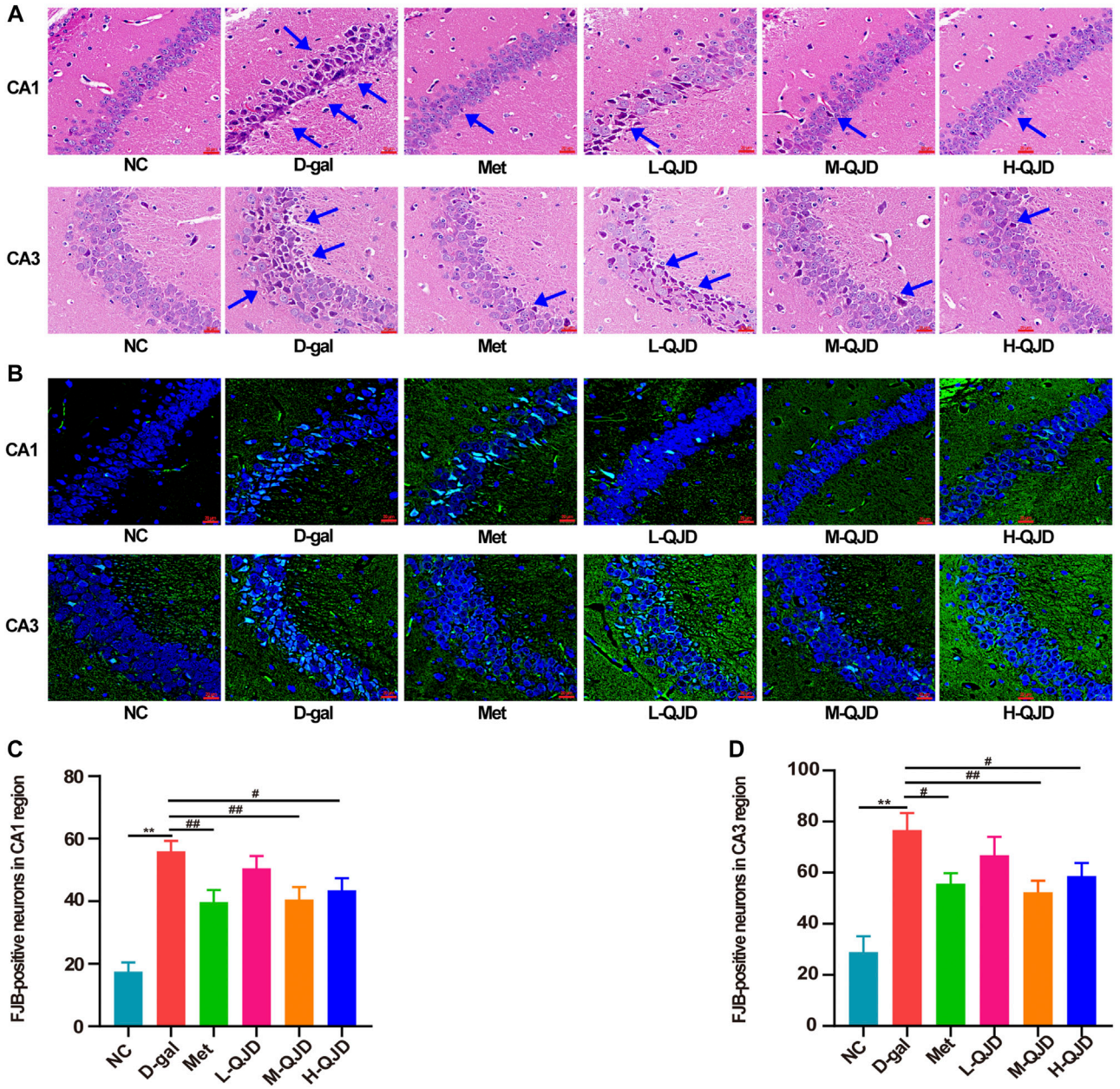


**FIGURE 2 |** QJD alleviated the pathological alterations in the hippocampus of D-gal–induced mice. **(A)** Representative HE staining images in the hippocampus of CA1 and CA3 regions (magnification × 400; scale bar = 20 μm). **(B)** Representative FJB staining images (labeled in green) in the hippocampus of CA1 and CA3 regions (magnification × 400; scale bar: 20 μm). **(C)** Number of FJB-positive neurons in the hippocampus CA1 region. **(D)** Number of FJB-positive neurons in the hippocampus CA3 region. The blue arrows indicate damaged neurons in the hippocampus. All data were presented as mean ± SEM ($n$ = 4/group). $^{**}p < 0.01$ vs. NC group; $^{\#}p < 0.05$ and $^{\#\#}p < 0.01$ vs. D-gal group.

obvious alteration in the escape latency among all groups during 3 days of consecutive training ($p > 0.05$, **Figure 1B**). Starting from the fourth day, the D-gal treatment significantly increased the escape latency, whereas this phenomenon was significantly reversed by the metformin, M-QJD, and H-QJD ($p < 0.05$ or 0.01; **Figures 1B, C**). The representative path tracings of each group in the navigation test were presented in **Figure 1D**, which indicated the M-QJD significantly shortened the escape latency in D-gal-induced mice. Besides, we examined the spatial memory ability of mice by using the spatial probe test. According to the spatial probe test, we found the M-QJD group and H-QJD group had a higher number of crossing platform when compared to the D-gal group ($p < 0.05$ or 0.01; **Figure 1E**). Meanwhile, the M-QJD group and H-QJD group significantly increased the time that mice spent in the target quadrant ($p < 0.05$ or 0.01; **Figure 1F**). Nevertheless, the L-QJD group did not significantly change the

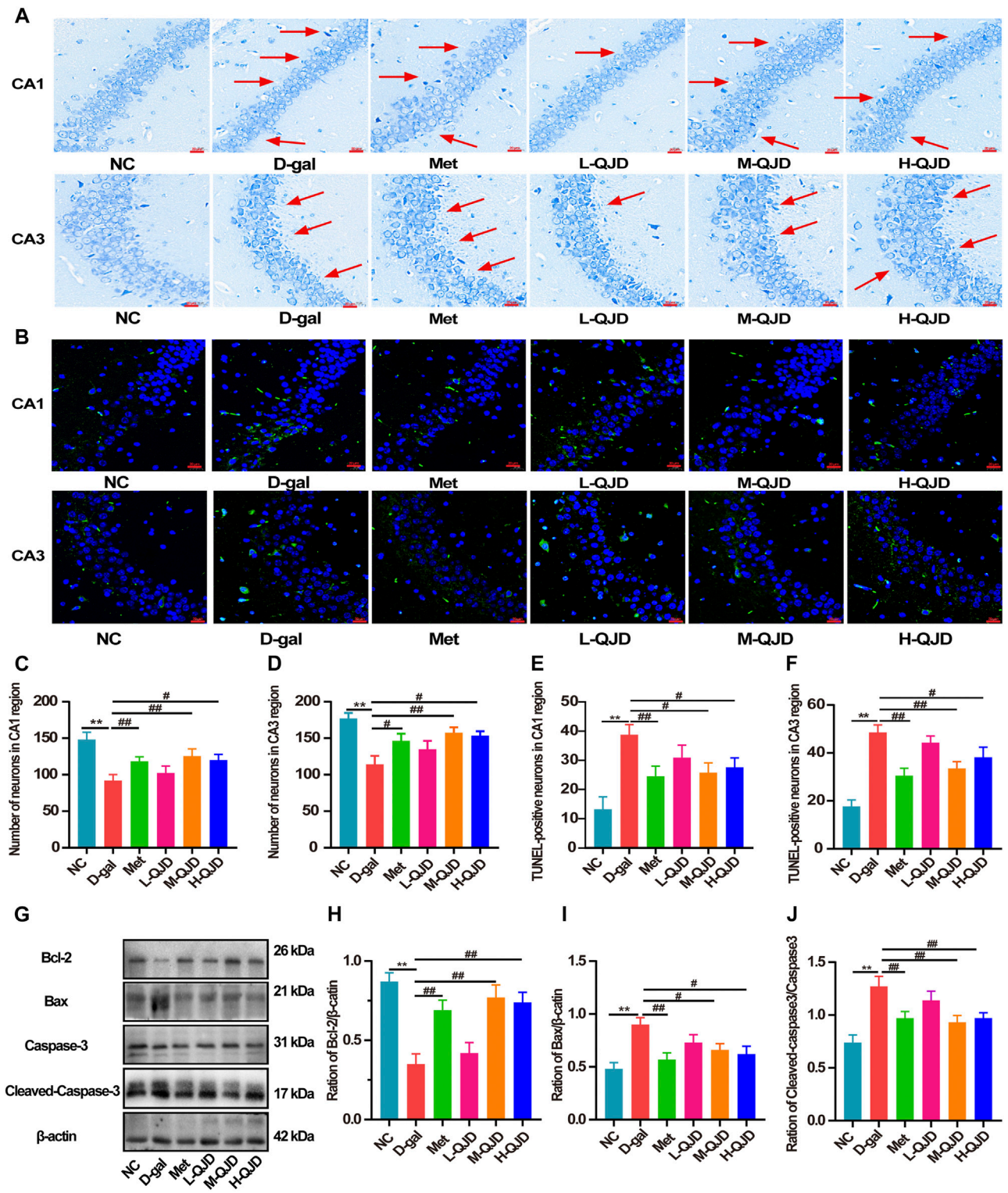


**FIGURE 3 |** QJD alleviated the hippocampal neuron loss and apoptosis in D-gal–induced mice. **(A)** Representative Nissl staining images in the hippocampus of CA1 and CA3 regions (magnification × 400; scale bar = 20 μm). **(B)** Representative TUNEL staining images (labeled in green) in the hippocampus of CA1 and CA3 regions (magnification × 400; scale bar = 20 μm). **(C)** Number of neurons in the hippocampus CA1 region. **(D)** Number of neurons in the hippocampus CA3 region. **(E)** Number of TUNEL-positive neurons in the hippocampus CA1 region. **(F)** Number of TUNEL-positive neurons in the hippocampus CA3 region. **(G)** Representative Western blot bands showing the protein expression levels of Bcl-2, Bax, caspase-3 and cleaved caspase-3 in the hippocampus. **(H)** Relative protein expression level of Bcl-2. **(I)** Relative protein expression level of Bax. **(J)** Relative protein expression level of cleaved caspase-3/caspase-3. The red arrows indicate the hippocampal neuron loss. All data were presented as mean ± SEM ($n$ = 4 or 6/group). $^{**}p < 0.01$ vs. NC group; $^{\#}p < 0.05$ and $^{\#\#}p < 0.01$ vs. D-gal group.

abovementioned results ($p > 0.05$; **Figures 1E,F**). In mean swimming speed, no statistical difference was found among all groups ($p > 0.05$; **Figure 1G**), which implies that mice's swimming ability had no difference. These results indicated that chronic D-gal administration could induce the cognitive impairment, and the QJD, especially the M-QJD, reversed this phenomenon, whereas the L-QJD did not mitigate the cognitive impairment in D-gal–induced mice.

## QJD Alleviates the Pathological Alterations in the Hippocampus of D-Gal–Induced Mice

The MWM test results show that the QJD could alleviate the cognitive deficits induced by D-gal, and thereby, the HE staining and FJB staining were utilized to evaluate whether QJD could rescue the pathological alterations of the hippocampus induced by D-gal. In HE staining, we noticed that the D-gal group's neurons in the hippocampal CA1 and CA3 regions were degenerated with dark staining, deformed, and denatured nuclei in comparison with the NC group (**Figure 2A**). However, the neuronal damages in these regions of the M-QJD group and H-QJD group were decreased in comparison to the D-gal group, and the stained neurons and deformed nuclei were also alleviated. In addition, neurodegenerative changes in the hippocampus were detected by using FJB staining. As showed in FJB staining, compared with the NC group, there were remarkably increased FJB-positive cells in the hippocampal CA1 and CA3 regions of D-gal group ($p < 0.01$, **Figures 2B–D**). However, after treatment with M-QJD and H-QJD, the number of FJB-positive cells in these regions were significantly diminished ($p < 0.05$ or 0.01; **Figures 2B–D**). The above findings manifested that QJD could relieve the pathological alterations of hippocampus induced by D-gal.

## QJD Alleviates the Hippocampal Neuron Loss and Apoptosis in D-Gal–Induced Mice

We also employed Nissl staining and TUNEL staining to investigate whether QJD could improve the hippocampal neuron loss and apoptosis in D-gal–induced mice. In Nissl staining, we found that there was a decreased number of neurons in the CA1 and CA3 regions, when compared to the NC group ($p < 0.01$; **Figures 3A,C,D**). Whereas compared to the D-gal group, the decreased neurons were rescued by the M-QJD and the H-QJD ($p < 0.05$ or 0.01; **Figures 3A,C,D**). We also used the TUNEL staining to evaluate whether QJD could restrain neuronal apoptosis and quantified the number of TUNEL-positive cells by using Image-Pro Plus 7.0 software. The TUNEL staining results showed that the decreased TUNEL-positive neurons in the CA1 and CA3 regions were inhibited by the M-QJD and the H-QJD ($p < 0.05$ or 0.01; **Figures 3B,E,F**). In addition, the apoptotic markers including Bcl-2 (anti-apoptotic protein), Bax (apoptosis regulator), and cleaved caspase-3 (pro-apoptotic protein) were detected by Western blot (Ullah et al., 2020). Our finding verified that the D-gal treatment could upregulate the protein levels of Bax and cleaved caspase-3 in the hippocampus compared to the NC group ($p < 0.01$; **Figures 3G,I,J**), while the protein levels of Bcl-2 were significantly downregulated ($p < 0.01$; **Figures 3G,H**). After 4 weeks of M-QJD and H-QJD treatment, the above phenomenon was reversed ($p < 0.05$ or 0.01; **Figures 3G–J**). These results implied that the QJD could alleviate the hippocampal neuron loss and apoptosis in D-gal–induced mice.

## QJD Alleviates the Neuroinflammation Through Suppressing Microglial and Astrocytes Activation in D-Gal–Induced Mice

Neuroinflammation acts as the contributor in accelerating the pathological progression of aging-related neurodegenerative diseases, and the increasing researches have demonstrated that chronic D-gal administration can stimulate the microglia and astrocytes activation in central nervous system, thereby inducing chronic neuroinflammation (Lu et al., 2010; Cao et al., 2019; Yahfoufi et al., 2020). Therefore, in this study, we measured the contents of TNF-α, IL-1β, and IL-6 in the hippocampus through ELISA. When compared to the D-gal group, the NC group had a lower level of TNF-α, IL-1β, and IL-6 ($p < 0.01$; **Figures 4A–C**). However, after treatment with M-QJD and H-QJD, these pro-inflammatory cytokines were suppressed ($p < 0.05$ or 0.01; **Figures 4A–C**). The microglia and astrocytes activation is the critical factor for the release of pro-inflammatory cytokines. Growing researches have confirmed that chronic D-gal administration can induce the microglia and astrocytes activation, thereby accelerating the release of pro-inflammatory cytokines (Lu et al., 2010; Jeong et al., 2021; Oskouei et al., 2021). So, we used the immunofluorescence staining to detect the levels of IBA1 and GFAP. Our findings showed that the D-gal group had higher fluorescence intensity of IBA1-positive microglia and GFAP-positive astrocytes ($p < 0.01$; **Figures 4D–I**), when compared to the NC group. After treatment with M-QJD and H-QJD, the fluorescence intensity of IBA1-positive microglia and GFAP-positive astrocytes was significantly decreased ($p < 0.05$ or 0.01; **Figures 4D–I**). Collectively, these results manifested that QJD could alleviate chronic neuroinflammation through suppressing the activation of microglial and astrocytes in D-gal–induced mice.

## QJD Activates the AMPK/SIRT1 Signaling Pathway in the Hippocampus of D-Gal–Induced Mice

In the aging-related neurodegenerative diseases, the AMPK/SIRT1 signaling pathway acts as a crucial role in regulating energy metabolism, apoptosis as well as neuroinflammation (Domise and Vingtdeux, 2016; Chen et al., 2020). Previous research has confirmed that the inactivation of this signal pathway can accelerate neuroinflammation, while the activation of this signal pathway can naturally inhibit neuroinflammation (Peixoto et al., 2017). In this study, we examined the levels of AMPK and SIRT1 and the phosphorylation of APMK in the hippocampus by using Western blot. Compared with NC group, the levels of SIRT1

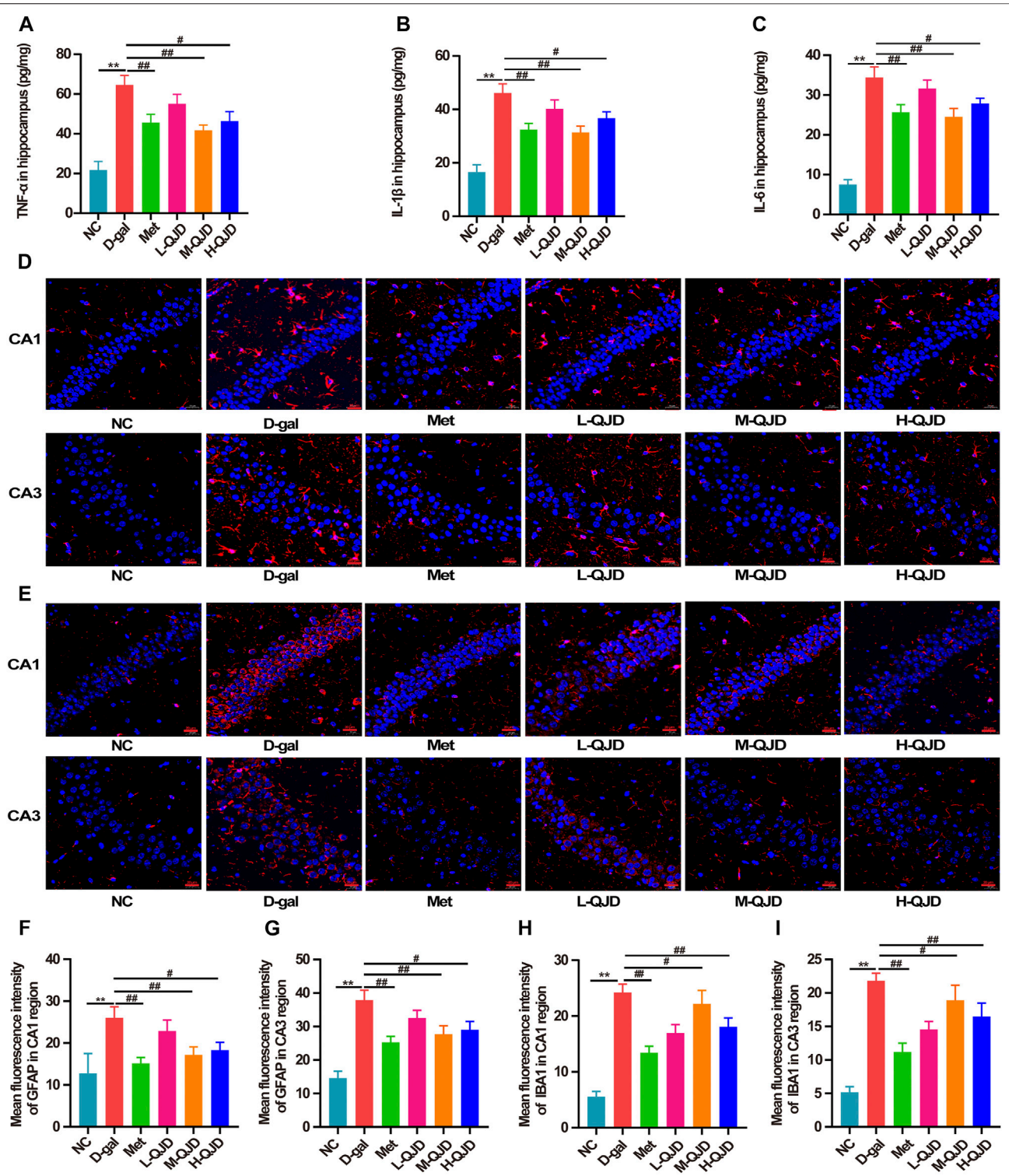


**FIGURE 4 |** QJD alleviated the neuroinflammation through suppressing microglial and astrocytic activation in D-gal–induced mice. **(A)** Protein expression of TNF-α in hippocampus. **(B)** Protein expression of IL-1β in hippocampus. **(C)** Protein expression of IL-6 in hippocampus. **(D)** Representative immunofluorescence staining images of GFAP (labeled in red) in the hippocampus of CA1 and CA3 regions (magnification × 400; scale bar = 20 μm). **(E)** Representative immunofluorescence staining images of IBA1 (labeled in red) in the hippocampus of CA1 and CA3 regions (magnification × 400; scale bar = 20 μm). **(F)** Mean fluorescence intensity of GFAP in the hippocampus of CA1 region. **(G)** Mean fluorescence intensity of GFAP in the hippocampus of CA3 region. **(H)** Mean fluorescence intensity of IBA1 in the hippocampus of CA1 region. **(I)** Mean fluorescence intensity of IBA1 in the hippocampus of CA3 region. All data were presented as mean ± SEM ($n$ = 4 or 6/group). $^{**}p < 0.01$ vs. NC group; $^{\#}p < 0.05$ and $^{\#\#}p < 0.01$ vs. D-gal group.

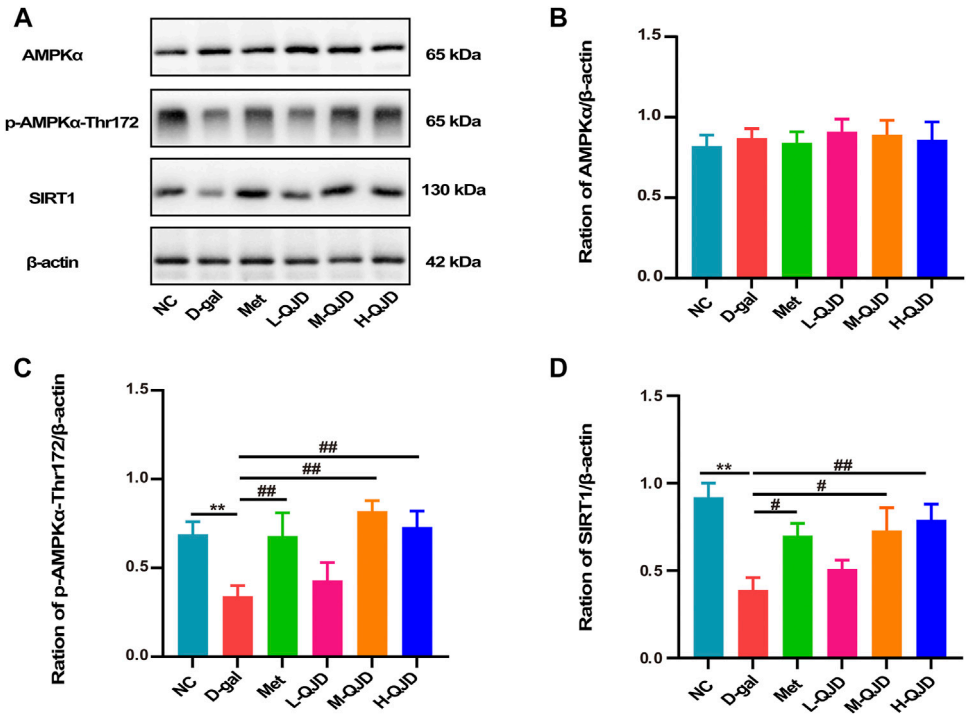


**FIGURE 5 |** QJD activated the AMPK/SIRT1 signaling pathway in the hippocampus of D-gal–induced mice. **(A)** Representative Western blot bands showing the protein expression levels of AMPKα, *p*-AMPKα-Thr172, and SIRT1 in the hippocampus. **(B)** Relative protein expression level of AMPKα. **(C)** Relative protein expression level of *p*-AMPKα-Thr172. **(D)** Relative protein expression level of SIRT1. All data were presented as mean ± SEM ($n$ = 6/group). $^{**}p < 0.01$ vs. NC group; $^{\#}p < 0.05$ and $^{\#\#}p < 0.01$ vs. D-gal group.

and the phosphorylation of APMK in the D-gal group were significantly decreased ($p < 0.01$; **Figures 5A–D**), which indicated that the AMPK/SIRT1 signaling pathway was inhibited by D-gal. After treatment with QJD, the M-QJD and H-QJD had a higher levels of SIRT1 and the phosphorylation of APMK, when compared to the D-gal group ($p < 0.05$ or 0.01; **Figures 5A–D**). Furthermore, we noticed that the H-QJD had the similar effect with M-QJD. Those results showed that QJD could activate the AMPK/SIRT1 signaling pathway in the hippocampus of D-gal–induced mice.

## QJD Inhibits the NF-κB Signaling Pathway in the Hippocampus of D-Gal–Induced Mice

AMPK/SITR1 signaling pathway is an important regulator of NF-κB, and the activity of NF-κB can be restrained by the AMPK/SITR1 signaling pathway. Growing researches have suggested that the activation of the AMPK/SITR1 signaling pathway can inhibit the activation of NF-κB, so we further investigate whether QJD alleviates the neuroinflammation through regulating the AMPK/SITR1–mediated NF-κB signaling pathway. In this study, we first used Western blot to examine the IκBα and NF-κB p65 in the hippocampus. Subsequently, the phosphorylated IκBα (Ser32) and NF-κB p65 (Ser536) were also detected by Western blot. As revealed by **Figures 6A–E**, the D-gal treatment significantly increased the levels of phosphorylated IκBα and phosphorylated NF-κB p65 in the hippocampus of the D-gal group, when compared to the NC group ($p < 0.01$). However, the H-QJD, especially the M-QJD, suppressed the levels of phosphorylated IκBα and phosphorylated NF-κB p65 ($p < 0.05$ or 0.01; **Figures 6A–E**). These data indicated that QJD could inhibit the NF-κB signaling pathway activation in the hippocampus of D-gal–induced mice.

# DISCUSSION

Cognitive and memory deficits are one of the major clinical symptoms in brain aging. Numerous studies have confirmed that long-term D-gal subcutaneous injection (100 mg/kg) can induce memory impairment of rodents, so we employed the D-gal to establish the model of brain aging, and the mice were treated with D-gal by subcutaneous injection for 8 weeks in the present research (Chen et al., 2019; Jeong et al., 2021; Oskouei et al., 2021). Metformin is the activator of AMP-activated protein kinase (AMPK) (Steinberg and Carling., 2019). Simultaneously, previous studies have confirmed that metformin can alleviate the memory impairment of brain aging models in rodents by inhibiting oxidative stress and neuroinflammation, so it was used as a controlled drug in this research (Pan et al., 2016; Mudgal et al., 2019; Saffari et al., 2020). After treatment with metformin and QJD, we applied the MWM test to examine the learning and memory of mice in each group. As showed in **Figure 1**, there was no obvious difference in average escape latency to platform among all groups

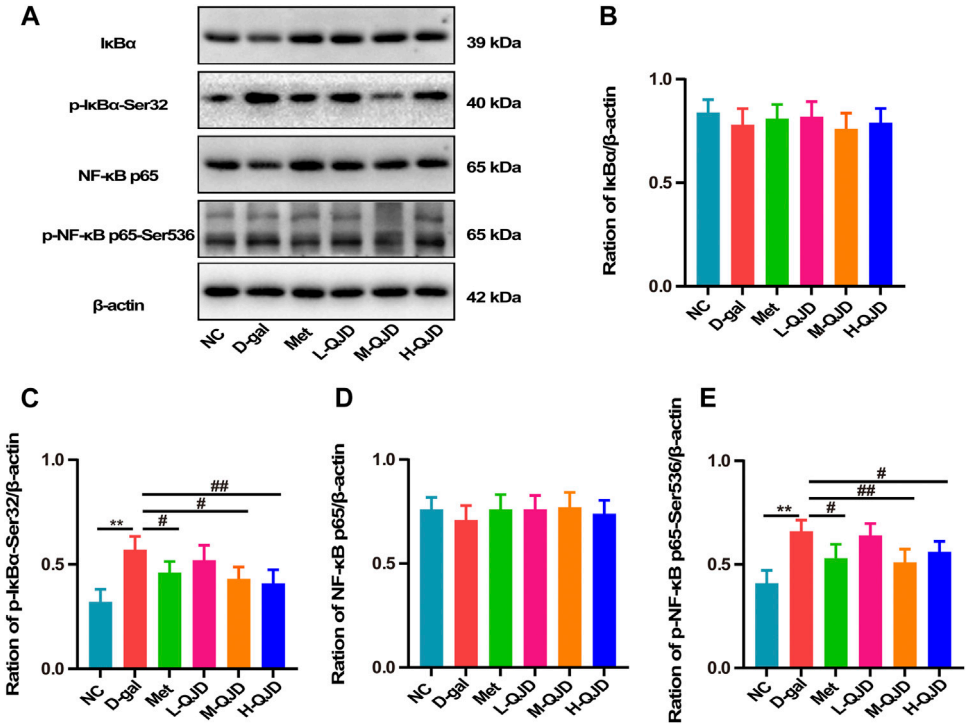


**FIGURE 6 |** QJD inhibited the NF-κB signaling pathway in the hippocampus of D-gal–induced mice. **(A)** Representative Western blot bands showing the protein expression levels of IκBα, p-IκBα-Ser32, NF-κB p65, and p-NF-κB p65-Ser536 in the hippocampus. **(B)** Relative protein expression level of IκBα. **(C)** Relative protein expression level of *p*-IκBα-Ser32. **(D)** Relative protein expression level of NF-κB p65. **(E)** Relative protein expression level of p-NF-κB p65-Ser536. All data were presented as mean ± SEM ($n$ = 6/group). $^{**}p < 0.01$ vs. NC group; $^{\#}p < 0.05$ and $^{\#\#}p < 0.01$ vs. D-gal group.

during the first to third days of the navigation test, whereas the D-gal group significantly increased the escape latency to the platform from the fourth day compared with the NC group. Taken together, our data implied that we have successfully established the model of brain aging by subcutaneous injection of D-gal. After 4-week treatment, the M-QJD group and the H-QJD group had shortened escape latency to platform compared with the D-gal group, while we did not find a considerable alteration in the L-QJD group. The navigation test showed that M-QJD and H-QJD could mitigate the spatial learning impairment of the model of brain aging. As for the spatial probe test, the H-QJD, especially the M-QJD, had significantly increased the number of crossing platform and time spent in the target quadrant, when compared with the D-gal group. Both of above data indicated that M-QJD and H-QJD could alleviate the spatial memory impairment in the model of brain aging. In addition, the metformin group has a similar effect to the M-QJD group. Collectively, the metformin and QJD, especially the M-QJD, could alleviate the cognitive impairment in the model of brain aging induced by D-gal.

The structure and function of neurons are critical for the hippocampus-dependent learning and memory, and the damage of neuronal structure and function can induce the learning and memory dysfunction. Growing researches have demonstrated that pathological alterations in hippocampus can be induced by long-term D-gal subcutaneous injection (Bei et al., 2018; Wang L. et al., 2020). To evaluate whether QJD can alleviate the pathological changes in the hippocampus induced by D-gal, we used HE staining to detect the pathologically degenerated neurons in the hippocampus. In the HE staining, we found that the D-gal group had obvious histopathological degenerative changes in hippocampal CA1 and CA3 regions. Furthermore, FJB staining was also employed to detect degenerative neurons, and the number of FJB-positive neurons in the hippocampus was analyzed by Image-Pro Plus 7.0 software. As showed in FJB staining, the D-gal group had a higher number of FJB-positive neurons in hippocampal CA1 and CA3 regions than the NC group. Therefore, the FJB staining's results were consistent with the HE staining, both of which indicated that D-gal could induce hippocampal neurodegenerative changes. After treatment with QJD for 4 weeks, we find that the hippocampal neurodegenerative changes were improved compared to the D-gal group. The FJB staining also confirmed that QJD could reduce the number of FJB-positive cells of CA1 and CA3 regions in hippocampus. Taken together, the above experiments clearly suggested that QJD could alleviate the pathological alterations in the hippocampus induced by the D-gal.

Neuronal loss and apoptosis are other pathological features of the brain aging (Shruster et al., 2010; Grimm and Eckert, 2017). Thus, the Nissl staining and TUNEL staining were carried out to evaluate whether QJD could ameliorate the neuron loss and apoptosis, respectively. As showed in Nissl staining, compared

with the NC group, the number of neurons in the hippocampal CA1 and CA3 regions in the D-gal group was decreased. However, we found that the number of TUNEL-positive cells in hippocampal CA1 and CA3 regions of the D-gal group was prominently higher than the NC group. In short, both Nissl staining and TUNEL staining demonstrated that long-term D-gal subcutaneous injection (100 mg/kg) can induce the neuron loss and apoptosis. After 4-week treatment, the H-QJD group, especially the M-QJD group, increased the neurons in the hippocampal CA1 and CA3 regions, whereas the TUNEL-positive cells in hippocampal CA1 and CA3 regions were significantly reduced. Thus, our present study indicated that QJD could inhibit neurodegenerative changes and hippocampal neuron apoptosis induced by D-gal. Besides, Western blot was carried out to detect the apoptotic markers including Bcl-2 (anti-apoptotic protein), Bax (apoptosis regulator), and cleaved caspase-3 (pro-apoptotic protein). We noticed that the QJD groups had lower protein expression level of Bax in hippocampus in comparison with the D-gal group, and protein expression level of cleaved caspase-3 in hippocampus showed a similar trend to the Bax. However, the M-QJD and H-QJD increased the protein expression level of Bcl-2. Collectively, the above data suggested that QJD could relieve the hippocampal neuron loss and apoptosis induced by the D-gal.

Neuroinflammation is significantly involved in aggravating cognitive impairment and neurodegenerative changes of brain aging (Singhal et al., 2014). Accumulated researches have confirmed that long-term D-gal subcutaneous injection can induce neuroinflammation by stimulating the activation of microglia and astrocytes (Lu et al., 2010; Jeong et al., 2021; Oskouei et al., 2021). Meanwhile, the activation of microglia and astrocytes will further trigger neuroinflammation, and finally releasing the pro-inflammatory factors, such as TNF-α, IL-1β, and IL-6, in D-gal–induced mice. Thus, we used ELISA to detect the levels of TNF-α, IL-1β, and IL-6 in the hippocampus. The ELISA results suggested that QJD-treated groups, especially the M-QJD remarkably, suppressed the contents of TNF-α, IL-1β, and IL-6 in the hippocampus, when compared with the D-gal group. Besides, the IBA1 and GFAP expression in the hippocampus of each group was examined through immunofluorescence staining. By analyzing the fluorescence intensity of microglia and astrocytes, we noticed that the M-QJD group and the H-QJD group had a decreased level of IBA1 and GFAP in the hippocampal CA1 and CA3 regions in comparison with the D-gal group. These obtained findings demonstrated that QJD could alleviate the neuroinflammation through suppressing microglial and astrocytes activation in D-gal–induced mice.

AMP-activated protein kinase (AMPK) known as the crucial factor in the regulation of cellular energy metabolism in hippocampal tissues, but it has been demonstrated to ameliorate brain aging by regulating energy metabolism, oxidative stress, neuroinflammation, apoptosis, and autophagy (Shah et al., 2017; Stern and Mcnew, 2021). AMPKα, the representative member of the AMPK family, and the phosphorylated AMPKα at the Thr172 site can inhibit neuroinflammation and apoptosis by activating silent information regulator of transcription 1 (SIRT1). In this research, we employed the Western blot to examine the protein expression level of *p*-AMPKα-Thr172 as well as a total of AMPKα and SIRT1 in the hippocampus of mice. Our findings showed that the D-gal group had a lower protein expression level of *p*-AMPKα-Thr172 and SIRT1 in comparison with the NC group. Thus, the present research suggested that the D-gal could suppress the AMPK/SIRT1 signaling pathway. After treatment with the QJD, compared with the D-gal group, we noticed that the protein expression level of *p*-AMPKα-Thr172 and SIRT1 was remarkably increased in the M-QJD group. Collectively, our study showed that QJD could activate the AMPK/SIRT1 signaling pathway.

Nuclear factor-kappa beta (NF-κB) can be regulated by the AMPK/SIRT1 signaling pathway, and the activation of the AMPK/SIRT1 signaling pathway can inhibit the NF-κB, thereby suppressing the neuroinflammation (Li et al., 2020; Zhang et al., 2020). Under physiological conditions, NF-κB combines with IκBα in the cytoplasm. However, IκBα can be phosphorylated at serine 32 site by TNF-α, IL-1β, and IL-6. Subsequently, phosphorylated IκBα further promotes the activation of NF-κB p65 at serine 536, thereby inducing the neuroinflammation (Sivandzade et al., 2019; Ding et al., 2020). Hence, we employed Western blot to detect the protein expression levels of *p*-IκBα-Ser32 and p-NF-κB p65-Ser536 as well as the total of IκBα and NF-κB p65. As shown in **Figure 6**, the increased *p*-IκBα-Ser32 and p-NF-κB p65-Ser536 were rescued in the M-QJD group and the H-QJD group. The above results showed that QID could mitigate neuroinflammation through inhibiting the NF-κB signaling pathway in D-gal–induced mice.

## CONCLUSIONS

In short, the present study showed that QJD alleviated cognitive impairment and neurodegenerative changes induced by D-gal. Furthermore, QJD attenuated the neuroinflammation by regulating the AMPK/SIRT1/NF-κB signaling pathway. Hence, our present study suggested that QJD may offer a promising therapeutic intervention in preventing cognitive impairment of brain aging.

## DATA AVAILABILITY STATMENT

The original contributions presented in the study are included in the article/supplementary material, and further inquiries can be directed to the corresponding author/s.

## ETHICS STATEMENT

The animal study was reviewed and approved by the Animal Ethics Review Committee of Hubei University of Chinese Medicine (No. 8217150845; Hubei, China).

## AUTHOR CONTRIBUTIONS

L-LH, Y-CW, and Y-TA contributed equally to this work and should be considered by co-first authors; Q-HL and HH co-designed the study and should be considered co-corresponding authors; L-LH, Y-CW, and Y-TA carried out the experiments and wrote the

manuscript; S-MG provided technical support for FJB staining in this study; PW provided experimental equipment and technology for this study; L-LH, Y-CW, Y-TA, and LW conducted the analysis of data. All authors have revised and approved the manuscript.

## FUNDING

This work was sponsored by the National Natural Science Foundation of China (81973921).

## REFERENCES


Ahmad, S., Khan, A., Ali, W., Jo, M. H., Park, J., Ikram, M., et al. (2021). Fisetin Rescues the Mice Brains against D-Galactose-Induced Oxidative Stress, Neuroinflammation and Memory Impairment. *Front. Pharmacol.* 12, 612078. doi:10.3389/fphar.2021.612078

Baeta-Corral, R., Castro-Fuentes, R., and Giménez-Llort, L. (2018). Sexual Dimorphism in the Behavioral Responses and the Immunoendocrine Status in D-Galactose-Induced Aging. *J. Gerontol. A. Biol. Sci. Med. Sci.* 73, 1147–1157. doi:10.1093/gerona/gly031

Bei, Y., Wu, X., Cretoiu, D., Shi, J., Zhou, Q., Lin, S., et al. (2018). miR-21 Suppression Prevents Cardiac Alterations Induced by D-Galactose and Doxorubicin. *J. Mol. Cell Cardiol.* 115, 130–141. doi:10.1016/j.yjmcc.2018.01.007

Cao, P., Zhang, J., Huang, Y., Fang, Y., Lyu, J., and Shen, Y. (2019). The Age-Related Changes and Differences in Energy Metabolism and Glutamate-Glutamine Recycling in the D-Gal-Induced and Naturally Occurring Senescent Astrocytes *In Vitro*. *Exp. Gerontol.* 118, 9–18. doi:10.1016/j.exger.2018.12.018

Chen, C., Zhou, M., Ge, Y., and Wang, X. (2020). SIRT1 and Aging Related Signaling Pathways. *Mech. Ageing Dev.* 187, 111215. doi:10.1016/j.mad.2020.111215

Chen, S., Zhou, H., Zhang, G., Meng, J., Deng, K., Zhou, W., et al. (2019). Anthocyanins from Lycium Ruthenicum Murr. Ameliorated D-Galactose-Induced Memory Impairment, Oxidative Stress, and Neuroinflammation in Adult Rats. *J. Agric. Food Chem.* 67, 3140–3149. doi:10.1021/acs.jafc.8b06402

Ding, B., Lin, C., Liu, Q., He, Y., Ruganzu, J. B., Jin, H., et al. (2020). Tanshinone IIA Attenuates Neuroinflammation via Inhibiting RAGE/NF-κB Signaling Pathway *In Vivo* and *In Vitro*. *J. Neuroinflammation* 17, 302. doi:10.1186/s12974-020-01981-4

Domise, M., and Vingtdeux, V. (2016). AMPK in Neurodegenerative Diseases. *Exp. Suppl.* 107, 153–177. doi:10.1007/978-3-319-43589-3_7

El-Far, A. H., Lebda, M. A., Noreldin, A. E., Atta, M. S., Elewa, Y. H. A., Elfeky, M., et al. (2020). Quercetin Attenuates Pancreatic and Renal D-Galactose-Induced Aging-Related Oxidative Alterations in Rats. *Int. J. Mol. Sci.* 21, 4348. doi:10.3390/ijms21124348

Farr, S. A., Roesler, E., Niehoff, M. L., Roby, D. A., Mckee, A., and Morley, J. E. (2019). Metformin Improves Learning and Memory in the SAMP8 Mouse Model of Alzheimer's Disease. *Jad* 68, 1699–1710. doi:10.3233/jad-181240

Fung, I. T. H., Sankar, P., Zhang, Y., Robison, L. S., Zhao, X., D'Souza, S. S., et al. (2020). Activation of Group 2 Innate Lymphoid Cells Alleviates Aging-Associated Cognitive Decline. *J. Exp. Med.* 217, e20190915. doi:10.1084/jem.20190915

Garthe, A., and Kempermann, G. (2013). An Old Test for New Neurons: Refining the Morris Water Maze to Study the Functional Relevance of Adult Hippocampal Neurogenesis. *Front. Neurosci.* 7, 63. doi:10.3389/fnins.2013.00063

Grimm, A., and Eckert, A. (2017). Brain Aging and Neurodegeneration: from a Mitochondrial point of View. *J. Neurochem.* 143, 418–431. doi:10.1111/jnc.14037

Gu, B., Wang, M., and Zhang, W. (2008). Effect of Qiangji Decoction on Learning and Lemory Impaiment Induced by D-Galactose in Mice. *Guiding J. Chin. Med. Pharm.*, 616–618. doi:10.3969/j.issn.1672-951X.2008.08.003

Jeong, J.-H., Koo, J.-H., Yook, J. S., Cho, J.-Y., and Kang, E.-B. (2021). Neuroprotective Benefits of Exercise and MitoQ on Memory Function, Mitochondrial Dynamics, Oxidative Stress, and Neuroinflammation in D-Galactose-Induced Aging Rats. *Brain Sci.* 11, 164. doi:10.3390/brainsci11020164

Li, F., Chen, Y., Li, Y., Huang, M., and Zhao, W. (2020). Geniposide Alleviates Diabetic Nephropathy of Mice through AMPK/SIRT1/NF-κB Pathway. *Eur. J. Pharmacol.* 886, 173449. doi:10.1016/j.ejphar.2020.173449

Li, F., Wu, Z., Li, Y., Chen, M., and Yang, M. (2008). Effect of Qiangji Decoction on Learning and Lemory Impaiment Induced by D-Galactose in Mice. *J. Beijing Univ. Chin. Med.* 886, 9–11. doi:10.3321/j.issn:1006-2157.2008.09.010

Li, H., Lei, T., Zhang, J., Yan, Y., Wang, N., Song, C., et al. (2021). Longan (Dimocarpus Longan Lour.) Aril Ameliorates Cognitive Impairment in AD Mice Induced by Combination of D-gal/AlCl3 and an Irregular Diet via RAS/MEK/ERK Signaling Pathway. *J. Ethnopharmacology* 267, 113612. doi:10.1016/j.jep.2020.113612

Li, W., Chaudhari, K., Shetty, R., Winters, A., Gao, X., Hu, Z., et al. (2019). Metformin Alters Locomotor and Cognitive Function and Brain Metabolism in Normoglycemic Mice. *Aging Dis.* 10, 949–963. doi:10.14336/ad.2019.0120

Lima Giacobbo, B., Doorduin, J., Klein, H. C., Dierckx, R. A. J. O., Bromberg, E., and De Vries, E. F. J. (2019). Brain-Derived Neurotrophic Factor in Brain Disorders: Focus on Neuroinflammation. *Mol. Neurobiol.* 56, 3295–3312. doi:10.1007/s12035-018-1283-6

Lin, J.-Y., Kuo, W.-W., Baskaran, R., Kuo, C.-H., Chen, Y.-A., Chen, W. S.-T., et al. (2020). Swimming Exercise Stimulates IGF1/PI3K/Akt and AMPK/SIRT1/PGC1α Survival Signaling to Suppress Apoptosis and Inflammation in Aging hippocampus. *Aging* 12, 6852–6864. doi:10.18632/aging.103046

Long, Q.-H., Wu, Y.-G., He, L.-L., Ding, L., Tan, A.-H., Shi, H.-Y., et al. (2021). Suan-Zao-Ren Decoction Ameliorates Synaptic Plasticity through Inhibition of the Aβ Deposition and JAK2/STAT3 Signaling Pathway in AD Model of APP/PS1 Transgenic Mice. *Chin. Med.* 16, 14. doi:10.1186/s13020-021-00425-2

Lu, J., Wu, D.-m., Zheng, Y.-l., Hu, B., Zhang, Z.-f., Ye, Q., et al. (2010). Ursolic Acid Attenuates D-Galactose-Induced Inflammatory Response in Mouse Prefrontal Cortex through Inhibiting AGEs/RAGE/NF- B Pathway Activation. *Cereb. Cortex* 20, 2540–2548. doi:10.1093/cercor/bhq002

Mudgal, J., Nampoothiri, M., Basu Mallik, S., Kinra, M., Hall, S., Grant, G., et al. (2019). Possible Involvement of Metformin in Downregulation of Neuroinflammation and Associated Behavioural Changes in Mice. *Inflammopharmacol* 27, 941–948. doi:10.1007/s10787-019-00638-w

Oskouei, Z., Mehri, S., Kalalinia, F., and Hosseinzadeh, H. (2021). Evaluation of the Effect of Thymoquinone in D -galactose-induced Memory Impairments in Rats: Role of MAPK , Oxidative Stress, and Neuroinflammation Pathways and Telomere Length. *Phytotherapy Res.* 35, 2252–2266. doi:10.1002/ptr.6982

Pan, Y., Sun, X., Jiang, L., Hu, L., Kong, H., Han, Y., et al. (2016). Metformin Reduces Morphine Tolerance by Inhibiting Microglial-Mediated Neuroinflammation. *J. Neuroinflammation* 13, 294. doi:10.1186/s12974-016-0754-9

Peixoto, C. A., Oliveira, W. H. d., Araújo, S. M. d. R., and Nunes, A. K. S. (2017). AMPK Activation: Role in the Signaling Pathways of Neuroinflammation and Neurodegeneration. *Exp. Neurol.* 298, 31–41. doi:10.1016/j.expneurol.2017.08.013

Rong, S., Wan, D., Fan, Y., Liu, S., Sun, K., Huo, J., et al. (2019). Amentoflavone Affects Epileptogenesis and Exerts Neuroprotective Effects by Inhibiting NLRP3 Inflammasome. *Front. Pharmacol.* 10, 856. doi:10.3389/fphar.2019.00856

Saffari, P. M., Alijanpour, S., Takzaree, N., Sahebgharani, M., Etemad-Moghadam, S., Noorbakhsh, F., et al. (2020). Metformin Loaded Phosphatidylserine Nanoliposomes Improve Memory Deficit and Reduce Neuroinflammation in Streptozotocin-Induced Alzheimer's Disease Model. *Life Sci.* 255, 117861. doi:10.1016/j.lfs.2020.117861

Salami, A., Papenberg, G., Sitnikov, R., Laukka, E. J., Persson, J., and Kalpouzos, G. (2021). Elevated Neuroinflammation Contributes to the Deleterious Impact of Iron Overload on Brain Function in Aging. *Neuroimage* 230, 117792. doi:10.1016/j.neuroimage.2021.117792

Shah, S. Z. A., Zhao, D., Hussain, T., and Yang, L. (2017). Role of the AMPK Pathway in Promoting Autophagic Flux via Modulating Mitochondrial Dynamics in Neurodegenerative Diseases: Insight into Prion Diseases. *Ageing Res. Rev.* 40, 51–63. doi:10.1016/j.arr.2017.09.004

Shruster, A., Melamed, E., and Offen, D. (2010). Neurogenesis in the Aged and Neurodegenerative Brain. *Apoptosis* 15, 1415–1421. doi:10.1007/s10495-010-0491-y

Shwe, T., Pratchayasakul, W., Chattipakorn, N., and Chattipakorn, S. C. (2018). Role of D-Galactose-Induced Brain Aging and its Potential Used for Therapeutic Interventions. *Exp. Gerontol.* 101, 13–36. doi:10.1016/j.exger.2017.10.029

Singhal, G., Jaehne, E. J., Corrigan, F., Toben, C., and Baune, B. T. (2014). Inflammasomes in Neuroinflammation and Changes in Brain Function: a Focused Review. *Front. Neurosci.* 8, 315. doi:10.3389/fnins.2014.00315

Sivandzade, F., Prasad, S., Bhalerao, A., and Cucullo, L. (2019). NRF2 and NF-Ƙb Interplay in Cerebrovascular and Neurodegenerative Disorders: Molecular Mechanisms and Possible Therapeutic Approaches. *Redox Biol.* 21, 101059. doi:10.1016/j.redox.2018.11.017

Steinberg, G. R., and Carling, D. (2019). AMP-activated Protein Kinase: the Current Landscape for Drug Development. *Nat. Rev. Drug Discov.* 18, 527–551. doi:10.1038/s41573-019-0019-2

Stern, M., and Mcnew, J. A. (2021). A Transition to Degeneration Triggered by Oxidative Stress in Degenerative Disorders. *Mol. Psychiatry* 26, 736–746. doi:10.1038/s41380-020-00943-9

Sun, K., Yang, P., Zhao, R., Bai, Y., and Guo, Z. (2018). Matrine Attenuates D-Galactose-Induced Aging-Related Behavior in Mice via Inhibition of Cellular Senescence and Oxidative Stress. *Oxidative Med. Cell Longevity* 2018, 1–12. doi:10.1155/2018/7108604

Trevisan, C., Limongi, F., Siviero, P., Noale, M., Cignarella, A., Manzato, E., et al. (2021). Mild Polypharmacy and MCI Progression in Older Adults: the Mediation Effect of Drug-Drug Interactions. *Aging Clin. Exp. Res.* 33, 49–56. doi:10.1007/s40520-019-01420-2

Ullah, R., Jo, M. H., Riaz, M., Alam, S. I., Saeed, K., Ali, W., et al. (2020). Glycine, the Smallest Amino Acid, Confers Neuroprotection against D-Galactose-Induced Neurodegeneration and Memory Impairment by Regulating C-Jun N-Terminal Kinase in the Mouse Brain. *J. Neuroinflammation* 17, 303. doi:10.1186/s12974-020-01989-w

Wahl, D., Coogan, S., Solon-Biet, S., De Cabo, R., Haran, J., Raubenheimer, D., et al. (2017). Cognitive and Behavioral Evaluation of Nutritional Interventions in Rodent Models of Brain Aging and Dementia. *Clin. Interview. Aging* Vol. 12, 1419–1428. doi:10.2147/cia.S145247

Wang, L., Chen, Q., Zhuang, S., Wen, Y., Cheng, W., Zeng, Z., et al. (2020a). Effect of Anoectochilus Roxburghii Flavonoids Extract on H2O2 - Induced Oxidative Stress in LO2 Cells and D-Gal Induced Aging Mice Model. *J. Ethnopharmacology* 254, 112670. doi:10.1016/j.jep.2020.112670

Wang, W., Liu, F., Xu, C., Liu, Z., Ma, J., Gu, L., et al. (2021). Lactobacillus Plantarum 69-2 Combined with Galacto-Oligosaccharides Alleviates D-Galactose-Induced Aging by Regulating the AMPK/SIRT1 Signaling Pathway and Gut Microbiota in Mice. *J. Agric. Food Chem.* 69, 2745–2757. doi:10.1021/acs.jafc.0c06730

Wang, Y., Yang, Z., Yang, L., Zou, Q., Zhao, S., Hu, N., et al. (2020b). Liuweidihuang Pill Alleviates Inflammation of the Testis via AMPK/SIRT1/NF-κB Pathway in Aging Rats. *Evidence-Based Complement. Altern. Med.* 2020, 1–9. doi:10.1155/2020/2792738

Xie, B. S., Wang, Y. Q., Lin, Y., Mao, Q., Feng, J. F., Gao, G. Y., et al. (2019). Inhibition of Ferroptosis Attenuates Tissue Damage and Improves Long-term Outcomes after Traumatic Brain Injury in Mice. *CNS Neurosci. Ther.* 25, 465–475. doi:10.1111/cns.13069

Yahfoufi, N., Matar, C., and Ismail, N. (2020). Adolescence and Aging: Impact of Adolescence Inflammatory Stress and Microbiota Alterations on Brain Development, Aging, and Neurodegeneration. *J. Gerontol. A. Biol. Sci. Med. Sci.* 75, 1251–1257. doi:10.1093/gerona/glaa006

Yiannopoulou, K. G., and Papageorgiou, S. G. (2020). Current and Future Treatments in Alzheimer Disease: An Update. *J. Cent. Nerv Syst. Dis.* 12, 117957352090739. doi:10.1177/1179573520907397

Zhang, F., Feng, J., Zhang, J., Kang, X., and Qian, D. (2020). Quercetin Modulates AMPK/SIRT1/NFκB Signaling to Inhibit Inflammatory/oxidative Stress Responses in Diabetic High Fat Dietinduced Atherosclerosis in the Rat Carotid Artery. *Exp. Ther. Med.* 20, 1. doi:10.3892/etm.2020.9410

**Conflict of Interest:** The authors declare that the research was conducted in the absence of any commercial or financial relationships that could be construed as a potential conflict of interest.

**Publisher's Note:** All claims expressed in this article are solely those of the authors and do not necessarily represent those of their affiliated organizations, or those of the publisher, the editors, and the reviewers. Any product that may be evaluated in this article, or claim that may be made by its manufacturer, is not guaranteed or endorsed by the publisher.

frontiers in Pharmacology

ORIGINAL RESEARCH
published: 22 November 2021
doi: 10.3389/fphar.2021.698833

# Modulatory Effects of Alpha- and Gamma-Tocopherol on the Mitochondrial Respiratory Capacity and Membrane Potential in an *In Vitro* Model of Alzheimer's Disease

*Aslina Pahrudin Arrozi, Wan Zurinah Wan Ngah, Hanafi Ahmad Damanhuri and Suzana Makpol**

*Department of Biochemistry, Faculty of Medicine, Universiti Kebangsaan Malaysia Medical Centre, Kuala Lumpur, Malaysia*

Increased amyloid-beta (Aβ) and amyloid precursor protein (APP) in the brains of Alzheimer's disease (AD) patients are common pathological hallmarks mediating the disease progression. Growing evidence also suggests that mitochondrial abnormalities are an early feature in the pathogenesis of AD. Intervention with antioxidants has received great interest as a molecular strategy for the manipulation of mitochondrial function. Our previous preliminary study using *in vitro* cell models expressing different types of APP demonstrated that treatment with alpha-tocopherol (ATF) or gamma-tocopherol (GTF) modulates mitochondrial function by reducing mitochondrial reactive oxygen species (ROS), increasing the production of ATP and preventing apoptosis events, especially in cells expressing the mutant APP form. Thus, we hypothesized that ATF or GTF treatment might also alter mitochondrial metabolic pathways such as oxidative phosphorylation. The present study aimed to investigate the role of ATF and GTF in modulating mitochondrial oxidative metabolism using high-resolution respirometry. Our results showed that both ATF and GTF increased the respiratory capacity and membrane potential in the ROUTINE and $OXPHOS_{CI\text{-}LINKED}$ states as well as complex IV enzyme activity in wild-type and mutant APP-overexpressing SH-SY5Y cells. Although preliminary, these findings indicate that ATF and GTF modulate mitochondrial oxidative metabolism in APP-overexpressing cells and, in part, may contribute to the planning of strategies for utilizing vitamin E isomers against mitochondrial-related diseases such as AD.

**Keywords: tocopherol, amyloid precursor proteins, respiratory capacity, membrane potential, Alzheimer's disease**

OPEN ACCESS

***Edited by:***
*Shijun Xu,*
*Chengdu University of Traditional Chinese Medicine, China*

***Reviewed by:***
*Ning Jia,*
*Xi'an Jiaotong University, China*
*Heather M. Wilkins,*
*University of Kansas Medical Center Research Institute, United States*

****Correspondence:***
*Suzana Makpol*
*suzanamakpol@ppukm.ukm.edu.my*

***Specialty section:***
*This article was submitted to Neuropharmacology, a section of the journal Frontiers in Pharmacology*

***Received:*** *22 April 2021*
***Accepted:*** *29 October 2021*
***Published:*** *22 November 2021*

***Citation:***
*Pahrudin Arrozi A, Wan Ngah WZ, Ahmad Damanhuri H and Makpol S (2021) Modulatory Effects of Alpha- and Gamma-Tocopherol on the Mitochondrial Respiratory Capacity and Membrane Potential in an* In Vitro *Model of Alzheimer's Disease. Front. Pharmacol. 12:698833. doi: 10.3389/fphar.2021.698833*

## INTRODUCTION

The accumulation of insoluble amyloid-beta (Aβ) protein in extracellular amyloid plaques in the brains of Alzheimer's disease (AD) patients is well known as the classical pathological hallmark of the disease (Tiwari et al., 2019) together with the presence of neurofibrillary tangles (NFTs) (Gao et al., 2018). In addition to abnormalities in protein aggregation, other pathological changes are seen in this condition, such as alterations in mitochondrial function (Bell et al., 2021). A recent study showed that overexpression of the β-secretase-derived APP-CTF fragment (C99) in

neuroblastoma SH-SY5Y cells triggers excessive mitochondrial morphology alterations associated with enhanced mitochondrial reactive oxygen species production independent of Aβ (Vaillant-Beuchot et al., 2021). Another study showed that overexpression of the human amyloid precursor protein (APP) with the familial Swedish mutation (APPswe) in a mouse neuroblastoma cell line (N2A) altered the structure and function of mitochondria-associated membranes, mitochondrial dynamics, biogenesis and protein import as well as the stress response (Fernandes et al., 2021). Previously, our group showed that the level of reactive oxygen species (ROS) in the mitochondria, activity of complex V enzyme, and cyclophilin D (CypD) and pro-caspase 3 protein expression as well as cytochrome c release were increased, followed by a decrease in ATP levels in SH-SY5Y cells overexpressing the mutant APP form (Pahrudin Arrozi et al., 2020), suggesting that the mitochondrial function in these *in vitro* models of AD was also altered. Thus, we hypothesized that mitochondrial metabolic pathways, such as oxidative phosphorylation and membrane potential, were also altered, as mitochondrial oxidative metabolism is the major site of ATP synthesis.

Several previous studies have demonstrated the tremendous role of alpha-tocopherol (ATF) as a radical-scavenging antioxidant to protect cells against ROS (Ulatowski and Manor, 2015) and as a signalling molecule that influences the expression of genes involved in disease development (Pédeboscq et al., 2012; Zingg, 2019). ATF is the most widely studied vitamin E isomer, as it has the highest biological activity in the body (Reboul, 2017) and is related to vitamin E deficiency syndrome (Jilani and Iqbal, 2018). In addition to ATF, other isomers of vitamin E, such as gamma-tocopherol (GTF), have also demonstrated unique functions in preventing oxidative stress in the brain related to reactive nitrogen species (RNS) (Williamson et al., 2002) regardless of their low bioavailability in the body (Ashley et al., 2019). Furthermore, a previous study also demonstrated that lower brain GTF in combination with higher ATF was associated with higher AD neuropathology (Morris et al., 2015), and higher GTF levels were found to be associated with higher presynaptic protein levels in the elderly human midfrontal cortex (de Leeuw et al., 2020), supporting the important role of GTF in the brain.

Studies on the role of ATF or GTF treatment on mitochondria are still limited. A recent *in vitro* study showed that treatment with different vitamin E isoforms, including ATF, had protective effects by reducing oxidative stress and increasing metabolic activity *via* oxidative metabolism in a human endothelial cell line under conditions mimicking sepsis (Minter et al., 2020). In addition, an *in vivo* study with preadministration of high-dose ATF showed significantly improved memory and mitochondrial membrane potential impairment as well as reduced ROS levels in the rat hippocampus induced with lactacystin, a proteasome inhibitor (Nesari et al., 2019). Our previous preliminary study revealed that treatment with ATF or GTF for 24 h reduced the Aβ42 and mitochondrial ROS levels, increased the activity of complex V enzyme and ATP levels, and prevented apoptotic events in SH-SY5Y cells overexpressing mutant APP (Pahrudin Arrozi et al., 2020), suggesting the protective effects of vitamin E on mitochondria. Therefore, in the present study, we aimed to investigate the potential effects of ATF and GTF in modulating mitochondrial oxidative metabolism to further elucidate the protective role of both vitamin E isomers, which may contribute to strategies against mitochondrial-related diseases such as AD.

# MATERIALS AND METHODS

## Development of SH-SY5Y Cells Overexpressing Wild-type and Mutant APP Genes

The development of SH-SY5Y cells stably expressing the wild-type or mutant APP gene was described in our previous study (Pahrudin Arrozi et al., 2017). Briefly, SH-SY5Y cells were transfected with three different plasmids carrying the wild-type (WT), Swedish (Swe), or Swedish/Indiana (Swe/Ind) form of the APP gene using Lipofectamine 3000 (Invitrogen, Carlsbad, United States). After 72 h of transfection, the positive green fluorescent protein (GFP)-expressing cells were selected using selection medium containing 400 μg/ml geneticin (G418) (Gibco, Calrsbad, United States). The steady state APP gene and protein expression as well as the production of secreted Aβ42/Aβ40 were measured for verification. The methodology and results of these evaluations have been published, whereby the levels of APP mRNA and protein expression were increased in all cells stably expressing the different types of APP genes, while the ratio of Aβ42/40 was found to be increased in the following order: SH-SY5Y-APP WT < SH-SY5Y-APP Swe < SH-SY5Y-APP Swe/Ind (Pahrudin Arrozi et al., 2017).

## Cell Culture

The nontransfected SH-SY5Y cells were grown in complete culture medium (CCM) containing a 1:1 ratio of Dulbecco's modified Eagle's medium (DMEM) and Ham's F-12 medium with 1% penicillin/streptomycin (Gibco) and 10% foetal bovine serum (FBS) (HyClone, Utah, United States). The stably transfected SH-SY5Y cell lines were grown in CCM without penicillin/streptomycin but with 400 μg/ml geneticin (Gibco). All types of cells were cultured in a humidified atmosphere of 5% $CO_2$ at 37°C.

## Treatment of Cells With Tocopherol Isomers

Stock solutions of ATF (98.9% pure d-ATF) and GTF (95% pure d-GTF) (ChromaDex, California, United States) were freshly prepared in 100% ethanol (EtOH) to a final stock solution concentration of 0.5 M and stored at −20°C for not more than 1 month. Prior to treatment, 15 μl of each isomer from the stock solution was incubated overnight with 20 μl of FBS at 37°C and then diluted to 0.1 M with 18 μl of CCM and 21 μl of 100% ethanol. The isomer solution was further diluted to 0.05 M with a 72 μl mixture of CCM and 100% ethanol in a 1:1 ratio (50% ethanol). Subsequently, the isomer solution was diluted to 0.025 M with 146 μl of CCM only. Next, 60 μl from the

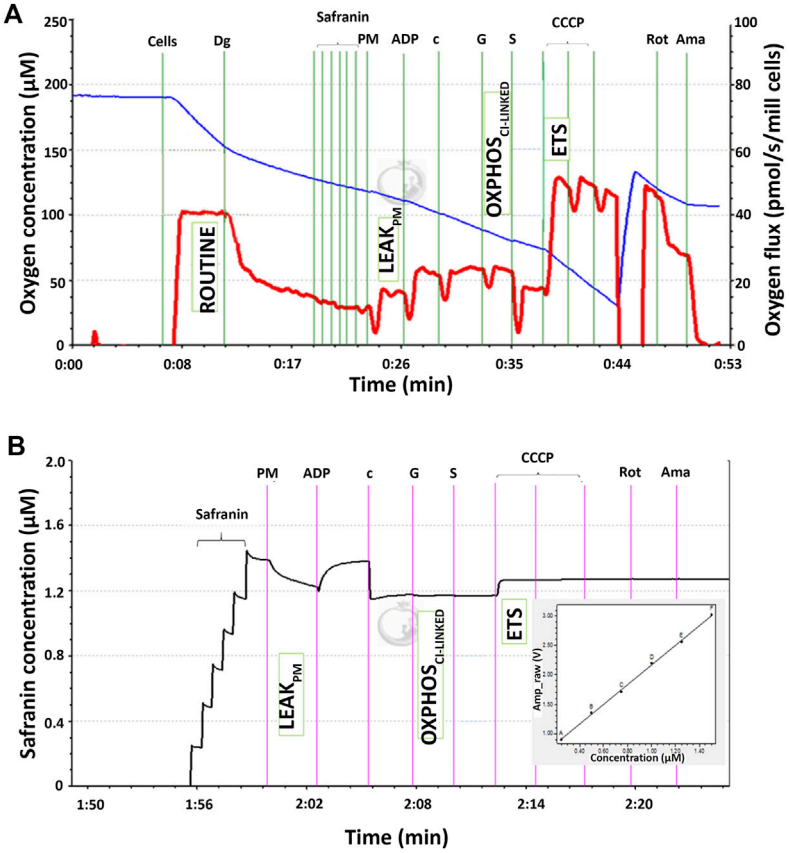


**FIGURE 1 |** Qualitative data for simultaneous high-resolution respirometry analysis of **(A)** the respiratory capacity at four selected mitochondrial bioenergetics states: ROUTINE, $LEAK_{PM}$, $OXPHOS_{CI-LINKED}$, and ETS expressed as the oxygen flux (pmol/s/mill cells) represented by the red line and **(B)** membrane potential at three selected mitochondrial bioenergetic states: $LEAK_{PM}$, $OXPHOS_{CI-LINKED}$, and ETS. The black line corresponds to the safranin concentration in the chamber medium and is directly proportional to the safranin signal expressed as amperes (amp). The membrane potential was inversely proportional to the safranin signal and thus calculated as 1/amp.

0.025 M isomer stock solution was removed and transferred into a new microcentrifuge tube. Then, 240 µl of CCM was added to prepare the 0.005 M stock solution. Two more stocks solutions (0.004 and 0.00025 M) were prepared by taking out 80 and 5 µL from the 0.005 M stock solution and combining them with 20 and 95 µL of CCM, respectively. Finally, the desired working concentrations of each isomer (5, 80, and 100 µM) were prepared from their respective stock solution (0.00025, 0.004, and 0.005 M), to give the final concentration of each tocopherol isomer in the culture media added to the cells. The final concentrations of ethanol and FBS were kept constant at 0.1 and 0.027%, respectively (calculated from the overnight incubation with 20 µL of FBS). Tocopherol treatment was carried out for 24 h. The cytotoxicity assay was performed in our previous study, and the results showed that ATF or GTF at concentrations from 1 to 100 µM were not toxic to the cells (Pahrudin Arrozi et al., 2020).

## Chemicals and Reagents Used in the Oxygraph-2k Experiment

All chemicals and reagents used in Oxygraph-2k (O2k), such as ethylene-glycol-bis(β-aminoetyl ether)-N,N,N′,N′-tetraacetic acid (EGTA), magnesium chloride hexahydrate ($MgCl_26H_2O$), lactobionic acid, taurine, potassium dihydrogen phosphate ($KH_2PO_4$), HEPES, D-sucrose, free fatty acid bovine serum albumin (BSA), sodium pyruvate (P), malate (M), glutamate (G), succinate (S), cytochrome c, catalase, adenosine 5′-diphosphate (ADP), carbonyl cyanide 3-chlorophenylhydrazone (CCCP), rotenone, antimysin-A, digitonin, safranin, ascorbate, tetramethyl-p-phenylenediamine dihydrochloride (TMPD) and sodium azide ($NaN_3$), were from Sigma–Aldrich, Missouri, United States. The preparation of all the substances is described in **Supplementary Table S1**.

## Simultaneous Determination of the Mitochondrial Respiratory Capacity and Membrane Potential

The simultaneous determination of the respiratory capacity and membrane potential was carried out using an Oxygraph-2k (O2k) (Oroboros Instruments, Innsbruck, Austria) according to the standard protocol as elaborated previously

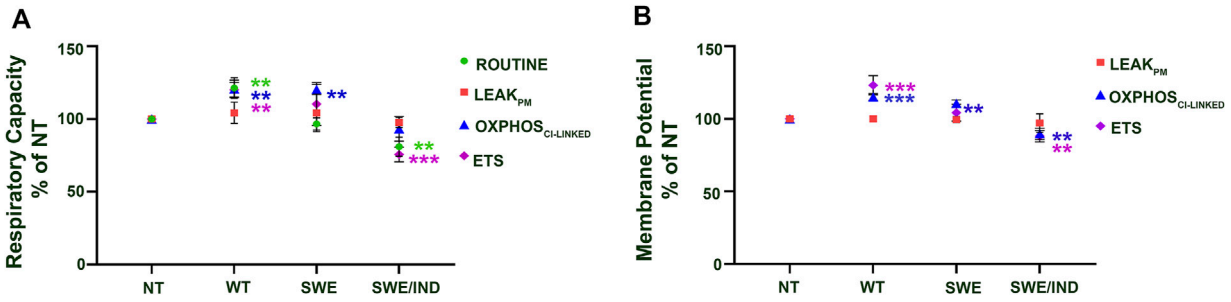


**FIGURE 2 |** Comparison between SH-SY5Y cells overexpressing different types of APP (WT, Swe and Swe/Ind) at different mitochondrial bioenergetic states (ROUTINE, $LEAK_{PM}$, $OXPHOS_{CI-LINKED}$ and ETS) expressed as % of nontransfected control (NT). **(A)** Respiratory capacity and **(B)** membrane potential. **: $p < 0.01$, ***: $p < 0.001$. Data are expressed as the mean ± SD, (N = 3).

(Krumschnabel et al., 2014; Lemieux et al., 2017). Briefly, at the beginning of each experiment, the O2k chambers were filled with 2.5 ml of Mir05 solution (**Supplementary Table S2**), excess solution was removed (final volume of Mir05 in the chamber was ~2.0 ml), calibrated with air at 37°C (9.72 µM O2/kPa) and constantly stirred using white PVDF-coated stirrers at 750 rpm. Each group of cells was trypsinized, and the cell pellet was then resuspended in 300 µL of Mir05 solution. The number of cells was calculated for normalization, and the cell suspension was titrated into chambers. Substrate–uncoupler–inhibitor titration (SUIT) protocols were then applied for the simultaneous determination of mitochondrial respiratory capacity and membrane potential analysis (**Supplementary Figure S1**).

After cell permeabilization with digitonin, nonphosphorylating LEAK respiration ($LEAK_{PM}$) was induced by adding the CI-linked substrates pyruvate (5 mM) and malate (2 mM). Subsequently, the OXPHOS capacity of CI-linked activity ($OXPHOS_{CI-LINKED}$) was measured after the addition of saturating concentrations of ADP (2.5 mM), cytochrome c (10 µM) and glutamate (10 mM). The OXPHOS capacity with combined CI and CII-linked substrates ($OXPHOS_{CI-CII-LINKED}$) was assessed by the addition of succinate (10 mM). Stepwise titration of CCCP (3 steps; 0.5, 1 and 1.5 µM), 0.5 µM) leads to proton leakage through the inner mitochondrial membrane and was used to measure the capacity of the electron transfer system (ETS), which is the noncoupled state at the optimum uncoupler concentration for maximum oxygen flux. Subsequent inhibition of CI by rotenone (0.5 µM) provided measurement of the CII-linked ETS capacity ($ETS_{CII-LINKED}$). To control for other oxygen-consuming processes, CIII was inhibited by antimycin A (2.5 µM). The resulting residual oxygen consumption (ROX) reflects oxygen consumption from undefined sources and was subtracted from mitochondrial respiratory states. Meanwhile, for membrane potential, the safranin signal was corrected manually using the value of cytochrome c acquired when injected into the chamber alone. The respiratory flux was expressed per million cells (pmol/s/mill cells). The fluorescence of the safranin signal was detected at an excitation wavelength of 495 nm and emission wavelength of 587 nm. The safranin signal (ampere) was inversely proportional to the membrane potential. The membrane potential was calculated as 1/Amp. Each experiment was repeated three times.

## Determination of Complex IV Enzyme Activity

Determination of complex IV enzyme activity was carried out using Oxygraph-2k (O2k) (Oroboros Instruments, Innsbruck, Austria). At the beginning of each experiment, 5 µL of 112,000 µ/mL catalase solution was titrated into O2k chambers filled with 2.5 ml Mir05 (final volume of Mir05 in the chamber was ~2.0 ml), calibrated with air at 37°C (9.72 µM $O_2$/kPa) and constantly stirred using white PVDF-coated stirrers at 750 rpm. Each group of cells was trypsinized, and the cell pellet was then resuspended in 300 µL of Mir05. The number of cells was calculated for normalization followed by titration protocols (**Supplementary Figure S2**). All substance preparations are presented in **Supplementary Table S3**. The final concentrations of all the substances were as follows: digitonin (0.01 mg/ml), rotenone (0.5 µM), CCCP (0.5 µM), ascorbate (2 mM), TMPD (0.5 mM), cytochrome c (10 µM), and $NaN_3$ (0.2 M). The value of oxygen flux was corrected automatically by Datlab 7 software using the value recorded after the inhibition of complex IV activity due to substrate autooxidation. Each experiment was repeated three times.

## Statistical Analysis

Statistical analyses were performed using GraphPad PRISM v.8 software (GraphPad Software, La Jolla, California, United States). Data obtained were expressed as the mean ± SD. Statistical comparisons between groups were performed using one-way ANOVA followed by the Sidak post hoc test. The statistical significance of all tests was set at $p < 0.05$.

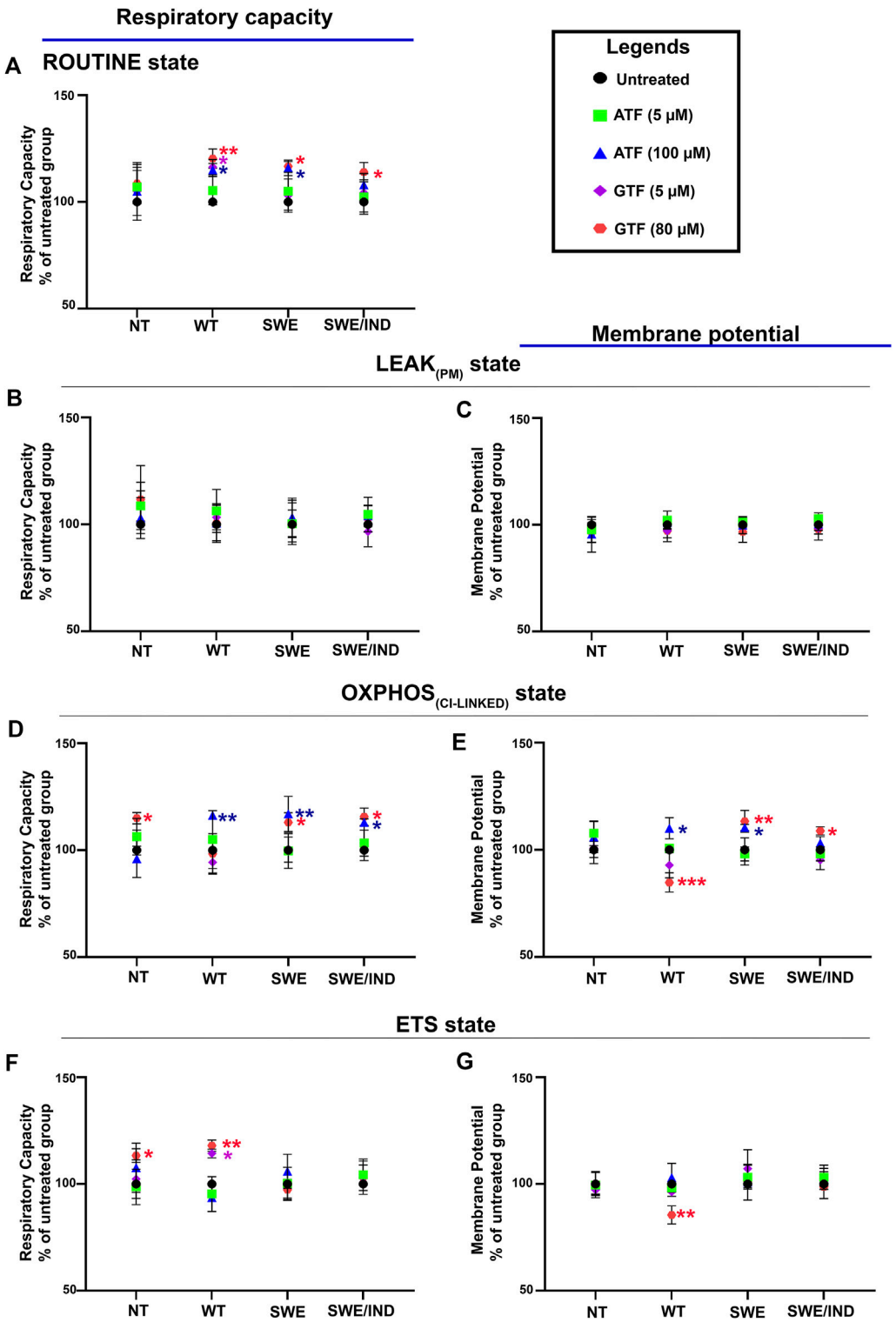


**FIGURE 3 |** Effects of ATF and GTF treatment on the mitochondrial respiratory capacity and membrane potential in nontransfected SH-SY5Y cells (NT) and cells overexpressing different types of APP (WT, Swe, and Swe/Ind) expressed as % of untreated group in the respective type of cells at **(A)** ROUTINE, **(B, C)** $LEAK_{PM}$, **(D, E)** $OXPHOS_{CI\text{-}LINKED}$ and **(F, G)** ETS. *: $p < 0.05$, **: $p < 0.01$, ***: $p < 0.001$. Data are expressed as the mean ± SD, (N = 3).

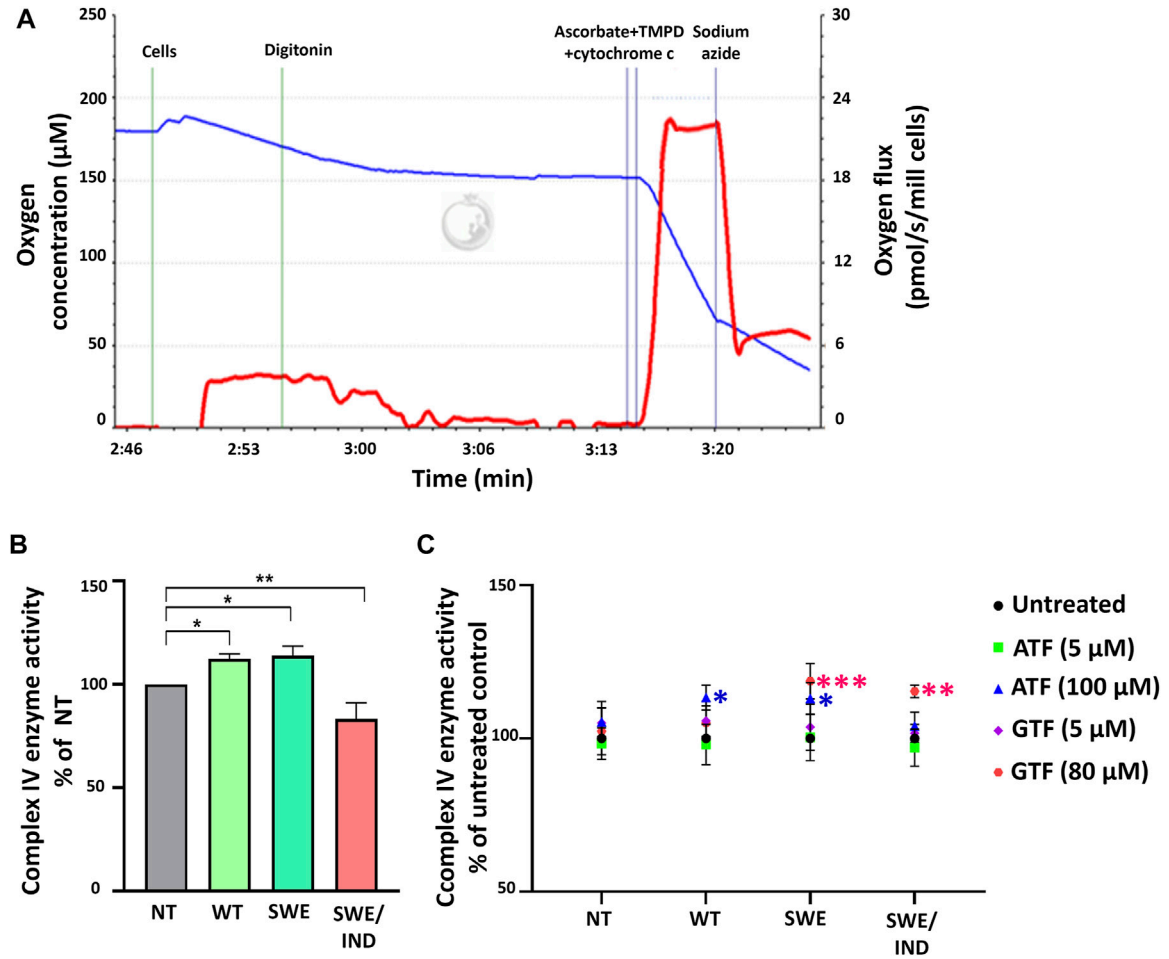


**FIGURE 4 |** Analysis of complex IV enzyme activity by high-resolution respirometry. **(A)** Qualitative data of complex IV enzyme activity were recorded after the addition of ascorbate, TMPD and cytochrome c expressed as the oxygen flux (pmol/s/mill cells) with chemical background correction using the value recorded after the addition of sodium azide. **(B)** The level of complex IV enzyme activity in SH-SY5Y cells overexpressing different types of APP (WT, Swe, and Swe/Ind) expressed as % of the nontransfected SH-SY5Y control cells (NT). *: $p < 0.05$, **: $p < 0.01$. **(C)** Effects of ATF and GTF treatment on complex IV enzyme activity in nontransfected SH-SY5Y (NT) and cells overexpressing different types of APP (WT, Swe, and Swe/Ind) expressed as % of the untreated group in respective type of cells. *: $p < 0.05$, **: $p < 0.01$, ***$p < 0.001$. Data are expressed as the mean ± SD, (N = 3).

## RESULTS

### An Abnormally Higher Respiratory Capacity and Membrane Potential Was Found in SH-SY5Y Cells Overexpressing APP Wt or APP Swe but Was Impaired in APP Swe/Ind Relative to the Non-transfected SH-SY5Y Control

The mitochondrial respiratory capacity and membrane potential were measured simultaneously in this study. **Figure 1A** shows qualitative data of high-resolution respiration (HRR) using an O2k respirometer with the SUIT protocol. The red line represents the oxygen flux to indicate the volume of oxygen converted by the cells per time per number of cells (pmol/s/mill cells), whereas the blue line represents the level of oxygen concentration inside the chamber. **Figure 1B** shows the signal of safranin in the chamber medium represented by the black line. The concentration of safranin is directly proportional to the safranin signal (amp) but inversely proportional to the membrane potential.

There were four respiratory capacities measured in the present study including ROUTINE, respiratory capacity in living cells controlled by cellular energy demand, energy turnover and the degree of coupling to phosphorylation, whereas the other three respiratory capacities were measured in cells that selectively permeabilized the plasma membrane of cells while the mitochondrial membrane remain intact thus allowing direct access to the mitochondria, which then required the supply from exogenous substrates/substances to measure mitochondrial respiration. The mitochondrial respiratory capacities are $LEAK_{PM}$, the respiratory capacity by which cation cycling and electron leakage lead to heat production

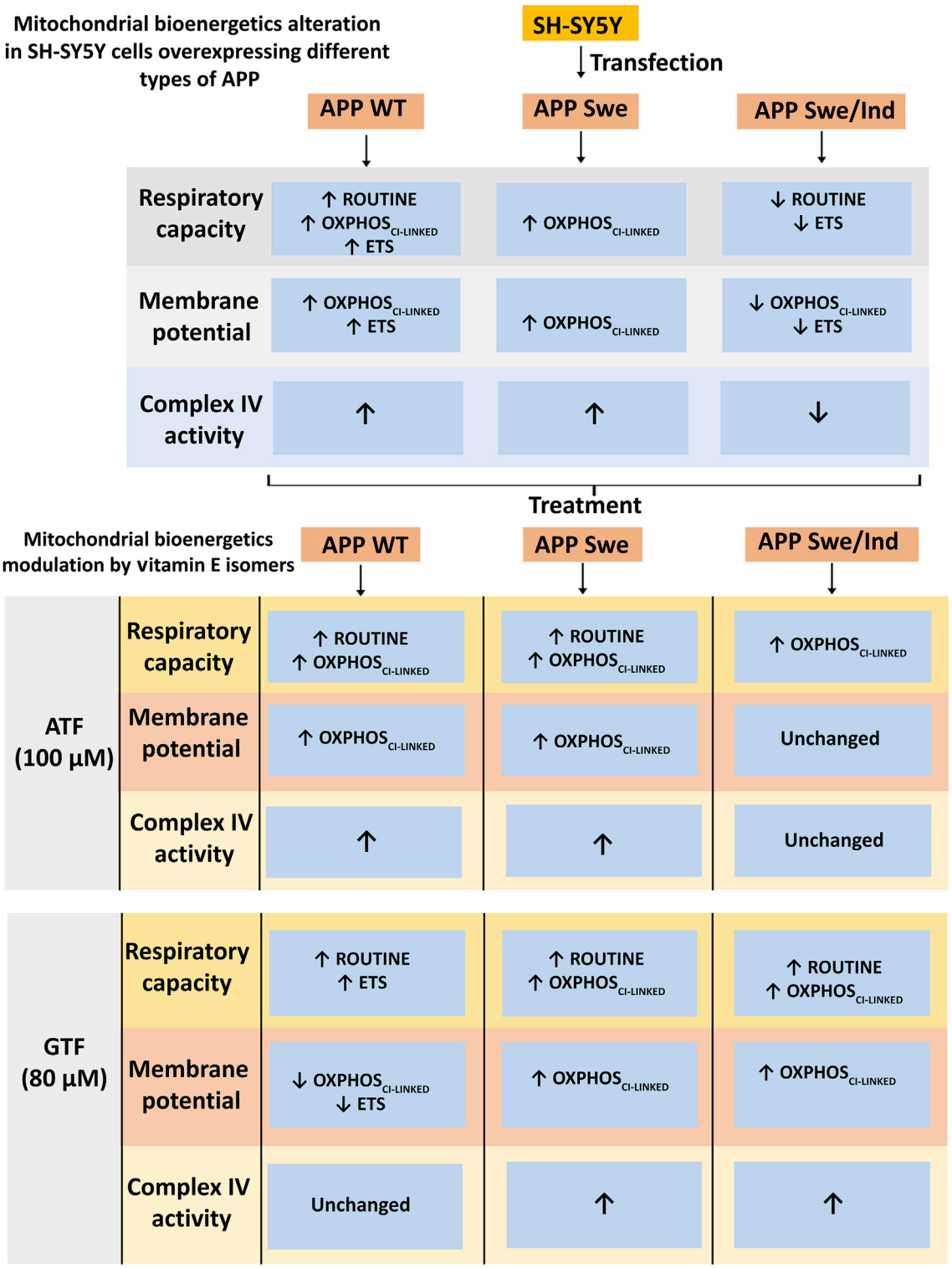


**FIGURE 5 |** Schematic diagram of mitochondrial bioenergetics alteration in SH-SY5Y cells overexpressing different types of APP and modulation by vitamin E isomers. The APP WT and Swe overexpressing cells showed increased in mitochondrial bioenergetics at $OXPHOS_{CI\text{-}LINKED}$ state accompanied by an increased in complex IV enzyme activity whereas the APP Swe/Ind overexpressing cells showed decreased in mitochondrial bioenergetics at ETS state followed by a decreased in complex IV enzyme activity. ATF and GTF modulated mitochondrial bioenergetics differently in different types of APP overexpressing cells generally by increasing the respiratory capacity, membrane potential and complex IV enzyme activity.

instead of biochemical work. This state was measured in the presence of reducing substrates such as pyruvate and malate but absence of ADP, a component described as the non-phosphorylating resting state when ATP synthase is not active; $OXPHOS_{CI\text{-}LINKED}$, the respiratory capacity supported by NADH-generating substrates (pyruvate, malate and glutamate) through complex I to the Q-junction, with further electron transfer through complex III and complex IV to oxygen coupled with phosphorylation in the presence of saturating ADP, a component described as oxidative phosphorylation; and ETS, the respiratory capacity of mitochondria measured as oxygen consumption in the noncoupled state supported by NADH-generating substrates and succinate at optimum uncoupler (CCCP) concentration and is not limited by the capacity of the phosphorylation system, a component described as the electron-transfer-pathway capacity.

At the baseline level without treatment with ATF and GTF, relative to the nontransfected control, the APP WT cells showed significantly higher respiratory capacity in the ROUTINE, $OXPHOS_{CI\text{-}LINKED,}$ and ETS states, whereas APP Swe cells showed significantly higher respiratory capacity only in the $OXPHOS_{CI\text{-}LINKED}$ state (**Figure 2A**). Meanwhile, for APP Swe/Ind cells, the respiratory capacity ROUTINE and ETS states were significantly lower relative to the nontransfected control (**Figure 2A**). In parallel to higher/lower respiratory capacity, the membrane potential was also higher in APP WT but lower in APP Swe/Ind at $OXPHOS_{CI\text{-}LINKED}$ and ETS states relative to the non-transfected control (**Figure 2B**). However, in APP Swe cells, the membrane potential was higher only in the $OXPHOS_{CI\text{-}LINKED}$ state relative to the nontransfected control (**Figure 2B**). There was no significant difference in respiratory capacity or membrane potential under the permeabilized conditions of the $LEAK_{PM}$ state in all SH-SY5Y cells overexpressing different types of APP relative to the nontransfected control (**Figures 2A,B**). These results showed that different forms of the APP gene expressed in the cells have different alterations in the level of respiratory capacity and membrane potential, such as abnormally higher expression in cells overexpressing APP without or with a single mutation in the $OXPHOS_{CI\text{-}LINKED}$ state but lower expression in cells overexpressing APP with double mutations in the ETS state.

## Treatment With ATF and GTF at Higher Concentrations Increased the Respiratory Capacity and Membrane Potential in SH-SY5Y Cells Overexpressing Different Types of APP

Our previous data demonstrated that ATF at 100 μM and GTF at 80 μM significantly increased cell viability and decreased the Aβ42 level in SH-SY5Y cells expressing different forms of APP (WT, APP Swe, and APP Swe/Ind) compared to untreated nontransfected controls (Pahrudin Arrozi et al., 2020); therefore, these cells were chosen to further elucidate their effect on the mitochondrial respiratory capacity and membrane potential. The respiratory capacity in the ROUTINE state was significantly increased in APP WT and Swe cells treated with 100 μM ATF compared to their respective untreated controls (**Figure 3A**). A similar observation was also shown when the same group of cells, including APP Swe/Ind cells, was treated with GTF at 80 μM (**Figure 3A**). There were no significant differences in the mitochondrial respiratory capacity and membrane potential in the $LEAK_{PM}$ state when all types of cells were treated with ATF or GTF compared to their respective untreated controls (**Figures 3B,C**).

The mitochondrial respiratory capacity in the $OXPHOS_{CI\text{-}LINKED}$ state was significantly increased in all types of APP-overexpressing cells, followed by an increase in the membrane potential in APP WT and Swe cells treated with 100 μM ATF compared to their respective untreated controls (**Figures 3D,E**). However, treatment with GTF at 80 μM significantly increased the mitochondrial respiratory capacity and membrane potential in the $OXPHOS_{CI\text{-}LINKED}$ state in cells overexpressing mutant APP (**Figures 3D,E**) but significantly decreased the membrane potential in APP WT cells (**Figure 3E**) compared to their respective untreated controls. Meanwhile, the mitochondrial respiratory capacity and membrane potential in the ETS state were significantly altered with only GTF treatment at 80 μM in APP WT cells compared to the untreated control (**Figures 3F,G**). These results indicated that treatment with ATF and GTF at higher concentrations modulated the mitochondrial respiratory capacity and membrane potential in different types of APP-overexpressing cells. In addition, lower concentrations of ATF and GTF at 5 μM did not cause any changes to the mitochondrial respiratory capacity and membrane potential, suggesting the dose dependency of the effect of ATF and GTF.

## Treatment With ATF and GTF at Higher Concentrations Increased the Activity of Complex IV Enzyme in SH-SY5Y Cells Overexpressing Different Types of APP

As oxygen is consumed by respiring cells and its loss was used to measure the rate of respiration, we further investigated the role of ATF and GTF on the key regulatory enzyme responsible for the conversion of oxygen to water molecules. The activity of complex IV was measured using an O2k instrument. **Figure 4A** demonstrates the graph of complex IV enzyme activity measured as the rate of oxygen consumption (pmol/s/mill cells) shown by the red line. The activity of complex IV was recorded after the addition of ascorbate, TMPD and cytochrome c. Data were corrected using the value recorded after the addition of sodium azide. At the baseline level without treatment with ATF or GTF, the activity of complex IV was higher in SH-SY5Y-APP Wt and SH-SY5Y-APP Swe cells but lower in SH-SY5Y-APP Swe/Ind cells than in nontransfected SH-SY5Y cells (**Figure 4B**). Treatment with ATF at higher concentrations significantly increased the activity of complex IV enzyme in SH-SY5Y-APP Wt and Swe cells compared to their respective untreated controls (**Figure 4C**). A similar result was obtained with GTF treatment at higher concentrations, which significantly increased the activity of complex IV enzyme in SH-SY5Y-overexpressing mutant APP forms compared to their respective untreated controls

(**Figure 4C**). These results indicate that ATF and GTF might act as signalling molecules in regulating the complex IV enzyme activation/deactivation pathway.

## DISCUSSION

In this study, we demonstrated that the mitochondrial respiratory capacity and membrane potential were abnormally higher in APP WT or Swe cells, particularly in the $OXPHOS_{CI\text{-}LINKED}$ state, but lower in APP Swe/Ind cells, particularly in the ETS state. A similar observation was also shown for complex IV enzyme activity, which is the major regulator of oxidative phosphorylation; it was higher in APP WT or Swe cells but lower in APP Swe/Ind cells. We also demonstrated that treatment with ATF and GTF at higher concentrations modulated the respiratory capacity and membrane potential, particularly in the ROUTINE and $OXPHOS_{CI\text{-}LINKED}$ states, as well as complex IV enzyme activity in APP-overexpressing cells.

We assessed mitochondrial oxidative metabolism using a cell suspension instead of isolated mitochondria, as this required a mild detergent, such as digitonin, to selectively permeabilize the cell plasma membrane *via* interaction with cholesterol, thus allowing free exchange of organic molecules and inorganic ions between the cytosol and the immediate cell environment while maintaining the integrity and localization of organelles, the cytoskeleton, and the nucleus. In the preparation of isolated mitochondria, however, the mitochondria are separated from other cell fractions and purified by differential centrifugation, entailing the loss of mitochondria; thus, this might compromise the mitochondrial yield or structural and functional integrity (Gnaiger, 2020).

The different alterations in the mitochondrial respiratory capacity and membrane potential were probably influenced by the types of APP accumulated in the cells. It has become generally accepted that the accumulation of Aβ is responsible for mitochondrial impairment (Cieślik et al., 2020; Quintana et al., 2020; Zhang et al., 2018); however, there is also evidence for the relationship between APP processing and mitochondrial bioenergetic regulation (Puig and Combs, 2013; Wilkins and Swerdlow, 2017). Our data highlight the need for a better understanding of the cellular function of APP and its metabolites, and further work is needed to elucidate their potential contribution to the alteration of mitochondrial bioenergetics. A study by Reddy et al. (Reddy et al., 2004) demonstrated the upregulation of gene expression involved in the regulation of mitochondrial metabolism in a Tg2576 transgenic mouse model transfected with the APP Wt gene as early cellular changes during the progression of Alzheimer's disease (Swerdlow, 2018). Meanwhile, a study by Hauptmann et al. (Hauptmann et al., 2009) showed a decreased mitochondrial respiration rate in the ETS state followed by a decrease in the mitochondrial membrane potential, complex IV enzyme activity and ATP levels in isolated mitochondria of transgenic mouse models carrying Swedish and London APP mutations (similar mutation position to Indiana mutation with different amino acid substitutions) as late cellular changes in disease progression.

The subsequent mechanism of action of ATF or GTF in this study was unclear, as the gene or protein expression involved in mitochondrial bioenergetic regulation was not measured. We speculated that ATF or GTF might act as signalling molecules in the transcriptional alteration of mitochondrial genes involved in mitochondrial energy metabolism, as shown by the increased/decreased complex IV enzyme activity in different types of APP-overexpressing cells (**Figure 5**). A previous study demonstrated that aged mice supplemented with different antioxidants, including ATF, modulate age-related changes in the activity of complex enzymes in the cerebral ETS composed of complexes I, II, III and IV (Sharman and Bondy, 2001). Furthermore, oral treatment with a combination of ATF and folic acid in an *in vivo* model of AD also modulated mitochondrial complex activity, especially complexes I and IV (Figueiredo et al., 2011). In addition, the gene expression profiles obtained in the brains of aged mice supplemented with ATF or a mixture of ATF and GTF showed a significant modulation effect by the combination of both isomers but not ATF alone on genes involved in mitochondrial energy metabolism, including ATP synthesis, which is primarily dependent on oxidative phosphorylation (Park et al., 2008), thus suggesting that the combination of vitamin E isomers might have better modulation than a single isomer. Moreover, ATF supplementation in aged rats was restored in a dose-dependent manner, and the decreases in tissue and mitochondrial respiration as well as complex I and IV activities in both the hippocampus and frontal cortex region (Navarro et al., 2011) supported the modulatory effect of ATF on mitochondrial bioenergetics.

There are several limitations in the present study. First, an *in vivo* study was not included to further confirm the role of ATF and GTF in modulating mitochondrial oxidative metabolism in a higher model system. Second, the expression of the genes or proteins involved in the regulation of mitochondrial oxidative metabolism was also not measured to further elucidate the mechanism of action of ATF or GTF. Third, only complex IV enzyme was measured, as this is the major enzyme regulator in ETS that permits the transfer of electrons from reduced cytochrome c to the final acceptor of electrons, oxygen, which is important to characterize the function of mitochondrial respiration.

## CONCLUSION

Both ATF and GTF modulated the mitochondrial respiratory capacity and membrane potential as well as the activity of the complex IV enzyme in different types of APP-overexpressing cells. Although preliminary, these findings may indicate the possible health benefits of ATF or GTF and, in part, may contribute to planning for a strategy of utilizing vitamin E isomers against mitochondrial-related diseases such as AD.

## DATA AVAILABILITY STATEMENT

The original contributions presented in the study are included in the article/**Supplementary Material**, further inquiries can be directed to the corresponding author.

## AUTHOR CONTRIBUTIONS

SM designed the study and supervised the project. APA performed the experiments and prepared the figures. SM, WZWN and HAD provided experimental technical assistance and commented on the results. APA and SM wrote the paper. All authors contributed to the article and approved the submitted version.

## FUNDING

This article is part of a research study financially supported by the Universiti Kebangsaan Malaysia Grants DIP-2013-003 and FF-2015-025.

## ACKNOWLEDGMENTS

The authors would like to express their gratitude to the research officer and medical laboratory technologists of the Biochemistry Department, Faculty of Medicine, Universiti Kebangsaan Malaysia Medical Centre for technical assistance.

## SUPPLEMENTARY MATERIAL

The Supplementary Material for this article can be found online at: https://www.frontiersin.org/articles/10.3389/fphar.2021.698833/full#supplementary-material

## REFERENCES

Ashley, S., Bradburn, S., and Murgatroyd, C. (2019). A Meta-Analysis of Peripheral Tocopherol Levels in Age-Related Cognitive Decline and Alzheimer's Disease. *Nutr. Neurosci.* 24, 1–15. doi:10.1080/1028415X.2019.1681066

Bell, S. M., Barnes, K., De Marco, M., Shaw, P. J., Ferraiuolo, L., Blackburn, D. J., et al. (2021). Mitochondrial Dysfunction in Alzheimer's Disease: A Biomarker of the Future? *Biomedicines* 9, 63. doi:10.3390/biomedicines9010063

Cieślik, M., Czapski, G. A., Wójtowicz, S., Wieczorek, I., Wencel, P. L., Strosznadjer, R. P., et al. (2020). Alterations of Transcription of Genes Coding Anti-oxidative and Mitochondria-Related Proteins in Amyloid β Toxicity: Relevance to Alzheimer's Disease. *Mol. Neurobiol.* 57, 1374–1388. doi:10.1007/s12035-019-01819-y

de Leeuw, F. A., Honer, W. G., Schneider, J. A., and Morris, M. C. (2020). Brain γ-Tocopherol Levels Are Associated with Presynaptic Protein Levels in Elderly Human Midfrontal Cortex. *J. Alzheimers. Dis.* 77, 619–627. doi:10.3233/JAD-200166

Fernandes, T., Resende, R., Silva, D. F., Marques, A. P., Santos, A. E., Cardoso, S. M., et al. (2021). Structural and Functional Alterations in Mitochondria-Associated Membranes (MAMs) and in Mitochondria Activate Stress Response Mechanisms in an *In Vitro* Model of Alzheimer's Disease. *Biomedicines* 9, 881. doi:10.3390/biomedicines9080881

Figueiredo, C. P., Bicca, M. A., Latini, A., Prediger, R. D., Medeiros, R., and Calixto, J. B. (2011). Folic Acid Plus α-tocopherol Mitigates Amyloid-β-Induced Neurotoxicity through Modulation of Mitochondrial Complexes Activity. *J. Alzheimers. Dis.* 24, 61–75. doi:10.3233/JAD-2010-101320

Gao, Y., Tan, L., Yu, J. T., and Tan, L. (2018). Tau in Alzheimer's Disease: Mechanisms and Therapeutic Strategies. *Curr. Alzheimer Res.* 15, 283–300. doi:10.2174/1567205014666170417111859

Gnaiger, E. (2020). Mitochondrial Pathways and Respiratory Control. An Introduction to OXPHOS Analysis. 5th ed. *Bioenerg. Commun.* 2, 122. doi:10.26124/bec:2020-0002

Hauptmann, S., Scherping, I., Dröse, S., Brandt, U., Schulz, K. L., Jendrach, M., et al. (2009). Mitochondrial Dysfunction: An Early Event in Alzheimer Pathology Accumulates with Age in AD Transgenic Mice. *Neurobiol. Aging* 30, 1574–1586. doi:10.1016/j.neurobiolaging.2007.12.005

Jilani, T., and Iqbal, M. P. (2018). Vitamin E Deficiency in South Asian Population and the Therapeutic Use of Alpha-Tocopherol (Vitamin E) for Correction of Anemia. *Pak J. Med. Sci.* 34, 1571–1575. doi:10.12669/pjms.346.15880

Krumschnabel, G., Eigentler, A., Fasching, M., and Gnaiger, E. (2014). "Use of Safranin for the Assessment of Mitochondrial Membrane Potential by High-Resolution Respirometry and Fluorometry," in *Conceptual Background and Bioenergetic/Mitochondrial Aspects of Oncometabolism*. Editors L. Galluzzi and G. Kroemer (Academic Press), 163–181. doi:10.1016/B978-0-12-416618-9.00009-1

Lemieux, H., Blier, P. U., and Gnaiger, E. (2017). Remodeling Pathway Control of Mitochondrial Respiratory Capacity by Temperature in Mouse Heart: Electron Flow through the Q-junction in Permeabilized Fibers. *Sci. Rep.* 7, 2840. doi:10.1038/s41598-017-02789-8

Minter, B. E., Lowes, D. A., Webster, N. R., and Galley, H. F. (2020). Differential Effects of MitoVitE, α-Tocopherol and Trolox on Oxidative Stress, Mitochondrial Function and Inflammatory Signalling Pathways in Endothelial Cells Cultured under Conditions Mimicking Sepsis. *Antioxidants (Basel)* 9, 1. doi:10.3390/antiox9030195

Morris, M. C., Schneider, J. A., Li, H., Tangney, C. C., Nag, S., Bennett, D. A., et al. (2015). Brain Tocopherols Related to Alzheimer's Disease Neuropathology in Humans. *Alzheimers. Dement.* 11, 32–39. doi:10.1016/j.jalz.2013.12.015

Navarro, A., Bandez, M. J., Lopez-Cepero, J. M., Gómez, C., and Boveris, A. (2011). High Doses of Vitamin E Improve Mitochondrial Dysfunction in Rat hippocampus and Frontal Cortex upon Aging. *Am. J. Physiol. Regul. Integr. Comp. Physiol.* 300, R827–R834. doi:10.1152/ajpregu.00525.2010

Nesari, A., Mansouri, M. T., Khodayar, M. J., and Rezaei, M. (2019). Preadministration of High-Dose Alpha-Tocopherol Improved Memory Impairment and Mitochondrial Dysfunction Induced by Proteasome Inhibition in Rat hippocampus. *Nutr. Neurosci.* 24, 1–11. doi:10.1080/1028415X.2019.1601888

Pahrudin Arrozi, A., Shukri, S. N. S., Wan Ngah, W. Z., Mohd Yusof, Y. A., Ahmad Damanhuri, M. H., Jaafar, F., et al. (2020). Comparative Effects of Alpha- and Gamma-Tocopherol on Mitochondrial Functions in Alzheimer's Disease *In Vitro* Model. *Sci. Rep.* 10, 8962. doi:10.1038/s41598-020-65570-4

Pahrudin Arrozi, A., Shukri, S. N. S., Wan Ngah, W. Z., Mohd Yusof, Y. A., Ahmad Damanhuri, M. H., and Makpol, S. (2017). Evaluation of the Expression of Amyloid Precursor Protein and the Ratio of Secreted Amyloid Beta 42 to Amyloid Beta 40 in SH-Sy5y Cells Stably Transfected with Wild-type, Single-Mutant and Double-Mutant Forms of the APP Gene for the Study of Alzheimer's Disease Pathology. *Appl. Biochem. Biotechnol.* 183, 853–866. doi:10.1007/s12010-017-2468-6

Park, S. K., Page, G. P., Kim, K., Allison, D. B., Meydani, M., Weindruch, R., et al. (2008). Alpha- and Gamma-Tocopherol Prevent Age-Related Transcriptional Alterations in the Heart and Brain of Mice. *J. Nutr.* 138, 1010–1018. doi:10.1093/jn/138.6.1010

Pédeboscq, S., Rey, C., Petit, M., Harpey, C., De Giorgi, F., Ichas, F., et al. (2012). Non-antioxidant Properties of α-tocopherol Reduce the Anticancer Activity of Several Protein Kinase Inhibitors *In Vitro*. *PLoS One* 7, e36811. doi:10.1371/journal.pone.0036811

Puig, K. L., and Combs, C. K. (2013). Expression and Function of APP and its Metabolites outside the central Nervous System. *Exp. Gerontol.* 48, 608–611. doi:10.1016/j.exger.2012.07.009

Quintana, D. D., Garcia, J. A., Anantula, Y., Rellick, S. L., Engler-Chiurazzi, E. B., Sarkar, S. N., et al. (2020). Amyloid-β Causes Mitochondrial Dysfunction via a Ca2+-Driven Upregulation of Oxidative Phosphorylation and Superoxide Production in Cerebrovascular Endothelial Cells. *J. Alzheimers. Dis.* 75 (1), 119–138. doi:10.3233/JAD-190964

Reboul, E. (2017). Vitamin E Bioavailability: Mechanisms of Intestinal Absorption in the Spotlight. *Antioxidants (Basel)* 6, 95. doi:10.3390/antiox6040095

Reddy, P. H., McWeeney, S., Park, B. S., Manczak, M., Gutala, R. V., Partovi, D., et al. (2004). Gene Expression Profiles of Transcripts in Amyloid Precursor Protein Transgenic Mice: Up-Regulation of Mitochondrial Metabolism and

Apoptotic Genes Is an Early Cellular Change in Alzheimer's Disease. *Hum. Mol. Genet.* 13, 1225–1240. doi:10.1093/hmg/ddh140

Sharman, E. H., and Bondy, S. C. (2001). Effects of Age and Dietary Antioxidants on Cerebral Electron Transport Chain Activity. *Neurobiol. Aging* 22, 629–634. doi:10.1016/s0197-4580(01)00226-3

Swerdlow, R. H. (2018). Mitochondria and Mitochondrial Cascades in Alzheimer's Disease. *J. Alzheimers. Dis.* 62, 1403–1416. doi:10.3233/JAD-170585

Tiwari, S., Atluri, V., Kaushik, A., Yndart, A., and Nair, M. (2019). Alzheimer's Disease: Pathogenesis, Diagnostics, and Therapeutics. *Int. J. Nanomedicine* 14, 5541–5554. doi:10.2147/IJN.S200490

Ulatowski, L. M., and Manor, D. (2015). Vitamin E and Neurodegeneration. *Neurobiol. Dis.* 84, 78–83. doi:10.1016/j.nbd.2015.04.002

Vaillant-Beuchot, L., Mary, A., Pardossi-Piquard, R., Bourgeois, A., Lauritzen, I., Eysert, F., et al. (2021). Accumulation of Amyloid Precursor Protein C-Terminal Fragments Triggers Mitochondrial Structure, Function, and Mitophagy Defects in Alzheimer's Disease Models and Human Brains. *Acta Neuropathol.* 141, 39–65. doi:10.1007/s00401-020-02234-7

Wilkins, H. M., and Swerdlow, R. H. (2017). Amyloid Precursor Protein Processing and Bioenergetics. *Brain. Res. Bull.* 133, 71–79. doi:10.1016/j.brainresbull.2016.08.009

Williamson, K. S., Gabbita, S. P., Mou, S., West, M., Pye, Q. N., Markesbery, W. R., et al. (2002). The Nitration Product 5-nitro-gamma-tocopherol Is Increased in the Alzheimer Brain. *Nitric Oxide* 6, 221–227. doi:10.1006/niox.2001.0399

Zhang, L., Trushin, S., Christensen, T. A., Tripathi, U., Hong, C., and Geroux, R. E. (2018). Differential Effect of Amyloid Beta Peptides on Mitochondrial Axonal Trafficking Depends on Their State of Aggregation and Binding to the Plasma Membrane. *Neurobiol. Dis.* 114, 1–16. doi:10.1016/j.nbd.2018.02.003

Zingg, J. M. (2019). Vitamin E: Regulatory Role on Signal Transduction. *IUBMB Life* 71, 456–478. doi:10.1002/iub.1986

**Conflict of Interest:** The authors declare that the research was conducted in the absence of any commercial or financial relationships that could be construed as a potential conflict of interest.

**Publisher's Note:** All claims expressed in this article are solely those of the authors and do not necessarily represent those of their affiliated organizations, or those of the publisher, the editors and the reviewers. Any product that may be evaluated in this article, or claim that may be made by its manufacturer, is not guaranteed or endorsed by the publisher.

frontiers in Pharmacology

ORIGINAL RESEARCH
published: 29 November 2021
doi: 10.3389/fphar.2021.772576

# Danzhi Xiaoyao Powder Promotes Neuronal Regeneration by Downregulating Notch Signaling Pathway in the Treatment of Generalized Anxiety Disorder

*Chao Liu[1†], Zhenhao Ying[2†], Zifa Li[3,4,5], Long Zhang[1], Xin Li[6], Wenbo Gong[1], Jiang Sun[1], Xuejing Fan[6], Ke Yang[6], Xingchen Wang[7,8]*, Sheng Wei[3,4,5]* and Ning Dong[7,8]**

[1]The First Clinical Medical College, Shandong University of Traditional Chinese Medicine, Ji'nan, China, [2]School of Rehabilitation Science, Shandong University of Traditional Chinese Medicine, Ji'nan, China, [3]Experimental Center, Shandong University of Traditional Chinese Medicine, Ji'nan, China, [4]Key Laboratory of Traditional Chinese Medicine Classical Theory, Ministry of Education, Shandong University of Traditional Chinese Medicine, Ji'nan, China, [5]Shandong Provincial Key Laboratory of Traditional Chinese Medicine for Basic Research, Shandong University of Traditional Chinese Medicine, Ji'nan, China, [6]College of Traditional Chinese Medicine, Shandong University of Traditional Chinese Medicine, Ji'nan, China, [7]Department of Neurology, The Second Affiliated Hospital of Shandong University of Traditional Chinese Medicine, Ji'nan, China, [8]The Second Clinical Medical College, Shandong University of Traditional Chinese Medicine, Ji'nan, China

**Background:** Generalized anxiety disorder (GAD) is one of the most common types of anxiety disorders with unclear pathogenesis. Our team's previous research found that extensive neuronal apoptosis and neuronal regeneration disorders occur in the hippocampus of GAD rats. Danzhi Xiaoyao (DZXYS) Powder can improve the anxiety behavior of rats, but its molecular mechanism is not well understood.

**Objective:** This paper discusses whether the pathogenesis of GAD is related to the abnormal expression of Notch signal pathway, and whether the anti-anxiety effect of DZXYS promotes nerve regeneration in the hippocampus by regulating the Notch signaling pathway.

**Methods:** The animal model of GAD was developed by the chronic restraint stress and uncertain empty bottle stimulation method. After the model was successfully established, the rats in the model preparation group were divided into the buspirone, DZXYS, DZXYS + DAPT, and model groups, and were administered the corresponding drug intervention. The changes in body weight and food intake of rats were continuously monitored throughout the process. The changes in anxiety behavior of rats were measured by open field experiment and elevated plus-maze test, and morphological changes and regeneration of neurons in the rat hippocampus were observed by HE staining and double immunofluorescence staining. Changes in the expression of key targets of the Notch

**Abbreviations:** BrdU, 5-bromo-2-deoxyuridine; CE, closed arm entry times; CMC-Na, sodium carboxymethyl cellulose; CT, time in the closed arm; DZXYS, Danzhi Xiaoyao Powder; DAPT, γ-secretase inhibitor; DG, dentate gyrus; EPM, elevated plus maze; GAD, generalized anxiety disorder; NSCs, neural stem cells; OE, open-arm entry times; OFT, open-field test; OT time in the open arm.

OPEN ACCESS

**Edited by:**
Fushun Wang,
Nanjing University of Chinese Medicine, China

**Reviewed by:**
Qian Li,
American Academy of Acupuncture and Oriental Medicine, United States
Raquel Romay-Tallon,
University of Illinois at Chicago, United States
Miao Qu,
Capital Medical University, China

***Correspondence:**
Xingchen Wang
sdlcwxc@163.com
Sheng Wei
weisheng@sdutcm.edu.cn
Ning Dong
72030320@sdutcm.edu.cn

[†]These authors contributed equally to this work and share the first authorship

**Specialty section:**
This article was submitted to Neuropharmacology, a section of the journal Frontiers in Pharmacology

**Received:** 08 September 2021
**Accepted:** 22 October 2021
**Published:** 29 November 2021

**Citation:**
Liu C, Ying Z, Li Z, Zhang L, Li X, Gong W, Sun J, Fan X, Yang K, Wang X, Wei S and Dong N (2021) Danzhi Xiaoyao Powder Promotes Neuronal Regeneration by Downregulating Notch Signaling Pathway in the Treatment of Generalized Anxiety Disorder. Front. Pharmacol. 12:772576. doi: 10.3389/fphar.2021.772576

signaling pathway in the hippocampus were monitored by real-time fluorescence quantitative PCR and western blotting.

**Results:** In this study, we verified that the GAD model was stable and reliable, and found that the key targets of the Notch signaling pathway (Notch1, Hes1, Hes5, etc.) in the hippocampus of GAD rats were significantly upregulated, leading to the increased proliferation of neural stem cells in the hippocampus and increased differentiation into astrocytes, resulting in neuronal regeneration. DZXYS intervention in GAD rats can improve appetite, promote weight growth, and significantly reverse the anxiety behavior of GAD rats, which can inhibit the upregulation of key targets of the Notch signaling pathway, promote the differentiation of neural stem cells in the hippocampus into neurons, and inhibit their differentiation into astrocytes, thus alleviating anxiety behavior.

**Conclusion:** The occurrence of GAD is closely related to the upregulation of the Notch signaling pathway, which hinders the regeneration of normal neurons in the hippocampus, while DZXYS can downregulate the Notch signaling pathway and promote neuronal regeneration in the hippocampus, thereby relieving anxiety behavior.

**Keywords: Generalized anxiety disorder, DZXYS, hippocampus, Notch, neuron regeneration**

## 1 INTRODUCTION

Generalized anxiety disorder (GAD) is a chronic anxiety disorder characterized by persistent significant tension, accompanied by autonomic nervous function excitement and over alertness. According to the World Health Organization (WHO) World Mental Health Survey, anxiety disorder is the most common cause of mental illness and disability worldwide, and generalized anxiety disorder (GAD) is one of the most common types of anxiety disorders (Demyttenaere et al., 2004). The global prevalence of anxiety disorder was 7.3% (Stein et al., 2017). The lifetime prevalence of GAD ranged from 0.8 to 5.1% (Kessler, 2000; Hidalgo and Sheehan, 2012), seriously affecting the quality of life of patients. At the same time, GAD is a risk factor for many other diseases, such as alcohol dependence and drug dependence (benzodiazepine dependence) (Tyrer and Baldwin, 2006). Although GAD is common in clinics, it has not been studied as much detail in neurobiology as many other emotional disorders such as depression (Menard et al., 2016), and its pathogenesis remains to be unclear. At present, it is generally believed that its pathogenesis is closely related to neurotransmitter disorders, and neurotransmitter regulating drugs are often used as treatment, and their effects are not ideal and side effects may be obvious, such as drowsiness, dizziness, nausea, and addiction, etc. (Bandelow, 2020).

Traditional Chinese medicine has been widely used in the treatment of emotional diseases for thousands of years. Danzhi Xiaoyao Powder is a classic Chinese prescription that has been used in the clinic. It originated from Xue Ji's Internal Medicine Abstract during the Ming Dynasty. It was modified by the "Xiaoyao Powder." The entire prescription consisted of 10 g danpi, 10 g gardenia, 15 g bupleurum, 10 g Poria cocos, 15 g fried Atractylodes macrocephala, 10 g Angelica sinensis, 10 g white peony, 10 g licorice, 3 g mint, and 9 g ginger, which is widely used in clinical and experimental research on anxiety and depression disorder (Xu et al., 2020). Our team's previous research found extensive neuronal apoptosis and neuronal regeneration disorders in the hippocampus of GAD rats. DZXYS can improve the anxiety behavior of GAD rats, but its mechanism remains to be explored (Dong, 2015).

In recent years, some scholars have found that the occurrence of depression is related to the decline of adult hippocampal neurons, and stimulating hippocampal neurons is a new strategy for antidepressant treatment (Tanti and Belzung, 2013; Hill et al., 2015; Anacker et al., 2018). The hippocampus has become the focus of research on mental diseases because of its nerve regeneration function and unique regulation of emotion and cognition (Toda et al., 2019). In view of the similarities between depression and anxiety disorders in pathophysiological mechanisms and neuroanatomical changes (Hettema, 2008), we speculate that neuronal apoptosis and neuronal regeneration disorder in the hippocampus of GAD rats found in the previous team's research are also important pathological mechanisms leading to GAD. Hippocampal newborn neurons do not appear spontaneously; they are the result of proliferation and differentiation of neural stem cells in the granular cell layer (subgranular cells of the dentate gyrus, SGZ) of the hippocampal dentate gyrus (Aguilar-Arredondo et al., 2015; Zupanc et al., 2019). The maintenance of neural stem cell proliferation and its differentiation direction and timing are regulated by the Notch signaling pathway (Lutolf et al., 2002; Niessen and Karsan, 2007), which are expressed in the two neurogenic sites of the SGZ and the subventricular zone (SVZ) in the adult brain (Stump et al., 2002), and participate in adult neurogenesis. The activated Notch signaling pathway can maintain the cellular characteristics of NSCs, inhibit their fate of neuronal differentiation, and promote their differentiation into astrocytes (Guo et al., 2009; Snyder et al., 2012). Astrocytes are the type with the largest number of glial

cells, and the ratio of their number to the number of neurons is 3: 1 in rodents and 1.4:1 in the human central nervous system (Sofroniew and Vinters, 2010). Under normal conditions, astrocytes can regulate the concentration of ions inside and outside neurons, nutritional repair, synaptic transmission, and construct a neural tissue grid, forming the blood-brain barrier; however, excessive proliferation can form glial scars, secrete nerve axon regeneration inhibitors, inhibit neuron and nerve axon regeneration, and lead to nerve regeneration disorder (Pekny et al., 2007; Singh and Joshi, 2017). We speculate that the Notch signaling pathway plays an important role in the pathogenesis and treatment of GAD. Therefore, this manuscript discusses the role of Notch signaling pathway in the pathogenesis of GAD and whether the anti-anxiety effect of DZXYS is related to the regulation of Notch signaling pathway to promote nerve regeneration in the hippocampus and improve anxiety behavior (Ren and Zuo, 2012).

# 2 MATERIALS AND METHODS

## 2.1 Animal Preparation

All the experiments were approved by the ethics review committee of Shandong University of Traditional Chinese Medicine (No. DWSY201703013) and carried out in accordance with "the Guidelines for the Care and Use of Experimental Animals of the National Institutes of Health". All the studies attempted to reduce the pain felt by the animals. Animals: Male Wistar rats ($n$ = 120, 6 weeks old, 200 ± 10 g) were purchased from Beijing Vital River Experimental Animal Technology Co., Ltd (Beijing, people's Republic of China; No. SCXK 2016–0006). During the standard 12 h light/dark cycle, the animals were kept at a room temperature of 21 ± 1°C and relative humidity of 30–40%. After 1 week of adaptation, the rats were randomly divided into two groups according to their body weight: control group ($n$ = 24) and model preparation group ($n$ = 96). The control group did not have a model, a free diet, or drinking water.

## 2.2 GAD Modeling Method

The GAD model was established in the model preparation group according to the uncertain empty bottle stimulation method and chronic restraint stress. The specific methods were as follows: first, 7 days of regular water feeding training, the rats were given a water bottle filled with water at 9:00–9:10 and 21:00–21:10 every day to drink for 10 min, and the rest of the time spent on removing the water bottle without water, so that the rats were in a thirsty state. After the rats were used to drinking water at two time points every day, from the 8th day to the 28th day, randomly select one time period to feed water to the water bottle for 10 min, and the other time period to stimulate the rats with empty water bottle, observe the rats' behavior of attacking the cage, looking around the water bottle and modification behavior, etc. At the same time, from 9:30 am to 15:30 pm every day, the rats were fixed with tubular rat fixator (Model: HL-DTS, Specification: 20*6 cm, Material: plexiglass, Heli Kechuang Technology Development Co., Ltd, Beijing) for 6 h for 21 days. On the 28th day, the elevated plus maze (EPM) and open field test (OFT) behavioral tests were performed after restraint, and the rats in the model preparation group were divided into DZXYS group, DZXYS + DAPT group, buspirone group, and model group with the time for rats to open arms in the EPM as the baseline, with 24 rats in each group. Different drug interventions were performed. During the drug intervention, the uncertain empty bottle stimulation and restraint methods were still carried out synchronously until the end of the drug intervention. From the beginning of the experiment to the 42nd day, the changes in body weight and food intake were measured every week (**Figure 1**).

## 2.3 Drug Preparation

The traditional Chinese medicine compound used in the experiment was Danzhi Xiaoyao Powder Formula Granule (1,035,073, Yifang Pharmaceutical Co., Ltd., Guangzhou, China). The granule was dissolved in the distilled water at a concentration of 1.05 g/ml. The drug concentration has been verified by a previous experiment conducted by the research group, and the curative effect is ideal (Dong Ning, 2015). The dose of Buspirone hydrochloride tablets (H19991024, Enhua Pharmaceutical Co., Ltd., Jiangsu, Beijing) were calculated to be 7 times the adult dosage (20 mg/60 kg/d), i.e., the dosage of rats was 2 mg/kg/d, which was dissolved in distilled water at a concentration of 0.2 mg/ml (Garakani et al., 2020). The drug has no addiction and has good anti-anxiety effects and has been found to promote neuronal regeneration in the hippocampus as a 5-HT1A receptor agonist (Masayoshi et al., 2014). 5-Bromo-2-deoxyuridine (BrdU Sigma Chemical Company, St. Louis, MO) was injected intraperitoneally into rats to label proliferating cells. BrdU solution was prepared from 0.9% NS at a concentration of 15 mg/ml and a rat injection dose of 50 mg/kg/time.DAPT (r-secret inhibitor) (D7230, Solarbio, Beijing, China)is a Notch signaling pathway inhibitor, dissolve 50 mg DAPT in 1 ml DMSO before use, and then add 0.9% NS to dilute it into a solution with a concentration of 4.54 mg/ml, and the dosage of intraperitoneal injection was 20 mg/kg/d (Breunig et al., 2007; Zhang et al., 2019).

In this experiment, only Notch signaling pathway inhibitors were used without agonists, for two reasons. Firstly, by consulting the literature, we have learned that the activated Notch signaling pathway can maintain the cellular characteristics of NSCs and inhibit their fate of differentiation into neurons, so as to promote the differentiation into astrocytes (Guo et al., 2009; Snyder et al., 2012). We speculate that excessive upregulation of the Notch signaling pathway is an important reason for the excessive proliferation and differentiation of neural stem cells into astrocytes, resulting in the obstacle of neuronal regeneration, and the application of Notch signaling pathway inhibitors can often inhibit the excessive proliferation of neural stem cells and restore the normal differentiation of neural stem cells into neurons (Breunig et al., 2007). If the application of the signal pathway inhibitor can help Chinese medicine reverse anxiety behavior, it confirms our hypothesis, so as to avoid excessive sacrifice of experimental animals, which is also in line with our animal ethical practices. In addition, the commonly used and

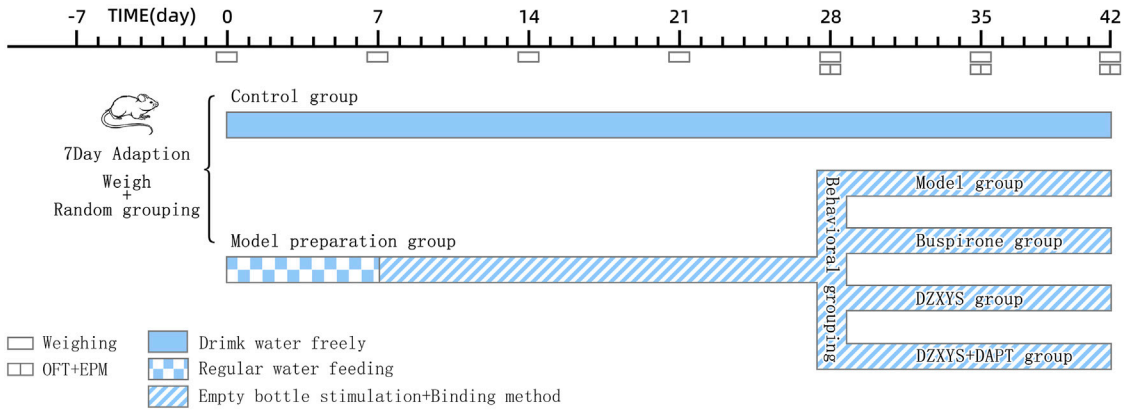


**FIGURE 1 |** Schedule for the model preparation protocol and behavioural testing. OFT, open field test; EPM, elevated plus-maze test.

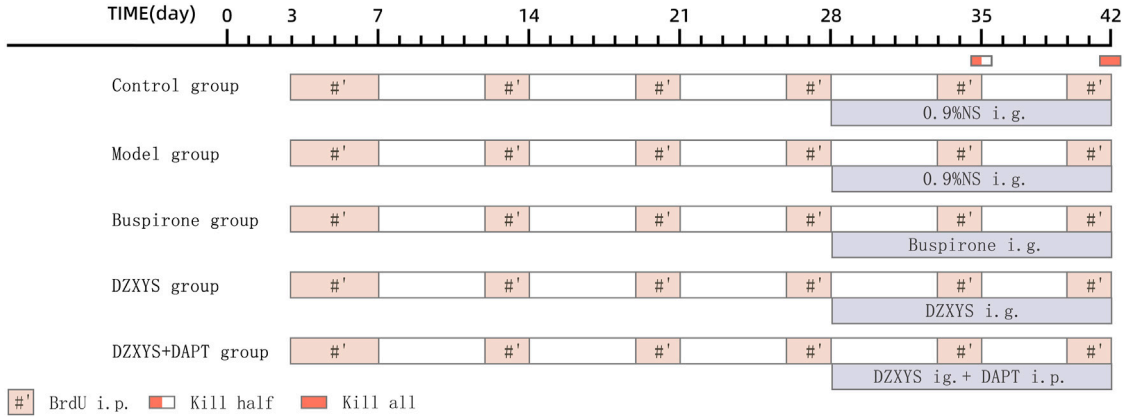


**FIGURE 2 |** Schedule for the drug administration. Abbreviations: i. p, intraperitoneal injection; ig, intragastric administration.

stable Notch signaling pathway agonists are Notch signal pathway ligands such as Jagged1 and Dll4 (Saffarzadeh et al., 2019). Another important topic of our team was to explore whether DZXYS can regulate Notch ligands. If such agonists are used, our research will be disturbed.

## 2.4 Drug Administration

From the 28th day after successful modeling, the rats in each group were given an oral stainless steel gavage needle 30 min before stimulation with an uncertain empty bottle of water every day. The DZXYS, DZXYS + DAPT and buspirone groups were given DZXYS solution and buspirone solution respectively according to the dosage of 1 ml/100 g body weight, and the blank group and model group were also given 0.9% NS according to 1 ml/100 g body weight, lasting for 14 days. In addition, rats in the DZXYS + DAPT group were intraperitoneally injected with DAPT and the rats in each group were injected intraperitoneally with BrdU during the modeling period. The injection frequency was as follows: BrdU was injected intraperitoneally twice a day, 5 days before the start of modeling, and then twice a week. One day before death, the rats were injected every 8 h three times (**Figure 2**).

## 2.5 Animal Behavior Test

Open-field test: The OFT experiment was conducted on the 28th day after modeling, 7 days after intragastric administration (35th day), and 14 days after administration (42nd day). The animals were placed in a quiet test room illuminated by red light for 30 min in advance to adapt to the environment. The open field is a black square device (length*width*height is 100 cm*100 cm*50 cm), and the bottom of the field is divided into nine equal squares. Each rat was placed separately in the center of the site and allowed to explore freely for 6 min. A camera was installed directly above the open field and connected to a computer on the side. The XR super-maze tracking system records the total distance, speed, time, number of times entering the central area, number of times standing up, and the number of times the horizontal grids were crossed (Ennaceur et al., 2009). After each rat was tested, the site was disinfected with 75% ethanol to remove any residual odor. When the animals stayed around the open field for a significantly longer time than in the central area, it proved that the rats had anxiety tendencies.

Elevated Plus Maze: The experiment was conducted in a quiet room illuminated by red light. EPM is a polypropylene plastic

cross-shaped device 76 cm above the ground and consists of two closing arms (50 × 10 cm), two open arms (50 × 10 cm), and a central platform (10 × 10 cm). We put the rat's head towards the closed arm on the central platform, and used the XR-super Maze tracking system to record the action track of rats within 6 min, including the frequency (OE) and time (OT) of entering the open arm, and the frequency (CE) and time (CT) of entering the closing arm (Biedermann et al., 2017). OE% and OT% were calculated as follows: OE% = OE/(OE + CE) × 100% and OT% = OT/(OT + CT) × 100%. If the OE% and OT% of rats were low, the anxiety behavior of rats was obvious.

## 2.6 Sample Collection and Preparation

Pentobarbital (2%) was injected into the abdominal cavity of rats to induce deep anesthesia (40 mg/kg). Some rats were decapitated, and their brains were removed. The hippocampus in the brain tissue was quickly stripped and stored in liquid nitrogen for subsequent western blotting and RT qPCR detection. The remaining rats in each group were perfused with 0.9% NS 500 ml and 4% paraformaldehyde 150 ml, the brain tissue was quickly removed and soaked in 4% paraformaldehyde, fixed for 24 h, and the area of the hippocampus was trimmed into small pieces with a thickness of 5 mm. The small pieces were dehydrated with gradient concentration of ethanol (75, 85, 95% for 2 h, 100% for 1 h), transparent in xylene (45 min), and soaked in paraffin (three times, 1 h each time). The tissues were embedded in an embedding machine to make paraffin blocks (Mohamed et al., 2017). Each paraffin block was cut into four 4 um pathological sections using a Leica paraffin slicer (Histocore Biocut Paraffin Slicer, Leica, United States).

## 2.7 HE Staining

First, paraffin sections of brain tissue from each rat were taken, dewaxed and hydrated, washed with 0.1 M PBS three times, then immersed in hematoxylin dye for 5 min, washed with tap water after removal, differentiated with 1% hydrochloric acid alcohol for several seconds, returned to blue with 0.6% ammonia, and rinsed with running water for 5 s. They were dyed in eosin solution for 2 min and rinsed with running water. Finally, the slices were successively placed in gradient alcohol and xylene, dehydrated, transparent, and sealed with neutral gum (Feldman and Delia, 2014).

## 2.8 Double Immunofluorescence

Three paraffin sections were obtained from the brain tissue of each rat. Each section was double-stained with anti-BrdU/anti Nestin (anti-BrdU mouse mAb, GB12051, Servicebio; Anti-Nestin Mouse mAb, GB12137, Servicebio), anti-BrdU/anti NeuN (Anti-NeuN Mouse mAb, GB11138, Servicebio), and anti-BrdU/anti GFAP (anti-GFAP rabbit pAb, GB11096, Servicebio). The staining steps of immunofluorescence double staining are briefly described as follows: First, the sections were dewaxed and hydrated, repaired with EDTA antigen repair solution, and the sections were washed with 0.1 M PBS, and then incubated in goat serum for 30 min. Each slice was then incubated with different pairs of primary antibodies at 4°C overnight. The next day, after recovery to room temperature, they were washed with 0.1 M PBS three times, and mixed secondary antibody (Alexa Fluor® 488 labeled goat anti-rabbit IgG, GB25303, Servicebio; Cy3 labeled goat anti-rabbit IgG, GB21303, Servicebio), incubated in the dark at room temperature for 20 min, washed with 0.1 M PBS for 3 times, Cy3-TSA was added dropwise and incubated at room temperature for 10 min, and the nuclei treated with 4′,6-diamidino-2-phenylindole (DAPI; ThermoFisher Scientific, Waltham, MA, United States). Finally, two drops of fluorescence quencher were added to each slice to seal it and was observed under an upright fluorescence microscope (Leica SP8, Hamburg, Germany)(Mohan et al., 2008; Lightbody and Nicol, 2019).

## 2.9 Real Time-qPCR

Total RNA was extracted from 60 rat hippocampal tissues using Trizol (CWBIO, CW0580s) according to the manufacturer's instructions. A large amount of cDNA was obtained using a HiFiScript cDNA Synthesis Kit. In the ultrasound mixture real-time fluorescence quantitative PCR system, the detection of fluorescence quantitative PCR is efficient and sensitive. Using $2^{-\Delta\Delta CT}$, the relative expression of each gene was calculated by the CT method, and the expression of each protein was standardized by the GAPDH housekeeping gene (Derveaux et al., 2010).

Gene-specific primers for quantitative RT-PCR included: GAPDH forward, 5-CCTTCCGTGTTCCTACCCC-3, GAPDH reverse, 5-GCCCAGGATGCCCTTTAGTG-3; Notch1 forward,5′-TGGATGCCGCTGACCTACG-3, Notch1 reverse, 5-TGGATGCCGCTGACCTACG-3; Hes1 forward, 5′-TTG AGCCAACTGAAAACACTGATT- 3′, Hes1 reverse, 5-GTG CTTCACTGTCATTTCCAGAAT-3; Hes5 forward, 5-GAT GCTCAGTCCCAAGGAGAAAA-3, Hes5 reverse, 5-CCACGA GTAACCCTCGCTGTAGT-3'.

## 2.10 Western Blotting

Hippocampal samples were dissected on ice, homogenized in ice-cold lysis buffer, and the protein concentration of the supernatant was measured on a spectrophotometer. A loading buffer was added to the samples to boil them. Then, 50 ug protein was loaded into 10% Bis-Tris gel, and the strip was transferred to a polyvinylidene fluoride membrane (PVDF) and sealed with sealing solution. The primary antibodies Hes1(1:300) (#11988, CST, American), Hes5 (1:300) (22666-1-AP, Proteintech, China), and Notch1 (1:1000) (#36081, CST, United States) were incubated at 4°C overnight. The secondary antibodies conjugated with horseradish peroxidase were added dropwise on the next day and visualized by enhanced chemiluminescence. The expression of each target gene was standardized using the GAPDH housekeeping gene (Pillai-Kastoori et al., 2020).

## 2.11 Statistical Analysis

The data were analyzed using Graph Pad Prism 7.00 software (Graph Pad Software, Inc, San Diego, California, United States). Outliers were eliminated by the statistical elution method (values that deviate from the mean ±2 times the standard deviation are excluded) (Nakagawa and Cuthill, 2009). The data were expressed as Mean ± SEM. In all group tests, whether using parametric analysis of variance or repeated measurement of parameters, the

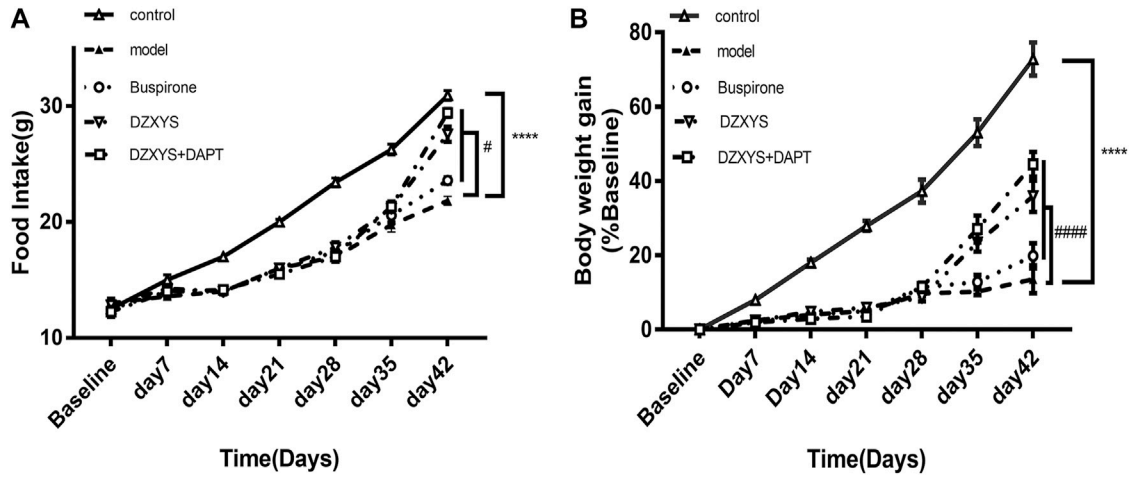


**FIGURE 3 |** Food intake of rats **(A)** and body weight growth rate **(B)** of rats in each group at the end of stress and drug intervention up to the 42nd day. Control: control group (Hollow triangle); model: model group (Solid triangle); Buspirone: Buspirone group (Hollow circle); DZXYS: DZXYS group (Inverted hollow triangle); DZXYS + DAPT: DZXYS + DAPT Group (Hollow square); ****$p < 0.0001$ vs control group. #$p < 0.05$, ####$p < 0.0001$ vs model group.

data before analysis of variance were subject to a normality test (Kolmogorov-Smirnov test) and variance homogeneity test (Levene test). If not, a nonparametric test was used. All data in this study were normal and homogeneous in terms of variance. The transcriptional expression levels of Notch1, Hes1, and Hes5 mRNA and the protein expression levels of Notch1, Hes1, and Hes5 in the hippocampus were analyzed by one-way ANOVA. Repeated measurement two-way ANOVA was used to analyze the food intake, body mass growth rate, total distance of exercise, distance to the central area, residence time in the central area, number of upright, and BrdU+/Nestin+, BrdU+/NeuN+, BrdU+/GFAP + expression in the DG area of the hippocampus. For all analyses, if appropriate, post hoc comparisons were performed using the Bonferroni posthoc tests test. The significance level of ANOVA and post-test was set at $p < 0.05$.

# 3 RESULTS

## 3.1 DZXYS Increased Food Intake and Weight Gain in GAD Rats

There are significant differences in food intake between groups (**Figure 3A**).

The Bonferroni post hoc test showed that the model group was significantly lower than the control group ($p < 0.0001$). There was no significant difference between the drug intervention groups and the model group after 7 days of drug intervention. After 14 days of DZXYS and DZXYS + DAPT intervention, the loss of appetite was reversed ($p < 0.0001$ and $p < 0.0001$, respectively). This shows that chronic stress stimulation affects the appetite of rats. The intervention of DZXYS or DZXYS + DAPT for a long time can improve the appetite of rats in the model group. Two-way ANOVA showed a drug treatment effect ($F_{4,52} = 90.72$, $p < 0.0001$) and time effect ($F_{6,312} = 673.5$, $p < 0.0001$). The growth rate of the body mass of the rats in each group was significantly different (**Figure 3B**). On the 42nd day, after stress and drug intervention, there was a significant difference in body mass growth rate between the groups. The Bonferroni post hoc test showed that the model group was significantly lower than the control group ($p < 0.0001$). After intervention with buspirone, DZXYS and DZXYS + DAPT, weight gain retardation was reversed on Day 35 and Day 42 respectively ($p = 0.0103$, $p < 0.0001$, $p < 0.0001$; $p < 0.0001$, $p < 0.0001$, $p < 0.0001$). The results showed that stress had an impact on the normal physiological metabolism of rats, and the three drug interventions corrected the abnormal physiological metabolism of stressed rats to varying degrees. Two-way ANOVA showed significant drug treatment effect ($F_{4,52} = 1631$, $p < 0.0001$)And time effect ($F_{6,312} = 2,700$, $p < 0.0001$).

## 3.2 DZXYS Reverses Anxiety Behavior in GAD Rats

In order to observe the effect of DZXYS on the improvement of anxiety behavior in GAD rats, we used the internationally widely used OFT and EPM behavioral testing methods to detect the changes in anxiety behavior in rats. As shown in **Figure 4B**, there was no significant difference in the total movement distance of rats in each group in the open field at each time node. Two-way ANOVA showed no significant treatment effect ($F_{4,52} = 1.935$, $p = 0.1184$).

There were significant differences among the groups in the central area exercise distance in the open field experiment (**Figure 4C**). The Bonferroni post hoc test showed that the model group was significantly lower than the control group ($p < 0.0001$), and buspirone, DZXYS, and DZXYS + DAPT were significantly higher than the model group after 7 days (Day 35) and 14 days (Day 42) ($p = 0.0010$, $p = 0.0009$, $p < 0.0001$; $p < 0.0001$, $p < 0.0001$, $p < 0.0001$, respectively). Two-way ANOVA showed that the movement distance of the central area had a significant processing effect ($F_{4,52} = 63.28$, $p < 0.0001$) and time effect ($F_{2,104} = 147.2$, $p < 0.0001$).

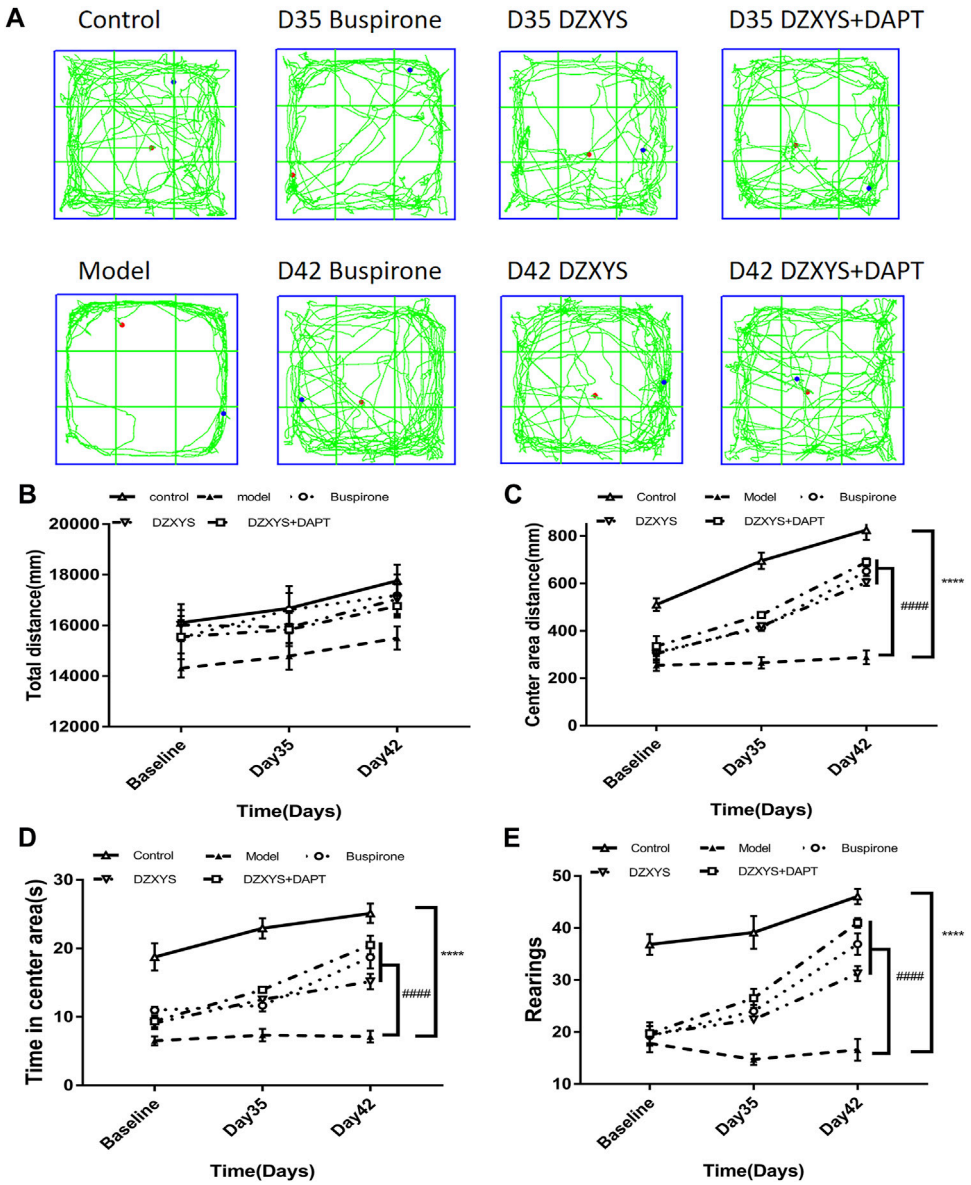


**FIGURE 4 |** Shows the results of the OFT experiment **(A)** The trajectory of OFT in each group **(B)** Total distance (mm) traveled in a 6 min period **(C)** Center area distance (mm) **(D)** Time in center area(s) **(E)** Number of rearings. ****$p < 0.0001$ vs control group. ####$p < 0.0001$ vs. model group, repeated measurements of two-way ANOVA.

The residence time in the central area of the rats in each group was significantly different between the groups (**Figure 4D**). The Bonferroni post hoc test showed that the model group was significantly lower than the control group ($p < 0.0001$), and buspirone, DZXYS, and DZXYS + DAPT were significantly higher than the model group on the 35th and 42nd days after intervention ($p = 0.0377$, $p = 0.0115$, $p = 0.0006$; $p < 0.0001$, $p < 0.0001$, $p < 0.0001$, respectively). The treatment effect of residence time in the central area was as significant as the time effect ($F_{4,52} = 51.7$, $p < 0.0001$) ($F_{2,104} = 51.29$, $p < 0.0001$). The results showed that the model group rats had obvious anxiety-like behaviors. Buspirone, DZXYS, DZXYS, and DAPT alleviated anxiety-like behavior in stressed rats.

The number of upright times in the open field of rats in each group was significantly different between the groups (**Figure 4E**). Bonferroni post hoc analysis showed that the model group was significantly lower than the control group ($p < 0.0001$), and buspirone, DZXYS, DZXYS + DAPT were significantly higher than the model group after 7 days (Day 35) and 14 days (Day 42) ($p = 0.0021$, $p = 0.0252$, $p < 0.0001$; $p < 0.0001$, $p < 0.0001$, $p < 0.0001$, respectively). Two-way ANOVA showed that the number of upright rats had a significant treatment effect ($F_{4,52} = 60.87$, $p < 0.0001$) and time effect ($F_{2,104} = 65.22$, $p < 0.0001$).

The behavioral trajectories of rats in the different treatment groups in the EPM device are shown in **Figure 4**. In the EPM test, significant differences are observed in the percentage of time

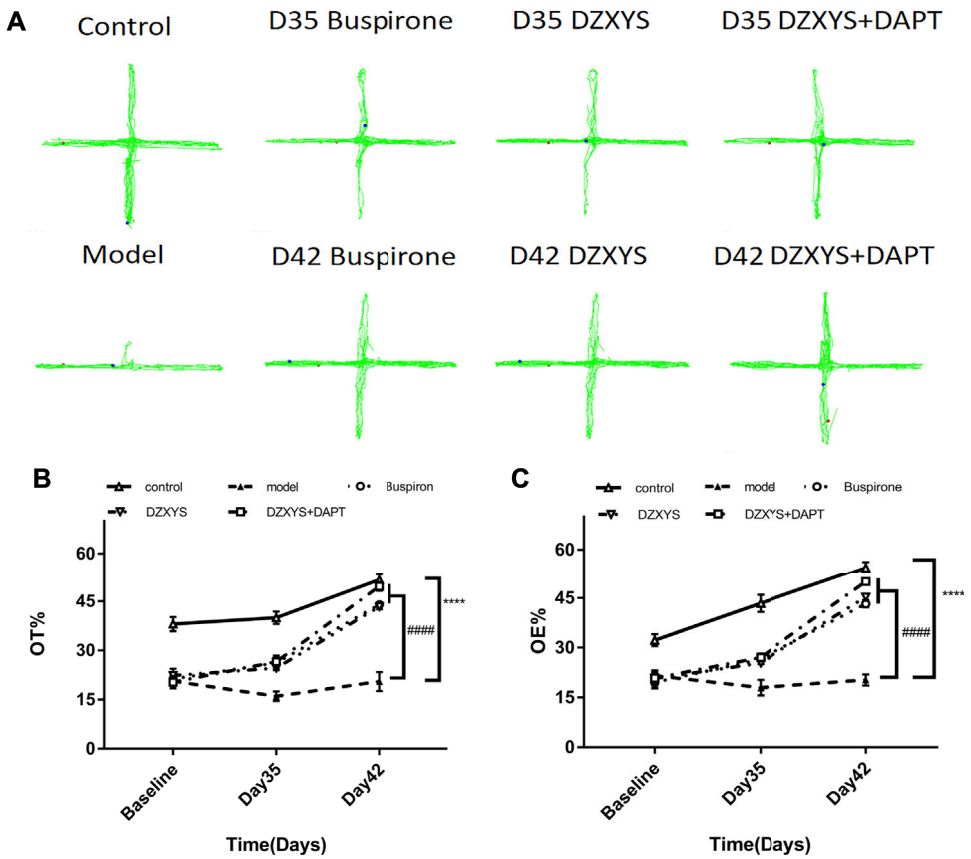


**FIGURE 5 |** The results of the EPM experiment. **(A)** The movement track of rats in the EPM experimental device. **(B)** The percentage of time in the open arm in the EPM test **(C)** Percentage of open arm entries in the EPM test. ****$p < 0.0001$ vs control group. ####$p < 0.0001$ vs. model group, two-way ANOVA of repeated data measurements.

entering the open arm (OT%) (**Figure 5B**) and the percentage of frequency entering the open arm entrance (OE%) (**Figure 5C**). Bonferroni post-test results showed that the OT% and OE% values of the model group were significantly lower than those of the control group ($p < 0.0001$, $p < 0.0001$), including buspirone and DZXYS after DZXYS + DAPT intervention for 7 days (Day 35) and 14 days (Day 42), The OT% value was significantly higher than that in the model group ($p < 0.0001$, $p = 0.0046$, $p < 0.0001$; $p < 0.0001$, $p < 0.0001$, $p < 0.0001$), and OE% was significantly higher than that in the model group ($p = 0.0035$,$p = 0.0176$, $p = 0.0048$; $p < 0.0001$, $p < 0.0001$, $p < 0.0001$).

Two-way ANOVA showed that OT% had a significant treatment effect ($F_{4,52} = 80.39$, $p < 0.0001$) and time effect ($F_{2,104} = 140$, $p < 0.0001$). The OE% value drug treatment effect was as significant as the time effect ($F_{4,52} = 85.93$, $p < 0.0001$) ($F_{2,104} = 174.6$, $p < 0.0001$).

## 3.3 DZXYS Improves the Morphology of Hippocampal DG Neurons in GAD Rats

We found that after HE staining in the hippocampus of rats in each group (**Figure 6**), the pyramidal nucleus in the hippocampus of rats in the normal group was large and round, the morphology was intact, the cytoplasm was pink, the nucleus was blue, the chromatin was evenly distributed, the nucleolus was obvious, and the connection between cells was tight and arranged neatly, while in the model group, the number and layers of cells in the hippocampus decreased and were disorderly arranged. It can be seen that a large number of neurons have nuclear chromatin gathering on the lower edge of the nuclear membrane, nuclear pyknosis, deep staining, irregular morphology, cytoplasmic concentration, dark red, and even apoptotic bodies. Neurons lack blindness, the arrangement between cells is disordered, loose, and irregular, and there are gaps around the cells. This is especially true in the DG area of the hippocampus. After 7 days of drug intervention (Day 35), the morphology of neurons in the hippocampus of the buspirone, DZXYS, and DZXYS + DAPT groups was slightly improved compared with that of the model group, but the number of cell layers were still less than that of the control group. Some nuclear chromatin gathered under the nuclear membrane, along with nuclear pyknosis, deep staining, and irregular morphology. After 14 days of drug intervention (Day 42), the morphology of hippocampal neurons in the DZXYS + DAPT and buspirone groups was significantly improved compared to that in the model group. Most cells had a clear outline and were arranged closely. Only a small number of nuclei had slight pyknosis and deep staining of the cytoplasm, which was similar to that in the control

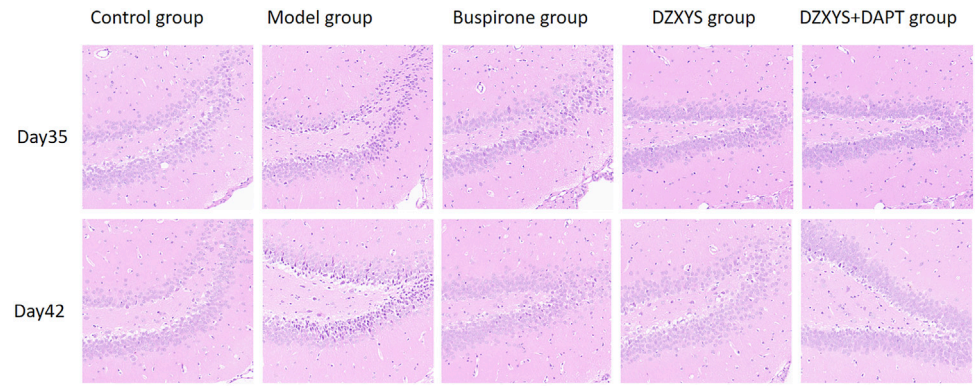


**FIGURE 6 |** Comparison of HE staining images of neurons in the DG area of the hippocampus in five groups on the 35th and 42nd day after modeling.

group. The morphology of hippocampal neurons in the DZXYS group was further improved compared to that at 7 days, but the arrangement was loose, which was slightly worse than that in the DZXYS + DAPT and buspirone groups.

## 3.4 DZXYS Promotes Neurogenesis in DG Region of Hippocampus in GAD Rats

To observe the proliferation of neural stem cells (NSCs), we labeled newly proliferating cells with BrdU (red) antibody and neural stem cells with nestin antibody (neural progenitor cell-specific marker; green) (Bernal and Arranz, 2018) in the dentate gyrus of rats. There were significant differences in the number of newborn NSCs in the DG area of the hippocampus between the groups (**Figures 7A–C**). The Bonferroni post hoc test showed that the number of newborn NSCs in the model group was significantly higher than that in the control group ($p < 0.0001$), and the number of buspirone, DZXYS, DZXYS + DAPT on the 35th and 42nd days after intervention was significantly lower than that in the model group ($p = 0.0004$, $p = 0.0004$, $p < 0.0001$; $p < 0.0001$, $p < 0.0001$, $p < 0.0001$, respectively). Two-way ANOVA showed that the number of neonatal NSCs in the DG area of rats had a significant treatment effect ($F_{4,20} = 52.16$, $p < 0.0001$) and time effect ($F_{1,20} = 5.488$, $p = 0.0296$).

To observe the differentiation of newborn NSCs into neurons (Zupanc et al., 2019), we double-labeled with anti-BrdU (red) and NeuN (neuron specific protein; green) (Gusel'nikova and Korzhevskiy, 2015) antibodies. After 7 days (Day 35) and 14 days (Day 42) of drug intervention, the number of newborn neurons in the DG of the hippocampus in each group was significantly different between the groups (**Figures 8A–C**). The Bonferroni post hoc test showed that the model group was significantly lower than the control group ($p < 0.0001$), and the number of newborn neurons in buspirone, DZXYS, and DZXYS + DAPT was significantly higher than that in the model group ($p < 0.0001$, $p < 0.0001$, $p < 0.0001$; $p < 0.0001$, $p < 0.0001$, $p < 0.0001$, respectively). Two-way ANOVA showed that the number of newborn neurons in the DG area had a significant processing effect ($F_{4,20} = 50.39$, $p < 0.0001$) and a significant time effect ($F_{1,20} = 11.64$, $p = 0.0028$). To observe the differentiation of neonatal NSCs into astrocytes in the rat hippocampus, we double-labeled them with antibodies against BrdU (red) and GFAP (a specific marker of astrocytes; green) (Baba et al., 1997). There was a significant difference in the number of new astrocytes in the DG area of the hippocampus between groups on the 35th and 42nd days after modeling (**Figures 9A–C**). Bonferroni post hoc analysis showed that the number of new astrocytes in the model group was significantly higher than that in the control group ($p < 0.0001$), and it was significantly lower than that in the model group after buspirone, DZXYS, and DZXYS + DAPT intervention for 7 days (Day 35) and 14 days (Day 42) ($p < 0.0001$, $p < 0.0001$, $p < 0.001$; $p < 0.0001$, $p < 0.0001$, $p < 0.0001$). Two-way ANOVA showed that the number of newborn neurons in the hippocampus had a significant processing effect ($F_{4,20} = 119.2$, $p < 0.0001$) and a significant time effect ($F_{1,20} = 39.06$, $p < 0.0001$).

## 3.5 DZXYS Downregulated the Expression of Notch1, Hes1, and Hes5 in the Hippocampus

DZXYS upregulated the expression of Notch1, Hes1, and Hes5 in the hippocampus, and there was a significant difference in the expression of Notch1 mRNA in the hippocampus of rats in each group ($F_{7,16} = 29.57$, $p < 0.0001$) (**Figure 10A**). The Bonferroni post hoc test showed that the expression of Notch1 mRNA in the model group was significantly higher than that in the control group ($1.783 \pm 0.093$ vs. $1.000 \pm 0.058$, $p < 0.0001$), and decreased compared to the model group after 7 days of intervention with buspirone, DZXYS, and DZXYS + DAPT ($1.370 \pm 0.012$ vs. $1.783 \pm 0.093$, $p = 0.0019$; $1.380 \pm 0.047$ vs. $1.783 \pm 0.093$, $p = 0.0025$; $1.270 \pm 0.017$ vs. $1.783 \pm 0.093$, $p = 0.0002$), and decreased significantly compared with that in the model group after 14 days of drug intervention ($0.970 \pm 0.017$ vs. $1.783 \pm 0.093$, $p < 0.0001$; $1.010 \pm 0.067$ vs. $1.783 \pm 0.093$, $p < 0.0001$; $0.900 \pm 0.069$ vs. $1.783 \pm 0.093$, $p < 0.0001$).

There was a significant difference in the expression of Hes1 mRNA in the hippocampus of rats in different treatment groups ($F_{7,16} = 24.13$, $p < 0.0001$) (**Figure 10B**). Bonferroni post test showed that the expression of Hes1 mRNA in the model group

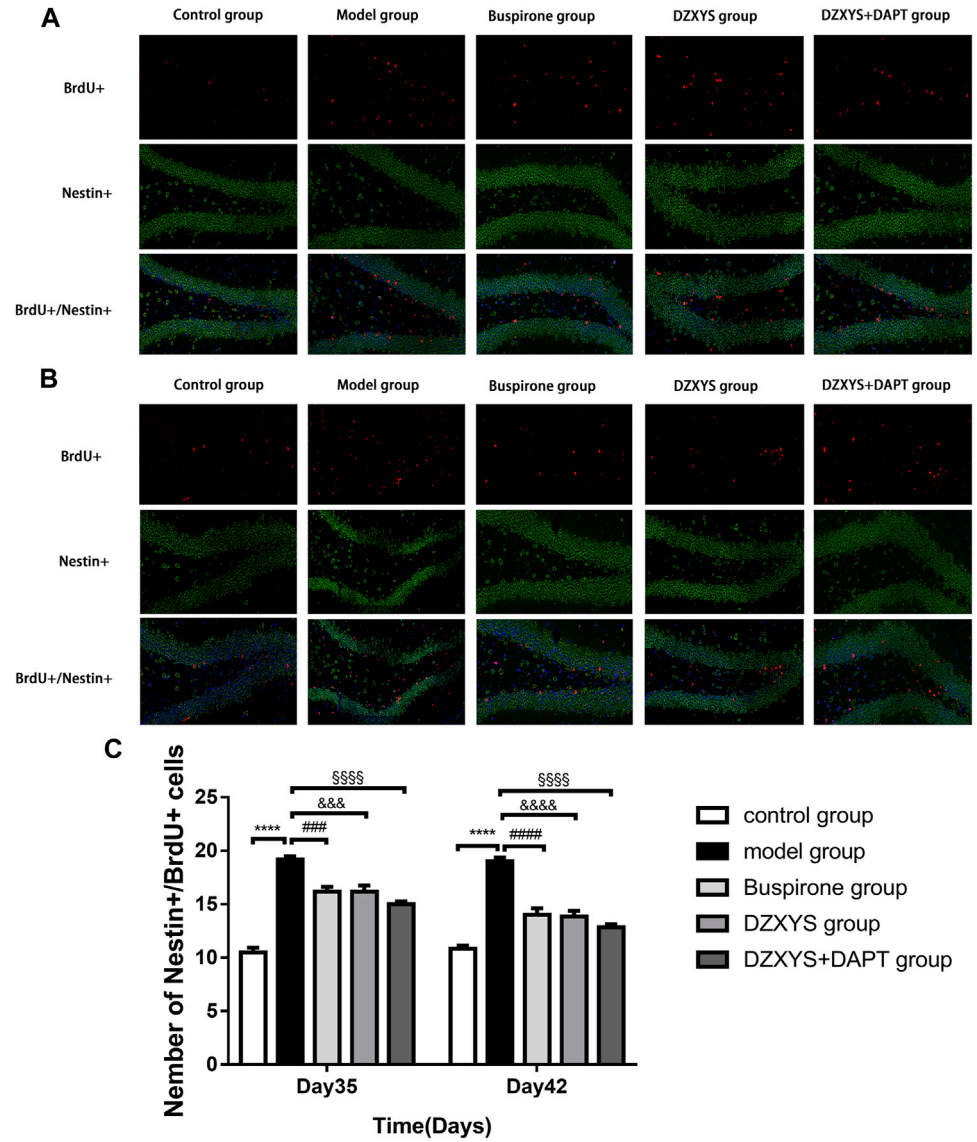


**FIGURE 7 |** The number of new neural stem cells in the dentate gyrus of hippocampus in each group was shown. BrdU (red) labeled newly formed cells, Nestin (green) labeled neural stem cells. The nuclei were labeled with DAPI (blue) **(A)** On the 35th day, the number of neural stem cells was increased **(B)** On the 42nd day, the number of neural stem cells was increased **(C)** The number of neural stem cell positive cells in dentate gyrus of hippocampus was observed on the 35th and 42nd day.****$p < 0.0001$, model group vs. control group; ###$p < 0.001$, ####$p < 0.0001$, Buspirone group vs Model group; &&&$p < 0.001$, &&&&$p < 0.0001$, DZXYS group vs. model group; §§§§$p < 0.0001$, DZXYS + DAPT group vs model group.

was significantly higher than that in the control group (1.7 ± 0.10 vs. 1.000 ± 0.115, $p < 0.0001$), and decreased after 7 days of intervention with Buspirone, DZXYS, and DZXYS + DAPT (1.317 ± 0.017 vs. 1.7 ± 0.10, $p = 0.0144$; 1.293 ± 0.007 vs. 1.7 ± 0.10, $p = 0.0083$; 1.28 ± 0.042 vs. 1.7 ± 0.10, $p = 0.0061$). After 14 days of drug intervention (Day 42), it was significantly lower than that in the model group (0.867 ± 0.073 vs. 1.7 ± 0.10, $p < 0.0001$; 0.913 ± 0.019 vs. 1.7 ± 0.10, $p < 0.0001$; 0.783 ± 0.017 vs. 1.7 ± 0.10, $p < 0.0001$).

There was a significant difference in the expression of Hes5 mRNA in the hippocampus of each group ($F_{7,16} = 23.86$, $p < 0.0001$) (**Figure 10C**). The Bonferroni post-test showed that the expression of Hes1 mRNA in the model group was significantly higher than that in the control group (1.600 ± 0.052 vs. 1.000 ± 0.115, $p < 0.0001$), and decreased after 7 days of intervention with Buspirone, DZXYS, and DZXYS + DAPT (1.18 ± 0.02 vs 1.600 ± 0.052, $p = 0.0023$; 1.3 ± 0.058 vs. 1.600 ± 0.052, $p = 0.0494$; 1.227 ± 0.064 vs. 1.600 ± 0.052, $p = 0.0073$). After 14 days of drug intervention (Day 42), the expression was significantly lower than that in the model group (0.820 ± 0.035 vs. 1.600 ± 0.052, $p < 0.0001$; 0.913 ± 0.019 vs. 1.600 ± 0.052, $p < 0.0001$; 0.783 ± 0.017 vs. 1.600 ± 0.052, $p < 0.0001$).

There was a significant difference in the amount of Notch1 protein in the hippocampus of rats in different treatment groups

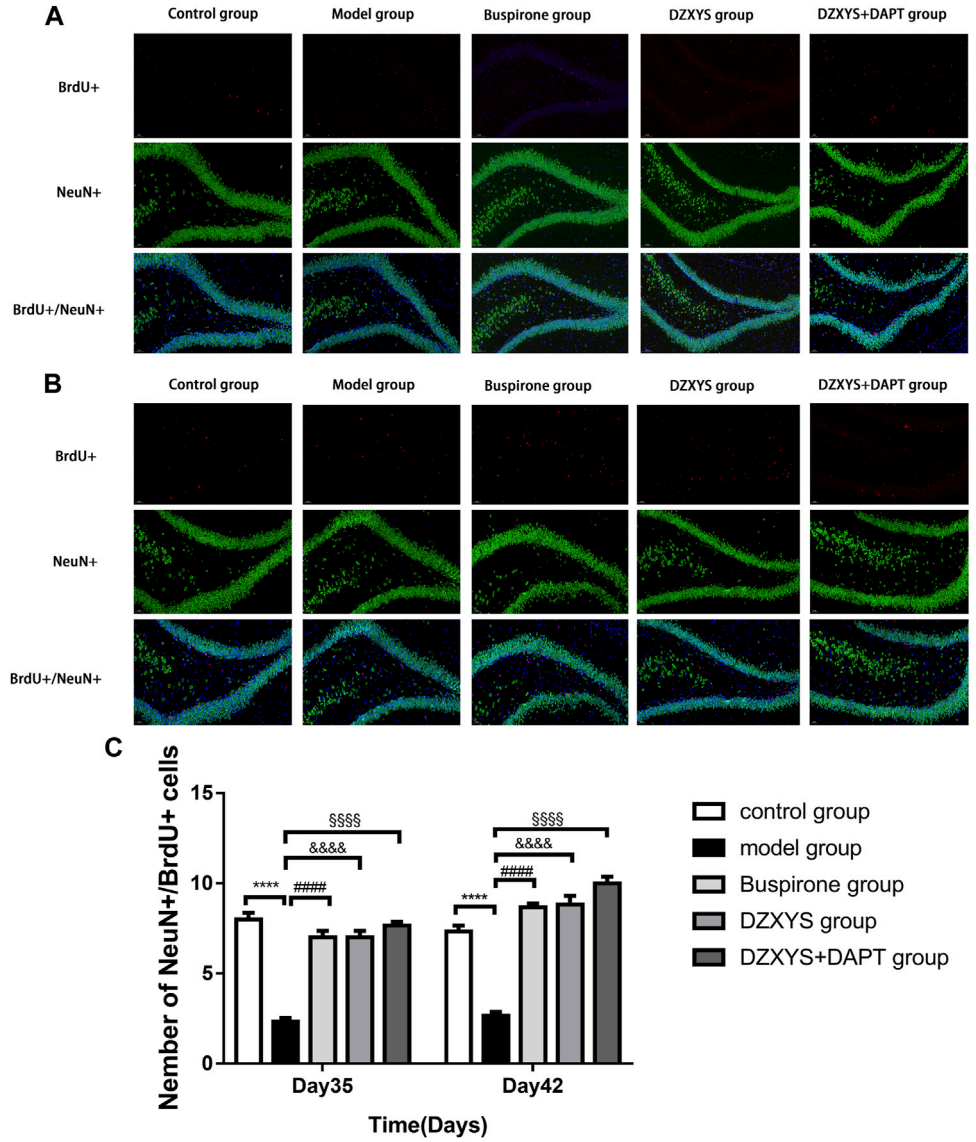


**FIGURE 8 |** The number of new neurons in the dentate gyrus of the hippocampus in each group. BrdU (red) labeled newly formed cells and NeuN (green)-labeled neurons. The nuclei were labeled with DAPI (blue) **(A)** The regeneration of neurons was observed on the 35th day **(B)** Regeneration of neurons on day 42 **(C)** The number of newborn neurons in the dentate gyrus of the hippocampus on the 35th and 42nd day. ****$p < 0.0001$, model group vs. control group; ####$p < 0.0001$, Buspirone group vs Model group; &&&&$p < 0.0001$, DZXYS group vs. model group; §§§§$p < 0.0001$, DZXYS + DAPT group vs model group.

($F_{7,16}$ = 207.3, $p < 0.0001$) (**Figure 10D**). Bonferroni post hoc analysis showed that the amount of Notch1 protein in the model group was significantly higher than that in the control group (2.828 ± 0.037 vs. 1.000 ± 0.028, $p < 0.0001$, $p < 0.0001$). The amount of Notch1 protein in the model group was significantly lower than that in the model group on the 35th day of the experiment after the intervention with buspirone, DZXYS, and DZXYS + DAPT (1.718 ± 0.035 vs. 2.828 ± 0.037, $p < 0.0001$; 1.957 ± 0.078 vs. 2.828 ± 0.037, $p < 0.0001$; 1.440 ± 0.059 vs. 2.828 ± 0.037, $p < 0.0001$). It continued to decline on the 42nd day of the intervention (1.302 ± 0.049 vs. 2.828 ± 0.037, $p < 0.0001$; 1.255 ± 0.033 vs. 2.828 ± 0.037, $p < 0.0001$; 0.714 ± 0.026 vs. 2.828 ± 0.037, $p < 0.0001$).

There was a significant difference in the amount of Hes1 protein in the hippocampus of rats in different treatment groups ($F_{7,16}$ = 46.57, $p < 0.0001$) (**Figure 10E**). Bonferroni's post hoc test showed that the amount of Hes1 protein in the model group was significantly higher than that in the control group (2.633 ± 0.033 vs. 0.995 ± 0.058, $p < 0.0001$). After 7 days of buspirone, DZXYS, and DZXYS + DAPT intervention (Day 35), the amount of Hes1 protein in the model group was significantly lower than that in the model group, especially in the DZXYS + DAPT group (2.067 ± 0.067 vs. 2.633 ± 0.033, $p = 0.02$; 2.067 ± 0.033 vs. 2.633 ± 0.033, $p = 0.02$; 1.643 ± 0.054 vs. 2.633 ± 0.033, $p < 0.0001$). Fourteen days after drug intervention (Day 42), the amount of Hes1 protein in the model group was significantly

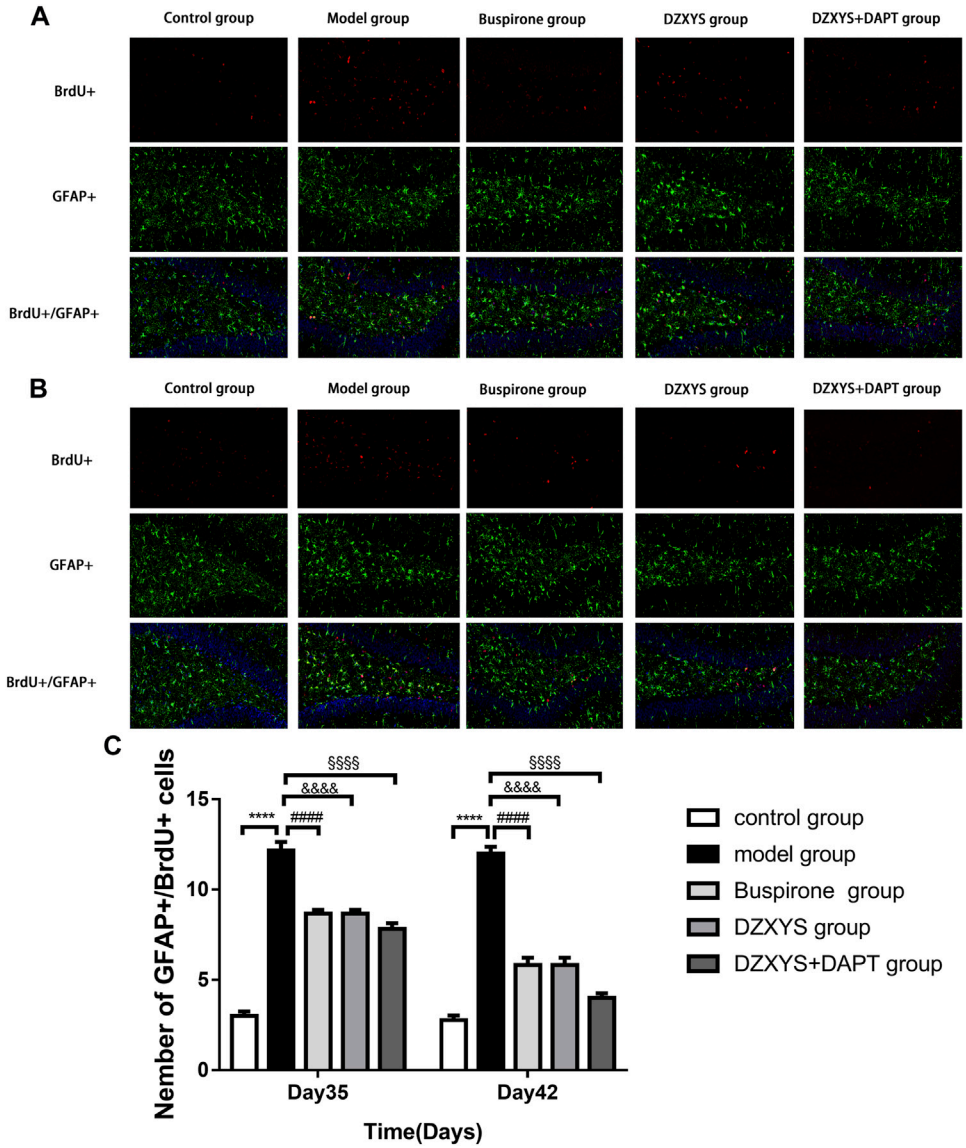


**FIGURE 9 |** The number of newborn astrocytes in the dentate gyrus of the hippocampus in each group. BrdU (red) labeled newly formed cells, GFAP (green) labeled astrocytes **(A)** The condition of newborn astrocytes on the 35th day **(B)** The condition of newborn astrocytes on the 42nd day **(C)** The number of new GFAP positive cells in the dentate gyrus on the 35th day and 42nd day. ****$p < 0.0001$, model group vs. control group; ####$p < 0.0001$, Buspirone group vs Model group; &&&&$p < 0.0001$, DZXYS group vs. model group; §§§§$p < 0.0001$, DZXYS + DAPT group vs model group.

lower than that in the model group (1.327 ± 0.037 vs. 2.633 ± 0.033, $p < 0.0001$; 1.427 ± 0.239 vs. 2.633 ± 0.033, $p < 0.0001$; 0.587 ± 0.047 vs. 2.633 ± 0.033, $p < 0.0001$).

There was a significant difference in the amount of Hes5 protein in the hippocampus of rats in each group ($F_{7,16} = 74.51$, $p < 0.0001$) (**Figure 10F**). Bonferroni post hoc analysis showed that the protein content of Hes1 in the model group was significantly higher than that in the control group (1.751 ± 0.055 vs. 1.000 ± 0.011, $p < 0.0001$). After 7 days of intervention with buspirone, DZXYS, and DZXYS + DAPT (Day 35), the protein content was lower than that in the model group, and the most significant was the DZXYS + DAPT group (1.542 ± 0.059 vs. 1.751 ± 0.055, $p = 0.0295$; 1.542 ± 0.025 vs. 1.751 ± 0.055, $p = 0.0304$; 1.260 ± 0.020 vs. 1.751 ± 0.055, $p < 0.0001$). Fourteen days after drug intervention (Day 42), the protein content of Hes1 in the model group was significantly lower than that in the model group (1.063 ± 0.037 vs. 1.751 ± 0.055, $p < 0.0001$; 0.995 ± 0.039 vs. 1.751 ± 0.055, $p < 0.0001$; 0.882 ± 0.025 vs. 1.751 ± 0.055, $p < 0.0001$).

## 4 DISCUSSION

The purpose of this study was to explore whether the pathogenesis of GAD is related to the abnormal expression of

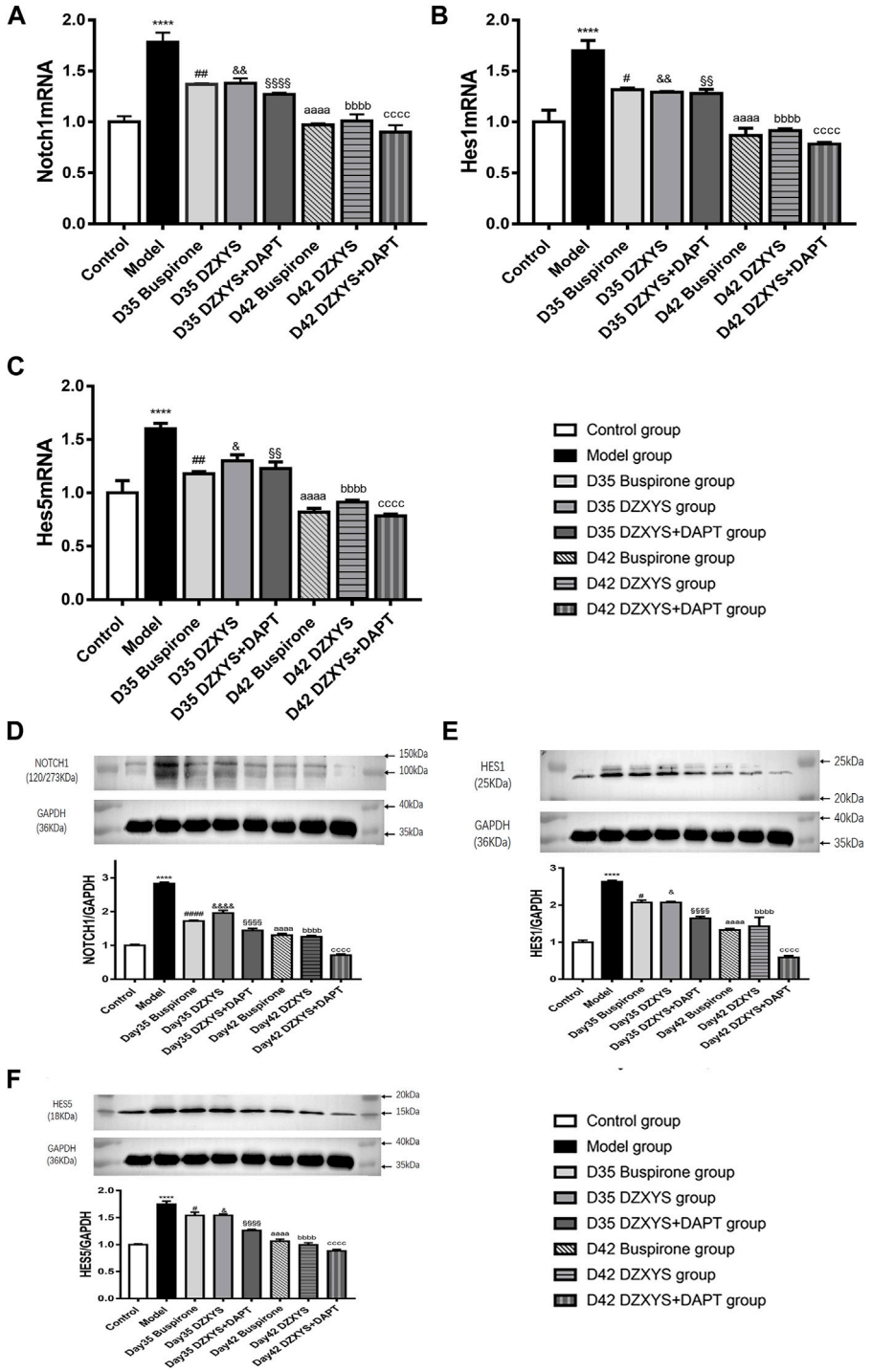


**FIGURE 10 |** The expression levels of Notch1, Hes1 and Hes5 mRNA transcripts in the hippocampus of rats in each group on the 35th and 42nd days after modeling were measured **(A)** Notch1 mRNA expression **(B)** Hes1 mRNA expression **(C)** Hes5 mRNA expression. **Figures D–F** show the electrophoretic bands of target protein and GAPDH in hippocampus of rats in different treatment groups, and the relative optical density of target protein in hippocampus of rats in different treatment groups were compared. The results were expressed as the percentage of the optical density of the target protein in the hippocampus of rats, including Notch1 **(Figure D)**、Hes1 **(Figure E)**、Hes5 **(Figure F)**. All data are expressed as the mean ± SEM from independent experiments performed in triplicate.****$p < 0.0001$, model group vs. control group; #$p < 0.05$, ##$p < 0.01$, ####$p < 0.0001$, Day 35 Buspirone group vs Model group; and $p < 0.05$, &&$p < 0.01$, &&&&$p < 0.0001$, Day 35 DZXYS group vs. model group; §§$p < 0.01$,§§§§$p < 0.0001$, Day 35 DZXYS + DAPT group vs model group; aaaa$p < 0.0001$, Day 42 Buspirone group vs Model group; bbbb$p <$ 0.0001, Day 42 DZXYS group vs. model group; cccc$p < 0.0001$, Day 42 DZXYS + DAPT group vs model group.

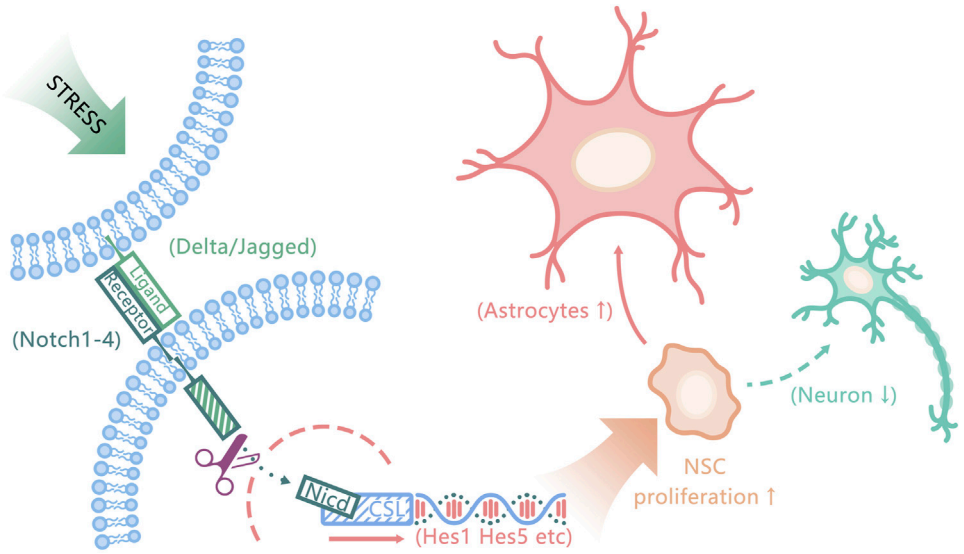


**FIGURE 11 |** Schematic diagram of molecular pathological mechanism of generalized anxiety disorder. Chronic stress activates Notch signaling pathway, which promotes the proliferation of neural stem cells and massive transformation to astrocytes, resulting in impaired neuronal regeneration (Louvi and Artavanis-Tsakonas, 2006).

the Notch signaling pathway, and whether the anti-anxiety effect of Danzhi Xiaoyao Powder can promote nerve regeneration in the hippocampus by regulating the Notch signaling. In this animal experiment, we found that after the intervention of DZXYS and DZXYS + DAPT, the food intake and body weight of rats increased significantly compared with the model group; the anxiety-like behavior of the buspirone, DZXYS, and DZXYS + DAPT groups was significantly reversed after 14 days of drug intervention, especially DZXYS + DAPT; immunofluorescence double staining of the hippocampal DG area of rats in each group showed that there was more proliferation of neonatal NSCs in the DG area of rats in the model group, and a large number of them transformed into astrocytes, resulting in obstacles to neurons. After 14 days of treatment with the three groups of drugs, the number of neonatal NSCs in the DG area of rats gradually decreased, the number of neonatal neurons increased significantly, the number of neonatal astrocytes decreased, and the protein expression of key targets of the Notch signaling pathway (Notch1, Hes1, and Hes5) in the hippocampus was gradually lower than that in the model group, and the protein expression of DZXYS + DAPT group was the most significant.

At present, the etiology of GAD is unclear, but it is certain that environmental pressure is an important reason for its onset, repeated fluctuation, and deterioration (Wittchen et al., 2000). Based on this, this study used the uncertain empty bottle drinking water stimulation method (Lin Wenjuan, 2003; Zhang et al., 2020) and chronic restraint stress (Ma et al., 2019) preparation of the GAD rat model. After 21 days of chronic stress stimulation, we found that GAD rats showed significant changes compared with the control group, such as decreased body weight growth rate (Morris, 2019), reduced exploration behavior in the central area of the open field experiment (Deacon, 2013), and significantly reduced exploration time to the open arm in the elevated cross maze (Gasnas, 2021), and there were statistical differences, which proved that the physiological metabolism of the model group was disordered. Moreover, there was anxiety of decreased desire for exploration and fear and timidity, which was consistent with the behavioral performance of anxiety disorder rats prepared by Wenjuan Lin (Lin Wenjuan, 2003) and Shuichi Chiba (Chiba et al., 2012). In addition, during the modeling period, the rats in the model group showed characteristics of depressed expression, easy frightening, dark yellow hair color, loss of luster, curling up in corners, and loose stool (Zhang et al., 2020). It can be seen from the above that the GAD model prepared in our study is accurate and reliable, and the characterization is consistent with clinical symptoms (Luyten et al., 2011).

Observing the changes of food intake of rats after drug intervention, we found that the food intake of rats in the DZXYS and DZXYS + DAPT groups increased significantly compared with the model group after 14 days of drug intervention; It was found that after 7 and 14 days of drug intervention, the body weight of rats in the buspirone, DZXYS and DZXYS + DAPT groups increased steadily compared with the model group, and had a time effect. DZXYS, the combination of DZXYS and DAPT had the most significant effect, indicating that the traditional Chinese medicine DZXYS, and the combination of DZXYS and DAPT can significantly improve appetite, restore normal physiological metabolism, and increase the body weight of rats, which is consistent with the animal experimental results of Yan et al. Yan et al. found that after the intervention of traditional Chinese medicine, the appetite and digestive ability of anxiety and depression rats can be significantly improved. It is speculated that this change is related to the change in the microbial population in the gastrointestinal tract, and its change is closely related to changes in brain metabolites (Qu et al., 2019). This phenomenon reflects the advantages of the multi-target treatment of traditional Chinese medicine.

Through the classical open field experiment, the exploratory behavior and tension of rats in novel and unfamiliar environments were observed, and it was found that the overall activity of rats after modeling showed no significant change compared with the control group, It shows that the limb activity of rats is normal and can move freely (Ann-Katrin et al., 2019), but the activity distance, residence time, and standing times of the central area in the open field were significantly lower than those in the control group after 28 days of modeling. After 7 days (Day 35) and 14 days (Day 42) of drug intervention, the activity distance of the central area in the buspirone, DZXYS, and DZXYS + DAPT groups were higher than those in the model group; the residence time and standing times increased significantly, and the activity of the central area increased most significantly in the DZXYS + DAPT group. This is currently the gold standard for investigating the anxiety of animals at present (Biedermann et al., 2017). The values of OT% and OE% in the model group were significantly lower than those in the control group. After 14 days of drug intervention, the values of OT% and OE% in the buspirone, DZXYS, and DZXYS + DAPT groups were significantly and continuously increased, and the treatment effect and time effect were significant (**Figure 5**) (Taylor et al., 1985). The above behavioral experimental results show that DZXYS can increase the ability of exploration, reduce the tension, and improve the anxiety behavior of rats. This is consistent with the experimental results obtained by (Zhao et al., 2017). Among them, the anti-anxiety effect of DZXYS + DAPT was better than that of DZXYS alone.

5-HT1A receptor agonists, such as buspirone and tandospirone, have been shown to promote the formation of neurons in the hippocampus of anxiety and depression rats and improve anxiety and depression. As shown in **Figure 6**, HE staining of rat hippocampus showed that the morphology of neurons in DG area of DZXYS group was slightly improved compared with that of the model group, most cells had clear outline and were closely arranged, only a small amount of nuclear pyknosis and deep staining of cytoplasm were seen, and the number and number of cell layers in DZXYS group were slightly lower than those in the control group (Kai et al., 2020). To understand the anti-anxiety role of DZXYS, we used double immunofluorescence staining (Donaldson, 2015) to observe neurogenesis in the DG area of the hippocampus of rats in each group at 7 days (Day 35) and 14 days (Day 42) after drug intervention. Proliferation of new neural stem cells (NSCs): Compared with the control group, the number of new NSCs in the GAD model group increased significantly. On the 35th day, the number of new NSCs in the DZXYS + DAPT group was lower than that in the model group. On the 42nd day, the number of new NSCs in the hippocampus of the buspirone, DZXYS, and DZXYS + DAPT groups decreased, especially in the DZXYS + DAPT group. This shows that compared with normal rats, neural stem cells in the DG area of the hippocampus of GAD rats had compensatory proliferation, while the proliferation of neural stem cells decreased or was successfully transformed into other neural cells after drug intervention. Proliferation of newborn neurons: Compared with the control group, the number of newborn neurons in the model group decreased significantly. After 7 and 14 days of drug intervention, the number of newborn neurons in the buspirone, DZXYS, and DZXYS + DAPT groups continued to increase significantly, with significant treatment effect and time effect; proliferation of new astrocytes: Compared with the control group, the number of new astrocytes in the DG area of the model group increased significantly. After 7 and 14 days of drug intervention, the number of new astrocytes in the hippocampus of the buspirone, DZXYS, and DZXYS + DAPT groups decreased significantly compared with the model group, and the time effect was significant, especially in the buspirone group which decreased most significantly. According to the above three fluorescent double-standard results, it can be seen that at all time points after the model was built by the model group, a large number of NSCs proliferated and mainly transformed into star-type glial cells, and a small number of them were transformed into new neurons. After DZXYS intervention for 7 days, the proliferation of NSCs decreased, and the number of newly proliferated NSCs in the early stage was transformed into new neurons, The transformation to the new astrocytes decreased significantly and the trend was more obvious with time. We speculate that the neural stem cells in the hippocampus of the model group that received adverse stimulation were over-proliferated and differentiated into astrocytes in large quantities, which could not be transformed into new neurons. Astrocytes are the most widely used glial cells in the brain. An appropriate number of astrocytes can maintain potassium homeostasis around neurons, regulate synaptic transmission, promote the supply of neuronal sugar, and have the ability to divide (Vasile et al., 2017). However, excessive proliferation of reactive astrocytes can form glial scars and secrete growth factors and interleukins, interferons, and other factors that inhibit nerve regeneration, inhibiting the regeneration of neurons and nerve axons (Rossi et al., 2007). Therefore, astrocyte activation plays a "double-edged" effect in the process of central nervous system injury and repair, and it is very important to ensure a steady state of astrocyte number (Lee et al., 2014; Pekny et al., 2016). Neurogenesis in the hippocampus is particularly important in cognition, emotion, and reproductive behavior, and dysfunctional neurogenesis leads to emotional and mental disorders, leading to the emergence of an anxious state. This is similar to Gisele's observation of neurons in the hippocampus of GAD rats (Dias et al., 2014). DZXYS, especially the combination of DZXYS and DAPT, dynamically reversed the excessive differentiation of neural stem cells into astrocytes, turned into newborn neurons, and improved anxiety behavior, which is similar to the mechanism of hippocampal neuron regeneration in the treatment of depression (Tanti and Belzung, 2013; Hill et al., 2015; Anacker et al., 2018). Therefore, we propose an important question as to how DZXYS dynamically reverses the differentiation direction of newborn neural stem cells at the molecular level.

It is generally recognized that Notch signaling plays an important role in maintaining the proliferation state of neural stem cells, regulating the timing of differentiation, and determining the fate of neural precursor cells (Lutolf et al.,

2002; Niessen and Karsan, 2007). Previous studies have shown that the Notch signaling pathway is expressed in the SGZ and SVZ regions of the adult brain (Stump et al., 2002) and participates in adult neurogenesis. The Notch signaling pathway is composed of the Notch receptor, ligand, and CSL (CBF1-suppressor of hairless-lag-1) DNA-binding protein (Ehebauer et al., 2006). This pathway is initiated by the combination of the Notch receptor and its ligand, after which the Notch receptor releases the active Notch intracellular domain (NICD) into the cytoplasm, and the released NICD is transferred to the nucleus to directly regulate the functions of transcription factors CSL [CBF-1, Su(H), and LAG-1] and a series of downstream target genes, including Hes1 Hes5 and Hes related protein (HERP/HEY) genes (Louvi and Artavanis-Tsakonas, 2006). In this study, we observed fluctuations in Notch1, Hes1 and Hes5 mRNA transcription levels and protein expression in the rat hippocampus by PCR and western blotting. The transcription levels of Notch1, Hes1 and Hes5 mRNA in the model group were significantly higher than those in the control group. After 7 and 14 days of drug intervention, Notch1, Hes1 and the expression of Hes5 mRNA decreased gradually, with an obvious time effect. Among them, the transcriptional levels of Notch1, Hes1, and Hes5 mRNA in the hippocampus of rats in the DZXYS + DAPT group decreased most significantly. The changes in the expression of the three proteins detected by western blotting were consistent with the PCR results.

Previous studies have shown that the activated Notch signaling pathway can maintain the cellular characteristics of NSCs and inhibit their differentiation into neurons, while promoting their differentiation into astrocytes (Guo et al., 2009; Snyder et al., 2012). The overexpression of Notch1 protein observed in this experiment will lead to a large number of transformations of newborn neural stem cells into astrocytes and neurogenesis disorder (Louvi and Artavanis-Tsakonas, 2006) as shown in **Figure 11**. Hes1 and Hes5, the main downstream targets of Notch signaling, are essential for regulating neurogenesis. They inhibit the transcription of precursor genes, leading to the inhibition of neuronal differentiation (Ohtsuka et al., 1999), the emergence of new astrocytes also depends on the activities of Notch downstream effectors Hes1 and Hes5 (Givogri et al., 2006). The transcriptional levels of Notch 1, Hes1, and Hes5 mRNA in the model group were significantly higher than those in the control group, which revealed that the deep-seated molecular mechanism of GAD was related to the activation of the Notch signaling pathway and the overexpression of key targets. DZXYS can downregulate the Notch signaling pathway, inhibit the continuous proliferation of neural stem cells, and promote their differentiation into neurons, thus improving the anxiety behavior of rats. DAPT in the DZXYS + DAPT group ($\gamma$-secretase inhibitors) can inhibit the transmission of Notch 1 signaling, inhibit the activation of the Notch signaling pathway, reduce the excessive proliferation of neural stem cells, and promote their transformation to newborn neurons (Breunig et al., 2007). Therefore, the decrease in protein expression of the main target of the Notch signaling pathway in the hippocampus of rats in the combination group of DZXYS and DAPT was more significant than that in other drug intervention groups. The Notch signaling pathway was most effectively inhibited, the proliferation level of neural stem cells decreased, and then differentiated into a large number of newborn neurons. The anxiety behavior was most significantly improved, which also confirmed that inhibiting the overexpression of the Notch signaling pathway and promoting the regeneration of newborn neurons is the key to alleviating anxiety behavior. Many common active ingredients in DZXYS can regulate Notch signaling pathway and promote neuronal regeneration. It has been found that sodium ferulate combined with bone marrow stromal cells can down regulate Notch signaling pathway and promote neural regeneration after focal cerebral ischemia in rats (Zhao et al., 2013); It was also found that baicalin could down regulate the expression of basic helix-loop-helix (bHLH) protein downstream of Notch signaling pathway and induce the differentiation of human iPS cells into neurons (Morita et al., 2015). At present, mental diseases are less associated with the Notch signaling pathway, and there is a great controversy about how the Notch signaling pathway plays a therapeutic role in limited studies. For example, Guo et al. observed the Notch signaling pathway in the hippocampus of post-stroke depression rats and found that the Notch signaling pathway in the hippocampus of depression rats is inhibited, neuronal apoptosis and necrosis are increased, and there are few newborn neurons; after intervention with antidepressants, the Notch signaling pathway was activated, and the protein expression of key targets (especially Hes1 and Hes5) increased, which promoted the increase of newborn neurons and alleviated depressive behavior (Guo et al., 2009). We speculate that the differential expression of the Notch signaling pathway protein is related to the special pathological state of post-stroke brain tissue in this study.

The neuronal hypothesis has been the focus of international psychiatry research in the past 10 years, and it is also one of the most challenging research fields. For the treatment of depression, experimental and theoretical research on promoting hippocampal neuron regeneration and improving depressive symptoms has gradually matured. Whether it can effectively promote hippocampal neuron generation has become an important new target to determine the effectiveness of antidepressants. As a chronic mental disease (Fenton, 1996), generalized anxiety disorder (GAD) usually precedes depression. Some experts believe that the emergence of depression may indicate that compensatory activities cannot protect themselves from the chronic pressure imposed by GAD and eventually develop into depressive disorder (Kessler et al., 1999; Maron and Nutt, 2017). If GAD symptoms can be reversed in the early stage of the disease, it can not only greatly alleviate the great mental pain experienced by patients with GAD, but also avoid the occurrence of depression to a certain extent. DZXYS has been widely used in the clinical treatment of GAD and has a definite curative effect on the disease, but it has not received extensive international attention because of its unclear treatment mechanism (Xu et al., 2020). Through this study, we found that the deep-seated molecular mechanism of DZXYS promotes neuronal regeneration in the hippocampus to treat

GAD by downregulating the Notch signaling pathway, which not only opens up new ideas for the development of more effective anti-anxiety drugs in the future, but also lays a foundation for further exploration of the effective components in the prescription. In addition, imaging tools can be developed to detect the level of adult hippocampal neurogenesis in patients with GAD, so that the degree of increased adult hippocampal neurogenesis can become a new biomarker for the efficacy of anti-anxiety drugs.

### 4.1 Summary and Limitations of Current Study

This study shows that the excessive up regulation of Notch signaling pathway in the hippocampus of GAD rats leads to a large number of proliferation and differentiation of neural stem cells into astrocytes, and neuronal regeneration is impaired; DZXYS can play a positive role in neurogenesis by inhibiting the overexpression of Notch signal pathway in hippocampus, promoting neuronal regeneration in hippocampus and inhibiting the differentiation into astrocytes, and has a significant time effect.

There are still three deficiencies in the design of this subject. Firstly, the experimental model was prepared using the chronic mild stress paradigm. Therefore, at the end of 21 days, we should not only use OFT and EPM to detect the formation of anxiety behavior in rats, but also use sucrose preference test to eliminate the depression phenotype (Hyeonwi et al., 2019), so as to eliminate the interference of depression phenotype rats to the experiment, In the future experimental design, we will supplement the sucrose preference experiment; Secondly, we only mechanically observed that DZXYS can downregulate the Notch signaling pathway, promote the increase of neuron number, but ignored the important part of neuronal synaptic plasticity, which is an important part of nerve regeneration. In the next experimental study, we need to focus on whether DZXYS can regulate NMDA receptor to a certain extent after intervening in Notch signal pathway in anxiety rats, promote neuronal synaptic plasticity without inducing its excitotoxic effects (Corlew et al., 2008; Moreau and Kullmann, 2013; Deutschenbaur et al., 2016). At the same time, in the next experiment, we will co locate Notch1 with BrdU, Nestin and NeuN by immunofluorescence in various regions of hippocampus, observe the specific expression changes of Notch1, and find the specific regions with elevated Notch1 level. At last, the abnormal expression of a single Notch signaling pathway is not sufficient to reveal the pathogenesis of generalized anxiety disorder. The therapeutic effect of traditional Chinese medicine is also multi-target and multi-channel. We should seek other effective multi-signal transduction pathways and explore the cross connection and interaction between various pathways to further explore the pathogenesis of GAD and explore the deep treatment mechanism of traditional Chinese medicine.

## DATA AVAILABILITY STATEMENT

The original contributions presented in the study are included in the article/Supplementary Material, further inquiries can be directed to the corresponding authors.

## ETHICS STATEMENT

The animal study was reviewed and approved by the Ethics review committee of Shandong University of Traditional Chinese Medicine.

## AUTHOR CONTRIBUTIONS

ND designed the subject, CL completed the manuscript, ZY conducted data sorting and statistical analysis, XW reviewed the data, ZL guided the animal experiment, LZ, XL, WG, JS, XF, and KY finished the experiment and SW supervised the animal experiment and revised the manuscript. All authors read and approved the final manuscript.

## FUNDING

This work was supported by the National Natural Science Foundation of China (Nos. 81904108, 81974553), The Project of Shandong Traditional Chinese Medicine Science and Technology Development Plan (Nos. 2017-097, 2019-0240), the Natural Science Foundation of Shandong Province (Nos. ZR2020ZD17, ZR2019MH053), The Youth Scientific Research Innovation Team specializing in nerve regeneration mechanism based on SUI cognition of TCM and TCM neurological rehabilitation strategy, Shandong University of Traditional Chinese Medicine (University No. 54 (2020)), and The Chinese Medicine and Brain Science Youth Scientific Research Innovation Team, Shandong University of Traditional Chinese Medicine (No. 22202101).

## ACKNOWLEDGMENTS

Thank Servicebio Technology Co., Ltd. for its help in the immunofluorescence experiment in this experiment. Thank Ran Xue for his guidance in the production of this picture.

## REFERENCES

Aguilar-Arredondo, A., Arias, C., and Zepeda, A. (2015). Evaluating the Functional State of Adult-Born Neurons in the Adult Dentate Gyrus of the hippocampus: from Birth to Functional Integration. *Rev. Neurosci.* 26, 269–279. doi:10.1515/revneuro-2014-0071

Anacker, C., Luna, V. M., Stevens, G. S., Millette, A., Shores, R., Jimenez, J. C., et al. (2018). Hippocampal Neurogenesis Confers Stress Resilience by Inhibiting the Ventral Dentate Gyrus. *Nature* 559, 98–102. doi:10.1038/s41586-018-0262-4

Baba, H., Nakahira, K., Morita, N., Tanaka, F., Akita, H., and Ikenaka, K. (1997). GFAP Gene Expression during Development of Astrocyte. *Dev. Neurosci.* 19, 49–57. doi:10.1159/000111185

Bandelow, B. (2020). Current and Novel Psychopharmacological Drugs for Anxiety Disorders. *Adv. Exp. Med. Biol.* 1191, 347–365. doi:10.1007/978-981-32-9705-0_19

Bernal, A., and Arranz, L. (2018). Nestin-expressing Progenitor Cells: Function, Identity and Therapeutic Implications. *Cell Mol Life Sci* 75, 2177–2195. doi:10.1007/s00018-018-2794-z

Biedermann, S. V., Biedermann, D. G., Wenzlaff, F., Kurjak, T., Nouri, S., Auer, M. K., et al. (2017). An Elevated Plus-Maze in Mixed Reality for Studying Human Anxiety-Related Behavior. *BMC Biol.* 15, 125. doi:10.1186/s12915-017-0463-6

Breunig, J. J., Silbereis, J., Vaccarino, F. M., Sestan, N., and Rakic, P. (2007). Notch Regulates Cell Fate and Dendrite Morphology of Newborn Neurons in the Postnatal Dentate Gyrus. *Proc. Natl. Acad. Sci. U S A.* 104, 20558–20563. doi:10.1073/pnas.0710156104

Chiba, S., Numakawa, T., Ninomiya, M., Richards, M. C., Wakabayashi, C., and Kunugi, H. (2012). Chronic Restraint Stress Causes Anxiety- and Depression-like Behaviors, Downregulates Glucocorticoid Receptor Expression, and Attenuates Glutamate Release Induced by Brain-Derived Neurotrophic Factor in the Prefrontal Cortex. *Prog. Neuropsychopharmacol. Biol. Psychiatry* 39, 112–119. doi:10.1016/j.pnpbp.2012.05.018

Corlew, R., Brasier, D. J., Feldman, D. E., and Philpot, B. D. (2008). Presynaptic NMDA Receptors: Newly Appreciated Roles in Cortical Synaptic Function and Plasticity. *Neuroscientist* 14 (6), 609–625. doi:10.1177/1073858408322675

Deacon, R. M. J. (2013). The Successive Alleys Test of Anxiety in Mice and Rats. *Jove-Journal of Visualized Experiments* 76, e2705. doi:10.3791/2705

Demyttenaere, K., Bruffaerts, R., Posada-Villa, J., Gasquet, I., Kovess, V., Lepine, J. P., et al. (2004). Prevalence, Severity, and Unmet Need for Treatment of Mental Disorders in the World Health Organization World Mental Health Surveys. *Jama-Journal Am. Med. Assoc.* 291, 2581–2590. doi:10.1001/jama.291.21.2581

Derveaux, S., Vandesompele, J., and Hellemans, J. (2010). How to Do Successful Gene Expression Analysis Using Real-Time PCR. *Methods* 50, 227–230. doi:10.1016/j.ymeth.2009.11.001

Deutschenbaur, L., Beck, J., Kiyhankhadiv, A., Mühlhauser, M., Borgwardt, S., Walter, M., et al. (2016). Role of Calcium, Glutamate and NMDA in Major Depression and Therapeutic Application. *Prog. Neuropsychopharmacol. Biol. Psychiatry* 64, 325–333. doi:10.1016/j.pnpbp.2015.02.015

Dias, G. P., Bevilaqua, M. C. D., Da Luz, A., Fleming, R. L., De Carvalho, L. A., Cocks, G., et al. (2014). Hippocampal Biomarkers of Fear Memory in an Animal Model of Generalized Anxiety Disorder. *Behav. Brain Res.* 263, 34–45. doi:10.1016/j.bbr.2014.01.012

Donaldson, J. G. (2015). Immunofluorescence Staining. *Curr. Protoc. Cel Biol.* 69, 431–437. doi:10.1002/0471143030.cb0403s69

Dong, N. (2015). *Study on the Intervention Mechanism of Shugan Qingre Jianpi Method on the Repair and Regeneration of Papez Loop Nerve in Rats with Generalized Anxiety*. Doctor: Beijing University of traditional Chinese medicine.

Ehebauer, M., Hayward, P., and Martinez-Arias, A. (2006). Notch Signaling Pathway. *Sci. STKE* 2006. cm7doi:doi:10.1126/stke.3642006cm7

Ennaceur, A., Michalikova, S., and Chazot, P. L. (2009). Do rats Really Express Neophobia towards Novel Objects? Experimental Evidence from Exposure to novelty and to an Object Recognition Task in an Open Space and an Enclosed Space. *Behav. Brain Res.* 197, 417–434. doi:10.1016/j.bbr.2008.10.007

Feldman, A. T., and Delia, W. (2014). Tissue Processing and Hematoxylin and Eosin Staining. *Methods Mol. Biol. (Clifton, N.J.).* 1180, 31–43. doi:10.1007/978-1-4939-1050-2_3

Fenton, W. S. (1996). DSM-IV Training Guide; DSM-IV Guidebook; DSM-IV Handbook of Differential Diagnosis; Diagnostic and Statistical Manual of Mental Disorders, 4th ed.: Primary Care Version. *Am. J. Psychiatry* 153, 960–961. doi:10.1176/ajp.153.7.960-a

Garakani, A., Murrough, J. W., Freire, R. C., Thom, R. P., Larkin, K., Buono, F. D., et al. (2020). Pharmacotherapy of Anxiety Disorders: Current and Emerging Treatment Options. *Front. Psychiatry* 11, 595584. doi:10.3389/fpsyt.2020.595584

Gasnas, A. (2021). Effects of Low-Frequency Repetitive Transcranial Magnetic Stimulation on Motor Recovery in Early Stroke Patients. *Eur. J. Neurol.* 28, 534–535.

Givogri, M. I., De Planell, M., Galbiati, F., Superchi, D., Gritti, A., Vescovi, A., et al. (2006). Notch Signaling in Astrocytes and Neuroblasts of the Adult Subventricular Zone in Health and after Cortical Injury. *Dev. Neurosci.* 28, 81–91. doi:10.1159/000090755

Guo, Y. J., Zhang, Z. J., Wang, S. H., Sui, Y. X., and Sun, Y. (2009). Notch(1) Signaling, Hippocampal Neurogenesis and Behavioral Responses to Chronic Unpredicted Mild Stress in Adult Ischemic Rats. *Prog. Neuro-Psychopharmacology Biol. Psychiatry* 33, 688–694. doi:10.1016/j.pnpbp.2009.03.022

Gusel'nikova, V. V., and Korzhevskiy, D. E. (2015). NeuN as a Neuronal Nuclear Antigen and Neuron Differentiation Marker. *Acta Naturae* 7, 42–47. doi:10.1159/000111185

Hettema, J. M. (2008). The Nosologic Relationship between Generalized Anxiety Disorder and Major Depression. *Depress. Anxiety* 25, 300–316. doi:10.1002/da.20491

Hidalgo, R. B., and Sheehan, D. V. (2012). Generalized Anxiety Disorder. *Handb Clin. Neurol.* 106, 343–362. doi:10.1016/B978-0-444-52002-9.00019-X

Hill, A. S., Sahay, A., and Hen, R. (2015). Increasing Adult Hippocampal Neurogenesis Is Sufficient to Reduce Anxiety and Depression-like Behaviors. *Neuropsychopharmacology* 40, 2368–2378. doi:10.1038/npp.2015.85

Hyeonwi, S., Hwan, Y. J., Joon, K. H., and Kun, L. D. (2019). A Chronic Immobilization Stress Protocol for Inducing Depression-like Behavior in Mice. *J. visualized experiments : JoVE* 147. doi:10.3791/59546

Kai, K., Pengfei, X., Mengxia, W., Jian, C., Xu, S., Guiping, R., et al. (2020). FGF21 Attenuates Neurodegeneration through Modulating Neuroinflammation and Oxidant-Stress. *Biomed. Pharmacother.* 129, 110439. doi:10.1016/J.BIOPHA.2020.110439

Kessler, R. C., Dupont, R. L., Berglund, P., and Wittchen, H. U. (1999). Impairment in Pure and Comorbid Generalized Anxiety Disorder and Major Depression at 12 Months in Two National Surveys. *Am. J. Psychiatry* 156, 1915–1923. doi:10.1176/ajp.156.12.1915

Kessler, R. C. (2000). The Epidemiology of Pure and Comorbid Generalized Anxiety Disorder: a Review and Evaluation of Recent Research. *Acta Psychiatrica Scand.* 102, 7–13. doi:10.1111/j.0065-1591.2000.acp29-02.x

Kraeuter, A. K., Guest, P. C., and Sarnyai, Z. (2019). The Open Field Test for Measuring Locomotor Activity and Anxiety-like Behavior. *Methods Mol. Biol.* 1916, 99–103. doi:10.1007/978-1-4939-8994-2_9

Lee, S., Yang, M. Y., Kim, J., Kim, J., Son, Y., Kwon, S., et al. (2014). Nestin Expression and Glial Response in the hippocampus of Mice after Trimethyltin Treatment. *Acta Histochem.* 116, 1276–1288. doi:10.1016/j.acthis.2014.07.009

Lightbody, E. D., and Nicol, C. J. B. (2019). Immunofluorescence Labeling of Nuclear Receptor Expression in Formalin-Fixed, Paraffin-Embedded Tissue. *Methods Mol. Biol.* 1966, 101–105. doi:10.1007/978-1-4939-9195-2_8

Lin Wenjuan, W. W. S. F. (2003). New Animal Model of Emotional Stress: Behavioral, Neuroendocrine and Immunological Consequences. *Chin. Sci. Bull.* 15, 1565–1568. doi:10.1360/03wc0007

Louvi, A., and Artavanis-Tsakonas, S. (2006). Notch Signalling in Vertebrate Neural Development. *Nat. Rev. Neurosci.* 7, 93–102. doi:10.1038/nrn1847

Lutolf, S., Radtke, F., Aguet, M., Suter, U., and Taylor, V. (2002). Notch1 Is Required for Neuronal and Glial Differentiation in the Cerebellum. *Development* 129, 373–385.

Luyten, L., Vansteenwegen, D., Van Kuyck, K., Gabriels, L., and Nuttin, B. (2011). Contextual Conditioning in Rats as an Animal Model for Generalized Anxiety Disorder. *Cogn. Affective Behav. Neurosci.* 11, 228–244. doi:10.3758/s13415-011-0021-6

Ma, Q. Y., Li, X. J., Yan, Z. Y., Jiao, H. Y., Wang, T. Y., Hou, Y. J., et al. (2019). Xiaoyaosan Ameliorates Chronic Immobilization Stress-Induced Depression-like Behaviors and Anorexia in Rats: The Role of the Nesfatin-1-Oxytocin-Proopiomelanocortin Neural Pathway in the Hypothalamus. *Front. Psychiatry* 10, 13. doi:10.3389/fpsyt.2019.00910

Maron, E., and Nutt, D. (2017). Biological Markers of Generalized Anxiety Disorder. *Dialogues Clin. Neurosci.* 19, 147–157. doi:10.1176/appi.focus.16205

Masayoshi, M., Yusuke, M., Asami, M., Tomoyo, T., and Kazunori, M. (2014). Chronic Treatment with the 5-HT1A Receptor Partial Agonist Tandospirone

Increases Hippocampal Neurogenesis. *Neurol. Ther.* 3 (1), 67–77. doi:10.1007/s40120-013-0015-0

Menard, C., Hodes, G. E., and Russo, S. J. (2016). Pathogenesis of Depression: Insights from Human and Rodent Studies. *Neuroscience* 321, 138–162. doi:10.1016/j.neuroscience.2015.05.053

Mohamed, S., Anne-Laure, B., and Laurence, F. (2017). Tissue Sampling and Processing for Histopathology Evaluation. *Methods Mol. Biol.* 1641, 101–114. doi:10.1007/978-1-4939-7172-5_4

Mohan, K. H., Pai, S., Rao, R., Sripathi, H., and Prabhu, S. (2008). Techniques of Immunofluorescence and Their Significance. *Indian J. Dermatol. Venereol. Leprol.* 74, 415–419. doi:10.4103/0378-6323.42898

Moreau, A. W., and Kullmann, D. M. (2013). NMDA Receptor-dependent Function and Plasticity in Inhibitory Circuits. *Neuropharmacology* 74, 23–31. doi:10.1016/j.neuropharm.2013.03.004

Morita, A., Soga, K., Nakayama, H., Ishida, T., Kawanishi, S., and Sato, E. F. (2015). Neuronal Differentiation of Human iPS Cells Induced by Baicalin via Regulation of bHLH Gene Expression. *Biochem. Biophysical Res. Commun.* 465 (3), 458–463. doi:10.1016/j.bbrc.2015.08.039

Morris, A. (2019). Anxiety-induced Weight Loss. *Nat. Rev. Endocrinol.* 15, 130. doi:10.1038/s41574-019-0169-7

Nakagawa, S., and Cuthill, I. C. (2009). Effect Size, Confidence Interval and Statistical Significance: a Practical Guide for Biologists. *Biol. Rev.* 84, 515. doi:10.1038/s41574-019-0169-7

Niessen, K., and Karsan, A. (2007). Notch Signaling in the Developing Cardiovascular System. *Am. J. Physiology-Cell Physiol.* 293, C1–C11. doi:10.1152/ajpcell.00415.2006

Ohtsuka, T., Ishibashi, M., Gradwohl, G., Nakanishi, S., Guillemot, F., and Kageyama, R. (1999). Hes1 and Hes5 as Notch Effectors in Mammalian Neuronal Differentiation. *Embo J.* 18, 2196–2207. doi:10.1093/emboj/18.8.2196

Pekny, M., Pekna, M., Messing, A., Steinhauser, C., Lee, J. M., Parpura, V., et al. (2016). Astrocytes: a central Element in Neurological Diseases. *Acta Neuropathologica* 131, 323–345. doi:10.1007/s00401-015-1513-1

Pekny, M., Wilhelmsson, U., Bogestal, Y. R., and Pekna, M. (2007). The Role of Astrocytes and Complement System in Neural Plasticity. *Int. Rev. Neurobiol.* 82, 95–111. doi:10.1016/S0074-7742(07)82005-8

Pillai-Kastoori, L., Schutz-Geschwender, A. R., and Harford, J. A. (2020). A Systematic Approach to Quantitative Western Blot Analysis. *Anal. Biochem.* 2020, 593. doi:10.1016/j.ab.2020.113608

Qu, W., Liu, S., Zhang, W. J., Zhu, H. W., Tao, Q., Wang, H., et al. (2019). Impact of Traditional Chinese Medicine Treatment on Chronic Unpredictable Mild Stress-Induced Depression-like Behaviors: Intestinal Microbiota and Gut Microbiome Function. *Food Funct.* 10, 5886–5897. doi:10.1039/c9fo00399a

Ren, Z. L., and Zuo, P. P. (2012). Neural Regeneration: Role of Traditional Chinese Medicine in Neurological Diseases Treatment. *J. Pharmacol. Sci.* 120, 139–145. doi:10.1254/jphs.12R06CP

Rossi, D. J., Brady, J. D., and Mohr, C. (2007). Astrocyte Metabolism and Signaling during Brain Ischemia. *Nat. Neurosci.* 10, 1377–1386. doi:10.1038/nn2004

Saffarzadeh, F., Mousavi, S. M. M., Lotfinia, A. A., Alipour, F., Ravandi, H. H., and Karimzadeh, F. (2019). Discrepancies of Notch 1 Receptor during Development of Chronic Seizures. *J. Cell Physiol.* 234, 13773–13780. doi:10.1002/jcp.28056

Singh, S., and Joshi, N. (2017). Astrocytes: Inexplicable Cells in Neurodegeneration. *Int. J. Neurosci.* 127, 204–209. doi:10.3109/00207454.2016.1173692

Snyder, J. L., Kearns, C. A., and Appel, B. (2012). Fbxw7 Regulates Notch to Control Specification of Neural Precursors for Oligodendrocyte Fate. *Neural Dev.* 7, 15. doi:10.1186/1749-8104-7-15

Sofroniew, M. V., and Vinters, H. V. (2010). Astrocytes: Biology and Pathology. *Acta Neuropathologica* 119, 7–35. doi:10.1007/s00401-009-0619-8

Stein, D. J., Scott, K. M., De Jonge, P., and Kessler, R. C. (2017). Epidemiology of Anxiety Disorders: from Surveys to Nosology and Back. *Dialogues Clin. Neurosci.* 19, 127–135.

Stump, G., Durrer, A., Klein, A. L., Lutolf, S., Suter, U., and Taylor, V. (2002). Notch1 and its Ligands Delta-like and Jagged Are Expressed and Active in Distinct Cell Populations in the Postnatal Mouse Brain. *Mech. Dev.* 114, 153–159. doi:10.1016/s0925-4773(02)00043-6

Tanti, A., and Belzung, C. (2013). Hippocampal Neurogenesis: a Biomarker for Depression or Antidepressant Effects? Methodological Considerations and Perspectives for Future Research. *Cel Tissue Res.* 354, 203–219. doi:10.1007/s00441-013-1612-z

Taylor, D. P., Eison, M. S., Riblet, L. A., and Vandermaelen, C. P. (1985). Pharmacological and Clinical Effects of Buspirone. *Pharmacol. Biochem. Behav.* 23 (4), 687–694. doi:10.1016/0091-3057(85)90438-1

Toda, T., Parylak, S. L., Linker, S. B., and Gage, F. H. (2019). The Role of Adult Hippocampal Neurogenesis in Brain Health and Disease. *Mol. Psychiatry* 24, 67–87. doi:10.1038/s41380-018-0036-2

Tyrer, P., and Baldwin, D. (2006). Generalised Anxiety Disorder. *The Lancet* 368, 2156–2166. doi:10.1016/S0140-6736(06)69865-6

Vasile, F., Dossi, E., and Rouach, N. (2017). Human Astrocytes: Structure and Functions in the Healthy Brain. *Brain Struct. Funct.* 222, 2017–2029. doi:10.1007/s00429-017-1383-5

Wittchen, H. U., Carter, R. M., Pfister, H., Montgomery, S. A., and Kessler, R. C. (2000). Disabilities and Quality of Life in Pure and Comorbid Generalized Anxiety Disorder and Major Depression in a National Survey. *Int. Clin. Psychopharmacol.* 15, 319–328. doi:10.1097/00004850-200015060-00002

Xu, M. B., Liu, Y. F., Guo, Y., Liu, C. Y., Liu, Y. Y., Yan, Z. Y., et al. (2020). Study on Urinary Metabolomics of Premenstrual Dysphoric Disorder Patients with Liver-Qi Depression Syndrome Treated with Xiaoyaosan Study Protocol Clinical Trial(SPIRIT Compliant). *Medicine* 99 (16). doi:10.1097/md.0000000000019425

Zhang, W., Yu, W. J., Liu, X. F., Wang, Q., Bai, X., Cui, X., et al. (2020). Effect of Jian-Pi-Zhi-Dong Decoction on the Amino Acid Neurotransmitters in a Rat Model of Tourette Syndrome and Comorbid Anxiety Disorder. *Front. Psychiatry* 11, 515. doi:10.3389/fpsyt.2020.00515

Zhang, Y., Xiang, Z., Jia, Y., He, X., Wang, L., and Cui, W. (2019). The Notch Signaling Pathway Inhibitor Dapt Alleviates Autism-like Behavior, Autophagy and Dendritic Spine Density Abnormalities in a Valproic Acid-Induced Animal Model of Autism. *Prog. Neuropsychopharmacol. Biol. Psychiatry* 94, 109644. doi:10.1016/j.pnpbp.2019.109644

Zhao, H. B., Jiang, Y. M., Li, X. J., Liu, Y. Y., Bai, X. H., Li, N., et al. (2017). Xiao Yao San Improves the Anxiety-like Behaviors of Rats Induced by Chronic Immobilization Stress: The Involvement of the JNK Signaling Pathway in the Hippocampus. *Biol. Pharm. Bull.* 40, 187–194. doi:10.1248/bpb.b16-00694

Zhao, Y., Lai, W., Xu, Y., Li, L., Chen, Z., and Wu, W. (2013). Exogenous and Endogenous Therapeutic Effects of Combination Sodium Ferulate and Bone Marrow Stromal Cells (BMSCs) Treatment Enhance Neurogenesis after Rat Focal Cerebral Ischemia. *Metab. Brain Dis.* 28 (4), 655–666. doi:10.1007/s11011-013-9425-z

Zupanc, G. K. H., Monaghan, J. R., and Stocum, D. L. (2019). Adult Neural Stem Cells in Development, Regeneration, and Aging. *Dev. Neurobiol.* 79, 391–395. doi:10.1002/dneu.22702

**Conflict of Interest:** The authors declare that the research was conducted in the absence of any commercial or financial relationships that could be construed as a potential conflict of interest.

frontiers in Pharmacology

ORIGINAL RESEARCH
published: 15 December 2021
doi: 10.3389/fphar.2021.791059

# Yi-Zhi-Fang-Dai Formula Exerts Neuroprotective Effects Against Pyroptosis and Blood–Brain Barrier–Glymphatic Dysfunctions to Prevent Amyloid-Beta Acute Accumulation After Cerebral Ischemia and Reperfusion in Rats

*Zhongkuan Lyu[1†], Qiyue Li[1†], Zhonghai Yu[2†], Yuanjin Chan[1], Lei Fu[3], Yaming Li[1*] and Chunyan Zhang[4*]*

[1]Geriatrics Department of Chinese Medicine, Huadong Hospital Affiliated to Fudan University, Shanghai, China, [2]Department of Traditional Chinese Medicine, Shanghai Jiao Tong University Affiliated Sixth People's Hospital, Shanghai, China, [3]Shanghai Key Laboratory of Clinical Geriatric Medicine, Huadong Hospital Affiliated to Fudan University, Shanghai, China, [4]International Medical Center of Traditional Chinese Medicine, Haikou Hospital of Traditional Chinese Medicine, Haikou, China

OPEN ACCESS

**Edited by:**
Fang Pan,
Shandong University, China

**Reviewed by:**
Brad A. Sutherland,
University of Tasmania, Australia
Lumei Liu,
North Carolina Agricultural and Technical State University, United States

***Correspondence:**
Yaming Li
doctorymli@163.com
Chunyan Zhang
cyzhang0810@163.com

[†]These authors have contributed equally to this work and share first authorship

**Specialty section:**
This article was submitted to Ethnopharmacology, a section of the journal Frontiers in Pharmacology

**Received:** 07 October 2021
**Accepted:** 29 November 2021
**Published:** 15 December 2021

**Citation:**
Lyu Z, Li Q, Yu Z, Chan Y, Fu L, Li Y and Zhang C (2021) Yi-Zhi-Fang-Dai Formula Exerts Neuroprotective Effects Against Pyroptosis and Blood–Brain Barrier–Glymphatic Dysfunctions to Prevent Amyloid-Beta Acute Accumulation After Cerebral Ischemia and Reperfusion in Rats. Front. Pharmacol. 12:791059. doi: 10.3389/fphar.2021.791059

**Background:** The dysfunctional blood–brain barrier (BBB)–glymphatic system is responsible for triggering intracerebral amyloid-beta peptide (Aβ) accumulation and acts as the key link between ischemic stroke and dementia dominated by Alzheimer's disease (AD). Recently, pyroptosis in cerebral ischemia and reperfusion (I/R) injury is demonstrated as a considerable mechanism causing BBB–glymphatic dysfunctions and Aβ acute accumulation in the brain. Targeting glial pyroptosis to protect BBB–glymphatic functions after cerebral I/R could offer a new viewpoint to prevent Aβ accumulation and poststroke dementia. Yi-Zhi-Fang-Dai formula (YZFDF) is an herbal prescription used to cure dementia with multiple effects of regulating inflammatory responses and protecting the BBB against toxic Aβ-induced damage. Hence, YZFDF potentially possesses neuroprotective effects against cerebral I/R injury and the early pathology of poststroke dementia, which evokes our current study.

**Objectives:** The present study was designed to confirm the potential efficacy of YZFDF against cerebral I/R injury and explore the possible mechanism associated with alleviating Aβ acute accumulation.

**Methods:** The models of cerebral I/R injury in rats were built by the method of middle cerebral artery occlusion/reperfusion (MCAO/R). First, neurological function assessment and cerebral infarct measurement were used for confirming the efficacy of YZFDF on cerebral I/R injury, and the optimal dosage (YZFDF-H) was selected to conduct the experiments, which included Western blotting detections of pyroptosis, $A\beta_{1\text{-}42}$ oligomers, and NeuN, immunofluorescence observations of glial pyroptosis, aquaporin-4 (AQP-4), and Aβ locations, brain water content measurement, SMI 71 (a specific marker for BBB)/

AQP-4 immunohistochemistry, and Nissl staining to further evaluate BBB–glymphatic functions and neuronal damage.

**Results:** YZFDF obviously alleviated neurological deficits and cerebral infarct after cerebral I/R in rats. Furthermore, YZFDF could inactivate pyroptosis signaling via inhibiting caspase-1/11 activation and gasdermin D cleavage, ameliorate glial pyroptosis and neuroinflammation, protect against BBB collapse and AQP-4 depolarization, prevent Aβ acute accumulation and $A\beta_{1\text{-}42}$ oligomers formation, and reduce neuronal damage and increase neurons survival after reperfusion.

**Conclusion:** Our study indicated that YZFDF could exert neuroprotective effects on cerebral I/R injury and prevent Aβ acute accumulation in the brain after cerebral I/R associated with inhibiting neuroinflammation-related pyroptosis and BBB–glymphatic dysfunctions.

**Keywords: Yi-Zhi-Fang-Dai formula, cerebral ischemia and reperfusion injury, dementia, neuroinflammation, pyroptosis, blood–brain barrier–glymphatic system, aquaporin-4, amyloid-beta peptide**

## INTRODUCTION

Alzheimer's disease (AD), a common neurodegenerative disease, comprises the major type of dementia and is causing a high socioeconomic impact with the advancement of world population aging (Alzheimer's Association, 2021). It is known that amyloid-beta peptide (Aβ) accumulation acts as a core factor among the multifaceted etiology of AD, which is closely associated with the cerebrovascular dysfunctions, especially brain microcirculation disturbance (Bell and Zlokovic, 2009; Yamazaki and Kanekiyo, 2017; Jack et al., 2018; Hampel et al., 2021; Kim et al., 2021). Experimental and clinical research is emerging to indicate that cerebral ischemia and reperfusion (I/R) can trigger both acute and chronic accumulation of Aβ in the brain which exacerbates cerebral I/R injury and accounts for the occurrence of dementia induced by ischemic stroke (van Groen et al., 2005; Song et al., 2013; Liu et al., 2015; Martins et al., 2019). Thus, maintaining the clearance of Aβ after cerebral I/R could offer a new therapeutic approach to prevent poststroke cognitive impairment and development into dementia (Goulay et al., 2020).

The normal blood–brain barrier (BBB) is an essential condition for keeping the balance of intracerebral and extracerebral Aβ, and accordingly BBB breakdown has been demonstrated as an early biomarker prior to appearance of cognitive impairment (Nation et al., 2019; Hussain et al., 2021). In addition to the BBB, the glymphatic system is another considerable pathway for the clearance of Aβ in the brain (Tarasoff-Conway et al., 2015). Endfeet of astrocytes are the main components of both the BBB and glymphatic system which contribute to maintain the homeostasis of brain microenvironments, and aquaporin-4 (AQP-4) on astrocytic endfeet is a water channel protein with high polarization and essential for neurovascular coupling and glymphatic flow to facilitate the clearance of metabolites such as Aβ (Nakada et al., 2017). Thus, in cerebral I/R injury, the loss of AQP-4 polarization on astrocytic endfeet is considered as an important factor of BBB–glymphatic dysfunctions that are the vital pathological change causing the onset and development of dementia (Verheggen et al., 2018; Goulay et al., 2020).

Inflammation is inherent across the whole course of both ischemia and reperfusion stages, and accordingly neuroinflammation acts as the fundamental cause and meanwhile as the consequence of cerebral I/R injury (Liu et al., 2014; Du et al., 2021). Recently, pyroptosis, a pro-inflammatory cell death, has been demonstrated as a crucial pathological link and gasdermin D (GSDMD) as its key effector in cerebral I/R injury (Zhang et al., 2019). Canonical pyroptosis was deemed to rely on the activation of inflammasomes represented by nucleotide-binding oligomerization domain-like receptors pyrin domain-containing 3 (NLRP3)/apoptosis-associated speck-like protein containing a caspase activation and recruitment domain (ASC)/caspase-1 to cleave GSDMD, causing the secretion of pro-inflammatory mediators such as cleaved interleukin-1β (IL-1β) (Shi J. et al., 2015). However, in the noncanonical pyroptosis pathway, GSDMD is the direct substrate of caspase-11 (orthologous caspase-4/5 in humans), and the N-terminal fragment (GSDMD-N) from the cleavage of full length GSDMD (GSDMD-FL) is critical for the formation of membrane nanopores leading to cell death. Meanwhile, as the upstream signaling, GSDMD-N activates the NLRP3/ASC/caspase-1 pathway and then results in the maturation and secretion of cleaved IL-1β (Kayagaki et al., 2015; Yi, 2018; Matikainen et al., 2020). Our recent study (Lyu et al., 2021) indicated that caspase-11-mediated pyroptosis after cerebral I/R focuses on glial cells (microglia and astrocytes) and is a considerable factor aggravating BBB–glymphatic dysfunctions and Aβ accumulation.

As one hallmark of cerebral I/R injury, BBB breakdown in the ischemic period is exacerbated by reperfusion and followed by a no-reflow phenomenon of capillaries (Mohamed Mokhtarudin and Payne, 2015; Burrows et al., 2016; Huang et al., 2020). In addition to intracerebral Aβ retention caused by microcirculation disturbance, activated platelets contained in microthrombosis during the ischemic period and after I/R are demonstrated as the potential

**TABLE 1 |** Components of Yi-Zhi-Fang-Dai formula.

| Latin name | English name | Chinese name | Part used | Ratio (%) |
|---|---|---|---|---|
| *Ginkgo biloba* | Ginkgo biloba leaves | Yinxingye | Dry leaves | 30 |
| *Panax ginseng* C. A. Meyer | Ginseng | Renshen | Root and rhizome | 30 |
| *Cistanche deserticola* Ma | Cistanches Herba | Roucongrong | Succulent stem | 30 |
| *Acorus tatarinowii* | Grassleaf sweetflag rhizome | Shichangpu | Rhizome | 10 |

peripheral source of acute Aβ accumulation in blood vessels including capillaries and nearby brain tissues (Martins et al., 2019; Carbone et al., 2021). Aβ accumulation in the brain can raise the formation of a toxic Aβ-like $Aβ_{1-42}$ oligomer, cause swelling in astrocytic endfeet, and also lead to dysregulation of capillaries by acting on pericytes, impairing energy supply for neurons (Merlini et al., 2011; Cavallucci et al., 2012; Nortley et al., 2019). Therefore, early protection of microcirculation and elimination of thromboinflammation in microcirculation after cerebral I/R are both crucial therapeutic strategies for the clearance of metabolites such as Aβ and the prevention of poststroke dementia.

According to traditional Chinese medicine (TCM) theories, blood stasis in brain collaterals with stagnancy of collateral-Qi in a deficiency condition is regarded as the basic pathogenesis of cerebral I/R injury (Wang B. et al., 2021), thus invigorating Qi and dredging brain collaterals are basic TCM therapeutic principles which consist of current therapeutic strategies emphasizing on microcirculation protection and removal of obstructions. Herbs have been widely used for thousands of years and are suitable for treating complex diseases such as ischemic stroke and dementia with the multicomponent and multitarget advantages (Yu et al., 2020; Singh et al., 2021). Yi-Zhi-Fang-Dai formula (YZFDF) is an experiential herbal prescription (Chan et al., 2020) commonly used to cure dementia cases by multiple efficacies of invigorating Qi, dredging brain collaterals, and promoting neurological function recovery. YZFDF is purely composed of herbal medicines with various bioactive ingredients, such as bilobalide, ginkgolide A, ginsenoside Rg1, cistanoside A, and α-asarone (Liu et al., 2016a). Our previous work showed that YZFDF and EGb761, the extracts from its main herb (*Ginkgo biloba* leaves), can inhibit microglial activation, regulate inflammatory responses, and protect the BBB against toxic Aβ-induced damage *in vitro* and *in vivo* (Wan WB. et al., 2014; Wan et al., 2016; Chan et al., 2020). Therefore, based on our previous studies, the present study was designed to confirm the potential therapeutic effects of YZFDF against cerebral I/R injury and further preliminarily explore the possible mechanism associated with alleviating Aβ acute accumulation by anti-neuroinflammation–related pyroptosis and BBB–glymphatic dysfunctions.

# MATERIALS AND METHODS

## Components and Drug Powder Preparation of YZFDF

YZFDF comprises four herbs as shown in **Table 1**, including *Ginkgo Biloba* leaves, Ginseng, Cistanches Herba, and grassleaf sweetflag rhizome, which were purchased from Shanghai Hongqiao Pharmaceutical Co., Ltd. (Shanghai, China). These herbal medicines were identified by the TCM Preparation Room of Shanghai Geriatric Institute of Chinese Medicine, Shanghai University of Traditional Chinese Medicine. The main active ingredient analysis of YZFDF by the methods of high-performance liquid chromatography (HPLC) and mass spectrometry (MS), as well as the chemical structures of each ingredient were introduced in detail in our previous work (Liu et al., 2016a). The YZFDF drug powder was prepared as previously described (Liu et al., 2016a; Chan et al., 2020). In brief, four herbal medicines were subjected twice to extraction with 75% ethanol for 2 h. The herbal dregs of the extract solution were removed after filtering. Subsequently, the filtered liquid was concentrated using a rotary evaporator (BÜCHI Labortechnik AG, Flawil, Switzerland) and then dried to get a drug powder by the freeze-drying method. The YZFDF power was kept in an airtight container in the deep freezer (−36°C) for long-term storage, and the powder was made into a suspension liquid nearing usage and then stored at 4°C.

## Animals

All animal experiments in this study were approved by the Ethics Committee of Shanghai Jiao Tong University Affiliated Sixth People's Hospital and performed in accordance with the relevant guidelines and regulations. Efforts were made as well to minimize animal suffering during the whole experiments. Specific pathogen-free (SPF) male Sprague–Dawley (SD) rats, weighing 200–230 g, were purchased from the Shanghai Laboratory Animal Research Center (Shanghai, China). The rats were housed in a SPF barrier environment under standard conditions at a controlled temperature (23 ± 1°C) on a 12:12 h light–dark cycle. Experimental operations were carried out after the acclimation of animals for several days with free access to food and water.

## Drug Administration and Experimental Design

The common human daily dosage of raw YZFDF herbs is 100 g/75 kg bodyweight. According to the formula (Lan et al., 2013) $d_{rat} = d_{human} \times 0.7/0.11$, the common dosage of raw YZFDF herbs in rats should be 8.48 g/kg/day, and the corresponding drug powder dosage is 2.69 g/kg/day. The drug tolerance of a rat is generally higher than that of the human, and thus we selected 2.8, 5.6, and 11.2 g/kg/day as the low, medium, and high drug powder dosages of YZFDF in the present study, respectively. Accordingly, at the first stage of this study, forty rats were randomly divided into five groups: sham group (Sham), ischemia and reperfusion group (I/

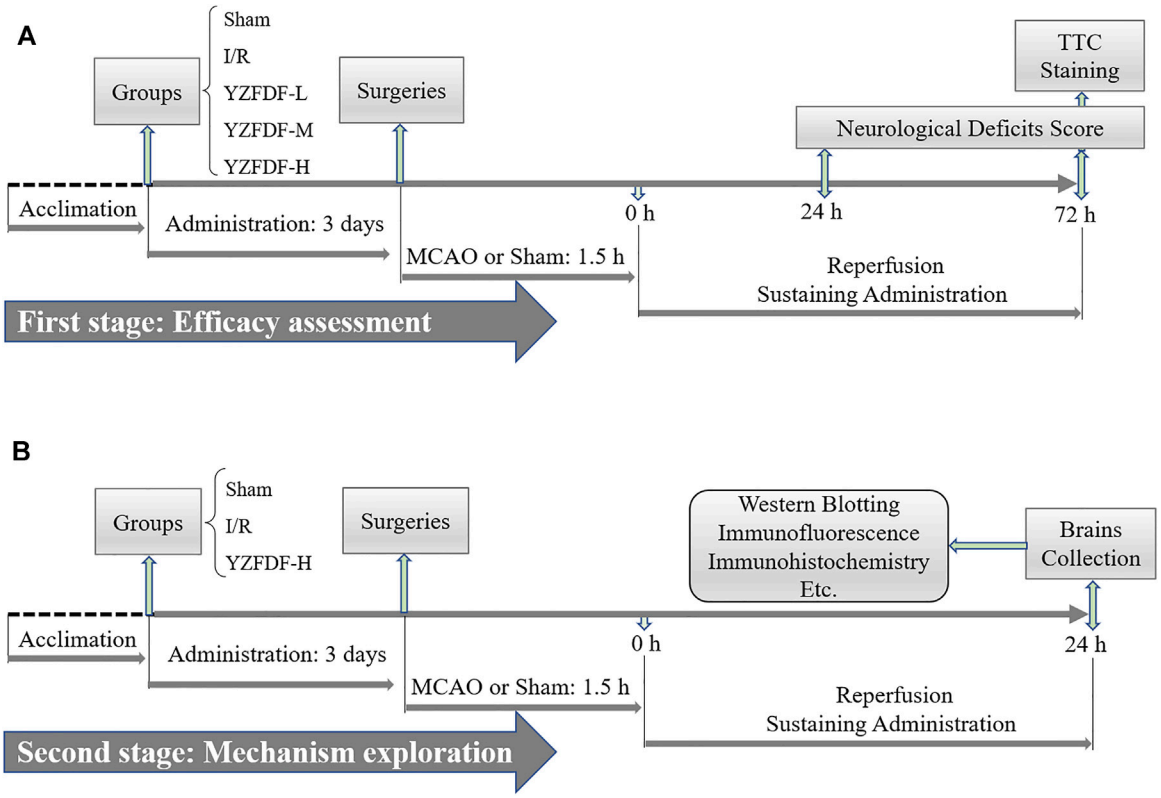


**FIGURE 1 |** Schematic diagram of this study. **(A)** First stage aiming at the efficacy assessment of YZFDF against I/R injury. **(B)** Second stage of this study for further preliminarily exploring the possible mechanism.

R), YZFDF low-dosage group (YZFDF-L), YZFDF medium-dosage group (YZFDF-M), and YZFDF high-dosage group (YZFDF-H). The rats in the YZFDF-treated groups were orally administered with the corresponding drug powder dosage of YZFDF (dissolved in distilled water), and the other rats were given the same volume of distilled water. Drug administration was performed twice a day at 9:00 and 16:00 for 3 days before the surgery and lasted 3 days after the surgery until animal sacrifice. According to the results of neurological function assessment and measurement of cerebral infarct area, the optimal dosage of YZFDF (YZFDF-H) was selected to conduct the following experiments.

At the second stage of this study, forty-five rats were randomly divided into three groups: sham group (Sham), ischemia and reperfusion group (I/R), and YZFDF high-dosage group (YZFDF-H). Drug administration was performed as previously mentioned for 3 days before the surgery and lasted until animal sacrifice for 24 h after reperfusion. The schematic diagram of this study is exhibited in **Figure 1**.

## Focal Cerebral I/R Injury Models

The models of focal cerebral I/R injury were built by the method of left middle cerebral artery occlusion/reperfusion (MCAO/R) as described in our previous studies (Yu et al., 2016; Yu et al., 2018). In brief, rats were anesthetized with pentobarbital sodium (0.5%, 1 ml/100 g). After the skin disinfection and incision, the left common carotid artery (CCA) was identified and exposed by separation from surrounding tissues. Subsequently, the external carotid artery (ECA) and internal carotid artery (ICA) were dissected and exposed carefully. At first, the ICA was occluded using a microvascular clip and the far end of the ECA was fastened, followed by the ECA being cut at 1 cm away from the bifurcation between the ECA and ICA. Then, a nylon monofilament (Beijing Sunbio Biotech, China) was inserted into the ICA from the incision of the ECA with the microvascular clip removed. At last, resistance could be felt when the rounded tip of the monofilament reached the origin of the middle cerebral artery (MCA) at the length of 18.5–19.5 mm from the bifurcation, and then the monofilament was fastened at ECA stump. After MCAO of 1.5 h, the monofilament was withdrawn to implement reperfusion. In the present study, the rats in I/R and YZFDF-treated groups were subjected to blinded MCAO/R surgeries, while rats in the Sham group only underwent the same operation with no insertion of the monofilament. During the whole course, the cardiovascular rate and rectal temperature of all rats were monitored and maintained.

## Neurological Function Assessment

Neurological examinations were performed after reperfusion. In order to exclude the interference of surgery failures, the rats subjected to MCAO/R with no detectable neurological deficits

were eliminated. The neurological deficit scores of rats at 24 and 72 h after reperfusion in the present study were evaluated on a 5-point scale as previously described (Longa et al., 1989; Cai et al., 2016): 0 = no deficit; 1 = failure to extend right forepaw; 2 = circling to the right; 3 = falling to the right; 4 = no spontaneous walking with a depressed level of consciousness.

## Measurement of the Cerebral Infarct Area

The measurement of the cerebral infarct area by 2, 3, 5-triphenyl tetrazolium chloride (TTC; Nanjing Jiancheng Bioengineering Institute, Nanjing, Jiangsu, China) staining was carried out as previously described (Yu et al., 2016). In brief, at 72 h after reperfusion, the rats under deep anesthesia went through cardiac perfusion with 200 ml normal saline. Subsequently, their brains were taken out quickly and placed at −20°C for 20 min. Then, each brain was sliced into five coronal slices (2 mm thickness) from the rostral to the caudal on the frozen ice pack, and then the slices were stained with TTC solution away from light for 20 min at 37°C. As a result, the infarct brain tissue was stained to the white-colored area distinguished from the red-colored non-infarct area. After the fixation of stained brain slices with 4% paraformaldehyde for 24 h, the percentages of the cerebral infarct area were calculated by microscope image analysis software (Image-Pro Plus, United States) according to the following formula (Yu et al., 2016): [contralateral hemisphere area-(ipsilateral hemisphere area-infarct area)/2×contralateral hemisphere area] × 100%.

## Brain Water Content Measurement

The dry–wet weight method was used to measure the brain water content. In Brief, the rats were sacrificed under deep anesthesia, and their brains were quickly taken out. Then, ischemic and nonischemic cerebral hemispheres were separated, immediately weighed to obtain the wet weight (WW), and then placed in an oven at 60°C for 24 h to obtain the dry weight (DW). The brain water content was calculated with the following formula (Lan et al., 2013): 100% × (WW−DW)/WW.

## Western Blotting Analysis

After 24 h reperfusion, the rats were deeply anesthetized and went through cardiac perfusion. The brains were taken out, and the ischemic core and normal brain tissue were obviously visible to the naked eye. Then, the transition zone neighboring the ischemic core (ischemic penumbra) and the equivalent area under sham were quickly peeled off and stored at −80°C. Western blotting (WB) analysis was used to detect the expression levels of neuroinflammation-related pyroptosis signaling molecules, $A\beta_{1\text{-}42}$ monomer/oligomers, and NeuN (a marker of neurons). In brief, the brain tissues from ischemic penumbra and the equivalent area under sham were prepared for protein samples followed by the concentration measurement. Subsequently, corresponding protein samples with equal amounts were separated by 10% sodium dodecyl sulfate-polyacrylamide gel electrophoresis and then electrotransferred onto the poly-vinylidnene fluoride membranes. Then, the membranes were blocked by 5% bovine serum albumin (BSA) at room temperature for 1 h and incubated at 4°C overnight with the following primary antibodies (**Supplementary Table S1** for details): caspase-11 (Santa Cruz, United States), GSDMD (CST, United States), NLRP3 (ProteinTech, United States), ASC (Santa Cruz), caspase-1 (ProteinTech), IL-6 (Santa Cruz), IL-1β (Santa Cruz), ionized calcium-binding adapter molecule-1 (Iba-1) (Abcam, United Kingdom), $A\beta_{1\text{-}42}$ (Abcam), NeuN (ProteinTech), and β-actin (CST). Then, the membranes were washed and incubated with the corresponding secondary antibodies (Signalway Antibody, United States) for 1 h at room temperature. Finally, the enhanced chemiluminescence kit (Millipore, United States) was used to develop WB bands, and the intensities of bands were analyzed with ImageJ software (National Institutes of Health, United States).

## Immunofluorescence

After deep anesthetization, the rats went through cardiac perfusion with 200 ml normal saline and then 4% paraformaldehyde. Subsequently, the brains were taken out and immersed in 4% paraformaldehyde for 24 h fixation and then prepared for paraffin slices. The procedure for immunofluorescence (IF) staining of proteins colocalization was as follows: after dewaxing and rehydration with gradient ethanol (100% ethanol for 5 min, 95% ethanol for 5 min, 80% ethanol for 5 min, 60% ethanol for 5 min, and $H_2O$ for 5 min), the slices further went through antigen retrieval and permeation by 0.3% triton-X 100 followed by blockage with 5% BSA. Subsequently, the slices were incubated with the first antibodies (**Supplementary Table S1** for details) mixed with GSDMD/Iba-1, GSDMD/glial fibrillary acidic protein (GFAP), AQP-4/GFAP, and Aβ/GFAP overnight at 4°C followed by incubations with corresponding mixed secondary antibodies (Beyotime, China) for 1 h at room temperature. After DAPI staining, the laser scanning confocal microscope (Leica Wetzlar, Germany) was used for capturing fluorescent pictures in the same brain area with blinding. Three fields were randomly selected for the analysis of double-positive staining cell number or fluorescent density by ImageJ software.

## Immunohistochemistry

An endothelial barrier antigen (EBA, clone: SMI 71) is a specific marker for the BBB, and AQP-4 polarization loss is an important cause of BBB–glymphatic dysfunctions responsible for Aβ accumulation. Thus, we further made evaluations of BBB–glymphatic functions by immunohistochemistry (IHC) staining of SMI 71 and AQP-4. In brief, after dewaxing and rehydration, the slices were subjected in sequence to antigen retrieval, permeation, inactivation of the endogenous catalase, and then blockage by 5% BSA. Subsequently, the slices were incubated with the anti-rat BBB antibody (SMI 71) (BioLegend, United States) and AQP-4 antibody (Santa Cruz) overnight at 4°C (**Supplementary Table S1** for details), followed by incubations with the corresponding secondary antibodies for 1 h at room temperature. Then, 3,3-diaminobenzidine tetrahydrochloride and hematoxylin were used for visualizing the slices. Finally, the light microscope was used for observing the slices and capturing the pictures in the same brain area with blinding. Three fields were randomly selected for the analysis of SMI 71 and AQP-4 staining density by ImageJ software.

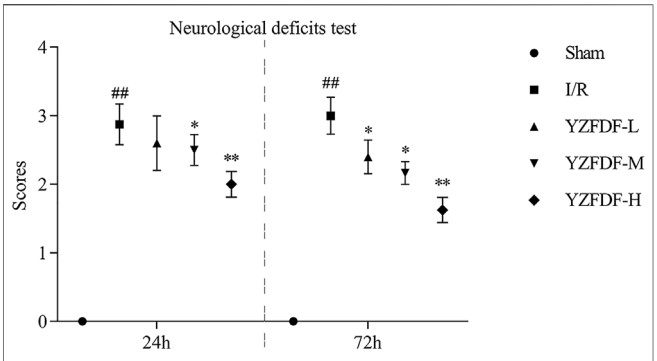


**FIGURE 2 |** YZFDF alleviated neurological deficits at 24 and 72 h after cerebral I/R in rats, $n = 5–8$. $^{\#\#}p < 0.01$ vs. Sham group; $^{*}p < 0.05$, $^{**}p < 0.01$ vs. I/R group.

## Nissl Staining

Nissl staining was used to evaluate neuronal damage as described in our previous study (Yu et al., 2016). In brief, after dewaxing and rehydration, the slices were stained with Nissl staining solution (Sangon Biotech, China) for 20 min at room temperature. Subsequently, the slices were rinsed in graded ethanol, transparentized by xylene, and coverslipped under Permount. Finally, the pictures in the same brain area were captured with blinding using the light microscope. Four fields were randomly selected for the analysis of damaged neurons.

## Statistical Analysis

All data were expressed as the mean ± standard deviation (SD) or standard error of the means (SEM). GraphPad Prism 8.0 (GraphPad Software Inc. United States) was used for statistical analysis. The differences among groups were analyzed by one-way ANOVA or unpaired Student's t-test. A value of $p < 0.05$ was considered to be statistically significant.

# RESULTS

## Yi-Zhi-Fang-Dai Formula Alleviated Neurological Deficits After Cerebral I/R in Rats

First, the effects of YZFDF on neurological deficits were assessed at 24 and 72 h after reperfusion in the present study. As exhibited in **Figure 2**, the rats in the Sham group had no performance of neurological deficits, and the rats in the I/R group showed obvious neurological deficits at both 24 and 72 h after reperfusion. However, compared with that of the I/R group, YZFDF-treated groups showed significantly low neurological deficit scores at 24 h (YZFDF-M group, $p < 0.05$; YZFDF-H group, $p < 0.01$) and 72 h (YZFDF-L and YZFDF-M groups, $p < 0.05$; YZFDF-H group, $p < 0.01$) after reperfusion. Thus, the result of neurological deficit assessment indicated that YZFDF could alleviate neurological deficits after cerebral I/R in a dosage- and time-dependent manner.

## Yi-Zhi-Fang-Dai Formula Reduced Cerebral Infarct After Cerebral I/R in Rats

The effects of YZFDF on cerebral infarct were measured following neurological deficit assessment at 72 h after reperfusion. The result (**Figures 3A,B**) showed that the rats in the Sham group had no cerebral infarct, and the rats in the I/R group exhibited obvious cerebral infarct (white-colored area). However, compared with that of the I/R group, YZFDF-treated groups showed significantly little cerebral infarct area with the YZFDF-H group exerting optimal effects (YZFDF-L and YZFDF-M groups, $p < 0.05$; YZFDF-H group, $p < 0.01$), which was consistent with the result of neurological deficit assessment.

Based on the outcomes at the first stage of this study and our previous work, the following experiments selected the optimal dosage of YZFDF (YZFDF-H) to further explore the potential effects of YZFDF against the fundamental and crucial links in cerebral I/R injury represented by neuroinflammation-related pyroptosis, BBB–glymphatic dysfunctions, and Aβ acute accumulation and thus to preliminarily probe into its neuroprotective mechanism for preventing early pathological changes of poststroke dementia.

## Yi-Zhi-Fang-Dai Formula Alleviated Cerebral I/R–Induced Pyroptosis *via* Inhibiting the Activation of Caspase-11/1 and Cleavage of GSDMD

Our previous study revealed that cerebral I/R activates the caspase-11/GSDMD-mediated pyroptosis pathway. In the present study, the result showed that YZFDF could obviously downregulate the increased protein levels of GSDMD-FL/N (the key effector of pyroptosis) and the related upstream or downstream signaling including pro/cleaved-caspase-11, NLRP3, ASC, and pro/cleaved-caspase-1 after cerebral I/R (**Figures 4A–D**), indicating that YZFDF could exert inhibitory effects on cerebral I/R–induced pyroptosis.

## Yi-Zhi-Fang-Dai Formula Blocked Overactivation and Pyroptosis of Microglia and Alleviated Inflammatory Responses After Reperfusion

The inflammatory microenvironment mediated by microglial activation is inherent across the whole course of cerebral I/R injury and deteriorated by pyroptosis after reperfusion, which can be reflected by the expressions of Iba-1 (microglial biomarker), IL-6, and pyroptosis-related pro-inflammatory factors such as IL-1β. The result in the present study showed that YZFDF treatment could reduce the raised immunofluorescent co-staining of GSDMD and Iba-1 in ischemic cortex and hippocampus-CA1 areas (**Figures 5A,B**) and downregulate the expression levels of Iba-1, IL-6, and cleaved IL-1β after reperfusion (**Figures 5C,D**), indicating that YZFDF could exert inhibitory effects on inflammatory responses during cerebral I/R by regulating microglial overactivation and pyroptosis.

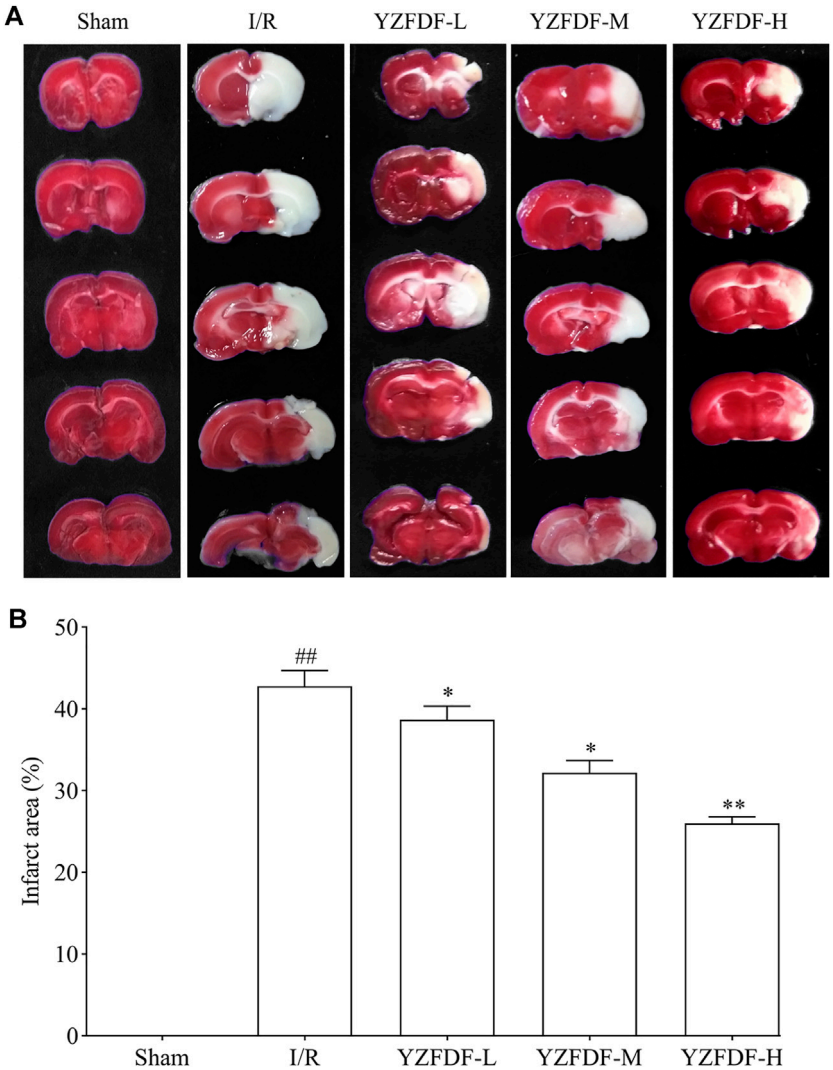


**FIGURE 3 |** YZFDF reduced cerebral infarct at 72 h after cerebral I/R in rats. **(A)** Representative pictures of cerebral infarct by TTC staining in each group. The red-colored area represents normal cerebral tissue with non-infarct, and the white-colored area represents cerebral infarct. **(B)** Comparative analysis of the cerebral infarct area between groups, $n$ = 5–8. *$p$ < 0.05, **$p$ < 0.01 vs. I/R group.

## Yi-Zhi-Fang-Dai Formula Inhibited Astrocytic Pyroptosis and Protected Against BBB Collapse After Reperfusion

Astrocytic endfeet envelop the cerebral capillaries that form the BBB. Our previous study indicated that astrocytic pyroptosis after I/R is the considerable pathological factor of BBB disruption and shriveled capillaries leading to brain microcirculation disturbance. The result in the present study showed that YZFDF treatment could reduce the GSDMD-positive immunofluorescent staining in astrocytes in ischemic cortex and hippocampus-CA1 areas (**Figures 6A,C**), indicating that YZFDF could exert inhibitory effects on cerebral I/R–induced astrocytic pyroptosis. Accordingly, YZFDF protected against BBB collapse and reduction after reperfusion which could be observed by immunohistochemical staining of SMI 71 in cortex and hippocampus-CA1 areas of the ischemic hemisphere (**Figures 6B,D,E**), potentially promoting blood flow circulation in capillaries of ischemic cerebral tissues.

## Yi-Zhi-Fang-Dai Formula Restored AQP-4 Polarization and Reduced Astrocytic Endfeet Swelling and Brain Edema After Reperfusion

The loss of AQP-4 polarization on astrocytic endfeet is closely associated with BBB–glymphatic dysfunctions which promote accumulation of metabolites and brain edema. In the present study, our results exhibited the loss of AQP-4 polarization with obvious dispersion, perturbed expressions, and astrocytic endfeet swelling in the ischemic brain tissues, which could be observed by immumohistochemical staining of AQP-4 (**Figures 7A–C**) and

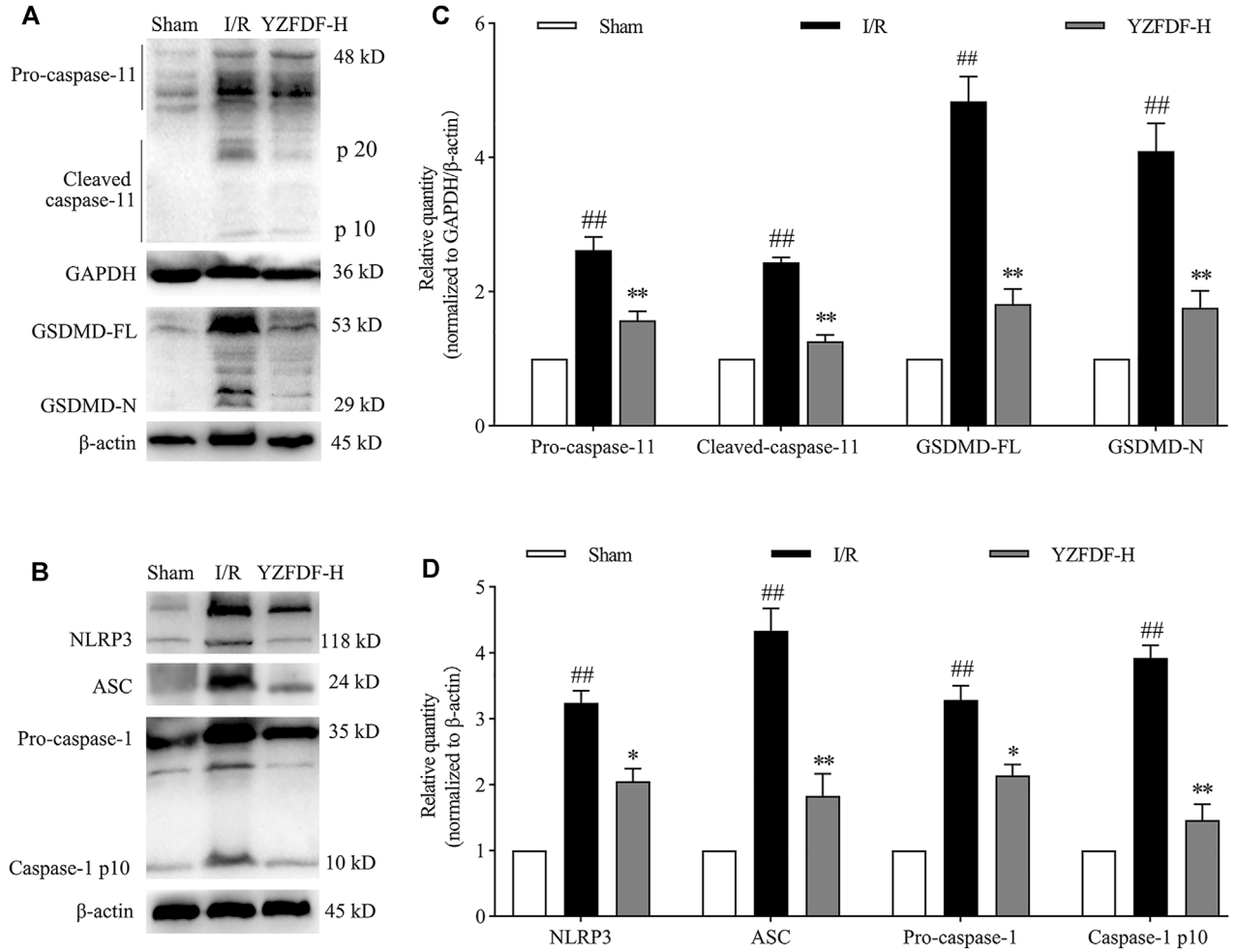


**FIGURE 4 |** YZFDF inhibited the activation of caspase-11/1 and cleavage of GSDMD at 24 h after cerebral I/R in rats. **(A)** Representative Western blots for pro/cleaved-caspase-11 and GSDMD-FL/N. **(B)** Representative Western blots for NLRP3, ASC, pro-caspase-1, and caspase-1 p10. **(C)** Quantitative analysis of pro/cleaved-caspase-11 and GSDMD-FL/N, $n = 6$. **(D)** Quantitative analysis of NLRP3, ASC, pro-caspase-1, and caspase-1 p10, $n = 6$. $^{\#\#}p < 0.01$ vs. Sham group; $^{*}p < 0.05$, $^{**}p < 0.01$ vs. I/R group.

double fluorescence staining of AQP-4 and GFAP in ischemic cortex and hippocampus-CA1 areas (**Figure 7D**, **Supplementary Figure S6**), while YZFDF intervention could restore AQP-4 polarization and accordingly reduce astrocytic endfeet swelling and brain edema in the ischemic hemisphere after reperfusion (**Figures 7A–E**).

## Yi-Zhi-Fang-Dai Formula Promoted Aβ Clearance and Prevented the Formation of $A\beta_{1\text{-}42}$ Oligomers After Reperfusion

Based on the above results in the present study, our study further exhibited that Aβ accumulates in the sites of swelling astrocytic endfeet, which was consistent with the situation of AQP-4 polarization loss (**Figures 8A–C**). However, YZFDF treatment could alleviate Aβ acute accumulation around astrocytes within 24 h after reperfusion in ischemic cortex and hippocampus-CA1 areas (**Figures 8A–C**). Furthermore, YZFDF could prevent the formation of $A\beta_{1\text{-}42}$ oligomers (the main form of toxic Aβ) in ischemic brain tissues after reperfusion (**Figures 8D,E**).

## Yi-Zhi-Fang-Dai Formula Alleviated Neuronal Damage and Promoted Neuron Survival After Reperfusion

The above results in the present study have revealed that YZFDF could inhibit cerebral I/R–induced pyroptosis, damage of the BBB–glymphatic system, and Aβ accumulation after reperfusion. Accordingly, our study further showed that YZFDF could alleviate neuronal damage after reperfusion (**Figures 9A–C**) and promote neuron survival in ischemic cortex and hippocampus-CA1 areas (**Figures 9D,E**), which was consistent with the results of the neurological function assessment and measurement of the cerebral infarct area.

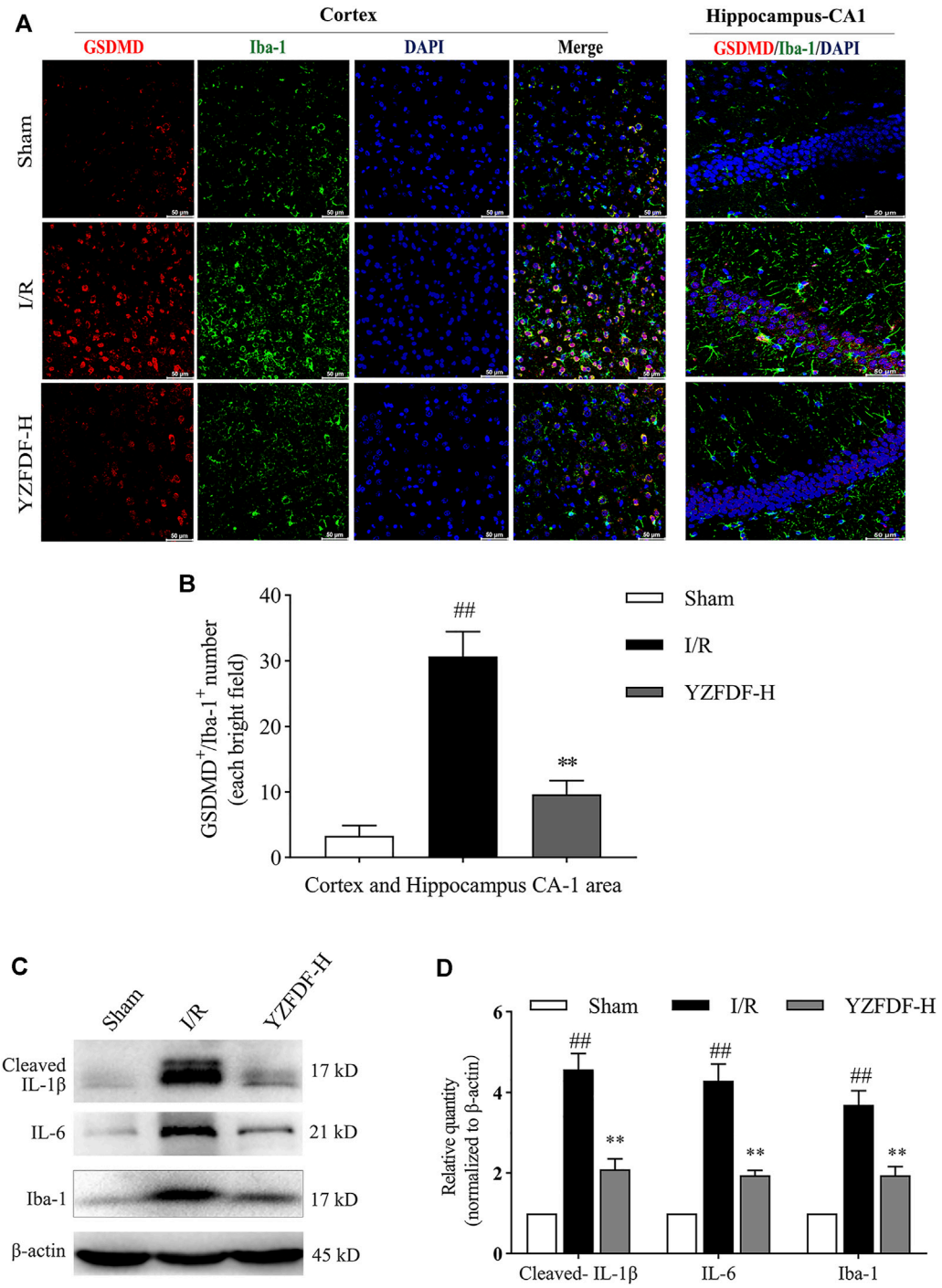


**FIGURE 5 |** YZFDF blocked overactivation and pyroptosis of microglia and alleviated inflammatory responses at 24 h after cerebral I/R in rats. **(A)** Representative pictures of double immunofluorescence staining of GSDMD (red) colocalized with Iba-1 (green) in cortex and hippocampus-CA1 areas, scale bar = 50 μm. **(B)** Quantitative analysis of double-positive staining of $GSDMD^{+}/Iba\text{-}1^{+}$ cell number, $n = 3$. **(C)** Representative Western blots for cleaved-IL-1β, IL-6, and Iba-1. **(D)** Quantitative analysis of cleaved-IL-1β, IL-6, and Iba-1, $n = 6$. $^{\#\#}p < 0.01$ vs. Sham group; $^{**}p < 0.01$ vs. I/R group.

## DISCUSSION

AD is a chronic cerebral disease affected by multifaceted etiological factors, among which cerebrovascular diseases represented by ischemic stroke have been attracting great attention (Wang R. et al., 2021; Eskandari et al., 2021; Zupanic et al., 2021). Despite the apparent association between AD and ischemic stroke, it remains unclear how the latter induces the

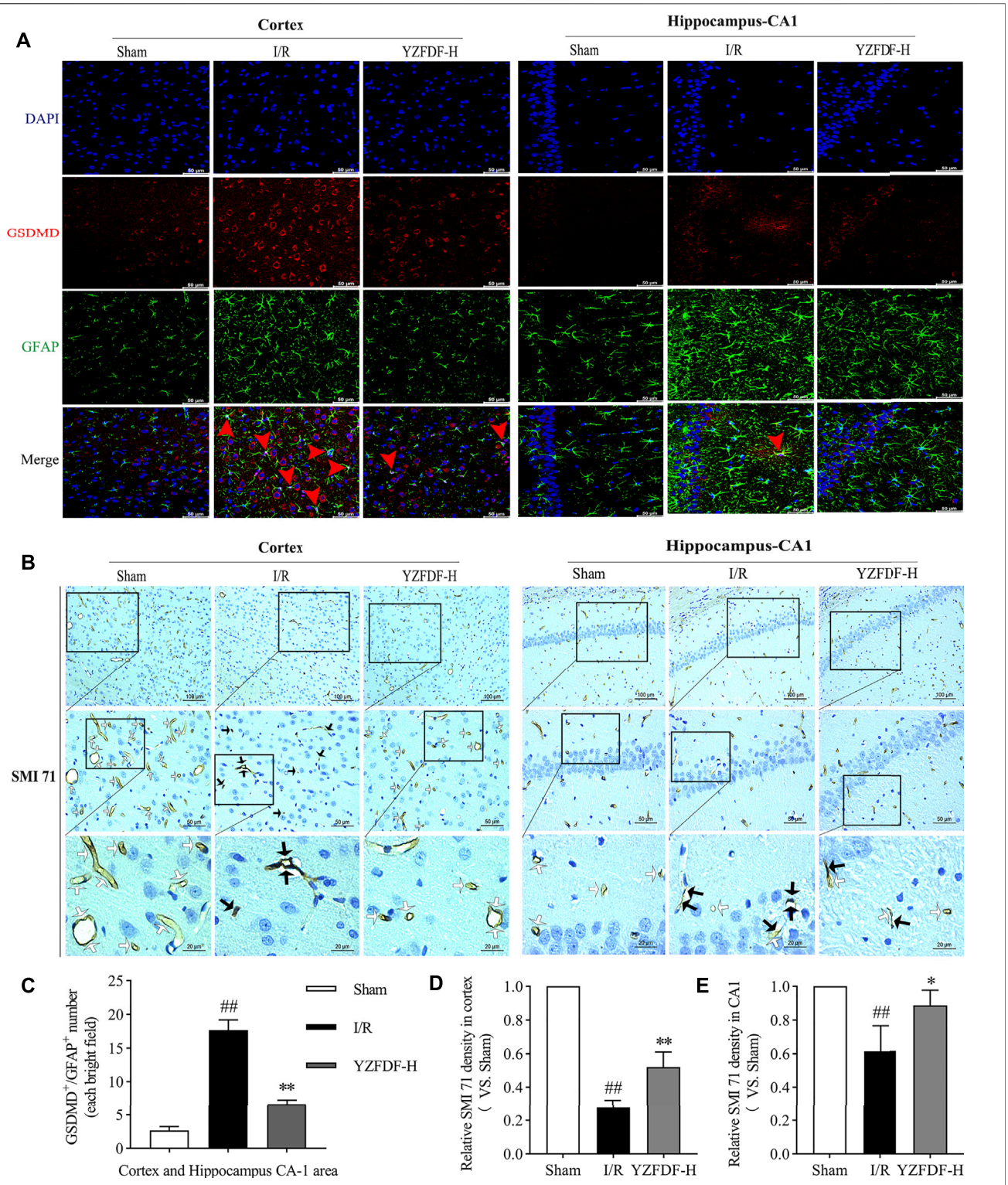


**FIGURE 6 |** YZFDF inhibited astrocytic pyroptosis and protected against BBB collapse at 24 h after cerebral I/R in rats. **(A)** Representative pictures of double immunofluorescence staining of GSDMD (red) with GFAP (green) in cortex and hippocampus-CA1 areas, scale bars = 50 μm. Red arrows show the GSDMD positive staining localized with the astrocytic nucleus. **(B)** Representative pictures of immunohistochemical staining of SMI 71 (a specific marker for BBB) in cortex and hippocampus-CA1 areas. White arrows show smooth and intact capillaries which represent normal BBB integrity, and black arrows indicate the damage of BBB integrity with unsmoothed, shriveled, or ruptured capillaries, scale bars = 100, 50, and 20 μm, as shown in pictures. **(C)** Quantitative analysis of astrocyte number with GSDMD-positive staining, $n = 3$. **(D)** Quantitative analysis of relative SMI 71 density in the cortex (scale bar = 50 μm), $n = 3$. **(E)** Quantitative analysis of relative SMI 71 density in the hippocampus-CA1 (scale bar = 50 μm), $n = 3$. $^{\#\#}p < 0.01$ vs. Sham group; $^{*}p < 0.05$, $^{**}p < 0.01$ vs. I/R group.

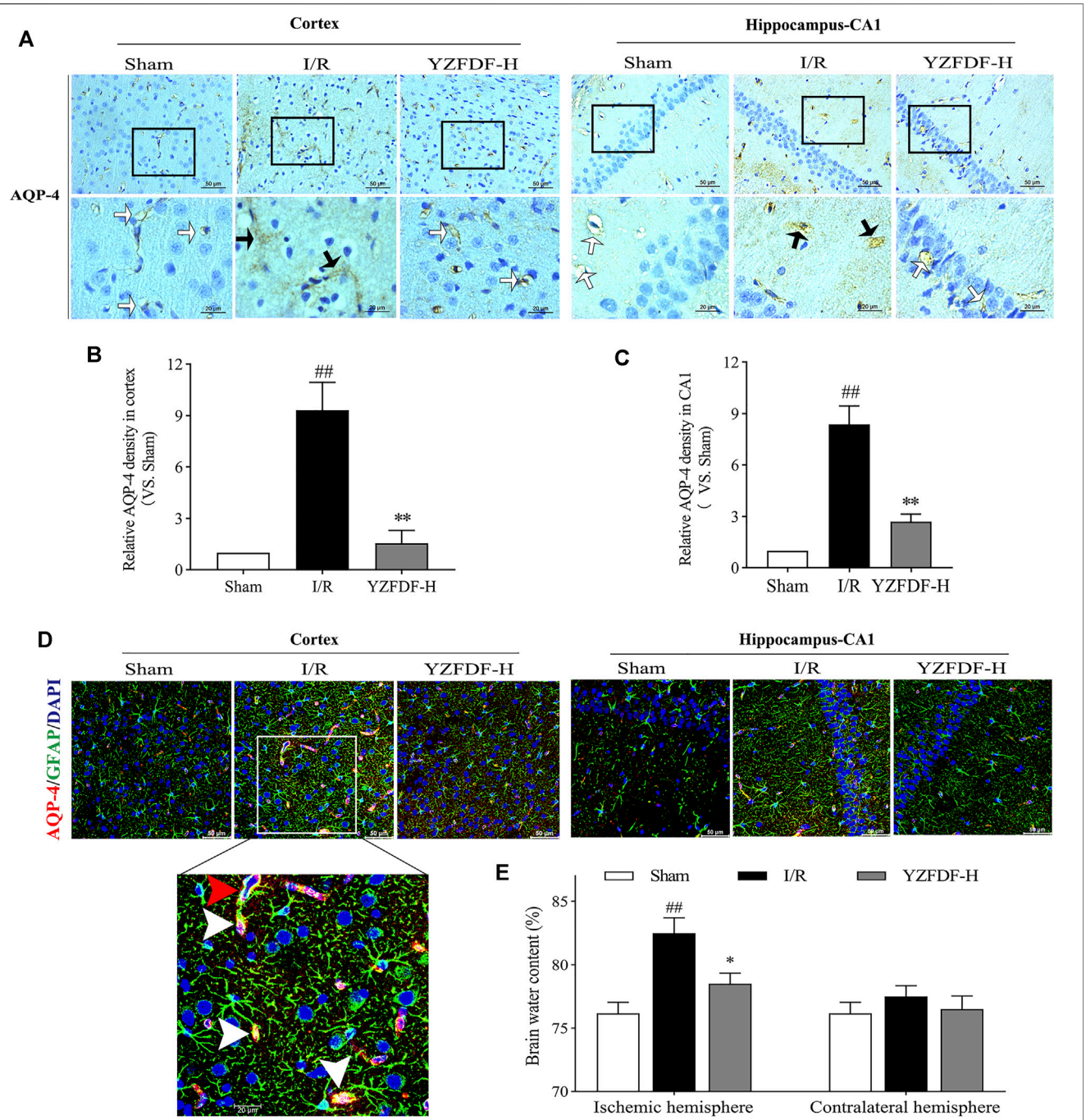


**FIGURE 7 |** YZFDF restored AQP-4 polarization and reduced astrocytic endfeet swelling and brain edema at 24 h after cerebral I/R in rats. **(A)** Representative pictures of immunohistochemical staining of AQP-4 in cortex and hippocampus-CA1 areas. White straight arrows represent normal AQP-4 polarization, and black arrows represent AQP-4 depolarization with obvious dispersion and perturbed expression, scale bars = 50 and 20 μm, as shown in pictures. **(B)** Quantitative analysis of relative AQP-4 density in the cortex (scale bar = 50 μm), $n = 3$. **(C)** Quantitative analysis of relative AQP-4 density in the hippocampus-CA1 (scale bar = 50 μm), $n = 3$. $^{\#\#}p < 0.01$ vs. Sham group; $^{**}p < 0.01$ vs. I/R group. **(D)** Representative pictures of double immunofluorescence staining of AQP-4 (red) with GFAP (green) in cortex and hippocampus-CA1 areas. Red triangle arrow indicates depolarized AQP-4 colocalizes with retracted GFAP and distributes around the astrocytic nucleus, and white triangle arrows indicate depolarized AQP-4 colocalizes with swelling of astrocytic endfeet, scale bars = 50 and 20 μm, as shown in pictures. **(E)** Brain water content analysis of ischemic and contralateral hemispheres, $n = 4$. $^{\#\#}p < 0.01$ vs. Sham group; $^{*}p < 0.05$ vs. I/R group.

onset and development of AD. However, accumulated evidence has showed that the neuroinflammation-related dysfunctional BBB–glymphatic system is responsible for triggering Aβ accumulation in the brain and may represent key link between ischemic stroke and dementia (Goulay et al., 2020; Ronaldson and Davis, 2020).

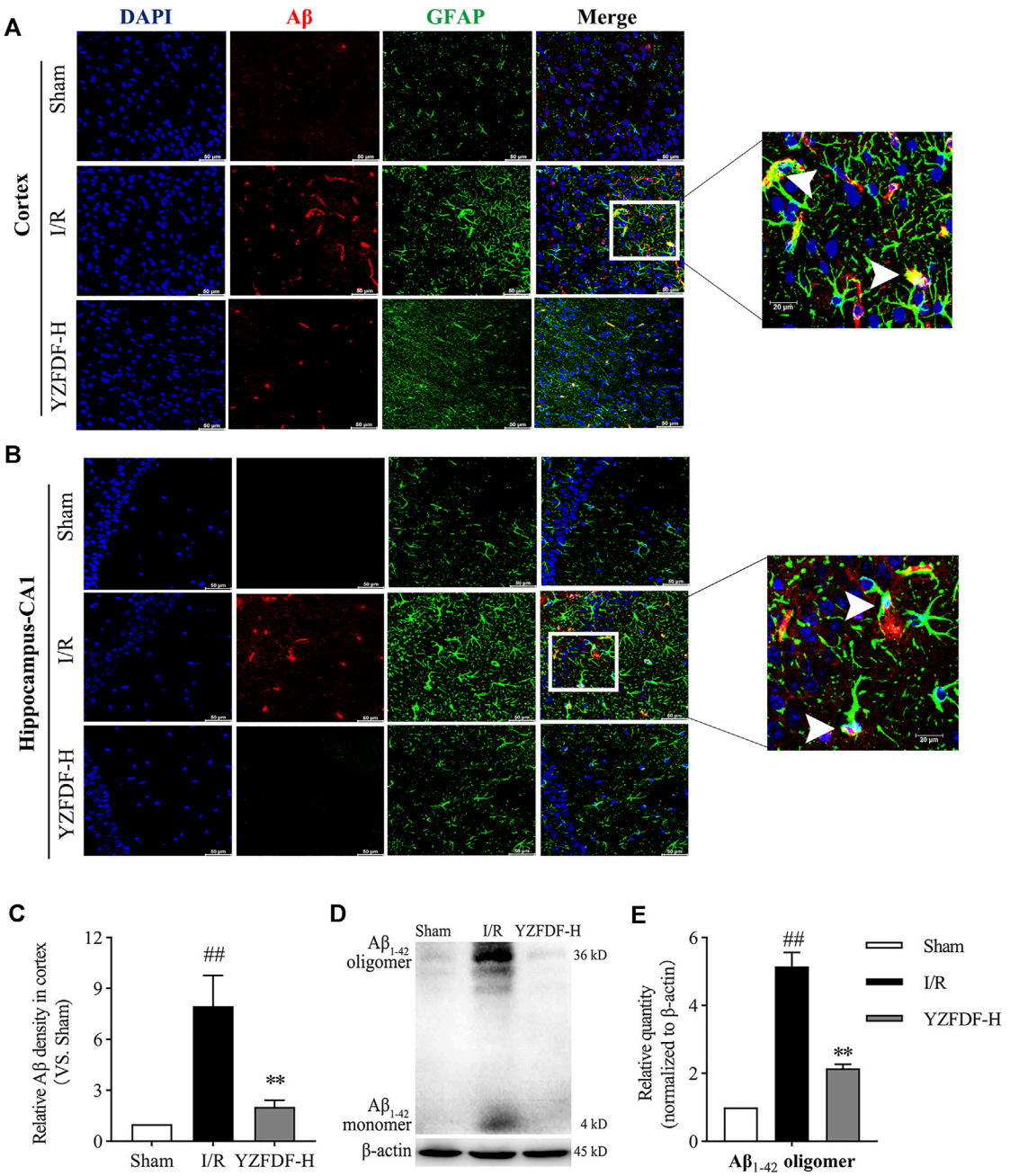


**FIGURE 8 |** YZFDF promoted Aβ clearance and prevented the formation of $A\beta_{1\text{-}42}$ oligomers at 24 h after cerebral I/R in rats. **(A,B)** Representative pictures of double immunofluorescence staining of Aβ (red) with GFAP (green) in cortex and hippocampus-CA1 areas, and white arrows represent Aβ accumulation in sites of swelling astrocytic endfeet, scale bars = 50 and 20 μm, as shown in pictures. **(C)** Quantitative analysis of relative Aβ density in the cortex (scale bar = 50 μm), $n = 3$. **(D)** Representative Western blots for the $A\beta_{1\text{-}42}$ monomer and $A\beta_{1\text{-}42}$ oligomer. **(E)** Quantitative analysis of $A\beta_{1\text{-}42}$ oligomers, $n = 6$. $^{\#\#}p < 0.01$ vs. Sham group; $^{**}p < 0.01$ vs. I/R group.

Restoring blood flow of the ischemic cerebral tissue in a short-time window is the most important therapeutic measure for patients suffering from acute cerebral ischemia. However, the potential additional injury following ischemia/reperfusion (I/R) has a great impact on the therapeutic efficacy of restoring blood flow (Kalogeris et al., 2016). I/R injury is the common pathophysiological phenomenon liable to occur in multiple organs including brain, and deterioration of microvasculature damage after reperfusion and the following non-reflow phenomenon of capillaries is the basic pathological change of I/R injury (Kloner et al., 2018). In the brain, the BBB is the main structure of microvasculature, and microcirculation disturbance resulting from BBB breakdown plays a crucial role in cerebral I/R injury (Mohamed Mokhtarudin and Payne, 2015; Huang et al., 2020; Xiao et al., 2020). Furthermore, BBB

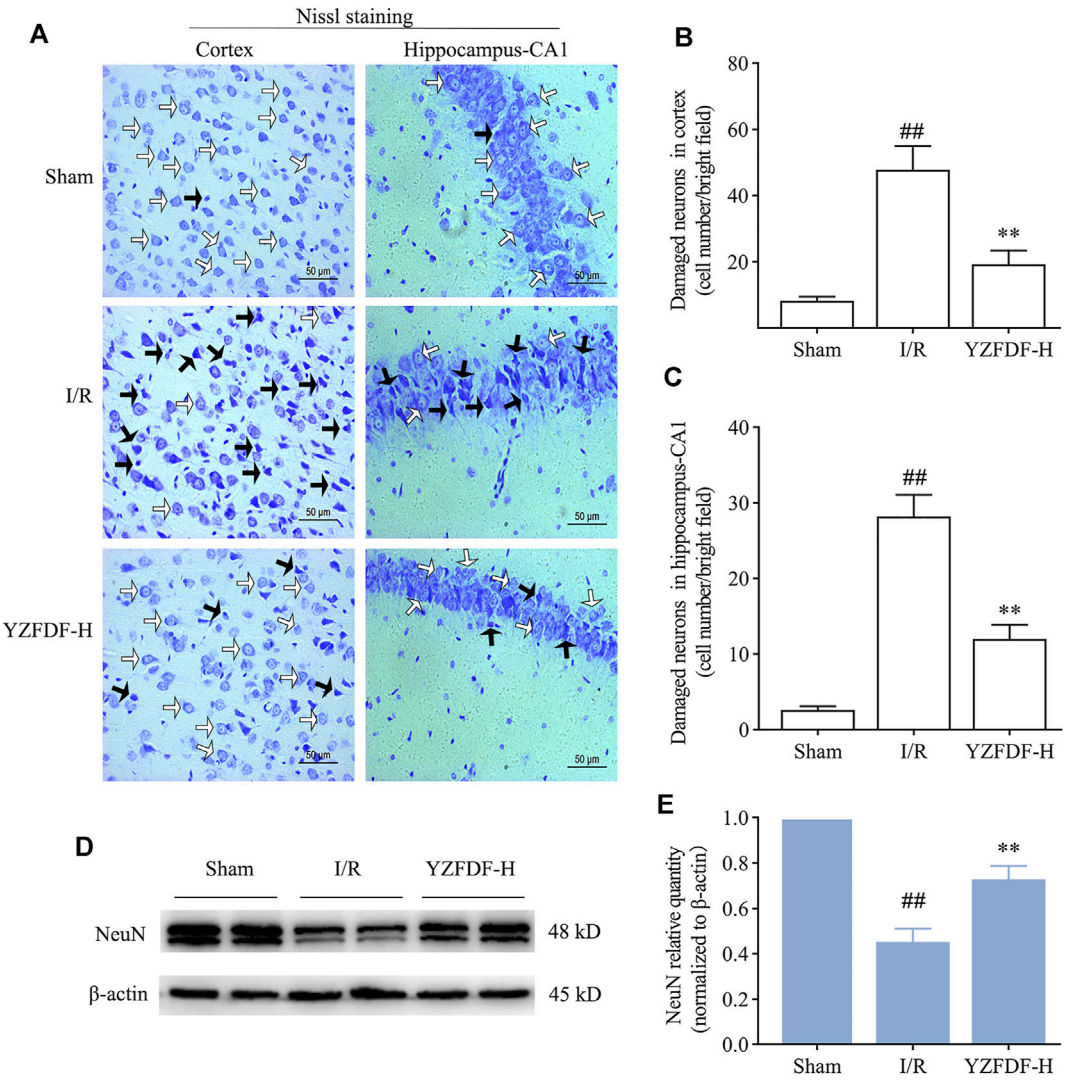


**FIGURE 9 |** YZFDF alleviated neuronal damage and promoted neuron survival at 24 h after cerebral I/R in rats. **(A)** Representative pictures of Nissl staining in ischemic cortex and hippocampus-CA1 areas. White arrows represent normal morphology of neurons with the clear nucleolus, abundant cytoplasm, and intact structure, and black arrows represent damaged neurons appearing shrunken and deep stained, scale bars = 50 μm. **(B,C)** Quantitative analysis of damaged neurons in cortex and hippocampus-CA1 areas, $n = 4$. $^{\#\#}p < 0.01$ vs. Sham group; $^{**}p < 0.01$ vs. I/R group. **(D)** Representative Western blots for NeuN. **(E)** Quantitative analysis of NeuN, $n = 6$. $^{\#\#}p < 0.01$ vs. Sham group; $^{**}p < 0.01$ vs. I/R group.

breakdown is recognized as an early marker for the onset of AD (Bell and Zlokovic, 2009; Sagare et al., 2012; Nation et al., 2019). Therefore, BBB protection during cerebral I/R injury is considered an important strategy for the prevention and treatment of ischemic stroke and poststroke dementia (Gursoy-Ozdemir et al., 2012; Goulay et al., 2020; Ronaldson and Davis, 2020).

As for the medication of cerebral I/R injury and BBB protection, amounts of literature indicated that various extracts or compound medicines from natural products show beneficial effects (Li Y. et al., 2019; Yu et al., 2020). For instance, Buyang Huanwu decoction (BHD) and Tongxinluo (TXL), both consisting of herbal and animal medicines, are common TCM prescriptions used for treating Qi deficiency and blood stasis syndrome of ischemic stroke by efficacies of invigorating Qi and activating blood circulation (Su et al., 2011; Wang Y. et al., 2020). Experimental studies revealed that BHD and TXL could alleviate cerebral I/R injury and exert protective effects on the BBB (Liu et al., 2013; Chen et al., 2019). In studies about the therapeutic efficacy of TCM compound medicines or extracts, such as BHD and TXL mentioned above for cerebral I/R injury, drug administration for 3–7 days starting before MCAO is the common means to enhance intervention effects (Liu et al., 2013; Yu et al., 2018; Chen et al., 2019; She et al., 2019; Zheng et al., 2019; Zhang S. et al., 2021). Accordingly, based on these literatures, we select YZFDF pretreatment to carry out the present study. However, different from BHD and TXL, YZFDF is purely composed of several plant-derived natural products, but the preliminary results in the present study showed that YZFDF could also exert significant neuroprotective effects against cerebral I/R injury by dose-

dependently alleviating neurological deficits and cerebral infarct after reperfusion. Our previous work revealed that pyroptosis of glial cells (microglia and astrocytes) is a considerable pathological mechanism causing BBB damage after cerebral I/R, and abating pyroptosis contributes to protect against BBB breakdown and maintains the homeostasis of brain microenvironments (Lyu et al., 2021). Our present study further indicated that YZFDF could protect ischemic cerebral tissues against pyroptotic cell death and accordingly exert protective effects against BBB collapse in damaged cortex and hippocampus areas after cerebral I/R, potentially promoting blood flow reperfusion in microcirculation of ischemic cerebral tissues, which probably owed to the multiple efficacies of invigorating Qi, removing blood stasis, and dredging brain collaterals.

As pro-inflammatory programmed cell death is distinguished from apoptosis and necrosis, pyroptosis manifests as nanopore formation on the cytomembrane leading to cell swelling and death, which is executed by the N-terminal fragments of gasdermin family represented by GSDMD-N (Feng et al., 2018). Upon stimulation, NLRP3 recruits pro-caspase-1 through the adapter molecule ASC to form the NLRP3/ASC/caspase-1 inflammasome, resulting in the activation of caspase-1 to cleave GSDMD and then leads to the secretion of pro-inflammatory cytokines, which is called canonical pyroptosis (Patel et al., 2017; Cong et al., 2020). However, in the caspase-11/GSDMD-mediated noncanonical pyroptosis pathway, GSDMD-N formed by the activation of caspase-11 acts as the upstream signaling that activates the NLRP3/ASC/caspase-1 inflammasome to further cause the maturation and secretion of pro-inflammatory cytokines such as IL-1β (Kayagaki et al., 2015; Aglietti et al., 2016). Caspase-11 is previously considered to be activated by lipopolysaccharide in infectious diseases (Hagar et al., 2013). Cerebral I/R injury is a noninfectious pathological process (Dong et al., 2018), and thus previous studies attributed cerebral I/R–induced pyroptosis to its canonical pathway (She et al., 2019). However, emerging literature has proven that caspase-11/GSDMD-mediated noncanonical pyroptosis is involved in acute kidney injury and hepatic injury induced by some endogenous pathophysiological factors including I/R injury (Miao et al., 2019; Wang X. et al., 2020). Our recent work revealed that caspase-11/GSDMD-mediated noncanonical pyroptosis also involves in cerebral I/R injury (Lyu et al., 2021). In the present study, we observed that YZFDF could obviously inactivate caspase-11 as well as cut off NLRP3/ASC/caspase-1 signaling and thus inhibit the cleavage of GSDMD to reduce the formation of GSDMD-N, indicating that YZFDF could exert inhibitory effects on cerebral I/R–induced canonical and noncanonical pyroptosis.

BBB breakdown in the cerebral ischemic period mainly results from the interaction between blood components (activated leukocytes and platelets) and microvascular endothelial cells, leading to inflammatory response and microthrombosis, which are exacerbated by blood flow reperfusion and then followed by the no-reflow phenomenon (Kalogeris et al., 2016). Following the initial ischemic damage, a wave of detrimental secondary events is caused by reperfusion such as oxidative stress and acute inflammation. Because inflammatory response is inherent across the whole course of cerebral I/R injury, and additionally due to the exacerbation of thromboinflammation and no-reflow after reperfusion in capillaries, neuroinflammation is recognized as the most vital pathological factor impacting on the BBB and the fundamental therapeutic target during both ischemic period and reperfusion (Liu et al., 2014; Li WH. et al., 2019; Stoll and Nieswandt, 2019). The results in our present study showed that YZFDF pretreatment could obviously downregulate the levels of IL-6 and inhibit the aberrant activation of microglia, reflecting that YZFDF alleviated the acute neuroinflammation during the course of cerebral I/R. There are intimate relationships between inflammation and pyroptosis (Kesavardhana et al., 2020). Research has proven that infectious or sterile inflammation can stimulate occurrence of pyroptosis, while pyroptosis reversely aggravates inflammatory responses by further generating and releasing certain pro-inflammatory mediators (Patel et al., 2017). In present study, our results further indicated that YZFDF could exert obvious inhibitory effects on microglial pyroptosis and the generation of IL-1β, which provided evidence for the blocking effect of YZFDF on cross talks between neuroinflammation and pyroptosis after reperfusion.

In addition to microglia, astrocytes are as well the main locations of cerebral I/R–induced pyroptosis which peaks at 24 h after reperfusion (Zhang et al., 2019; Lyu et al., 2021). As the most abundant glial cells in the mammalian brain, astrocytes are the major supporter of energy supply and nutrition for neurons in neuro-glial-vascular coupling (Nortley and Attwell, 2017; Allen and Lyons, 2018), and moreover astrocytic endfeet function as essential components of both the BBB and glymphatic system to clear metabolites such as Aβ and maintain brain microenvironmental homeostasis, in which aquaporin-4 (AQP-4) on astrocytic endfeet plays an important role (Gleiser et al., 2016; Rasmussen et al., 2021). Thus, in our previous study (Lyu et al., 2021), astrocytic pyroptosis was considered a vital factor causing the BBB further disruption and AQP-4 polarization loss, which account for Aβ accumulation, brain edema formation, non-reflow phenomenon of capillaries, and neuronal damage after cerebral I/R. In the present study, our results showed that YZFDF could obviously inhibit astrocytic pyroptosis after reperfusion which contributed to restore AQP-4 polarization and reduce brain edema. Moreover, the results as well showed that based on the protective effects against BBB–glymphatic dysfunctions, YZFDF could further significantly promote Aβ clearance and prevented the formation of $A\beta_{1\text{-}42}$ oligomers after reperfusion.

Aβ accumulation is the essential factor in the biological definition of AD, which can further cause tau pathology and neuron loss (Jack et al., 2018). Furthermore, Aβ accumulation in the brain can lead to extensive damages of the neurovascular unit (NVU) which comprises neurons, perivascular microglia, and BBB including cerebral microvascular endothelial cells (CMECs), pericytes, and surrounding astrocytes (Yamazaki and Kanekiyo, 2017). As mentioned previously, accumulated Aβ can act on pericytes via evoking reactive oxygen species generation in the form of oligomers to constrict capillaries which further promotes energy lack of neurons and neurodegeneration (Nortley et al., 2019). Aβ accumulation in capillaries, associated with cerebral amyloid angiopathy (CAA), also affect NVU astrocytes to cause mislocalization of AQP-4 expression (Wilcock et al., 2009), which was consistent with the acute accumulation of Aβ around swelling astrocytic endfeet as shown in our present study. Our previous study indicated that $A\beta_{1\text{-}42}$ oligomers are the main form of toxic Aβ and that $A\beta_{1\text{-}42}$ oligomers could damage tight junction scaffold proteins

among CMECs to induce BBB leakage via the receptor for advanced glycation end product (RAGE) (Wan W. et al., 2014; Wan et al., 2015; Chan et al., 2018; Chen et al., 2018). Previous studies demonstrated that Aβ increasingly accumulates around astrocytes along with both BBB breakdown and delayed neuronal death in the hippocampus within 6 months after cerebral I/R and even deposits as plaques with time further extension (van Groen et al., 2005; Pluta et al., 2010), which provides experimental evidence for stroke-inducing sporadic AD. Furthermore, recently, Martins et al. revealed that Aβ oligomers potentially resulting from activated platelets in microthrombosis massively accumulate in brain tissues including capillaries within 24 h after cerebral I/R, and they further demonstrated that Aβ oligomers are responsible for some of the brain damage during stroke by the property of forming ion channels on the cytomembrane (in a non-receptor–dependent way) to affect cellular osmotic balance and promote brain edema formation (Martins et al., 2019). Our recent study revealed that pyroptosis accounts for dysfunctions of the BBB–glymphatic system and the acute accumulation of toxic Aβ within 24 h after cerebral I/R (Lyu et al., 2021). However, on the other hand, toxic Aβ has been identified as a cause of pyroptosis and neuroinflammation in previous studies (Halle et al., 2008; Shi F. et al., 2015), which suggests a magnified effect of Aβ accumulation after cerebral I/R.

Large amounts of evidence mentioned previously indicate that Aβ accumulation is not only the consequence but also the further cause of the dysfunctional BBB–glymphatic system and neuronal damage in the course of cerebral I/R injury and in the process of ischemic stroke–inducing dementia. Therefore, maintaining Aβ clearance and protecting brain tissues against Aβ toxicity after cerebral I/R could offer a new viewpoint to alleviate ischemic stroke and prevent poststroke dementia. TCM herbal formulas or extracts have shown unique advantages in the prevention and treatment of complex brain diseases including acute ischemic stroke and dementia (Li Y. et al., 2019; Yu et al., 2020). Our previous study demonstrated that YZFDF could exert protective effects against $A\beta_{1\text{-}42}$ oligomer–induced BBB and neuronal damages (Liu et al., 2016a; Chan et al., 2020). The present study showed that YZFDF could promote Aβ clearance to prevent Aβ acute accumulation and the formation of $A\beta_{1\text{-}42}$ oligomers and thus block the potential interaction between the BBB–glymphatic dysfunctions and Aβ accumulation. Viewed from the macro perspective of TCM holism, the four herbal medicines of YZFDF potentially possess the neuroprotective effects against cerebral I/R injury by synergistically exerting efficacies of invigorating Qi, removing blood stasis, and dredging brain collaterals based on their drug properties. From the modern pharmacological and microcosmic perspective, our previous study had identified the bioactive ingredients in YZFDF, which contain bilobalide and ginkgolide A of *Ginkgo biloba* leaves, ginsenoside Rg1 of ginseng, cistanoside A of Cistanches Herba, and α-asarone of grassleaf sweetflag, which have a wide range of activities including anti-inflammation, anti-aggregation of platelets and proteins, neurovascular protections, and neurotrophic effects against cerebral I/R injury (Kimura et al., 1988; Zhou et al., 2014; Liu et al., 2016a; Zheng et al., 2019; Sarkar et al., 2020; Zhang K. et al., 2021). Our previous studies indicated that EGb761, a product extracted from *Ginkgo biloba* leaves (the main herb of YZFDF), could regulate Aβ-induced microglial inflammatory responses, BBB disruption, and alleviate neuronal damage (Wan WB. et al., 2014; Liu et al., 2016b; Wan et al., 2016). As a consequence, in this study, YZFDF potentially exerted advantages of multiple bioactive ingredients, multiple effects, and multiple targets on the whole NVU to alleviate cerebral I/R–induced neuroinflammation, pyroptosis, BBB–glymphatic dysfunctions, Aβ accumulation, and their interactions. Nevertheless, the action on body systems of YZFDF in this study and post-treatment and long-term effects as well as the more detailed targets and mechanism remain to be clarified and deserve our further explorations in future research.

## CONCLUSION

In summary, we demonstrated the neuroprotective properties of YZFDF against cerebral I/R injury at the first stage, and the following study further indicated that YZFDF pretreatment could exert inhibitory effects on microglial and astrocytic pyroptosis and acute neuroinflammation, which fundamentally contribute to restore the BBB–glymphatic functions, promote Aβ clearance and prevent the formation of Aβ oligomers via protecting against BBB breakdown, and AQP-4 polarization loss and thus facilitates to maintain the homeostasis of brain microenvironments and neuron survival after cerebral I/R.

## DATA AVAILABILITY STATEMENT

The original contributions presented in the study are included in the article/**Supplementary Material**, further inquiries can be directed to the corresponding authors.

## ETHICS STATEMENT

The animal study was reviewed and approved by the Animal Care Committee of Shanghai Jiao Tong University Affiliated Sixth People's Hospital.

## AUTHOR CONTRIBUTIONS

YL and CZ conceived and designed the project. ZL, QL, and ZY performed the experiments, analyzed the data, and wrote the manuscript. YC and LF contributed to assist the implementation of experiments. All authors read and approved the final manuscript.

## FUNDING

This work was supported by the National Natural Science Foundation of China (Grant Nos 81473739 and 81703857).

## SUPPLEMENTARY MATERIAL

The Supplementary Material for this article can be found online at: https://www.frontiersin.org/articles/10.3389/fphar.2021.791059/full#supplementary-material

## REFERENCES


Aglietti, R. A., Estevez, A., Gupta, A., Ramirez, M. G., Liu, P. S., Kayagaki, N., et al. (2016). GsdmD P30 Elicited by Caspase-11 during Pyroptosis Forms Pores in Membranes. *Proc. Natl. Acad. Sci. U S A.* 113 (28), 7858–7863. doi:10.1073/pnas.1607769113

Allen, N. J., and Lyons, D. A. (2018). Glia as Architects of central Nervous System Formation and Function. *Science* 362 (6411), 181–185. doi:10.1126/science.aat0473

Alzheimer's Association (2021). 2021 Alzheimer's Disease Facts and Figures. *Alzheimers Dement* 17 (3), 327–406. doi:10.1002/alz.12328

Bell, R. D., and Zlokovic, B. V. (2009). Neurovascular Mechanisms and Blood-Brain Barrier Disorder in Alzheimer's Disease. *Acta Neuropathol.* 118 (1), 103–113. doi:10.1007/s00401-009-0522-3

Burrows, F., Haley, M. J., Scott, E., Coutts, G., Lawrence, C. B., Allan, S. M., et al. (2016). Systemic Inflammation Affects Reperfusion Following Transient Cerebral Ischaemia. *Exp. Neurol.* 277, 252–260. doi:10.1016/j.expneurol.2016.01.013

Cai, M., Yu, Z., Wang, L., Song, X., Zhang, J., Zhang, Z., et al. (2016). Tongxinluo Reduces Brain Edema and Inhibits post-ischemic Inflammation after Middle Cerebral Artery Occlusion in Rats. *J. Ethnopharmacol* 181, 136–145. doi:10.1016/j.jep.2016.01.026

Carbone, M. G., Pagni, G., Tagliarini, C., Imbimbo, B. P., and Pomara, N. (2021). Can Platelet Activation Result in Increased Plasma Aβ Levels and Contribute to the Pathogenesis of Alzheimer's Disease? *Ageing Res. Rev.* 71, 101420. doi:10.1016/j.arr.2021.101420

Cavallucci, V., D'Amelio, M., and Cecconi, F. (2012). Aβ Toxicity in Alzheimer's Disease. *Mol. Neurobiol.* 45 (2), 366–378. doi:10.1007/s12035-012-8251-3

Chan, Y., Chen, W., Chen, Y., Lv, Z., Wan, W., Li, Y., et al. (2020). Yi-Zhi-Fang-Dai Formula Exerts a Protective Effect on the Injury of Tight Junction Scaffold Proteins *In Vitro* and *In Vivo* by Mediating Autophagy through Regulation of the RAGE/CaMKKβ/AMPK/mTOR Pathway. *Biol. Pharm. Bull.* 43 (12), 1847–1858. doi:10.1248/bpb.b20-00379

Chan, Y., Chen, W., Wan, W., Chen, Y., Li, Y., and Zhang, C. (2018). Aβ1-42 Oligomer Induces Alteration of Tight junction Scaffold Proteins via RAGE-Mediated Autophagy in bEnd.3 Cells. *Exp. Cel Res* 369 (2), 266–274. doi:10.1016/j.yexcr.2018.05.025

Chen, W., Chan, Y., Wan, W., Li, Y., and Zhang, C. (2018). Aβ1-42 Induces Cell Damage via RAGE-dependent Endoplasmic Reticulum Stress in bEnd.3 Cells. *Exp. Cel Res* 362 (1), 83–89. doi:10.1016/j.yexcr.2017.11.005

Chen, Z. Z., Gong, X., Guo, Q., Zhao, H., and Wang, L. (2019). Bu Yang Huan Wu Decoction Prevents Reperfusion Injury Following Ischemic Stroke in Rats via Inhibition of HIF-1 α, VEGF and Promotion β-ENaC Expression. *J. Ethnopharmacol* 228, 70–81. doi:10.1016/j.jep.2018.09.017

Cong, L., Gao, Z., Zheng, Y., Ye, T., Wang, Z., Wang, P., et al. (2020). Electrical Stimulation Inhibits Val-boroPro-Induced Pyroptosis in THP-1 Macrophages via Sirtuin3 Activation to Promote Autophagy and Inhibit ROS Generation. *Aging (Albany NY)* 12 (7), 6415–6435. doi:10.18632/aging.103038

Dong, Z., Pan, K., Pan, J., Peng, Q., and Wang, Y. (2018). The Possibility and Molecular Mechanisms of Cell Pyroptosis after Cerebral Ischemia. *Neurosci. Bull.* 34 (6), 1131–1136. doi:10.1007/s12264-018-0294-7

Du, H., He, Y., Pan, Y., Zhao, M., Li, Z., Wang, Y., et al. (2021). Danhong Injection Attenuates Cerebral Ischemia-Reperfusion Injury in Rats through the Suppression of the Neuroinflammation. *Front. Pharmacol.* 12, 561237. doi:10.3389/fphar.2021.561237

Eskandari, S., Sajadimajd, S., Alaei, L., Soheilikhah, Z., Derakhshankhah, H., and Bahrami, G. (2021). Targeting Common Signaling Pathways for the Treatment of Stroke and Alzheimer's: a Comprehensive Review. *Neurotox Res.* 39 (5), 1589–1612. doi:10.1007/s12640-021-00381-7

Feng, S., Fox, D., and Man, S. M. (2018). Mechanisms of Gasdermin Family Members in Inflammasome Signaling and Cell Death. *J. Mol. Biol.* 430 (18 Pt B), 3068–3080. doi:10.1016/j.jmb.2018.07.002

Gleiser, C., Wagner, A., Fallier-Becker, P., Wolburg, H., Hirt, B., and Mack, A. F. (2016). Aquaporin-4 in Astroglial Cells in the CNS and Supporting Cells of Sensory Organs-A Comparative Perspective. *Int. J. Mol. Sci.* 17 (9), 1411. doi:10.3390/ijms17091411

Goulay, R., Mena Romo, L., Hol, E. M., and Dijkhuizen, R. M. (2020). From Stroke to Dementia: a Comprehensive Review Exposing Tight Interactions between Stroke and Amyloid-β Formation. *Transl Stroke Res.* 11 (4), 601–614. doi:10.1007/s12975-019-00755-2

Gursoy-Ozdemir, Y., Yemisci, M., and Dalkara, T. (2012). Microvascular protection Is Essential for Successful Neuroprotection in Stroke. *J. Neurochem.* 123 (Suppl. 2), 2–11. doi:10.1111/j.1471-4159.2012.07938.x

Hagar, J. A., Powell, D. A., Aachoui, Y., Ernst, R. K., and Miao, E. A. (2013). Cytoplasmic LPS Activates Caspase-11: Implications in TLR4-independent Endotoxic Shock. *Science* 341 (6151), 1250–1253. doi:10.1126/science.1240988

Halle, A., Hornung, V., Petzold, G. C., Stewart, C. R., Monks, B. G., Reinheckel, T., et al. (2008). The NALP3 Inflammasome Is Involved in the Innate Immune Response to Amyloid-Beta. *Nat. Immunol.* 9 (8), 857–865. doi:10.1038/ni.1636

Hampel, H., Hardy, J., Blennow, K., Chen, C., Perry, G., Kim, S. H., et al. (2021). The Amyloid-β Pathway in Alzheimer's Disease. *Mol. Psychiatry*. doi:10.1038/s41380-021-01249-0

Huang, Y., Chen, S., Luo, Y., and Han, Z. (2020). Crosstalk between Inflammation and the BBB in Stroke. *Curr. Neuropharmacol* 18 (12), 1227–1236. doi:10.2174/1570159X18666200620230321

Hussain, B., Fang, C., and Chang, J. (2021). Blood-Brain Barrier Breakdown: An Emerging Biomarker of Cognitive Impairment in Normal Aging and Dementia. *Front. Neurosci.* 15, 688090. doi:10.3389/fnins.2021.688090

Jack, C. R., Jr., Bennett, D. A., Blennow, K., Carrillo, M. C., Dunn, B., Haeberlein, S. B., et al. (2018). NIA-AA Research Framework: Toward a Biological Definition of Alzheimer's Disease. *Alzheimers Dement* 14 (4), 535–562. doi:10.1016/j.jalz.2018.02.018

Kalogeris, T., Baines, C. P., Krenz, M., and Korthuis, R. J. (2016). Ischemia/Reperfusion. *Compr. Physiol.* 7 (1), 113–170. doi:10.1002/cphy.c160006

Kayagaki, N., Stowe, I. B., Lee, B. L., O'Rourke, K., Anderson, K., Warming, S., et al. (2015). Caspase-11 Cleaves Gasdermin D for Non-canonical Inflammasome Signalling. *Nature* 526 (7575), 666–671. doi:10.1038/nature15541

Kesavardhana, S., Malireddi, R. K. S., and Kanneganti, T. D. (2020). Caspases in Cell Death, Inflammation, and Pyroptosis. *Annu. Rev. Immunol.* 38, 567–595. doi:10.1146/annurev-immunol-073119-095439

Kim, D., Hughes, T. M., Lipford, M. E., Craft, S., Baker, L. D., Lockhart, S. N., et al. (2021). Relationship between Cerebrovascular Reactivity and Cognition Among People with Risk of Cognitive Decline. *Front. Physiol.* 12, 645342. doi:10.3389/fphys.2021.645342

Kimura, Y., Okuda, H., and Arichi, S. (1988). Effects of Various Ginseng Saponins on 5-hydroxytryptamine Release and Aggregation in Human Platelets. *J. Pharm. Pharmacol.* 40 (12), 838–843. doi:10.1111/j.2042-7158.1988.tb06285.x

Kloner, R. A., King, K. S., and Harrington, M. G. (2018). No-reflow Phenomenon in the Heart and Brain. *Am. J. Physiol. Heart Circ. Physiol.* 315 (3), H550–H562. doi:10.1152/ajpheart.00183.2018

Lan, R., Xiang, J., Wang, G. H., Li, W. W., Zhang, W., Xu, L. L., et al. (2013). Xiao-Xu-Ming Decoction Protects against Blood-Brain Barrier Disruption and Neurological Injury Induced by Cerebral Ischemia and Reperfusion in Rats. *Evid. Based Complement. Alternat Med.* 2013, 629782. doi:10.1155/2013/629782

Li, W. H., Cheng, X., Yang, Y. L., Liu, M., Zhang, S. S., Wang, Y. H., et al. (2019a). Kaempferol Attenuates Neuroinflammation and Blood Brain Barrier Dysfunction to Improve Neurological Deficits in Cerebral Ischemia/reperfusion Rats. *Brain Res.* 1722, 146361. doi:10.1016/j.brainres.2019.146361

Li, Y., Zhong, W., Jiang, Z., and Tang, X. (2019b). New Progress in the Approaches for Blood-Brain Barrier protection in Acute Ischemic Stroke. *Brain Res. Bull.* 144, 46–57. doi:10.1016/j.brainresbull.2018.11.006

Liu, L., Wan, W., Chen, W., Chan, Y., Shen, Q., and Li, Y. (2016a). Yi-Zhi-Fang-Dai Formula Protects against Aβ1-42 Oligomer Induced Cell Damage via Increasing Hsp70 and Grp78 Expression in SH-Sy5y Cells. *Evid. Based Complement. Alternat Med.* 2016, 8591656. doi:10.1155/2016/8591656

Liu, L., Zhang, C., Kalionis, B., Wan, W., Murthi, P., Chen, C., et al. (2016b). EGb761 Protects against Aβ1-42 Oligomer-Induced Cell Damage via Endoplasmic Reticulum Stress Activation and Hsp70 Protein Expression Increase in SH-Sy5y Cells. *Exp. Gerontol.* 75, 56–63. doi:10.1016/j.exger.2016.01.003

Liu, T., Zhang, T., Yu, H., Shen, H., and Xia, W. (2014). Adjudin Protects against Cerebral Ischemia Reperfusion Injury by Inhibition of Neuroinflammation and

Blood-Brain Barrier Disruption. *J. Neuroinflammation* 11, 107. doi:10.1186/1742-2094-11-107

Liu, W., Wong, A., Au, L., Yang, J., Wang, Z., Leung, E. Y., et al. (2015). Influence of Amyloid-β on Cognitive Decline after Stroke/Transient Ischemic Attack: Three-Year Longitudinal Study. *Stroke* 46 (11), 3074–3080. doi:10.1161/STROKEAHA.115.010449

Liu, Y., Tang, G. H., Sun, Y. H., Lin, X. J., Wei, C., Yang, G. Y., et al. (2013). The Protective Role of Tongxinluo on Blood-Brain Barrier after Ischemia-Reperfusion Brain Injury. *J. Ethnopharmacol* 148 (2), 632–639. doi:10.1016/j.jep.2013.05.018

Longa, E. Z., Weinstein, P. R., Carlson, S., and Cummins, R. (1989). Reversible Middle Cerebral Artery Occlusion without Craniectomy in Rats. *Stroke* 20 (1), 84–91. doi:10.1161/01.str.20.1.84

Lyu, Z., Chan, Y., Li, Q., Zhang, Q., Liu, K., Xiang, J., et al. (2021). Destructive Effects of Pyroptosis on Homeostasis of Neuron Survival Associated with the Dysfunctional BBB-Glymphatic System and Amyloid-Beta Accumulation after Cerebral Ischemia/Reperfusion in Rats. *Neural Plast.* 2021, 4504363. doi:10.1155/2021/4504363

Martins, A. H., Zayas-Santiago, A., Ferrer-Acosta, Y., Martinez-Jimenez, S. M., Zueva, L., Diaz-Garcia, A., et al. (2019). Accumulation of Amyloid Beta (Aβ) Peptide on Blood Vessel Walls in the Damaged Brain after Transient Middle Cerebral Artery Occlusion. *Biomolecules* 9 (8), 350. doi:10.3390/biom9080350

Matikainen, S., Nyman, T. A., and Cypryk, W. (2020). Function and Regulation of Noncanonical Caspase-4/5/11 Inflammasome. *J. Immunol.* 204 (12), 3063–3069. doi:10.4049/jimmunol.2000373

Merlini, M., Meyer, E. P., Ulmann-Schuler, A., and Nitsch, R. M. (2011). Vascular β-amyloid and Early Astrocyte Alterations Impair Cerebrovascular Function and Cerebral Metabolism in Transgenic arcAβ Mice. *Acta Neuropathol.* 122 (3), 293–311. doi:10.1007/s00401-011-0834-y

Miao, N., Yin, F., Xie, H., Wang, Y., Xu, Y., Shen, Y., et al. (2019). The Cleavage of Gasdermin D by Caspase-11 Promotes Tubular Epithelial Cell Pyroptosis and Urinary IL-18 Excretion in Acute Kidney Injury. *Kidney Int.* 96 (5), 1105–1120. doi:10.1016/j.kint.2019.04.035

Mohamed Mokhtarudin, M. J., and Payne, S. J. (2015). Mathematical Model of the Effect of Ischemia-Reperfusion on Brain Capillary Collapse and Tissue Swelling. *Math. Biosci.* 263, 111–120. doi:10.1016/j.mbs.2015.02.011

Nakada, T., Kwee, I. L., Igarashi, H., and Suzuki, Y. (2017). Aquaporin-4 Functionality and Virchow-Robin Space Water Dynamics: Physiological Model for Neurovascular Coupling and Glymphatic Flow. *Int. J. Mol. Sci.* 18 (8), 1798. doi:10.3390/ijms18081798

Nation, D. A., Sweeney, M. D., Montagne, A., Sagare, A. P., D'Orazio, L. M., Pachicano, M., et al. (2019). Blood-brain Barrier Breakdown Is an Early Biomarker of Human Cognitive Dysfunction. *Nat. Med.* 25 (2), 270–276. doi:10.1038/s41591-018-0297-y

Nortley, R., and Attwell, D. (2017). Control of Brain Energy Supply by Astrocytes. *Curr. Opin. Neurobiol.* 47, 80–85. doi:10.1016/j.conb.2017.09.012

Nortley, R., Korte, N., Izquierdo, P., Hirunpattarasilp, C., Mishra, A., Jaunmuktane, Z., et al. (2019). Amyloid β Oligomers Constrict Human Capillaries in Alzheimer's Disease via Signaling to Pericytes. *Science* 365 (6450). doi:10.1126/science.aav9518

Patel, M. N., Carroll, R. G., Galván-Peña, S., Mills, E. L., Olden, R., Triantafilou, M., et al. (2017). Inflammasome Priming in Sterile Inflammatory Disease. *Trends Mol. Med.* 23 (2), 165–180. doi:10.1016/j.molmed.2016.12.007

Pluta, R., Januszewski, S., Jabłoński, M., and Ułamek, M. (2010). Factors in Creepy Delayed Neuronal Death in hippocampus Following Brain Ischemia-Reperfusion Injury with Long-Term Survival. *Acta Neurochir Suppl.* 106, 37–41. doi:10.1007/978-3-211-98811-4_5

Rasmussen, M. K., Mestre, H., and Nedergaard, M. (2021). Fluid Transport in the Brain. *Physiol. Rev.* doi:10.1152/physrev.00031.2020

Ronaldson, P. T., and Davis, T. P. (2020). Regulation of Blood-Brain Barrier Integrity by Microglia in Health and Disease: A Therapeutic Opportunity. *J. Cereb. Blood Flow Metab.* 40 (1_Suppl. l), S6–S24. doi:10.1177/0271678X20951995

Sagare, A. P., Bell, R. D., and Zlokovic, B. V. (2012). Neurovascular Dysfunction and Faulty Amyloid β-peptide Clearance in Alzheimer Disease. *Cold Spring Harb Perspect. Med.* 2 (10), a011452. doi:10.1101/cshperspect.a011452

Sarkar, C., Quispe, C., Jamaddar, S., Hossain, R., Ray, P., Mondal, M., et al. (2020). Therapeutic Promises of Ginkgolide A: A Literature-Based Review. *Biomed. Pharmacother.* 132, 110908. doi:10.1016/j.biopha.2020.110908

She, Y., Shao, L., Zhang, Y., Hao, Y., Cai, Y., Cheng, Z., et al. (2019). Neuroprotective Effect of Glycosides in Buyang Huanwu Decoction on Pyroptosis Following Cerebral Ischemia-Reperfusion Injury in Rats. *J. Ethnopharmacol* 242, 112051. doi:10.1016/j.jep.2019.112051

Shi, F., Kouadir, M., and Yang, Y. (2015a). NALP3 Inflammasome Activation in Protein Misfolding Diseases. *Life Sci.* 135, 9–14. doi:10.1016/j.lfs.2015.05.011

Shi, J., Zhao, Y., Wang, K., Shi, X., Wang, Y., Huang, H., et al. (2015b). Cleavage of GSDMD by Inflammatory Caspases Determines Pyroptotic Cell Death. *Nature* 526 (7575), 660–665. doi:10.1038/nature15514

Singh, A. K., Rai, S. N., Maurya, A., Mishra, G., Awasthi, R., Shakya, A., et al. (2021). Therapeutic Potential of Phytoconstituents in Management of Alzheimer's Disease. *Evid. Based Complement. Alternat Med.* 2021, 5578574. doi:10.1155/2021/5578574

Song, B., Ao, Q., Niu, Y., Shen, Q., Zuo, H., Zhang, X., et al. (2013). Amyloid Beta-Peptide Worsens Cognitive Impairment Following Cerebral Ischemia-Reperfusion Injury. *Neural Regen. Res.* 8 (26), 2449–2457. doi:10.3969/j.issn.1673-5374.2013.26.006

Stoll, G., and Nieswandt, B. (2019). Thrombo-inflammation in Acute Ischaemic Stroke - Implications for Treatment. *Nat. Rev. Neurol.* 15 (8), 473–481. doi:10.1038/s41582-019-0221-1

Su, L., Li, Y., Lv, B., Ji, H., Ding, H., Hu, L., et al. (2011). Clinical Study on Naoxintong Capsule for Stroke Recovery of Qi-Deficiency and Blood-Stasis Syndrome. *Zhongguo Zhong Yao Za Zhi* 36 (11), 1530–1533.

Tarasoff-Conway, J. M., Carare, R. O., Osorio, R. S., Glodzik, L., Butler, T., Fieremans, E., et al. (2015). Clearance Systems in the Brain-Implications for Alzheimer Disease. *Nat. Rev. Neurol.* 11 (8), 457–470. doi:10.1038/nrneurol.2015.119

van Groen, T., Puurunen, K., Mäki, H. M., Sivenius, J., and Jolkkonen, J. (2005). Transformation of Diffuse Beta-Amyloid Precursor Protein and Beta-Amyloid Deposits to Plaques in the Thalamus after Transient Occlusion of the Middle Cerebral Artery in Rats. *Stroke* 36 (7), 1551–1556. doi:10.1161/01.STR.0000169933.88903.cf

Verheggen, I. C. M., Van Boxtel, M. P. J., Verhey, F. R. J., Jansen, J. F. A., and Backes, W. H. (2018). Interaction between Blood-Brain Barrier and Glymphatic System in Solute Clearance. *Neurosci. Biobehav Rev.* 90, 26–33. doi:10.1016/j.neubiorev.2018.03.028

Wan, W., Cao, L., Liu, L., Zhang, C., Kalionis, B., Tai, X., et al. (2015). Aβ(1-42) Oligomer-Induced Leakage in an *In Vitro* Blood-Brain Barrier Model Is Associated with Up-Regulation of RAGE and Metalloproteinases, and Down-Regulation of Tight junction Scaffold Proteins. *J. Neurochem.* 134 (2), 382–393. doi:10.1111/jnc.13122

Wan, W., Chen, H., and Li, Y. (2014a). The Potential Mechanisms of Aβ-Receptor for Advanced Glycation End-Products Interaction Disrupting Tight Junctions of the Blood-Brain Barrier in Alzheimer's Disease. *Int. J. Neurosci.* 124 (2), 75–81. doi:10.3109/00207454.2013.825258

Wan, W., Zhang, C., Danielsen, M., Li, Q., Chen, W., Chan, Y., et al. (2016). EGb761 Improves Cognitive Function and Regulates Inflammatory Responses in the APP/PS1 Mouse. *Exp. Gerontol.* 81, 92–100. doi:10.1016/j.exger.2016.05.007

Wan, W. B., Cao, L., Liu, L. M., Kalionis, B., Chen, C., Tai, X. T., et al. (2014b). EGb761 Provides a Protective Effect against Aβ1-42 Oligomer-Induced Cell Damage and Blood-Brain Barrier Disruption in an *In Vitro* bEnd.3 Endothelial Model. *PLoS One* 9 (11), e113126. doi:10.1371/journal.pone.0113126

Wang, B., Lyu, Z., Chan, Y., Li, Q., Zhang, L., Liu, K., et al. (2021a). Tongxinluo Exerts Inhibitory Effects on Pyroptosis and Amyloid-β Peptide Accumulation after Cerebral Ischemia/Reperfusion in Rats. *Evid. Based Complement. Alternat Med.* 2021, 5788602. doi:10.1155/2021/5788602

Wang, R., Qiu, C., Dintica, C. S., Shang, Y., Calderón Larrañaga, A., Wang, H. X., et al. (2021b). Shared Risk and Protective Factors between Alzheimer's Disease and Ischemic Stroke: A Population-Based Longitudinal Study. *Alzheimers Dement* 17 (2), 191–204. doi:10.1002/alz.12203

Wang, X., Liu, Z., and Shen, L. (2020a). Isoflurane Preconditioning Inhibits Caspase-11-Related Noncanonical Pyroptosis Pathway to Alleviate Hepatic Ischemia-Reperfusion Injury in Mice. *Nan Fang Yi Ke Da Xue Xue Bao* 40 (5), 670–675. doi:10.12122/j.issn.1673-4254.2020.05.09

Wang, Y., Zhang, L., Pan, Y. J., Fu, W., Huang, S. W., Xu, B., et al. (2020b). Investigation of Invigorating Qi and Activating Blood Circulation Prescriptions in Treating Qi Deficiency and Blood Stasis Syndrome of Ischemic Stroke Patients: Study Protocol for a Randomized Controlled Trial. *Front. Pharmacol.* 11, 892. doi:10.3389/fphar.2020.00892

Wilcock, D. M., Vitek, M. P., and Colton, C. A. (2009). Vascular Amyloid Alters Astrocytic Water and Potassium Channels in Mouse Models and Humans with Alzheimer's Disease. *Neuroscience* 159 (3), 1055–1069. doi:10.1016/j.neuroscience.2009.01.023

Xiao, M., Xiao, Z. J., Yang, B., Lan, Z., and Fang, F. (2020). Blood-Brain Barrier: More Contributor to Disruption of Central Nervous System Homeostasis Than Victim in Neurological Disorders. *Front. Neurosci.* 14, 764. doi:10.3389/fnins.2020.00764

Yamazaki, Y., and Kanekiyo, T. (2017). Blood-Brain Barrier Dysfunction and the Pathogenesis of Alzheimer's Disease. *Int. J. Mol. Sci.* 18 (9), 1965. doi:10.3390/ijms18091965

Yi, Y. S. (2018). Regulatory Roles of the Caspase-11 Non-canonical Inflammasome in Inflammatory Diseases. *Immune Netw.* 18 (6), e41. doi:10.4110/in.2018.18.e41

Yu, L., Tao, J., Zhao, Q., Xu, C., and Zhang, Q. (2020). Confirmation of Potential Neuroprotective Effects of Natural Bioactive Compounds from Traditional Medicinal Herbs in Cerebral Ischemia Treatment. *J. Integr. Neurosci.* 19 (2), 373–384. doi:10.31083/j.jin.2020.02.63

Yu, Z., Cai, M., Li, X., Zhang, J., Wu, T., Yang, F., et al. (2018). Neuroprotective Effects of Tongxinluo on Focal Cerebral Ischemia and Reperfusion Injury in Rats Associated with the Activation of the MEK1/2/ERK1/2/p90RSK Signaling Pathway. *Brain Res.* 1685, 9–18. doi:10.1016/j.brainres.2018.01.036

Yu, Z. H., Cai, M., Xiang, J., Zhang, Z. N., Zhang, J. S., Song, X. L., et al. (2016). PI3K/Akt Pathway Contributes to Neuroprotective Effect of Tongxinluo against Focal Cerebral Ischemia and Reperfusion Injury in Rats. *J. Ethnopharmacol* 181, 8–19. doi:10.1016/j.jep.2016.01.028

Zhang, D., Qian, J., Zhang, P., Li, H., Shen, H., Li, X., et al. (2019). Gasdermin D Serves as a Key Executioner of Pyroptosis in Experimental Cerebral Ischemia and Reperfusion Model Both *In Vivo* and *In Vitro*. *J. Neurosci. Res.* 97 (6), 645–660. doi:10.1002/jnr.24385

Zhang, K., Liu, Q., Luo, L., Feng, X., Hu, Q., Fan, X., et al. (2021a). Neuroprotective Effect of Alpha-Asarone on the Rats Model of Cerebral Ischemia-Reperfusion Stroke via Ameliorating Glial Activation and Autophagy. *Neuroscience* 473, 130–141. doi:10.1016/j.neuroscience.2021.08.006

Zhang, S., Jiang, X., Wang, Y., Lin, K., Zhang, Z., Zhang, Z., et al. (2021b). Protective Effect of An-Gong-Niu-Huang Wan Pre-treatment against Experimental Cerebral Ischemia Injury via Regulating GSK-3β/HO-1 Pathway. *Front. Pharmacol.* 12, 640297. doi:10.3389/fphar.2021.640297

Zheng, T., Jiang, H., Jin, R., Zhao, Y., Bai, Y., Xu, H., et al. (2019). Ginsenoside Rg1 Attenuates Protein Aggregation and Inflammatory Response Following Cerebral Ischemia and Reperfusion Injury. *Eur. J. Pharmacol.* 853, 65–73. doi:10.1016/j.ejphar.2019.02.018

Zhou, Y., Li, H. Q., Lu, L., Fu, D. L., Liu, A. J., Li, J. H., et al. (2014). Ginsenoside Rg1 Provides Neuroprotection against Blood Brain Barrier Disruption and Neurological Injury in a Rat Model of Cerebral Ischemia/reperfusion through Downregulation of Aquaporin 4 Expression. *Phytomedicine* 21 (7), 998–1003. doi:10.1016/j.phymed.2013.12.005

Zupanic, E., von Euler, M., Winblad, B., Xu, H., Secnik, J., Kramberger, M. G., et al. (2021). Mortality after Ischemic Stroke in Patients with Alzheimer's Disease Dementia and Other Dementia Disorders. *J. Alzheimers Dis.* 81 (3), 1253–1261. doi:10.3233/JAD-201459

**Conflict of Interest:** The authors declare that the research was conducted in the absence of any commercial or financial relationships that could be construed as a potential conflict of interest.

**Publisher's Note:** All claims expressed in this article are solely those of the authors and do not necessarily represent those of their affiliated organizations, or those of the publisher, the editors, and the reviewers. Any product that may be evaluated in this article, or claim that may be made by its manufacturer, is not guaranteed or endorsed by the publisher.

frontiers in Pharmacology

ORIGINAL RESEARCH
published: 26 January 2022
doi: 10.3389/fphar.2021.774795

# Berberine Alleviate Cisplatin-Induced Peripheral Neuropathy by Modulating Inflammation Signal *via* TRPV1

*Jing Meng*[1,2], *Siyan Qiu*[1], *Ling Zhang*[1], *Min You*[1], *Haizhu Xing*[1] *and Jing Zhu*[1,3]*

[1]*Jiangsu Key Laboratory for Pharmacology and Safety Evaluation of Chinese Materia Medica, Department of Pharmacy, Nanjing University of Chinese Medicine, Nanjing, China,* [2]*Jiangsu Province Key Laboratory of Anesthesia and Analgesia Application Technology, Xuzhou Medical University, Xuzhou, China,* [3]*Department of Neurology and Neuroscience, Johns Hopkins School of Medicine, Baltimore, MD, United States*

Chemotherapy induced peripheral neuropathy (CIPN) is a severe neurodegenerative disorder caused by chemotherapy drugs. Berberine is a natural monomer compound of Coptis chinensis, which has anti-tumor effect and can improve neuropathy through anti-inflammatory mechanisms. Transient receptor potential vanilloid (TRPV1) can sense noxious thermal and chemical stimuli, which is an important target for the study of pathological pain. In both vivo and *in vitro* CIPN models, we found that berberine alleviated peripheral neuropathy associated with dorsal root ganglia inflammation induced by cisplatin. We confirmed that berberine mediated the neuroinflammatory reaction induced by cisplatin by inhibiting the overexpression of TRPV1 and NF-κB and activating the JNK/p38 MAPK pathways in early injury, which inhibited the expression of *p*-JNK and mediated the expression of p38 MAPK/ERK in late injury *in vivo*. Moreover, genetic deletion of *TRPV1* significantly reduced the protective effects of berberine on mechanical and heat hyperalgesia in mice. In *TRPV1* knockout mice, the expression of NF-κB increased in late stage, and berberine inhibited the overexpression of NF-κB and *p*-ERK in late injury. Our results support berberine can reverse neuropathic inflammatory pain response induced by cisplatin, TRPV1 may be involved in this process.

**Keywords: chemotherapy-induced peripheral neuropathy, neurodegenerative disorders, medicine plant, berberine, dorsal root ganglia**

OPEN ACCESS

***Edited by:***
*Shijun Xu,*
*Chengdu University of Traditional Chinese Medicine, China*

***Reviewed by:***
*Gang Chen,*
*Jinan University, China*
*Baohan Pan,*
*Johns Hopkins Medicine, United States*
*Saijilafu,*
*Soochow University Medical College, China*

***Correspondence:**
*Jing Zhu*
*830640@njucm.edu.cn*

***Specialty section:***
*This article was submitted to Neuropharmacology, a section of the journal Frontiers in Pharmacology*

***Received:*** *13 September 2021*
***Accepted:*** *06 December 2021*
***Published:*** *26 January 2022*

***Citation:***
*Meng J, Qiu S, Zhang L, You M, Xing H and Zhu J (2022) Berberine Alleviate Cisplatin-Induced Peripheral Neuropathy by Modulating Inflammation Signal via TRPV1. Front. Pharmacol. 12:774795. doi: 10.3389/fphar.2021.774795*

## 1 INTRODUCTION

The platinum analogue cisplatin (cis-di-amino-di-chloro-platinum, CDDP) was the first platinum-based cytotoxic agent (Quasthoff and Hartung, 2002). Long-term use of CDDP can cause peripheral nerve injury (Staff et al., 2017), known as chemotherapy-induced peripheral neuropathy (CIPN). Platinum-based chemotherapeutics are notably toxic to neurons. Platinum leads to the dysfunction of neuronal membrane excitability and disruption of neurotransmission, induction of inflammation *via* release of proinflammatory chemokines, and alteration of voltage-gated ion channels expression (Ibrahim and Ehrlich, 2020). Platinum ion accumulation leads to DNA damage in dorsal root ganglia (DRG) of the spinal cord. And platinum also induces apoptosis in sensory neurons (Fukuda et al., 2017), resulting in chronic dose-dependent pain and sensory changes. At present, there is no specific clinic drug for treating CIPN. The main clinical treatment is analgesia, supplemented with other sedative drugs. Nonsteroidal anti-inflammatory drugs can temporarily control symptoms for some patients, but the treatment effect in most patients is not satisfactory. Although a variety of

pharmacologic agents have been evaluated for the treatment of CIPN, only duloxetine (DLX) has been recommended to treat CIPN by American Society of Clinical Oncology.

CIPN is one type of chronic neuropathic pain, the expression of transient receptor potential vanilloid (TRPV1) in DRG is an important target which initiates neuron inflammation and paraesthesia. TRPV1 is widely expressed in the middle- and small-diameter neurons of DRG, as well as trigeminal ganglia (TG) (Xu et al., 2013). As a capsaicin receptor and non-selective cation channel, TRPV1 is the primary detector of chemical stimuli and thermally (>43°C) evoked pain sensations (Caterina et al., 1997; Caterina et al., 2000; Davis et al., 2000). By using the mouse model of CDDP-induced neuropathy, researchers found that treatment with CDDP results in an increase of TRPV1 mRNA level in cultured DRG neurons and the similar up-regulation of TRPV1 occurs in CDDP-treated mice (Ta et al., 2009; Ta et al., 2010). Thus, TRPV1 plays a key role in CDDP-induced thermal hyperalgesia in animal models.

In our preliminary works, we found that berberine (BBR) protects DRG nerve cells from damage by chemotherapeutic drugs. Therefore, the protective effect of BBR and its role in inflammation associated with CIPN were explored. BBR is the main active monomer in *Coptis chinensis* and a quaternary ammonium isoquinoline alkaloid, with a wide range of clinical applications (Wu et al., 2016). Recently, more indications of positive effects of BBR have been found. BBR can inhibit the expression and transcription of pro-inflammatory factors IL-1$\alpha$, IL-1$\beta$, IL-8, and TNF-$\alpha$ by inhibiting JNK and TAK1/NF-κB signalling pathways (Zhang et al., 2014; Ni et al., 2021). Other studies have shown that BBR can inhibit the activity of COX-2 and exert anti-inflammatory effects through the PKC pathway, which regulates TRPV1 receptors (Zan et al., 2017). In this study, we observed the protective effects of BBR on neuroinflammatory injury induced by chemotherapeutic drugs and BBR treatment of CIPN does not affect the anti-tumour effect of chemotherapy drugs.

In summary, using CDDP peripheral nerve injury animal and cell models *via TRPV1* gene knockout, we observed changes in inflammatory factors and signals after chronic nerve injury and found the neuroprotective effects of BBR on CIPN.

# 2 MATERIALS AND METHODS

## 2.1 Experimental Animals

All procedures involving animals were performed in accordance with the ethical guidelines established by the International Association for the Study of Pain. This study was approved by the Animal Care and Use Committee of Nanjing University of Chinese Medicine (Nanjing, China). Male C57BL/6 [wild-type (WT)] and *TRPV1*$^{-/-}$ mice weighing 20–22 g was used for these experiments. C57BL/6 mice were purchased from Qinglongshan Animal Centre, Nanjing, China. *TRPV1* knockout mice were obtained from Johns Hopkins University (Baltimore, MD, United States). After backcrossing *TRPV1*$^{-/-}$ mice with WT mice for six generations, *TRPV1*$^{-/-}$ mice were mated with each other to generate null mutant offspring for use in the present study. All animals were held in a humidity- and temperature-controlled environment and maintained in a 12: 12 h light and dark cycle with free access to food and water. All behavioural experiments were performed by an individual blinded to the treatment groups.

## 2.2 Cisplatin Induced Peripheral Neuropathy Model and Drug Administration

Mice were randomly divided into six groups ($n$ = 8 per group). CDDP was dissolved in 0.9% sterile saline to obtain a final concentration of 0.3 mg/ml. CDDP (3 mg/kg) was injected intraperitoneally (i.p.) 8 times (Ta et al., 2009; Carozzi et al., 2014). Normal control mice were injected with sterile saline, consistent with the quantities injected into mice in the drug treated groups. Low (60 mg/kg), medium (90 mg/kg), and high (120 mg/kg) concentrations of BBR were administered orally daily in the first 2 weeks and every other day after 2 weeks. Mice in the duloxetine positive control group were intraperitoneally injected with duloxetine (20 mg/kg, prepared with normal saline). Behavioural tests were performed weekly. The thermal pain threshold in mice were measured at 1, 2, 3, 4, and 8 h after the first administration of CDDP.

## 2.3 Behavioral Assay

### 2.3.1 The Radiant Heat Assay

The thermal radiation tester (37370-001, Ugo Basile, Italy) was used to measure heat hyperalgesia. Mice were placed in a 3 mm thick plexiglass box for 30 min, the light source was directed at the skin of the middle and posterior part of the hind foot of mice, the paw withdrawal latency (PWL) of mice were recorded.

### 2.3.2 Hot Plate Assay

The hot plate (35150-001, Ugo Basile, Italy) was used to determine heat thresholds of mice. Mice were placed on a metal surface maintained at a constant temperature (55 ± 0.5°C). The time from feet touching the hot plate to responding of the hind foot (paw withdrawal or licking, stamping) were recorded. A cut-off time of 60 s was applied to prevent pelma pain.

### 2.3.3 Cold Plate Assay

The cold plate (35150-001, Ugo Basile, Italy) was used to determine heat thresholds of mice. Mice were placed on a metal surface maintained at a constant temperature (4 ± 0.5°C). The time from feet touching the cold plate to responding of the hind foot (paw withdrawal or licking, stamping) were recorded. A cut-off time of 60 s was applied to prevent pelma pain.

### 2.3.4 Tail Flick Test

Half of the tail of each mouse was placed in a 48°C constant temperature water bath. The tail flick latency (TFL) of mice were determined according to the time of immersion into water to tail flick out of the water. A cut-off time of 40 s was applied to prevent tail pain.

### 2.3.5 Mechanical Allodynia

Mechanical allodynia was evaluated using von Frey filaments (37450-001, Ugo Basile, Italy) according to a previously reported method. Mice were placed individually in small cages with a mesh floor for 30 min. A monofilament was applied perpendicularly to the plantar surface of the hind paw, gradually increase the intensity of the stimulus. The time from the beginning of stimulation to raising, licking, or jumping was considered the paw withdrawal latency (PWL, s) time, and the stimulus intensity was the paw withdrawal threshold (PWH, g). Measurements were repeated three times at 5-min intervals, and the mean value was calculated.

## 2.4 Western Blot

DRG tissues were collected from mice and later disrupted in RIPA mixed with PMSF and protease inhibitor cocktail (1×) on ice. Total protein (20 μg) was separated by 10% SDS polyacrylamide gels and then transferred to PVDF membranes (Bio-Rad). After the membranes were blocked for 1 h at room temperature in Tris-buffered saline Tween-20 (TBST) containing 5% skim milk, followed by incubation with primary antibodies specific for p38MAPK (1:4000, CST, Danvers, MA, United States), *p*-p38MAPK (1:4000, CST), ERK1/2 (1:4000, Abcam, MA, United States), *p*-ERK1/2 (1:4000, CST), JNK (1: 3000, Abcam), *p*-JNK (1:3000, Abcam), NF-κB (1:4000, Abcam), TRPV1 (1:2000, Neuromics, INA), and GAPDH (1:8000, CST) at 4°C overnight. After being washed with TBST three times, the membranes were incubated with secondary antibodies (1:10,000, Proteintech, WH, CHN) for 1 h at room temperature. After being washed with TBST three times, the antibodies were detected with ECL reagents (Tanon, SH, CHN). Immunoreactivity was detected by chemiluminescence. The results were quantified using ImageJ software.

## 2.5 Total RNA Extraction and Polymerase Chain Reaction (PCR)

Total RNA was extracted from DRG tissues using Trizol/ chloroform reagent (Thermo-Scientific, United States). RT-PCR was proceeded according to a First Strand cDNA Synthesis Kit (TOYOBO, Japan) and Polymerase Chain Reactor (ABI, United States). Q-PCR was using TransStart Top Green qPCR SuperMix (TransGen Biotech, Beijing, CHN) on a Real-Time PCR System (Applied Biosystems, Foster City, CA, United States). The GAPDH was used as an endogenous reference, its forward primer was TTC CTA CCC CCA ATG TAT CCG, and the reverse primer was CAT GAG GTC CAC CAC CCT GTT. The mRNA expression levels of *NF-κB* and *TRPV1* in DRG tissues were determined using quantitative RT-PCR. The NF-κB forward primer was CTG GTG CAT TCT GAC CTT GC, and the reverse primer was GGT CCA TCT CCT TGG TCT GC. The *TRPV1* forward primer was AAG AGC AAG AAG CGC CTG AC, and the reverse primer was GCA GAG CAA TGG TGT CGT TC. The relative quantification of real-time RT-PCR products was performed using the $2^{-\Delta\Delta CT}$ method (Livak and Schmittgen, 2001).

## 2.6 Immunofluorescence

DRG tissues and primary DRG neurons were fixed with 4% paraformaldehyde for 20 min and washed with phosphate-buffered saline (PBS). The sections were immersed in 0.4% Triton X-100 for 15 min and blocked in 5% BSA for 1 h at room temperature. The sections were then stained with βIII-tubulin mouse monoclonal antibody (1:500, Abcam), anti-TRPV1 (VR1-C)-mouse specific antibody (1:300, Neuromics, INA), and anti-NF-κB antibody (1:500, Abcam, United States) at 4°C overnight, followed by incubation with FITC-conjugated goat anti-mouse IgG (1:200, Proteintech, CHN) for 1 h at room temperature. Sections were treated with DAPI, and immunofluorescence images were visualised using a fluorescence microscope (IX71, Olympus, Japan).

## 2.7 Enzyme-Linked Immunosorbent Assay (ELISA)

The serum levels of inflammatory factors, including nerve growth factor (NGF), NF-κB, TNF-α, IL-1β, IL-6, and IL-10, were assayed using ELISA kits (MaiBo, Nanjing, CHN). The standard curve was drawn in Excel, the regression equation and *R* values were obtained, and the concentration of each test sample was calculated.

## 2.8 Cell Culture and Treatments

Newborn rats were anaesthetised with isoflurane and then decapitated and quickly cut with surgical scissors to isolated DRG. All the above operations were performed on ice. DRG tissues were transferred to L15 (Gibco, United States) for centrifugation, and the supernatant was discarded. Collagenase I (Worthington Biochemical Corporation, United States) was added to cells for 50 min, then the foetal bovine serum (FBS, Gibco) was added to terminate digestion. The deposit was washed with L15. The DRG cells were suspended in neurobasal medium (Gibco, United States) with 10% FBS and 10 ng/ml glial cell line-derived neurotrophic factor (GDNF, Gibco, United States). After suspension, 10,000 cells/mL were counted on a blood count plate and inoculated into poly-L-lysine (Sigma, United States) coated slides or orifice plates. After 24 h of incubation in a 37°C and 5% $CO_2$ incubator, the DRG neuron culture medium was exchanged for drug-containing culture medium.

CDDP was diluted in 2% FBS neurobasal culture medium to a final concentration of 3 μM. BBR was diluted to concentrations of 10 nM, 30 nM, 100 nM, 300 nM, 1 μM, 3 μM, 10 μM, and 30 μM in neurobasal medium containing 3 μM CDDP and 2% FBS. In the control group, 2% FBS-containing neuron culture medium was added. The cells were then incubated at 37°C and 5% $CO_2$ incubator for 48 h. Cell viability was measured using a 3-(4,5-dimethylthiazol-2-yl)-2, 5-diphenyltetrazolium bromide (MTT) assay.

## 2.9 Data Analysis

All data are expressed as means ± standard errors of means. One-way ANOVA with correction for multiple comparisons was performed in GraphPad Prism 8. Animal behaviour data were

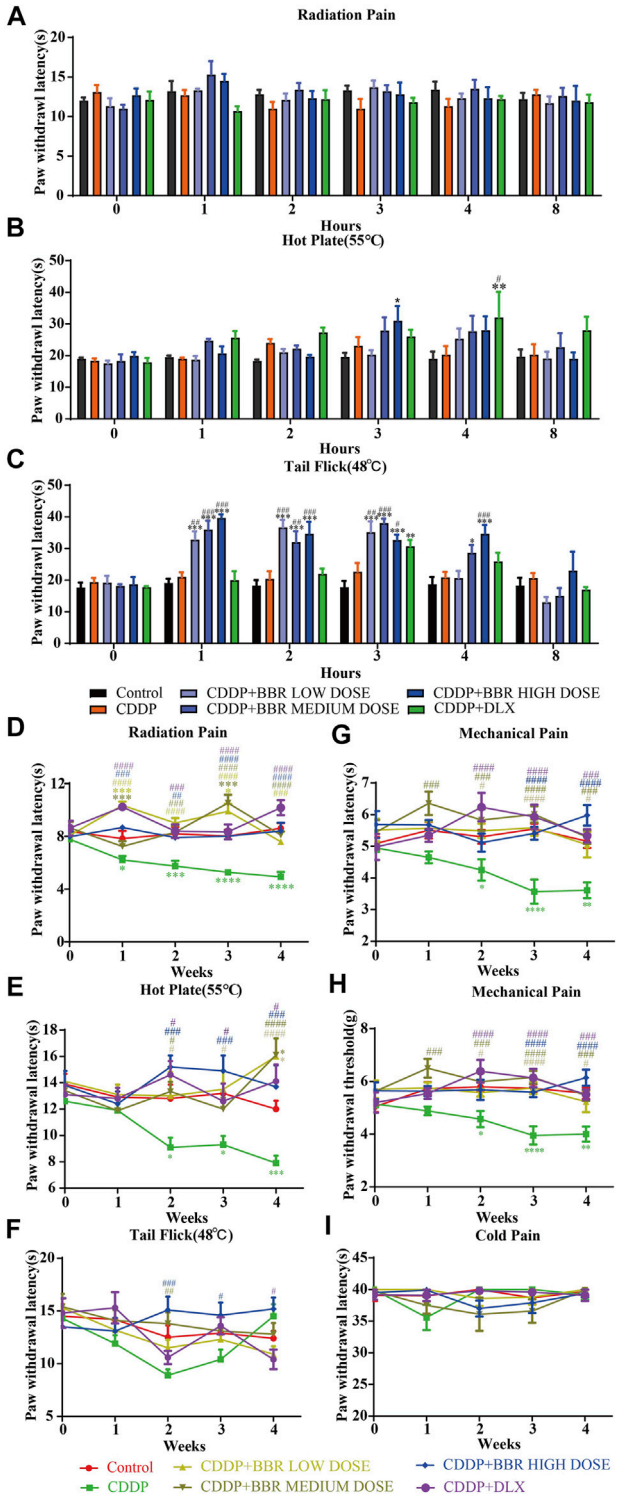


**FIGURE 1 |** BBR increased the pain threshold and inhibited thermal hyperalgesia induced by CDDP. **(A)** The latent period of paw withdrawal induced by light radio stimulation. **(B)** The paw withdrawal latency stimulated by 55°C hot plate. **(C)** Preventive administration of BBR increased the latency of tail flick of mice for 2–3 h after immersion in a 48°C water bath. The thermal pain threshold of the pelma [**(D)**: $F = 4.983$, $p < 0.0001$] and tail [**(E)**: *(Continued)*

**FIGURE 1 |** F = *1.927*, p = *0.0007*] ***[(F)****: F = 2.086, p = 0.004] in CDDP mice decreased significantly after 2 weeks treatment, and the tail thermal heat pain threshold gradually increased after the third week.* ***(G,H)*** *The foot mechanical pain threshold in CDDP model mice was significantly lower than that of control* ***[(G)****: F = 1.994, p = 0.008]. After berberine treatment, the pain improved significantly* ***[(H)****: F = 2.206, p = 0.0059].* ***(I)*** *The latency of tail responses to cold pain was no significant difference. Statistical analysis was performed using repeated ANOVA (n = 6–8; *p < 0.05, **p < 0.01, ***p < 0.001, ****p < 0.0001, compared with control group. #p < 0.05, ##p < 0.01; ###p < 0.001 compared with the CDDP group). CBL: CDDP + BBR low dose; CBM: CDDP + BBR medium dose; CBH: CDDP + BBR high dose.*

analysed using repeated ANOVA. Statistical significance was set at $p < 0.05$.

# 3 RESULTS

## 3.1 Berberine Protects Against CDDP-Induced Hyperalgesia

A significant ($p < 0.05$, $p < 0.001$) development of thermal hyperalgesia was observed in the CDDP group compared to the control (**Figure 1**). Preventive administration of BBR significantly increased the pain threshold of mice for 2–3 h ($p < 0.01$, $p < 0.001$) (**Figure 1C**). Duloxetine treatment also increased the thermal heat pain threshold of mice ($p < 0.01$, $p < 0.001$) (**Figure 1**). The above results suggest that CDDP can induce thermal hyperalgesia in mice after a single administration for 2 h, and the pain disappears gradually after 3–4 h. All doses of BBR (low dose 60 mg/kg, medium dose 90 mg/kg, high dose 120 mg/kg) can increase the pain threshold and inhibit thermal hyperalgesia induced by CDDP. The effect of BBR was similar to that of duloxetine group.

After 1 week of administration, the thermal heat pain threshold of the pelma and tail decreased in the CDDP group mice. However, the difference from the control was not significant. Two weeks later, the thermal pain threshold of the pelma and tail in CDDP mice decreased significantly ($p < 0.05$, $p < 0.01$, $p < 0.001$) (**Figures 1D–F**), and the tail thermal heat pain threshold gradually increased after the third week, possibly because of severe tail injury and sensory numbness. Duloxetine only alleviated CDDP-induced pain behaviour with radiation heat and hot plate test (**Figures 1D,E**), but showed no significant effect on tail withdrawal latencies (**Figure 1F**). BBR can improve hypersensitivity induced by radiation heat and thermal stimulation at 55°C (**Figures 1D,E**), and BBR (90 mg/kg and 120 mg/kg) increased the tail flick threshold by the second week ($p < 0.01$, $p < 0.001$) (**Figure 1F**).

At the second, third, and fourth week, the foot mechanical pain threshold in CDDP model mice was significantly lower than that of control, and the mechanical pain threshold in the duloxetine group was significantly higher than that in the CDDP group ($p < 0.001$) (**Figures 1G,H**). Compared with the CDDP group, BBR increased the threshold of mechanical pain, and 90 mg/kg BBR was found to be the optimum concentration for this increase (**Figures 1G,H**). There was no significant difference in tail responses to cold pain (**Figure 1I**).

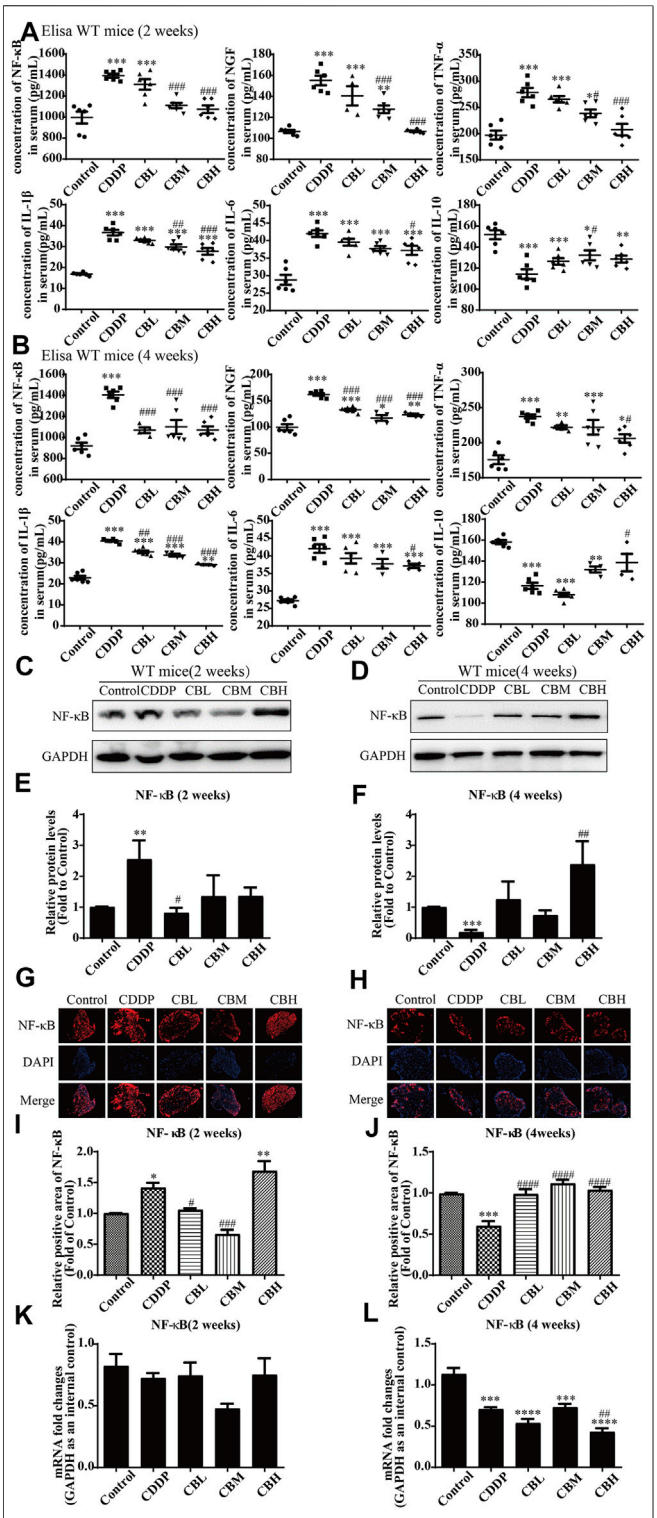


**FIGURE 2 |** BBR reduces inflammation in serum and the overexpression of NF-κB protein in DRG in CDDP model of WT mice. **(A,B)** The effect of BBR on serum levels of inflammatory factors NF-κB, NGF, TNF-$\alpha$, IL-1$\beta$, IL-6 and IL-10 were in CDDP-induced mice by ELISA. CDDP induced NF-κB ($F$ = 17.81, $p < 0.001$), NGF ($F$ = 28.46, $p < 0.001$), TNF-$\alpha$ ($F$ = 17.34, $p < 0.001$), IL-1$\beta$ ($F$ = 49.53, $p < 0.001$), and IL-6($F$ = 20.90, $p < 0.001$) up-regulation in

(*Continued*)

**FIGURE 2 |** DRG for 2 and 4 weeks, and BBR reversed inflammatory factors up-expression in DRG. CDDP induced IL-10 under-regulation in DRG for 2 and 4 weeks, and BBR inhibited IL-10 under-regulation in DRG ($F$ = 11.30, $p <$ 0.001). **(C,E)** Western blot results and their quantitative data show CDDP induced NF-κB up-regulation in spinal DRG for 2 weeks, and BBR inhibited NF-κB over-expression in DRG, after 2 weeks of treatment. **(D,F)** Western blot results and their quantitative data show CDDP induced NF-κB under-regulation lasted for 4 weeks ($F$ = 3.645, $p$ = 0.0288). **(G,I)** Immunofluorescence results and the quantitative data show CDDP induced NF-κB up-regulation, and BBR inhibited NF-κB over-expression in DRG after 2 weeks of treatment. **(H,J)** Immunofluorescence results and their quantitative data show CDDP induced NF-κB under-regulation lasted for 4 weeks. **(K)** There was no significant difference in the expression of NF-κB mRNA after 2 weeks of BBR treatment ($p > 0.05$). **(L)** The expression of NF-κB protein and mRNA decreased at 4 weeks ($F$ = 30.54, $p < 0.0001$). Statistical analysis was performed using one-way ANOVA (*$p < 0.05$, **$p < 0.01$, ***$p < 0.001$, ****$p < 0.0001$, compared with the control group; $^{\#}p < 0.05$, $^{\#\#}p < 0.01$, $^{\#\#\#}p < 0.001$, $^{\#\#\#\#}p <$ 0.0001, compared with the CDDP group). CBL: CDDP + BBR low dose; CBM: CDDP + BBR medium dose; CBH: CDDP + BBR high dose.

## 3.2 Berberine Inhibits CDDP-Induced Serum Pro-inflammatory Factors

Compared with the CDDP group, BBR 2- and 4-weeks treatment group decreased the levels of pro-inflammatory factor NF-κB, NGF, IL-1$\beta$, IL-6, and TNF-$\alpha$ in mice serum and increased the level of anti-inflammatory factor IL-10 (**Figures 2A,B**). This suggests that the anti-inflammatory effect of BBR may be mediated by the mobilisation of serum inflammatory factors.

## 3.3 Berberine Regulates Nuclear Factor NF-κB and JNK/p38MAPK/ERK Inflammatory Pathways

Long-term use of CDDP causes a neuroinflammatory response and interferes with inflammatory signalling. Western blot results showed that the expression of NF-κB in DRG increased significantly after 2 weeks of CDDP use (**Figures 2C,E**), and the expression of NF-κB protein (**Figures 2D,F**) and mRNA (**Figure 2L**) decreased at 4 weeks ($p < 0.001$). This suggested that NF-κB participated in neurological damage induced by CDDP, but there were opposing effects at early and late stages of treatment. A high dose of BBR can reverse the expression of NF-κB induced by CDDP (**Figures 2G–I**). Moreover, after 2 weeks of BBR treatment, the overexpression of proteins (JNK, *p*-JNK, and p38) induced by CDDP were alleviated in the DRG (**Figures 3A,B**). At 4 weeks of BBR treatment, CDDP-induced DRG inflammation (**Figures 3C,D**) was ameliorated mainly by promoting the expression of ERK1/2 and *p*-p38 and inhibiting JNK phosphorylation. JNK/ERK/p38MAPK signalling pathways play crucial roles in BBR protection against CDDP-induced neuroinflammatory injury.

## 3.4 Effect of Berberine on TRPV1 Expression in Dorsal Root Ganglia

CDDP induced TRPV1 up-regulation (**Figures 4A,C**) in spinal DRG for 2 weeks, and this effect lasted for 4 weeks (**Figures**

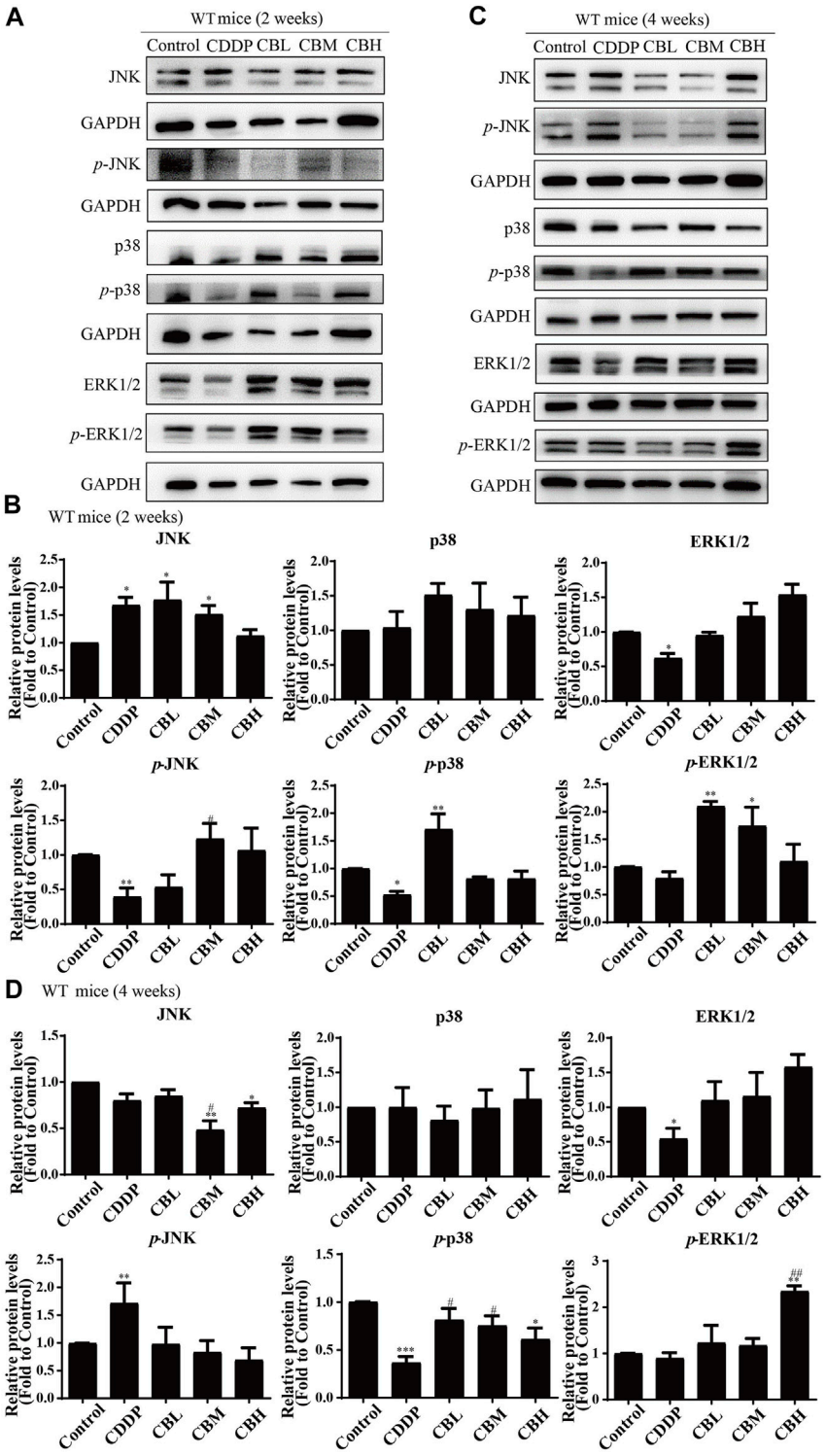


**FIGURE 3 |** BBR regulates JNK/p38MAPK signaling pathway. **(A,B)** Western blot results and their quantitative data show CDDP induced *p*-JNK and *p*-p38 under-regulation in spinal DRG for 2 weeks, and BBR inhibited *p*-JNK and *p*-p38 under-expression in DRG. **(C,D)** Western blot results and their quantitative data show CDDP induced ERK1/2 ($F = 2.817$, $p = 0.0838$) and *p*-p38($F = 6.596$, $p = 0.0029$) under-regulation in spinal DRG for 4 weeks, and BBR inhibited ERK1/2 and *p*-p38 under-expression in DRG. Statistical analysis was performed using one-way ANOVA ($n = 6$, $^{*}p < 0.05$, $^{**}p < 0.01$, $^{***}p < 0.001$, compared with the control group; $^{\#}p < 0.05$, $^{\#\#}p < 0.01$, $^{\#\#\#}p < 0.001$, compared with the CDDP group). CBL: CDDP + BBR low dose; CBM: CDDP + BBR medium dose; CBH: CDDP + BBR high dose.

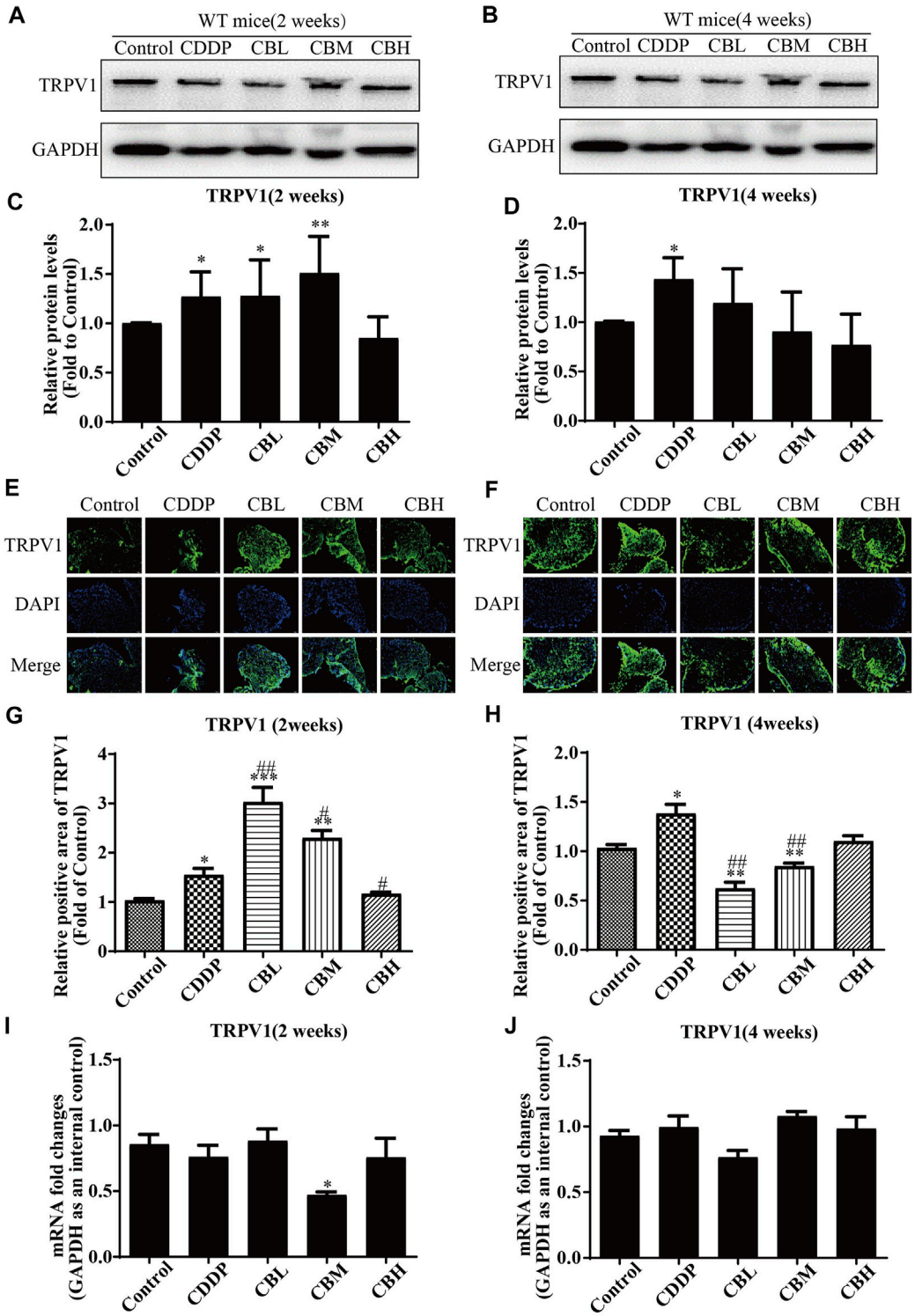


**FIGURE 4 |** BBR inhibits up-regulation of TRPV1 protein in CDDP-induced DRG of WT mice. **(A,C)** Western blot results and their quantitative data show CDDP induced TRPV1 up-regulation in spinal DRG for 2 weeks. **(B,D)** Western blot results and their quantitative data show CDDP induced TRPV1 up-regulation lasted for 4 weeks, and BBR inhibited TRPV1 over-expression in DRG after 4 weeks of treatment. **(E,G)** Immunofluorescence results and their quantitative data show CDDP induced TRPV1 up-regulation in DRG for 2 weeks. **(F,H)** Immunofluorescence results and their quantitative data show CDDP induced TRPV1 up-regulation lasted for 4 weeks, and BBR inhibited TRPV1 over-expression in DRG after 4 weeks of treatment. Statistical analysis was performed using one-way ANOVA (*$p < 0.05$, **$p < 0.01$, ***$p < 0.001$, compared with the control group; $^{\#}p < 0.05$, $^{\#\#}p < 0.01$, $^{\#\#\#}p < 0.001$, compared with the CDDP group). CBL: CDDP + BBR low dose; CBM: CDDP + BBR medium dose; CBH: CDDP + BBR high dose.

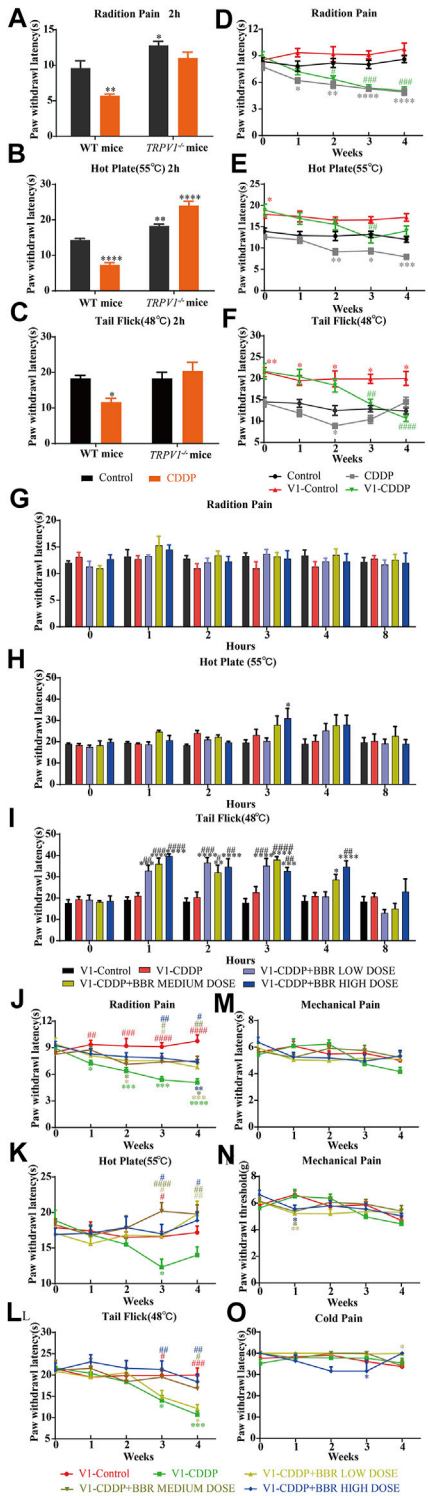


**FIGURE 5 |** BBR increased the pain threshold and inhibited thermal hyperalgesia induced by CDDP in *TRPV1*$^{-/-}$ mice. **(A–C)** Heat pain thresholds in *TRPV1*$^{-/-}$ mice increased 2 h and 4 weeks after initial administration. *TRPV1*$^{-/-}$ mice were less sensitive to heat pain than WT mice. ($F = 2.039$; $^{*}p < 0.05$; $^{**}p < 0.01$, $^{****}p < 0.0001$, compared with the control group of WT mice). **(D–F)** Heat pain thresholds in *TRPV1*$^{-/-}$ mice increased 4 weeks after

(*Continued*)

**FIGURE 5 |** initial administration. *TRPV1*$^{-/-}$ mice were less sensitive to heat pain than WT mice ($F = 1.54$; $^{*}p < 0.05$; $^{**}p < 0.01$; $^{***}p < 0.001$, $^{****}p < 0.0001$, compared with the control group of WT mice; $^{\#}p < 0.05$, $^{\#\#}p < 0.01$, $^{\#\#\#}p < 0.001$, $^{\#\#\#\#}p < 0.0001$, V1-CDDP group compared with the V1-control group). **(G–L)** After single administration and 4 weeks, BBR effectively increased the heat pain threshold of *TRPV1*$^{-/-}$ mice ($F = 4.527$, $p < 0.0001$). **(M–O)** There was no significant change in mechanical and thermal pain thresholds in *TRPV1*$^{-/-}$ mice ($F = 2.378$, $p = 0.0028$). Statistical analysis was performed using repeated ANOVA ($n = 6$; $^{*}p < 0.05$, $^{**}p < 0.01$, $^{***}p < 0.001$, $^{****}p < 0.0001$, compared with the control group, $^{\#}p < 0.05$, $^{\#\#}p < 0.01$, $^{\#\#\#}p < 0.001$, $^{\#\#\#\#}p < 0.0001$, compared with the CDDP group). CBL: CDDP + BBR low dose; CBM: CDDP + BBR medium dose; CBH: CDDP + BBR high dose.

**4B,D**). BBR inhibited TRPV1 over-expression only in the high-dose treatment group by the second week. After 4 weeks of treatment, BBR inhibited TRPV1 over-expression in DRG (**Figures 4B,D**). The results of immunofluorescence staining of TRPV1 were consistent with those of western blotting (**Figures 4E–H**). There was no significant difference between *TRPV1* mRNA expression in DRG in all groups (**Figures 4I,J**).

## 3.5 Behavioural Changes Associated With Pain in TRPV1 $^{-/-}$ Mice

*TRPV1* knockout mice had a higher thermal heat pain threshold than WT mice. WT mice were hypersensitive to heat at 2 h after a single injection of CDDP, but *TRPV1* knockout mice were not (**Figures 5A–C**). After continuous injection of CDDP, a hypersensitivity to heat stimulation in WT mice was apparent at approximately 2 weeks, the *TRPV1* knockout mice were delayed to about 3 weeks (**Figures 5D–F**). The behavioural results suggest that CDDP-induced neurofibrillary hyperalgesia may be associated with increased expression of *TRPV1*. After the *TRPV1* gene is deleted, hyperalgesia can be controlled within 2 weeks, but other thermal hyperalgesia responses can occur after 3 weeks.

The BBR treatment groups were similar to the control group in their thermal pain thresholds on the first day of administration in *TRPV1*$^{-/-}$ mice (**Figures 5G–I**). The tail-flick latency was significantly increased at 1–3 h after BBR administration in *TRPV1*$^{-/-}$ mice (**Figure 5I**). This indicated that the *TRPV1* gene knockout has a synergistic effect with BBR.

After continuous administration, there was no difference in the pain threshold between the BBR group and the control group in *TRPV1* gene knockout mice. BBR led to remission of CDDP-induced thermal hyperalgesia after 3 weeks (**Figures 5J,K,L**). There was no difference in the responses of the mice in different groups to mechanical and cold stimuli (**Figures 5M–O**). This suggested that BBR treatment in the late stage of CIPN may involve other mechanisms besides that associated with TRPV1.

## 3.6 Effect of Inflammatory Factors in the Sera of TRPV1$^{-/-}$ Mice

The levels of pro-inflammatory factors (NF-κB, NGF, IL-1$\beta$, IL-6, and TNF-$\alpha$) in serum were decreased in a dose-dependent

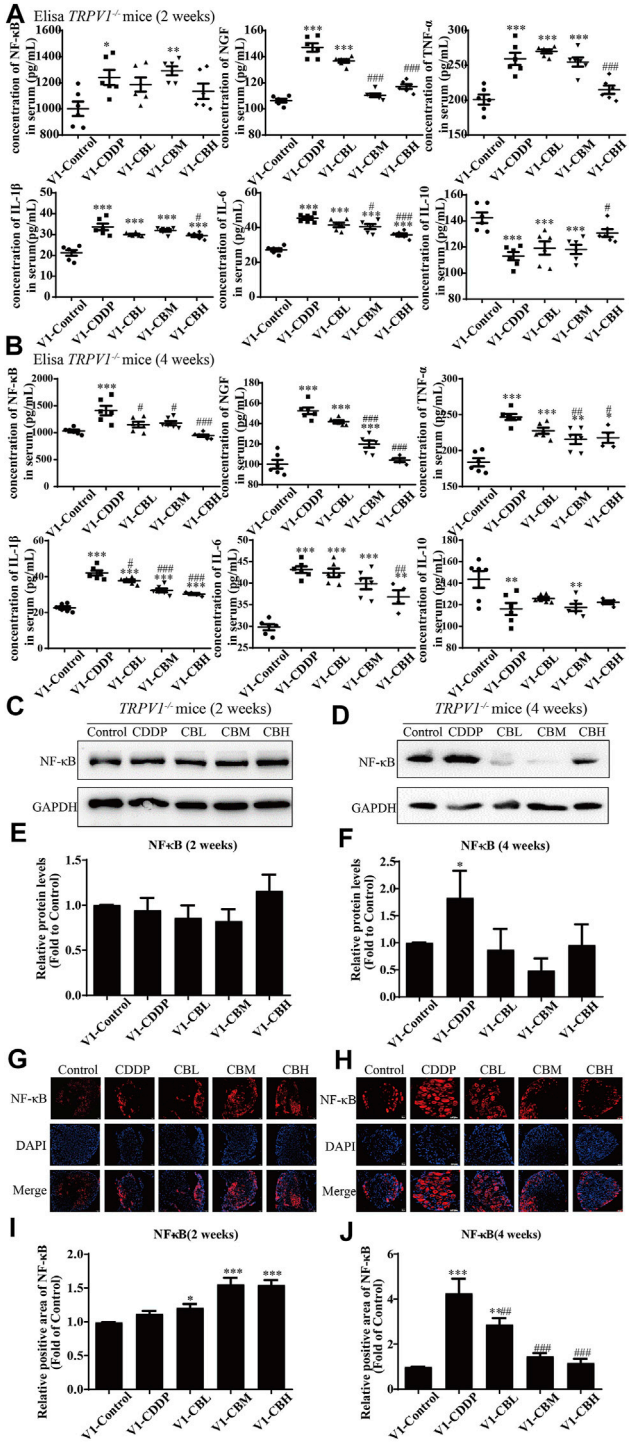


**FIGURE 6 |** BBR reduces inflammation in mice and inhibits the overexpression of NF-κB in *TRPV1*$^{-/-}$ mice induced by CDDP. **(A,B)** Expression of inflammatory cytokines NF-κB, NGF, IL-1$\beta$, IL-6, TNF-$\alpha$ and IL-10 in serum were determined by ELISA ($n$ = 4–6). BBR can down-regulate the expression of pro-inflammatory cytokines NGF, TNF-$\alpha$, IL-1$\beta$, IL-6 and up-regulate the expression of anti-inflammatory cytokines IL-10 in the serum of *TRPV1*$^{-/-}$ mice. **(C–F)** Western blot showed the levels of NF-κB in the DRGs of *TRPV1*$^{-/-}$ mice. **(G–J)** Immunofluorescence staining showed NF-κB relative abundance in DRG of *TRPV1*$^{-/-}$ mice. Section Thickness = 10 mm, Scale bar = 50 μm. **(C,E,G,I)** There was no difference in the protein expression of NF-κB in DRG of mice in each group at the second week after *TRPV1* knockout. **(D,F,H,J)** At the fourth week after *TRPV1* knockout, the expression of NF-κB was significantly increased in the CDDP group, while BBR treatment could inhibit its overexpression ($F$ = 17.24, $p$ = 0.0002). Statistical analysis was performed using one-way ANOVA ($n$ = 3; $^{*}p < 0.05$, $^{**}p < 0.01$, $^{***}p < 0.001$, compared with the control group; $^{\#}p < 0.05$, $^{\#\#}p < 0.01$; $^{\#\#\#}p < 0.001$, compared with the CDDP group). CBL: CDDP + BBR low dose; CBM: CDDP + BBR medium dose; CBH: CDDP + BBR high dose.

manner for 2 weeks and, after 4 weeks of treatment with BBR, the level of anti-inflammatory factor IL-10 was increased. There was no difference between wild type group and *TRPV1*$^{-/-}$ group (**Figures 2A**,**2B**, **6A**,**6B**). These results suggested that serum inflammatory factors may be upstream factors that triggered intracellular signal transduction in DRG, so they were not affected by deletion of TRPV1.

## 3.7 Effect of Berberine on the NF-κB and JNK/p38 MAPK/ERK Pathways in Dorsal Root Ganglia of TRPV1 $^{-/-}$ Mice

There was no difference in the protein expression of NF-κB in DRG of *TRPV1* $^{-/-}$ mice at the second week (**Figures 6C,E,G,I**). At the fourth week, NF-κB expression was increased in the CDDP group, and BBR was shown to relieve neurological symptoms by inhibiting NF-κB expression (**Figures 6D,F,H,J**). In our previous study, BBR inhibited the expression of NF-κB induced by CDDP after 2 weeks of treatment and promoted the expression of NF-κB after 4 weeks of treatment in WT mice (**Figure 2**). This indicated that NF-κB expression was completely blocked by *TRPV1* knockout at an early stage in CDDP animals (**Figures 2C**,E, **6C**,E). However, even the *TRPV1* gene was knocked out, the level of NF-κB protein was still elevated in the late model of CDDP (**Figures 3D**,F, **6D**,F), and BBR inhibited the high expression of NF-κB in late-stage CIPN. Moreover, the expression of JNK, p38, and ERK1/2 decreased and $p$-p38 and $p$-ERK1/2 increased in response to CDDP in DRG of *TRPV1*$^{-/-}$ mice. After 2 weeks of treatment, BBR maintained the expression of JNK, p38, and ERK1/2, and inhibited the phosphorylation of p38 and ERK1/2 in *TRPV1*$^{-/-}$ mice (**Figures 7A,B**). In contrast, BBR treatment promoted the phosphorylation of p38 and ERK1/2 in WT mice at 2 weeks (**Figures 3A,B**). This suggested that BBR may regulate JNK/p38 MAPK/ERK inflammatory signalling mediated by the *TRPV1* receptor in CIPN. At 4 weeks, there was no significant difference in MAPK signalling pathways proteins expression in *TRPV1* knockout mice before and after BBR treatment (**Figures 7C,D**).

## 3.8 Berberine Alleviates Cultured Dorsal Root Ganglia Neuron Damage Induced by CDDP

To study whether BBR directly exerts anti-inflammatory effects on DRG, we cultured DRG neurons *in vitro* and observed changes in intracellular inflammatory signals. After incubation with 3 μM

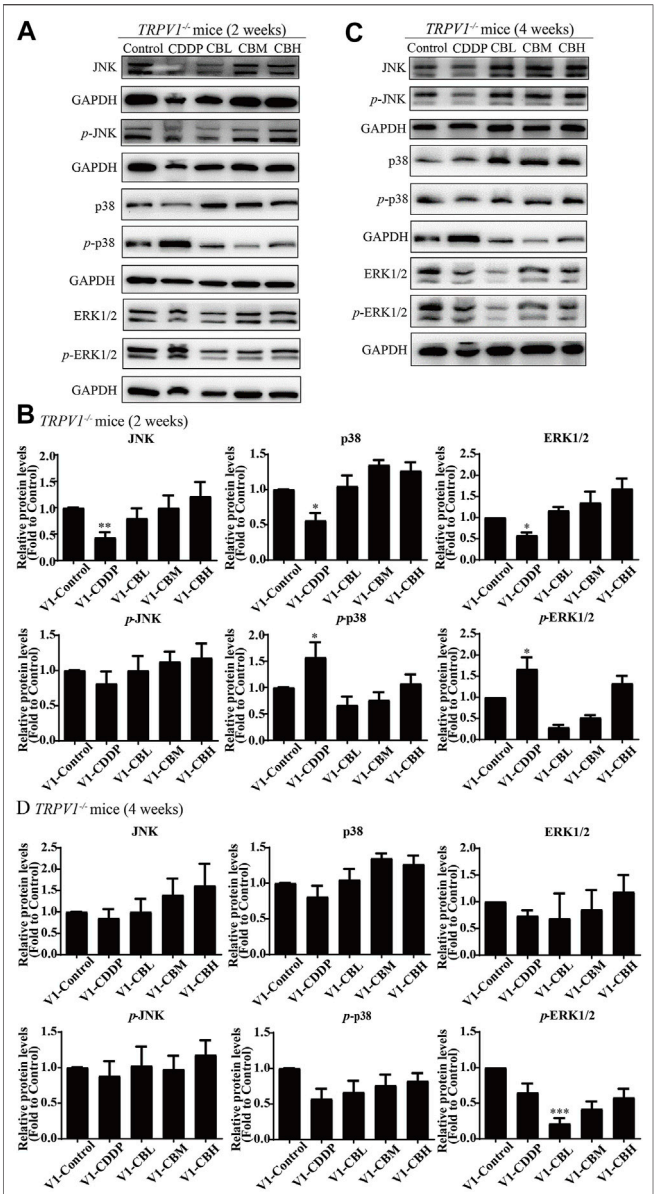


**FIGURE 7 |** BBR regulates TRPV1-mediated MAPKs signaling pathway in mice. Western blot showed the levels of MAPKs inflammatory pathway protein in the DRGs of *TRPV1*$^{-/-}$ mice ($n$ = 3). **(A,B)** After 2 weeks of treatment, BBR up-regulated the downregulation expression of JNK, p38, ERK1/2 induced by CDDP, and inhibited the phosphorylation of p38($F$ = 8.702, $p$ = 0.0008) and ERK1/2 ($F$ = 6.228, $p$ = 0.0037) in *TRPV1*$^{-/-}$ mice. **(C,D)** There was no significant difference in MAPKs signaling pathway protein expression in each group of mice after 4 weeks of treatment. Statistical analysis was performed using one-way ANOVA ($^{*}p < 0.05$, $^{**}p < 0.01$, $^{***}p < 0.001$, compared with the control group; $^{\#}p < 0.05$, $^{\#\#}p < 0.01$; $^{\#\#\#}p < 0.001$, compared with the CDDP group). CBL: CDDP + BBR low dose; CBM: CDDP + BBR medium dose; CBH: CDDP + BBR high dose.

CDDP for 48 h, the neuronal cell viability was decreased to 40–50% (**Figure 8A**). 3 μM BBR treatment significantly enhanced cell viability (**Figure 8B**) compared with CDDP group using the MTT assay. Then, the morphology of DRG neurons was examined (**Figure 8C**). Measuring the axon length of neurons, 3 μM CDDP was found to cause axon degeneration, whereas 3 μM BBR co-incubated with CDDP protected normal axon growth in neurons (**Figure 8D**), which was consistent with the results of βIII-tubulin immunofluorescence staining (**Figure 8E**).

## 3.9 Effect of Berberine on the NF-κB and JNK/p38 MAPK/ERK Pathways in Dorsal Root Ganglia Neurons

Western blot and immunofluorescence staining were used to examine the expression of NF-κB 48 h after treatment with BBR. The results showed that CDDP caused overexpression of NF-κB in neurons, and BBR normalized the protein level (**Figures 9A–D**). Hence BBR may reduce the inflammatory damage of DRG neurons induced by CDDP by inhibiting NF-κB signalling. Furthermore, the expression of JNK, p38, and *p*-p38 increased and the expression of *p*-JNK decreased in DRG neurons incubated with 3 μM CDDP for 48 h. Co-incubation with 3 μM BBR inhibited the expression of *p*-ERK1/2 and p38 (**Figures 9E,F**). The results indicate that BBR can reduce damage to DRG neurons by regulating JNK/p38 MAPK/ERK inflammatory signalling *in vitro*.

# 4 DISCUSSION

This study showed that a single dose of CDDP caused thermal hyperalgesia for 2 h in mice, and then the thermal hyperalgesia gradually disappeared in 1–2 h. Long-term administration of CDDP for 2 weeks can cause peripheral nerve pain abnormalities. BBR attenuated peripheral hyperalgesia induced by CDDP (single dose and long-term) in mice, and its improvement was similar to the duloxetine group. Experiments *in vitro* demonstrated that BBR can increase the activity of DRG neurons and reduce the damage of CDDP to cells. Previous studies have shown that BBR has neuroprotective effects, it can alleviate diabetic peripheral neuropathy (Yang wt al., 2020) and protect DRG neuronal cells from high glucose damage (Yerra et al., 2018). And other studies have suggested that BBR can reduce paclitaxel induced peripheral nerve injury (Singh et al., 2018). Our study indicates that BBR can be used to prevent and treat cisplatin induced peripheral neuropathy.

The success of CDDP injury model of primary cultured DRG neuronal cell can be identified by cell viability and morphological changes. Neuronal cell bodies and axons were identified respectively with neuron-specific nuclear protein NeuN and β-III tubulin (Guo et al., 2017). More and more studies have shown that oxidative stress in spinal dorsal root ganglion may underlie the pathogenesis of platinum induced peripheral neurotoxicity. The binding of platinum ions bind to DNA leads to mitochondrial dysfunction and DRG energy failure (Carozzi et al., 2010). *In vitro* and *in vivo* studies have shown that CDDP induced neuronal apoptosis in DRG was associated with changes in cyclin expression (Fischer et al., 2001; Mcdonald et al., 2005), and MAPK family members

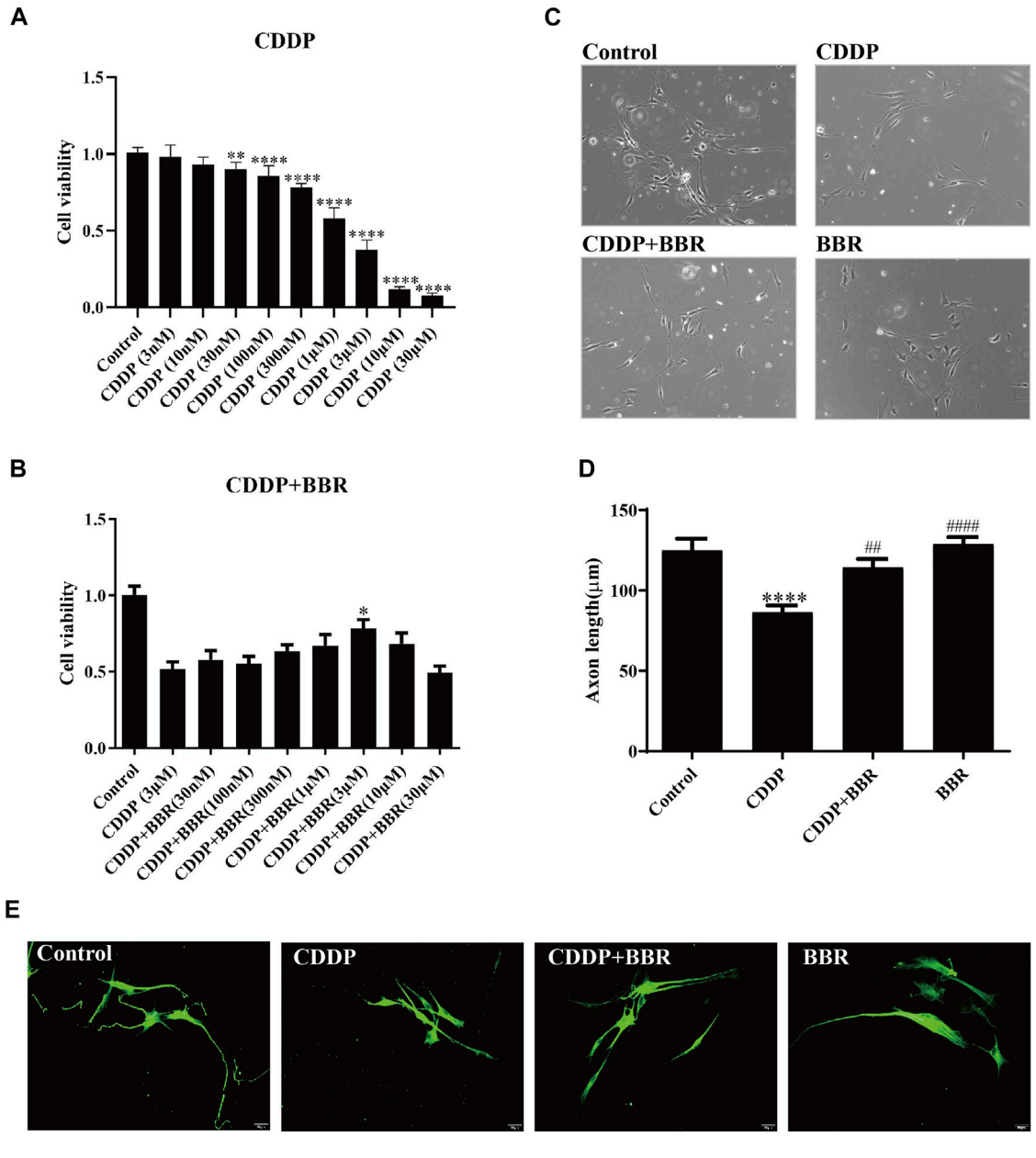


**FIGURE 8 |** BBR protects DRG cells from damage induced by CDDP. **(A)** The MTT assay was used to measure the survival rate of neurons. DRG neurons were cultured with CDDP (3 μM) for 48 h, the cell viability was decreased to 40–50% ($n = 6$, $F = 301.7$, $p < 0.0001$). **(B)** An injury model of neurons cultured with CDDP (3 μM) was established, and then DRG was cultured with different concentration gradient BBR for 48 h. The results showed that BBR (3 μM) enhanced cell viability ($F = 8.034$, $p < 0.0001$). **(C)** Primary DRG neuronal cell were cultured with CDDP (3 μM). **(D)** CDDP (3 μM) contributes to the axon growth, whereas BBR (3 μM) co-incubated with CDDP protected normal axon growth in neurons or BBR (3 μM) for 48 h ($F = 13.59$, $p < 0.0001$). **(E)** Neuron specific nucleoprotein βIII-tubulin staining was used to identify primary DRG cell axons. BBR (3 μM) attenuates the damage of CCDP to primary DRG cells. Statistical analysis was performed using one-way ANOVA ($^{*}p < 0.05$, $^{**}p < 0.01$, $^{***}p < 0.001$, $^{****}p < 0.0001$, compared with the control group; $^{\#\#}p < 0.01$, $^{\#\#\#\#}p < 0.0001$, compared with the CDDP group). CBL: CDDP + BBR low dose; CBM: CDDP + BBR medium dose; CBH: CDDP + BBR high dose.

(ERK1/2, JNK, p38) are involved in peripheral nerve injury (Myers et al., 2003; Zielinska, 2003; Cavaletti et al., 2010; Belair, 2021). Platinum induced apoptosis of DRG neuronal is mediated by the early activation of p38 and ERK1/2 (Scuteri et al., 2009), whereas JNK/SAPK is involved in cell repair and protects neurons from platinum ion damage (Middlemas et al., 2003; Potapova et al., 1997). All of the above studies suggest that platinum ion induced peripheral neuropathy triggers oxidative stress and apoptosis of DRG neurons through the MAPK signalling pathways.

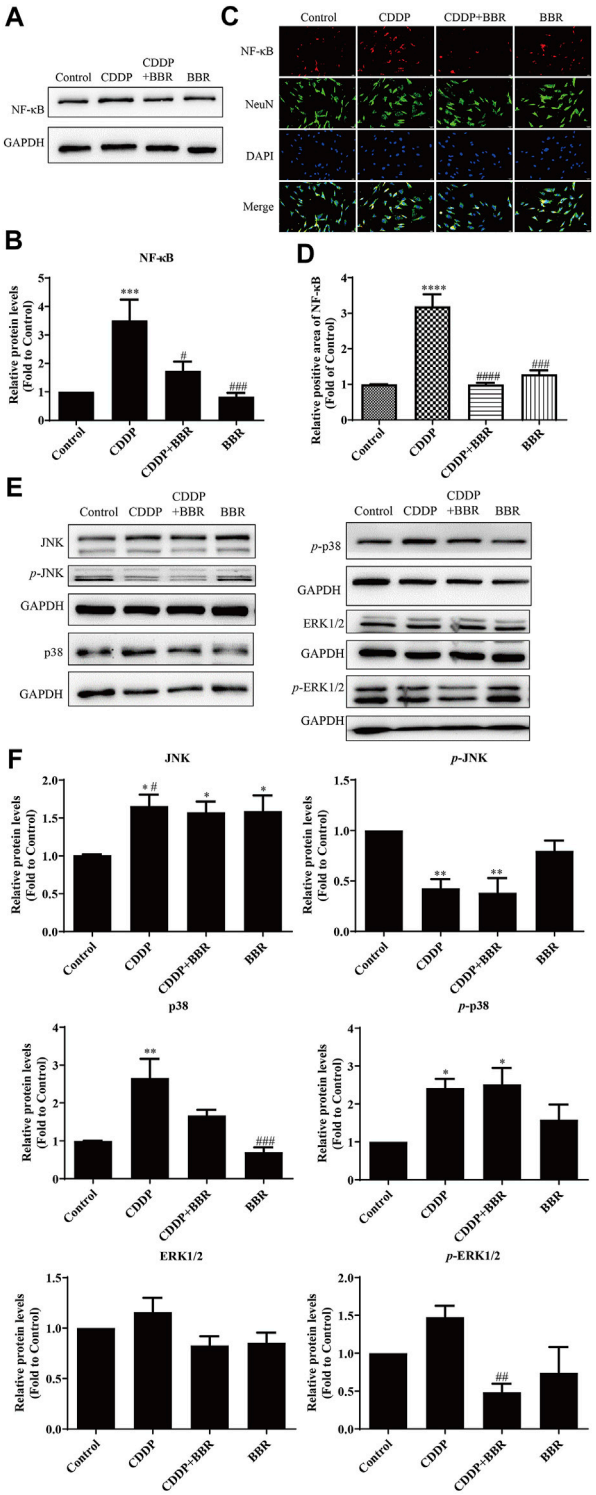


**FIGURE 9 |** BBR inhibits the overexpression of NF-κB in DRG neurons induced by CDDP. **(A,B)** BBR inhibits the overexpression of NF-κB induced by CDDP ($F = 9.178$, $p = 0.0002$). **(C)** Immunofluorescence staining showed NF-κB relative abundance induced by CDDP and BBR stimulation in DRG cells NeuN labeled neurons. Scale bar = 20 μm. **(D)** The quantitative of immunofluorescence showed that 3 μM BBR alleviates the expression of NF-

(*Continued*)

**FIGURE 9 |** ?B in DRG tissue ($F = 43.49$, $p < 0.0001$). **(E,F)** CDDP (3 μM, 48 h) increased the expression of JNK, p38, and *p*-p38, and decreased the expression of *p*-JNK, *p*-ERK1/2 and p38. Co-incubation with 3 μM BBR inhibited the expression of *p*-ERK1/2 ($F = 4.764$, $p = 0.0207$) and p38 ($F = 10.3$, $p = 0.0005$). Statistical analysis was performed using one-way ANOVA ($n = 3$; $^{*}p < 0.05$, $^{**}p < 0.01$, $^{***}p < 0.001$, $^{****}p < 0.0001$, compared with the control group; $^{\#}p < 0.05$, $^{\#\#}p < 0.01$, $^{\#\#\#}p < 0.001$, $^{\#\#\#\#}p < 0.0001$, compared with the CDDP group). CBL: CDDP + BBR low dose; CBM: CDDP + BBR medium dose; CBH: CDDP + BBR high dose.

Previous studies have shown that BBR can protect neurons by anti-apoptotic, anti-oxidative, and anti-inflammatory effects through PI3K/Akt/Bcl-2, Akt/NF-κB, and MAPK signalling (Zhang et al., 2018). BBR have reduced neuronal damage both *in vivo* and *in vitro* by inhibiting inflammatory responses and reducing the production of inflammatory mediators rather than directly exerting anti-inflammatory effects on neuronal cells. BBR have inhibited the expression and activity of tissue factors induced by lipopolysaccharide, whereas NF-κB, AKT, and JNK/p38 MAPK/ERK pathways were downregulated (Gao et al., 2014). BBR have also exerted anti-inflammatory effects by inhibiting COX-2 (Feng et al., 2012). As a treatment for traumatic inflammation, BBR inhibited TAK1/JNK and TAK1/NF-κB signalling by reducing phosphorylation of JNK and NF-κB, and reducing the expression of inflammation factors IL-1$\beta$, IL-6, IL-8, TNF-$\alpha$, and TGF-$\beta$ to inhibit inflammation (Akhter et al., 1977; Zhang et al., 2014). In addition, BBR have blocked TLR4 receptors to decrease TLR4 mRNA and protein expression, attenuated NF-κB activity, reduced secretion of inflammatory factors IL-1 and IL-6, and preventd macrophage involvement in inflammatory response (Fu et al., 2015). BBR have significantly inhibited the MAPK pathways by blocking phosphorylation of p38 and JNK rather than phosphorylation of ERK1/2 (Feng et al., 2017). BBR have partially inhibited activation of TRPV1 by inhibiting inflammation and blocking the PKC pathway, thereby protecting peripheral neurons from damage caused by diabetes (Zan et al., 2017). Although these studies were not primarily directed at CIPN, they suggest that the mechanism by which BBR reduces CIPN nerve injury is associated with regulation of inflammatory signalling pathways.

Our study showed that BBR can inhibit the CDDP induced neuroinflammatory response by inhibiting TRPV1 and NF-κB protein overexpression, activating the JNK/p38 MAPK pathways, and promoting NF-κB expression in early-stage injury. In late-stage injury, BBR inhibited the expression of *p*-JNK, promoted NF-κB expression, and regulated the p38 MAPK/ERK signalling pathways. BBR dose-dependently decreased pro-inflammatory factors NF-κB, IL-1$\alpha$, IL-1$\beta$, and IL-6 in the serum of mice. The increase in the anti-inflammatory factor IL-10 improved hyperalgesia symptoms in mice. To sum up, our results indicate that BBR can inhibit NF-κB protein expression by blocking TRPV1, decrease

phosphorylation of p38 and ERK1/2, and ameliorate thermal hyperalgesia induced by CDDP.

The expression of TRPV1 in DRG is an important target for pain research. Studies have shown that upregulation of *TRPV1* and *TRPA1* mRNA was associated with thermal hyperalgesia and mechanical hypersensitivity in CDDP treated mice (Bölcskei et al., 2005; Ta et al., 2009). This suggests that TRPV1 plays an important role in signalling associated with thermal heat pain after CDDP induced neuronal injury. In this study, we compared CDDP induced thermal heat pain motility behaviour changes before and after *TRPV1* gene knockout in mice, and found that nerve fibres expressed thermal hyperalgesia induced by CDDP. After knocking out the *TRPV1* gene, the hyperalgesia response was controlled within 2 weeks, but the thermal heat pain threshold was still reduced 3 weeks after treatment. BBR reversed CDDP induced pain sensation throughout the course of the experiment. These results suggest that TRPV1 receptors are only involved in regulating CDDP induced hyperalgesia in the early stage of BBR therapy. Other mechanisms may be involved in the later stages of CIPN treatment.

We found that BBR decreased the levels of proinflammatory factors NF-κB, IL-1$\alpha$, IL-1$\beta$, IL-6, and TNF-$\alpha$ in mice serum and increased the levels of anti-inflammatory factor IL-10 in a dose-dependent manner. It indicates that the anti-inflammatory effect of BBR is not only expressed in DRG, but also involved in regulating blood. Previous studies have shown that NGF acted as an inflammatory mediator, activating PKA, PKC, MAPK/ERK, and PI3K signalling through sensitising TRPV1 receptors, leading to thermal hyperalgesia (Bölcskei et al., 2005; Zan et al., 2017). NGF can also upregulate TRPV1 expression through p38 MAPK signalling. With the activation of TRPV1 channel, calcium influx increases, and the TRPV1 channel threshold is reduced significantly during inflammation (Davis et al., 2000; Brederson et al., 2013; Maeda and Ozaki, 2014; Taguchi, 2016). Although many studies have shown that platinum drugs can increase expression of TRPV1 in animals (Chen et al., 2011; Khasabova et al., 2012; Naziroğlu and Braidy, 2017), there are no reports on these changes (Lu et al., 2020) or even a reduction in *TRPV1* mRNA expression in DRG neurons *in vitro* (Ta et al., 2009). The role of TRPV1 in CIPN remains to be clarified.

## DATA AVAILABILITY STATEMENT

The original contributions presented in the study are included in the article/Supplementary Material, further inquiries can be directed to the corresponding author.

## ETHICS STATEMENT

The animal study was reviewed and approved by The Animal Care and Use Committee at the Nanjing University of Chinese Medicine (Approval number AUC171001).

## AUTHOR CONTRIBUTIONS

JZ and JM designed and planned the experiments, JM wrote the manuscript, JM, SQ, LZ, MY, and HX carried out experiments, JZ gave critical revision of the manuscript.

## FUNDING

This study was supported by Key Project of Jiangsu Province for Fundamental Research and Development (BE2018717), Specially-appointed Professor Grant by Jiang Su province (2014, JZ), Jiangsu Six Talent Peak Award (2015, JZ).

## ACKNOWLEDGMENTS

We are grateful to Zongxiang Tang (Nanjing University of Chinese Medicine) Ahmet Hoke (The Johns Hopkins University) for assistance.

## REFERENCES

Akhter, M. H., Sabir, M., and Bhide, N. K. (1977). Anti-Inflammatory Effect of Berberine in Rats Injected Locally with Cholera Toxin. *Indian J. Med. Res.* 65 (1), 133–141.

Belair, D. G. (2021). *Investigation into the Role of ERK in Tyrosine Kinase Inhibitor-Induced Neuropathy*. London: Oxford University Press.

Brederson, J. D., Kym, P. R., and Szallasi, A. (2013). Targeting TRP Channels for Pain Relief. *Eur. J. Pharmacol. Int. J.* 716 (1–3), 61–76. doi:10.1016/j.ejphar.2013.03.003

Bölcskei, K., Helyes, Z., Szabó, A., Sándor, K., Elekes, K., Németh, J., et al. (2005). Investigation of the Role of TRPV1 Receptors in Acute and Chronic Nociceptive Processes Using Gene-Deficient Mice. *Pain.* 117 (3), 368–376. doi:10.1016/j.pain.2005.06.024

Carozzi, V. A., Chiorazzi, A., Canta, A., Meregalli, C., Oggioni, N., Cavaletti, G., et al. (2014). Chemotherapy-induced Peripheral Neurotoxicity in Immune-Deficient Mice: New Useful Ready-To-Use Animal Models. *Exp. Neurol.* 264 (2), 92–102. doi:10.1016/j.expneurol.2014.11.002

Carozzi, V. A., Marmiroli, P., and Cavaletti, G. (2010). The Role of Oxidative Stress and Anti-Oxidant Treatment in Platinum-Induced Peripheral Neurotoxicity. *Curr. Cancer Drug Targets.* 10 (7), 670–682. doi:10.2174/156800910793605820

Caterina, M. J., Leffler, A., Malmberg, A. B., Martin, W. J., Trafton, J., Petersen-Zeitz, K. R., et al. (2000). Impaired Nociception and Pain Sensation in Mice Lacking the Capsaicin Receptor. *Science.* 288 (5464), 306–313. doi:10.1126/science.288.5464.306

Caterina, M. J., Schumacher, M. A., Tominaga, M., Rosen, T. A., Levine, J. D., and Julius, D. (1997). The Capsaicin Receptor: a Heat-Activated Ion Channel in the Pain Pathway. *Nature.* 389 (6653), 816–824. doi:10.1038/39807

Cavaletti, G., Miloso, M., Nicolini, G., Scuteri, A., and Tredici, G. (2010). Emerging Role of Mitogen-Activated Protein Kinases in Peripheral Neuropathies. *J. Peripher. Nerv Syst.* 12 (3), 175–194. doi:10.1111/j.1529-8027.2007.00138.x

Chen, Y., Yang, C., and Wang, Z. J. (2011). Proteinase-Activated Receptor 2 Sensitizes Transient Receptor Potential Vanilloid 1, Transient Receptor Potential Vanilloid 4, and Transient Receptor Potential Ankyrin 1 in Paclitaxel-Induced Neuropathic Pain. *Neuroscience.* 193 (1), 440–451. doi:10.1016/j.neuroscience.2011.06.085

Davis, J. B., Gray, J., Gunthorpe, M. J., Hatcher, J. P., Davey, P. T., Overend, P., et al. (2000). Vanilloid Receptor-1 Is Essential for Inflammatory Thermal Hyperalgesia. *Nature.* 405 (6783), 183–187. doi:10.1038/35012076

Feng, A. W., Gao, W., Zhou, G. R., Yu, R., Li, N., Huang, X. L., et al. (2012). Berberine Ameliorates COX-2 Expression in Rat Small Intestinal Mucosa Partially Through PPARγ Pathway During Acute Endotoxemia. *Int. Immunopharmacology.* 12 (1), 182–188. doi:10.1016/j.intimp.2011.11.009

Feng, M., Kong, S. Z., Wang, Z. X., He, K., Zou, Z. Y., Hu, Y. R., et al. (2017). The Protective Effect of Coptisine on Experimental Atherosclerosis ApoE-/- Mice Is Mediated by MAPK/NF-κB-Dependent Pathway. *Biomed. Pharmacother.* 93, 721–729. doi:10.1016/j.biopha.2017.07.002

Fischer, S. J., McDonald, E. S., Gross, L., and Windebank, A. J. (2001). Alterations in Cell Cycle Regulation Underlie Cisplatin Induced Apoptosis of Dorsal Root Ganglion Neurons *In Vivo*. *Neurobiol. Dis.* 8 (6), 1027–1035. doi:10.1006/nbdi.2001.0426

Fu, K., Lv, X., Li, W., Wang, Y., Li, H., Tian, W., et al. (2015). Berberine Hydrochloride Attenuates Lipopolysaccharide-Induced Endometritis in Mice by Suppressing Activation of NF-Kb Signal Pathway. *Int. Immunopharmacol.* 24 (1), 128–132. doi:10.1016/j.intimp.2014.11.002

Fukuda, Y., Li, Y., and Segal, R. A. (2017). A Mechanistic Understanding of Axon Degeneration in Chemotherapy-Induced Peripheral Neuropathy. *Front. Neurosci.* 11, 481. doi:10.3389/fnins.2017.00481

Gao, M. Y., Chen, L., Yang, L., Yu, X., Kou, J. P., and Yu, B. Y. (2014). Berberine Inhibits LPS-Induced TF Procoagulant Activity and Expression through NF-κB/p65, Akt and MAPK Pathway in THP-1 Cells. *Pharmacol. Rep.* 66 (3), 480–484. doi:10.1016/j.pharep.2013.12.004

Guo, L., Hamre, J., Eldridge, S., Behrsing, H. P., Cutuli, F. M., Mussio, J., et al. (2017). Multiparametric Image Analysis of Rat Dorsal Root Ganglion Cultures to Evaluate Peripheral Neuropathy-Inducing Chemotherapeutics. *Toxicol. Sci.* 156 (1), 275–288. doi:10.1093/toxsci/kfw254

Ibrahim, E. Y., and Ehrlich, B. E. (2020). Prevention of Chemotherapy-Induced Peripheral Neuropathy: A Review of Recent Findings. *Crit. Rev. Oncol. Hematol.* 145, 102831. doi:10.1016/j.critrevonc.2019.102831

Khasabova, I. A., Khasabov, S., Paz, J., Harding-Rose, C., Simone, D. A., and Seybold, V. S. (2012). Cannabinoid Type-1 Receptor Reduces Pain and Neurotoxicity Produced by Chemotherapy. *J. Neurosci.* 32 (20), 7091–7101. doi:10.1523/JNEUROSCI.0403-12.2012

Livak, K. J., and Schmittgen, T. D. (2001). Analysis of Relative Gene Expression Data Using Real-Time Quantitative PCR and the 2(-Delta Delta C(T)) Method. *Methods.* 25 (4), 402–408. doi:10.1006/meth.2001.1262

Lu, Y., Zhang, P., Zhang, Q., Yang, C., Qian, Y., Suo, J., et al. (2020). Duloxetine Attenuates Paclitaxel-Induced Peripheral Nerve Injury by Inhibiting P53-Related Pathways. *J. Pharmacol. Exp. Ther.* 373 (3), 453265082–453265462. doi:10.1124/jpet.120.265082

Maeda, T., and Ozaki, M. (2014). Study on Novel Mechanism Underlying Analgesia Targeting TRPV1. *Yakugaku Zasshi.* 134 (3), 373–378. doi:10.1248/yakushi.13-00236-1

Mcdonald, E. S., Randon, K. R., Knight, A., and Windebank, A. J. (2005). Cisplatin Preferentially Binds to DNA in Dorsal Root Ganglion Neurons *In Vitro* and *In Vivo*: a Potential Mechanism for Neurotoxicity. *Neurobiol. Dis.* 18 (2), 305–313. doi:10.1016/j.nbd.2004.09.013

Middlemas, A., Delcroix, J. D., Sayers, N. M., Tomlinson, D. R., and Fernyhough, P. (2003). Enhanced Activation of Axonally Transported Stress-Activated Protein Kinases in Peripheral Nerve in Diabetic Neuropathy Is Prevented by Neurotrophin-3. *Brain.* 126 (7), 1671–1682. doi:10.1093/brain/awg150

Myers, R. R., Sekiguchi, Y., Kikuchi, S., Scott, B., Medicherla, S., Protter, A., et al. (2003). Inhibition of P38 MAP Kinase Activity Enhances Axonal Regeneration. *Exp. Neurol.* 184 (2), 606–614. doi:10.1016/S0014-4886(03)00297-8

Naziroğlu, M., and Braidy, N. (2017). Thermo-Sensitive TRP Channels: Novel Targets for Treating Chemotherapy-Induced Peripheral Pain. *Front. Physiol.* 8, 1040. doi:10.3389/fphys.2017.01040

Ni, W., Zheng, X., Hu, L., Kong, C., and Xu, Q. (2021). Preventing Oxaliplatin-Induced Neuropathic Pain: Using Berberine to Inhibit the Activation of NF-Kb and Release of Pro-Inflammatory Cytokines in Dorsal Root Ganglions in Rats. *Exp. Ther. Med.* 21 (2), 135. doi:10.3892/etm.2020.9567

Potapova, O., Haghighi, A., Bost, F., Liu, C., Birrer, M. J., Gjerset, R., et al. (1997). The Jun Kinase/Stress-Activated Protein Kinase Pathway Functions to Regulate DNA Repair and Inhibition of the Pathway Sensitizes Tumor Cells to Cisplatin. *J. Biol. Chem.* 272 (22), 14041–14044. doi:10.1074/jbc.272.22.14041

Quasthoff, S., and Hartung, H. P. (2002). Chemotherapy-induced Peripheral Neuropathy. *J. Neurol.* 249 (1), 9–17. doi:10.1007/pl00007853

Scuteri, A., Galimberti, A., Maggioni, D., Ravasi, M., Pasini, S., Nicolini, G., et al. (2009). Role of MAPKs in Platinum-Induced Neuronal Apoptosis. *Neurotoxicology.* 30 (2), 312–319. doi:10.1016/j.neuro.2009.01.003

Singh, J., Saha, L., Singh, N., Kumari, P., Bhatia, A., and Chakrabarti, A. (2019). Study of Nuclear Factorerythroid Related Factoractivator, Berberine, in Paclitaxel Induced Peripheral Neuropathy Pain Model in Rats. *J. Pharm. Pharmacol.* 71 (5), 797–805. doi:10.1111/jphp.13047

Staff, N. P., Grisold, A., Grisold, W., and Windebank, A. J. (2017). Chemotherapy-Induced Peripheral Neuropathy: A Current Review. *Ann. Neurol.* 81 (6), 772–781. doi:10.1002/ana.24951

Ta, L. E., Bieber, A. J., Carlton, S. M., Loprinzi, C. L., Low, P. A., and Windebank, A. J. (2010). Transient Receptor Potential Vanilloid 1 Is Essential for Cisplatin-Induced Heat Hyperalgesia in Mice. *Mol. Pain.* 6 (1), 15. doi:10.1186/1744-8069-6-15

Ta, L. E., Low, P. A., and Windebank, A. J. (2009). Mice with Cisplatin and Oxaliplatin-Induced Painful Neuropathy Develop Distinct Early Responses to thermal Stimuli. *Mol. Pain.* 5 (1), 9. doi:10.1186/1744-8069-5-9

Taguchi, K. (2016). Role of Transient Receptor Potential Channels in Paclitaxel- and Oxaliplatin-Induced Peripheral Neuropathy. *Yakugaku Zasshi.* 136 (2), 287–296. doi:10.1248/yakushi.15-00214

Wu, J., Zhang, H., Hu, B., Yang, L., Wang, P., Wang, F., et al. (2016). Coptisine from Coptis Chinensis Inhibits Production of Inflammatory Mediators in Lipopolysaccharide-Stimulated RAW 264.7 Murine Macrophage Cells. *Eur. J. Pharmacol.* 780, 106–114. doi:10.1016/j.ejphar.2016.03.037

Xu, Q., Zhang, X. M., Duan, K. Z., Gu, X. Y., Han, M., Liu, B. L., et al. (2013). Peripheral TGF-ß 1 Signaling Is a Critical Event in Bone Cancer-Induced Hyperalgesia in Rodents. *J. Neurosci.* 33 (49), 19099–19111. doi:10.1523/JNEUROSCI.4852-12.2013

Yang, S., Yu, Z., Sun, W., Jiang, C., Ba, X., and Zhou, Q. (2020). The Antiviral Alkaloid Berberine Ameliorates Neuropathic Pain in Rats with Peripheral Nerve Injury. *Acta Neurol. Belgica.* 120 (3), 557–567. doi:10.1007/s13760-018-1006-9

Yerra, V. G., Kalvala, A. K., Sherkhane, B., Areti, A., and Kumar, A. (2018). Adenosine Monophosphate-Activated Protein Kinase Modulation by Berberine Attenuates Mitochondrial Deficits and Redox Imbalance in Experimental Diabetic Neuropathy. *Neuropharmacology.* 131, 256–270. doi:10.1016/j.neuropharm.2017.12.029

Zan, Y., Kuai, C. X., Qiu, Z. X., and Huang, F. (2017). Berberine Ameliorates Diabetic Neuropathy: TRPV1 Modulation by PKC Pathway. *Am. J. Chin. Med.* 45, 1709–1723. doi:10.1142/S0192415X17500926

Zhang, Y., Li, X., Zhang, Q., Li, J., Ju, J., Du, N., et al. (2014). Berberine Hydrochloride Prevents Postsurgery Intestinal Adhesion and Inflammation in Rats. *J. Pharmacol. Exp. Ther.* 349 (3), 417–426. doi:10.1124/jpet.114.212795

Zhang, H. N., Sun, Y. J., He, H. Q., Li, H. Y., Xie, Q. L., Liu, Z. M., et al. (2018). Berberine Promotes Nerve Regeneration Through IGFR-Mediated JNK-AKT Signal Pathway. *Mol. Med. Rep.* 18 (6), 5030–5036. doi:10.3892/mmr.2018.9508

Zielinska, M. (2003). Role of N-Methyl-D-Aspartate Receptors in the Neuroprotective Activation of Extracellular Signal-Regulated Kinase 1/2 by Cisplatin. *J Biol Chem.* 278, 43663. doi:10.1074/jbc.M301554200

**Conflict of Interest:** The authors declare that the research was conducted in the absence of any commercial or financial relationships that could be construed as a potential conflict of interest.

**Publisher's Note:** All claims expressed in this article are solely those of the authors and do not necessarily represent those of their affiliated organizations, or those of the publisher, the editors and the reviewers. Any product that may be evaluated in this article, or claim that may be made by its manufacturer, is not guaranteed or endorsed by the publisher.

frontiers in Pharmacology

REVIEW
published: 04 February 2022
doi: 10.3389/fphar.2022.841110

# Therapeutic Potential and Molecular Mechanisms of Echinacoside in Neurodegenerative Diseases

*Jin Li*[1†], *Hongni Yu*[2†], *Chuan Yang*[3†], *Tao Ma*[2*] *and Yuan Dai*[1*]

[1]School of Health Preservation and Rehabilitation, Chengdu University of Traditional Chinese Medicine, Chengdu, China, [2]Dongfang Hospital, Beijing University of Chinese Medicine, Beijing, China, [3]School of Pharmacy, Chengdu University of Traditional Chinese Medicine, Chengdu, China

Echinacoside (ECH) is a natural phenylethanoid glycoside (PhG) in *Cistanche tubulosa*. A large number of studies have shown that ECH has very promising potential in the inhibition of neurodegenerative disease progression. Experimental studies strongly suggest that ECH exhibits a variety of beneficial effects associated with in neuronal function, including protecting mitochondrial function, anti-oxidative stress, anti-inflammatory, anti-endoplasmic reticulum stress (ERS), regulating autophagy and so on. The aim of this paper is to provide an extensive and actual summarization of ECH and its neuroprotective efficacy in prevention and treatment of neurodegenerative diseases, including Alzheimer's disease (AD), Parkinson's disease (PD), amyotrophic lateral sclerosis (ALS), and so on, based on published data from both *in vivo* and *in vitro* studies. There is a growing evidence that ECH may serve as an efficacious and safe substance in the future to counteract neurodegenerative disease.

**Keywords: echinacoside, neurodegenerative diseases, Alzheimer's disease, Parkinson's disease, amyotrophic lateral sclerosis, vascular dementia**

OPEN ACCESS

***Edited by:***
*Fushun Wang,*
*Nanjing University of Chinese Medicine, China*

***Reviewed by:***
*Wenqiang Chen,*
*Georgetown University, United States*
*Chunhe Wang,*
*Shanghai Institute of Materia Medica (CAS), China*

***Correspondence:**
*Tao Ma*
*matao@bucm.edu.cn*
*Yuan Dai*
*daiyuan@cdutcm.edu.cn*

*[†]These authors have contributed equally to this work*

***Specialty section:***
*This article was submitted to Neuropharmacology, a section of the journal Frontiers in Pharmacology*

***Received:*** *21 December 2021*
***Accepted:*** *03 January 2022*
***Published:*** *04 February 2022*

***Citation:***
*Li J, Yu H, Yang C, Ma T and Dai Y (2022) Therapeutic Potential and Molecular Mechanisms of Echinacoside in Neurodegenerative Diseases. Front. Pharmacol. 13:841110. doi: 10.3389/fphar.2022.841110*

## 1 INTRODUCTION

With the increase in population aging, neurodegenerative diseases are the most prevalent and fastest growing disorders of the elderly worldwide, which are endangering human health and cause a heavy financial burden on society (Erkkinen et al., 2018). The number of the dementia elderly is expected to increase to 130 million by 2050, and the annual socio-economic cost per patient is US$19,144.36, the global cost is estimated to reach US$9.12 trillion by 2050 (Jia et al., 2018; Hansson, 2021). Neurodegenerative diseases mainly include Alzheimer's disease (AD), Parkinson's disease (PD), Huntington's disease (HD), amyotrophic lateral sclerosis (ALS), multiple sclerosis (MS), vascular dementia (VD), and so on (Gitler et al., 2017). Neuronal damage, mitochondrial dysfunction, oxidative stress and neuroinflammation are their common pathogenesis feature. The neurodegenerative diseases are mainly manifested as memory and cognitive impairment, and abnormal movement in clinic (Enogieru et al., 2018). Up to now, the therapeutic strategy for neurodegenerative diseases mainly focuses on improving symptoms. Therefore, it is urgent to explore and develop novel drugs with therapeutic potential directed at the pathogenesis of neurodegenerative disease.

Echinacoside (ECH, **Figure 1**) is a phenylethanoid glycoside (PhG), and was first extracted from the rhizome of *Echinacea angustifolia* DC. It is not only one of the key effective components of *Echinacea* (Jiang and Tu, 2009; Zhu et al., 2013; Li et al., 2018), but also abundant in other natural plants, such as *Scrophulariae Radix*, *Rehmanniae Radix*, *Cistanches Herba*, etc. Among them, *Cistanche tubulosa* contains

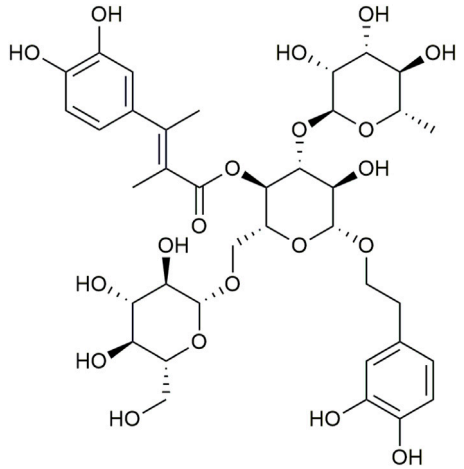

**FIGURE 1 |** Chemical structure of Echinacoside (ECH).

the highest content of ECH reaching about 30% (w/w) (Tian XY et al., 2021). The molecular formula of ECH is $C_{35}H_{46}O_{20}$ (**Figure 1**) and its chemical structure is composed of a sugar group, a phenylpropenyl group, and a phenylethanol group (Wu et al., 2020). Recently, ECH has shown a variety of important pharmacological activities, such as anti-inflammatory, protection of mitochondrial function, anti-oxidation, anti-neurotoxicity, anti-endoplasmic reticulum stress (ERS), anti-apoptosis, and neuroprotective effect (Wang et al., 2015; Chen et al., 2018; Ma et al., 2019; Wei et al., 2019; Wu et al., 2020). In addition, the metabolites of ECH C6-C3 and C6-C2 may have certain neuroprotective activities, which can directly supplement the neurotransmitter defects (Song et al., 2019). This review presented current and innovative results concerning the pharmacology and the efficacy of ECH in the treatment of neurodegenerative diseases, focusing on its mechanism of action in AD, PD, VD, and ALS, etc.

## 2 ALZHEIMER'S DISEASE

AD is an irreversible and progressive chronic central neurodegenerative disease. It is the most common type of dementia and is becoming a major challenge to global health and social care (Alzheimer's Association, 2020). Patients with AD usually suffer from significant memory impairment, language difficulties, decreased executive and visuospatial functions, and other degrees of cognitive impairment, as well as personality and behavior changes (Hansson, 2021). The pathogenesis mainly includes oxidative stress, mitochondrial abnormalities, neuroinflammation, abnormal accumulation of extracellular Amyloid-β (Aβ) plaques, and so on (Lane et al., 2018; Magalingam et al., 2018). AD involves multiple pathogeneses. The current treatment strategy for a single pathway has been proved to be insufficient. Recent evidences indicate that ECH has very extensive neuropharmacological activities. It may be a potential natural active ingredient with broad-spectrum and multiple target effects in the treatment of AD.

### 2.1 The Production and Toxicity of Amyloid-β

Excessive accumulation of Aβ oligomers and soluble aggregates outside the central nerve cells of the brain is one

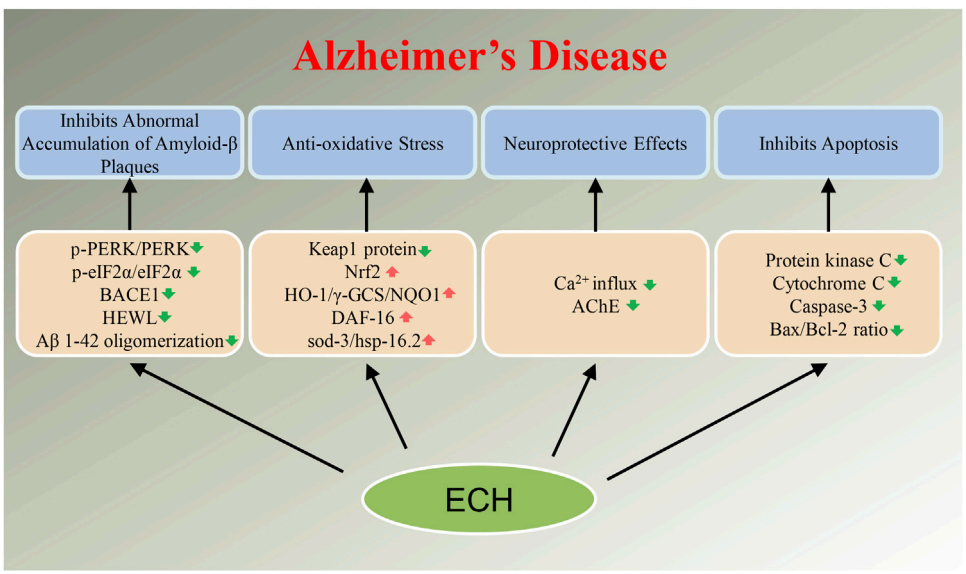


**FIGURE 2 |** Diagram with neuroprotective mechanisms of Echinacoside (ECH) in Alzheimer's disease (AD). ECH can improve neurodegenerative diseases by regulating target genes or target proteins on abnormal accumulation of Amyloid-β plaques, oxidative stress, apoptosis, and neurotoxicity signaling pathways.

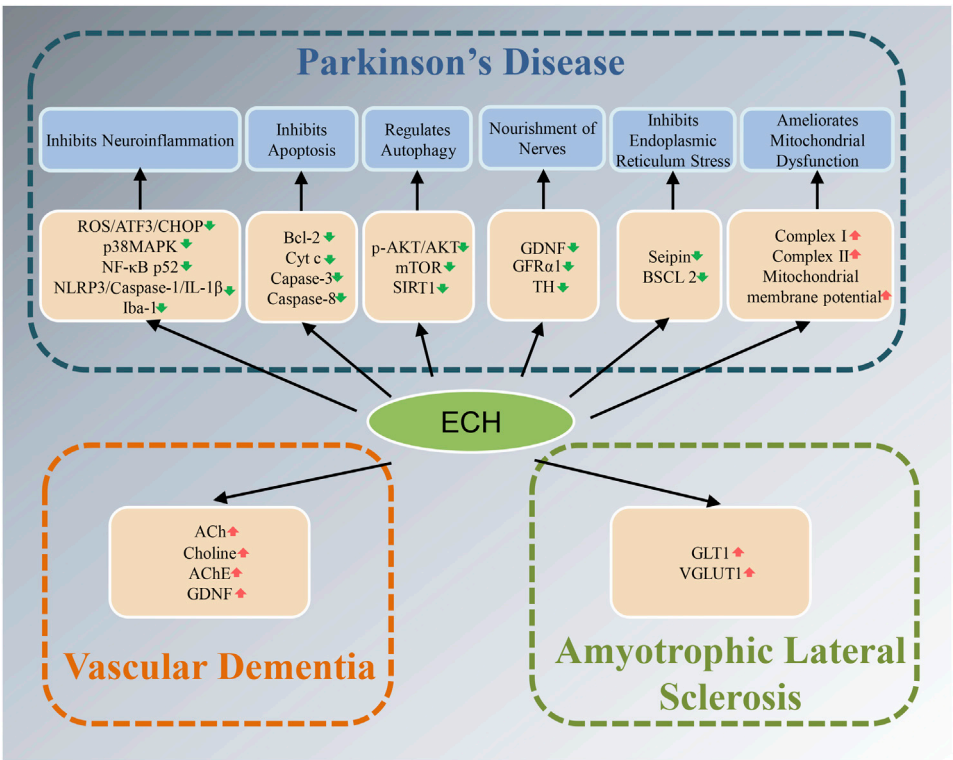


**FIGURE 3 |** Diagram with neuroprotective mechanisms of Echinacoside (ECH) in Parkinson's disease (PD), amyotrophic lateral sclerosis (ALS), and vascular dementia (VD). ECH can improve neurodegenerative diseases by improving oxidative stress, neuroinflammation, apoptosis, autophagy, nourishment of nerves, and mitochondrial dysfunction signaling pathways.

of the important causes of AD (Imbimbo and Watling, 2019). Beta site amyloid precursor protein cleaving enzyme 1 (BACE1) is the key rate-limiting enzyme for amyloid precursor protein (APP) processing to produce Aβ, which can catalyze the initial cleavage of APP and produce Aβ. Dai et al. confirm that ECH affects Protein kinase-like endoplasmic reticulum kinase (PERK), inhibits the PERK/eIF2α pathway to reduce ERS, and regulates F-actin remodeling to reduce the excessive accumulation of Aβ and the expression of BACE1 protein by using immunohistochemistry, Aβ plaque load quantification, Aβ ELISA, RNA isolation, quantitative PCR, Western blot analysis, BACE1 activity assay and Transmission Electron Microscopy in APPswe/PS1dE9 (2 × Tg-AD) mice (Dai et al., 2020). In the hen egg-white lysozyme (HEWL) model system, Zhang et al. used spectroscopic analyses, electron microscopy, cell viability assay, and hemolysis assay to find that ECH can inhibit the conversion of HEWL in a dose-dependent manner, antagonize amyloidosis, destroy the structure of fibrils, and convert amyloid fibrils into amorphous aggregates (Zhang et al., 2015). In addition, in Amyloid β peptide 1-42 (Aβ 1-42)-treated SH-SY5Y cells, Shiao et al. found that ECH inhibited $A\beta_{1\text{-}42}$ oligomerization, restored the cell viability that was reduced by $A\beta_{1\text{-}42}$, and reduced acetylcholinesterase activity, which in turn reverses cortical cholinergic dysfunction caused by $A\beta_{1\text{-}42}$ in $A\beta_{1\text{-}42}$-infused rat (Shiao et al., 2017). Wu et al. used the AD rats induced by injecting $A\beta_{1\text{-}42}$ and found ECH can ameliorate the cognitive deficits, decrease amyloid deposition and reverse cholinergic and hippocampal dopaminergic dysfunction caused by $A\beta_{1\text{-}42}$ (Wu et al., 2014).

## 2.2 Oxidative Stress

The central nervous system requires high energy, so it is one of the organs that is vulnerable to hypoxia (Wilson et al., 2009). The presence of oxidative damage in neuronal lipids and proteins is an important feature of AD. The binding of redox-active metal ions to Aβ and mitochondrial dysfunction can catalyze the production of reactive oxygen species (ROS) (Cheignon et al., 2018). Studies have shown that ECH has significant antioxidant and free radical scavenging properties. Nuclear factor-erythroid 2-related factor 2 (Nrf2) is one of the most important transcription factors in oxidative stress. ECH significantly decreased the Kelch-like ECH-associated protein-1 (Keap1) protein expression along with the substantial nuclear accumulation of Nrf2 in hippocampus. ECH further elevated the expression of heme oxygenase-1 (HO-1), NAD(P)H quinone oxidoreductase 1 (NQO1) and γ-glutamyl cysteine Synthetase (γ-GCS). Then, Nrf2 promotes the transcription of key antioxidative enzymes, such as

superoxide dismutase (SOD) and phase II detoxifying genes (such as NQO1), and regulates the Keap1-Nrf2-ARE pathway to depress oxidative stress and mitochondrial dysfunction (Zheng et al., 2019). In the *Caenorhabditis elegans*, ECH suppressed oxidative stress via the DR pathway and the insulin/IGF signaling (IIS) pathway, which triggers the nuclear localization of DAF-16. Then DAF-16 regulates target genes which participate in lifespan regulation and stress resistance. ECH also increased its two downstream targets, namely superoxide dismutase (sod-3) and small heat shock protein 16.2 (hsp-16.2) which involved in oxidative damage (Mukhopadhyay et al., 2006; Chen et al., 2018). Furthermore, ECH could ameliorate the pathology of AD through decreasing the formation of ROS and the accumulation of intracellular free $Ca^{2+}$, and improving the mitochondrial membrane integrity (Kuang et al., 2009).

## 2.3 Neuroprotection

Glutamate is the main excitatory neurotransmitter. Excessive release of glutamate and excessive excitement of N-methyl-D-aspartate receptor (NMDAR) can cause depolarization of nerve cell membranes and cause a large amount of $Ca^{2+}$ influx, which is an important cause of neuronal degeneration and death (Cobley et al., 2018). According to the research results of Lu and others, in the rat cerebral cortex, ECH can reduce voltage-dependent $Ca^{2+}$ influx and inhibit protein kinase C activity (Lu et al., 2016). Shiao et al. infuse $A\beta_{1\text{-}42}$ into the brain cistern by an osmotic pump and found that ECH can inhibit AChE activity, reverse cortical cholinergic neuron dysfunction caused by Aβ deposition, and improve cognitive dysfunction caused by $A\beta_{1\text{-}42}$. Achieve protection of nerves from toxic effects (Shiao et al., 2017).

## 2.4 Apoptosis

ECH can inhibit the release of cytochrome c (Cyt c) and the activation of caspase-3 through the extracellular signal-regulated kinase (ERK) pathway *in vitro* (Zhu et al., 2013). The members of the Bcl-2 family-like Bax and Bcl-2 have participated in apoptosis induced by the accumulation of ROS through the mitochondrial apoptotic pathway (Deng et al., 2004; Soane et al., 2008). ECH prevents a $H_2O_2$-induced increase of the Bax/Bcl-2 ratio to depress apoptosis in rat pheochromocytoma cell line (PC12 cells) (Kuang et al., 2009).

# 3 PARKINSON'S DISEASE

PD is a chronic progressive neurodegenerative disease. Its clinical symptoms mainly include resting tremor, bradykinesia, muscle rigidity, and postural and gait disorders. The typical neuropathological features of PD are the degeneration of dopaminergic neurons located in the substantial nigra pars compacta (SNpc) of the midbrain and the formation of Lewy bodies, and α-synuclein and ubiquitin are the main components of Lewy bodies (Dunnett and Björklund, 1999). Recent studies have shown that the loss of dopaminergic terminals in the striatum, rather than the loss of SNpc neurons, is crucial for the occurrence of motor symptoms. With the aging of the global population, the prevalence of PD is expected to double in the next 20 years (Simon et al., 2020).

## 3.1 Neuroinflammation

ECH inhibits the activation of microglia and astrocytes in 6-hydroxydopamine (6-OHDA) subacute PD model mice and promotes the nerves of dopamine (DA), 3,4-dihydroxyphenylacetic acid (DOPAC), high vanillic acid (HVA), norepinephrine (NE), and serotonin (5-HT) in the striatum and extracellular fluid of the hippocampus. Secretion of nutritional factors (Chen et al., 2007), and finally, the apoptosis of DA neurons is reduced, and the pathological state of PD is improved. It is also reported in the literature that ECH can prevent the level of DA, DOPAC, and HVA in the right striatum of 1-methyl-4-phenyl-1,2,3,6-tetrahydropyridine (MPTP) model mice from decreasing (Zhang et al., 2021a). At the same time, inhibiting the reduction of striatal fibers, DA and DA transporters can improve gait disorders. *In vitro* experiments show that ECH can improve 6-OHDA-induced PC12 cell model cell viability, significantly enhance redox activity and mitochondrial membrane potential, reduce ROS production, and inhibit mitochondrial-mediated apoptosis (Chen et al., 2019). MPTP is converted into 1-methyl-4-phenylpyridinium ($MPP^+$) by monoamine oxidase B in glial cell species. $MPP^+$ produces neurotoxicity by generating ROS in DA neuron mitochondria (Ahmed et al., 2017). $MPP^+$ is now widely used to induce damage in SH-SY5Y cell line to mimic the pathogenesis of PD. After ECH administration, it has been shown to attenuate DA neuron damages. Zhang et al. used proteomics to detect pro-inflammatory cytokines and found that seven cytokines including c5/c5a, interleukin-1beta (IL-1β), tumor necrosis factor-alpha (TNF-α), interleukin-2 (IL-2), and interleukin-4 (IL-4) were down-regulated by down-regulating p38 mitogen Pro-activated protein kinase (p38MAPK) and nuclear factor-kappa B (NF-κB) p52 (Zhang J et al., 2017; Liang et al., 2019) or regulate the activation of ROS/ATF3/CHOP pathway participate in the inhibition of inflammation in dopaminergic neurons in the midbrain the occurrence of the reaction, thereby inhibiting the occurrence of apoptosis, has a neuroprotective effect (Zhao et al., 2016). The excessive activation of microglia is closely related to neurotoxicity and participates in the main pathological development of PD. The inflammatory response mediated by activated microglia is the main component of the pathological process of PD. In the ECH group of MPTP model mice, the specific marker Iba-1 of microglia in the midbrain decreased, and ECH treatment inhibited the small activation of glial cells which improves inflammation in the brain (Ho, 2019). There are also reports in the literature that ECH improves the neuropathological state of PD mice through neuroprotective cell survival and inhibiting activated microglia-mediated NLRP3/CASP-1/IL-1β inflammation signals (Gao et al., 2020). In summary, ECH can depress the neuroinflammation that involved in the pathological progress of PD by multiple ways.

## 3.2 Apoptosis

Bcl-2 is the coding product of the Bcl-2 proto-oncogene and is an apoptosis-inhibiting protein. It promotes cell survival by

inhibiting the permeability of the outer mitochondrial membrane, regulates the release of mitochondrial apoptotic factors, participates in the regulation of apoptosis, and promotes cells' survive (Liu et al., 2019). In MPTP subacute PD model mice, ECH inhibits the release of mitochondrial Cyt c and caspase-8 and the lysis of caspase-3 by reducing the ratio of Bax/Bcl-2 in dopamine neurons in the substantia nigra and plays a role of inhibiting apoptosis.

## 3.3 Autophagy

In the pathological process of PD, the disorder of autophagy regulation will eventually lead to the accumulation of misfolded proteins and the damage of organelles. The autophagy-lysosome pathway can not only degrade proteins that cannot be degraded by the ubiquitin-proteasome pathway, but also degrade α-synuclein (Webb et al., 2003). Autophagy is the main pathway for the degradation of intracellular aggregates, and mechanistic target of rapamycin (mTOR) kinase is the key regulatory site for autophagy (Glick et al., 2010). By regulating the autophagy-lysosome pathway and increasing the degradation of autophagy and α-synuclein, the addition of ECH has significant advantages in improving the clinical efficacy and clinical symptoms of PD. Zhang et al. used MPTP to create a subacute PD mouse model. ECH can significantly improve the neurobehavior of PD mice by upregulating the survival signal p-AKT/AKT The expression of mTOR inhibits the expression of mTOR, thereby promoting the clearance of α-synuclein and the degradation of the autophagy substrate P62, exerting a neuroprotective effect (Zhang et al., 2021b). Sirtuins are nicotinamide adenine dinucleotide ($NAD^+$)-dependent deacetylases that play an important role in neuronal development and aging, which also have neuroprotective effects in PD models *in vivo* and *in vitro* (Donmez and Outeiro, 2013). It has been proved that sirtuin 1 (SIRT1) promotes the transcription of HSP70 (heat shock protein) and other molecular chaperones by deacetylating heat shock factor 1, and is an effective regulator of autophagy. Experiments have shown that ECH binds to SIRT1, and the binding product activates forkhead box subgroup O1 (FoxO1) to cause autophagy gene transcription. And translation, promote the autophagic degradation of α-synuclein, which can reverse the damage of dopaminergic neurons (Chen et al., 2019).

## 3.4 Nourishment of Nerves

The neurotrophic factor is a protein for the growth and survival of neurons, including nerve growth factor (NGF), brain-derived neurotrophic factor (BDNF), and glial cell-derived neurotrophic factor (GDNF). It can promote the growth and development of nerves and axons. The increased incidence of neuronal apoptosis and the decreased protective effect of neurotrophic factors caused by various pathological factors are the basis of dopaminergic neuron degeneration (Barker et al., 2020). GDNF has the strongest neurotrophic factor that protects and promotes the repairment of dopaminergic neurons. ECH improved the viability of $MPP^+$-treated cell *in vivo*, and increased the expression of tyrosine hydroxylase (TH), GDNF, GDNF family receptor α (GFRα1) and Ret in cells of substantia nigra (SN) of MPTP-induced PD mouse model (Xu et al., 2016).

## 3.5 Endoplasmic Reticulum Stress

Seipin/BSCL2 has been identified as the pathogenic gene for Berardinelli-Seip congenital lipodystrophy type 2 (BSCL2) and induces the most severe form of lipodystrophy, characterized by an almost complete absence of adipose tissue and associated metabolic disorders. Seipin is a global membrane protein of the endoplasmic reticulum (ER) that plays a key role in adipogenesis, lipid droplet homogenization, and cellular triglyceride lipolysis (Wang et al., 2018). Seipin accumulation strongly impaired adipocyte isotropy and leads to lipodystrophy, showing potential neural involvement. Chronic ERS leads to the accumulation of α-synuclein, and unfolded proteins in ER further leads to neuronal death (Licker et al., 2014). ECH attenuates the accumulation of Seipin (BSCL2) in 6-OHDA-induced rat models by promoting its ubiquitination and degradation, thereby reducing the activation of ERS related pathways (Zhang Y et al., 2017).

## 3.6 Mitochondrial Dysfunction

Mitochondria are key organelles for adenosine 5′-triphosphate (ATP) production through oxidative phosphorylation (OXPHOS), which is necessary for normal cellular functions. OXPHOS generates electron donor NADH and flavin adenine dinucleotide ($FADH_2$) through electron transport chain (ETC) transmission to produce ATP (Filograna et al., 2021). The spare respiratory capacity (SRC) that mitochondria reserve under normal physiological conditions is critical for cell survival under stress when energy needs increase or oxygen depletion occurs. Complex I is the main entry point of ETC and is the site that mainly produces lesions or injuries. MMP induces the mouse model of PD by inhibiting complex I, suggesting that complex I may be the core of PD pathogenesis (Iverson, 2013), and it is another entry point for ETC and is used to reduce equivalents. There is evidence that complex II is a key regulator of neuroprotection, and complex II is a major source of SRC. In the human neuroblastoma SH-SY5Y cell line, ECH selectively attenuated cell damage and reversed complex I by increasing the activity of complex II to ameliorate the mitochondrial respiratory disorder and bioenergy shortage (Ma et al., 2019). ECH could also increase the mitochondrial membrane potential, and restore the mitochondrial energy supply in 6-OHDA-treated PC12 cells.

# 4 OTHER NEURODEGENERATIVE DISEASE

Compared with the study of the mechanism that ECH is used to treat AD and PD, the mechanism of ECH's potential therapeutic effect on ALS, VD, and other diseases research is still very few.

**TABLE 1 |** Neuroprotective effects of Echinacoside against neurodegenerative diseases.

| Disease | Model | Mechanism | Target protein | Result | References |
|---|---|---|---|---|---|
| AD | APPswe/PS1dE9 (2 × Tg-AD) mice | inhibit the abnormal accumulation of Aβ plaques | PERK/eIF2α | reduce ERS and regulate F-actin remodeling to reduce the excessive accumulation of Aβ and the expression of BACE1 | Dai et al. (2020) |
| | $Aβ_{1-42}$-injected AD rats | inhibit the abnormal accumulation of Aβ plaques | AChE | ameliorate the cognitive deficits, decrease Aβ deposition and reverse cholinergic and hippocampal dopaminergic dysfunction caused by $Aβ_{1-42}$ | Wu et al. (2014) |
| | $Aβ_{1-42}$-treated SH-SY5Y cells | inhibit the abnormal accumulation of Aβ plaques | AChE | inhibit $Aβ_{1-42}$ oligomerization, restore the cell viability | Shiao et al. (2017) |
| | *Caenorhabditis elegans* | inhibit the abnormal accumulation of Aβ plaques | — | improve the survival of CL4176 worms in response to proteotoxic-stress induced by Aβ protein aggregation | Chen et al. (2018) |
| | HEWL model system | inhibit the abnormal accumulation of Aβ plaques | — | antagonize amyloidosis, destroy the fibril structure, and convert amyloid fibrils into non-Shape aggregates, and inhibits the conversion of HEWL in a dose-dependent manner | Zhang et al. (2015) |
| | Acute hypobaric hypoxia C57 mice | anti-oxidative stress | HO-1, NQO1, γ-GCS, Nrf2 | reduce HH-induced memory decline, increase the expression of nuclear factor E2 p45- related factor 2, heme oxygenase-1, NAD(P)H: quinone oxidoreductase 1, and γ-GCS synthetase in mRNA and protein levels | Zheng et al. (2019) |
| | *Caenorhabditis elegans* | anti-oxidative stress | DAF-16 | trigger the nuclear localization of DAF-16. DAF-16 regulates target genes to participate in lifespan regulation and stress resistance | Mukhopadhyay et al. (2006) |
| | *Caenorhabditis elegans* | anti-oxidative stress | sod-3, hsp-16.2 | extend the mean lifespan of worms and increase their survival under oxidative stress | Chen et al. (2018) |
| | Rats | neuroprotective effects | glutamate | reduce the 4-aminopyridine-evoked (4-AV) increase in cytoplasmic free $Ca^{2+}$ concentration, decrease 4-AV-induced phosphorylation of protein kinase C | Lu et al. (2016) |
| | SH-SY5Y cells | inhibits apoptosis | TrkA/TrkB | inhibit the release of Cyt c and the activation of caspase-3 through the ERK pathway to achieve neuroprotection | Zhu et al. (2013) |
| | PC12 cells | | Bax, Bcl-2 | prevent a $H_2O_2$-induced increase of the Bax/Bcl-2 ratio, the formation of ROS, and accumulation of intracellular free $Ca^{2+}$ ($[Ca^{2+}]$ i) | Kuang et al. (2009) |
| PD | 6-OHDA subacute PD model mice | inhibits neuroinflammation | DA, DOPAC, HVA, NE, and 5-HT | the apoptosis of DA neurons is reduced, and the pathological state of PD is improved | Chen et al. (2007) |
| | MPTP model mice | inhibits neuroinflammation | DA, DOPAC, and HVA | prevent the level of DA, DOPAC, and HVA in the right striatum of MPTP model mice from decreasing | Zhang et al. (2021a) |
| | 6-OHDA-induced PC12 cell model cell | inhibits neuroinflammation | DA | improve 6-OHDA-induced PC12 cell model cell viability, enhance redox activity and mitochondrial membrane potential, reduce ROS production, and inhibit mitochondrial-mediated apoptosis | Chen et al. (2019) |
| | SH-SY5Y cells | inhibits neuroinflammation | c5/c5a, IL-1β, IL-4, TNF-α, IL-2, p52, p38MAPK, NF-κB | attenuate DA neuron damage, regulate the activation of ROS/ATF3/CHOP pathway participate in the inhibition of inflammation in dopaminergic neurons, inhibits the occurrence of apoptosis and neuroprotective effect | Zhao et al. (2016), Zhang J et al. (2017), Liang et al. (2019) |
| | MPTP model mice | inhibits neuroinflammation | Iba-1 | inhibit the small activation of glial cells improve inflammation in the brain | Ho, (2019) |
| | PD mice | inhibits neuroinflammation | NLRP3/CASP-1/IL-1β | improve the neuropathological state of PD mice through neuroprotective cell survival and inhibit activated microglia-mediated NLRP3/CASP-1/IL-1β pathway | Gao et al. (2020) |
| | MPTP subacute PD model mice | inhibits apoptosis | Bcl-2 | inhibit the release of mitochondrial Cyt c and caspase-8 and the lysis of caspase-3 by | Liu et al. (2019) |

(Continued on following page)

**TABLE 1 |** (*Continued*) Neuroprotective effects of Echinacoside against neurodegenerative diseases.

| Disease | Model | Mechanism | Target protein | Result | References |
|---|---|---|---|---|---|
| | | | | reducing the ratio of Bax/Bcl-2 in dopamine neurons in the substantia nigra | |
| | SH-SY5Y cells | inhibits apoptosis | c5/c5a, IL-1β, IL-4, TNF-α, IL-2, p52, p38MAPK, NF-κB | inhibits the occurrence of apoptosis, and neuroprotective effect | Zhao et al. (2016) |
| | MPTP subacute PD model mice | regulates autophagy | p-AKT/AKT, P62 | improve the neurobehavior of PD mice by upregulating the survival signal p-AKT/AKT, promoting the clearance of α-synuclein and the degradation of the autophagy substrate P62, exerting a neuroprotective effect | Zhang et al. (2021b) |
| | PD models | regulates autophagy | SIRT1, HSP70 | activate FoxO1 to cause autophagy gene transcription, promote the autophagic degradation of α-synuclein, which can reverse the damage of dopaminergic neurons | Donmez and Outeiro (2013); Chen et al. (2019) |
| | MPTP model mice | regulates autophagy | GDNF | GFRα1 and TH in their brains, improve the pathological state of PD | Xu et al. (2016) |
| | 6-OHDA-induced rat models | nourishment of nerves | BSCL2 | reduce the activation of ERS related pathways | Zhang Y et al. (2017) |
| | MPTP model mice | improves mitochondrial dysfunction | mitochondria complex | reduce equivalents | Iverson (2013) |
| | SH-SY5Y cell line | improves mitochondrial dysfunction | mitochondria complex | attenuate cell damage and reverse complex I by increasing the activity of complex II to inhibit the induction of mitochondrial respiratory disorder and bioenergy weakness | Ma et al. (2019) |
| | 6-OHDA-induced PC12 cells | improves mitochondrial dysfunction | — | The mitochondrial membrane potential was increased in 6-OHDA-induced PC12 cells and the state of mitochondrial energy disorder was improved | Ma et al. (2019) |
| ALS | neurons in SOD1 astrocyte conditioned medium | neuroprotective effects | GLT1 | improve neuron survival and synapse loss treated with SOD1 astrocyte conditioned medium | Tian Y et al. (2021) |
| VD | VD model rats | neuroprotective effects | AChE | promote effect on the restoration of ACh and choline levels in the hippocampus and striatum of VD model rats, increase the activity of AChE | Liu et al. (2013) |
| | VD model rats | neuroprotective effects | GDNF | up-regulate the expression of GDNF in the hippocampus by regulating the level of mitochondrial oxidation, thereby reducing the ischemic damage | Liu et al. (2017) |

ALS is a type of motor neuron disease characterized by the degeneration of more than motor neurons and lower motor neurons. Yang Tian's research team found that 10 μM ECH promoted the expression of glutamate transporter 1 (GLT1) in astrocytes, and found that ECH can significantly improve neuron survival and synapse loss treated with superoxide dismutase 1 (SOD1) astrocyte conditioned medium. Western blot and MTS were used. As well as immunohistochemistry and confocal imaging, this clarifies to a certain extent that ECH has a potential therapeutic effect on ALS (Tian Y et al., 2021). However, the molecular mechanism of 10 μM ECH promoting GLT1 expression needs more exploration. VD is a disease of severe cognitive impairment often caused by cerebrovascular diseases such as hemorrhagic or ischemic stroke. In previous studies, ECH has been found to have a certain promoting effect on the restoration of ACh and choline levels in the hippocampus and striatum of VD model rats, and it can also significantly increase the activity of AChE. The recovery of the cholinergic nervous system of VD rats has a promoting effect, but the specific molecular mechanism remains to be further discovered (Liu et al., 2013). And Xu Liu et al. also showed that ECH can up-regulate the expression of GDNF in the hippocampus by regulating the level of mitochondrial oxidation, thereby reducing the ischemic damage of VD rat neurons and improving learning and memory function (Liu et al., 2017).

## 5 CONCLUSION AND FUTURE DIRECTIONS

Neurodegenerative diseases have caused a tremendous burden to patient's family and society worldwide. Up to now, therapeutic drugs remain very scarce. Natural active ingredients may be one of the promising drug discovery strategies for AD treatment. As a natural PhG, ECH has been confirmed to be have multiple neuroprotective effects such as anti-oxidative stress, anti-apoptosis, anti-neuroinflammation, inhibit the accumulation of toxic protein and regulate autophagy and ERS (**Figure 2,3**). All of this implied that ECH possess broad-spectrum and multiple target neuropharmacological effects, suggesting ECH may be a potential candidate compounds to develop therapeutic drug for treating neurodegenerative diseases with multi-target collaborative intervention. Here, we enumerate the neuroprotective effects of ECH against neurodegenerative diseases based on current reports and results (**Table 1**).

## AUTHOR CONTRIBUTIONS

YD conceived, planned, critically reviewed, edited, and revised the manuscript; TM critically reviewed and revised the manuscript; JL planned, wrote the original manuscript and edited manuscript; HY reviewed and edited manuscript; CY contributed significantly to the manuscript preparation and revision of the manuscript.

## FUNDING

This work was supported by Applied basic Research project of Sichuan Province (2021YJ0009), National Natural Science Foundation of China (No. 81973786), Key R&D project of Sichuan Province (2019YFS0173) and Chengdu technology innovation R&D project (2021-YF05-01985-SN).

## REFERENCES

Ahmed, H., Abushouk, A. I., Gabr, M., Negida, A., and Abdel-Daim, M. M. (2017). Parkinson's Disease and Pesticides: A Meta-Analysis of Disease Connection and Genetic Alterations. *Biomed. Pharmacother.* 90, 638–649. doi:10.1016/j.biopha.2017.03.100

Alzheimer's Association (2020). 2020 Alzheimer's Disease Facts and Figures. *Alzheimers Dement* (16), 391–460. doi:10.1002/alz.12068

Barker, R. A., Björklund, A., Gash, D. M., Whone, A., Van Laar, A., Kordower, J. H., et al. (2020). GDNF and Parkinson's Disease: Where Next? A Summary from a Recent Workshop. *J. Parkinsons Dis.* 10 (3), 875–891. doi:10.3233/jpd-202004

Cheignon, C., Tomas, M., Bonnefont-Rousselot, D., Faller, P., Hureau, C., and Collin, F. (2018). Oxidative Stress and the Amyloid Beta Peptide in Alzheimer's Disease. *Redox Biol.* 14, 450–464. doi:10.1016/j.redox.2017.10.014

Chen, H., Jing, F. C., Li, C. L., Tu, P. F., Zheng, Q. S., and Wang, Z. H. (2007). Echinacoside Prevents the Striatal Extracellular Levels of Monoamine Neurotransmitters from Diminution in 6-hydroxydopamine Lesion Rats. *J. Ethnopharmacol.* 114 (3), 285–289. doi:10.1016/j.jep.2007.07.035

Chen, W., Lin, H. R., Wei, C. M., Luo, X. H., Sun, M. L., Yang, Z. Z., et al. (2018). Echinacoside, a Phenylethanoid Glycoside from Cistanche Deserticola, Extends Lifespan of *Caenorhabditis elegans* and Protects from Aβ-Induced Toxicity. *Biogerontology* 19 (1), 47–65. doi:10.1007/s10522-017-9738-0

Chen, C., Xia, B., Tang, L., Wu, W., Tang, J., Liang, Y., et al. (2019). Echinacoside Protects against MPTP/MPP+-induced Neurotoxicity via Regulating Autophagy Pathway Mediated by Sirt1. *Metab. Brain Dis.* 34 (1), 203–212. doi:10.1007/s11011-018-0330-3

Cobley, J. N., Fiorello, M. L., and Bailey, D. M. (2018). 13 Reasons Why the Brain Is Susceptible to Oxidative Stress. *Redox Biol.* 15, 490–503. doi:10.1016/j.redox.2018.01.008

Dai, Y., Han, G., Xu, S., Yuan, Y., Zhao, C., and Ma, T. (2020). Echinacoside Suppresses Amyloidogenesis and Modulates F-Actin Remodeling by Targeting the ER Stress Sensor PERK in a Mouse Model of Alzheimer's Disease. *Front. Cel Dev. Biol.* 8, 593659. doi:10.3389/fcell.2020.593659

Deng, M., Zhao, J. Y., Tu, P. F., Jiang, Y., Li, Z. B., and Wang, Y. H. (2004). Echinacoside Rescues the SHSY5Y Neuronal Cells from TNFalpha-Induced Apoptosis. *Eur. J. Pharmacol.* 505 (1-3), 11–18. doi:10.1016/j.ejphar.2004.09.059

Donmez, G., and Outeiro, T. F. (2013). SIRT1 and SIRT2: Emerging Targets in Neurodegeneration. *EMBO Mol. Med.* 5 (3), 344–352. doi:10.1002/emmm.201302451

Dunnett, S. B., and Björklund, A. (1999). Prospects for New Restorative and Neuroprotective Treatments in Parkinson's Disease. *Nature* 399 (6738 Suppl. l), A32–A39. doi:10.1038/399a032

Enogieru, A. B., Haylett, W., Hiss, D. C., Bardien, S., and Ekpo, O. E. (2018). Rutin as a Potent Antioxidant: Implications for Neurodegenerative Disorders. *Oxid. Med. Cel Longev.* 2018, 6241017. doi:10.1155/2018/6241017

Erkkinen, M. G., Kim, M. O., and Geschwind, M. D. (2018). Clinical Neurology and Epidemiology of the Major Neurodegenerative Diseases. *Cold Spring Harb. Perspect. Biol.* 10 (4), a033118. doi:10.1101/cshperspect.a033118

Filograna, R., Mennuni, M., Alsina, D., and Larsson, N. G. (2021). Mitochondrial DNA Copy Number in Human Disease: the More the Better? *FEBS Lett.* 595 (8), 976–1002. doi:10.1002/1873-3468.14021

Gao, M. R., Wang, M., Jia, Y. Y., Tian, D. D., Liu, A., Wang, W. J., et al. (2020). Echinacoside Protects Dopaminergic Neurons by Inhibiting NLRP3/Caspase-1/IL-1β Signaling Pathway in MPTP-Induced Parkinson's Disease Model. *Brain Res. Bull.* 164, 55–64. doi:10.1016/j.brainresbull.2020.08.015

Gitler, A. D., Dhillon, P., and Shorter, J. (2017). Neurodegenerative Disease: Models, Mechanisms, and a new hope. *Dis. Model. Mech.* 10 (5), 499–502. doi:10.1242/dmm.030205

Glick, D., Barth, S., and Macleod, K. F. (2010). Autophagy: Cellular and Molecular Mechanisms. *J. Pathol.* 221 (1), 3–12. doi:10.1002/path.2697

Hansson, O. (2021). Biomarkers for Neurodegenerative Diseases. *Nat. Med.* 27 (6), 954–963. doi:10.1038/s41591-021-01382-x

Ho, M. S. (2019). Microglia in Parkinson's Disease. *Adv. Exp. Med. Biol.* 1175, 335–353. doi:10.1007/978-981-13-9913-8_13

Imbimbo, B. P., and Watling, M. (2019). Investigational BACE Inhibitors for the Treatment of Alzheimer's Disease. *Expert Opin. Investig. Drugs* 28 (11), 967–975. doi:10.1080/13543784.2019.1683160

Iverson, T. M. (2013). Catalytic Mechanisms of Complex II Enzymes: a Structural Perspective. *Biochim. Biophys. Acta* 1827 (5), 648–657. doi:10.1016/j.bbabio.2012.09.008

Jia, J., Wei, C., Chen, S., Li, F., Tang, Y., Qin, W., et al. (2018). The Cost of Alzheimer's Disease in China and Re-estimation of Costs Worldwide. *Alzheimers Dement* 14 (4), 483–491. doi:10.1016/j.jalz.2017.12.006

Jiang, Y., and Tu, P. F. (2009). Analysis of Chemical Constituents in Cistanche Species. *J. Chromatogr. A.* 1216 (11), 1970–1979. doi:10.1016/j.chroma.2008.07.031

Kuang, R., Sun, Y., Yuan, W., Lei, L., and Zheng, X. (2009). Protective Effects of Echinacoside, One of the Phenylethanoid Glycosides, on H(2)O(2)-induced Cytotoxicity in PC12 Cells. *Planta Med.* 75 (14), 1499–1504. doi:10.1055/s-0029-1185806

Lane, C. A., Hardy, J., and Schott, J. M. (2018). Alzheimer's Disease. *Eur. J. Neurol.* 25 (1), 59–70. doi:10.1111/ene.13439

Li, L., Wan, G., Han, B., and Zhang, Z. (2018). Echinacoside Alleviated LPS-Induced Cell Apoptosis and Inflammation in Rat Intestine Epithelial Cells by Inhibiting the mTOR/STAT3 Pathway. *Biomed. Pharmacother.* 104, 622–628. doi:10.1016/j.biopha.2018.05.072

Liang, Y., Chen, C., Xia, B., Wu, W., Tang, J., Chen, Q., et al. (2019). Neuroprotective Effect of Echinacoside in Subacute Mouse Model of Parkinson's Disease. *Biomed. Res. Int.* 2019, 4379639. doi:10.1155/2019/4379639

Licker, V., Turck, N., Kövari, E., Burkhardt, K., Côte, M., Surini-Demiri, M., et al. (2014). Proteomic Analysis of Human Substantia Nigra Identifies Novel Candidates Involved in Parkinson's Disease Pathogenesis. *Proteomics* 14 (6), 784–794. doi:10.1002/pmic.201300342

Liu, C. L., Chen, H., Jiang, Y., Tu, P. F., Zhong, M., Ma, J. Y., et al. (2013). Effects of Echinacoside on Extracellular Acetylcholine and Choline Levels of hippocampus and Striatum of Cerebral Ischemia Rats. *Yao Xue Xue Bao* 48 (5), 790–793.

Liu, X., Luo, Q. H., Zhou, J., Wan, X. L., Zhang, H. Y., Wan, Z. G., et al. (2017). Effects of Echinacoside on GDNF Expression and Mitochondrial Oxidative Stress Levels in Vascular Dementia Rats. *Int. J. Clin. Exp. Med.* 10 (5), 7752–7759.

Liu, J., Liu, W., and Yang, H. (2019). Balancing Apoptosis and Autophagy for Parkinson's Disease Therapy: Targeting BCL-2. *ACS Chem. Neurosci.* 10 (2), 792–802. doi:10.1021/acschemneuro.8b00356

Lu, C. W., Lin, T. Y., Huang, S. K., and Wang, S. J. (2016). Echinacoside Inhibits Glutamate Release by Suppressing Voltage-dependent Ca(2+) Entry and Protein Kinase C in Rat Cerebrocortical Nerve Terminals. *Int. J. Mol. Sci.* 17 (7), 1006. doi:10.3390/ijms17071006

Ma, H., Liu, Y., Tang, L., Ding, H., Bao, X., Song, F., et al. (2019). Echinacoside Selectively Rescues Complex I Inhibition-Induced Mitochondrial Respiratory Impairment via Enhancing Complex II Activity. *Neurochem. Int.* 125, 136–143. doi:10.1016/j.neuint.2019.02.012

Magalingam, K. B., Radhakrishnan, A., Ping, N. S., and Haleagrahara, N. (2018). Current Concepts of Neurodegenerative Mechanisms in Alzheimer's Disease. *Biomed. Res. Int.* 2018, 3740461. doi:10.1155/2018/3740461

Mukhopadhyay, A., Oh, S. W., and Tissenbaum, H. A. (2006). Worming Pathways to and from DAF-16/FOXO. *Exp. Gerontol.* 41 (10), 928–934. doi:10.1016/j.exger.2006.05.020

Shiao, Y. J., Su, M. H., Lin, H. C., and Wu, C. R. (2017). Echinacoside Ameliorates the Memory Impairment and Cholinergic Deficit Induced by Amyloid Beta Peptides via the Inhibition of Amyloid Deposition and Toxicology. *Food Funct.* 8 (6), 2283–2294. doi:10.1039/c7fo00267j

Simon, D. K., Tanner, C. M., and Brundin, P. (2020). Parkinson Disease Epidemiology, Pathology, Genetics, and Pathophysiology. *Clin. Geriatr. Med.* 36 (1), 1–12. doi:10.1016/j.cger.2019.08.002

Soane, L., Siegel, Z. T., Schuh, R. A., and Fiskum, G. (2008). Postnatal Developmental Regulation of Bcl-2 Family Proteins in Brain Mitochondria. *J. Neurosci. Res.* 86 (6), 1267–1276. doi:10.1002/jnr.21584

Song, Q., Li, J., Huo, H., Cao, Y., Wang, Y., Song, Y., et al. (2019). Retention Time and Optimal Collision Energy Advance Structural Annotation Relied on LC-MS/MS: An Application in Metabolite Identification of an Antidementia Agent Namely Echinacoside. *Anal. Chem.* 91 (23), 15040–15048. doi:10.1021/acs.analchem.9b03720

Tian, X. Y., Li, M. X., Lin, T., Qiu, Y., Zhu, Y. T., Li, X. L., et al. (2021). A Review on the Structure and Pharmacological Activity of Phenylethanoid Glycosides. *Eur. J. Med. Chem.* 209, 112563. doi:10.1016/j.ejmech.2020.112563

Tian Y, Y., Jin, S., Promes, V., Liu, X., and Zhang, Y. (2021). Astragaloside IV and Echinacoside Benefit Neuronal Properties via Direct Effects and through Upregulation of SOD1 Astrocyte Function *In Vitro*. *Naunyn Schmiedebergs Arch. Pharmacol.* 394 (5), 1019–1029. doi:10.1007/s00210-020-02022-w

Wang, X., Zhang, J., Lu, L., and Zhou, L. (2015). The Longevity Effect of Echinacoside in *Caenorhabditis elegans* Mediated through Daf-16. *Biosci. Biotechnol. Biochem.* 79 (10), 1676–1683. doi:10.1080/09168451.2015.1046364

Wang, L., Hong, J., Wu, Y., Liu, G., Yu, W., and Chen, L. (2018). Seipin Deficiency in Mice Causes Loss of Dopaminergic Neurons via Aggregation and Phosphorylation of α-synuclein and Neuroinflammation. *Cell Death Dis.* 9 (5), 440. doi:10.1038/s41419-018-0471-7

Webb, J. L., Ravikumar, B., Atkins, J., Skepper, J. N., and Rubinsztein, D. C. (2003). Alpha-Synuclein Is Degraded by Both Autophagy and the Proteasome. *J. Biol. Chem.* 278 (27), 25009–25013. doi:10.1074/jbc.M300227200

Wei, W., Lan, X. B., Liu, N., Yang, J. M., Du, J., Ma, L., et al. (2019). Echinacoside Alleviates Hypoxic-Ischemic Brain Injury in Neonatal Rat by Enhancing Antioxidant Capacity and Inhibiting Apoptosis. *Neurochem. Res.* 44 (7), 1582–1592. doi:10.1007/s11064-019-02782-9

Wilson, M. H., Newman, S., and Imray, C. H. (2009). The Cerebral Effects of Ascent to High Altitudes. *Lancet Neurol.* 8 (2), 175–191. doi:10.1016/s1474-4422(09)70014-6

Wu, C. R., Lin, H. C., and Su, M. H. (2014). Reversal by Aqueous Extracts of Cistanche Tubulosa from Behavioral Deficits in Alzheimer's Disease-like Rat Model: Relevance for Amyloid Deposition and central Neurotransmitter Function. *BMC Complement. Altern. Med.* 14, 202. doi:10.1186/1472-6882-14-202

Wu, L., Georgiev, M. I., Cao, H., Nahar, L., El-Seedi, H. R., Sarker, S. D., et al. (2020). Therapeutic Potential of Phenylethanoid Glycosides: A Systematic Review. *Med. Res. Rev.* 40 (6), 2605–2649. doi:10.1002/med.21717

Xu, Q., Fan, W., Ye, S. F., Cong, Y. B., Qin, W., Chen, S. Y., et al. (2016). Cistanche Tubulosa Protects Dopaminergic Neurons through Regulation of Apoptosis and Glial Cell-Derived Neurotrophic Factor: *In Vivo* and *In Vitro*. *Front. Aging Neurosci.* 8, 295. doi:10.3389/fnagi.2016.00295

Zhang, D., Li, H., and Wang, J. B. (2015). Echinacoside Inhibits Amyloid Fibrillization of HEWL and Protects against Aβ-Induced Neurotoxicity. *Int. J. Biol. Macromol.* 72, 243–253. doi:10.1016/j.ijbiomac.2014.08.034

Zhang, Z. N., Hui, Z., Chen, C., Liang, Y., Tang, L. L., Wang, S. L., et al. (2021a). Neuroprotective Effects and Related Mechanisms of Echinacoside in MPTP-Induced PD Mice. *Neuropsychiatr. Dis. Treat.* 17, 1779–1792. doi:10.2147/ndt.S299685

Zhang, Z. N., Hui, Z., Chen, C., Liang, Y., Tang, L. L., Wang, S. L., et al. (2021b). Mechanism of Autophagy Regulation in MPTP-Induced PD Mice via the mTOR Signaling Pathway by Echinacoside. *Neuropsychiatr. Dis. Treat.* 17, 1397–1411. doi:10.2147/ndt.S299810

Zhang J, J., Zhang, Z., Xiang, J., Cai, M., Yu, Z., Li, X., et al. (2017). Neuroprotective Effects of Echinacoside on Regulating the Stress-Active p38MAPK and NF-κB P52 Signals in the Mice Model of Parkinson's Disease. *Neurochem. Res.* 42 (4), 975–985. doi:10.1007/s11064-016-2130-7

Zhang Y, Y., Long, H., Zhou, F., Zhu, W., Ruan, J., Zhao, Y., et al. (2017). Echinacoside's Nigrostriatal Dopaminergic protection against 6-OHDA-Induced Endoplasmic Reticulum Stress through Reducing the Accumulation of Seipin. *J. Cel Mol. Med.* 21 (12), 3761–3775. doi:10.1111/jcmm.13285

Zhao, Q., Yang, X., Cai, D., Ye, L., Hou, Y., Zhang, L., et al. (2016). Echinacoside Protects against MPP(+)-Induced Neuronal Apoptosis via ROS/ATF3/CHOP Pathway Regulation. *Neurosci. Bull.* 32 (4), 349–362. doi:10.1007/s12264-016-0047-4

Zheng, H., Su, Y., Sun, Y., Tang, T., Zhang, D., He, X., et al. (2019). Echinacoside Alleviates Hypobaric Hypoxia-Induced Memory Impairment in C57 Mice. *Phytother Res.* 33 (4), 1150–1160. doi:10.1002/ptr.6310

Zhu, M., Lu, C., and Li, W. (2013). Transient Exposure to Echinacoside Is Sufficient to Activate Trk Signaling and Protect Neuronal Cells from Rotenone. *J. Neurochem.* 124 (4), 571–580. doi:10.1111/jnc.12103

**Conflict of Interest:** The authors declare that the research was conducted in the absence of any commercial or financial relationships that could be construed as a potential conflict of interest.

**Publisher's Note:** All claims expressed in this article are solely those of the authors and do not necessarily represent those of their affiliated organizations, or those of the publisher, the editors and the reviewers. Any product that may be evaluated in this article, or claim that may be made by its manufacturer, is not guaranteed or endorsed by the publisher.

## GLOSSARY

**5-HT** serotonin
**6-OHDA** 6-hydroxydopamine
**AD** Alzheimer's disease
**ALS** amyotrophic lateral sclerosis
**APP** amyloid precursor protein
**ARE** antioxidant response element
**ATP** adenosine 5′-triphosphate
**Aβ** Amyloid-β
**BACE1** Beta site amyloid precursor protein cleaving enzyme 1
**BDNF** brain-derived neurotrophic factor
**BSCL2** Berardinelli-Seip congenital lipodystrophy type 2
**Cyt c** cytochrome c
**DA** dopamine
**DOPAC** 3,4-dihydroxyphenylacetic acid
**ECH** Echinacoside
**eIF2α** eukaryotic initiation factor-2α
**ER** endoplasmic reticulum
**ERK** extracellular signal-regulated kinase
**ERS** endoplasmic reticulum stress
**ETC** electron transport chain
**$FADH_2$** flavin adenine dinucleotide
**FoxO1** forkhead box subgroup O1
**GDNF** glial cell-derived neurotrophic factor
**GFRα1** GDNF family receptor α
**GLT1** glutamate transporter 1
**HD** Huntington's disease
**HEWL** hen egg-white lysozyme
**HO-1** heme oxygenase-1
**HVA** high vanillic acid
**IIS** insulin/IGF signaling
**IL-1β** Interleukin-1 beta
**IL-2** Interleukin-2
**IL-4** Interleukin-4
**Keap1** Kelch-like ECH-associated protein-1
**$MPP^+$** 1-methyl-4-phenylpyridinium
**MPTP** 1-methyl-4-phenyl-1,2,3,6-tetrahydropyridine
**MS** multiple sclerosis
**mTOR** mechanistic target of rapamycin
**$NAD^+$** nicotinamide adenine dinucleotide
**NE** norepinephrine
**NF-κB** nuclear factor-kappa B
**NGF** nerve growth factor
**NMDAR** N-methyl-D-aspartate receptor
**NQO1** NAD(P)H quinone oxidoreductase 1
**Nrf2** Nuclear factor-erythroid 2-related factor 2
**OXPHOS** oxidative phosphorylation
**p38MAPK** p38 mitogen Pro-activated protein kinase
**PD** Parkinson's disease
**PERK** Protein kinase-like endoplasmic reticulum kinase
**PhG** phenylethanoid glycoside
**ROS** reactive oxygen species
**SIRT1** sirtuin 1
**SN** substantia nigra
**SNpc** substantial nigra pars compacta
**SOD1** superoxide dismutase 1
**SRC** spare respiratory capacity
**TH** tyrosine hydroxylase
**TNF-α** tumor necrosis factor-alpha
**VD** vascular dementia
**γ-GCS** γ-glutamyl cysteine Synthetase

frontiers in Pharmacology

REVIEW
published: 15 February 2022
doi: 10.3389/fphar.2021.825330

# Progress in the Mechanism of Autophagy and Traditional Chinese Medicine Herb Involved in Dementia

*Pengyu Tao[1†], Jing Ji[2†], Simeng Gu[3†], Qian Wang[4] and Yuzhen Xu[5*]*

[1]Basic Medical School, Shanghai University of Traditional Chinese Medicine, Shanghai, China, [2]Department of Nephrology, Yueyang Hospital Affiliated to Shanghai University of Traditional Chinese Medicine, Shanghai, China, [3]Department of Psychology, Jiangsu University Medical School, Zhenjiang, China, [4]Postdoctoral Workstation, Department of Central Laboratory, Taian City Central Hospital, Shandong First Medical University and Shandong Academy of Medical Sciences, Taian, China, [5]Department of Rehabilitation, The Second Affiliated Hospital of Shandong First Medical University, Taian, China

Dementias is a kind of neurodegenerative disease, which occurs among the aging population. Current therapeutic outcome for dementia is limited. The medical use of herbal plant has a rich history in traditional Chinese medicine practice for thousands of years. Herbal medicine (HM) may provide a positive effect for prevention and treatment in dementia. As an alternative treatment to dementia, there has been a growing interest in HM extracts in scientific community as a result of its promising study results, mainly in animal experiment. At the molecular level, HM extracts trigger autophagy and reduce generation of reactive oxygen species (ROS) while inhibiting inflammation and reduce neurotoxicity. Experiments both *in vivo* and *in vitro* have identified certain potential of HM extracts and natural products as an important regulator factor in mediating autophagy, which might contribute to the improvement of dementia. This brief review not only summarizes the mechanism of autophagy in dementia but also offers a general understanding of the therapeutic mechanism of HM extracts in treating dementia and evaluates the potential clinical practice of HM in general.

**Keywords: autophagy, Chinese herbal medicine extracts, dementia, inflammation, oxidative stress, apoptosis**

OPEN ACCESS

***Edited by:***
*Fang Pan,*
*Shandong University, China*

***Reviewed by:***
*Tao Liu,*
*Hainan General Hospital, China*
*Wei Li,*
*Shanghai Jiao Tong University, China*

****Correspondence:***
*Yuzhen Xu*
*tianyayizhe@126.com*

*†These authors have contributed equally to this work*

***Specialty section:***
*This article was submitted to Neuropharmacology, a section of the journal Frontiers in Pharmacology*

***Received:*** *30 November 2021*
***Accepted:*** *24 December 2021*
***Published:*** *15 February 2022*

***Citation:***
*Tao P, Ji J, Gu S, Wang Q and Xu Y (2022) Progress in the Mechanism of Autophagy and Traditional Chinese Medicine Herb Involved in Dementia. Front. Pharmacol. 12:825330. doi: 10.3389/fphar.2021.825330*

## INTRODUCTION

Dementias, mainly including Alzheimer's disease (AD) and vascular dementia (VaD) (the two major form of dementia), are characterized by memory loss, damaged judgment, and language barrier seriously affecting daily life (Xu et al., 2019). It is estimated by the WHO report based on epidemiological data that the number of people across the world suffering from dementias will jump to 81.1 million by 2040 (Le Couteur et al., 2020). It is universally acknowledged that heart attack, stroke, atherosclerosis, hypertension, obesity, smoking, and cardiac problems are vital risk factors contributing to the cause of vascular dementia (Sahyouni et al., 2021). Clinically, dementia covers a wide range of brain abnormalities, ranging from slow progressive loss of memory, cognitive function, to a failure to conduct personal daily activities. The hallmark of dementia is characterized by accumulation of β-amyloid (Aβ) and hyper-phosphorylated Tau protein. The overexpression of these hallmarks often indicate neurodegenerative disorders that may turn into severe pathology. Thus, targeting these hallmarks may relieve the symptoms of dementias on the whole, and triggering autophagy by HM extracts is likely to be an alternative treatment for dementias (Padilla, 2019; Paik et al., 2020).

Autophagy has been interfered in the pathogenesis of dementias (He and Klionsky, 2009). It is generally assumed that autophagy is activated and acts as a protective mechanism in response to stimulating factors, thus attenuating toxic damage to the neuron. A variety of methods can be the promoter of autophagy, such as less food intake, regular sport, rapamycin, and AMP-activated protein kinase (AMPK)-activated protein kinase (Papandreou et al., 2008; Wang et al., 2021). However, once the autophagy pathway is impaired by stroke, atherosclerosis, and hypertension, this might lead to the progressive accumulation of toxic proteins in neuron, which finally contribute to the development of VaD (Romeo et al., 2019). Moreover, the activation of autophagy plays a key role in protecting and maintaining vascular integrity, and inhibition of autophagy is acting as a negative regulator in vascular degeneration, aging, and related pathological conditions (Levine and Kroemer, 2008; Ju and Weihl, 2010; Wang et al., 2021).

The incidence rate and mortality of dementias experienced a fast growth year by year. Current therapies simply offer symptomatic relief and fail to achieve a desired efficacy against dementias. Thus, there is an urgent need to seek an alternative treatment (Levine and Kroemer, 2008). Traditional Chinese medicine (TCM) is rooted in yin-yang theory and has been broadly used for the prevention and treatment of neurodegenerative disease in China for centuries (Han et al., 2012; Wang et al., 2021). As some Chinese medicines act as alternative approach in treating dementia and show effects on relieving dementia-related syndrome (Bai and Zhang, 2021), it has drawn great attention among researchers. It is the plant elements or extracts that carry out therapeutic function (Li and Zhang, 2009). The derivations of medicinal herbs have shown potential in alleviating dementia; the herb-plant-derived natural products tested in clinical trials have obtained positive results of improving dementias (Lin et al., 2017). Recently, studies have suggested that medicinal herb extracts could slow down the development of dementia *via* activating different pathways, which might provide a guideline of TCM for VaD therapy (Shen and Li, 2005; Zhu et al., 2006).

## THE ROLE OF AUTOPHAGY AND ITS RELATED SIGNALING PATHWAY IN DEMENTIA

Autophagy is a highly conserved self-digestion process involved in physiology to maintain cellular homeostasis *via* delivering dispensable or potentially damaged intracellular components, such as proteins and organelles to lysosomes for degradation, clearance, and recycling (He and Klionsky, 2009). Macroautophagy, microautophagy, and chaperone-mediated autophagy are three main forms of autophagy, all of which vary from their mechanisms to functions (Morita et al., 2010). Of these three types, macroautophagy is the most intensively studied autophagy process (Wang et al., 2020a); thus, it is generally referred to as autophagy. Autophagy is a normal physiological activity occurring in most cells to maintain homeostasis. But under some extreme situation, autophagy is usually activated to act as an adaptive and protective mechanism in alleviating damage of cells exposed to risky factors, such as oxidative stress, inflammation, or metabolic disorders (Morita et al., 2010). Researchers found that the dysfunction of autophagy contributes to the pathogenesis of neurodegenerative disease, such as vascular dementia (**Figure 1**). Thus, restoring autophagy activation may improve the prognosis of dementia (Cuervo, 2013; Caberlotto and Nguyen, 2014).

The mammalian neuron system depends on autophagy to maintain its normal functions and homeostasis (Jiang and Chang, 2019). Numerous specific-gene knockout animal models have been established to show that deletion of core autophagy-related genes leads to neonatal and embryonic lethality (Alirezaei et al., 2008). Three major steps are necessary for the formation of autophagosome: initiation, nucleation, and elongation. With more than 30 autophagy-related genes (ATGs) participating in autophagy activation, this complex process is strictly regulated to keep dynamic balance between synthesis and degradation, use, and recycling of intracellular substances (Caberlotto and Nguyen, 2014). The ULK1/2–ATG13–FIP200–ATG101 complex is important for activating autophagy. The Becl-1–PI3K complex is necessary for the phagophore nucleation step. The Atg12–Atg5–Atg16 complex and LC3/Atg8 cascade are employed in the autophagosomes elongation step (Cuervo, 2013; Liu et al., 2014; Nussenzweig et al., 2015). The conversion of LC3-I to LC3-II is recognized as a marker of autophagy activation and autophagosome formation (Levine and Kroemer, 2008).

mTOR is the best known mammalian target of rapamycin and also considered one of the most significant autophagy regulators in eukaryotic cells that includes two mTOR complexes, the mTOR complex 1 (mTORC1) and complex 2 (mTORC2); mTORC1 is the most extensive studied complex (Cao, 2010). Under most normal conditions, mTORC1 suppresses autophagy function *via* phosphorylating ULK1 and thereby inhibiting its activity (Alers et al., 2012). However, once cells are exposed to oxidative stress stimuli, the autophagy process can be initiated *via* the inactivation of mTORC1 (Kim et al., 2011). In the nervous system, the autophagy function can be neuroprotective *via* the inhibition of mTORC1. The high expression of mTORC1 is frequently observed in animals with nervous system diseases, such as vascular dementia (Guo et al., 2021; Perluigi et al., 2021). Thus, autophagy activation with the inhibition of mTOR expression can lead to neural tissue protection (Cao, 2010). Results from experimental models of AD indicated that disease progression seems to have a connection with dysfunctional autophagic processes and be improved by inhibition of mTOR activity (Joungmok and Kun-Liang, 2019).

Sirtuin1 (SIRT1), a homolog of Sir2, regulates energy metabolism, longevity, and autophagy in an NAD+-dependent manner (Ji et al., 2020). The sirt1 activity promotes life survival in organisms and protects neuronal cells from oxidative stress (Salminen and Kaarniranta, 2009). SIRT1 is responsible for the homeostasis of neural systems (Kim et al., 2007). If sirt1 activity is lost, this leads to impaired cognitive abilities, elevated Aβ production, and accumulation in AD patients (Qin et al., 2006). The increased sirt1 level can induce autophagy *via*

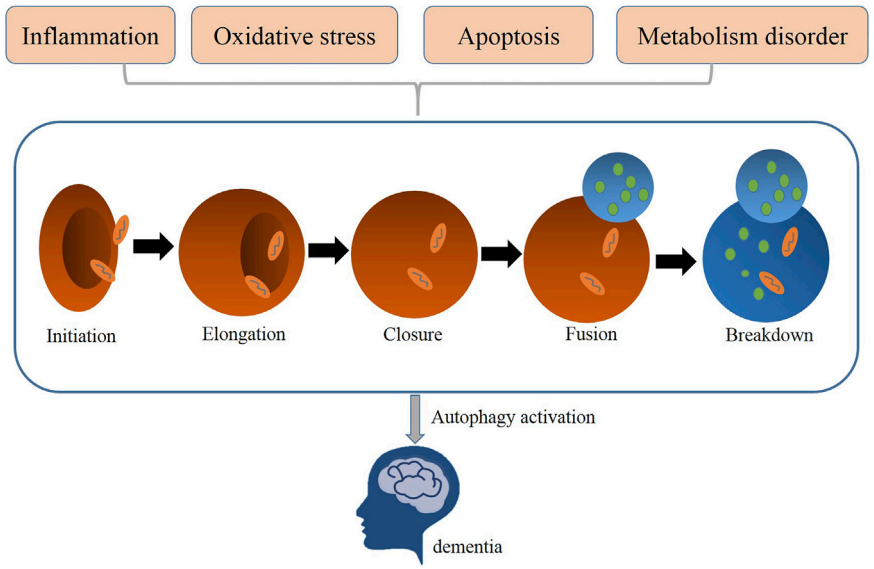


**FIGURE 1 |** Related pathological processes (metabolism disorder, oxidative stress, apoptosis, inflammation) mediated autophagy in dementia.

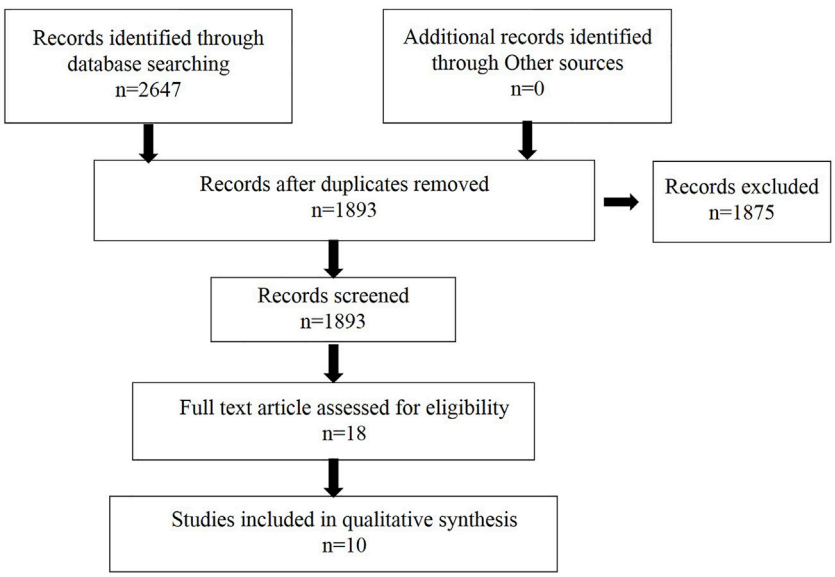


**FIGURE 2 |** Flow chart of literature research used to retrieve information to identify potential extracts for dementia treatment.

prohibiting mTOR pathways to protect cells exposed to oxidative stress (Preeti et al., 2017). Overexpression of sirt1 can promote nerve cell growth and regulate cellular metabolism by suppressing mTOR level (Süleyman et al., 2012). The enhanced SIRT1 activity could reduce the toxic damage imposing on nerve cells by activating AMPK-mediated autophagy process, which is essential for cell survival (Cantó et al., 2009; Dong et al., 2015). The sirt1-mediated autophagy may represent a promising therapeutic treatment to block the neurodegenerative disease (Kilic et al., 2018).

## TCM FOR DEMENTIA

We searched the relevant literature to determine the extracts that may be used to treat dementia. The flow chart is shown in **Figure 2**, and the specific extracts are summarized in **Table 1**. The cholinesterase inhibitors approved by FDA have been put into clinical use for relieving the symptoms of dementia rather than therapeutic drugs (Eglit, 1999). Patients with progressive dementia may need to take more doses of cholinesterase inhibitors than before, which bring some unwanted effects,

**TABLE 1 |** Herbal medicine exerts protective effect on dementia.

| Herb name | Effective ingredients and protective mechanism |
|---|---|
| Salviae Miltiorrhizae | Tanshinone IIA blocking the expression of iNOS and MMP-2 protein and reduce the production of ROS (Kong et al., 2021) |
| Mulberry | Resveratrol inhibit inflammation *via* decreasing expression of IL-1β, IL-6, and TNF-α (Zhao et al., 2019) |
| Cortex *Phellodendron amurensis* | Ethanol extract of Cortex *Phellodendron amurensis* promote the survival of nerve cells under toxic situation by increasing the level of Bcl-2/Bax protein (Xian et al., 2013) |
| *Ganoderma lucidum* | *Ganoderma lucidum* triterpenoids attenuated neuronal damage through decreasing the expression of antioxidative protein Nrf2, HO1, and NQO1 (Yu et al., 2020) |
| *Curcuma longa* | Curcumin improved spatial learning and memory *via* upregulating the expression of IGF-1R, IRS-2, and Akt (Natascia et al., 2014) |

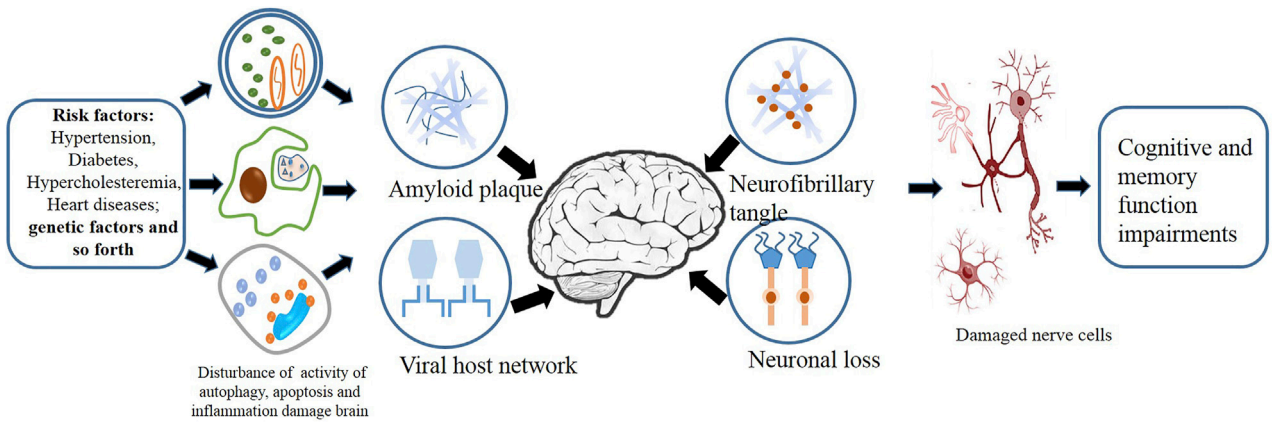


**FIGURE 3 |** Factors including inflammation, autophagy, and apoptosis act on the complex cellular network of the brain.

such as nausea, vomiting, and diarrhea; these adverse events limit its clinical treatment (Skaljo et al., 2009; Lu and Herr, 2012). The combination multi-targets therapy is essential to slow down the progression of the pathogenesis of dementia from multiple perspectives (Li, 2018). TCM has become a hot point in research due to its representative of multiple targets and multiple pathway, and they play a significant role in discovering new drugs against dementia. The combination and application of various herbs are the core heart of TCM, and this process is complex, which produces different outcomes, since the complexity of formulas often reacts to different targets or pathways (**Figure 3**). In order to get a satisfactory efficacy, some bioactive extracts derived from herbal plants have already shown promising results in study on dementias (Ma et al., 2019; Wang et al., 2020b). In this study, we will summarize some protective function of active extracts isolated form Chinese herbal plan on dementia.

## HM EXTRACTS ON OXIDATIVE STRESS

Numerous studies have shown that the overgeneration of reactive oxygen species and inactive antioxidant defenses result in the failure in removing free radicals or fixing organ damage that leads to the occurrence of oxidative stress, which is considered as a key role in the pathogenesis of dementias (Mao, 2012).

Salviae Miltiorrhizae is a popular Chinese herbal plant that is widely employed in the treatment of nerve system disease including dementia (Paudel et al., 2020). Tanshinone IIA (Tan IIA) is an active compound isolated from Salviae Miltiorrhizae (Kong et al., 2021). It is reported that Tan IIA could effectively delay the progression of AD in rats through blocking the expression of inducible nitric oxide synthase (iNOS) and matrix metallopeptidase 2 (MMP-2) protein and also improve memory function and learning ability of rats with AD *via* reducing the generation of ROS contributed to oxidative stress (Zhi et al., 2009; Jiang et al., 2014; Tang et al., 2017).

Rehmanniae Radix is one of the commonly used Chinese herbal medicine, which could nourish kidney yin to make the brain clearer based on Chinese medicine theory (Sun et al., 2014). Rehmannioside A (ReA) is a main compound isolated from Rehmanniae Radix, which offers protection against various diseases (Jung et al., 2013). AD rats treated with Rehmannioside A have shown a great improvement in cognitive function and memory by promoting neuro growth; the mechanism is partially associated with the inhibition of NOS and superoxide dismutase (SOD) activity (Sun et al., 2014; Sun et al., 2019).

## HM EXTRACTS ON APOPTOSIS

The integrity of nerve cell is vital to the normal functional activities of the nerve system (Heydarabadi et al., 2020). Thus, progressive accumulation of impaired nerve cell will inevitably lead to a series of neurological dysfunction (Wang et al., 2019). Recent studies indicate that oxidative stress and metabolic disorder are related to the apoptosis of nerve cells, which is the main factor responsible for the neuron loss in patients with dementia. Handling apoptosis is recognized as an effective therapy in alleviating dementia (Zhang et al., 2019).

Fucoidan is a natural polysaccharide mainly isolated from brown algae with various bioactive functions, including anti-inflammatory (Lee et al., 2012). A study indicated that fucoidan could protect nerve cell survival from being exposed to oxidative stress through inhibiting the expression of capase-3, which is considered to be vital role in the regulation of apoptosis (Subaraja et al., 2020).

Cortex *Phellodendron amurensis* (CPA), also known as "Huang Bai," is employed in Chinese medicine clinical practice as anti-heat herb for relieving inflammatory conditions and calming spirit (Xian et al., 2011). The ethanol extract of Cortex *Phellodendron amurensis* shows great potential in reducing neurotoxicity in beta-amyloid (Aβ)-induced PC12 cells. The mechanism by which the ethanol extract of CPA affects the survival of PC12 cells are likely to be associated with increasing the level of Bcl-2/Bax protein and decreasing the level of capase-3 protein so as to inhibit the occurrence of nerve cell apoptosis and exert neuroprotective effect against toxicity (Xian et al., 2013).

Salviae Miltiorrhizae-derived Tanshinone IIA (Tan IIA) exhibited a strong potential to ameliorate beta-amyloid peptides (Aβ)-induced cytotoxicity in PC-12 cells, which is generally used as AD research model (Dong et al., 2012). Treatment of Tan IIA in dementia is capable of protecting the brain under chronic injury and inhibiting apoptosis occurring among cells, with a repression of PI3K/Akt pathways and a down-level of anti-autophagic regulator mTOR (Dong et al., 2012).

## HM EXTRACTS ON INFLAMMATION

Inflammation observed in the development of dementia is recognized as a typical pathological feature (Lee et al., 2020). The beta-amyloid peptides (Aβ)-induced inflammation in nerve cells causes the neuron loss and cognitive impairment. The injured nerve cells with low autophagy activity produce proinflammatory cytokines and chemokines, which further enhance the activity of inflammation (Lee et al., 2020). Targeted inflammation and restoration of autophagy activity could be a promising therapy in alleviating dementia.

Dioscin is an active compound derived from Polygonatum Zanlanscianense Pamp. Dioscin could remarkably prohibit the beta-amyloid peptides (Aβ)-induced neurotoxicity in animals with dementia and the decline in number of apoptotic cell and reactive oxygen species (ROS) production (Zhang et al., 2020). The mechanism is linked to the suppression of inflammation by downregulation of interleukin (IL)-1β, IL-6, and tumor necrosis factor alpha (TNF-α) protein. In addition, further findings indicated that the administration of Dioscin upregulates the expression of Beclin-1 and LC3-II level and sequentially restore autophagy activity (Zhang et al., 2020).

Resveratrol is a polyphenolic ascorbic acid derived from plants, such as wine, apples, and peanuts, which exert a strong protective effect against inflammation (Moussa et al., 2017). The accumulation of evidence indicated that Resveratrol is capable of blocking inflammation in the brain of animals with dementia, and the reduction in expression of IL-1β, IL-6, and TNF-α (Zhao et al., 2019). In addition, resveratrol is reported to restore autophagy activity through enhancing the expression of Beclin-1 and LC3-II level and suppressing nuclear factor kappa B (NF-κB)-mediated inflammation (Fisher, 2021), suggesting that restoration of autophagy activity could be used as a treatment against inflammation-induced dementia.

## HM EXTRACTS ON ENERGY DYSFUNCTION

Mitochondria is a kind of organelle serving as the energy source of cellular function. Differences in the number, structure, and enzyme activity of mitochondria are existing between AD patients and non-AD patients (Eckert, 2019). Mitochondrial dysfunction induced by beta-amyloid peptides (Aβ) has been identified as an early marker during the development of AD, mainly characterized by the brain metabolism disorder, the dysregulation of calcium homeostasis, and the rising ROS level (Guo et al., 2019).

Curcumin is an active compound derived from *Curcuma longa* and shows therapeutic potential in regulating metabolism (Isik et al., 2009). Numerous studies investigating the effect of curcumin on glucose metabolism indicated that treatment of APP/PS1 double transgenic mice with curcumin enhanced glucose uptake and ameliorated impaired insulin signaling pathway in the brain and improved spatial learning and memory *via* upregulating the expression of IGF-1R, IRS-2, and Akt protein expression (Miyasaka et al., 2010; Natascia et al., 2014). These findings lead to a conclusion that targeting metabolism-related signaling may act as an innovative method for preventing Alzheimer's-related dementia.

Ganoderma lucidum triterpenoids (GLTs) are the major meditative compounds extracted from *Ganoderma lucidum*, which is documented in Chinese medicine therapy as a folk remedy based on its multifunctional health-promoting abilities (Yu et al., 2020). Multiple studies on neuroprotective effect of GLTs implied that GLTs improved cognitive impairment, attenuated nerve damage, and suppressed cell apoptosis in the nerve cells in AD animals through decreasing expression of anti-oxidative protein Nrf2, HO1, and NQO1 to inhibit the generation of ROS in the brain and promote nerve cell survival under oxidative stress situation (Yu et al., 2020).

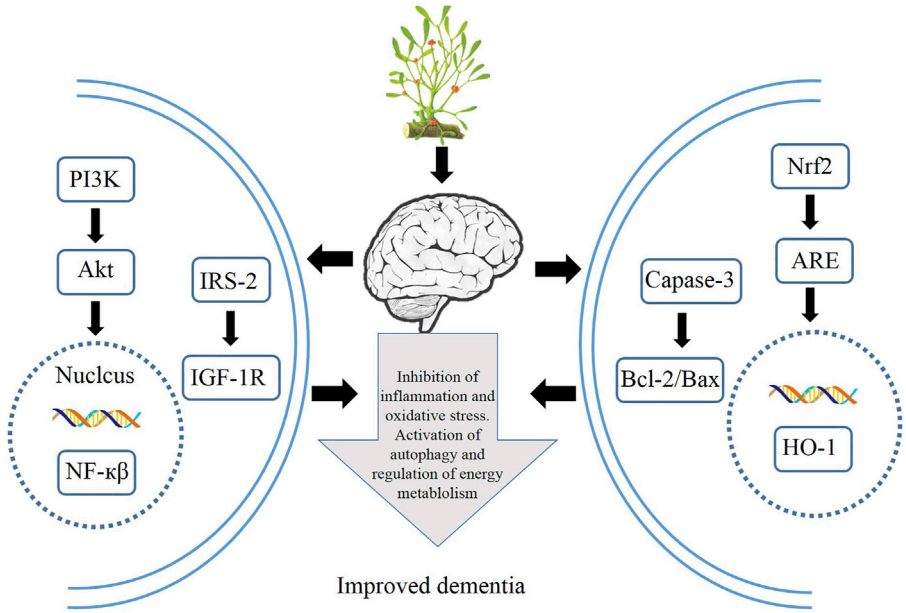


**FIGURE 4 |** Therapeutic applications of HMs *via* modulation of autophagy, inflammation, oxidative stress, and energy metabolism.

## CONCLUSION AND PERSPECTIVE

HM extracts have shown its great efficacy in improving dementia, although the mechanisms are still under exploration. Recent findings highlight the role of HM extracts *via* activating various signaling pathways to attenuate cognitive barrier, spatial learning, and energy metabolism in both animal experiments and cell lines. The generally used HM extracts, such as resveratrol, Tanshinone IIA, dioscin, and curcumin, are potential candidates for new drug screening against dementia, and numerous results have demonstrated their therapeutic efficacy to attenuate nerve cell damage in both animal mode and cell lines *via* activating autophagy and anti-inflammation and inhibiting apoptosis. The relevant mechanisms of the therapeutic application of HMs are summarized in **Figure 4**. Although these results sounds promising, further studies into the safety of HM extracts should be carried out, since multiple targets are involved, and most of the results are obtained from experiments; clinical practices are in great need to assess the therapeutic efficacy and safety on the human body. Therefore, HM extracts offer an alternative solution to the treatment of dementias *via* mediating various signaling pathways.

## AUTHOR CONTRIBUTIONS

All authors listed have made a substantial, direct, and intellectual contribution to the work and approved it for publication.

## FUNDING

This work was supported by grants from the China Postdoctoral Science Foundation (2020M681398), Youth Project of National Natural Science Foundation of China (82101602), and Medical and Health Science and Technology Development Project of Shandong Province (2018WS147).

## REFERENCES

Alers, S., Löffler, A. S., Wesselborg, S., and Stork, B. (2012). Role of AMPK-mTOR-Ulk1/2 in the Regulation of Autophagy: Cross Talk, Shortcuts, and Feedbacks. *Mol. Cel Biol* 32, 2–11. doi:10.1128/MCB.06159-11

Alirezaei, M., Kiosses, W. B., and Fox, H. S. (2008). Decreased Neuronal Autophagy in HIV Dementia: A Mechanism of Indirect Neurotoxicity. *Autophagy* 4, 963–966. doi:10.4161/auto.6805

Bai, X., and Zhang, M. (2021). Traditional Chinese Medicine Intervenes in Vascular Dementia: Traditional Medicine Brings New Expectations. *Front. Pharmacol.* 12, 689625. doi:10.3389/fphar.2021.689625

Caberlotto, L., and Nguyen, T. P. (2014). A Systems Biology Investigation of Neurodegenerative Dementia Reveals a Pivotal Role of Autophagy. *BMC Syst. Biol.* 8, 65. doi:10.1186/1752-0509-8-65

Cantó, C., Gerhart-Hines, Z., Feige, J. N., Lagouge, M., Noriega, L., Milne, J. C., et al. (2009). AMPK Regulates Energy Expenditure by Modulating NAD+ Metabolism and SIRT1 Activity. *Nature* 458, 1056–1060. doi:10.1038/nature07813

Cao, J. (2010). mTOR Regulation of Autophagy. *FEBS Lett.* 2010, 584.

Cuervo, A. M. (2013). Autophagy and Neurodegeneration. *Alzheimer\\"s Demen.* 9, P512. doi:10.1016/j.jalz.2013.04.219

Dong, H., Mao, S., Mao, S., Wei, J., Liu, B., Zhang, Z., et al. (2012). Tanshinone IIA Protects PC12 Cells from β-amyloid(25-35)-induced Apoptosis via PI3K/Akt

Signaling Pathway. *Mol. Biol. Rep.* 39, 6495–6503. doi:10.1007/s11033-012-1477-3

Dong, W., Wang, R., Ma, L. N., Xu, B. L., Zhang, J. S., Zhao, Z. W., et al. (2015). Autophagy Involving Age-Related Cognitive Behavior and hippocampus Injury Is Modulated by Different Caloric Intake in Mice. *Int. J. Clin. Exp. Med.* 8, 11843–11853.

Eckert, A. (2019). C.11.02 the Role of Mitochondria in Aging, MCI and Dementia. *Eur. Neuropsychopharmacol.* 29, S626–S627. doi:10.1016/j.euroneuro.2018.11.992

Eglit, H. C. (1999). *Diagnosis, Management and Treatment of Dementia*.

Fisher, L. (2021). Retraction: Resveratrol Attenuates Inflammation and Reduces Matrix-Metalloprotease Expression by Inducing Autophagy via Suppressing the Wnt/β-Catenin Signaling Pathway in IL-1β-induced Osteoarthritis Chondrocytes. *RSC Adv.* 11. doi:10.1039/d1ra90015c

Guo, M., Xu, J., Wang, S., and Dong, B. (2021). Asiaticoside Reduces Autophagy and Improves Memory in a Rat Model of Dementia through mTOR Signaling Pathway Regulation. *Mol. Med. Rep.* 24, 284. doi:10.3892/mmr.2021.12284

Guo, Y., Wang, S., Zhang, H., Gao, W., and Fan, F. (2019). Abstract P3016: High Glucose Induced Diabetic Dementia Is Mediated by Mitochondria Dysfunction. *Hypertension* 74, 3016. doi:10.1161/hyp.74.suppl_1.p3016

Han, J., Pan, X. Y., Xu, Y., Xiao, Y., An, Y., Tie, L., et al. (2012). Curcumin Induces Autophagy to Protect Vascular Endothelial Cell Survival from Oxidative Stress Damage. *Autophagy* 8, 812–825. doi:10.4161/auto.19471

He, C., and Klionsky, D. J. (2009). Regulation Mechanisms and Signaling Pathways of Autophagy. *Annu. Rev. Genet.* 43, 67–93. doi:10.1146/annurev-genet-102808-114910

Heydarabadi, F. H., Abdoli, A., Gharibzadeh, S., Sayyah, M., Bashar, R., and Sheikholeslami, F. (2020). Role of Autophagy in Nerve Cell Apoptosis in Mice Infected with Street Rabies Virus. *Arch. Virol.* 165, 2857–2867. doi:10.1007/s00705-020-04815-z

Isik, A. T., Celik, T., Ulusoy, G., Ongoru, O., Elibol, B., Doruk, H., et al. (2009). Curcumin Ameliorates Impaired Insulin/IGF Signalling and Memory Deficit in a Streptozotocin-Treated Rat Model. *Age (Dordr)* 31, 39–49. doi:10.1007/s11357-008-9078-8

Ji, J., Tao, P., Wang, Q., Li, L., and Xu, Y. (2020). SIRT1: Mechanism and Protective in Diabetic Nephropathy. *Endocr. Metab. Immune Disord. Drug Targets* 21, 835. doi:10.2174/1871530320666201029143606

Jiang, P., Li, C., Xiang, Z., and Jiao, B. (2014). Tanshinone IIA Reduces the Risk of Alzheimer's Disease by Inhibiting iNOS, MMP-2 and NF-κBp65 T-ranscription and T-ranslation in the T-emporal L-obes of R-at M-odels of Alzheimer's D-isease. *Mol. Med. Rep.* 10, 689–694. doi:10.3892/mmr.2014.2254

Jiang, W., and Chang, C. (2019). Discussion on Treatment of Vascular Dementia by Autophagy and Detoxification. *Liaoning J. Traditional Chin. Med.*

Joungmok, K., and Kun-Liang, G. (2019). mTOR as a central Hub of Nutrient Signalling and Cell Growth. *Nat. Cel. Biol.* 21, 63. doi:10.1038/s41556-018-0205-1

Ju, J. S., and Weihl, C. C. (2010). Inclusion Body Myopathy, Paget's Disease of the Bone and Fronto-Temporal Dementia: a Disorder of Autophagy. *Hum. Mol. Genet.* 19, R38–R45. doi:10.1093/hmg/ddq157

Jung, E. Y., Lee, M. S., Ahn, C. J., Cho, S. H., Bae, H., and Shim, I. (2013). The Neuroprotective Effect of Gugijihwang-Tang on Trimethyltin-Induced Memory Dysfunction in the Rat. *Evid. Based Complement. Alternat Med.* 2013, 542081. doi:10.1155/2013/542081

Kilic, U., Elibol, B., Uysal, O., Kilic, E., Yulug, B., Sayin Sakul, A., et al. (2018). Specific Alterations in the Circulating Levels of the SIRT1, TLR4, and IL7 Proteins in Patients with Dementia. *Exp. Gerontol.* 111, 203–209. doi:10.1016/j.exger.2018.07.018

Kim, D., Nguyen, M. D., Dobbin, M. M., Fischer, A., Sananbenesi, F., Rodgers, J. T., et al. (2007). SIRT1 Deacetylase Protects against Neurodegeneration in Models for Alzheimer's Disease and Amyotrophic Lateral Sclerosis. *EMBO J.* 26, 3169–3179. doi:10.1038/sj.emboj.7601758

Kim, J., Kundu, M., Viollet, B., and Guan, K. L. (2011). AMPK and mTOR Regulate Autophagy through Direct Phosphorylation of Ulk1. *Nat. Cel Biol.* 13, 132. doi:10.1038/ncb2152

Kong, D., Luo, J., Shi, S., and Huang, Z. (2021). Efficacy of Tanshinone IIA and Mesenchymal Stem Cell Treatment of Learning and Memory Impairment in a Rat Model of Vascular Dementia. *J. Tradit Chin. Med.* 41, 133–139. doi:10.19852/j.cnki.jtcm.2021.01.015

Le Couteur, D. G., Doust, J., Creasey, H., and Brayne, C. (2020). Political Drive to Screen for Pre-dementia: Not Evidence Based and Ignores the Harms of Diagnosis. *BMJ* 347, f5125. doi:10.1136/bmj.f5125

Lee, B., Sur, B., Park, J., Shin, H., Kwon, S., Yeom, M., et al. (2012). Fucoidan Ameliorates Scopolamine-Induced Neuronal Impairment and Memory Dysfunction in Rats via Activation of Cholinergic System and Regulation of cAMP-Response Element-Binding Protein and Brain-Derived Neurotrophic Factor Expressions. *J. Korean Soc. Appl. Biol. Chem.* 55, 711–720. doi:10.1007/s13765-012-2137-y

Lee, J. H., Choi, S. H., Lee, C. J., and Oh, S. S. (2020). Recovery of Dementia Syndrome Following Treatment of Brain Inflammation. *Dement Geriatr. Cogn. Dis. Extra* 10, 1–12. doi:10.1159/000504880

Levine, B., and Kroemer, G. (2008). Autophagy in the Pathogenesis of Disease. *Cell* 132, 27–42. doi:10.1016/j.cell.2007.12.018

Li, Q. (2018). Research Overview on Treating Vascular Dementia in TCM. *Clin. J. Chin. Med.*

Li, X. J., and Zhang, H. Y. (2009). Potential Anti-dementia Agents in Traditional Chinese Medicine. *Nat. Prod. Commun.* 4, 877–886. doi:10.1177/1934578x0900400629

Lin, S. K., Lin, P. H., Hsu, R. J., Chuang, H. C., and Liu, J. M. (2017). Traditional Chinese Medicine Therapy Reduces the Catheter Indwelling Risk in Dementia Patients with Difficult Voiding Symptoms. *J. Ethnopharmacol* 203, 120–126. doi:10.1016/j.jep.2017.03.040

Liu, B., Tang, J., Zhang, J., Li, S., Yuan, M., and Wang, R. (2014). Autophagy Activation Aggravates Neuronal Injury in the hippocampus of Vascular Dementia Rats. *Neural Regen. Res.* 9, 1288–1296. doi:10.4103/1673-5374.137576

Lu, D. F., and Herr, K. (2012). Pain in Dementia: Recognition and Treatment. *J. Gerontol. Nurs.* 38, 8–13. doi:10.3928/00989134-20120113-01

Ma, J., Wang, Y., Zhang, Y., Guo, Q., Zhen, X., and Shi, M. (2019). Neuropsychological Features in post-stroke Cognitive Impairment with No Dementia Patients with Different Traditional Chinese Medicine Syndromes. *J. Traditional Chin. Med.* 39, 97.

Mao, P. (2012). Oxidative Stress and its Clinical Applications in Dementia. *J. Neurodegener Dis.* 2013, 319898. doi:10.1155/2013/319898

Miyasaka, T., Yoshimura, S., Saka, A., Shinzaki, Y., Yoshina, S., Kage-Nakadai, E., et al. (2010). Curcumin Improves Tau-Mediated Neuronal Dysfunction in Nematode. *Alzheimer's Demen.* 6, e27–e28. doi:10.1016/j.jalz.2010.08.086

Morita, T., Watanabe, K., Asai, M., Iwata, N., and Shirotani, K. (2010). *Autophagy and its Significance on Dementia*.

Moussa, C., Hebron, M., Huang, X., Ahn, J., Rissman, R. A., Aisen, P. S., et al. (2017). Resveratrol Regulates Neuro-Inflammation and Induces Adaptive Immunity in Alzheimer's Disease. *J. Neuroinflammation* 14, 1. doi:10.1186/s12974-016-0779-0

Natascia, B., Simona, R., Annalisa, B., Antonella, C., Niccolò, L., Francesco, B., et al. (2014). Curcumin as a Therapeutic Agent in Dementia: A Mini Systematic Review of Human Studies. *Scientific World J.* 2014, 174282.

Nussenzweig, S. C., Verma, S., and Finkel, T. (2015). The Role of Autophagy in Vascular Biology. *Circ. Res.* 116, 480–488. doi:10.1161/CIRCRESAHA.116.303805

Padilla, R. (2019). "Working with Elders Who Have Dementia and Alzheimer's Disease," in *Occupational Therapy with Elders*. Fourth Edition, 282–297. doi:10.1016/b978-0-323-49846-3.00020-2

Paik, J. S., Ha, M., Jung, Y. H., Kim, G. H., Han, K. D., Kim, H. S., et al. (2020). Low Vision and the Risk of Dementia: a Nationwide Population-Based Cohort Study. *Sci. Rep.* 10, 9109. doi:10.1038/s41598-020-66002-z

Papandreou, I., Lim, A. L., Laderoute, K., and Denko, N. C. (2008). Hypoxia Signals Autophagy in Tumor Cells via AMPK Activity, Independent of HIF-1, BNIP3, and BNIP3L. *Cell Death Differ* 15, 1572–1581. doi:10.1038/cdd.2008.84

Paudel, P., Park, C. H., Jung, H. A., Yokozawa, T., and Choi, J. S. (2020). A Systematic Review on Anti-Alzheimer's Disease Activity of Prescription Kangen-Karyu. *Drug Discov. Ther.* 14, 61–66. doi:10.5582/ddt.2020.03013

Perluigi, M., Di Domenico, F., Barone, E., and Butterfield, D. A. (2021). mTOR in Alzheimer Disease and its Earlier Stages: Links to Oxidative Damage in the Progression of This Dementing Disorder. *Free Radic. Biol. Med.* 169, 382. doi:10.1016/j.freeradbiomed.2021.04.025

Preeti, S., Peter, S., and Hanson, M. (2017). SIRT1 Ameliorates Oxidative Stress Induced Neural Cell Death and Is Down-Regulated in Parkinson's Disease. *BMC Neurosci.* 18, 46.

Qin, W., Yang, T., Ho, L., Zhao, Z., Wang, J., Chen, L., et al. (2006). Neuronal SIRT1 Activation as a Novel Mechanism Underlying the Prevention of Alzheimer Disease Amyloid Neuropathology by Calorie Restriction. *J. Biol. Chem.* 281, 21745–21754. doi:10.1074/jbc.M602909200

Romeo, M. A., Faggioni, A., and Cirone, M. (2019). Could Autophagy Dysregulation Link Neurotropic Viruses to Alzheimer's Disease? *Neural Regen. Res.* 14, 1503–1506. doi:10.4103/1673-5374.253508

Sahyouni, R., Chen, J., Verma, A., and Brown, N. (2021). *Alzheimer's Disease Decoded: The History, Present, and Future of Alzheimer's Disease and Dementia, Alzheimer's Disease Decoded: The History, Present, and Future of Alzheimer's Disease and Dementia*.

Salminen, A., and Kaarniranta, K. (2009). SIRT1: Regulation of Longevity via Autophagy. *Cell Signal* 21, 1356–1360. doi:10.1016/j.cellsig.2009.02.014

Shen, Y. J., and Li, C. Y. (2005). Experimental Study of Traditional Chinese Medicine in the Treatment of Vascular Dementia. *Zhongguo Zhong Yao Za Zhi* 30, 725–728.

Skaljo, E., Hodzic, M., and Bektas, I. (2009). "Treatment Guidelines for Agitation in Dementia Patients," in International Conference on Ultra Modern Telecommunications & Workshops.

Subaraja, M., Anantha Krishnan, D., Edwin Hillary, V., William Raja, T. R., Mathew, P., Ravikumar, S., et al. (2020). Fucoidan Serves a Neuroprotective Effect in an Alzheimer's Disease Model. *Front. Biosci. Elite Ed.* 12, 1–34.

Süleyman, C., Hai, E., Dang, W., Le, S., and Widlund, A. L. (2012). *The Relation between Resveratrol, Sirt1, mTOR and Autophagy*.

Sun, M., Shen, X., and Ma, Y. (2019). Rehmannioside A Attenuates Cognitive Deficits in Rats with Vascular Dementia (VD) through Suppressing Oxidative Stress, Inflammation and Apoptosis. *Biomed. Pharmacother.* 120, 109492. doi:10.1016/j.biopha.2019.109492

Sun, W., Hongmei, A. N., and Hospital, L. (2014). Effects of Prepared Radix Rehmanniae and Related Herbal Formula in Treatment of Senile Dementia. *Chin. Arch. Traditional Chin. Med.*.

Tang, L. M., Wang, L. X., Wang, Z. Y., Sun, L. F., Pan, X. D., and Pan, G. Q. (2017). Tanshinone IIA Ameliorates lead (Pb)-Induced Cognitive Deficits and Oxidative Stress in a Rat Pup Model. *Bratisl Lek Listy* 118, 196–201. doi:10.4149/BLL_2017_039

Wang, H., Yu, H., Song, K., Xiong, F., and Zhang, H. (2020). Traditional Chinese Medicine for Mild Cognitive Impairment: A Protocol for Systematic Review and Network Meta-Analysis. *Medicine (Baltimore)* 99, e22187. doi:10.1097/MD.0000000000022187

Wang, Q. C., Lu, L., and Zhou, H. J. (2019). Relationship between the MAPK/ERK Pathway and Neurocyte Apoptosis after Cerebral Infarction in Rats. *Eur. Rev. Med. Pharmacol. Sci.* 23, 5374. doi:10.26355/eurrev_201906_18206

Wang, W., Qiao, O., Ji, H., Zhang, X., Han, X., Zhang, Y., et al. (2021). Autophagy in Vascular Dementia and Natural Products with Autophagy Regulating Activity. *Pharmacol. Res.* 170, 105756. doi:10.1016/j.phrs.2021.105756

Wang, X. X., Zhang, B., Xia, R., and Jia, Q. Y. (2020). Inflammation, Apoptosis and Autophagy as Critical Players in Vascular Dementia. *Eur. Rev. Med. Pharmacol. Sci.* 24, 9601–9614. doi:10.26355/eurrev_202009_23048

Xian, Y. F., Lin, Z. X., Ip, S. P., Su, Z. R., Chen, J. N., and Lai, X. P. (2013). Comparison the Neuropreotective Effect of Cortex Phellodendri Chinensis and Cortex Phellodendri Amurensis against Beta-Amyloid-Induced Neurotoxicity in PC12 Cells. *Phytomedicine* 20, 187–193. doi:10.1016/j.phymed.2012.09.028

Xian, Y. F., Mao, Q. Q., Ip, S. P., Lin, Z. X., and Che, C. T. (2011). Comparison on the Anti-inflammatory Effect of Cortex Phellodendri Chinensis and Cortex Phellodendri Amurensis in 12-O-Tetradecanoyl-Phorbol-13-Acetate-Induced Ear Edema in Mice. *J. Ethnopharmacol* 137, 1425–1430. doi:10.1016/j.jep.2011.08.014

Xu, Y., Wang, Q., Qu, Z., Yang, J., Zhang, X., and Zhao, Y. (2019). Protective Effect of Hyperbaric Oxygen Therapy on Cognitive Function in Patients with Vascular Dementia. *Cel Transpl.* 28, 1071–1075. doi:10.1177/0963689719853540

Yu, N., Huang, Y., Jiang, Y., Zou, L., Liu, X., Liu, S., et al. (2020). Ganoderma Lucidum Triterpenoids (GLTs) Reduce Neuronal Apoptosis via Inhibition of ROCK Signal Pathway in APP/PS1 Transgenic Alzheimer's Disease Mice. *Oxid Med. Cel Longev* 2020, 9894037. doi:10.1155/2020/9894037

Zhang, H., Zhang, Y., Zhou, L., Ruipeng, W. U., Wei, J., Juanjuan, L. U., et al. (2019). Effects of Total Alkaloids of Rhizoma Corydalis on Hippocampal Cell Apoptosis and Cognitive Function in Vascular Dementia Rats. *J. Zhengzhou Univ. (Medical Sciences)*.

Zhang, Z., Han, K., Wang, C., Sun, C., and Jia, N. (2020). Dioscin Protects against Aβ1-42 Oligomers-Induced Neurotoxicity via the Function of SIRT3 and Autophagy. *Chem. Pharm. Bull. (Tokyo)* 68, 717–725. doi:10.1248/cpb.c20-00046

Zhao, Z., Zou, Z., Mao, C., Liu, J., Hao, G., Shi, Z., et al. (2019). Resveratrol Alleviates the Nervous System Inflammation by SIRT1 in Rats with Subarachnoid Hemorrhage. *Chin. J. Neuroanat*.

Zhi, H., Pan, Z., and Lu, W. (2009). Neuroprotective Effects of Tanshinone IIA on Vascular Dementia in Rats. *Pharmacol. Clin. Chin. Materia Med*.

Zhu, A. H., Tian, J. Z., Zhong, J., Yang, C. Z., Shi, J., and Yin, J. X. (2006). A Clinical Study on a Randomized, Double-Blind Control of Chinese Medicine Granules in Treatment of Vascular Dementia. *Zhongguo Zhong Yao Za Zhi* 31, 1722.

**Conflict of Interest:** The authors declare that the research was conducted in the absence of any commercial or financial relationships that could be construed as a potential conflict of interest.

**Publisher's Note:** All claims expressed in this article are solely those of the authors and do not necessarily represent those of their affiliated organizations, or those of the publisher, the editors, and the reviewers. Any product that may be evaluated in this article, or claim that may be made by its manufacturer, is not guaranteed or endorsed by the publisher.

frontiers | Frontiers in Pharmacology

ORIGINAL RESEARCH
published: 26 April 2022
doi: 10.3389/fphar.2022.859244

# Tanhuo Formula Inhibits Astrocyte Activation and Apoptosis in Acute Ischemic Stroke

*Yuting Nie*[1,2†], *Lulu Wen*[1,2†], *Hui Li*[3], *Juexian Song*[1], *Ningqun Wang*[1], *Liyuan Huang*[1], *Li Gao*[1*] *and Miao Qu*[1*]

[1]Department of Neurology, Xuanwu Hospital, Capital Medical University, Beijing, China, [2]Capital Medical University, Beijing, China, [3]Institute of Chinese Materia Medica, China Academy of Chinese Medical Sciences, Beijing, China

Tanhuo formula (THF), a traditional Chinese medicinal formula, has been demonstrated to be effective in the clinical treatment of acute ischemic stroke (AIS). However, its active ingredients, potential targets, and molecular mechanisms remain unknown. Based on the validation of active ingredient concentrations, our study attempted to elucidate the possible mechanisms of THF based on network pharmacological analysis and experimental validation. Components of THF were screened using network pharmacological analysis, and a compound–target network and protein–protein interaction (PPI) network were constructed. In total, 42 bioactive compounds and 159 THF targets related to AIS were identified. The PPI network identified AKT1, TNF, IL6, IL1B, and CASP3 as key targets. Kyoto Encyclopedia of Genes and Genomes pathway enrichment analysis demonstrated that the inflammation and apoptotic pathways were enriched by multiple targets. The main components of THF were identified *via* high-performance liquid chromatography. Subsequently, a validation experiment was conducted, and the expressions of GFAP, C3, TNF-α, and IL-6 were detected *via* immunofluorescence staining, confirming the inflammatory response at 30 min and 3 days post injury. Immunohistochemical staining for caspase-3 and TUNEL was also performed to assess apoptosis at the same time points. These results indicate that THF can effectively decrease neural cell apoptosis through the caspase-3 pathway and restrain excessive abnormal activation of astrocytes and the release of TNF-α and IL-6, which might be accompanied by the recovery of motor function. Thus, THF may serve as a promising therapeutic strategy for AIS through multiple targets, components, and pathways.

**Keywords: Tanhuo formula (THF), inflammation, astrocyte, apoptosis, network pharmacology**

OPEN ACCESS

***Edited by:***
*Fushun Wang,*
*Nanjing University of Chinese Medicine, China*

***Reviewed by:***
*Wenqiang Chen,*
*Georgetown University, United States*
*Xiaoyan Gao,*
*Beijing University of Chinese Medicine, China*

***Correspondence:**
*Miao Qu*
*qumiaotcm@126.com*
*Li Gao*
*xuanwugaoli@126.com*

*[†]These authors have contributed equally to this work*

***Specialty section:***
*This article was submitted to Ethnopharmacology, a section of the journal Frontiers in Pharmacology*

***Received:*** *21 January 2022*
***Accepted:*** *15 March 2022*
***Published:*** *26 April 2022*

***Citation:***
*Nie Y, Wen L, Li H, Song J, Wang N, Huang L, Gao L and Qu M (2022) Tanhuo Formula Inhibits Astrocyte Activation and Apoptosis in Acute Ischemic Stroke. Front. Pharmacol. 13:859244. doi: 10.3389/fphar.2022.859244*

## INTRODUCTION

Acute ischemic stroke (AIS), characterized by high morbidity, disability, and mortality, is one of the leading causes of human death and disability worldwide; it, thereby, imposes an immense financial burden on society and severe psychological stress on individuals (Herpich and Rincon, 2020; Gao et al., 2020). According to the World Health Organization, approximately 15 million people experience an ischemic stroke each year, of which approximately 5 million die (Esquiva et al., 2018; Krishnamurthi et al., 2020; Morovatdar et al., 2021). Recombinant tissue–type plasminogen

activator, a unique, FDA-approved drug for the treatment of AIS, can only benefit approximately 5% of patients owing to the narrow treatment window for thrombolysis and the risk of cerebral hemorrhage induced by the drug (Saberi et al., 2021). Therefore, it is essential to develop more effective and safe drugs with minimal side effects for AIS treatment.

Increasing evidence has demonstrated that intervening inflammatory reactions are important targets in the clinical treatment of AIS. Astrocytes are important regulators of the neuroinflammatory response and have also been found to be effective targets for therapeutic intervention in ischemic stroke (Patabendige et al., 2021). Owing to the widespread distribution and intrinsic features of the central nervous system (CNS), astrocytes are rapidly activated and proliferated after ischemic stroke (Stary and Giffard, 2015). Activated astrocytes can immediately differentiate into two polarization phenotypes, A1 and A2. The former has pro-inflammatory and neurotoxic effects, whereas the latter has anti-inflammatory and neural restoration effects. Overactivated A1 astrocytes secrete various types of inflammatory cytokines and a large number of cytotoxic substances, such as ROS, iNOS, and glutamate. These substances amplify the inflammatory cascade reaction, aggravate the redistribution or degradation of key tight junctions (such as claudin-5 and occludin), and deteriorate the leakage of the blood–brain barrier, ultimately causing severe tissue damage and neuronal death (Xu et al., 2020; Qiu et al., 2021; Sun et al., 2021). Apoptosis is the major type of cell death at the location of cerebral infarction (Radak et al., 2017). Neurons are sensitive to the deterioration of the microenvironment and undergo massive apoptosis after a series of ischemia, hypoxia, oxidative stress, and inflammatory responses following AIS (Xu et al., 2020). Thus, inhibition of apoptosis and activation of A1 astrocytes are an essential neuroprotective strategy for AIS.

For many years, Tanhuo formula (THF), a traditional Chinese medicinal formula, has been generally acknowledged as an effective prescription for AIS caused by phlegm-heat syndrome in Xuanwu Hospital. Although our previous study confirmed that THF reduced infarct volume and attenuated neuronal damage in cerebral ischemic rats, the mechanism of antiapoptosis and astrocyte regulation has not yet been elucidated (Cong et al., 2021). THF comprises five herbal medicines: dried rhizome of *Coptis chinensis Franch.* [*Ranunculaceae*; Coptidis rhizoma; Huang-Lian (HL)], dried roots and rhizomes of *Rheum officinale Baill.*, [*Polygonaceae*, Rhei radix et rhizoma, Da-Huang (DH)], dried fruits of *Forsythia suspensa (Thunb.) Vahl* [*Oleaceae*; Forsythiae fructus; Lian-Qiao (LQ)], dried leaves of *Lophatherum gracile Brongn.* [*Poaceae*; Lophatheri herba; Dan-Zhu-Ye (DZY)], and *Rhizoma Arisaematis Cum Bile* [*Araceae*; Arisaema cum bile; Dan-Nan-Xing (DNX)]. The herbal components of THF, such as aloe emodin in DH, phillyrin in LQ, berberine, and palmatine in HL, have been shown to inhibit inflammatory responses and neuronal apoptosis in the brain (Zhu et al., 2019; Guo X. et al., 2021; Jiang et al., 2021; Tang et al., 2021; Xian et al., 2021; Zhao et al., 2021). We determined the relatively high concentrations of these key components in THF using high-performance liquid chromatography (HPLC). Based on the required concentrations to exert pharmacological effects, it is reasonable to infer that these THF components can exert pharmacological effects in the human body and promote recovery by inhibiting inflammatory response and reducing apoptosis in AIS. However, THF consists of several herbs and contains a variety of components that act *via* multiple pathways and may influence each other. Therefore, we comprehensively investigated the pharmacodynamics of THF on AIS by considering a variety of components and using network pharmacology methods. Based on bioinformatics and systems biology, network pharmacology is used to study the multilevel network relationship of "drug–target–disease" by screening potential pharmacodynamic components, action targets, and pathways in a database. Although the formula for THF has multiple ingredients and targets, network pharmacology can help address this challenge by precisely determining the research target of THF and revealing the underlying mechanisms for AIS effectively. However, current network pharmacology studies focus on the chemical composition of herbal medicines instead of the dose–effect relationship, and the content of compounds also affects the effect of herbal medicines. Therefore, the prediction results of network pharmacology may be biased and need to be experimentally verified (Zhang et al., 2019). Herein, combined with content determination of the known active components, a comparative experiment of two doses was designed in this study to enhance the reliability of network pharmacology and further analyze the mechanisms of THF in AIS. The framework of this study is shown in **Figure 1**.

# MATERIALS AND METHODS

## Materials and Reagents

LC-20AT HPLC (Shimadzu Corporation, Japan), Welch Ultimate XB-C18 column (250 mm × 4.6 mm, 5 μm), methanol and acetonitrile (chromatographic purity, Thermo Fisher Scientific, Shanghai, China), ultrapure water (Hangzhou Wahaha Beverage Co., Ltd., Hangzhou, China), ethanol, and other reagents were used as analytical reagents. LQ (batch number 140610003, purchased from Beijing Qiancao Chinese Medicine Tablet Co.), DNX (batch number 409051, purchased from Sinopharm Group Beijing Huamiao Pharmaceutical Co. Ltd.). HL (batch number 1402001), DZY (batch number 1406001), and DH (batch number 1402001) were purchased from Anguo Changda Chinese herbal medicine Pieces Co. Ltd. (Baoding, China). The identity of all the herbs was confirmed by a botanical expert, Professor Hui Li (Institute of Chinese Materia Medica, China Academy of Chinese Medical Sciences, Beijing, China), and the specimens were archived in the institute. Berberine hydrochloride (lot:110713-201212, purity: 86.7%) and phillyrin (lot:110821-201213, purity: 95.3%), obtained from the National Institutes for Food and Drug Control (Beijing, China), were used as reference standards.

## Preparation of THF

The composition of THF was HL (9 g), DH (5 g), LQ (10 g), DZY (9 g), and DNX (9 g). LQ (166.7 g) and DH (83.3 g), ratio: 2:1,

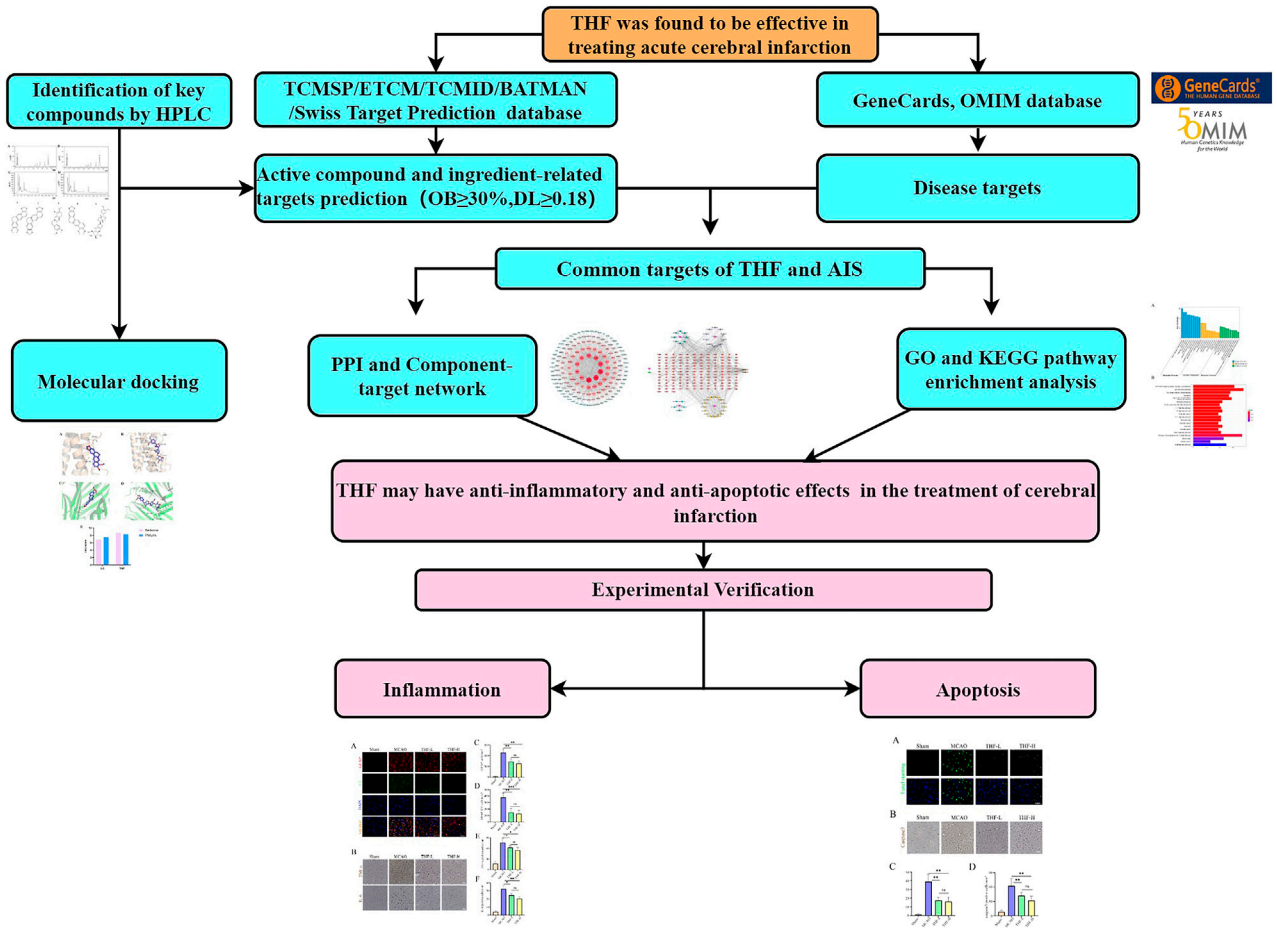


**FIGURE 1 |** Framework of this study.

were extracted three times by reflux extraction with 65% ethanol (eight times the volume) for 2 h at a time and filtered and concentrated into a filtrate with a relative density of 1.10–1.20 (50–60°C). HL (150 g), DNX (150 g, wrap-boiling), and DZY (150 g), ratio: 1:1:1, were extracted with water three times (2 h each time): the first time with 10 times the volume of water and the second and third times with eight times the volume of water. The extracts were filtered and concentrated into a filtrate with a relative density of 1.20–1.30 (60–70°C). The two filtrates were mixed, dried under reduced pressure, and finally crushed into a powder.

## Sample and Reference Solution Preparation

Preparation of standard solutions: berberine hydrochloride and phillyrin were prepared in methanol to yield 0.15 and 0.20 mg/ml control solution, respectively, and then filtered through a 0.45-μm membrane filter before HPLC analysis. To prepare a sample solution for berberine, epiberberine, coptisine, and palmatine: THF dried powder (0.5 g) was added to 50 ml of methanol-hydrochloric acid (100: 1) and then sonicated for 30 min. Methanol was added to restore the solution weight to the initial. After filtration, 2 ml of the filtrate was placed in a 10-ml volumetric flask and methanol was added till it reached the mark. The sample solution was obtained by filtration through a 0.45-μm membrane. To prepare a sample solution for phillyrin, 1.0 g of THF dried powder was weighed and 15 ml 70% methanol was added, follow by sonication for 30 min, 70% methanol was used to replace the lost weight, and ultimately the sample solution of phillyrin was obtained by filtration through a 0.45-μm membrane.

## HPLC Analysis

The concentrations of THF compounds were analyzed by HPLC. HPLC analysis was performed using a Welch Ultimate XB-C18 column (250 mm × 4.6 mm, 5 μm).

HPLC conditions for berberine, epiberberine, coptisine, and palmatine were as follows: octadecylsilane-bonded silica gel was used as the filler for the HPLC column. Acetonitrile (0.05 mol/L): potassium dihydrogen phosphate (50:50) ( 0.4 g sodium dodecyl sulfate per 100 ml is added and then the pH is adjusted to 4.0, with phosphoric acid) were used as the mobile phase. Chromatographic analysis was performed at 30°C with a flow rate of 1 ml/min, detection wavelength of 345 nm, and an injection volume of 10 μl.

To perform HPLC for phillyrin, the mobile phase consisted of water (A) and acetonitrile (B), and the gradient elution program was (time/B%): 0–30 min, 23–24%; 30–31 min, 24–95%; 31–39 min, 95%; 39–40 min, 95–23%; 10–15 min, 50–80%; and 40–50 min, 23%. Chromatographic analysis was performed at 30°C with a flow rate of 1 ml/min, detection wavelength of 277 nm, and an injection volume of 10 μl.

## Screening Conditions for Candidate Active Ingredients

The Traditional Chinese Medicine Database and Analysis Platform (TCMSP) was used to screen the active ingredients of THF. The TCMSP is a recognized Chinese herbal medicine platform that provides detailed pharmacokinetic data of herbal ingredients, such as oral bioavailability (OB), drug-likeness (DL), aqueous solubility, and the blood–brain barrier (BBB) *etc.*(Veber et al., 2002; Ru et al., 2014). Due to the breakdown of the neurovascular unit and BBB after cerebral infarction, huge amounts of herbal components directly enter the CNS without obstacles. Thus, the screening conditions on the platform were set as OB ≥30% and DL ≥0.18 (Huang et al., 2014).

## Candidate Active Compounds and Ingredient-Related Target Prediction

THF compounds were clarified from the TCMSP (https://old.tcmsp-e.com/tcmsp.php), ETCM (http://www.tcmip.cn/ETCM/index.php/Home/Index/), TCMID (http://www.megabionet.org/tcmid/), and BATMAN (http://bionet.ncpsb.org/batman-tcm/index.php) databases and literature search. Subsequently, the TCMSP platform was used to identify target genes. In addition, the targets were predicted using the Swiss Target Prediction database (http://www.swisstargetprediction.ch/) for the quality marker (Q-maker) of each herb in THF. Subsequently, different ID types of the targets were transformed into UniProt IDs using the UniProt database (https://www.uniprot.org/).

## Screening of Disease-Associated Targets

AIS-related targets were predicted using GeneCards (https://www.genecards.org) and OMIM (https://omim.org). "Cerebral infarction," "stroke," and "cerebral ischemia" were used as the keywords for target searching. The relevance score was set as greater than or equal to 5, duplicate targets were excluded, and cerebral infarction–related targets were screened out. Intersection of THF-AIS–related target genes was performed to verify common target genes.

## Protein–Protein Interaction (PPI) and Component–Target Network

Common targets of THF and AIS were uploaded into the STRING database (https://string-db.org/) for PPI network mapping by setting species as "Homo sapiens" and moderate confidence. Subsequently, the PPI network and component–target network were created and visualized using Cytoscape 3.8.0 software, and the degree centrality, betweenness centrality, and closeness centrality were calculated. The size and color of a node represent the degree value, which further reflects its importance and the number of connections with other nodes.

## Enrichment Analysis

The ClusterProfiler software package and R software were used to perform Gene Ontology (GO) function and Kyoto Encyclopedia of Genes and Genomes (KEGG) pathway enrichment analyses. GO function enrichment analysis involves biological processes (BP), molecular function (MF), and cellular component (CC) biology.

## Molecular Docking

The target receptors were retrieved by downloading them from the PDB database (PDB: https://www.rcsb.org/). The compounds were downloaded from PubChem (https://pubchem.ncbi.nlm.nih.gov/). Prior to docking, all receptor proteins were treated with PyMol 2.5, including the removal of water molecules, salt ions, and small molecules. Molecular docking was then accomplished using AutoDock Vina 1.1.2 software, and docking was performed using the default docking parameters. The docking results were visualized using PyMol 2.5.

## MCAO Models

All experimental procedures complied with the national guidelines for care and the use of laboratory animals were approved by the Experimental Animal Ethics Committee of Capital Medical University (Ethics Number: aeei-2019-086). All male 8-week-old Sprague–Dawley rats were obtained from Beijing Vital River Laboratory Animal Technology Co., Ltd. (License Number: scxk[Beijing]2016-0006) and raised in the experimental animal center of Capital Medical University in a specific pathogen-free SPF environment (18–22°C, 40–60% humidity, 12 h day/night). Twelve male rats were used to avoid the protective effects of estrogen. The rats were anesthetized using 5% isoflurane (Beyotime, China), and the right common carotid artery (CCA), internal carotid artery (ICA), and external carotid artery (ECA) were gently dissected and exposed. After permanent ligation of the CCA and ECA in the proximal portion, the distal end of the ICA was clamped using hemostatic forceps, and a small incision was made at the bifurcation of the CCA. The preprocessed nylon suture was then inserted from the CCA into the ICA for 18–22 mm until resistance was probed in the middle cerebral artery. Finally, a nylon suture (Beijing Shadong Biotechnology Co., Ltd., Beijing, China) was fixed to prevent spontaneous withdrawal, and the incision was sutured and disinfected. The sham group was treated using the same procedure but without MCAO.

## Drug Treatment

The THF dried powder (purity: 5.34 g crude drug/kg dried powder; batch number: 201809-jgf) was provided by the China Academy of Chinese Medical Sciences. The daily consumption of THF is 4.9 g crude drug/kg in rats, which is equivalent to 0.7 g crude drug/kg in patients. We set low dose of THF (THF-L) and high dose of THF (THF-H) groups in rats, approximately one and

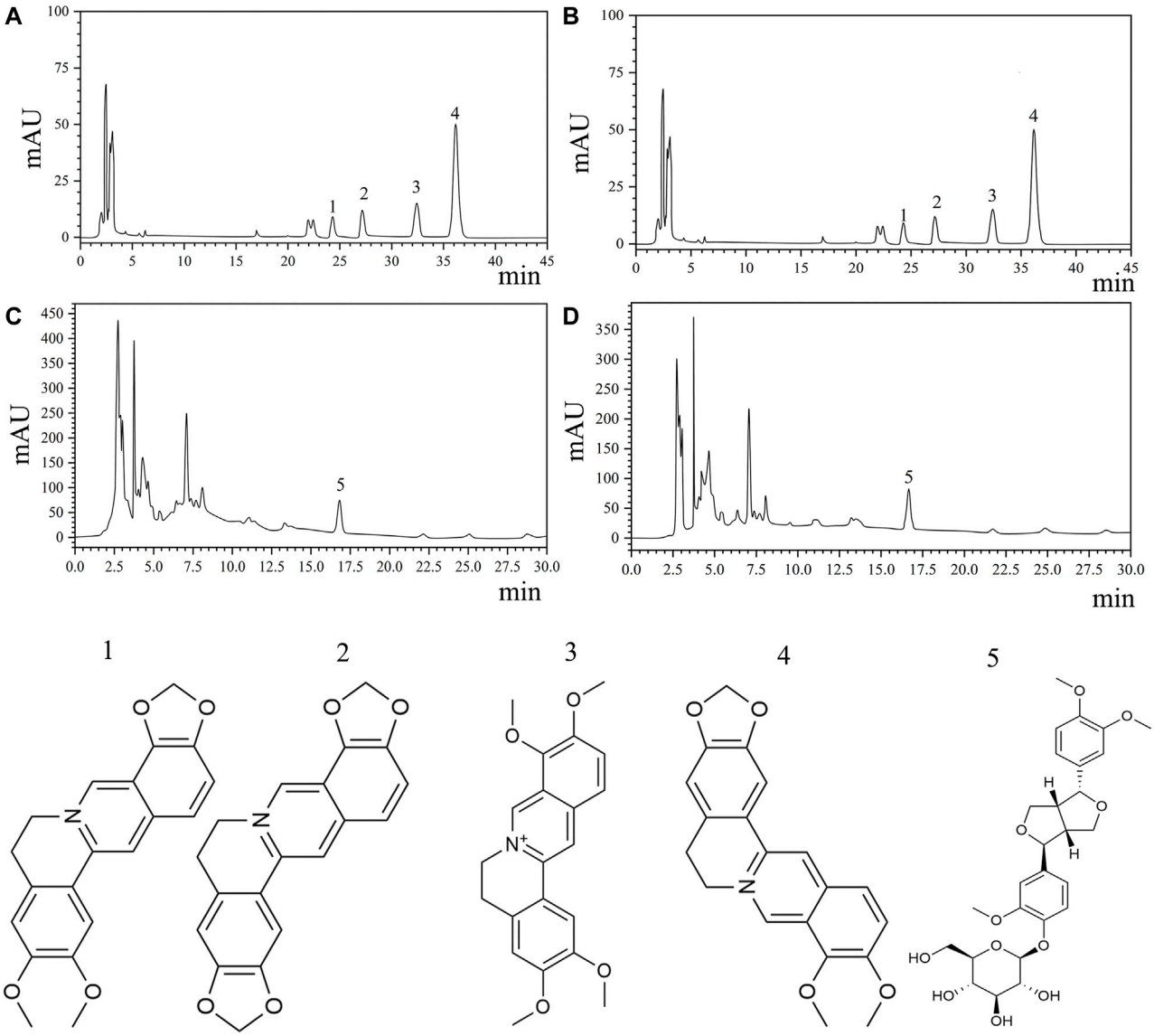


**FIGURE 2 |** Quantitative analysis of key compounds of THF by HPLC analysis. **(A,B)** HPLC analysis and chemical structures of four major ingredients of HL. 1. Epiberberine ($C_{20}H_{17}NO_4$). 2. Coptisine($C_{19}H_{13}NO_4$). 3. Palmatine ($C_{21}H_{21}NO_4$). 4. Berberine($C_{20}H_{17}NO_4$). **(C,D)** HPLC analysis and chemical structure of phillyrin. 5. Phillyrin($C_{20}H_{34}O_{11}$).

two times the dosage of clinical patients, respectively: 0.92 g dried powder/kg; 1.84 g dried powder/kg.

## Grouping

The animals were randomly assigned to four groups: sham group, model group (MCAO rats), THF-L group (0.92 g dried powder/kg), and THF-H group (1.84 g dried powder/kg). For the THF-L group, 9.2 g of dry powder was weighed and dissolved in 100 ml of deionized water, meaning 10 ml of the solution contained 0.92 g of the drug, and the volume administered to rats was 10 ml/kg/d. For the THF-H group, 18.4 g of dry powder was weighed and dissolved in 100 ml of deionized water, meaning 10 ml of the solution contained 1.84 g of the drug, and the volume administered to rats was 10 ml/kg/d. The rats in the administration group were intragastrically administered 6, 24, 48, and 72 h after cerebral ischemia surgery. The rats in the sham and model groups were administered the same volume of saline (10 ml/kg/day) at the same time points.

## Immunofluorescence

For immunofluorescence (Shah et al., 2017), the rats in each group were euthanized, rinsed with warm saline *via* rapid left ventricular perfusion, and fixed with 4% paraformaldehyde in PBS solution for 60 min. This process was carried out at 3 days and 30 min post injury (dpi) for immunofluorescence studies. The striatal level of the brain was then dissected and fixed with 4%

**TABLE 1** | Content of key compounds of THF.

| Ingredients | Content(mg/g)A | Content(mg/g)B | Mean |
|---|---|---|---|
| Epiberberine | 4.3425 | 4.1895 | 4.266 |
| Coptisine | 7.3395 | 7.0716 | 7.205 |
| Palmatine | 9.438 | 9.1455 | 9.291 |
| Berberine | 35.1382 | 33.7735 | 34.455 |
| Total alkaloids | 56.26 | 54.18 | 55.22 |
| | Content(mg/g)C | Content(mg/g)D | |
| Phillyrin | 4.16 | 4.27 | 4.22 |

paraformaldehyde in PBS solution for 1 week. After that, the tissues were dehydrated with gradient ethanol, made transparent with xylene, embedded in paraffin, and cut into 0.5-μm sections using a biological tissue microtome. After dewaxing and hydration, the slides were immersed in 5% BSA for 1 h to block nonspecific antibodies. All paraffin sections were then incubated with primary antibodies overnight at 4°C, namely, GFAP (1:1000, rabbit source, Servicebio, Wuhan, China) and C3(1:400, mouse source, Santa Cruz, United States). These sections were then incubated with Alexa Fluor 594 and Alexa Fluor 488 (1:300, goat anti-mouse and goat anti-rabbit source, Abcam, United Kingdom) for 2 h.

## Immunohistochemistry

For immunohistochemistry (Kusakawa et al., 2015), the slides were incubated with antibodies against caspase-3 (1:750, rabbit source, Servicebio, Wuhan, China), TNF-α (1:500, rabbit source, Servicebio, Wuhan, China), and IL-6 (1:1000, rabbit source, Servicebio, Wuhan, China) overnight at 4°C. Subsequently, paraffin sections of the tissues were washed with PBS, and the secondary antibody was added and incubated for 1 h.

## TUNEL Staining

TUNEL staining (Beyotime Biotechnology, Shanghai, China) was used to detect apoptosis in tissues (Lv et al., 2021). First, the slides were fixed with 4% paraformaldehyde for 30 min at room temperature. The tissue sections were then treated with permeabilization solution for 5 min, followed by TUNEL solution for 1 h at 37°C. Finally, the tissues were observed under a fluorescence microscope (Nikon Eclipse E600, Boston, United States).

## Statistical Analysis

Statistical analyses were performed using SPSS 26.0 (IBM Corp., Armonk, NY, United States). All data are expressed as the mean ± standard deviation. Homogeneity of variance was tested; one-way analysis of variance was used to compare multiple groups; and subsequently, the LSD test was performed for pairwise comparison. $P < 0.05$ was considered to be statistically significant.

# RESULTS

## Quantitative Analysis of Key Compounds

HL is a monarch medicine, and LQ has the highest dosage in THF. A qualitative study of HL and LQ is important for controlling the quality of the entire prescription. Therefore, berberine, epiberberine, coptisine, palmatine of HL, and phillyrin of LQ were selected as quality control indices according to the standards of the Chinese Pharmacopoeia 2015 edition. HPLC was used to determine the concentrations of the key compounds. The results are shown in **Figure 2** and **Table 1**. The average berberine, epiberberine, coptisine, palmatine, and phillyrin contents were 34.455, 4.266, 7.205, 9.291, and 4.22 mg/g, respectively.

## Candidate Active Compound of THF

Traditional Chinese medicine is a multitarget, multicomponent therapy model. By screening the TCMSP, ETCM, TCMID, and BATMAN databases, a total of 64 active ingredients were retrieved, of which 42 had regulatory effects on cerebral infarction. DH, HL, LQ, DNX, and DZY contained eight, 10, 16, five, and one chemical compounds/compound, respectively. Beta-sitosterol is a common component of DH and DNX, whereas quercetin is a common component of HL and LQ (**Supplementary Table S1**).

## Common Targets of THF and AIS

A total of 518 targets were obtained by eliminating duplicate targets (**Supplementary Table S2**). These drug targets were further converted into Uniport ID. A total of 986 AIS-related genes were obtained from the GeneCards and OMIM databases. Finally, 159 common target genes of THF and AIS were identified (**Figure 3A**).

## Protein–Protein Interaction Network

To identify the predominant common targets of THF and AIS, a network analysis of PPI was performed using the STRING database (**Figure 3B**). A total of 159 common target genes were imported into the STRING database platform, and the PPI network was constructed using Cytoscape 3.8.0 software. The network included 159 nodes and 2,779 edges, with an average degree value of 34.95 (**Supplementary Table S3**). The larger the node, the more important the role it plays in the network, and the top five targets contain AKT1, TNF, IL6, IL1B, and CASP3 (**Table 2**), which are not only important genes of THF for treating AIS but are also essential targets for experimental verification.

## Compound-Target Network Analysis

To establish the correlation between THF and potential targets, the "Compound–Target Network" was conducted using Cytoscape 3.8.0 (**Figure 3C**). This network includes 206 nodes and 604 edges, among which the regular hexagon, rhombus, and ellipse represent herbs, herb compounds, and genes, respectively. The degree values, which reflect the number of nodes directly linked to the compound, were used to evaluate the importance of the compound in the network. We selected the top 15 compounds based on their degree values, as shown in **Table 3**. The results showed that quercetin (MOL000098, degree = 70), coptisine (MOL001458, degree = 38), palmatine (MOL000785, degree = 38), berberine (MOL001454, degree = 36), epiberberine (MOL002897,

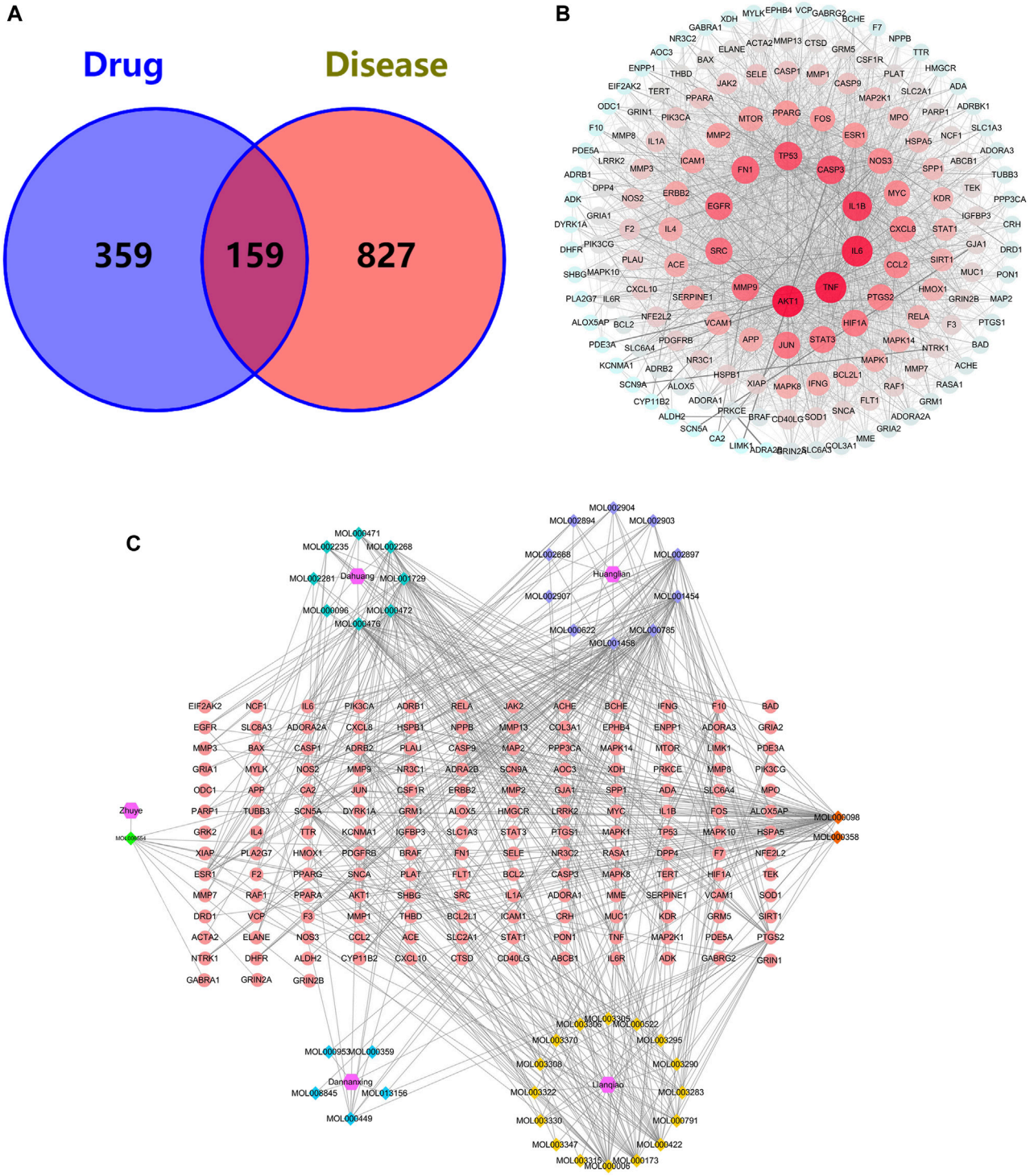


**FIGURE 3 | (A)** Venn diagram for common genes of THF and AIS. **(B)** PPI network of the potential targets of THF. **(C)** Compound–target network of THF on AIS. The regular hexagon, rhombus, and ellipse represent the herbs, herb compounds, and genes, respectively. The number of connected lines indicates the importance of the node.

degree = 36), physcion (MOL000476, degree = 35), emodin (MOL000472, degree = 30), and chrysophanol (MOL001729, degree = 29) were identified. These compounds exhibited high degree values, demonstrating that one herb can target multiple genes and play a crucial role in the treatment of cerebral infarction.

**TABLE 2 |** Topological parameters of the targets.

| Name | Degree | Betweenness centrality | Closeness centrality |
|---|---|---|---|
| AKT1 | 115 | 0.08234 | 0.782178 |
| TNF | 112 | 0.059641 | 0.76699 |
| IL6 | 110 | 0.056531 | 0.763285 |
| IL1B | 101 | 0.033635 | 0.731481 |
| CASP3 | 94 | 0.035664 | 0.705357 |
| TP53 | 93 | 0.022581 | 0.702222 |
| FN1 | 88 | 0.023245 | 0.686957 |
| EGFR | 86 | 0.022094 | 0.681034 |
| SRC | 84 | 0.023343 | 0.67234 |
| MMP9 | 84 | 0.018505 | 0.666667 |
| JUN | 83 | 0.017286 | 0.669492 |
| STAT3 | 81 | 0.013424 | 0.661088 |
| HIF1A | 81 | 0.011461 | 0.666667 |
| PTGS2 | 77 | 0.010596 | 0.650206 |
| CCL2 | 77 | 0.009268 | 0.647541 |
| CXCL8 | 77 | 0.011757 | 0.647541 |
| MYC | 75 | 0.014225 | 0.644898 |
| NOS3 | 74 | 0.033877 | 0.650206 |
| ESR1 | 71 | 0.01457 | 0.639676 |
| FOS | 71 | 0.020903 | 0.639676 |

**TABLE 3 |** Core compounds of THF.

| Name | Compound | Degree | Betweenness | Closeness |
|---|---|---|---|---|
| MOL000098 | Quercetin | 70 | 13738.66 | 0.465909 |
| MOL001458 | Coptisine | 38 | 4416.309 | 0.403543 |
| MOL000785 | Palmatine | 38 | 4259.88 | 0.403543 |
| MOL001454 | Berberine | 36 | 4012.556 | 0.406746 |
| MOL000476 | Physcion | 36 | 3922.645 | 0.395753 |
| MOL002897 | Epiberberine | 35 | 3346.933 | 0.405138 |
| MOL000472 | Emodin | 30 | 3200.005 | 0.386792 |
| MOL001729 | Crysophanol | 29 | 2903.895 | 0.382463 |
| MOL000006 | Luteolin | 26 | 2134.274 | 0.372727 |
| MOL000173 | Wogonin | 25 | 1742.017 | 0.382463 |
| MOL000422 | Kaempferol | 24 | 1383.854 | 0.370036 |
| MOL002268 | Rhein | 22 | 1666.857 | 0.375458 |
| MOL000358 | Beta-sitosterol | 17 | 1651.767 | 0.364769 |
| MOL000791 | Bicuculline | 14 | 1259.112 | 0.357143 |

## GO and KEGG Pathway Enrichment Analysis

To determine the biological characteristics of potential targets of THF on AIS, GO and KEGG pathway enrichment analyses on 159 common targets were performed using the ClusterProfiler software package of the R platform. A total of 2681 GO functional processes were obtained and annotated in terms of BP, MF, and CC ($p$ <0.05). The top 10 significant terms in the BP, CC, and MF categories are shown in **Figure 4A**. Among them, the top three enriched GO functions for target genes included cellular response to chemical stress, neuron death, response to oxidative stress in BP, membrane rafts, membrane microdomains, membrane regions in CC, phosphatase binding, protein phosphatase binding, and serine hydrolase activity in MF. KEGG pathway enrichment analysis showed that 168 pathways were associated with cerebral infarction. Detailed pathways related to cerebral infarction are shown in **Figure 4B** and **Supplementary Table S4**. Enrichment analysis suggested that the inflammation and apoptotic pathways were enriched by multiple targets. Collectively, these results suggest that restraining inflammation and apoptosis may be a promising therapeutic strategy for AIS treated with THF.

## Molecular Docking

Berberine (the most abundant component in HL) and phillyrin were used for molecular docking. The key targets IL-6 and TNF-α were also selected for analysis. It is generally accepted that the lower the Vina score, the more stable the binding of the compound is to the crucial target. The results indicated that berberine and phillyrin had good binding activity for IL-6 and TNF-α (**Figures 5A–E**).

## Inhibition of THF Activity in Apoptosis in Cerebral Infarction in the MCAO Model

As network pharmacology analysis suggested that THF may protect against neuronal damage by inhibiting the apoptotic pathway, TUNEL staining was used to estimate the number of apoptotic cells at the infarction locus. A marked increase in apoptotic cells was observed in the cortex of MCAO rats, whereas THF-L and THF-H remarkably reduced apoptosis (**Figures 6A,C**). Immunochemistry was further performed to determine the protective effect of THF on neural cells. The number of caspase-3–positive cells in the cortex was significantly lower than that in the MCAO group. In contrast to MCAO rats, the number of cells with positive expression of caspase-3 in the THF-L and THF-H groups was significantly decreased (**Figures 6B,D**). These results indicate that THF treatment significantly suppressed the expression of caspase-3 and protected neural cells from apoptosis in MCAO rats.

## Inhibitory Activity of THF on the Pro-inflammatory Activation of A1 Astrocyte and Release of IL-6 and TNF-α

In the network pharmacology analysis, IL-6 and TNF were the hub genes of the PPI network, and the TNF signaling pathway was the key pathway in the KEGG enrichment, suggesting that the inflammatory response may play a pivotal role in treating AIS by THF. To evaluate the inflammatory response after cerebral infarction, immunofluorescence was performed to determine the activation of A1 astrocytes that induce an evident inflammatory response in many CNS diseases. First, double immunofluorescence staining of GFAP and C3 was performed to label astrocytes, in which positive cells labeled with C3/GFAP represented A1-type pro-inflammatory astrocytes, whereas positive cells labeled with GFAP represented all types of astrocytes. In this study, a large number of C3-/GFAP-labeled positive cells were detected at the edge of the infarct foci in MCAO rats, but not in the ipsilateral brains of rats in the sham group. Furthermore, the statistical results showed that the cell density of GFAP and C3/GFAP positive cells around infarct lesions in the THF-L and THF-H groups was lower than that in MCAO rats (**Figures 7A,C,D**). Simultaneously, immunohistochemical staining was performed to evaluate the release of IL-6 and TNF-α. Significant differences were observed between the sham and model groups. Accordingly, IL-6 expression in the cortex was decreased in both the THF-L and THF-H groups

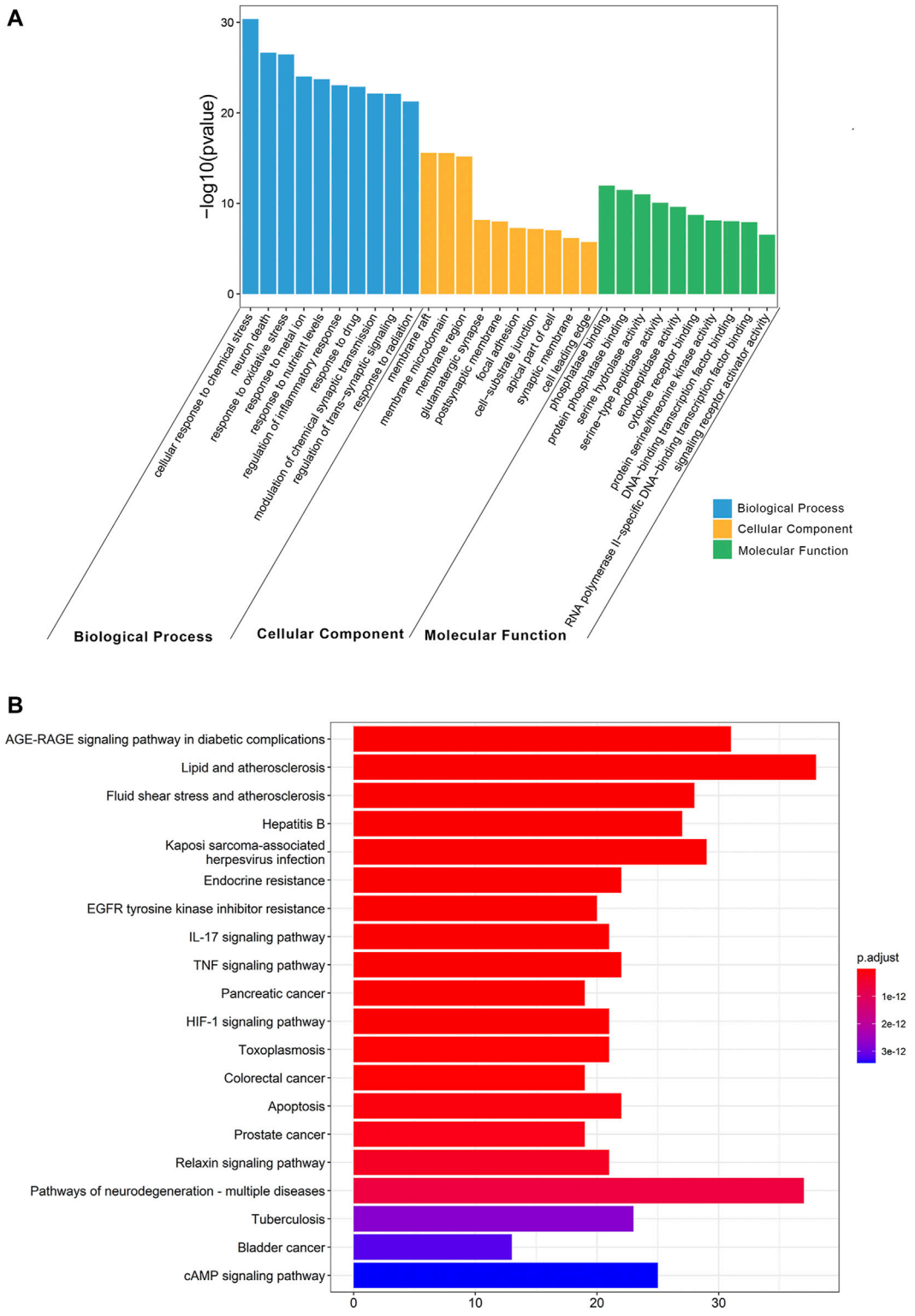


**FIGURE 4 |** Gene Ontology (GO) and Kyoto Encyclopedia of Genes and Genomes (KEGG) pathway enrichment analysis. **(A)** GO functional enrichment analysis. **(B)** KEGG pathway enrichment analysis.

compared with that in the MCAO group, whereas THF-H markedly reduced TNF-α expression, suggesting that THF inhibits the release of inflammatory factors (**Figures 7B,E,F**). Collectively, our study demonstrated that THF curbs the inflammatory response and thereby protects neural cells from apoptosis during cerebral infarction.

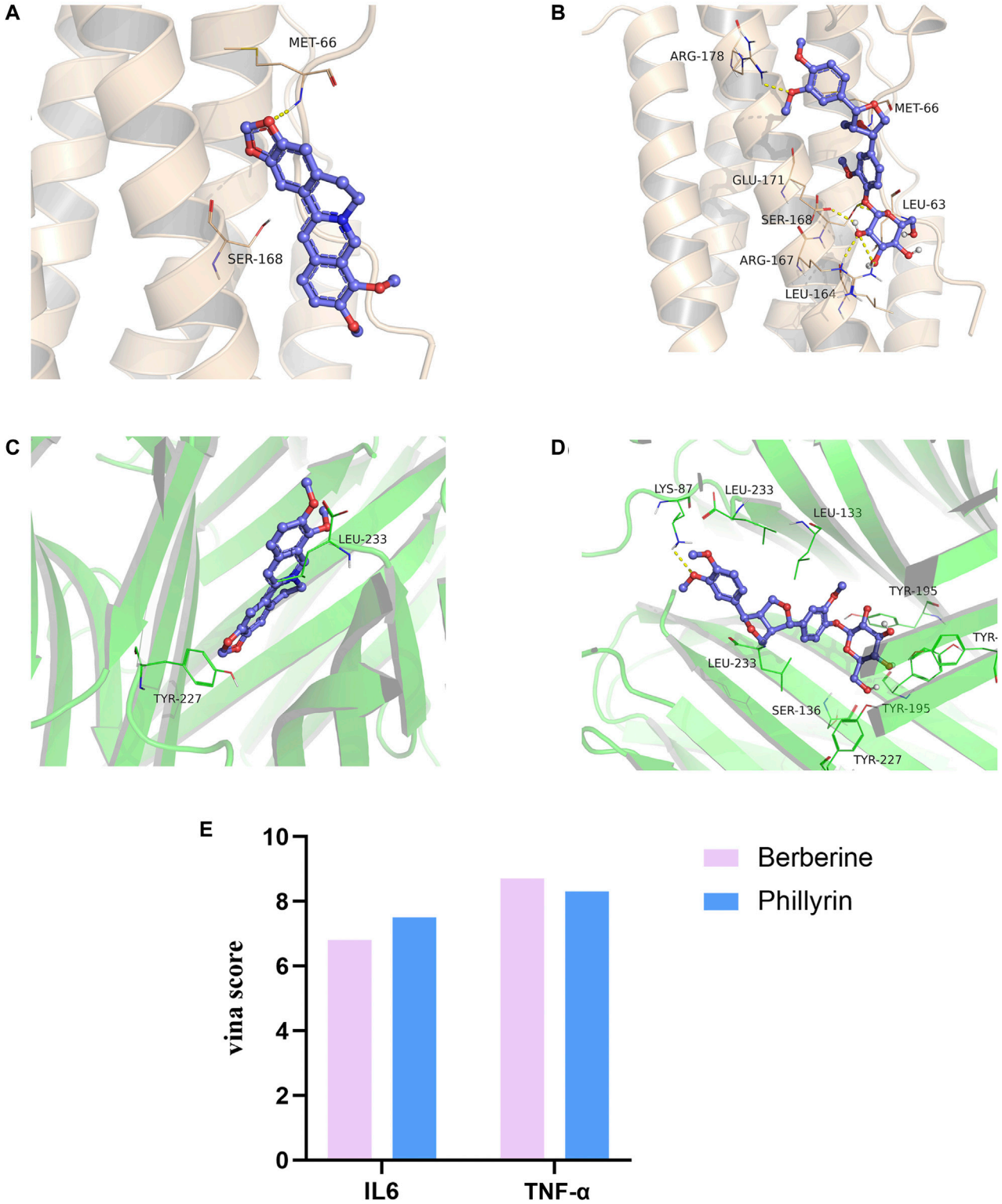


**FIGURE 5 |** Molecular docking. **(A)** Berberine-(IL-6). **(B)** Phillyrin-(IL-6). **(C)** Berberine-(TNF-α). **(D)** Phillyrin-(TNF-α). **(E)** Absolute value of vina score (kcal/mol).

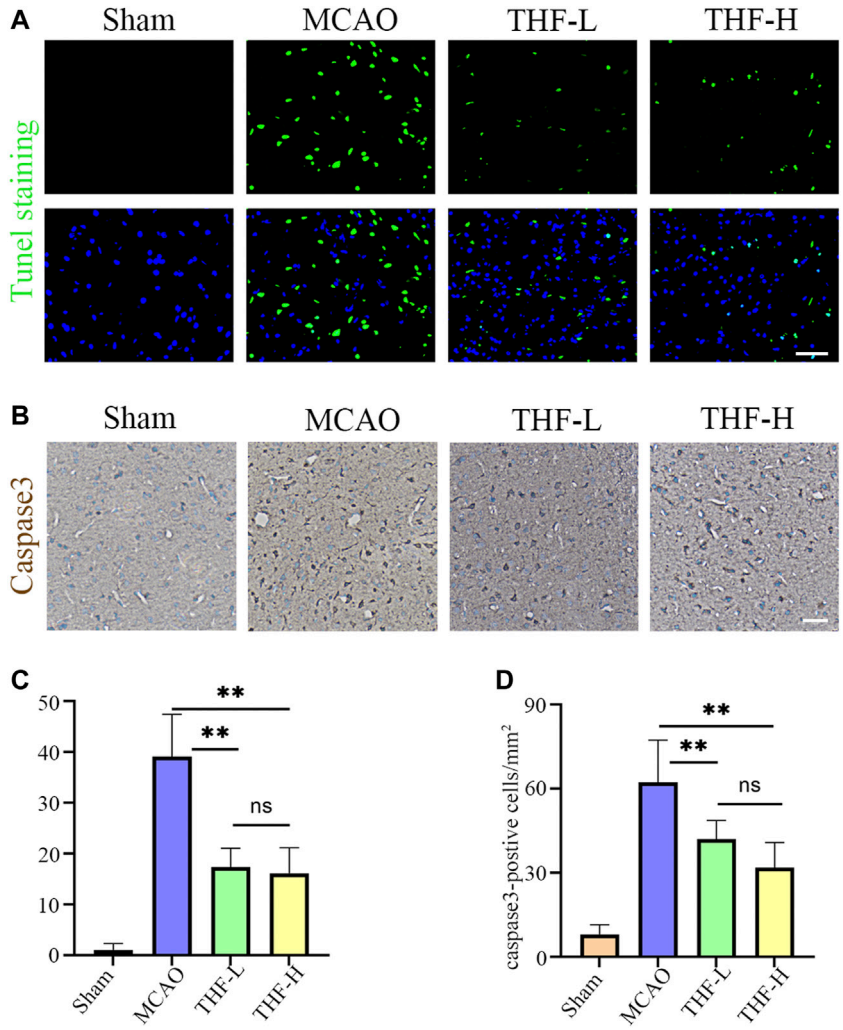


**FIGURE 6 |** Effects of THF on the neural cell apoptosis in infarction focus at 3 days and 30 min. **(A)** TUNEL staining of apoptotic cells in the cortex. Scale bar = 50 μm. **(B)** Representative immunohistochemistry images showing caspase-3–positive cells in the cortex. Scale bar = 100 μm. **(C)** Quantitative analysis of apoptotic cells in the cortex. **(D)** Quantification of the number of caspase-3–positive cells in each group. $n = 3$. (**$p < 0.01$, compared to the MCAO group).

## DISCUSSION

AIS is a common disease in elderly people, with a stepwise sequence of pathophysiological processes that are strongly correlated to inflammatory responses and apoptosis during development and progression (Ao et al., 2018; Uzdensky, 2019). THF is a traditional herbal medicine formula with multiple active compounds, which has been used in treating AIS for more than 10 years in China owing to its excellent efficacy in "heating–clearing, fire–purgingg, and detoxification." In this study, network pharmacology and experimental verification were applied to explore the underlying mechanism by which THF improves AIS outcomes.

Network pharmacological analysis was first used to predict and determine the active ingredients and potential targets of THF in AIS. First, 42 potential compounds associated with the therapeutic effects of cerebral infarction were identified. By constructing a PPI network for the common targets of THF and AIS, AKT1, TNF, IL6, IL1B, and CASP3 were predicted as pivotal targets. Finally, KEGG pathway enrichment analysis showed that inflammation- and apoptosis-related pathways were significantly enriched, and we focused on the TNF pathway. IL-6 is a pleiotropic cytokine primarily produced by activated microglia and astrocytes. Upregulation of IL-6 may act on microvascular endothelial cells and increase the expression of adhesion molecules and chemokines, thus mediating the inflammatory cascade and aggravating cerebral ischemic injury (Huang et al., 2006). CASP3 is generally recognized as a crucial molecule in apoptosis after cerebral ischemia. Thus, inhibition of the CASP3 pathway can simultaneously block neural cell apoptosis (Burguillos et al., 2011). TNF-α (tumor necrosis factor–α) is a cytokine associated with systemic inflammation, immune regulation, inhibition of tumor cell growth, and rejection of organ transplantation. There is

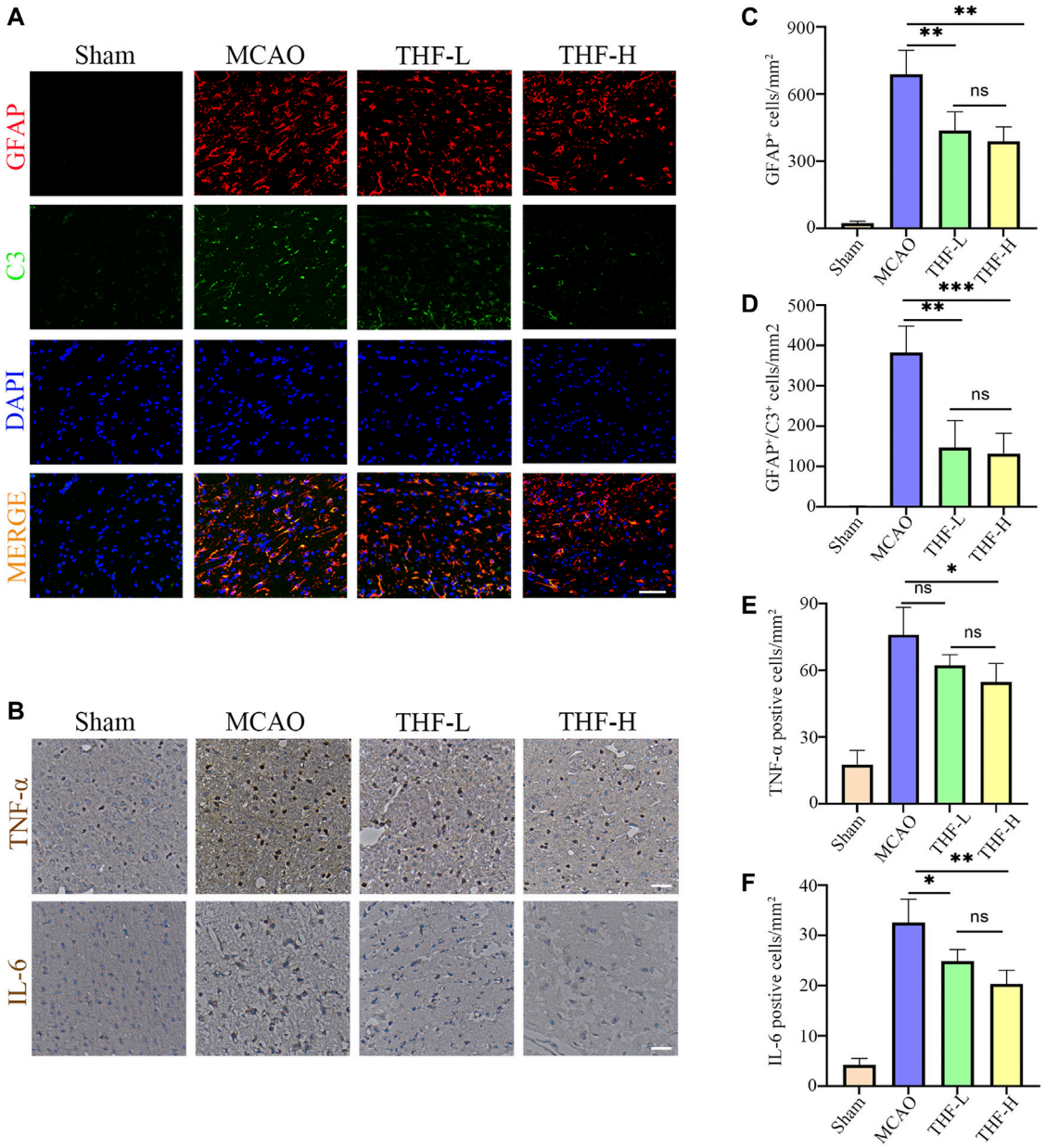


**FIGURE 7 |** THF inhibits the activation of A1 astrocytes and expression of IL-6 and TNF-α. **(A)** Representative immunofluorescence images represent GFAP (red) and C3 (green) staining in the cortex. GFAP, glial fibrillary acidic protein. Scale bar = 50 μm. **(B)** Immunohistochemistry of IL-6 and TNF-α in the cortex. Scale bar = 100 μm. **(C)** Quantification of the number of GFAP positive cells in each group. **(D)** Statistical diagram of GFAP/C3 positive cells. **(E)** Statistical diagram of TNF-α–positive cells. **(F)** Quantification of the density of IL-6–immunostained cells. IL-6, interleukin-6; TNF-α, tumor necrosis factor-α. $n = 3$. (*$p < 0.05$, **$p < 0.01$, ***$p < 0.001$compared to the MCAO group).

considerable evidence that TNF-α is significantly associated with ischemic stroke, which further increases sharply in the acute stage of stroke, resulting in serious tissue damage (Shishkova et al., 2018; Zuo et al., 2019). Based on the HPLC analysis and molecular docking results, we speculated that berberine and phillyrin are likely to play a pivotal role in inflammation. Previous studies have shown that berberine alleviates cerebral ischemic injury by attenuating apoptosis, inhibiting M1 glial cell polarization, and inhibiting the expression of pro-inflammatory cytokines (Simões Pires et al., 2014; Zhu et al., 2019). Similarly, *in vivo* experiments showed that phillyrin inhibits microglia-mediated inflammation by promoting the polarization of "M2" microglia. In addition, phillyrin has been reported to alleviate apoptosis by inhibiting apoptotic pathways such as caspase-3 (Du et al., 2020; Jiang et al., 2021). Altogether, the network pharmacology results showed that TNF, IL6, and CASP3 are hub genes in the PPI network. In addition, KEGG enrichment analysis showed that

the TNF inflammatory pathway was significantly enriched through multiple targets (including the hub targets CASP3 and IL6). These targets are actively involved in apoptotic and inflammatory pathways, suggesting that THF may exert anti-inflammatory and antiapoptotic effects on AIS by primarily regulating the TNF signaling pathway and targeting certain genes, such as CASP-3, IL-6, and TNF-α. Therefore, corresponding animal experiments were subsequently designed to validate the predictions of network pharmacology. Specifically, we emphasize that the CASP3 signaling pathway induces apoptosis and detects the activation of A1 astrocytes and the release of IL6 and TNF-α. CASP3, a marker of apoptosis, is located in the core of the apoptotic cascade pathway. Nerve cells are very sensitive to severe ischemia and hypoxia and die rapidly after ischemic stroke. In particular, the number of CASP3-positive neurons in the cerebral cortex and hippocampal CA1 area increased at 3 h, reached a peak at 48 h, and decreased to a stable level 14 days after MCAO (Liu et al., 2013). Therefore, inhibiting the expression of CASP3 and reducing neural cell apoptosis are important therapeutic targets for acute ischemic stroke (Akpan and Troy, 2013). Our findings confirm that THF alleviates apoptosis of neural cells by inhibiting the CASP3 pathway.

Numerous studies have demonstrated that abnormally activated A1 astrocytes exhibit a detrimental effect on the transmission of inflammatory mediators and glutamic acids, initiating immune cascade reactions and leading to increased tissue damage, such as the destruction of the BBB, brain edema, and neuronal degeneration and death (Hawkins and Davis, 2005; Buffo et al., 2010). TNF-α is an important mediator of the inflammatory response, which can activate microglia and astrocytes, leading to leakage of the BBB and aggravating the progression of stroke (Berti et al., 2002; Tuttolomondo et al., 2014). IL-6 is a pro-inflammatory cytokine that promotes the occurrence and development of neurovascular unit dysfunction and neuroinflammation (Pawluk et al., 2020). Therefore, restraining the abnormal activation of A1 astrocytes and production of TNF-α and IL-6 is conducive to alleviating neuronal damage after cerebral ischemia, which is also indispensable for functional rehabilitation. In our study, A1 astrocytes were significantly activated, and the levels of TNF-α and IL-6 were upregulated in MCAO rats, consequently causing neuronal death. However, this inflammation and tissue injury could be reversed by THF treatment. These data suggest a potential mechanism whereby THF can curb overactivation of A1 astrocytes and the release of TNF-α and IL-6 at an early stage after AIS.

Finally, although our study demonstrates that THF has an impact on the inflammatory response and apoptosis by targeting IL-6, TNF-α, and caspase-3 in MCAO rats, the upstream pathway has not been elucidated. In addition, a previous study showed that THF can improve clinical outcomes by altering the gut microbiota (Guo Q. et al., 2021). However, there is currently no evidence of the efficacy of THF in animals. Therefore, the effect of THF on improving animal prognosis and more in-depth mechanisms remain to be elucidated in the future.

## CONCLUSION

To the best of our knowledge, ischemic stroke is a complex pathological process mediated by multiple targets and multiple pathways, and the complicated pathophysiological mechanism of THF in treating AIS was explored based on network pharmacology analysis and experimental validation. According to network pharmacology analysis, 42 bioactive compounds and 159 targets of THF related to AIS were obtained. Simultaneously, AKT1, TNF, IL6, IL1B, and CASP3 were identified as hub targets. Inflammation and apoptosis were significantly enriched in multiple signaling pathways and multiple targets. Therefore, THF is likely to be involved in modulating AIS by primarily regulating the TNF signaling pathway and targeting certain genes such as CASP3, IL-6, and TNF-α. Based on experimental validation, this study provides new insights into the mechanisms by which THF can effectively decrease neural cell apoptosis through the caspase-3 pathway and restrain the excessive activation of A1 astrocytes. Therefore, THF may serve as a prospective treatment strategy for AIS through multiple targets, components, and pathways.

## DATA AVAILABILITY STATEMENT

The original contributions presented in the study are included in the article/**Supplementary Material**, further inquiries can be directed to the corresponding authors.

## ETHICS STATEMENT

The animal study was reviewed and approved by the Ethics Committee of Capital Medical University.

## AUTHOR CONTRIBUTIONS

MQ and LG designed this research; YN and LW analyzed the network pharmacology data, conducted the experiments, and wrote the manuscript; LH performed the preparation of herbal prescriptions; JS, NW and LH contributed to data analysis and interpretation of the results; LG and MQ reviewed the manuscript. All authors have read and approved the manuscript.

## FUNDING

This research was funded by the National Natural Science Foundation of China (81973759, 81573905), the National Key Research and Development Project (2020YFC2003100, 2020YFC2003103), and Capital's Funds for Health Improvement and Research (SF2020–1–2011).

## SUPPLEMENTARY MATERIAL

The Supplementary Material for this article can be found online at: https://www.frontiersin.org/articles/10.3389/fphar.2022.859244/full#supplementary-material

## REFERENCES


Akpan, N., and Troy, C. M. (2013). Caspase Inhibitors: Prospective Therapies for Stroke. *Neuroscientist* 19 (2), 129–136. doi:10.1177/1073858412447875

Ao, L. Y., Yan, Y. Y., Zhou, L., Li, C. Y., Li, W. T., Fang, W. R., et al. (2018). Immune Cells after Ischemic Stroke Onset: Roles, Migration, and Target Intervention. *J. Mol. Neurosci.* 66 (3), 342–355. doi:10.1007/s12031-018-1173-4

Berti, R., Williams, A. J., Moffett, J. R., Hale, S. L., Velarde, L. C., Elliott, P. J., et al. (2002). Quantitative Real-Time RT-PCR Analysis of Inflammatory Gene Expression Associated with Ischemia-Reperfusion Brain Injury. *J. Cereb. Blood Flow Metab.* 22 (9), 1068–1079. doi:10.1097/00004647-200209000-00004

Buffo, A., Rolando, C., and Ceruti, S. (2010). Astrocytes in the Damaged Brain: Molecular and Cellular Insights into Their Reactive Response and Healing Potential. *Biochem. Pharmacol.* 79 (2), 77–89. doi:10.1016/j.bcp.2009.09.014

Burguillos, M. A., Deierborg, T., Kavanagh, E., Persson, A., Hajji, N., Garcia-Quintanilla, A., et al. (2011). Caspase Signalling Controls Microglia Activation and Neurotoxicity. *Nature* 472 (7343), 319–324. doi:10.1038/nature09788

Cong, L., Zhao, T., Hui, Z., Xuefen, F., Yun, L., Le, Y., et al. (2021). Protective Effects of TanhuoFormula on Neuroglial Cells and Cerebral Per-Fusion in Rats with Cerebral Ischemia. *J. Beijing Univ. Tradit. Chin. Med.* 44 (7), 605–614. doi:10.3969/j.issn.1006-2157.2021.07.005

Du, Y., You, L., Ni, B., Sai, N., Wang, W., Sun, M., et al. (2020). Phillyrin Mitigates Apoptosis and Oxidative Stress in Hydrogen Peroxide-Treated RPE Cells through Activation of the Nrf2 Signaling Pathway. *Oxid. Med. Cel Longev.* 2020, 2684672. doi:10.1155/2020/2684672

Esquiva, G., Grayston, A., and Rosell, A. (2018). Revascularization and Endothelial Progenitor Cells in Stroke. *Am. J. Physiol. Cel Physiol.* 315 (5), C664–c674. doi:10.1152/ajpcell.00200.2018

Gao, Y., Xie, Y. M., Cai, Y. F., Shen, X. M., Zhao, D. X., and Xie, Y. Z. (2018). Risk factors associated with recurrence within 90 days of ischemic stroke onset in chinese medicine hospital: A national cross-sectional study in China. *World J. Trad. Chin. Med.* 6 (4), 441–447. doi:10.4103/wjtcm.wjtcm_32_20

Guo, Q., Jiang, X., Ni, C., Li, L., Chen, L., Wang, Y., et al. (2021a). Gut Microbiota-Related Effects of Tanhuo Decoction in Acute Ischemic Stroke. *Oxid. Med. Cel Longev.* 2021, 5596924. doi:10.1155/2021/5596924

Guo, X., Cao, P., Lian, X., Hu, M., Zhao, J., Shen, W., et al. (2021b). The Neuroprotective Effect of Phillyrin in Intracerebral Hemorrhagic Mice is Produced by Activation of the Nrf2 Signaling Pathway. *Eur. J. Pharmacol.* 909, 174439. doi:10.1016/j.ejphar.2021.174439

Hawkins, B. T., and Davis, T. P. (2005). The Blood-Brain Barrier/neurovascular Unit in Health and Disease. *Pharmacol. Rev.* 57 (2), 173–185. doi:10.1124/pr.57.2.4

Herpich, F., and Rincon, F. (2020). Management of Acute Ischemic Stroke. *Crit. Care Med.* 48 (11), 1654–1663. doi:10.1097/ccm.0000000000004597

Huang, J., Upadhyay, U. M., and Tamargo, R. J. (2006). Inflammation in Stroke and Focal Cerebral Ischemia. *Surg. Neurol.* 66 (3), 232–245. doi:10.1016/j.surneu.2005.12.028

Huang, C., Zheng, C., Li, Y., Wang, Y., Lu, A., and Yang, L. (2014). Systems Pharmacology in Drug Discovery and Therapeutic Insight for Herbal Medicines. *Brief Bioinform.* 15 (5), 710–733. doi:10.1093/bib/bbt035

Jiang, Q., Wei, D., He, X., Gan, C., Long, X., and Zhang, H. (2021). Phillyrin Prevents Neuroinflammation-Induced Blood-Brain Barrier Damage Following Traumatic Brain Injury via Altering Microglial Polarization. *Front. Pharmacol.* 12, 719823. doi:10.3389/fphar.2021.719823

Krishnamurthi, R. V., Ikeda, T., and Feigin, V. L. (2020). Global, Regional and Country-Specific Burden of Ischaemic Stroke, Intracerebral Haemorrhage and Subarachnoid Haemorrhage: A Systematic Analysis of the Global Burden of Disease Study 2017. *Neuroepidemiology* 54 (2), 171–179. doi:10.1159/000506396

Kusakawa, Y., Mikawa, S., and Sato, K. (2015). BMP5 Expression in the Adult Rat Brain. *Neuroscience* 284, 972–987. doi:10.1016/j.neuroscience.2014.07.057

Liu, G., Wang, T., Wang, T., Song, J., and Zhou, Z. (2013). Effects of Apoptosis-Related Proteins Caspase-3, Bax and Bcl-2 on Cerebral Ischemia Rats. *Biomed. Rep.* 1 (6), 861–867. doi:10.3892/br.2013.153

Lv, H., Li, Y., Cheng, Q., Chen, J., and Chen, W. (2021). Neuroprotective Effects against Cerebral Ischemic Injury Exerted by Dexmedetomidine via the HDAC5/NPAS4/MDM2/PSD-95 Axis. *Mol. Neurobiol.* 58 (5), 1990–2004. doi:10.1007/s12035-020-02223-7

Morovatdar, N., Avan, A., Azarpazhooh, M. R., Di Napoli, M., Stranges, S., Kapral, M. K., et al. (2021). Secular Trends of Ischaemic Heart Disease, Stroke, and Dementia in High-Income Countries from 1990 to 2017: the Global Burden of Disease Study 2017. *Neurol. Sci.* 43, 255–264. doi:10.1007/s10072-021-05259-2

Patabendige, A., Singh, A., Jenkins, S., Sen, J., and Chen, R. (2021). Astrocyte Activation in Neurovascular Damage and Repair Following Ischaemic Stroke. *Int. J. Mol. Sci.* 22 (8), 4280. doi:10.3390/ijms22084280

Pawluk, H., Woźniak, A., Grześk, G., Kołodziejska, R., Kozakiewicz, M., Kopkowska, E., et al. (2020). The Role of Selected Pro-inflammatory Cytokines in Pathogenesis of Ischemic Stroke. *Clin. Interv. Aging* 15, 469–484. doi:10.2147/cia.S233909

Qiu, Y. M., Zhang, C. L., Chen, A. Q., Wang, H. L., Zhou, Y. F., Li, Y. N., et al. (2021). Immune Cells in the BBB Disruption after Acute Ischemic Stroke: Targets for Immune Therapy? *Front. Immunol.* 12, 678744. doi:10.3389/fimmu.2021.678744

Radak, D., Katsiki, N., Resanovic, I., Jovanovic, A., Sudar-Milovanovic, E., Zafirovic, S., et al. (2017). Apoptosis and Acute Brain Ischemia in Ischemic Stroke. *Curr. Vasc. Pharmacol.* 15 (2), 115–122. doi:10.2174/1570161115666161104095522

Ru, J., Li, P., Wang, J., Zhou, W., Li, B., Huang, C., et al. (2014). TCMSP: a Database of Systems Pharmacology for Drug Discovery from Herbal Medicines. *J. Cheminform.* 6, 13. doi:10.1186/1758-2946-6-13

Saberi, A., Ghayegran, A., Ghayegran, A., Abbasalizade, M., Ehtiatkar, Z., Ghorbani Shirkouhi, S., et al. (2021). The Outcome of Treatment with Recombinant Tissue Plasminogen Activator in Acute Ischemic Stroke. *Caspian J. Neurol. Sci.* 7 (3), 148–156. doi:10.32598/CJNS.7.26.1

Shah, S. A., Khan, M., Jo, M. H., Jo, M. G., Amin, F. U., and Kim, M. O. (2017). Melatonin Stimulates the SIRT1/Nrf2 Signaling Pathway Counteracting Lipopolysaccharide (LPS)-Induced Oxidative Stress to Rescue Postnatal Rat Brain. *CNS Neurosci. Ther.* 23 (1), 33–44. doi:10.1111/cns.12588

Shishkova, V. N., Adasheva, T. V., Remenik, A. Y., Valyaeva, V. N., and Shklovsky, V. M. (2018). Prognostic Significance of Clinical-Anthropometric, Biochemical, Metabolic, Vascular-Inflammatory and Molecular-Genetic Markers in the Development of the First Ischemic Stroke. *Zh Nevrol Psikhiatr Im S S Korsakova* 118 (2), 4–11. doi:10.17116/jnevro2018118214-11

Simões Pires, E. N., Frozza, R. L., Hoppe, J. B., and Menezes, B. d. M. (2014). Berberine was Neuroprotective against an In Vitro Model of Brain Ischemia: Survival and Apoptosis Pathways Involved. *Brain Res.* 1557, 26–33. doi:10.1016/j.brainres.2014.02.021

Stary, C. M., and Giffard, R. G. (2015). Advances in Astrocyte-Targeted Approaches for Stroke Therapy: an Emerging Role for Mitochondria and microRNAS. *Neurochem. Res.* 40 (2), 301–307. doi:10.1007/s11064-014-1373-4

Sun, Q., Xu, X., Wang, T., Xu, Z., Lu, X., Li, X., et al. (2021). Neurovascular Units and Neural-Glia Networks in Intracerebral Hemorrhage: from Mechanisms to Translation. *Transl. Stroke Res.* 12 (3), 447–460. doi:10.1007/s12975-021-00897-2

Tang, C., Hong, J., Hu, C., Huang, C., Gao, J., Huang, J., et al. (2021). Palmatine Protects against Cerebral Ischemia/Reperfusion Injury by Activation of the AMPK/Nrf2 Pathway. *Oxid. Med. Cel Longev.* 2021, 6660193. doi:10.1155/2021/6660193

Tuttolomondo, A., Pecoraro, R., and Pinto, A. (2014). Studies of Selective TNF Inhibitors in the Treatment of Brain Injury from Stroke and Trauma: a Review of the Evidence to Date. *Drug Des. Devel. Ther.* 8, 2221–2238. doi:10.2147/dddt.S67655

Uzdensky, A. B. (2019). Apoptosis Regulation in the Penumbra after Ischemic Stroke: Expression of Pro- and Antiapoptotic Proteins. *Apoptosis* 24 (9-10), 687–702. doi:10.1007/s10495-019-01556-6

Veber, D. F., Johnson, S. R., Cheng, H. Y., Smith, B. R., Ward, K. W., and Kopple, K. D. (2002). Molecular Properties that Influence the Oral Bioavailability of Drug Candidates. *J. Med. Chem.* 45 (12), 2615–2623. doi:10.1021/jm020017n

Xian, M., Cai, J., Zheng, K., Liu, Q., Liu, Y., Lin, H., et al. (2021). Aloe-emodin Prevents Nerve Injury and Neuroinflammation Caused by Ischemic Stroke via the PI3K/AKT/mTOR and NF-κB Pathway. *Food Funct.* 12 (17), 8056–8067. doi:10.1039/d1fo01144h

Xu, S., Lu, J., Shao, A., Zhang, J. H., and Zhang, J. (2020). Glial Cells: Role of the Immune Response in Ischemic Stroke. *Front. Immunol.* 11, 294. doi:10.3389/fimmu.2020.00294

Zhang, R., Zhu, X., Bai, H., and Ning, K. (2019). Network Pharmacology Databases for Traditional Chinese Medicine: Review and Assessment. *Front. Pharmacol.* 10, 123. doi:10.3389/fphar.2019.00123

Zhao, L., Li, H., Gao, Q., Xu, J., Zhu, Y., Zhai, M., et al. (2021). Berberine Attenuates Cerebral Ischemia-Reperfusion Injury Induced Neuronal Apoptosis by Down-Regulating the CNPY2 Signaling Pathway. *Front. Pharmacol.* 12, 609693. doi:10.3389/fphar.2021.609693

Zhu, J., Cao, D., Guo, C., Liu, M., Tao, Y., Zhou, J., et al. (2019). Berberine Facilitates Angiogenesis against Ischemic Stroke through Modulating Microglial Polarization via AMPK Signaling. *Cell Mol. Neurobiol.* 39 (6), 751–768. doi:10.1007/s10571-019-00675-7

Zuo, Y., Huang, L., Enkhjargal, B., Xu, W., Umut, O., Travis, Z. D., et al. (2019). Activation of Retinoid X Receptor by Bexarotene Attenuates Neuroinflammation via PPARγ/SIRT6/FoxO3a Pathway after Subarachnoid Hemorrhage in Rats. *J. Neuroinflammation* 16 (1), 47. doi:10.1186/s12974-019-1432-5

**Conflict of Interest:** The authors declare that the research was conducted in the absence of any commercial or financial relationships that could be construed as a potential conflict of interest.

frontiers | Frontiers in Pharmacology

MINI REVIEW
published: 19 May 2022
doi: 10.3389/fphar.2022.903119

# Curcumin as a Holistic Treatment for Tau Pathology

*Lovesha Sivanantharajah*[1]* *and Amritpal Mudher*[2]

[1]School of Natural Sciences, Bangor University, Bangor Gwynedd, United Kingdom, [2]Faculty of Natural and Environmental Sciences, University of Southampton, Southampton, United Kingdom

Global forecasts for prevalence of Alzheimer's Disease (AD) estimate that 152.8 million people will have dementia in 2050, a sharp rise from 57.4 million in 2019 (GBD 2019). This rise can be attributable to increases in population growth and aging, but in the absence of disease-modifying therapies it poses a huge societal challenge that must be addressed urgently. One way to combat this challenge is to explore the utility of holistic treatments that may protect against AD, including traditional herbs, spices and other nutraceuticals that are pharmacologically safe, inexpensive and readily available. In this light, the spice turmeric, and its active ingredient curcumin, has been investigated as a potential holistic treatment for AD over the past 2 decades; however, promising results with animal studies have not translated to success in clinical trials. One issue is that most animal models examining the effects of curcumin and curcumin derivatives in AD have been done with a focus at ameliorating amyloid pathology. Due to the limited success of Amyloid-β-based drugs in recent clinical trials, tau-focused therapeutics provide a promising alternative. In this article, we aim to provide a clearer picture of what is currently known about the effectiveness of curcumin and curcumin derivatives to ameliorate tau pathology. Tau focused studies may help inform more successful clinical studies by placing greater emphasis on the development and optimised delivery of curcumin derivatives that more effectively target tau pathology.

**Keywords: turmeric (Curcuma longa L), curcumin, Alzheheimer's disease, tauopathy, animal models, holistic medicine**

OPEN ACCESS

***Edited by:***
*Shijun Xu,*
*Chengdu University of Traditional Chinese Medicine, China*

***Reviewed by:***
*Ali Mohammad Pourbagher-Shahri,*
*Birjand University of Medical Sciences, Iran*

***Correspondence:**
*Lovesha Sivanantharajah*
*l.sivanantharajah@bangor.ac.uk*

***Specialty section:***
*This article was submitted to Neuropharmacology, a section of the journal Frontiers in Pharmacology*

***Received:*** *23 March 2022*
***Accepted:*** *02 May 2022*
***Published:*** *19 May 2022*

***Citation:***
*Sivanantharajah L and Mudher A (2022) Curcumin as a Holistic Treatment for Tau Pathology. Front. Pharmacol. 13:903119. doi: 10.3389/fphar.2022.903119*

## INTRODUCTION

Alzheimer's disease (AD) is the most common form of dementia, characterised clinically by progressive cognitive decline, and neuropathologically by amyloid plaques and neurofibrillary tau tangles (NFT). Global forecasts for prevalence of AD estimate that 152.8 million people will have dementia in 2050, a sharp rise from 57.4 million in 2019 (GBD 2019). Although this rise can be attributable to increases in population growth and aging, in the absence of disease-modifying therapies it poses a huge societal challenge we must urgently address. One approach is to implement public health measures that scale up modifiable lifestyle factors known to influence risk of AD (GBD 2019) (Livingston et al., 2020). Another is to explore the utility of holistic treatments that may protect against AD, including traditional herbs, spices and other nutraceuticals that are pharmacologically safe, inexpensive and readily available. The case for repurposing such nutraceuticals for dementia treatment first arose from the observation that the prevalence of dementia in countries like India, where such spices are regularly consumed, is remarkably low when compared to high income countries where these spices are not common (Kannappan et al., 2011). Although other factors,

including population ageing differences, have since been put forward to explain at least some of this differential dementia prevalence, there have been significant efforts to assess the disease-modifying potential of nutraceuticals in cellular and animal models of AD. Such research reveals that common Indian herbs and spices such as turmeric, garlic, ginger, black pepper, coriander and others, contain phytochemicals that display a range of neuroprotective properties (Kannappan et al., 2011). They have been shown to be antioxidant, anti-inflammatory, anti-amyloidogenic and also to upregulate protective cellular responses like heat shock responses (Forouzanfar et al., 2019). As misfolding and aggregation of tau and amyloid proteins, oxidative stress and aberrant inflammation are all implicated in AD, it is not surprising that these spice-derived nutraceuticals have shown some disease-modifying potential in AD models. This review summarises the research done to investigate the protective effects of the spice, curcumin, against tau pathology in AD.

## CURCUMIN AND ALZHEIMER'S DISEASE

The medicinal properties of the nutraceutical, turmeric, have been known for centuries, prompting its widespread use in holistic traditional medicines in India and China. It is derived from the rhizome of *Curcuma longa*, a member of the ginger family indigenous to South and Southeast Asia. The active ingredient in turmeric is the phytochemical, curcumin ((1E, 6E)-1, 7-bis (4-hydroxy-3-methoxyphenyl)-1, 6-heptadiene-3, 5-dione). As a key ingredient in Asian cooking, turmeric was first considered for prevention or treatment of AD because of reports that prevalence of AD in India was significantly lower than in the West where this spice is not routinely consumed (Kannappan et al., 2011). Although more recent studies have begun to show that several other lifestyle related factors modulate AD risk, and that prevalence may be increasing in Asian countries and decreasing in the West (Livingston et al., 2020), these original observations prompted research into the disease-modifying potential of turmeric and its active ingredient, curcumin. Further, as evidence mounts for the importance of diet on wellbeing and disease prevention, curcumin becomes a more attractive medicinal agent providing a cost-effective, easily accessible solution to promote resilience to dementia. This will have even greater significance for developing countries.

Curcumin has a wide variety of neuroprotective properties: it inhibits nuclear factor kB-mediated transcription of inflammatory cytokines (Singh and Aggarwal 1995), it behaves as an anti-oxidant by scavenging reactive oxygen species (ROS) (Scapagnini et al., 2010)and neutralising NO-based free radicals (Sreejayan and Rao 1997), it is capable of disrupting amyloids displaying anti-amyloidogenic and anti-fibrillogenic behaviour (Garcia-Alloza et al., 2007), and interacts with homeostatic pathways such as the unfolded protein response (UPR) and chaperones like Hsp70 to facilitate correct protein folding (Mukherjee et al., 2021). Curcumin has also been shown to play a protective role in aging and age-related disorders including atherosclerosis, diabetes and cancer (Olszanecki et al., 2005; He et al., 2015). One striking observation is the ability of dietary curcumin to extend life span in fly, nematode and mouse models (Suckow and Suckow 2006; Kitani et al., 2007; Lee et al., 2010; Liao et al., 2011). Therefore, it is not surprising that curcumin and its derivatives have been found to suppress phenotypes in multiple models of neurodegenerative disease in which aging is a substantive risk factor, including Huntington's Disease (Chongtham and Agrawal 2016; Labanca et al., 2021), Parkinson's Disease (Chetty et al., 2021; Nebrisi 2021)), and AD (Reddy et al., 2018; Chainoglou and Hadjipavlou-Litina 2020). The observation that curcumin treatment leads to suppression of phenotypes caused by a wide range of conditions, from aging-related to several different misfolded proteins characterising distinct proteinopathies, suggests that its disease-modifying actions may be affected through key overlapping mechanisms such as oxidative stress and neuroinflammation.

## THE STATUS QUO

In the absence of a cure for AD, there are four drugs in general use for the symptomatic treatment of AD. Three of these drugs—donepezil, galantamine and rivastigmine—are acetylcholinesterase (AChE) inhibitors, developed on the cholinergic hypothesis which proposed AD was due to preferential loss of cholinergic neurons (Bartus 2000). The fourth drug, memantine, is a N-methyl-D-aspartate (NMDA) receptor antagonist, which suppresses the neuronal excitotoxicity noted in AD caused by excess glutamate binding of NMDA receptors (Reisberg et al., 2003). More recently, the Federal Drug Administration (USA) granted accelerated approval to the drug, aducanumab, which works by reducing amyloid deposits in the brain that may slow the progression of AD; however, it's effectiveness in halting the progression of cognitive decline or dementia has yet to be clinically demonstrated.

Tau-directed treatments have also been investigated, and over the years a number of different tau-centric agents have entered clinical trials with limited success. (Panza et al., 2016). These include kinase inhibitors (Lovestone et al., 2015; Maqbool et al., 2016), phosphatase stimulators (Parekh et al., 2013), aggregation inhibitors like methylene blue (Wischik et al., 1996), tau vaccines (d'Abramo et al., 2015; Sankaranarayanan et al., 2015), and microtubule stabilising agents (Brunden et al., 2011; Quraishe et al., 2016). However, in the absence of approved tau-modifying treatments or in fact any disease modifying treatments, current medical treatments arguably provide small benefits at the cost of side effects and lack general accessibility. It is here that holistic medicines, such as curcumin, can play a key role.

To date, numerous animal studies have been conducted, mainly in rodent models, with promising results for the effectiveness of curcumin for therapeutic purposes (see comprehensive review of animal and clinical studies in Voulgaropoulou et al. (2019). Unfortunately, this has not translated to similar success in human clinical trials where study results are inconsistent, with some studies reporting a beneficial effect of curcumin on cognitive function (Cox et al., 2015; Rainey-Smith et al., 2016; Small et al., 2018) and others

reporting none (Baum et al., 2008; Ringman et al., 2012). Since so few clinical studies have actually been done, this may not be surprising. However, many factors may contribute to the observed discrepancy in translation with the first being issues with curcumin supplementation, which include low bioavailability of the compound, rapid metabolism in gut, and low penetration across the blood brain barrier (Anand et al., 2007). There are a number of ways in which these issues have been, and are currently being, addressed with the development of curcumin derivatives with greater bioavailability and optimisation of delivery methods, including isomerisation, liposomes, micelles, phospholipids, nanotechnology, vaporising and intravenous injection.

Coupled with the above issue is that much of the work examining the effects of curcumin in AD in animal models has been done with a focus at ameliorating amyloid pathology. However, the limited success of Amyloid-beta (Aβ)-based drugs in clinical trials suggests a shift in focus is needed. This is where tau-targeted therapeutics provide a promising alternative. Currently, few studies have directly examined the effectiveness of curcumin and curcumin derivatives in tauopathy models or to ameliorate tau pathology in animal and clinical studies. Here we provide a snapshot of this field with a view that tau-focused animal studies may help inform more successful clinical studies by emphasising development of curcumin derivatives and delivery mechanisms that more effectively target tau pathology.

## ANIMAL MODELS EXAMINING CURCUMIN AND TAU PATHOLOGY

Tauopathies are a class of over 20 degenerative disorders, including AD, marked by neuronal aggregation of abnormally phosphorylated forms of the protein tau, a microtubule associated protein (MAPT) essential for microtubule assembly and stability ((Grundke-Iqbal et al., 1986; Williams 2006; Spillantini and Goedert 2013). In pathological scenarios, there is evidence of both toxic loss of function (LOF) as well as gain of toxic functions (GOF) by pathogenic tau. Hyperphosphorylated tau detaches from microtubules and causes their destabilisation, consequently leading to disruption of cytoskeletal integrity, axonal transport and synaptic transmission (Mudher et al., 2004; Chee et al., 2005; Cowan et al., 2010; Hoover et al., 2010). Further, these abnormally hyperphosphorylated tau proteins aggregate to form higher order structures from soluble oligomers to paired helical filaments (PHFs) to insoluble neurofibrillary tangles (NFTs) ((Spillantini and Goedert 2013; von Bergen et al., 2000). While PHFs have historically been thought of as the main pathological species in tauopathies, more recent studies have suggested that it is their precursors, soluble tau oligomers, that are the toxic species spurring disease pathogenesis and progression through a variety of mechanisms including oxidative stress (Stamer et al., 2002; Cowan et al., 2021), mitochondrial dysfunction and transport (Ittner et al., 2008), nuclear dysfunction (Andorfer et al., 2005; Khurana et al., 2012), prion-like conversion and propagation of pathology (Holmes et al., 2014), inflammation (Nagele et al., 2004; Ismail et al., 2020), and induction of ER stress (Hoozemans et al., 2009) (Götz et al., 2019). Thus, finding ways to target toxic tau species is one solution for developing disease-modifying treatments that ameliorate or prevent these LOF and GOF pathogenic effects.

While the vast majority of animal studies with curcumin have been done in models of amyloid pathology, there are a handful that have examined the effects of curcumin in ameliorating tau pathology (**Table 1**, **Figure 1**). Using a nematode model of tauopathy, Miyasaka et al. (Miyasaka et al., 2016) expressed wild-type human tau isoform 0N4R (hTau0N4R) and hTau with the R406W (hTauR406W) mutation associated with frontotemporal lobe dementia (FTD). Worms were grown for 3 days on growth medium plates with or without curcumin (at concentrations of 0, 3, 30 uM) before collection of behavioural data. They found that htau-expressing worms grown on 30 uM of curcumin showed significant improvement in behavioural abnormalities (e.g., uncoordinated movement and touch sense). In addition, curcumin significantly decreased the number of morphological abnormalities (i.e., kinks and protrusions) noted in neurons expressing hTau. Interestingly, curcumin treatment had no effect on the phosphorylation of tau (AT100, AT8, AT180, pS262, PHF-1). However, further analysis found that curcumin significantly increased the levels of acetylated alpha-tubulin in worms. Since acetylation of alpha-tubulin occurs in association with microtubule stabilization, one possible mechanism for the therapeutic effects of curcumin is that it enhances microtubule stability.

The more common animal model for evaluating curcumin on tau pathology has been the mouse. Ma et al. (Ma et al., 2013) used a transgenic mouse model expressing human wild-type Tau (hTau) on a mouse-Tau knockout background, where synaptic and cognitive deficits and NFTs are present at 11–12 months and neuron loss occurs by 17 months. The mice used in this 4-months study were 15–16 months old at study commencement and were placed on diets without or with 500 ppm Longvida© (Verdure Sciences, Indianapolis, IN) curcumin, solid lipid curcumin particles showing higher bioavailability of free curcumin in the brain compared to other curcumin formulations. This study found that curcumin reduced the level of soluble tau dimers, reversed the disruption noted in htau-expressing mice in expression of the molecular chaperones, HSP90, HSP70, and HSP72, and improved cognitive performance in some behavioural assays. More specifically, they found that curcumin treatment improved spatial learning and memory, as measured using a Morris Water Maze (MWM), when compared to untreated htau mice. Also, curcumin treated htau mice showed normalisation of recognition memory toward wildtype measures using the Novel Object Recognition test (NORT).

Another study also using Longvida© examined abnormal accumulation of NFT's and Aβ in a p25 transgenic mouse model (Sundaram et al., 2017). The authors found that curcumin treatment significantly reduced p25-mediated tau hyperphosphorylation (AT8) and Aβ1-42 immunostaining in curcumin-treated p25Tg mice compared to their non-treated counterparts. One explanation for this reduction is the suppressed expression of neuroinflammatory cytokines. The authors found that the expression levels of the pro-

**TABLE 1 |** Summary of animal studies examining curcumin and tau pathology.

| References | Goal | Model | Study Design | Curcumin Treatment | Behavioural/ Cognitive Measurements | Summary Results |
|---|---|---|---|---|---|---|
| Ma et al. (2013) | Study effects of curcumin on tau pathology in a mouse model | Transgenic mouse model expressing human wild-type Tau (hTau) on a mouse-Tau knockout background | Wildtype versus hTau mice with and without compound for 4 months | 500 ppm Longvida in chow | Morris Water Maze (MWM), Y-Maze, Novel Object Recognition task (NORT) | Curcumin reduced the level of soluble tau dimers, reversed the disruption in expression of molecular chaperones (e.g., HSP90, HSP70, HSP72) that is noted in htau-expressing mice. Curcumin treatment improved spatial learning and memory (MWM), when compared to untreated htau mice. Also, curcumin treated htau mice showed normalisation of recognition memory toward wildtype measures (NORT) |
| Miyasaka et al. (2016) | Establish nematode tauopathy model and test effectiveness of curcumin in reducing tau induced phenotypes | Wildtype hTau0N4R and hTauR406W expressed in *C. elegans* | Worms grown on growth medium plates with or without curcumin for 3 days | 0, 3 uM, 30 uM Curcumin in growth medium | Measured uncoordinated movement, Touch sense | Curcumin significantly decreased the number of morphological abnormalities (kinks and protrusions) noted in neurons expressing hTau. hTau expressing worms grown on 30 uM of curcumin showed significant decreases in behavioural abnormalities. Curcumin treatment did not affect the phosphorylation of tau (AT100, AT8, AT180, pS262, PHF-1) |
| Okuda et al. (2017) | Test the efficiency of their curcumin derivative, PE859, a dual inhibitor of tau and amyloid pathology | Senescence-accelerated mouse prone 8 (SAMP8) model | 9-weeks study, SAMP8/TaSlc mice from 2 months of age to 4 months | 0, 1 mg/k/day, 3 mg/kg/day PE859, oral administration using gastric tube | Rotarod, MWM, Y-Maze, Grip strength | Saw a reduction in tau and A-beta1-40 aggregates with PE859 treatment. Mice given curcumin treatment did show a significant improvement in cognitive deficits in spatial working memory (Y-Maze). However, no differences noted with other behaviours assayed. |
| Sundaram et al. (2017) | Examine effects of Longvida® on mouse model of neuroinflammation and neurodegeneration | Transgenic mouse overexpressing p25 (p25Tg) | 12-weeks study, Wildtype versus p25Tg mice fed with and without compound | 4 g/kg Longvida (0.8 g curcumin/kg) in chow | 8-arm radial maze | Saw that curcumin-mediated suppression of neuroinflammation reduced the progression of p25-induced tau/amyloid pathology and ameliorated p25-induced cognitive impairments |
| Yanagisawa et al. (2018) | Test the effects of their curcumin derivative, Shiga-Y5 (SY5), in a mouse model of tauopathy | Transgenic mouse model rTg4510 expressing a repressible form of human tau with P301L mutation linked with familial frontotemporal dementia | 2 month-old male rTg4510 mice and 2 month-old male wild- type mice fed a standard chow diet with or without SY5 for 4 months | 500 ppm SY5 in chow | Rotarod, MWM, Y-Maze | Found no significant differences in behavioural performance between rTg4510 mice fed SY5 or a control diet. Further, histological and biochemical analyses found no significant changes in tau accumulation following curcumin treatment |

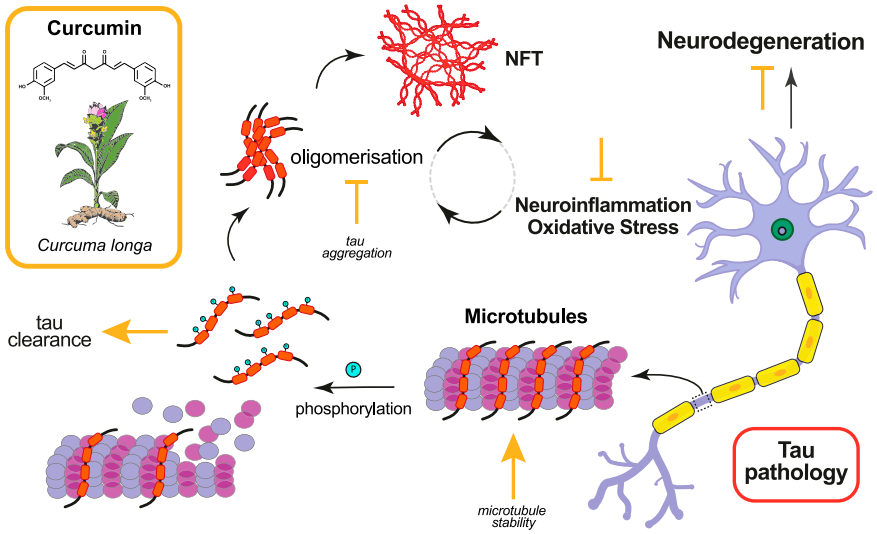


**FIGURE 1 |** Effects of curcumin in ameliorating tau pathology. Curcumin and its derivatives have been shown to ameliorate tau pathology in animal models by targeting various molecular mechanisms. The mode of action of curcumin, whether promotive (arrow) or inhibitive (falsum), is indicated in yellow next to the process it modifies.

inflammatory cytokines MIP-1α (macrophage inflammatory protein-1α), TNF-α (tumour necrosis factor-alpha), and IL-1β (Interleukin-1α) were significantly reduced in curcumin treated p25Tg mice. Further, behavioural studies using an 8-arm radial maze showed improved spatial and working memory with curcumin treatment.

Other labs have both developed and tested the effectiveness of curcumin derivatives in mouse models. Yanagisawa et al. (Yanagisawa et al., 2018) examined a novel curcumin derivative synthesised by the group called Shiga-Y5 (SY5), which they had previously found to be effective in inhibiting cognitive impairment and amyloid deposition in an AD mouse model (Yanagisawa et al., 2015). In this study, control and SY5-containing (500 ppm) chow diets were fed for 4 months to rTg4510 mice, a mouse tauopathy model expressing human four-repeat tau with P301L mutation in the forebrain at levels 13-fold higher than endogenous mouse tau (Ramsden et al., 2005). Behavioural tests were conducted from 5.5 months of age and mice sacrificed at 6 months. They found no significant differences in behavioural performance between rTg4510 mice fed SY5 or a control diet. Further, histological and biochemical analyses found no significant changes in tau accumulation following curcumin treatment. Given that SY5 was first designed as a fluorine-19 magnetic resonance imaging probe to detect amyloid deposition, it's effectiveness against tau accumulation may not be optimal (Yanagisawa et al., 2011).

Okuda et al. (2017) designed, synthesized and evaluated the efficacy of the curcumin derivative, PE859, a dual inhibitor of tau and Aβ aggregation, in a senescence-accelerated mouse prone 8 (SAMP8) model. In this 9-weeks study, SAMP8 mice were given oral administrations via gastric tube of PE859 at three concentrations: 0, 1 mg/k/day, 3 mg/kg/day, from 2 to 4 months of age. They reported a significant improvement in cognitive deficits in spatial working memory (i.e., using Y-maze tests), but not for any other behavioural measure. They did however note that PE859 reduced the amount of aggregated tau and Aβ1-40 in SAMP8 mice. It is possible that a more robust behavioural response would have been noted had curcumin treatment been extended.

## CLINICAL STUDIES EXAMINING CURCUMIN AND TAU PATHOLOGY

Conclusions on the efficacy of curcumin and its derivatives has been hindered by the limited number of clinical trials, and inconsistent reports on the effectiveness of these compounds in improving cognitive deficits (see Voulgaropoulou et al., 2019). The studies that have directly examined tau pathology in clinical studies have also reported mixed results. Ringman et al. (Ringman et al., 2012) evaluated the efficacy of the Curcumin 3 Complex® (Sabinsa Corporation, Piscataway, NJ), a curcuminoid mixture of curcumin, bisdemethoxycurcumin and demethoxycurcumin, in a population with mild to moderate AD. The compound was administered in three doses (placebo, 2 g/day and 4 g/day curcumin) for 24 weeks. However, Curcumin C3 Complex® did not improve cognitive deficits or reduce tau and Aβ levels in plasma and cerebrospinal fluid (CSF). In this study, low bioavailability of the compound was noted in plasma and patient dropout due to gastrointestinal complains was reported.

In contrast, Small et al. (Small et al., 2018) evaluated the effects of Theracurmin®, a form of curcumin with increased intestinal endothelium penetrability, and reported positive effects. In this study, non-demented adults between 51–84 years of age were given Theracurmin® or placebo twice a day for 18 months. The authors found that Theracurmin® improved verbal and visual

memory and attention. Further, 2-(1-ethylidene) malononitrile positron emission tomography (FDDNP-PET) scans performed pre- and post-treatment found a reduction in tau and amyloid accumulation in the amygdala of the curcumin treated group compared to placebo. In the hypothalamus, the curcumin treated group showed no change, while the placebo group showed an increase. Together, this indicates that curcumin can reduce pathogenic protein accumulation in the brain. The success of this latter study may be due to 1) it's length, indicating that extended curcumin usage may be key for improved cognitive function, and 2) it's use of non-demented adults, suggesting a more preventative than curative role for curcumin in allaying cognitive decline in human populations. For a stronger grasp on curcumin's effectiveness in treating AD, more clinical studies are necessary, especially in more severely affected populations.

## FUTURE DIRECTIONS

The general success of curcumin and curcumin derivatives in ameliorating AD pathology in animal studies is encouraging. Although, there has been limited success in clinical trials this may simply be attributable to the small number of such studies having been attempted and published to date. Given that curcumin provides a cost-effective, easily accessible solution to promote resilience to dementia, and that such a holistic treatment for AD will have even greater significance for developing countries, there is an urgent need to level the gap between animal and clinical studies. First, more clinical trials are required, especially with a focus on understanding the ability of curcumin to ameliorate cognitive deficits in severely affected populations and on the benefits of extended curcumin treatment. Other avenues for improvement include finding ways to increase the bioavailability of curcumin in the brain and considering dose dependent effects of curcumin in clinical studies (Voulgaropoulou et al., 2019).

Yet another approach of placing greater emphasis on tau-focused development of curcumin derivatives and subsequent validation in animal models may provide a more fruitful strategy. For example, a number of *in vitro* studies have demonstrated the effectiveness of curcumin derivatives in attenuating the formation of toxic tau oligomers, including tau-targeting biomimetic nanoparticles that reduce phospho-tau levels (Gao et al., 2020) and sugar-curcumin conjugates that suppress tau aggregation more efficiently at lower concentrations than curcumin (Dolai et al., 2011). A study by Cascio et al. (Lo Cascio et al., 2019) screened a small library of novel curcumin derivatives against pre-formed tau oligomers and identified six compounds that interacted with toxic tau species to further promote aggregation. Interestingly, these larger tau structures had decreased toxicity in human neuroblastoma SH-SY5Y cell lines and cultured primary cortical neurons. A subsequent paper examining these compounds and disease-relevant brain-derived tau oligomers (BDTOs) isolated from brain tissues of different tauopathies reported similar results but identified compound CL3 as effective in the formation of larger, less toxic tau aggregates with decreased seeding propensity (Lo Cascio et al., 2020). A thorough validation in animal and clinical studies will reveal if any of these tau-directed curcumin derivatives are more effective in reducing cognitive deficits caused by AD. In summary, the work summarised here highlights a great potential for curcumin as a therapeutic treatment for AD. With a continued push towards development and testing of more effective curcumin derivatives, future studies may finally bridge the gap in translation.

## AUTHOR CONTRIBUTIONS

LS ands AM cowrote this manuscript.

## FUNDING

This work was supported by the Salifu Dagarti Foundation, and by funding to LS from the Alzheimers Society United Kingdom [grant number 315 (AS-JF-16-004)].

## REFERENCES

Anand, P., Kunnumakkara, A. B., Newman, R. A., and Aggarwal, B. B. (2007). Bioavailability of Curcumin: Problems and Promises. *Mol. Pharm.* 4 (6), 807–818. doi:10.1021/mp700113r

Andorfer, C., Acker, C. M., Kress, Y., Hof, P. R., Duff, K., and Davies, P. (2005). Cell-cycle Reentry and Cell Death in Transgenic Mice Expressing Nonmutant Human Tau Isoforms. *J. Neurosci.* 25 (22), 5446–5454. doi:10.1523/JNEUROSCI.4637-04.2005

Bartus, R. T. (2000). On Neurodegenerative Diseases, Models, and Treatment Strategies: Lessons Learned and Lessons Forgotten a Generation Following the Cholinergic Hypothesis. *Exp. Neurol.* 163 (2), 495–529. doi:10.1006/exnr.2000.7397

Baum, L., Lam, C. W., Cheung, S. K., Kwok, T., Lui, V., Tsoh, J., et al. (2008). Six-month Randomized, Placebo-Controlled, Double-Blind, Pilot Clinical Trial of Curcumin in Patients with Alzheimer Disease. *J. Clin. Psychopharmacol.* 28 (1), 110–113. doi:10.1097/jcp.0b013e318160862c

Brunden, K. R., Yao, Y., Potuzak, J. S., Ferrer, N. I., Ballatore, C., James, M. J., et al. (2011). The Characterization of Microtubule-Stabilizing Drugs as Possible Therapeutic Agents for Alzheimer's Disease and Related Tauopathies. *Pharmacol. Res.* 63 (4), 341–351. doi:10.1016/j.phrs.2010.12.002

Chainoglou, E., and Hadjipavlou-Litina, D. (2020). Curcumin in Health and Diseases: Alzheimer's Disease and Curcumin Analogues, Derivatives, and Hybrids. *Int. J. Mol. Sci.* 21 (6), 1975. doi:10.3390/ijms21061975

Chee, F. C., Mudher, A., Cuttle, M. F., Newman, T. A., MacKay, D., Lovestone, S., et al. (2005). Over-expression of Tau Results in Defective Synaptic Transmission in Drosophila Neuromuscular Junctions. *Neurobiol. Dis.* 20 (3), 918–928. doi:10.1016/j.nbd.2005.05.029

Chetty, D., Abrahams, S., van Coller, R., Carr, J., Kenyon, C., and Bardien, S. (2021). Movement of Prion-like α-synuclein along the Gut-Brain axis in Parkinson's Disease: A Potential Target of Curcumin Treatment. *Eur. J. Neurosci.* 54 (2), 4695–4711. doi:10.1111/ejn.15324

Chongtham, A., and Agrawal, N. (2016). Curcumin Modulates Cell Death and Is Protective in Huntington's Disease Model. *Sci. Rep.* 6, 18736. doi:10.1038/srep18736

Cowan, C. M., Bossing, T., Page, A., Shepherd, D., and Mudher, A. (2010). Soluble Hyper-Phosphorylated Tau Causes Microtubule Breakdown and Functionally Compromises Normal Tau *In Vivo*. *Acta Neuropathol.* 120 (5), 593–604. doi:10.1007/s00401-010-0716-8

Cowan, C. M., Sealey, M. A., and Mudher, A. (2021). Suppression of Tau-Induced Phenotypes by Vitamin E Demonstrates the Dissociation of Oxidative Stress and Phosphorylation in Mechanisms of Tau Toxicity. *J. Neurochem.* 157 (3), 684–694. doi:10.1111/jnc.15253

Cox, K. H., Pipingas, A., and Scholey, A. B. (2015). Investigation of the Effects of Solid Lipid Curcumin on Cognition and Mood in a Healthy Older Population. *J. Psychopharmacol.* 29 (5), 642–651. doi:10.1177/0269881114552744

d'Abramo, C., Acker, C. M., Jimenez, H., and Davies, P. (2015). Passive Immunization in JNPL3 Transgenic Mice Using an Array of Phospho-Tau Specific Antibodies. *PLoS One* 10 (8), e0135774. doi:10.1371/journal.pone.0135774

Dolai, S., Shi, W., Corbo, C., Sun, C., Averick, S., Obeysekera, D., et al. (2011). "Clicked" Sugar-Curcumin Conjugate: Modulator of Amyloid-β and Tau Peptide Aggregation at Ultralow Concentrations. *ACS Chem. Neurosci.* 2 (12), 694–699. doi:10.1021/cn200088r

Forouzanfar, F., Barreto, G., Majeed, M., and Sahebkar, A. (2019). Modulatory Effects of Curcumin on Heat Shock Proteins in Cancer: A Promising Therapeutic Approach. *Biofactors* 45 (5), 631–640. doi:10.1002/biof.1522

Gao, C., Chu, X., Gong, W., Zheng, J., Xie, X., Wang, Y., et al. (2020). Neuron Tau-Targeting Biomimetic Nanoparticles for Curcumin Delivery to Delay Progression of Alzheimer's Disease. *J. Nanobiotechnology* 18 (1), 71. doi:10.1186/s12951-020-00626-1

Garcia-Alloza, M., Borrelli, L. A., Rozkalne, A., Hyman, B. T., and Bacskai, B. J. (2007). Curcumin Labels Amyloid Pathology *In Vivo*, Disrupts Existing Plaques, and Partially Restores Distorted Neurites in an Alzheimer Mouse Model. *J. Neurochem.* 102 (4), 1095–1104. doi:10.1111/j.1471-4159.2007.04613.x

Götz, J., Halliday, G., and Nisbet, R. M. (2019). Molecular Pathogenesis of the Tauopathies. *Annu. Rev. Pathol.* 14, 239–261. doi:10.1146/annurev-pathmechdis-012418-012936

Grundke-Iqbal, I., Iqbal, K., Tung, Y. C., Quinlan, M., Wisniewski, H. M., and Binder, L. I. (1986). Abnormal Phosphorylation of the Microtubule-Associated Protein Tau (Tau) in Alzheimer Cytoskeletal Pathology. *Proc. Natl. Acad. Sci. U. S. A.* 83 (13), 4913–4917. doi:10.1073/pnas.83.13.4913

He, Y., Yue, Y., Zheng, X., Zhang, K., Chen, S., and Du, Z. (2015). Curcumin, Inflammation, and Chronic Diseases: How Are They Linked? *Molecules* 20 (5), 9183–9213. doi:10.3390/molecules20059183

Holmes, B. B., Furman, J. L., Mahan, T. E., Yamasaki, T. R., Mirbaha, H., Eades, W. C., et al. (2014). Proteopathic Tau Seeding Predicts Tauopathy *In Vivo*. *Proc. Natl. Acad. Sci. U. S. A.* 111 (41), E4376–E4385. doi:10.1073/pnas.1411649111

Hoover, B. R., Reed, M. N., Su, J., Penrod, R. D., Kotilinek, L. A., Grant, M. K., et al. (2010). Tau Mislocalization to Dendritic Spines Mediates Synaptic Dysfunction Independently of Neurodegeneration. *Neuron* 68 (6), 1067–1081. doi:10.1016/j.neuron.2010.11.030

Hoozemans, J. J., van Haastert, E. S., Nijholt, D. A., Rozemuller, A. J., Eikelenboom, P., and Scheper, W. (2009). The Unfolded Protein Response Is Activated in Pretangle Neurons in Alzheimer's Disease hippocampus. *Am. J. Pathol.* 174 (4), 1241–1251. doi:10.2353/ajpath.2009.080814

Ismail, R., Parbo, P., Madsen, L. S., Hansen, A. K., Hansen, K. V., Schaldemose, J. L., et al. (2020). The Relationships between Neuroinflammation, Beta-Amyloid and Tau Deposition in Alzheimer's Disease: a Longitudinal PET Study. *J. Neuroinflammation* 17 (1), 151. doi:10.1186/s12974-020-01820-6

Ittner, L. M., Fath, T., Ke, Y. D., Bi, M., van Eersel, J., Li, K. M., et al. (2008). Parkinsonism and Impaired Axonal Transport in a Mouse Model of Frontotemporal Dementia. *Proc. Natl. Acad. Sci. U. S. A.* 105 (41), 15997–16002. doi:10.1073/pnas.0808084105

Kannappan, R., Gupta, S. C., Kim, J. H., Reuter, S., and Aggarwal, B. B. (2011). Neuroprotection by Spice-Derived Nutraceuticals: You Are what You Eat! *Mol. Neurobiol.* 44 (2), 142–159. doi:10.1007/s12035-011-8168-2

Khurana, V., Merlo, P., DuBoff, B., Fulga, T. A., Sharp, K. A., Campbell, S. D., et al. (2012). A Neuroprotective Role for the DNA Damage Checkpoint in Tauopathy. *Aging Cell.* 11 (2), 360–362. doi:10.1111/j.1474-9726.2011.00778.x

Kitani, K., Osawa, T., and Yokozawa, T. (2007). The Effects of Tetrahydrocurcumin and Green Tea Polyphenol on the Survival of Male C57BL/6 Mice. *Biogerontology* 8 (5), 567–573. doi:10.1007/s10522-007-9100-z

Labanca, F., Ullah, H., Khan, H., Milella, L., Xiao, J., Dajic-Stevanovic, Z., et al. (2021). Therapeutic and Mechanistic Effects of Curcumin in Huntington's Disease. *Curr. Neuropharmacol.* 19 (7), 1007–1018. doi:10.2174/1570159x18666200522201123

Lee, K. S., Lee, B. S., Semnani, S., Avanesian, A., Um, C. Y., Jeon, H. J., et al. (2010). Curcumin Extends Life Span, Improves Health Span, and Modulates the Expression of Age-Associated Aging Genes in *Drosophila melanogaster*. *Rejuvenation Res.* 13 (5), 561–570. doi:10.1089/rej.2010.1031

Liao, V. H., Yu, C. W., Chu, Y. J., Li, W. H., Hsieh, Y. C., and Wang, T. T. (2011). Curcumin-mediated Lifespan Extension in *Caenorhabditis elegans*. *Mech. Ageing Dev.* 132 (10), 480–487. doi:10.1016/j.mad.2011.07.008

Livingston, G., Huntley, J., Sommerlad, A., Ames, D., Ballard, C., Banerjee, S., et al. (2020). Dementia Prevention, Intervention, and Care: 2020 Report of the Lancet Commission. *Lancet* 396 (10248), 413–446. doi:10.1016/S0140-6736(20)30367-6

Lo Cascio, F., Garcia, S., Montalbano, M., Puangmalai, N., McAllen, S., Pace, A., et al. (2020). Modulating Disease-Relevant Tau Oligomeric Strains by Small Molecules. *J. Biol. Chem.* 295 (44), 14807–14825. doi:10.1074/jbc.RA120.014630

Lo Cascio, F., Puangmalai, N., Ellsworth, A., Bucchieri, F., Pace, A., Palumbo Piccionello, A., et al. (2019). Toxic Tau Oligomers Modulated by Novel Curcumin Derivatives. *Sci. Rep.* 9 (1), 19011. doi:10.1038/s41598-019-55419-w

Lovestone, S., Boada, M., Dubois, B., Hüll, M., Rinne, J. O., Huppertz, H. J., et al. (2015). A Phase II Trial of Tideglusib in Alzheimer's Disease. *J. Alzheimers Dis.* 45 (1), 75–88. doi:10.3233/JAD-141959

Ma, Q. L., Zuo, X., Yang, F., Ubeda, O. J., Gant, D. J., Alaverdyan, M., et al. (2013). Curcumin Suppresses Soluble Tau Dimers and Corrects Molecular Chaperone, Synaptic, and Behavioral Deficits in Aged Human Tau Transgenic Mice. *J. Biol. Chem.* 288 (6), 4056–4065. doi:10.1074/jbc.M112.393751

Maqbool, M., Mobashir, M., and Hoda, N. (2016). Pivotal Role of Glycogen Synthase Kinase-3: A Therapeutic Target for Alzheimer's Disease. *Eur. J. Med. Chem.* 107, 63–81. doi:10.1016/j.ejmech.2015.10.018

Miyasaka, T., Xie, C., Yoshimura, S., Shinzaki, Y., Yoshina, S., Kage-Nakadai, E., et al. (2016). Curcumin Improves Tau-Induced Neuronal Dysfunction of Nematodes. *Neurobiol. Aging* 39, 69–81. doi:10.1016/j.neurobiolaging.2015.11.004

Mudher, A., Shepherd, D., Newman, T. A., Mildren, P., Jukes, J. P., Squire, A., et al. (2004). GSK-3beta Inhibition Reverses Axonal Transport Defects and Behavioural Phenotypes in Drosophila. *Mol. Psychiatry* 9 (5), 522–530. doi:10.1038/sj.mp.4001483

Mukherjee, S., Mishra, A. K., Peer, G. D. G., Bagabir, S. A., Haque, S., Pandey, R. P., et al. (2021). The Interplay of the Unfolded Protein Response in Neurodegenerative Diseases: A Therapeutic Role of Curcumin. *Front. Aging Neurosci.* 13, 767493. doi:10.3389/fnagi.2021.767493

Nagele, R. G., Wegiel, J., Venkataraman, V., Imaki, H., Wang, K. C., and Wegiel, J. (2004). Contribution of Glial Cells to the Development of Amyloid Plaques in Alzheimer's Disease. *Neurobiol. Aging* 25 (5), 663–674. doi:10.1016/j.neurobiolaging.2004.01.007

Nebrisi, E. E. (2021). Neuroprotective Activities of Curcumin in Parkinson's Disease: A Review of the Literature. *Int. J. Mol. Sci.* 22 (20), 11248. doi:10.3390/ijms222011248

Okuda, M., Fujita, Y., Hijikuro, I., Wada, M., Uemura, T., Kobayashi, Y., et al. (2017). PE859, A Novel Curcumin Derivative, Inhibits Amyloid-β and Tau Aggregation, and Ameliorates Cognitive Dysfunction in Senescence-Accelerated Mouse Prone 8. *J. Alzheimers Dis.* 59 (1), 313–328. doi:10.3233/JAD-161017

Olszanecki, R., Jawień, J., Gajda, M., Mateuszuk, L., Gebska, A., Korabiowska, M., et al. (2005). Effect of Curcumin on Atherosclerosis in apoE/LDLR-Double Knockout Mice. *J. Physiol. Pharmacol.* 56 (4), 627–635.

Panza, F., Solfrizzi, V., Seripa, D., Imbimbo, B. P., Lozupone, M., Santamato, A., et al. (2016). Tau-Centric Targets and Drugs in Clinical Development for the Treatment of Alzheimer's Disease. *Biomed. Res. Int.* 2016, 3245935. doi:10.1155/2016/3245935

Parekh, K. D., Dash, R. P., Pandya, A. N., Vasu, K. K., and Nivsarkar, M. (2013). Implication of Novel Bis-Imidazopyridines for Management of Alzheimer's Disease and Establishment of its Role on Protein Phosphatase 2A Activity in Brain. *J. Pharm. Pharmacol.* 65 (12), 1785–1795. doi:10.1111/jphp.12149

Quraishe, S., Sealey, M., Cranfield, L., and Mudher, A. (2016). Microtubule Stabilising Peptides Rescue Tau Phenotypes *In-Vivo*. *Sci. Rep.* 6, 38224. doi:10.1038/srep38224

Rainey-Smith, S. R., Brown, B. M., Sohrabi, H. R., Shah, T., Goozee, K. G., Gupta, V. B., et al. (2016). Curcumin and Cognition: a Randomised, Placebo-Controlled, Double-Blind Study of Community-Dwelling Older Adults. *Br. J. Nutr.* 115 (12), 2106–2113. doi:10.1017/S0007114516001203

Ramsden, M., Kotilinek, L., Forster, C., Paulson, J., McGowan, E., SantaCruz, K., et al. (2005). Age-dependent Neurofibrillary Tangle Formation, Neuron Loss, and Memory Impairment in a Mouse Model of Human Tauopathy (P301L). *J. Neurosci.* 25 (46), 10637–10647. doi:10.1523/JNEUROSCI.3279-05.2005

Reddy, P. H., Manczak, M., Yin, X., Grady, M. C., Mitchell, A., Tonk, S., et al. (2018). Protective Effects of Indian Spice Curcumin against Amyloid-β in Alzheimer's Disease. *J. Alzheimers Dis.* 61 (3), 843–866. doi:10.3233/JAD-170512

Reisberg, B., Doody, R., Stöffler, A., Schmitt, F., Ferris, S., Möbius, H. J., et al. (2003). Memantine in Moderate-To-Severe Alzheimer's Disease. *N. Engl. J. Med.* 348 (14), 1333–1341. doi:10.1056/NEJMoa013128

Ringman, J. M., Frautschy, S. A., Teng, E., Begum, A. N., Bardens, J., Beigi, M., et al. (2012). Oral Curcumin for Alzheimer's Disease: Tolerability and Efficacy in a 24-week Randomized, Double Blind, Placebo-Controlled Study. *Alzheimers Res. Ther.* 4 (5), 43. doi:10.1186/alzrt146

Sankaranarayanan, S., Barten, D. M., Vana, L., Devidze, N., Yang, L., Cadelina, G., et al. (2015). Passive Immunization with Phospho-Tau Antibodies Reduces Tau Pathology and Functional Deficits in Two Distinct Mouse Tauopathy Models. *PLoS One* 10 (5), e0125614. doi:10.1371/journal.pone.0125614

Scapagnini, G., Caruso, C., and Calabrese, V. (2010). Therapeutic Potential of Dietary Polyphenols against Brain Ageing and Neurodegenerative Disorders. *Adv. Exp. Med. Biol.* 698, 27–35. doi:10.1007/978-1-4419-7347-4_3

Singh, S., and Aggarwal, B. B. (1995). Activation of Transcription Factor NF-Kappa B Is Suppressed by Curcumin (Diferuloylmethane) [corrected]. *J. Biol. Chem.* 270 (42), 24995–25000. doi:10.1074/jbc.270.42.24995

Small, G. W., Siddarth, P., Li, Z., Miller, K. J., Ercoli, L., Emerson, N. D., et al. (2018). Memory and Brain Amyloid and Tau Effects of a Bioavailable Form of Curcumin in Non-demented Adults: A Double-Blind, Placebo-Controlled 18-Month Trial. *Am. J. Geriatr. Psychiatry* 26 (3), 266–277. doi:10.1016/j.jagp.2017.10.010

Spillantini, M. G., and Goedert, M. (2013). Tau Pathology and Neurodegeneration. *Lancet Neurol.* 12 (6), 609–622. doi:10.1016/S1474-4422(13)70090-5

Sreejayan, R., and Rao, M. N. (1997). Nitric Oxide Scavenging by Curcuminoids. *J. Pharm. Pharmacol.* 49 (1), 105–107. doi:10.1111/j.2042-7158.1997.tb06761.x

Stamer, K., Vogel, R., Thies, E., Mandelkow, E., and Mandelkow, E. M. (2002). Tau Blocks Traffic of Organelles, Neurofilaments, and APP Vesicles in Neurons and Enhances Oxidative Stress. *J. Cell. Biol.* 156 (6), 1051–1063. doi:10.1083/jcb.200108057

Suckow, B. K., and Suckow, M. A. (2006). Lifespan Extension by the Antioxidant Curcumin in *Drosophila melanogaster*. *Int. J. Biomed. Sci.* 2 (4), 402–405.

Sundaram, J. R., Poore, C. P., Sulaimee, N. H. B., Pareek, T., Cheong, W. F., Wenk, M. R., et al. (2017). Curcumin Ameliorates Neuroinflammation, Neurodegeneration, and Memory Deficits in P25 Transgenic Mouse Model that Bears Hallmarks of Alzheimer's Disease. *J. Alzheimers Dis.* 60 (4), 1429–1442. doi:10.3233/JAD-170093

von Bergen, M., Friedhoff, P., Biernat, J., Heberle, J., Mandelkow, E. M., and Mandelkow, E. (2000). Assembly of Tau Protein into Alzheimer Paired Helical Filaments Depends on a Local Sequence Motif ((306)VQIVYK(311)) Forming Beta Structure. *Proc. Natl. Acad. Sci. U. S. A.* 97 (10), 5129–5134. doi:10.1073/pnas.97.10.5129

Voulgaropoulou, S. D., van Amelsvoort, T. A. M. J., Prickaerts, J., and Vingerhoets, C. (2019). The Effect of Curcumin on Cognition in Alzheimer's Disease and Healthy Aging: A Systematic Review of Pre-clinical and Clinical Studies. *Brain Res.* 1725, 146476. doi:10.1016/j.brainres.2019.146476

Williams, D. R. (2006). Tauopathies: Classification and Clinical Update on Neurodegenerative Diseases Associated with Microtubule-Associated Protein Tau. *Intern Med. J.* 36 (10), 652–660. doi:10.1111/j.1445-5994.2006.01153.x

Wischik, C. M., Edwards, P. C., Lai, R. Y., Roth, M., and Harrington, C. R. (1996). Selective Inhibition of Alzheimer Disease-like Tau Aggregation by Phenothiazines. *Proc. Natl. Acad. Sci. U. S. A.* 93 (20), 11213–11218. doi:10.1073/pnas.93.20.11213

Yanagisawa, D., Amatsubo, T., Morikawa, S., Taguchi, H., Urushitani, M., Shirai, N., et al. (2011). *In Vivo* detection of Amyloid β Deposition Using $^{19}$F Magnetic Resonance Imaging with a $^{19}$F-Containing Curcumin Derivative in a Mouse Model of Alzheimer's Disease. *Neuroscience* 184, 120–127. doi:10.1016/j.neuroscience.2011.03.071

Yanagisawa, D., Hamezah, H. S., Durani, L. W., Taguchi, H., and Tooyama, I. (2018). Study of Tau Pathology in Male rTg4510 Mice Fed with a Curcumin Derivative Shiga-Y5. *PLoS One* 13 (12), e0208440. doi:10.1371/journal.pone.0208440

Yanagisawa, D., Ibrahim, N. F., Taguchi, H., Morikawa, S., Hirao, K., Shirai, N., et al. (2015). Curcumin Derivative with the Substitution at C-4 Position, but Not Curcumin, Is Effective against Amyloid Pathology in APP/PS1 Mice. *Neurobiol. Aging* 36 (1), 201–210. doi:10.1016/j.neurobiolaging.2014.07.041

**Conflict of Interest:** The authors declare that the research was conducted in the absence of any commercial or financial relationships that could be construed as a potential conflict of interest.

frontiers | Frontiers in Pharmacology

REVIEW
published: 20 May 2022
doi: 10.3389/fphar.2022.845591

# Berberine: A Promising Treatment for Neurodegenerative Diseases

*Ziqian Cheng[1], Chenglan Kang[2], Songtian Che[1], Jingyun Su[1], Qihan Sun[1], Tongtong Ge[1], Yi Guo[1], Jiayin Lv[3], Zhihui Sun[4], Wei Yang[1], Bingjin Li[1], Xin Li[1]* and Ranji Cui[1]**

[1]Jilin Provincial Key Laboratory on Molecular and Chemical Genetic, Second Hospital of Jilin University, Changchun, China, [2]Department of Cardiology, The China-Japan Union Hospital of Jilin University, Changchun, China, [3]Department of Orthopedics, The China-Japan Union Hospital of Jilin University, Changchun, China, [4]Department of Pharmacy, The First Hospital of Jilin University, Changchun, China

Berberine, as a natural alkaloid compound, is characterized by a diversity of pharmacological effects. In recent years, many researches focused on the role of berberine in central nervous system diseases. Among them, the effect of berberine on neurodegenerative diseases has received widespread attention, for example Alzheimer's disease, Parkinson's disease, Huntington's disease, and so on. Recent evidence suggests that berberine inhibits the production of neuroinflammation, oxidative, and endoplasmic reticulum stress. These effects can further reduce neuron damage and apoptosis. Although the current research has made some progress, its specific mechanism still needs to be further explored. This review provides an overview of berberine in neurodegenerative diseases and its related mechanisms, and also provides new ideas for future research on berberine.

**Keywords: berberine, neurodegenerative diseases, neuroinflammation, neuroprotection, oxidative stress**

OPEN ACCESS

***Edited by:***
*Fang Pan,*
*Shandong University, China*

***Reviewed by:***
*Young-Ji Shiao,*
*National Research Institute of Chinese Medicine, Taiwan*
*George L. S. Oliveira,*
*Federal University of Piauí, Brazil*

****Correspondence:***
*Xin Li*
*xinli@jlu.edu.cn*
*Ranji Cui*
*cuiranji@jlu.edu.cn*

***Specialty section:***
*This article was submitted to Neuropharmacology, a section of the journal Frontiers in Pharmacology*

***Received:*** *30 December 2021*
***Accepted:*** *21 March 2022*
***Published:*** *20 May 2022*

***Citation:***
*Cheng Z, Kang C, Che S, Su J, Sun Q, Ge T, Guo Y, Lv J, Sun Z, Yang W, Li B, Li X and Cui R (2022) Berberine: A Promising Treatment for Neurodegenerative Diseases. Front. Pharmacol. 13:845591. doi: 10.3389/fphar.2022.845591*

## 1 INTRODUCTION

Berberine ($C_{20}H_{18}NO_4$, IUPAC name: 16,17-dimethoxy-5,7-dioxa-13-azoniapentacyclo [11.8.0.0$^{2,10}$.0$^{4,8}$.0$^{15,20}$] henicosa-1(13),2,4(8),9,14,16,18,20-octaene, PubChem CID: 2353), an isoquinoline quaternary alkaloid, isolated from different medicinal plants with a molar weight of 336.36 g/mol, including *Hydrastis canadensis*, *Xanthorhiza simplicissima*, *Berberis aristata*, *Coptis chinensis*, *Coptis japonica*, etc. (Ortiz et al., 2014; Cicero and Baggioni, 2016; Feng et al., 2019). Berberine is a yellow powder, slightly soluble in ethanol or methanol (Kong et al., 2004; Wang et al., 2017). It has been reported that berberine is widely used in many traditional medical systems, including Ayurvedic, Iranian, and Chinese medicine (Kunwar et al., 2006; Cicero and Baggioni, 2016), and it has been used in some cases like cancer, diabetes, cardiovascular diseases, hypertension, Alzheimer's disease, etc. (Imenshahidi and Hosseinzadeh, 2016; Wang et al., 2017; de Oliveira et al., 2019). Many preclinical studies conclusively shown that berberine plays a therapeutic role in many central nervous system disorders such as Alzheimer s disease, cerebral ischemia, depression, schizophrenia, epilepsy, and anxiety (Fan et al., 2017; Liu et al., 2017; Sedaghat et al., 2017; Fan J. et al., 2019a; Yuan et al., 2019; Rezaeian et al., 2020; Qiu et al., 2021; Zhao et al., 2021), however these experimental data are only obtained in animal models (Kulkarni and Dhir, 2010). Study elucidated that berberine can reduce the cognitive impairment caused by doxorubicin (DOX). In further research, it was found that berberine achieved antioxidant effects by reducing the expression of pro-inflammatory factors, apoptotic factors and nuclear transcription factor κ B (NF-κb), as well as up-regulating the expression of peroxlsome proliferator-activated receptor-γ coactlvator-1α (PGC-1α) and manganese superoxide dismutase. Berberine can also regulate cAMP response

element binding protein (CREB) and brain-derived neurotrophic factor (BDNF) to further regulate synaptic plasticity (Shaker et al., 2021). Moreover, the literature points out that berberine has inhibitory effects on four key enzymes related to the pathogenesis of Alzheimer s disease: monoamine oxidase B (MAO-B), acetylcholinesterase, monoamine oxidase A (MAO-A), and butyrylcholinesterase (Yuan et al., 2019). However, the effects of berberine on neurodegenerative diseases are rarely reported and further investigation is still needed.

Due to the increase of the senior population in recent years, age-related diseases such as neurodegenerative diseases have become more common and pose a serious threat to human health (Heemels, 2016). Among them, World Health Organization reported that Alzheimer's and other forms of dementia are currently among the top ten causes of death globally, ranking third in both the Americas and Europe in 2019 (World Health Organization, 2020). Moreover, neurodegenerative diseases, such as Alzheimer's disease, Parkinson's disease, bring a heavy burden to patients and their families, and become a public health problem that needs to be solved urgently. Neurodegenerative diseases are characterized by progressive damage to functions of synapses, neurons, glial cells (Marchesi et al., 2021; Pathak et al., 2021). Research on genome instability, autophagy, protein aggregation, and inflammation are currently a hot spot for the pathogenesis of neurodegenerative diseases (Hou et al., 2019). Although significant progress has been made in the research on the pathogenesis of neurodegenerative diseases such as Alzheimer's disease, Parkinson's disease, amyotrophic lateral sclerosis and Huntington's disease, and many drugs have found neuroprotective effects in cells and animal models, but there is still no drug that can produce clinical changes significantly in the pathogenesis. It is very urgent to develop a drug that can effectively treat neurodegenerative diseases with few side effects.

Therefore, we conducted a systematic review of research articles on the role of berberine in neurodegenerative diseases over the past decade. The main focus is on the two most common neurodegenerative diseases, Alzheimer's disease and Parkinson's disease, other neurodegenerative diseases are also involved in a small amount. This review was carried out by searching on the electronic databases (including PubMed, ScienceDirect, and Pubchem) for studies focusing on the molecular mechanism of berberine in the biological processes related to neurodegenerative diseases. Furthermore, this review provides a perspective for future research that may contribute to the development of new drugs for neurodegenerative disease treatments.

# 2 PHARMACOLOGICAL EFFECTS OF BERBERINE

## 2.1 Oxidative Stress

The effect of berberine on a variety of neurodegenerative diseases indicates that it may have a regulatory effect on the common pathways of these diseases. MAO-B inhibitors are believed to have a positive effect on patients with Alzheimer's and Parkinson's disease (Mangoni et al., 1991; Rabey et al., 2000; Jiang et al., 2015a). The dopamine metabolic pathway mediated by MAO-B can generate hydrogen peroxide ($H_2O_2$), and with the increase of MAO-B activity, excessive $H_2O_2$ leads to oxidative stress and neuronal damage (Jiang et al., 2015a). Therefore, the antioxidant effect of berberine has great effects on the treatment of neurodegenerative diseases.

The pathogenesis of neurodegenerative diseases has several common features, such as oxidative damage and mitochondrial dysfunction. Among them, oxidative stress refers to the excessive accumulation of reactive oxygen species (ROS) that leads to the imbalance of oxidants and antioxidants, oxidative stress has the ability to lead to mitochondrial dysfunction and lysosome dysfunction, and ultimately induces neurodegenerative disease (Caspersen et al., 2005; Poprac et al., 2017; Li Z. et al., 2020a). It has been reported that Berberine significantly reduces ROS production in the cytoplasm and mitochondria (Sun et al., 2017). This effect may be related to the activation of AMP-activated protein kinase (AMPK) and sirtuin1 (SIRT1)/forkhead box O1 (FOXO1) pathway (Li et al., 2018; Ma et al., 2018). In addition, in PC12 and N2a cells, low-concentration administration of berberine significantly reduced the amount of ROS generation, lipid peroxidation, and DNA fragmentation, and at the same time increased glutathione content and superoxide dismutase activity (Sadeghnia et al., 2017). As we all know, the body has both enzymatic (such as glutathione-S-transferase) and non-enzymatic (such as thiols and reduced glutathione) antioxidant mechanisms to combat oxidative damage. Once ROS overwhelms the antioxidant activity of the cell, oxidative stress occurs (Lee et al., 2012; de Oliveira et al., 2019). Berberine-induced increase in heme oxygenase-1 (HO-1, an antioxidant enzyme) mRNA and protein expression is positively correlated with concentration and continuous administration time. This effect can be antagonized by kinase-protein kinase B (AKT) inhibitors and phosphatidylinositol 3-kinase (PI3K) inhibitors (Chen et al., 2012). An *in-vitro* study found that berberine protected NSC34 cells from $H_2O_2$-induced cytotoxicity by reducing ROS production, restoring glutathione, and superoxide dismutase activity, and activating the production of antioxidant proteins nuclear factor erythroid 2-related factor-2 (Nrf2) and HO-1 (Hsu et al., 2012; Fan D. et al., 2019a).

Studies have found that berberine has an antidepressant effect (Kulkarni and Dhir, 2008; Fan et al., 2017), acute administration can increase dopamine, serotonin and norepinephrine levels in the whole brains of mice, and this effect can be antagonized by l-arginine or sildenafil pretreatment. In short, berberine can play an antidepressant effect by regulating brain biogenic amines and nitric oxide pathway (Kulkarni and Dhir, 2008). Besides, the treatment of berberine can reduce the activity of ecto-nucleoside triphosphate diphosphohydrolase (NTPDases) and 5′-nucleotidasein the cerebral cortex and hippocampus (de Oliveira et al., 2019). In brief, the application of berberine provides a promising neuroprotective therapy for neurodegenerative diseases induced by oxidative damage, such as Alzheimer's disease, Parkinson's disease (**Figure 1**). It may be playing an antioxidant role by reducing ROS, iNOS, COX-2, increasing HO-1, and activating SIRT/FOXO1 signal pathway.

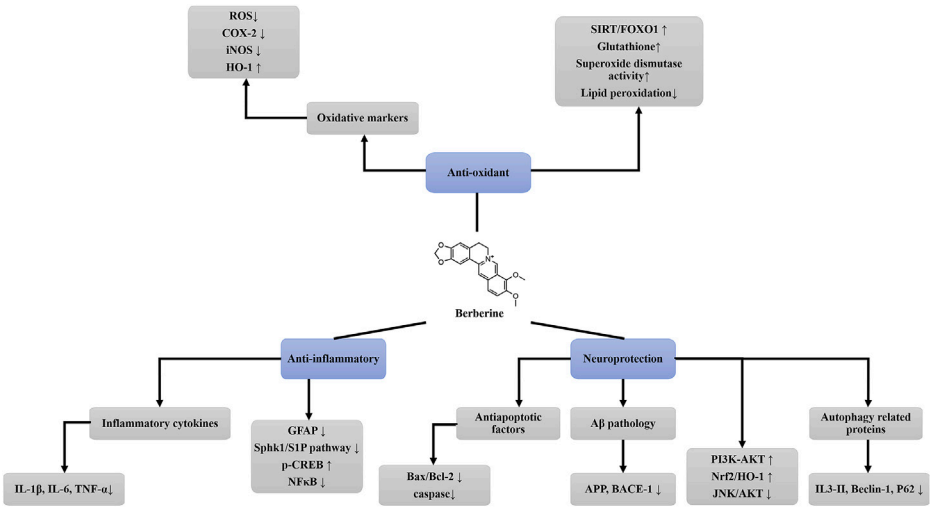


**FIGURE 1 |** The pharmacological effects of berberine. This schematic drawing shows the anti-oxidant, anti-inflammatory and neuroprotective effects of berberine and its related molecular mechanisms. ROS, reactive oxygen species; COX-2, cyclooxygenase-2; iNOS, initric oxide synthase; HO-1, heme oxygenase-1; SIRT1, sirtuin1; FOXO1, forkhead box O1; IL-1β, interleukin 1β; IL-6, interleukin 6; TNF-α, tumor necrosis factor-alpha; GFAP, glial fibrillary acidic protein; SphK1, sphingosine kinase-1; S1P, sphingosine-1-phosphate; p-CREB, phosphorylated cAMP response element binding protein; NF-κb, nuclear transcription factor kappa B; Aβ, amyloid β; APP, amyloid precursor protein; BACE1, beta-secretase 1; PI3K, phosphatidylinositol 3-kinase; AKT, kinase-protein kinase B; Nrf2, nuclear factor erythroid 2-related factor-2; JNK, jun amino-terminal kinases.

Berberine can also play a therapeutic role by increasing glutathione and superoxide dismutase activity. In addition, whether the antioxidant effect of berberine alters other markers needs to be further explored.

## 2.2 Neuroprotection

*In vitro* experimental results show that berberine can reduce 6-hydroxydopamine-induced reactive oxygen generation and caspase-3 activation in SH-SY5Y cell. In addition, berberine can induce activation of PI3K/AKT signaling pathway, which is related to Nrf2 expression and neuroprotection (Bae et al., 2013). Similarly, it has been confirmed in PC-12 cells that berberine exerts a neuroprotective effect by activating the PI3K/AKT signaling pathway and Nrf2/HO-1 antioxidant signaling pathway (Zhang et al., 2017). In BV2 and N2a cells treated with amyloid β (Aβ), berberine promotes cell proliferation, inhibits the activity of caspase-3, and reduces the rate of apoptosis, in addition, berberine promotes cell viability *via* the microRNA (miR)-188/nitric oxide synthase 1 (NOS1) pathway (Chen M. et al., 2020a). By analyzing the learning and memory of post-cerebral ischaemia. animals, the researchers discovered the neuroprotective effects of berberine (Ye et al., 2009; Zhang C. C. et al., 2018a). *In vitro* experiments (organotypic hippocampal culture exposed to oxygen and glucose deprivation), the culture treated with berberine has less cellular death. In further research, it was found that the neuroprotection mediated by berberine after ischemia involves the AKT/glycogen synthase kinase-3β (GSK3β)/extracellular signal-regulated kinase 1/2 (ERK 1/2) signal pathway, and inhibits Jun amino-terminal kinases (JNK) and caspase-3 activity (Simões Pires et al., 2014).

Berberine inhibits neuronal apoptosis by regulating autophagy-related proteins [Microtubule-associated protein 1A/1B-light chain 3 (LC3), Beclin-1, p62], and apoptosis regulatory proteins [caspase 3, caspase 8, caspase 9, poly ADP-ribose polymerase (PARP), and B-cell lymphoma 2 (Bcl-2)/Bcl-2 associated X (Bax)] (Zhang et al., 2016). Similarly, berberine shows anti-apoptotic effects by reducing the overexpression of caspase-3 and Bax/Bcl-2 (Sadeghnia et al., 2017). In 1-methyl-4-phenyl-1,2,3,6-tetrahydropyridine/probenecid (MPTP/P)-induced Parkinson's disease model mice, MPTP/P injection increased the ratio of Bax/Bcl-2 and the expression of caspase-3 in the hippocampus, while berberine administration reversed these effects (Kim et al., 2014).

In addition, animal experiments and cell experiments have confirmed that berberine reduces the levels of extracellular and intracellular Aβ, increases the levels of LC3-II, Beclin-1, hVps34 and cathepsin-D, and reduced the levels of P62, Bcl-2, amyloid precursor protein (APP), and beta-secretase 1 (BACE1). Briefly, berberine plays a neuroprotective effect by promoting autophagy clearance and reducing Aβ production (Huang et al., 2017).

Besides, it is indicating that berberine facilitates nerve regeneration via JNK-AKT signal pathway mediated by insulin-like growth factor receptor (Zhang H. N. et al., 2018b). In astrocytes, berberine reduces glutamate-induced cytotoxicity by reducing mitochondrial fragmentation and neurodegeneration (Campisi et al., 2011). Additionally, berberine prolongs the incubation period of epileptic seizures in a dose-dependent manner. Long-term administration of berberine reduces the level of malondialdehyde in epileptic mice and enhances the activities of glutathione and catalase (Gao et al., 2014). In addition, the neuroprotective role of berberine is related to the decrease in endoplasmic reticulum stress and oxidative stress (Liang et al., 2021). Berberine can also be used in combination with other drugs such as levetiracetam and curcumin to enhance

its neuroprotective effect by reducing inflammation and oxidative stress (Lin et al., 2020; Singh et al., 2021). *In vitro*, low-dose berberine significantly increased PC12 cell viability, whereas high-dose berberine did the opposite (Zhang et al., 2017). Additionally, low-dose berberine protected PC12 cells from 6-hydroxydopamine (6-OHDA, Parkinson's disease-related neurotoxin)-induced cytotoxicity and apoptosis, whereas high-dose berberine showed no neuroprotective activity. Further experiments found that low-dose berberine can promote cell survival and antioxidant effects by up-regulating PI3K/AKT/Bcl-2 and Nrf2/HO-1 signal pathways. In animal studies, low-dose berberine attenuated 6-OHDA-induced loss of dopaminergic neurons and hypokinesia in zebrafish, whereas high-dose berberine had no apparent effect (Zhang et al., 2017). These suggests that the neuroprotective effects of berberine may be related to an excitatory mechanism that promotes cell survival and antioxidant-related signaling pathways. Studies have found that berberine attenuates ischemia-reperfusion injury through NF-κB nuclear translocation in mice with transient cerebral artery occlusion, however, this neuroprotective effect was more pronounced at the high dose (50 mg/kg) than the low dose (25 mg/kg) (Zhu et al., 2018). These differences may be related to different concentrations of berberine and different models of nerve injury. In addition, berberine *in vivo* may be metabolized to make its active ingredients different from those used *in vitro*, resulting in inconsistent results.

In brief, berberine can reduce anti-apoptotic factors (Bax/bcl-2, caspase), autophagy related proteins (IL-3, Beclin, etc.), Aβ pathology, and activate PI3K-AKT and other signaling pathways, and then produce neuroprotective effect (**Figure 1**). However, whether berberine alleviates neurodegenerative disease symptoms by increasing neuroprotection requires further study.

## 2.3 Neuroinflammation

Some studies have shown that berberine activates macrophages and increases their phagocytic function, increases the production of interleukin (IL)-1, and enhances non-specific immunity, can be used as a neuroprotective agent to prevent Alzheimer's disease (Kumazawa et al., 1984; Panahi et al., 2013). Long-term administration of berberine increases the expression of IL-1β and inducible nitric oxide synthase (iNOS) in Alzheimer's disease mice hippocampus, and ameliorate memory impairment (Zhu and Qian, 2006). Besides, berberine down-regulates the expression of acetylcholinesterase and inhibits acetylcholinesterase activity in Alzheimer's disease model mice hippocampus which induced by heavy metals, in addition, berberine normalizes the production of inflammatory factors, such as tumor necrosis factor-alpha (TNF-α), IL-6, IL-1β (Hussien et al., 2018).

Studies demonstrated that berberine contributed to AMPK signaling pathway activation and participate in anti-neuroinflammation. In BV-2 microglia, berberine down-regulates lipopolysaccharide- or interferon-γ-induced iNOS and cyclooxygenase-2 (COX-2) level, and inhibits inflammatory cytokines expression (for example IL-6, IL-1β, TNF-α) (Lu et al., 2010). On the other hand, berberine can inhibit ERK phosphorylation (Lu et al., 2010), and induce the phosphorylation of Liver kinase B1 (LKB1) (Ser428), calcium/calmodulin-dependent protein kinase II (CaMKII) (Thr286), and AMPK (Thr172) (Lu et al., 2010). In animal experiments, berberine has the ability to improve learning and memory impairment in rats via lipopolysaccharide. Further studies showed that berberine enhanced the activities of glutathione peroxidase, glutathione, superoxide dismutase, and catalase, further reducing the activity of acetylcholinesterase and caspase-3, protein carbonyl, and DNA fragmentation in the hippocampus (Sadraie et al., 2019). In addition, berberine can properly restore the levels of 3-nitrotyrosine (3-NT), COX 2, glial fibrillary acidic protein (GFAP), and sirtuin 1 in the hippocampus (Sadraie et al., 2019). Besides, the protective effect of berberine resisting MTPT-induced toxicity may be related to the enhancement of autophagy by berberine through AMPK-dependent pathways (Deng and Ma, 2021).

The study found that berberine alleviated the severity of symptoms in the multiple sclerosis mouse model, and in primary astrocyte culture, berberine inhibited the increase in sphingosine kinase-1 (SphK1), and Sphingosine-1-phosphate (S1P) induced by lipopolysaccharide. A number of researchers have reported that the activation of the SphK1/S1P signaling pathway marks the occurrence of autoimmune diseases, and the up-regulation of SphK1 is related to the pathogenesis of multiple sclerosis (Luo et al., 2017). In Alzheimer's disease mice, GFAP and neuron loss increased and neuronal nuclei (NeuN) decreased significantly. Studies have found that under pathological conditions, astrocytes are activated by Aβ to produce cytoinflammatory factors, complement, oxygen free radicals, etc., which then trigger inflammation, promote nerve cell damage and death, and ultimately aggravate Alzheimer's disease (Do et al., 2014; Matuszyk et al., 2021). The latest research shows that berberine significantly decreases the expression of GFAP in the Alzheimer's disease mice hippocampus, indicating berberine inhibits the overexpression of astrocytes in Alzheimer's disease mice. These may be linked to the effect of berberine on improving local blood flow, reducing the production of Aβ and reducing cell apoptosis (Ye et al., 2021). Similarly, berberine treatment can significantly reduce the oxidative stress in diabetic rat hippocampus and suppress GFAP immunoreactive astrocytes (Moghaddam et al., 2014). Astrocytes treated with berberine can increase the expression of p85 and p-AKT. Berberine also increases the accumulation of Nrf2 and DNA binding activity in the nucleus. It is worth noting that the increase in Nrf2 DNA binding activity induced by berberine can be antagonized by PI3K inhibitors and AKT inhibitors. In other words, in astrocytes. the increase in HO-1 expression induced by berberine is activated by Nrf2 activation through PI3K/AKT signaling pathway (Chen et al., 2012). Similarly, in SH-SY5Y cells, berberine resists rotenone-induced neurotoxicity through antioxidant effects and activates the PI3K/AKT signaling pathway (Deng et al., 2020).

Studies have found that the combined treatment of DOX and berberine can significantly counteract the increase in acetylcholinesterase activity, oxidative stress, the decrease in glutathione content and CAT activity, and the increase in

GFAP, NF-κB and caspase-3 induced by DOX (Ibrahim Fouad and Ahmed, 2021). Zhang et al. found that berberine can increase the levels of neuroprotective factors, such as p-AKT and p-CREB, and down-regulate inflammatory response factors to inhibit inflammation, such as NF-κB (Zhang et al., 2012).

Neuroinflammation plays a pivotal role in the pathogenesis of neurodegenerative diseases. It is a central feature in the neurodegenerative process that leads to more neuronal loss over time. In previous studies, it was found that berberine can reduce the expression of inflammatory factors and GFAP, while inhibiting the Sphk1/S1P signaling pathway and activating CREB signaling pathway. These show that berberine is very likely to play a therapeutic role in neurodegenerative diseases by inhibiting neuroinflammation. However, there are few literatures about the effect of berberine on astrocytes, and further experimental verification is needed.

# 3 THERAPEUTIC EFFECTS OF BERBERINE ON NEURODEGENERATIVE DISEASE

In recent years, many studies surrounded the effect of berberine in central nervous system disease, including Alzheimer's disease, Parkinson's disease, Huntington disease, etc. (Jiang et al., 2011; Kim et al., 2014; Jiang et al., 2015b; Bandiwadekar et al., 2021). Berberine has proven its protective role on oxidative stress, neuroinflammation, neuroprotection, etc. (Zhang et al., 2012; Maleki et al., 2018; de Oliveira et al., 2019; Li Z. et al., 2020a; Qin et al., 2020; Rezaeian et al., 2020; Mohi-Ud-Din et al., 2021). And whether it can be used to improve the symptoms of neurodegenerative diseases has attracted widespread attention.

## 3.1 Alzheimer's Disease

Alzheimer's disease, an age-related neurodegenerative disease, affects the quality of life of patients, and their families. Patient with Alzheimer's disease suffer from memory loss, cognitive decline, energy metabolism dysregulation, changes in personality, and behavior (Goedert and Spillantini, 2006; Ribeiro et al., 2017; Shinjyo and Kita, 2021). Although a considerable new research progress has been made in Alzheimer's disease research, the pathogenesis remains unclear. Current typical histopathological changes in Alzheimer's disease include Aβ plaques and tau tangles, the accumulation of these proteins leads to neuroinflammation and normal dysfunction, leading to neuronal death (Ameen and Michniak-Kohn, 2017; Bandiwadekar et al., 2021; Ye et al., 2021). The hypotheses on the pathogenesis of Alzheimer's disease include cholinergic hypothesis, amyloid toxicity hypothesis, oxidative stress hypothesis, etc. (Ye et al., 2009; Guo et al., 2021). At present, the therapies of Alzheimer's disease include stem cell therapy, gene therapy, and chemotherapy, but these therapies have limitations inevitably such as inefficient and neurotoxicity (Bandiwadekar et al., 2021). At the same time, natural compounds have better compatibility with the human body and have fewer side effects. A number of studies have shown that some natural drugs have significant neuroprotective, anti-oxidant and anti-inflammatory characteristics, and are suitable for the treatment of different types of neurodegenerative diseases (Ahmed et al., 2015; Jiang et al., 2015b; Fan et al., 2017; Zhang et al., 2020). Many literatures have reported the improvement effect of berberine on Alzheimer's disease (Chen M. et al., 2020a; Chen Y. et al., 2020b; Xuan et al., 2020; Raju et al., 2021).

Aβ has a neurotoxic effect, which can lead to neuronal degeneration, death, apoptosis, and decrease in the number of synapses and ultimately lead to cognitive impairment and behavioral abnormalities (Li W. et al., 2020b; Ye et al., 2021). It has proved that activating microglia by reducing Aβ is an effective treatment for Alzheimer's disease. Microglia exerts a vital role on the repair of central nervous system damage. In Alzheimer's disease, the production of pro-inflammatory factors and Aβ can over-activate microglia, secrete inflammatory factors and neurotoxins, and then induce neuronal damage and even apoptosis, thereby triggering Alzheimer's disease. On the contrary, microglia can also protect the central nervous system by engulfing Aβ, slowing the development of Alzheimer's disease (Li et al., 2021). Study have shown berberine can inhibit Aβ-induced microglial activation mediated by suppressor of cytokine signaling 1 (SOCS1) (Guo et al., 2021). Berberine induces the production of antioxidant Aβ40 and inhibits the formation of Aβ42, which is the cause of Aβ plaque accumulation, and then exerts a neuroprotective effect (Hussien et al., 2018). Besides, berberine inhibits the p-ERK/Eukaryotic translation initiation factor 2alpha (eIF2α) pathway and then reduces BACE1 expression, the decrease in BACE1 protein expression inhibits the production of Aβ. In other words, berberine suppressed Aβ production via inhibiting protein kinase R (PKR)-like endoplasmic reticulum kinase (PERK)/ eukaryotic translation-initiation factor 2α (elF2α) signaling-mediated BACE1 translation (Liang et al., 2021). Berberine also restored protein phosphate 2A (PP2A) activity and glycogen synthase kinase 3 (GSK-3β) activity (GSK-3β Tyr216 and Ser9 site phosphorylation increased) (Yu et al., 2011).

Studies have shown that the severity of Alzheimer's disease has a connection with the degree of neurofibrillary tangles deposition, and most neurofibrillary tangles are caused by abnormal hyperphosphorylation of tau (Šimić et al., 2016; Šimić et al., 2017; Chen Y. et al., 2020b). In the meantime, a number of researchers have reported that tau dysfunction can trigger the production of Aβ, and the overproduction of Aβ and tau dysfunction synergistically induce Alzheimer's disease (Rajmohan and Reddy, 2017). Berberine can alleviate cognitive function of Alzheimer's disease mice via reducing the hyperphosphorylation of tau and promoting the autophagy clearance of tau (Chen Y. et al., 2020b). After 24 h of berberine administration, the hyperphosphorylation of tau at Ser198/199/ 202, Ser396, Ser404, Thr205, and Thr231 was significantly reduced (Yu et al., 2011). Besides, the effects of berberine in Alzheimer's mice may be related to the inhibition of NF-κB activity and lipid peroxidation, and the increase of glutathione activity in the hippocampus (He et al., 2017) (**Figure 2**).

*In vitro*, berberine can regulate mitochondrial bioenergetics, reduce primary energy and glutathione metabolic pathway dysfunction, inhibit basal respiration, and suppress the production of pro-inflammatory cytokines. Moreover, berberine and pioglitazone have similar binding affinity to peroxisome proliferator-activated receptor gamma (PPARγ) protein, have an overlapping effect on Alzheimer's disease (Wong et al., 2021).

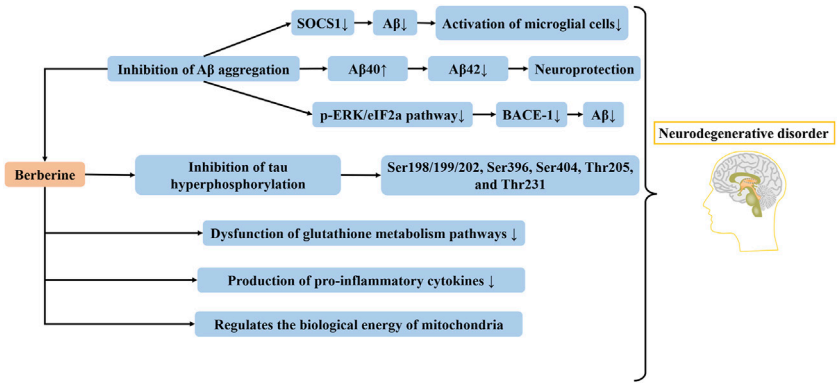


**FIGURE 2 |** The therapeutic effect of berberine on Alzheimer's disease. Berberine inhibits Aβ aggregation, tau hyperphosphorylation and pro-inflammatory cytokines production, in addition to regulating glutathione metabolism pathways and mitochondrial bioenergetics. SOCS1, suppressor of cytokine signaling 1; Aβ, amyloid β; BACE1, beta-secretase 1; p-ERK, phosphorylated extracellular signal-regulated kinase.

Under pathological conditions, long-term excessive stress can cause damage to the endoplasmic reticulum function, and endoplasmic reticulum stress activates the apoptosis pathway, which leads to nerve cell damage and even death (Cameron, 2013). Berberine treatment enhanced the cognitive ability in Alzheimer's disease rats, this effect is related to the reduction of endoplasmic reticulum stress. Berberine regulates the mRNA levels of glucose-regulated protein 78 (GRP78), CCAAT/enhancer binding protein (C/EBP) -homologous protein (CHOP), procaspase-3/9/12 in Alzheimer's disease rat's hippocampus, which involve in the endoplasmic reticulum stress pathway (Xuan et al., 2020).

Berberine conjugates, such as berberine-benzenediol derivatives, berberine-melatonin hybrid, and berberine-ferulic acid hybrid, exhibited anti-oxidant activity, and inhibited Aβ aggregation. Among them, the hydroquinone-berberine hybrid, had the greatest ability to suppress Aβ aggregation and inhibit oxidative stress (Jiang et al., 2011).

## 3.2 Parkinson's Disease

Parkinson's disease, a neurodegenerative disease characterized by muscle stiffness, tremor, speech and gait changes, and its risk factors include environmental factors, genetic factors, gender factors, age, etc. (Kalia and Lang, 2015; Hou et al., 2019). At present, the therapy of Parkinson's disease mainly uses dopamine agonists and MAO-B inhibitors to suppress the decomposition of dopamine, but they only target symptoms and have serious side effects (Jiang et al., 2015a). In the transcriptomics of *Microsporum canis*, there are 6 signaling pathways that have significant changes in Gene Ontology functional enrichment analysis after berberine treatment, including steroid biosynthesis, steroid hormone biosynthesis, Parkinson's disease, 2,4-Dichlorobenzoic acid (2,4-DCBA) degradation and biosynthesis of tropane, piperidine and isoquinoline alkaloids (Xiao et al., 2015).

Previous studies have found that berberine inhibits cell death induced by 6-OHDA, and increases the expression of HO-1, ultimately protecting dopaminergic neurons (Bae et al., 2013). In SH-SY5Y cells, berberine suppressed 6-OHDA-induced ROS production, caspase-3 activation, and cell death (Bae et al., 2013). These indicate that berberine can be used as an effective therapeutic agent for dopaminergic neuron degeneration. In MPTP/P-induced mouse model of Parkinson's disease, berberine reduced neuron loss in the substantia nigra pars compacta, dopaminergic fiber loss in the striatum, and apoptosis in the hippocampus. Animal behavior experiments have shown that the disorder of movement balance and coordination has been improved (Kim et al., 2014). However, when berberine is long-term administered to 6-OHDA-induced rat model of Parkinson's disease, monitoring for adverse symptoms is required. Preclinical studies have found that berberine increases the number of tyrosine hydroxylase (TH)-positive neurons in the substantia nigra, at the same time, berberine also increases striatum dopamine, norepinephrine, 3,4-dihydroxyphenylacetic acid (DOPAC) and homovanillic acid levels (Shin et al., 2013). Berberine is a potential therapeutic drug for alleviating motor dysfunction and memory impairment in patients with Parkinson's disease (Kim et al., 2014). Meanwhile, there are several studies offer some important insights into the neurotoxic effects of berberine. It is reported that in the Parkinson's disease model rats induced by 6-OHDA, berberine aggravate the degeneration of dopaminergic neuron in the substantia nigra of rats (Shin et al., 2013). In addition, berberine can aggravate the cytotoxicity induced by 6-OHDA in PC12 cells and aggravate of dopaminergic neuron death (Kwon et al., 2010).

Interestingly, Wang et al. pointed out that the application of berberine in Parkinson's disease may up-regulate the synthesis of L-dopa in the intestinal microbiota through vitamin-like effects, thereby exerting a therapeutic effect (Wang Y. et al., 2021a). Besides, berberine can prevent NACHT, LRR, and PYD domains-containing protein 3 (NLRP3) inflammasome from being activated during the inflammation process of Parkinson's disease and restore autophagy activity to protect dopamine neurons (Huang et al., 2020).

In addition to the above studies, in the zebrafish Parkinson's disease model, berberine derivatives can be used to treat Parkinson's disease. This is because berberine derivatives can cross the blood-brain barrier and target mitochondria in the meantime (Wang L. et al., 2021b).

### 3.4 Other Neurodegenerative Diseases

Huntington's disease is mainly caused by an autosomal dominant mutation in either of the two copies of the Huntingtin (HTT) gene (Cicchetti et al., 2014; Fan D. et al., 2019b). The pathogenesis of Huntington's disease is mainly related to striatal atrophy and neuron loss. Its symptoms include chorea, dystonia, cognitive decline, etc. (Duff et al., 2007; Subramaniam et al., 2009; Hou et al., 2019). In previous studies, the expansion of polyglutamine (polyQ) bundles to 36 or more glutamine repeats will cause the HTT protein to misfold and aggregate, leading to neuronal death and symptoms of Huntington's disease (Mangiarini et al., 1996). Recent evidence suggests that the autophagy-lysosome pathway is associated with the removal of aggregated polyQ-HTT (Sarkar and Rubinsztein, 2008; Fan D. et al., 2019b). Studies have found that berberine can effectively alleviate the motor dysfunction of HTT mice and prolong their survival time, further studies proves that berberine promote the degradation of mutant HTT protein through enhancing autophagy function, thereby reducing the accumulation of mutant huntingtin protein (Jiang et al., 2015b). Moreover, recent advances have revealed that berberine and its derivatives promote the elimination of neurotoxic misfolded proteins, which can be used as a potential treatment for neurodegenerative diseases (Rusmini et al., 2020).

Multiple sclerosis, characterized by multiple demyelinating lesions of the spinal cord and brain, has a progressive neurodegenerative pattern (Manu et al., 2021; Zahid et al., 2021). Berberine has been reported as a potential drug for the treatment of multiple sclerosis. In experimental autoimmune encephalomyelitis (a model of multiple sclerosis), berberine reduces the permeability of the blood-brain barrier and inhibits the activity of matrix metalloprotease 9 (MMP-9) in the cerebrospinal fluid and the brain of model mice (Ma et al., 2010). At the same time, berberine can inhibit gelatinase activity and reduce laminin degradation (Jiang et al., 2013). In addition, the severity of multiple sclerosis is positively correlated with the severity of reactive gliosis, and whether the anti-inflammatory effect of berberine has a connection with the treatment of multiple sclerosis still remains to be explored (Luo et al., 2017).

## 4 LIMITATIONS OF BERBERINE TREATMENT

Berberine has a variety of activities that may be involved in alleviating Alzheimer's disease, including antioxidant, neuroprotective, and anti-inflammatory effects (Campisi et al., 2014). As a natural pharmaceutical ingredient, berberine has the advantage of high safety (Rabbani et al., 1987), it is generally considered to be non-genotoxic and cytotoxic in clinical (Imanshahidi and Hosseinzadeh, 2008). So far, there have been no reports of serious adverse reactions caused by oral berberine in clinical practice, and in short-term and long-term trials, berberine is safe for most human subjects (Liu et al., 2016; Wang et al., 2017). In addition, berberine is small in size, so it can available through the blood-brain barrier and effectually act on molecular target, showing great therapeutic potential in the treatment of neurodegenerative diseases (Wang et al., 2005; Ji and Shen, 2011; Jiang et al., 2015a). However, due to the disadvantages of poor water solubility and solubility, the bioavailability of oral berberine is low (Kumar et al., 2015). At present, studies have designed formulations aimed at improving its bioavailability. For example, oral microemulsions containing berberine are 6.47 times more bioavailable than tablets and suspensions (Gui et al., 2008). Furthermore, studies have found that verapamil can enhance the neuroprotective effect of berberine by inhibiting the mechanism of P-glycoprotein efflux and preventing changes in calcium homeostasis (Kumar et al., 2016). Therefore, the changes in the dosage form or the combination with other drugs can further compensate for the weakness of low bioavailability of berberine.

## 5 CONCLUSION

The above evidences suggest that berberine has various roles in neurological diseases, including neuroinflammation, neuroprotection, oxidative stress, etc. At present, few studies to date have reported the pharmacological effects of berberine on neurodegenerative diseases, especially in human trials. In addition, most of the studies on berberine's use in the treatment of neurodegenerative diseases focus on Alzheimer's disease and Parkinson's disease, and few other diseases are involved. Therefore, the answers to some questions remain unclear. Berberine may be a valuable potential therapeutic target for various neurodegenerative diseases, as data based on both *in vitro* models and animal models of neurodegenerative diseases support the beneficial effects of berberine. In addition, it is easy to introduce natural products containing berberine into the diet because they are common enough to be used preventively. However, further research is still needed to fully understand the efficacy and dosage of berberine in clinical trials.

## AUTHOR CONTRIBUTIONS

ZC wrote the first draft. CK, SC, JS, QS, and TG provided writing reviewing and editing. YG, JL, ZS, WY, and BL provided conceptualization of ideas. XL and RC provided supervision. All authors approved the final version of the manuscript for submission.

## FUNDING

This work was supported by National Natural Science Foundation of China, China, 81871070. National Natural Science Foundation of China, 31971078. National Natural Science Foundation of China, 81971276. Jilin Science and Technology Agency funds in China, 20200301005RQ. Jilin Science and Technology Agency funds in China, 20190701078GH.

## REFERENCES


Ahmed, T., Gilani, A. U., Abdollahi, M., Daglia, M., Nabavi, S. F., and Nabavi, S. M. (2015). Berberine and Neurodegeneration: A Review of Literature. *Pharmacol. Rep.* 67, 970–979. doi:10.1016/j.pharep.2015.03.002

Ameen, D., and Michniak-Kohn, B. (2017). Transdermal Delivery of Dimethyl Fumarate for Alzheimer's Disease: Effect of Penetration Enhancers. *Int. J. Pharm.* 529, 465–473. doi:10.1016/j.ijpharm.2017.07.031

Bae, J., Lee, D., Kim, Y. K., Gil, M., Lee, J. Y., and Lee, K. J. (2013). Berberine Protects 6-Hydroxydopamine-Induced Human Dopaminergic Neuronal Cell Death through the Induction of Heme Oxygenase-1. *Mol. Cell* 35, 151–157. doi:10.1007/s10059-013-2298-5

Bandiwadekar, A., Jose, J., Khayatkashani, M., Habtemariam, S., Khayat Kashani, H. R., and Nabavi, S. M. (2021). Emerging Novel Approaches for the Enhanced Delivery of Natural Products for the Management of Neurodegenerative Diseases. *J. Mol. Neurosci.* 72, 653–676. doi:10.1007/s12031-021-01922-7

Cameron, N. E. (2013). Role of Endoplasmic Reticulum Stress in Diabetic Neuropathy. *Diabetes* 62, 696–697. doi:10.2337/db12-1469

Campisi, A., Acquaviva, R., Bonfanti, R., Raciti, G., Amodeo, A., Mastrojeni, S., et al. (20142014). Antioxidant Properties of Berberis Aetnensis C. Presl (Berberidaceae) Roots Extract and Protective Effects on Astroglial Cell Cultures. *ScientificWorldJournal* 2014, 315473. doi:10.1155/2014/315473

Campisi, A., Acquaviva, R., Mastrojeni, S., Raciti, G., Vanella, A., De Pasquale, R., et al. (2011). Effect of Berberine and Berberis Aetnensis C. Presl. Alkaloid Extract on Glutamate-Evoked Tissue Transglutaminase Up-Regulation in Astroglial Cell Cultures. *Phytother Res.* 25, 816–820. doi:10.1002/ptr.3340

Caspersen, C., Wang, N., Yao, J., Sosunov, A., Chen, X., Lustbader, J. W., et al. (2005). Mitochondrial Abeta: a Potential Focal point for Neuronal Metabolic Dysfunction in Alzheimer's Disease. *FASEB J.* 19, 2040–2041. doi:10.1096/fj.05-3735fje

Chen, J. H., Huang, S. M., Tan, T. W., Lin, H. Y., Chen, P. Y., Yeh, W. L., et al. (2012). Berberine Induces Heme Oxygenase-1 Up-Regulation through Phosphatidylinositol 3-kinase/AKT and NF-E2-Related Factor-2 Signaling Pathway in Astrocytes. *Int. Immunopharmacol* 12, 94–100. doi:10.1016/j.intimp.2011.10.019

Chen, M., Li, L., Liu, C., and Song, L. (2020a). Berberine Attenuates Aβ-Induced Neuronal Damage through Regulating miR-188/NOS1 in Alzheimer's Disease. *Mol. Cel Biochem* 474, 285–294. doi:10.1007/s11010-020-03852-1

Chen, Y., Chen, Y., Liang, Y., Chen, H., Ji, X., and Huang, M. (2020b). Berberine Mitigates Cognitive Decline in an Alzheimer's Disease Mouse Model by Targeting Both Tau Hyperphosphorylation and Autophagic Clearance. *Biomed. Pharmacother.* 121, 109670. doi:10.1016/j.biopha.2019.109670

Cicchetti, F., Lacroix, S., Cisbani, G., Vallières, N., Saint-Pierre, M., St-Amour, I., et al. (2014). Mutant Huntingtin Is Present in Neuronal Grafts in Huntington Disease Patients. *Ann. Neurol.* 76, 31–42. doi:10.1002/ana.24174

Cicero, A. F., and Baggioni, A. (2016). Berberine and its Role in Chronic Disease. *Adv. Exp. Med. Biol.* 928, 27–45. doi:10.1007/978-3-319-41334-1_2

de Oliveira, J. S., Abdalla, F. H., Dornelles, G. L., Palma, T. V., Signor, C., da Silva Bernardi, J., et al. (2019). Neuroprotective Effects of Berberine on Recognition Memory Impairment, Oxidative Stress, and Damage to the Purinergic System in Rats Submitted to Intracerebroventricular Injection of Streptozotocin. *Psychopharmacology (Berl)* 236, 641–655. doi:10.1007/s00213-018-5090-6

Deng, H., Jia, Y., Pan, D., and Ma, Z. (2020). Berberine Alleviates Rotenone-Induced Cytotoxicity by Antioxidation and Activation of PI3K/Akt Signaling Pathway in SH-Sy5y Cells. *Neuroreport* 31, 41–47. doi:10.1097/WNR.0000000000001365

Deng, H., and Ma, Z. (2021). Protective Effects of Berberine against MPTP-Induced Dopaminergic Neuron Injury through Promoting Autophagy in Mice. *Food Funct.* 12, 8366–8375. doi:10.1039/d1fo01360b

Do, T. M., Alata, W., Dodacki, A., Traversy, M. T., Chacun, H., Pradier, L., et al. (2014). Altered Cerebral Vascular Volumes and Solute Transport at the Blood-Brain Barriers of Two Transgenic Mouse Models of Alzheimer's Disease. *Neuropharmacology* 81, 311–317. doi:10.1016/j.neuropharm.2014.02.010

Duff, K., Paulsen, J. S., Beglinger, L. J., Langbehn, D. R., and Stout, J. C. (2007). Predict-HD Investigators of the Huntington Study GroupPsychiatric Symptoms in Huntington's Disease before Diagnosis: the Predict-HD Study. *Biol. Psychiatry* 62, 1341–1346. doi:10.1016/j.biopsych.2006.11.034

Fan, D., Liu, L., Wu, Z., and Cao, M. (2019b). Combating Neurodegenerative Diseases with the Plant Alkaloid Berberine: Molecular Mechanisms and Therapeutic Potential. *Curr. Neuropharmacol* 17, 563–579. doi:10.2174/1570159X16666180419141613

Fan, J., Li, B., Ge, T., Zhang, Z., Lv, J., Zhao, J., et al. (2017). Berberine Produces Antidepressant-like Effects in Ovariectomized Mice. *Sci. Rep.* 7, 1310. doi:10.1038/s41598-017-01035-5

Fan, J., Zhang, K., Jin, Y., Li, B., Gao, S., Zhu, J., et al. (2019a). Pharmacological Effects of Berberine on Mood Disorders. *J. Cel Mol Med* 23, 21–28. doi:10.1111/jcmm.13930

Feng, X., Sureda, A., Jafari, S., Memariani, Z., Tewari, D., Annunziata, G., et al. (2019). Berberine in Cardiovascular and Metabolic Diseases: From Mechanisms to Therapeutics. *Theranostics* 9, 1923–1951. doi:10.7150/thno.30787

Gao, F., Gao, Y., Liu, Y. F., Wang, L., and Li, Y. J. (2014). Berberine Exerts an Anticonvulsant Effect and Ameliorates Memory Impairment and Oxidative Stress in a Pilocarpine-Induced Epilepsy Model in the Rat. *Neuropsychiatr. Dis. Treat.* 10, 2139–2145. doi:10.2147/NDT.S73210

Goedert, M., and Spillantini, M. G. (2006). A century of Alzheimer's Disease. *Science* 314, 777–781. doi:10.1126/science.1132814

Gui, S. Y., Wu, L., Peng, D. Y., Liu, Q. Y., Yin, B. P., and Shen, J. Z. (2008). Preparation and Evaluation of a Microemulsion for Oral Delivery of Berberine. *Pharmazie* 63, 516–519.

Guo, Q., Wang, C., Xue, X., Hu, B., and Bao, H. (2021). SOCS1 Mediates Berberine-Induced Amelioration of Microglial Activated States in N9 Microglia Exposed to β Amyloid. *Biomed. Res. Int.* 2021, 9311855. doi:10.1155/2021/9311855

He, W., Wang, C., Chen, Y., He, Y., and Cai, Z. (2017). Berberine Attenuates Cognitive Impairment and Ameliorates Tau Hyperphosphorylation by Limiting the Self-Perpetuating Pathogenic Cycle between NF-Kb Signaling, Oxidative Stress and Neuroinflammation. *Pharmacol. Rep.* 69, 1341–1348. doi:10.1016/j.pharep.2017.06.006

Heemels, M. T. (2016). Neurodegenerative Diseases. *Nature* 539, 179. doi:10.1038/539179a

Hou, Y., Dan, X., Babbar, M., Wei, Y., Hasselbalch, S. G., Croteau, D. L., et al. (2019). Ageing as a Risk Factor for Neurodegenerative Disease. *Nat. Rev. Neurol.* 15, 565–581. doi:10.1038/s41582-019-0244-7

Hsu, Y. Y., Chen, C. S., Wu, S. N., Jong, Y. J., and Lo, Y. C. (2012). Berberine Activates Nrf2 Nuclear Translocation and Protects against Oxidative Damage via a Phosphatidylinositol 3-kinase/Akt-dependent Mechanism in NSC34 Motor Neuron-like Cells. *Eur. J. Pharm. Sci.* 46, 415–425. doi:10.1016/j.ejps.2012.03.004

Huang, M., Jiang, X., Liang, Y., Liu, Q., Chen, S., and Guo, Y. (2017). Berberine Improves Cognitive Impairment by Promoting Autophagic Clearance and Inhibiting Production of β-amyloid in APP/tau/PS1 Mouse Model of Alzheimer's Disease. *Exp. Gerontol.* 91, 25–33. doi:10.1016/j.exger.2017.02.004

Huang, S., Liu, H., Lin, Y., Liu, M., Li, Y., Mao, H., et al. (2020). Berberine Protects against NLRP3 Inflammasome via Ameliorating Autophagic Impairment in MPTP-Induced Parkinson's Disease Model. *Front. Pharmacol.* 11, 618787. doi:10.3389/fphar.2020.618787

Hussien, H. M., Abd-Elmegied, A., Ghareeb, D. A., Hafez, H. S., Ahmed, H. E. A., and El-Moneam, N. A. (2018). Neuroprotective Effect of Berberine against Environmental Heavy Metals-Induced Neurotoxicity and Alzheimer's-like Disease in Rats. *Food Chem. Toxicol.* 111, 432–444. doi:10.1016/j.fct.2017.11.025

Ibrahim Fouad, G., and Ahmed, K. A. (2021). Neuroprotective Potential of Berberine against Doxorubicin-Induced Toxicity in Rat's Brain. *Neurochem. Res.* 46, 3247–3263. doi:10.1007/s11064-021-03428-5

Imanshahidi, M., and Hosseinzadeh, H. (2008). Pharmacological and Therapeutic Effects of Berberis Vulgaris and its Active Constituent, Berberine. *Phytother Res.* 22, 999–1012. doi:10.1002/ptr.2399

Imenshahidi, M., and Hosseinzadeh, H. (2016). Berberis Vulgaris and Berberine: An Update Review. *Phytother Res.* 30, 1745–1764. doi:10.1002/ptr.5693

Ji, H. F., and Shen, L. (2011). Berberine: a Potential Multipotent Natural Product to Combat Alzheimer's Disease. *Molecules* 16, 6732–6740. doi:10.3390/molecules16086732

Jiang, H., Wang, X., Huang, L., Luo, Z., Su, T., Ding, K., et al. (2011). Benzenediol-berberine Hybrids: Multifunctional Agents for Alzheimer's Disease. *Bioorg. Med. Chem.* 19, 7228–7235. doi:10.1016/j.bmc.2011.09.040

Jiang, W., Li, S., and Li, X. (2015a). Therapeutic Potential of Berberine against Neurodegenerative Diseases. *Sci. China Life Sci.* 58, 564–569. doi:10.1007/s11427-015-4829-0

Jiang, W., Wei, W., Gaertig, M. A., Li, S., and Li, X. J. (2015b). Therapeutic Effect of Berberine on Huntington's Disease Transgenic Mouse Model. *PloS one* 10, e0134142. doi:10.1371/journal.pone.0134142

Jiang, Y., Wu, A., Zhu, C., Pi, R., Chen, S., Liu, Y., et al. (2013). The Protective Effect of Berberine against Neuronal Damage by Inhibiting Matrix Metalloproteinase-9 and Laminin Degradation in Experimental Autoimmune Encephalomyelitis. *Neurol. Res.* 35, 360–368. doi:10.1179/1743132812Y.0000000156

Kalia, L. V., and Lang, A. E. (2015). Parkinson's Disease. *Lancet* 386, 896–912. doi:10.1016/S0140-6736(14)61393-3

Kim, M., Cho, K. H., Shin, M. S., Lee, J. M., Cho, H. S., Kim, C. J., et al. (2014). Berberine Prevents Nigrostriatal Dopaminergic Neuronal Loss and Suppresses Hippocampal Apoptosis in Mice with Parkinson's Disease. *Int. J. Mol. Med.* 33, 870–878. doi:10.3892/ijmm.2014.1656

Kong, W., Wei, J., Abidi, P., Lin, M., Inaba, S., Li, C., et al. (2004). Berberine Is a Novel Cholesterol-Lowering Drug Working through a Unique Mechanism Distinct from Statins. *Nat. Med.* 10, 1344–1351. doi:10.1038/nm1135

Kulkarni, S. K., and Dhir, A. (2010). Berberine: a Plant Alkaloid with Therapeutic Potential for central Nervous System Disorders. *Phytother Res.* 24, 317–324. doi:10.1002/ptr.2968

Kulkarni, S. K., and Dhir, A. (2008). On the Mechanism of Antidepressant-like Action of Berberine Chloride. *Eur. J. Pharmacol.* 589, 163–172. doi:10.1016/j.ejphar.2008.05.043

Kumar, A., EkavaliChopra, K., Chopra, K., Mukherjee, M., Pottabathini, R., and Dhull, D. K. (2015). Current Knowledge and Pharmacological Profile of Berberine: An Update. *Eur. J. Pharmacol.* 761, 288–297. doi:10.1016/j.ejphar.2015.05.068

Kumar, A., EkavaliMishra, J., Mishra, J., Chopra, K., and Dhull, D. K. (2016). Possible Role of P-Glycoprotein in the Neuroprotective Mechanism of Berberine in Intracerebroventricular Streptozotocin-Induced Cognitive Dysfunction. *Psychopharmacology (Berl)* 233, 137–152. doi:10.1007/s00213-015-4095-7

Kumazawa, Y., Itagaki, A., Fukumoto, M., Fujisawa, H., Nishimura, C., and Nomoto, K. (1984). Activation of Peritoneal Macrophages by Berberine-type Alkaloids in Terms of Induction of Cytostatic Activity. *Int. J. Immunopharmacol* 6, 587–592. doi:10.1016/0192-0561(84)90069-9

Kunwar, R. M., Nepal, B. K., Kshhetri, H. B., Rai, S. K., and Bussmann, R. W. (2006). Ethnomedicine in Himalaya: a Case Study from Dolpa, Humla, Jumla and Mustang Districts of Nepal. *J. Ethnobiol. Ethnomed* 2, 27. doi:10.1186/1746-4269-2-27

Kwon, I. H., Choi, H. S., Shin, K. S., Lee, B. K., Lee, C. K., Hwang, B. Y., et al. (2010). Effects of Berberine on 6-Hydroxydopamine-Induced Neurotoxicity in PC12 Cells and a Rat Model of Parkinson's Disease. *Neurosci. Lett.* 486, 29–33. doi:10.1016/j.neulet.2010.09.038

Lee, D. H., Gold, R., and Linker, R. A. (2012). Mechanisms of Oxidative Damage in Multiple Sclerosis and Neurodegenerative Diseases: Therapeutic Modulation via Fumaric Acid Esters. *Int. J. Mol. Sci.* 13, 11783–11803. doi:10.3390/ijms130911783

Li, Q., Wu, Y., Chen, J., Xuan, A., and Wang, X. (2021). Microglia and Immunotherapy in Alzheimer's Disease. *Acta Neuro Scand.* 145, 273–278. doi:10.1111/ane.13551

Li, S., Gaur, U., Chong, C. M., Lin, S., Fang, J., Zeng, Z., et al. (2018). Berberine Protects Human Retinal Pigment Epithelial Cells from Hydrogen Peroxide-Induced Oxidative Damage through Activation of AMPK. *Int. J. Mol. Sci.* 19. doi:10.3390/ijms19061736

Li, W., Kui, L., Demetrios, T., Gong, X., and Tang, M. (2020b). A Glimmer of Hope: Maintain Mitochondrial Homeostasis to Mitigate Alzheimer's Disease. *Aging Dis.* 11, 1260–1275. doi:10.14336/AD.2020.0105

Li, Z., Jiang, T., Lu, Q., Xu, K., He, J., Xie, L., et al. (2020a). Berberine Attenuated the Cytotoxicity Induced by T-BHP via Inhibiting Oxidative Stress and Mitochondria Dysfunction in PC-12 Cells. *Cell Mol Neurobiol* 40, 587–602. doi:10.1007/s10571-019-00756-7

Liang, Y., Ye, C., Chen, Y., Chen, Y., Diao, S., and Huang, M. (2021). Berberine Improves Behavioral and Cognitive Deficits in a Mouse Model of Alzheimer's Disease via Regulation of β-Amyloid Production and Endoplasmic Reticulum Stress. *ACS Chem. Neurosci.* 12, 1894–1904. doi:10.1021/acschemneuro.0c00808

Lin, L., Li, C., Zhang, D., Yuan, M., Chen, C. H., and Li, M. (2020). Synergic Effects of Berberine and Curcumin on Improving Cognitive Function in an Alzheimer's Disease Mouse Model. *Neurochem. Res.* 45, 1130–1141. doi:10.1007/s11064-020-02992-6

Liu, C. S., Zheng, Y. R., Zhang, Y. F., and Long, X. Y. (2016). Research Progress on Berberine with a Special Focus on its Oral Bioavailability. *Fitoterapia* 109, 274–282. doi:10.1016/j.fitote.2016.02.001

Liu, Y. M., Niu, L., Wang, L. L., Bai, L., Fang, X. Y., Li, Y. C., et al. (2017). Berberine Attenuates Depressive-like Behaviors by Suppressing Neuro-Inflammation in Stressed Mice. *Brain Res. Bull.* 134, 220–227. doi:10.1016/j.brainresbull.2017.08.008

Lu, D. Y., Tang, C. H., Chen, Y. H., and Wei, I. H. (2010). Berberine Suppresses Neuroinflammatory Responses through AMP-Activated Protein Kinase Activation in BV-2 Microglia. *J. Cel Biochem* 110, 697–705. doi:10.1002/jcb.22580

Luo, J., Chen, R., Zeng, S., Yu, J., Jiang, G., Wang, L., et al. (2017). The Effects of Berberine on a Murine Model of Multiple Sclerosis and the SPHK1/S1P Signaling Pathway. *Biochem. Biophys. Res. Commun.* 490, 927–932. doi:10.1016/j.bbrc.2017.06.142

Ma, X., Chen, Z., Wang, L., Wang, G., Wang, Z., Dong, X., et al. (2018). The Pathogenesis of Diabetes Mellitus by Oxidative Stress and Inflammation: Its Inhibition by Berberine. *Front. Pharmacol.* 9, 782. doi:10.3389/fphar.2018.00782

Ma, X., Jiang, Y., Wu, A., Chen, X., Pi, R., Liu, M., et al. (2010). Berberine Attenuates Experimental Autoimmune Encephalomyelitis in C57 BL/6 Mice. *PloS one* 5, e13489. doi:10.1371/journal.pone.0013489

Maleki, S. N., Aboutaleb, N., and Souri, F. (2018). Berberine Confers Neuroprotection in Coping with Focal Cerebral Ischemia by Targeting Inflammatory Cytokines. *J. Chem. Neuroanat.* 87, 54–59. doi:10.1016/j.jchemneu.2017.04.008

Mangiarini, L., Sathasivam, K., Seller, M., Cozens, B., Harper, A., Hetherington, C., et al. (1996). Exon 1 of the HD Gene with an Expanded CAG Repeat Is Sufficient to Cause a Progressive Neurological Phenotype in Transgenic Mice. *Cell* 87, 493–506. doi:10.1016/s0092-8674(00)81369-0

Mangoni, A., Grassi, M. P., Frattola, L., Piolti, R., Bassi, S., Motta, A., et al. (1991). Effects of a MAO-B Inhibitor in the Treatment of Alzheimer Disease. *Eur. Neurol.* 31, 100–107. doi:10.1159/000116655

Manu, M. S., Hohjoh, H., and Yamamura, T. (2021). Extracellular Vesicles as Pro- and Anti-inflammatory Mediators, Biomarkers and Potential Therapeutic Agents in Multiple Sclerosis. *Aging Dis.* 12, 1451–1461. doi:10.14336/AD.2021.0513

Marchesi, N., Fahmideh, F., Boschi, F., Pascale, A., and Barbieri, A. (2021). Ocular Neurodegenerative Diseases: Interconnection between Retina and Cortical Areas. *Cells* 10, 2394. doi:10.3390/cells10092394

Matuszyk, M. M., Garwood, C. J., Ferraiuolo, L., Simpson, J. E., Staniforth, R. A., and Wharton, S. B. (2021). Biological and Methodological Complexities of Beta-amyloid Peptide: Implications for Alzheimer's Disease Research. *J. Neurochem.* 160, 434–453. doi:10.1111/jnc.15538

Moghaddam, H. K., Baluchnejadmojarad, T., Roghani, M., Khaksari, M., Norouzi, P., Ahooie, M., et al. (2014). Berberine Ameliorate Oxidative Stress and Astrogliosis in the hippocampus of STZ-Induced Diabetic Rats. *Mol. Neurobiol.* 49, 820–826. doi:10.1007/s12035-013-8559-7

Mohi-Ud-Din, R., Mir, R. H., Wani, T. U., Shah, A. J., Banday, N., and Pottoo, F. H. (2022). Berberine in the Treatment of Neurodegenerative Diseases and Nanotechnology Enabled Targeted Delivery. *Cchts* 25, 616–633. doi:10.2174/1386207324666210804122539

Ortiz, L. M., Lombardi, P., Tillhon, M., and Scovassi, A. I. (2014). Berberine, an Epiphany against Cancer. *Molecules* 19, 12349–12367. doi:10.3390/molecules190812349

Panahi, N., Mahmoudian, M., Mortazavi, P., and Hashjin, G. S. (2013). Effects of Berberine on β-secretase Activity in a Rabbit Model of Alzheimer's Disease. *Arch. Med. Sci.* 9, 146–150. doi:10.5114/aoms.2013.33354

Pathak, N., Vimal, S. K., Tandon, I., Agrawal, L., Hongyi, C., and Bhattacharyya, S. (2021). Neurodegenerative Disorders of Alzheimer, Parkinsonism, Amyotrophic Lateral Sclerosis and Multiple Sclerosis: An Early Diagnostic

Approach for Precision Treatment. *Metab. Brain Dis.* 37, 67–104. doi:10.1007/s11011-021-00800-w

Poprac, P., Jomova, K., Simunkova, M., Kollar, V., Rhodes, C. J., and Valko, M. (2017). Targeting Free Radicals in Oxidative Stress-Related Human Diseases. *Trends Pharmacol. Sci.* 38, 592–607. doi:10.1016/j.tips.2017.04.005

Qin, S., Tang, H., Li, W., Gong, Y., Li, S., Huang, J., et al. (2020). AMPK and its Activator Berberine in the Treatment of Neurodegenerative Diseases. *Curr. Pharm. Des.* 26, 5054–5066. doi:10.2174/1381612826666200523172334

Qiu, Y., Li, M., Zhang, Y., Liu, Y., Zhao, Y., Zhang, J., et al. (2022). Berberine Treatment for Weight Gain in Patients with Schizophrenia by Regulating Leptin rather Than Adiponectin. *Asian J. Psychiatr.* 67, 102896. doi:10.1016/j.ajp.2021.102896

Rabbani, G. H., Butler, T., Knight, J., Sanyal, S. C., and Alam, K. (1987). Randomized Controlled Trial of Berberine Sulfate Therapy for Diarrhea Due to Enterotoxigenic *Escherichia coli* and *Vibrio cholerae*. *J. Infect. Dis.* 155, 979–984. doi:10.1093/infdis/155.5.979

Rabey, J. M., Sagi, I., Huberman, M., Melamed, E., Korczyn, A., Giladi, N., et al. (2000). Rasagiline Mesylate, a New MAO-B Inhibitor for the Treatment of Parkinson's Disease: a Double-Blind Study as Adjunctive Therapy to Levodopa. *Clin. Neuropharmacol* 23, 324–330. doi:10.1097/00002826-200011000-00005

Rajmohan, R., and Reddy, P. H. (2017). Amyloid-Beta and Phosphorylated Tau Accumulations Cause Abnormalities at Synapses of Alzheimer's Disease Neurons. *J. Alzheimers Dis.* 57, 975–999. doi:10.3233/JAD-160612

Raju, M., Kunde, S. S., Auti, S. T., Kulkarni, Y. A., and Wairkar, S. (2021). Berberine Loaded Nanostructured Lipid Carrier for Alzheimer's Disease: Design, Statistical Optimization and Enhanced *In Vivo* Performance. *Life Sci.* 285, 119990. doi:10.1016/j.lfs.2021.119990

Rezaeian, L., Kalalian-Moghaddam, H., Mohseni, F., Khaksari, M., and Rafaiee, R. (2020). Effects of Berberine Hydrochloride on Methamphetamine-Induced Anxiety Behaviors and Relapse in Rats. *Iran J. Basic Med. Sci.* 23, 1480–1488. doi:10.22038/ijbms.2020.47285.10884

Ribeiro, F. M., Vieira, L. B., Pires, R. G., Olmo, R. P., and Ferguson, S. S. (2017). Metabotropic Glutamate Receptors and Neurodegenerative Diseases. *Pharmacol. Res.* 115, 179–191. doi:10.1016/j.phrs.2016.11.013

Rusmini, P., Cristofani, R., Tedesco, B., Ferrari, V., Messi, E., Piccolella, M., et al. (2020). Enhanced Clearance of Neurotoxic Misfolded Proteins by the Natural Compound Berberine and its Derivatives. *Int. J. Mol. Sci.* 21, 3443. doi:10.3390/ijms21103443

Sadeghnia, H. R., Kolangikhah, M., Asadpour, E., Forouzanfar, F., and Hosseinzadeh, H. (2017). Berberine Protects against Glutamate-Induced Oxidative Stress and Apoptosis in PC12 and N2a Cells. *Iran J. Basic Med. Sci.* 20, 594–603. doi:10.22038/IJBMS.2017.8847

Sadraie, S., Kiasalari, Z., Razavian, M., Azimi, S., Sedighnejad, L., Afshin-Majd, S., et al. (2019). Berberine Ameliorates Lipopolysaccharide-Induced Learning and Memory Deficit in the Rat: Insights into Underlying Molecular Mechanisms. *Metab. Brain Dis.* 34, 245–255. doi:10.1007/s11011-018-0349-5

Sarkar, S., and Rubinsztein, D. C. (2008). Huntington's Disease: Degradation of Mutant Huntingtin by Autophagy. *FEBS J.* 275, 4263–4270. doi:10.1111/j.1742-4658.2008.06562.x

Sedaghat, R., Taab, Y., Kiasalari, Z., Afshin-Majd, S., Baluchnejadmojarad, T., and Roghani, M. (2017). Berberine Ameliorates Intrahippocampal Kainate-Induced Status Epilepticus and Consequent Epileptogenic Process in the Rat: Underlying Mechanisms. *Biomed. Pharmacother.* 87, 200–208. doi:10.1016/j.biopha.2016.12.109

Shaker, F. H., El-Derany, M. O., Wahdan, S. A., El-Demerdash, E., and El-Mesallamy, H. O. (2021). Berberine Ameliorates Doxorubicin-Induced Cognitive Impairment (Chemobrain) in Rats. *Life Sci.* 269, 119078. doi:10.1016/j.lfs.2021.119078

Shin, K. S., Choi, H. S., Zhao, T. T., Suh, K. H., Kwon, I. H., Choi, S. O., et al. (2013). Neurotoxic Effects of Berberine on Long-Term L-DOPA Administration in 6-Hydroxydopamine-Lesioned Rat Model of Parkinson's Disease. *Arch. Pharm. Res.* 36, 759–767. doi:10.1007/s12272-013-0051-4

Shinjyo, N., and Kita, K. (2021). Infection and Immunometabolism in the Central Nervous System: A Possible Mechanistic Link between Metabolic Imbalance and Dementia. *Front Cel Neurosci* 15, 765217. doi:10.3389/fncel.2021.765217

Šimić, G., Babić Leko, M., Wray, S., Harrington, C., Delalle, I., Jovanov-Milošević, N., et al. (2016). Tau Protein Hyperphosphorylation and Aggregation in Alzheimer's Disease and Other Tauopathies, and Possible Neuroprotective Strategies. *Biomolecules* 6, 6. doi:10.3390/biom6010006

Šimić, G., Babić Leko, M., Wray, S., Harrington, C. R., Delalle, I., Jovanov-Milošević, N., et al. (2017). Monoaminergic Neuropathology in Alzheimer's Disease. *Prog. Neurobiol.* 151, 101–138. doi:10.1016/j.pneurobio.2016.04.001

Simões Pires, E. N., Frozza, R. L., Hoppe, J. B., and Menezes, B. d. M. (2014). Berberine Was Neuroprotective against an *In Vitro* Model of Brain Ischemia: Survival and Apoptosis Pathways Involved. *Brain Res.* 1557, 26–33. doi:10.1016/j.brainres.2014.02.021

Singh, A., Dhaneshwar, S., and Mazumder, A. (2021). Investigating Neuroprotective Potential of Berberine, Levetiracetam and Their Combination in the Management of Alzheimer's Disease Utilizing Drug Repurposing Strategy. *Crcep* 16. doi:10.2174/2772432816666210910104306

Subramaniam, S., Sixt, K. M., Barrow, R., and Snyder, S. H. (2009). Rhes, a Striatal Specific Protein, Mediates Mutant-Huntingtin Cytotoxicity. *Science* 324, 1327–1330. doi:10.1126/science.1172871

Sun, Y., Yuan, X., Zhang, F., Han, Y., Chang, X., Xu, X., et al. (2017). Berberine Ameliorates Fatty Acid-Induced Oxidative Stress in Human Hepatoma Cells. *Sci. Rep.* 7, 11340. doi:10.1038/s41598-017-11860-3

Wang, K., Feng, X., Chai, L., Cao, S., and Qiu, F. (2017). The Metabolism of Berberine and its Contribution to the Pharmacological Effects. *Drug Metab. Rev.* 49, 139–157. doi:10.1080/03602532.2017.1306544

Wang, L., Sheng, W., Tan, Z., Ren, Q., Wang, R., Stoika, R., et al. (2021b). Treatment of Parkinson's Disease in Zebrafish Model with a Berberine Derivative Capable of Crossing Blood Brain Barrier, Targeting Mitochondria, and Convenient for Bioimaging Experiments. *Comp. Biochem. Physiol. C: Toxicol. Pharmacol.* 249, 109151. doi:10.1016/j.cbpc.2021.109151

Wang, X., Wang, R., Xing, D., Su, H., Ma, C., Ding, Y., et al. (2005). Kinetic Difference of Berberine between hippocampus and Plasma in Rat after Intravenous Administration of Coptidis Rhizoma Extract. *Life Sci.* 77, 3058–3067. doi:10.1016/j.lfs.2005.02.033

Wang, Y., Tong, Q., Ma, S. R., Zhao, Z. X., Pan, L. B., Cong, L., et al. (2021a). Oral Berberine Improves Brain Dopa/dopamine Levels to Ameliorate Parkinson's Disease by Regulating Gut Microbiota. *Signal. Transduct Target. Ther.* 6, 77. doi:10.1038/s41392-020-00456-5

Wong, L. R., Tan, E. A., Lim, M. E. J., Shen, W., Lian, X. L., Wang, Y., et al. (2021). Functional Effects of Berberine in Modulating Mitochondrial Dysfunction and Inflammatory Response in the Respective Amyloidogenic Cells and Activated Microglial Cells - *In Vitro* Models Simulating Alzheimer's Disease Pathology. *Life Sci.* 282, 119824. doi:10.1016/j.lfs.2021.119824

World Health Organization (2020). *WHO Reveals Leading Causes of Death and Disability Worldwide: 2000-2019* (Accessed December 9, 2018).

Xiao, C. W., Ji, Q. A., Wei, Q., Liu, Y., Pan, L. J., and Bao, G. L. (2015). Digital Gene Expression Analysis of Microsporum canis Exposed to Berberine Chloride. *PloS one* 10, e0124265. doi:10.1371/journal.pone.0124265

Xuan, W. T., Wang, H., Zhou, P., Ye, T., Gao, H. W., Ye, S., et al. (2020). Berberine Ameliorates Rats Model of Combined Alzheimer's Disease and Type 2 Diabetes Mellitus via the Suppression of Endoplasmic Reticulum Stress. *3 Biotech.* 10, 359. doi:10.1007/s13205-020-02354-7

Ye, C., Liang, Y., Chen, Y., Xiong, Y., She, Y., Zhong, X., et al. (2021). Berberine Improves Cognitive Impairment by Simultaneously Impacting Cerebral Blood Flow and β-Amyloid Accumulation in an APP/tau/PS1 Mouse Model of Alzheimer's Disease. *Cells* 10, 1161. doi:10.3390/cells10051161

Ye, M., Fu, S., Pi, R., and He, F. (2009). Neuropharmacological and Pharmacokinetic Properties of Berberine: a Review of Recent Research. *J. Pharm. Pharmacol.* 61, 831–837. doi:10.1211/jpp/61.07.0001

Yu, G., Li, Y., Tian, Q., Liu, R., Wang, Q., Wang, J. Z., et al. (2011). Berberine Attenuates Calyculin A-Induced Cytotoxicity and Tau Hyperphosphorylation in HEK293 Cells. *J. Alzheimers Dis.* 24, 525–535. doi:10.3233/JAD-2011-101779

Yuan, N. N., Cai, C. Z., Wu, M. Y., Su, H. X., Li, M., and Lu, J. H. (2019). Neuroprotective Effects of Berberine in Animal Models of Alzheimer's Disease: a Systematic Review of Pre-clinical Studies. *BMC Complement. Altern. Med.* 19, 109. doi:10.1186/s12906-019-2510-z

Zahid, M., Busmail, A., Penumetcha, S. S., Ahluwalia, S., Irfan, R., Khan, S. A., et al. (2021). Tumor Necrosis Factor Alpha Blockade and Multiple Sclerosis: Exploring New Avenues. *Cureus* 13, e18847. doi:10.7759/cureus.18847

Zhang, C., Li, C., Chen, S., Li, Z., Jia, X., Wang, K., et al. (2017). Berberine Protects against 6-OHDA-Induced Neurotoxicity in PC12 Cells and Zebrafish through Hormetic Mechanisms Involving PI3K/AKT/Bcl-2 and Nrf2/HO-1 Pathways. *Redox Biol.* 11, 1–11. doi:10.1016/j.redox.2016.10.019

Zhang, C. C., Lu, F., Liang, J. Q., and Zhou, Y. F. (2018a). Research Progress of Histone Deacetylase 6 Inhibitors in the Therapy of Ischemic Stroke. *Sheng Li Xue Bao* 70, 301–309.

Zhang, H. N., Sun, Y. J., He, H. Q., Li, H. Y., Xue, Q. L., Liu, Z. M., et al. (2018b). Berberine Promotes Nerve Regeneration through IGFR-mediated JNK-AKT S-ignal P-athway. *Mol. Med. Rep.* 18, 5030–5036. doi:10.3892/mmr.2018.9508

Zhang, N., Gao, Y., Yu, S., Sun, X., and Shen, K. (2020). Berberine Attenuates Aβ42-Induced Neuronal Damage through Regulating circHDAC9/miR-142-5p axis in Human Neuronal Cells. *Life Sci.* 252, 117637. doi:10.1016/j.lfs.2020.117637

Zhang, Q., Bian, H., Guo, L., and Zhu, H. (2016). Pharmacologic Preconditioning with Berberine Attenuating Ischemia-Induced Apoptosis and Promoting Autophagy in Neuron. *Am. J. Transl Res.* 8, 1197–1207.

Zhang, X., Zhang, X., Wang, C., Li, Y., Dong, L., Cui, L., et al. (2012). Neuroprotection of Early and Short-Time Applying Berberine in the Acute Phase of Cerebral Ischemia: Up-Regulated pAkt, pGSK and pCREB, Down-Regulated NF-Kb Expression, Ameliorated BBB Permeability. *Brain Res.* 1459, 61–70. doi:10.1016/j.brainres.2012.03.065

Zhao, L., Li, H., Gao, Q., Xu, J., Zhu, Y., Zhai, M., et al. (2021). Berberine Attenuates Cerebral Ischemia-Reperfusion Injury Induced Neuronal Apoptosis by Down-Regulating the CNPY2 Signaling Pathway. *Front. Pharmacol.* 12, 609693. doi:10.3389/fphar.2021.609693

Zhu, F., and Qian, C. (2006). Berberine Chloride Can Ameliorate the Spatial Memory Impairment and Increase the Expression of Interleukin-1beta and Inducible Nitric Oxide Synthase in the Rat Model of Alzheimer's Disease. *BMC Neurosci.* 7, 78. doi:10.1186/1471-2202-7-78

Zhu, J. R., Lu, H. D., Guo, C., Fang, W. R., Zhao, H. D., Zhou, J. S., et al. (2018). Berberine Attenuates Ischemia-Reperfusion Injury through Inhibiting HMGB1 Release and NF-Kb Nuclear Translocation. *Acta Pharmacol. Sin* 39, 1706–1715. doi:10.1038/s41401-018-0160-1

**Conflict of Interest:** The authors declare that the research was conducted in the absence of any commercial or financial relationships that could be construed as a potential conflict of interest.

**Publisher's Note:** All claims expressed in this article are solely those of the authors and do not necessarily represent those of their affiliated organizations, or those of the publisher, the editors and the reviewers. Any product that may be evaluated in this article, or claim that may be made by its manufacturer, is not guaranteed or endorsed by the publisher.

frontiers | Frontiers in Pharmacology

MINI REVIEW
published: 23 May 2022
doi: 10.3389/fphar.2022.824420

# Current Evidence and Future Directions of Berberine Intervention in Depression

*Wen-Qian Zhu[1], Hui-Ying Wu[1], Zhi-Hui Sun[2], Yi Guo[3], Tong-Tong Ge[1], Bing-Jin Li[1], Xin Li[1]* and Ran-Ji Cui[1]**

[1]Jilin Provincial Key Laboratory on Molecular and Chemical Genetic, Second Hospital of Jilin University, Changchun, China, [2]Department of Pharmacy, The Eastern Division of First Hospital of Jilin University, Changchun, China, [3]Department of Breast Surgery, The Affiliated Hospital Changchun University of Chinese Medicine, Changchun, China

A major type of serious mood disorder, depression is currently a widespread and easily overlooked psychological illness. With the low side effects of natural products in the treatment of diseases becoming the pursuit of new antidepressants, natural Chinese medicine products have been paid more and more attention for their unique efficacy in improving depression. In a view from the current study, the positive antidepressant effects of berberine are encouraging. There is a lot of work that needs to be done to accurately elucidate the efficacy and mechanism of berberine in depression. In this review, the relevant literature reports on the treatment of depression and anxiety by berberine are updated, and the potential pharmacological mechanism of berberine in relieving depression has also been discussed.

**Keywords: berberine, bioamine, depression, natural active ingredients, neuroplasticity**

OPEN ACCESS

***Edited by:***
*Fushun Wang,*
*Nanjing University of Chinese Medicine, China*

***Reviewed by:***
*Malcolm Hopwood,*
*The University of Melbourne, Australia*
*Qi Xu,*
*Anhui Medical University, China*

****Correspondence:***
*Xin Li*
*Xinli@jlu.edu.cn*
*Ran-Ji Cui*
*cuiranji@jlu.edu.cn*

***Specialty section:***
*This article was submitted to Ethnopharmacology, a section of the journal Frontiers in Pharmacology*

***Received:*** *29 November 2021*
***Accepted:*** *01 February 2022*
***Published:*** *23 May 2022*

***Citation:***
*Zhu W-Q, Wu H-Y, Sun Z-H, Guo Y, Ge T-T, Li B-J, Li X and Cui R-J (2022) Current Evidence and Future Directions of Berberine Intervention in Depression. Front. Pharmacol. 13:824420. doi: 10.3389/fphar.2022.824420*

## INTRODUCTION

Depressive disorder is a heterogeneous disease based on symptoms forming a syndrome and causing bodily dysfunction, which has the characteristics of multiple phenotypes, biological and psychological susceptibilities, and indirect incidence (Kim 2021). The cardinal symptoms of patient include emotional instability, anhedonia, poor concentration, and tendency to commit suicide (Yang et al., 2015). With the increasing number of patients, depression has become a serious illness that threatens human health, and increases burden on families and society. A lot of research reports have made some breakthroughs in elucidating the underlying pathogenesis of depression, mainly including the widely accepted monoamine hypothesis, hypothalamic–pituitary–adrenal axis disorder hypothesis, neuroinflammation hypothesis, and neuroplasticity and neurogenesis hypothesis (Malhi and Mann 2018). These hypotheses show that depression is a rather complex medical disease caused by a combination of genetic and environmental factors, involving a variety of neurobiological substrates, brain regions, and circuits (Wang et al., 2019). Although multiple antidepressants are available, most patients do not respond with the desired effect to these treatments and even induced paradoxical effects, such as deterioration of symptoms and withdrawal symptoms (Chouinard and Chouinard 2015). In the search for better antidepressants, the lower side effects of drugs have become a pursuit of new antidepressants. Therefore, natural Chinese medicine products have been widely a concern by medical workers for their unique efficacy in improving depression. In particular, the research of safe and effective antidepressants in traditional herbal medicine has become a hot spot in the current medical field.

**TABLE 1 |** Representative examples of potential plant sources of berberine with medicinal value.

| No | Botanical name | Part used | Modal | Pharmacological properties | Reference |
|---|---|---|---|---|---|
| 1 | *Argemone mexicana* L | Leaves | Bacterial species (G+/G–) | Antibacterial activity | More et al. (2017) |
| 2 | *Berberis amurensis* | Root | Ear swelling mice | Anti-inflammatory and analgesic | Liao et al. (2021) |
| 3 | *Berberis aquifolium* | Root | HPV-positive and HPV-negative CaCx cell lines | Anticancer | Singh et al. (2021) |
| 4 | *Berberis aristate* L | Mixture of plant extracts | C57BL/6J mice/metabolic syndrome patients | Amelioration of metabolic parameters and of hepatic steatosis | Roshanravan et al., (2020) Cossiga et al. (2021) |
| 5 | *Berberis asiatica* | Air-dried root, stem | Multiple bacterial strains, fungi strains | Antibacterial activity, antifungal activity | Singh et al. (2007) |
| 6 | *Berberis chitria* | Air-dried root, stem | Multiple bacterial strains, fungi strains | Antibacterial activity, antifungal activity | Singh et al. (2007) |
| 7 | *Berberis croatica* Horvat | Root and twig | Bacterial species (G+/G–) and yeast | Antimicrobial activity | Kosalec et al. (2008) |
| 8 | *Berberis lycium* Royle | Root | HepG2 Cells | Anticancer | Mustafa et al. (2020) |
| 9 | *Berberis sibirica* Pall | Overground parts | Naive male Swiss mice | Neuroprotection | Szalak et al. (2021) |
| 10 | *Berberis thunbergii* DC. | Root | Multiple cancer cell lines | Anticancer | Suchomelova et al. (2007), Och et al. (2019) |
| 11 | *Berberis vulgaris* L | Root and twig | Bacterial species (G+/G–) and yeast | Antimicrobial activity | Kosalec et al. (2008) |
| 12 | *Coptidis rhizome* (Coptis chinensis Franch) | Dried roots | Rat/mice intestinal content | Antibacterial and antidiabetic activity | Lyu et al. (2021) |
| 13 | *Coscinium fenestratum* | Dried stems | HL-60 leukemia cells and PBMC cells | Anticancer | Tungpradit et al. (2010) |
| 14 | *Fibraurea recisa* Pierre | Fresh rattan stem | Multiple fungi strains | Antifungal activity | Rao et al. (2009) |
| 15 | *Hydrastis canadensis* L | Root and rhizomes | *Fusarium oxysporum* | Antifungal activity | Tims and Batista (2007), Douglas et al. (2010) |
| 16 | *Mahonia bealei* (Fort.) Carr | Leaves | HT-29 cells and human embryonic kidney cells | Antiproliferative activity | Hu et al. (2011) |
| 17 | *Thalictrum foliolosum* DC | Rhizomes or whole plant | β-carotene linoleate model system, goat liver, and bacterial species (G+/G–) | Antioxidant and antimicrobial activity | Pandey et al. (2018), Sharma et al. (2020) |
| 18 | *Tinospora sinensis* (Lour.) Merr | Fresh mature stems | Diabetic rat model | Antioxidant, anti-inflammatory, and antihyperglycemic activity | Banerjee et al. (2020) |

*Note. There are many plants potentially containing berberine, which is reflected in many folk medical records of different regions, well-documented pharmacopeia, and research reports. Among them, the plants containing berberine and used for pharmacological studies are listed in this table. Then research reports without models and therapeutic action were ignored. Note G+, Gram-positive bacterial species; G–, Gram-negative bacterial species; HL-60 leukemia cells, acute promyelocytic leukemia; PBMC cells, peripheral blood mononuclear cells; CaCx, cancer of the cervix; HPV, human papilloma virus; HepG2 cells, hepatocellular carcinoma cells; MCF7 cell lines, human breast adenocarcinoma cell line; HT-29, human colon cancer cells;*

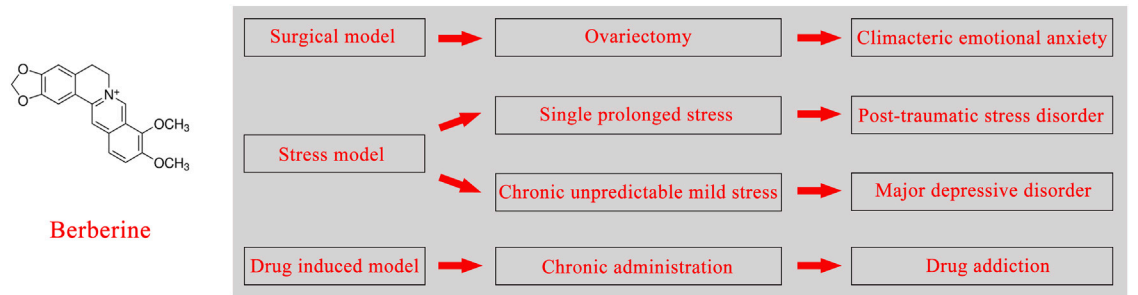


**FIGURE 1 |** Chemical structural formula of berberine, associated depression models, and clinical diseases.

The naturally effective ingredients tested in most studies were selected based on their multiple pharmacological actions, medicinal value, or as antidepressants. Berberine, an isoquinoline alkaloid, was extracted from the roots and aboveground parts of plants (**Table 1**), which are readily available from Berberidaceae, Papaveraceae, Menispermaceae, Ranunculaceae, and other botanical families (Kulkarni and Dhir 2010; Liu et al., 2016). Clinical studies of berberine have revealed multiple therapeutic actions, including anti-inflammatory, anticancer, relieving depression, hypolipidemic, and hypoglycemic actions, which indicate that berberine is a drug with multispectral activities (Mujtaba et al., 2021). Therefore, it is also a noteworthy candidate drug for the treatment of depression, which has been studied in several animal models of depression (**Figure 1**). The purpose of this review was to investigate the mechanism of berberine and its traditional Chinese medicine prescription in the treatment of depression in

recent literature reports, combined with the pathogenesis of depression. Meanwhile, we sought to present a summary of the current problems and feasible solutions of berberine in the clinical treatment of depression.

## The effect of berberine on symptom clusters of depression

The multi-angle regulatory mechanism of berberine may confer positive therapeutic effects against depression, due to its extensive range of biological effects. Many potential factors that are well known to increase the risk of depression, including the influence of sex hormones, a dulled response to stress in the hypothalamic–pituitary–adrenal axis, and a higher tendency to introspection, might boost the chances of women suffering from depression (Riecher-Rossler 2017). Moreover, findings from a Chinese woman-based cohort study showed that symptoms of anxiety and depression are more common during and after menopause than in premenopausal women (Tang et al., 2019). Therefore, the ovariectomized (OVX) mice model was used to mimic clinical postmenopausal condition (Rana et al., 2022). Researchers have found that after gavage administration of berberine (100 mg/kg), the increased content of equol (a chemical structure similar to the hormone estrogen that binds to estrogen receptors) in the OVX rat model transplanted with fecal microbiota, enriched the taxa involved in isoflavone biotransformation and significantly reduced anxiety-like behavior. The results suggest that berberine may alleviate anxiety-like behavior in perimenopausal rat partly through the microbiota–gut–brain axis system (Fang et al., 2021). In addition, our previous study showed that ovariectomy reduced the brain-derived neurotrophic factor (BDNF) protein expression levels in the hippocampus and phosphorylated cyclase adenosine monophosphate response element-binding protein (pCREB)/CREB ratio in the frontal cortex, but this change was reversed in the short term by berberine, considering that the rapid-onset antidepressant-like behavior is mediated by the decreased phosphorylation of eukaryotic elongation factor 2 (eEF2) and the increased translation of BDNF. In this case, we suggest that berberine may produce antidepressant-like effects in OVX mice via the BDNF-CREB and eEF2 pathways (Fan et al., 2017).

Depression is closely related to a decrease in neuronal plasticity. BDNF is associated with changes in neuroplasticity in certain areas, such as the amygdala and hippocampus (Camuso et al., 2021), and is deemed to be beneficial in neurogenesis, neural survival, and growth (Shen et al., 2020). A recent study showed that berberine was involved in the regulation of depression progression through miRNA and BDNF. Berberine treatment could effectively reverse the promotion effect of overexpression of miR-34b-5p/miR-470-5p on the depressive-like behavior of chronic unpredicted mild stress (CUMS) mice and regulate the growth of hippocampal neurons by mediating the expression of BDNF(Zhan et al., 2021). Clinical studies on major depression patients showed that their hippocampus was seriously damaged, and their neurogenesis function was impaired (Park 2019; Huang et al., 2020). The above pathologic phenomenon was reversed by antidepressant treatment, suggesting that neurogenesis is associated with the altered course of depression (Zeng et al., 2022). Neurogenesis, an important focus of hippocampal structural plasticity, produces full neural function that involves the proliferation and differentiation of neural stem cells (Li et al., 2020). Berberine was able to protect C17.2 neural stem cells from the 2,2′-azobis(2-amidinopropane)dihydrochloride-induced oxidative damage; to be more specific, it lowered the cellular reactive oxygen species level in C17.2 cells via the nuclear factor erythroid 2-related factor 1/2 (NRF1/2)-NAD(P)H quinone dehydrogenase 1–heme oxygenase 1 pathway. Besides, berberine enhanced the viability of C17.2 cells by upregulating the expression of extracellular signal-related kinase (ERK) and phosphor-ERK, which contributed to the activation of the WNT/β catenin pathway in C17.2 cells to promote neuronal differentiation (Shou et al., 2019).

In addition, berberine plays an antidepressant role by regulating brain neurotransmitters, especially biogenic amines. It has high affinity for dopamine receptors (Lee et al., 2018), and regulates hypothalamic corticotrophin-releasing factor and central norepinephrine systems (Lee et al., 2012). There is evidence that berberine increases the level of dopa/dopamine in blood, in which dopa enters the brain through the circulation and is converted into dopamine, so as to improve brain function. Generally, the increase in dopamine is closely related to positive emotions (Hamon and Blier 2013). Lee et al. found that single prolonged stress induced DAergic dysfunction in rats, leading to depression-like behavior. The concentration of dopamine in the hippocampus and striatum were significantly increased after intraperitoneal injection of berberine, which may alleviate anxiety to some extent (Lee et al., 2018). A recent study showed that oral berberine could promote the production of dopa/dopamine by improving the synthetic pathway of Phe–Tyr–dopa–dopamine in the gut flora, and the active compound produced by dopa/dopamine is dihydroberberine (an intestinal metabolite). In other words, dopa/dopamine in brain tissue was increased by dihydroberberine, but not berberine (Wang et al., 2021). These advances may lead to a deeper understanding of the role of berberine in regulating biogenic amines, gut–brain dialogue, and curing depression.

It is also well recognized that inflammation and weakened immunity are also key factors in the pathogenesis of depression (Chen et al., 2022). A line of evidence demonstrated that a significant proportion of patients with emotional-related diseases exhibit characteristics of chronic low-grade inflammation involving increased concentrations of peripheral and central inflammatory cytokines, inflammatory mediators, and acute-phase reactants (Felger 2018). For example, the levels of TNF-α, IL-1β, IL-6, IL-8 and other inflammatory cytokines in the serum of patients with depression is upregulated (Fan et al., 2017). Moreover, the study indicated that chronic methamphetamines (METH) induced anxiety-like behavior in rats, at least in part, by activating the immune Toll-like receptor 4 (TLR4) signaling pathway, which leads to the upregulation of the expression of several inflammatory agents, such as NF-κB and α-actin in the hippocampus (Wang et al., 2019; Rezaeian et al., 2020). Coincidentally, activation of NF-κB

by proinflammatory mediators creates a positive feedback loop that amplifies inflammatory signals (Azam et al., 2019). Based on the above research results, Rezaeian et al. suggested that oral berberine (100 mg/kg) modulated neuroinflammation and reduced anxiety behavior via suppressing the activation of TLR4 and NF-κB in METH-addicted rats (Rezaeian et al., 2020).

### The effect of Chinese medicine prescription of berberine on depression

The diversity of bioactive compounds contributes to prescriptions of traditional herbal medicines to perform multiple pharmacological effects. From this perspective, a simple theoretical conjecture is that herbal formula with several phytochemical components have more action targets than a single-compound Chinese medicine preparation. Although the action pathway or mechanism of Chinese medicine prescriptions with an antidepressant effect is relatively obscure owing to their multi-active ingredients or complexes and non-additivity, we cannot ignore the potential of prescriptions in antidepressants. Huang-Lian Jie-Du Decoction (HLJDD) is an ancient Chinese medicine prescription composed of *Coptis chinensis* Franch, *Scutellaria baicalensis* Georgi, *Phellodendron chinense* Schneid, and *Gardenia fructus* Ellis, which can ameliorate multiple central nervous system diseases, such as cerebral ischemia (Wang et al., 2013), Alzheimer's disease (Liu et al., 2019), and mental disorders (Qu et al., 2021). A study reported that the protective mechanism of HLJDD against neurotoxicity may be due to the protective effect of berberine, an important component of the formula, in alleviating the decrease in paraquat-induced mitochondrial membrane potential in human SH-SY5Y cells (Lee et al., 2021). In addition, previous studies on pharmacological properties of berberine have shown that it could reduce NADPH oxidase activity, attenuate mitochondrial defects and redox imbalance, and induce mitochondrial biogenesis, which may partially support the viewpoints mentioned above. The network pharmacology and metabolomics study showed that the main target of HLJDD-ameliorated depressive-like behaviors in CUMS mice was tryptophan metabolism, in which sodium-dependent serotonin transporter (SLC6A4) and monoamine oxidase A (MAOA) were regulated by active ingredients such as berberine (Qu et al., 2021).

## CHALLENGES AND POSSIBLE SOLUTIONS

In normal conditions, oral delivery and parenteral administration are relatively ideal routes of administration in treating chronic diseases. Although berberine has been researched for many years and received positive therapeutic feedback in an animal model of depression, there is poor bioavailability of oral or parenteral administration due to low absorption and intestinal first-pass effect, restricting its utilization in the treatment of depression (Fan et al., 2019). Therefore, it is necessary to overcome the problem of bioavailability and improve its therapeutic effects before it can be applied to clinical treatment. Nanotechnology-based drug delivery strategies constitute a potential approach to enhance the poor bioavailability of berberine. Many studies have demonstrated that topical delivery has the characteristics of targeting and performance release controllability, which plays an important role in medical treatment (Dare et al., 2020). Among them, intranasal delivery, as a form of topical delivery, bypasses the blood–brain barrier through the olfactory pathway and trigeminal nerve pathway, directly transporting drugs to the brain (Dhuria et al., 2010). Recent studies have shown that intranasal delivery of berberine was effective in the treatment of depression through a pre-prepared self-assembled thermosensitive *in situ* hydrogel (Wang et al., 2020; Xu et al., 2021). It is noteworthy that intranasal administration of hydrogel increased the bioavailability of berberine by approximately 135-fold, compared with intragastric administration of drug solution, which is probably the positive result of the synergistic effect of hydrogels in drug delivery.

## DISCUSSION

Depression is essentially a disease of the brain. Once its mechanisms of action with antidepressants are fully known, this disorder is likely to be effectively prevented and treated through some targets. In actual clinical treatment, antidepressants, such as selective serotonin reuptake inhibitor (SSRIs) or serotonin–noradrenaline reuptake inhibitors (SNRIs), are often applied to relieve symptoms. Actually, studies demonstrated that up to more than half of depression patients treated with SSRIs or SNRIs showed multiple common and well-documented adverse effects, such as some degree of emotional blunting (Christensen et al., 2021). For these reasons, while developing multitarget chemicals to reduce adverse reactions and long-term intolerance and improve the efficacy of depression drugs, a whole lot of attention is paid to the positive effects of active ingredients in natural products on depression. As a promising medicine ingredient candidate for the treatment of emotional disorders, berberine needs to be studied in substantive and long-term clinical practice with the help of neuroscience, genomics, and technologies. It exerts antidepressant effects through regulating monoamines, alleviating the dysfunction of nerve injury, ameliorating the dysregulation of immune and inflammation, and other regulatory mechanisms. Besides, it can also relieve depression-related complications, such as insomnia and cognitive impairment. Therefore, programs are necessary to increase knowledge on the use of natural antidepressants, formulate a treatment strategy for individual needs to reduce the adverse reactions of patients, as well as enhance the public's confidence in traditional Chinese medicine to cure emotional diseases, so as to improve the public's lack of trust in the health care system.

## CONCLUSION

We have reviewed the latest research progress of berberine in the treatment of depression, which may provide a reference for the

search of natural antidepressants. Although berberine has been revealed with multiple therapeutic actions, and it may be a potential drug for mood disorders, transformation research is needed to further address its safety concerns, poor bioavailability, and solubility.

## AUTHOR CONTRIBUTIONS

W-QZ wrote the manuscript. T-TG provided the critical revisions. H-Y W, Z-H S, Y G, B-J L, X L and R-J C provided supervision of entire manuscript. All authors approved the final version of the manuscript for submission.

## FUNDING

This project was funded by the National Key R&D Program of China, China (#2018YFC1311600), the National Natural Science Foundation of China, China (81871070), the National Natural Science Foundation of China, China (31971078), the National Natural Science Foundation of China, China (81971276), the Jilin Science and Technology Agency funds in China, China (20200301005RQ), The Jilin Science and Technology Agency funds in China, China (20190701078GH, 20210402003GH), and the Scientific Research Foundation of the Education Department of Jilin Province (JJKH20201032KJ). Jilin Provincial Finance Department, China(2020SCZT091, JLSCZ b2019051).

## REFERENCES

Azam, S., Jakaria, M., Kim, I. S., Kim, J., Haque, M. E., and Choi, D. K. (2019). Regulation of Toll-like Receptor (TLR) Signaling Pathway by Polyphenols in the Treatment of Age-Linked Neurodegenerative Diseases: Focus on TLR4 Signaling. *Front. Immunol.* 10, 1000. doi:10.3389/fimmu.2019.01000

Banerjee, A., Singh, S., Prasad, S. K., Kumar, S., Banerjee, O., Seal, T., et al. (2020). Protective Efficacy of Tinospora Sinensis against Streptozotocin Induced Pancreatic Islet Cell Injuries of Diabetic Rats and its Correlation to its Phytochemical Profiles. *J. Ethnopharmacol.* 248, 112356. doi:10.1016/j.jep.2019.112356

Camuso, S., La Rosa, P., Fiorenza, M. T., and Canterini, S. (2021). Pleiotropic Effects of BDNF on the Cerebellum and hippocampus: Implications for Neurodevelopmental Disorders. *Neurobiol. Dis.* 163, 105606. doi:10.1016/j.nbd.2021.105606

Chen, X., Chen, Y., Qi, D., and Cui, D. (2022). Multifaceted Interconnections between Macrophage Migration Inhibitory Factor and Psychiatric Disorders. *Prog. Neuropsychopharmacol. Biol. Psychiatry* 112, 110422. doi:10.1016/j.pnpbp.2021.110422

Chouinard, G., and Chouinard, V. A. (2015). New Classification of Selective Serotonin Reuptake Inhibitor Withdrawal. *Psychother. Psychosom.* 84, 63–71. doi:10.1159/000371865

Christensen, M. C., Fagiolini, A., Florea, I., Loft, H., Cuomo, A., and Goodwin, G. M. (2021). Validation of the Oxford Depression Questionnaire: Sensitivity to Change, Minimal Clinically Important Difference, and Response Threshold for the Assessment of Emotional Blunting. *J. Affect Disord.* 294, 924–931. doi:10.1016/j.jad.2021.07.099

Cossiga, V., Lembo, V., Nigro, C., Mirra, P., Miele, C., D'Argenio, V., et al. (2021). The Combination of Berberine, Tocotrienols and Coffee Extracts Improves Metabolic Profile and Liver Steatosis by the Modulation of Gut Microbiota and Hepatic miR-122 and miR-34a Expression in Mice. *Nutrients* 13, 1281. doi:10.3390/nu13041281

Daré, R. G., Costa, A., Nakamura, C. V., Truiti, M. C. T., Ximenes, V. F., Lautenschlager, S. O. S., et al. (2020). Evaluation of Lipid Nanoparticles for Topical Delivery of Protocatechuic Acid and Ethyl Protocatechuate as a New Photoprotection Strategy. *Int. J. Pharm.* 582, 119336. doi:10.1016/j.ijpharm.2020.119336

Dhuria, S. V., Hanson, L. R., and Frey, W. H., 2nd. (2010). Intranasal Delivery to the central Nervous System: Mechanisms and Experimental Considerations. *J. Pharm. Sci.* 99, 1654–1673. doi:10.1002/jps.21924

Douglas, J. A., Follett, J. M., Parmenter, G. A., Sansom, C. E., Perry, N. B., and Littler, R. A. (2010). Seasonal Variation of Biomass and Bioactive Alkaloid Content of Goldenseal, Hydrastis canadensis. *Fitoterapia* 81, 925–928. doi:10.1016/j.fitote.2010.06.006

Fan, J., Li, B., Ge, T., Zhang, Z., Lv, J., Zhao, J., et al. (2017). Berberine Produces Antidepressant-like Effects in Ovariectomized Mice. *Sci. Rep.* 7, 1310. doi:10.1038/s41598-017-01035-5

Fan, J., Zhang, K., Jin, Y., Li, B., Gao, S., Zhu, J., et al. (2019). Pharmacological Effects of Berberine on Mood Disorders. *J. Cel. Mol. Med.* 23, 21–28. doi:10.1111/jcmm.13930

Fan, Ni, N., Luo, Y., Ou, Y., and He, H. (2017). Altered Serum Levels of TNF-α, IL-6, and IL-18 in Depressive Disorder Patients. *Hum. Psychopharmacol.* 32. doi:10.1002/hup.2588

Fang, Y., Zhang, J., Zhu, S., He, M., Ma, S., Jia, Q., et al. (2021). Berberine Ameliorates Ovariectomy-Induced Anxiety-like Behaviors by Enrichment in Equol Generating Gut Microbiota. *Pharmacol. Res.* 165, 105439. doi:10.1016/j.phrs.2021.105439

Felger, J. C. (2018). Imaging the Role of Inflammation in Mood and Anxiety-Related Disorders. *Curr. Neuropharmacol.* 16, 533–558. doi:10.2174/1570159X15666171123201142

Hamon, M., and Blier, P. (2013). Monoamine Neurocircuitry in Depression and Strategies for New Treatments. *Prog. Neuropsychopharmacol. Biol. Psychiatry* 45, 54–63. doi:10.1016/j.pnpbp.2013.04.009

Hu, W., Yu, L., and Wang, M. H. (2011). Antioxidant and Antiproliferative Properties of Water Extract from Mahonia Bealei (Fort.) Carr. Leaves. *Food Chem. Toxicol.* 49, 799–806. doi:10.1016/j.fct.2010.12.001

Huang, Y. L., Zeng, N. X., Chen, J., Niu, J., Luo, W. L., Liu, P., et al. (2020). Dynamic Changes of Behaviors, Dentate Gyrus Neurogenesis and Hippocampal miR-124 Expression in Rats with Depression Induced by Chronic Unpredictable Mild Stress. *Neural Regen. Res.* 15, 1150–1159. doi:10.4103/1673-5374.270414

Kim, Y. K. (2021). Recent Advances and Challenges in Major Depressive Disorder. *Prog. Neuropsychopharmacol. Biol. Psychiatry* 111, 110403. doi:10.1016/j.pnpbp.2021.110403

Kosalec, I., Gregurek, B., Kremer, D., Zovko, M., Sanković, K., and Karlović, K. (2008). Croatian Barberry (Berberis Croatica Horvat): a New Source of Berberine-Analysis and Antimicrobial Activity. *World J. Microbiol. Biotechnol.* 25, 145–150. doi:10.1007/s11274-008-9860-x

Kulkarni, S. K., and Dhir, A. (2010). Berberine: a Plant Alkaloid with Therapeutic Potential for central Nervous System Disorders. *Phytother Res.* 24, 317–324. doi:10.1002/ptr.2968

Lee, B., Shim, I., Lee, H., and Hahm, D. H. (2018). Berberine Alleviates Symptoms of Anxiety by Enhancing Dopamine Expression in Rats with post-traumatic Stress Disorder. *Korean J. Physiol. Pharmacol.* 22, 183–192. doi:10.4196/kjpp.2018.22.2.183

Lee, B., Sur, B., Yeom, M., Shim, I., Lee, H., and Hahm, D. H. (2012). Effect of Berberine on Depression- and Anxiety-like Behaviors and Activation of the Noradrenergic System Induced by Development of Morphine Dependence in Rats. *Korean J. Physiol. Pharmacol.* 16, 379–386. doi:10.4196/kjpp.2012.16.6.379

Lee, I. J., Chao, C. Y., Yang, Y. C., Cheng, J. J., Huang, C. L., Chiou, C. T., et al. (2021). Huang Lian Jie Du Tang Attenuates Paraquat-Induced Mitophagy in Human SH-Sy5y Cells: A Traditional Decoction with a Novel Therapeutic Potential in Treating Parkinson's Disease. *Biomed. Pharmacother.* 134, 111170. doi:10.1016/j.biopha.2020.111170

Li, H., Li, X., Liu, Z., Wu, S., Guo, J., Shi, R., et al. (2020). Resveratrol Reserved Hypoxia-Ischemia Induced Childhood Hippocampal Dysfunction and Neurogenesis via Improving Mitochondrial Dynamics. *Neurosci. Res.* 161, 51–58. doi:10.1016/j.neures.2019.11.012

Liao, C.-P., Liu, X.-C., Dong, S.-Q., An, M., Zhao, L., Zhang, A.-J., et al. (2021). Investigation of the Metabolites of Five Major Constituents from Berberis Amurensis in normal and Pseudo Germ-free Rats. *Chin. J. Nat. Medicines* 19, 758–771. doi:10.1016/S1875-5364(21)60082-1

Liu, C. S., Zheng, Y. R., Zhang, Y. F., and Long, X. Y. (2016). Research Progress on Berberine with a Special Focus on its Oral Bioavailability. *Fitoterapia* 109, 274–282. doi:10.1016/j.fitote.2016.02.001

Liu, Y., Du, T., Zhang, W., Lu, W., Peng, Z., Huang, S., et al. (2019). Modified Huang-Lian-Jie-Du Decoction Ameliorates Aβ Synaptotoxicity in a Murine Model of Alzheimer's Disease. *Oxid Med. Cel. Longev.* 2019, 8340192. doi:10.1155/2019/8340192

Lyu, Y. F., Lin, L., Xie, Y. N., Li, D., Xiao, M., Zhang, Y. F., et al. (2021). Blood-Glucose-Lowering Effect of Coptidis Rhizoma Extracts from Different Origins via Gut Microbiota Modulation in Db/db Mice. *Front. Pharmacol.* 12, 684358. doi:10.3389/fphar.2021.684358

Malhi, G. S., and Mann, J. J. (2018). Depression. *Lancet* 392, 2299–2312. doi:10.1016/S0140-6736(18)31948-2

More, N. V., Kharat, K. R., and Kharat, A. S. (2017). Berberine from Argemone Mexicana L Exhibits a Broadspectrum Antibacterial Activity. *Acta Biochim. Pol.* 64, 653–660. doi:10.18388/abp.2017_1621

Mujtaba, M. A., Akhter, M. H., Alam, M. S., Ali, M. D., and Hussain, A. (2022). An Updated Review on Therapeutic Potential and Recent Advances in Drug Delivery of Berberine: Current Status and Future prospect. *Cpb* 23, 60–71. doi:10.2174/1389201022666210208152113

Mustafa, K., Mohamed, H., Shah, A. M., Yu, S. X., Akhlaq, M., Xiao, H. F., et al. (2020). *In Vitro* Anticancer Potential of Berberis Lycium Royle Extracts against Human Hepatocarcinoma (HepG2) Cells. *Biomed. Res. Int.*, 8256809. doi:10.1155/2020/8256809

Och, A., Zalewski, D., Komsta, Ł., Kołodziej, P., Kocki, J., and Bogucka-Kocka, A. (2019). Cytotoxic and Proapoptotic Activity of Sanguinarine, Berberine, and Extracts of Chelidonium Majus L. And Berberis Thunbergii DC. toward Hematopoietic Cancer Cell Lines. *Toxins (Basel)* 11, 485. doi:10.3390/toxins11090485

Pandey, G., Khatoon, S., Pandey, M. M., and Rawat, A. K. S. (2018). Altitudinal Variation of Berberine, Total Phenolics and Flavonoid Content in Thalictrum Foliolosum and Their Correlation with Antimicrobial and Antioxidant Activities. *J. Ayurveda Integr. Med.* 9, 169–176. doi:10.1016/j.jaim.2017.02.010

Park, S. C. (2019). Neurogenesis and Antidepressant Action. *Cell Tissue Res.* 377, 95–106. doi:10.1007/s00441-019-03043-5

Qu, S. Y., Li, X. Y., Heng, X., Qi, Y. Y., Ge, P. Y., Ni, S. J., et al. (2021). Analysis of Antidepressant Activity of Huang-Lian Jie-Du Decoction through Network Pharmacology and Metabolomics. *Front. Pharmacol.* 12, 619288. doi:10.3389/fphar.2021.619288

Rana, A. K., Sharma, S., Patial, V., and Singh, D. (2022). Lithium Therapy Subdues Neuroinflammation to Maintain Pyramidal Cells Arborization and Rescues Neurobehavioural Impairments in Ovariectomized Rats. *Mol. Neurobiol.* doi:10.1007/s12035-021-02719-w

Rao, G. X., Zhang, S., Wang, H. M., Li, Z. M., Gao, S., and Xu, G. L. (2009). Antifungal Alkaloids from the Fresh rattan Stem of Fibraurea Recisa Pierre. *J. Ethnopharmacol.* 123, 1–5. doi:10.1016/j.jep.2009.02.046

Rezaeian, L., Kalalian-Moghaddam, H., Mohseni, F., Khaksari, M., and Rafaiee, R. (2020). Effects of Berberine Hydrochloride on Methamphetamine-Induced Anxiety Behaviors and Relapse in Rats. *Iran J. Basic Med. Sci.* 23, 1480–1488. doi:10.22038/ijbms.2020.47285.10884

Riecher-Rössler, A. (2017). Sex and Gender Differences in Mental Disorders. *Lancet Psychiatry* 4, 8–9. doi:10.1016/S2215-0366(16)30348-0

Roshanravan, B., Yousefizadeh, S., Apaydin Yildirim, B., Farkhondeh, T., Amirabadizadeh, A., Ashrafizadeh, M., et al. (2020). The Effects of Berberis Vulgaris L. And Berberis Aristata L. in Metabolic Syndrome Patients: a Systematic and Meta-Analysis Study. *Arch. Physiol. Biochem.*, 1–12. doi:10.1080/13813455.2020.1828482

Sharma, N., Kumar, V., Chopra, M. P., Sourirajan, A., Dev, K., and El-Shazly, M. (2020). Thalictrum Foliolosum: A Lesser Unexplored Medicinal Herb from the Himalayan Region as a Source of Valuable Benzyl Isoquinoline Alkaloids. *J. Ethnopharmacol.* 255, 112736. doi:10.1016/j.jep.2020.112736

Shen, X., Hui, R., Luo, Y., Yu, H., Feng, S., Xie, B., et al. (2020). Berberine Facilitates Extinction of Drug-Associated Behavior and Inhibits Reinstatement of Drug Seeking. *Front. Pharmacol.* 11, 476. doi:10.3389/fphar.2020.00476

Shou, J. W., Cheung, C. K., Gao, J., Shi, W. W., and Shaw, P. C. (2019). Berberine Protects C17.2 Neural Stem Cells from Oxidative Damage Followed by Inducing Neuronal Differentiation. *Front. Cel. Neurosci.* 13, 3955. doi:10.3389/fncel.2019.00395

Singh, M., Srivastava, S., and Rawat, A. K. (2007). Antimicrobial Activities of Indian Berberis Species. *Fitoterapia* 78, 574–576. doi:10.1016/j.fitote.2007.03.021

Singh, T., Chhokar, A., Thakur, K., Aggarwal, N., Pragya, P., Yadav, J., et al. (2021). Targeting Aberrant Expression of STAT3 and AP-1 Oncogenic Transcription Factors and HPV Oncoproteins in Cervical Cancer by Berberis Aquifolium. *Front. Pharmacol.* 12, 757414. doi:10.3389/fphar.2021.757414

Suchomelová, J., Bochoráková, H., Paulová, H., Musil, P., and Táborská, E. (2007). HPLC Quantification of Seven Quaternary Benzo[c]phenanthridine Alkaloids in Six Species of the Family Papaveraceae. *J. Pharm. Biomed. Anal.* 44, 283–287. doi:10.1016/j.jpba.2007.02.005

Szalak, R., Kukula-Koch, W., Matysek, M., Kruk-Słomka, M., Koch, W., Czernicka, L., et al. (2021). Effect of Berberine Isolated from Barberry Species by Centrifugal Partition Chromatography on Memory and the Expression of Parvalbumin in the Mouse Hippocampus Proper. *Int. J. Mol. Sci.* 22, 4487. doi:10.3390/ijms22094487

Tang, R., Luo, M., Li, J., Peng, Y., Wang, Y., Liu, B., et al. (2019). Symptoms of Anxiety and Depression Among Chinese Women Transitioning through Menopause: Findings from a Prospective Community-Based Cohort Study. *Fertil. Steril.* 112, 1160–1171. doi:10.1016/j.fertnstert.2019.08.005

Tims, Mc., and Batista, C. (2007). Effects of Root Isoquinoline Alkaloids from Hydrastis canadensis on Fusarium Oxysporum Isolated from Hydrastis Root Tissue. *J. Chem. Ecol.* 33, 1449–1455. doi:10.1007/s10886-007-9319-9

Tungpradit, R., Sinchaikul, S., Phutrakul, S., Wongkham, W., and Chen, S. T. (2010). Anti-Cancer Compound Screening and Isolation: Coscinium Fenestratum, Tinospora Crispa and Tinospora Cordifolia. *Chiang Mai J. Sci.* 37, 476–488.

Wang, P. R., Wang, J. S., Zhang, C., Song, X. F., Tian, N., and Kong, L. Y. (2013). Huang-Lian-Jie-Du-Decotion Induced Protective Autophagy against the Injury of Cerebral Ischemia/reperfusion via MAPK-mTOR Signaling Pathway. *J. Ethnopharmacol.* 149, 270–280. doi:10.1016/j.jep.2013.06.035

Wang, Q. S., Li, K., Gao, L. N., Zhang, Y., Lin, K. M., and Cui, Y. L. (2020). Intranasal Delivery of Berberine via *In Situ* Thermoresponsive Hydrogels with Non-invasive Therapy Exhibits Better Antidepressant-like Effects. *Biomater. Sci.* 8, 2853–2865. doi:10.1039/c9bm02006c

Wang, Y., Tong, Q., Ma, S. R., Zhao, Z. X., Pan, L. B., Cong, L., et al. (2021). Oral Berberine Improves Brain Dopa/dopamine Levels to Ameliorate Parkinson's Disease by Regulating Gut Microbiota. *Signal. Transduct Target. Ther.* 6, 77. doi:10.1038/s41392-020-00456-5

Wang, Xiaohui, X., Northcutt, A. L., Cochran, T. A., Zhang, X., Fabisiak, T. J., Haas, M. E., et al. (2019). Methamphetamine Activates Toll-like Receptor 4 to Induce Central Immune Signaling within the Ventral Tegmental Area and Contributes to Extracellular Dopamine Increase in the Nucleus Accumbens Shell. *ACS Chem. Neurosci.* 10, 3622–3634. doi:10.1021/acschemneuro.9b00225

Wang, Y. S., Shen, C. Y., and Jiang, J. G. (2019). Antidepressant Active Ingredients from Herbs and Nutraceuticals Used in TCM: Pharmacological Mechanisms and Prospects for Drug Discovery. *Pharmacol. Res.* 150, 104520. doi:10.1016/j.phrs.2019.104520

Xu, D., Qiu, C., Wang, Y., Qiao, T., and Cui, Y. L. (2021). Intranasal Co-delivery of Berberine and Evodiamine by Self-Assembled Thermosensitive *In-Situ* Hydrogels for Improving Depressive Disorder. *Int. J. Pharm.* 603, 120667. doi:10.1016/j.ijpharm.2021.120667

Yang, L., Zhao, Y., Wang, Y., Liu, L., Zhang, X., Li, B., et al. (2015). The Effects of Psychological Stress on Depression. *Curr. Neuropharmacol.* 13, 494–504. doi:10.2174/1570159x1304150831150507

Zeng, N. X., Li, H. Z., Wang, H. Z., Liu, K. G., Gong, X. Y., Luo, W. L., et al. (2022). Exploration of the Mechanism by Which Icariin Modulates Hippocampal Neurogenesis in a Rat Model of Depression. *Neural Regen. Res.* 17, 632, doi:10.4103/1673-5374.320993

Zhan, Y., Han, J., Xia, J., and Wang, X. (2021). Berberine Suppresses Mice Depression Behaviors and Promotes Hippocampal Neurons Growth through Regulating the miR-34b-5p/miR-470-5p/BDNF Axis. *Neuropsychiatr. Dis. Treat.* 17, 613–626. doi:10.2147/NDT.S289444

**Conflict of Interest:** The authors declare that the research was conducted in the absence of any commercial or financial relationships that could be construed as a potential conflict of interest.

**Publisher's Note:** All claims expressed in this article are solely those of the authors and do not necessarily represent those of their affiliated organizations, or those of the publisher, the editors, and the reviewers. Any product that may be evaluated in this article, or claim that may be made by its manufacturer, is not guaranteed or endorsed by the publisher.

# Advantages of publishing in Frontiers

**OPEN ACCESS**
Articles are free to read for greatest visibility and readership

**FAST PUBLICATION**
Around 90 days from submission to decision

**HIGH QUALITY PEER-REVIEW**
Rigorous, collaborative, and constructive peer-review

**TRANSPARENT PEER-REVIEW**
Editors and reviewers acknowledged by name on published articles

**Frontiers**
Avenue du Tribunal-Fédéral 34
1005 Lausanne | Switzerland

**Visit us:** www.frontiersin.org
**Contact us:** frontiersin.org/about/contact

**REPRODUCIBILITY OF RESEARCH**
Support open data and methods to enhance research reproducibility

**DIGITAL PUBLISHING**
Articles designed for optimal readership across devices

**FOLLOW US**
@frontiersin

**IMPACT METRICS**
Advanced article metrics track visibility across digital media

**EXTENSIVE PROMOTION**
Marketing and promotion of impactful research

**LOOP RESEARCH NETWORK**
Our network increases your article's readership